THE TÜRKİYE EARTHQUAKE SEQUENCE OF FEBRUARY 2023

A LONGITUDINAL STUDY REPORT BY EEFIT

February 2024

EEFIT

THE TÜRKİYE EARTHQUAKE SEQUENCE OF FEBRUARY 2023

A LONGITUDINAL STUDY REPORT BY EEFIT

Cite as:
Aktaş, Y. D., So, E., Johnson, C., Dönmez, K., Özden, A. T., Vatteri, A. P., O'Kane, A., Kalkan, A., Andonov, A., Verrucci, E., Çabuk, E., Opabola, E., Malcıoğlu, F. S., Marko, H. P., Giardina, G., Madabhushi, G., Triantafyllou, I., Byun, J. E., Jones, J. N., Asinari, M., Free, M., Bashein, M., Bektaş, N., Adamidis, O., Gözenoğlu, Ö., Milillo, P., Dede, Ş., Boulton, S. J., Açıkgöz, S., Gökçe, T., Efeoğlu, T., Tetik, T., Novelli, V., Gonnuru, P., Voelker, B., Tavakkoli, A., Macchiarulo, V., Gutierrez-Urzua, F., Freddi, F. & Rossetto, T. (2024). The Türkiye Earthquake Sequence of February 2023: A Longitudinal Study Report by EEFIT. Earthquake Engineering Field Investigation Team (EEFIT), Institution of Structural Engineers (IStructE). DOI: 10.13140/RG.2.2.15906.40641

EEFIT

Dr Yasemin Didem AKTAŞ, University College London (UCL)

Prof Emily SO, University of Cambridge

Prof Cassidy JOHNSON, University College London (UCL)

Kökcan DÖNMEZ, University College London (UCL)

Dr Ali Tolga ÖZDEN, Canakkale Onsekiz Mart University

Dr Ahsana PARAMMAL VATTERI, University College London (UCL)

Dr Aisling O'KANE, University of Canterbury & GNS Science

Akbey KALKAN, Sellafield Ltd

Anton ANDONOV, Mott Macdonald

Dr Enrica VERRUCCI, University College London (UCL)

Eser ÇABUK, Dolfen Engineering

Dr Eyitayo Opabola, University College London (UCL)

Dr Fatma Sevil MALCIOĞLU, Boğaziçi University

Hristo Pavlov MARKOV, Willis Towers Watson (WTW)

Dr Giorgia GIARDINA, Delft University of Technology

Prof Gopal Madabhushi, University of Cambridge

Dr Ioanna TRIANTAFYLLOU, National & Kapodistrian University of Athens

Dr Ji-Eun BYUN, University of Glasgow

Dr Joshua Nathan JONES, AECOM

Mariana ASINARI, Mott Macdonald

Dr Matthew FREE, Arup

Mohammed Bashein, RedR

Nurullah BEKTAŞ, Széchenyi István University

Dr Orestis ADAMIDIS, University of Oxford

Özcan GÖZENOGLU, Arup

Prof Pietro MILILLO, University of Houston & German Aerospace Center (DLR)

Şahin DEDE, University College London (UCL)

Dr Sarah J. BOULTON, University of Plymouth

Dr Sinan AÇIKGÖZ, University of Oxford

Dr Tansu GÖKÇE, University of Bristol

Teoman EFEOĞLU, University of Bristol

Tuğce TETİK, Namık Kemal University & Boğaziçi University

Dr Viviana NOVELLI, Cardiff University

With support from:

Pratyusha Gonnuru (University of Houston)

Brandon Voelker (University of Houston)

Amin Tavakkoli (University of Houston)

Dr Valentina Macchiarulo (TU-Delft)

Dr Fernando Gutiérrez-Urzúa (UCL)

Dr Fabio FREDDI, University College London (UCL)

Prof Tiziana ROSSETTO, University College London (UCL)

EXECUTIVE SUMMARY

On 6 February 2023 at 4:17 am local time, a large area in southeastern Türkiye and northern Syria was hit by an Mw 7.8 earthquake, which was followed by an Mw 7.5 earthquake at 1:24 pm local time, causing the loss of more than 50,000 lives, some 100,000 injuries and significant damage to buildings and infrastructure, estimated to be in the range of 84.1 billion USD for Türkiye alone. The largest earthquake in Türkiye since the deadly 1939 Erzincan earthquake with however much larger losses, the sequence immediately attracted the attention of the global post-disaster reconnaissance/engineering communities. This included the Earthquake Engineering Field Investigation Team (EEFIT), who, within one week of the event, gathered a team with 30 people from academia and industry in the UK (19), Türkiye (5), New Zealand (1), Hungary (1), Bulgaria (1), Greece (1) and USA (1) with two support members from the UK and the Netherlands, to study the events and their impacts, and also to develop suggestions to reduce the existing vulnerabilities in the future. The team was organised in the form of 6 working groups as shown below, which were (1) strong ground motions and seismotectonics, (2) geotechnics, (3) structures, (4) infrastructure, (5) remote sensing and (6) relief response and recovery.

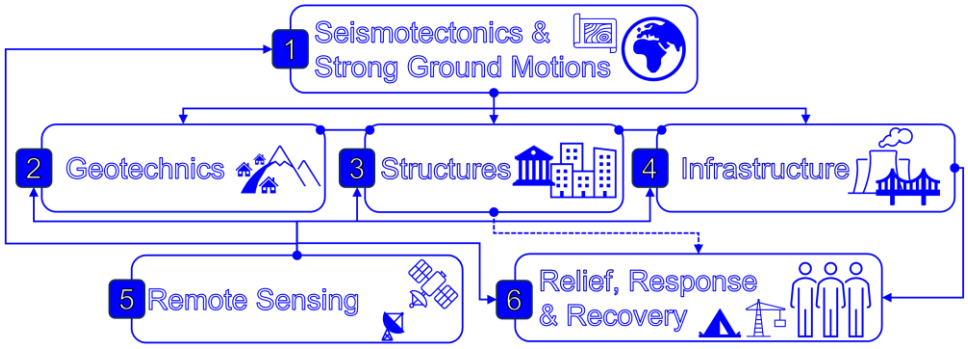

Established EEFIT working groups and organization of the team.

Following the EEFIT missions carried out during the height of the Covid-19 pandemic, this mission also followed a “hybrid” model with part of the team working remotely to assist the field crew. One of the objectives of the study is to identify and/or develop alternative data sources that are not typically consulted or used as primary sources during post-disaster work for formal data collection. Importantly, the primary objectives of the EEFIT mission were delineated considering parallel national and international efforts in order to make sure that EEFIT’s contribution is complementary. To this end, particular emphasis has been given to rural building stocks and communities.

The field team of 15 members deployed to the affected area on 13-17 March, where they visited city centres and villages in Hatay, Kahramanmaraş, Gaziantep and Adıyaman, to study geotechnics, structural and infrastructure response, and relief-response-recovery characteristics. The team also collected data to support remote sensing team. This was followed by three other field deployments with smaller teams: on 12-20 April to study the performance of monumental heritage buildings in Osmaniye and Hatay, on 16-24 June to study the performance of vernacular/traditional buildings in Kahramanmaraş, Malatya and Antakya and to monitor recovery, and lastly on 29 September-4 October to study the performance of vernacular/traditional buildings in Kahramanmaraş, Osmaniye and Antakya.

The key findings emerging from these field studies and other remotely conducted studies are given below:

- Strong motivation for embedding **scientific knowledge in policies**. The well-distributed seismic network in the area allowed us to comprehend the characteristics of ground motions and be able to correlate the shaking with damage. The very high **vertical acceleration** and further provisions regarding **soft soil conditions** need to be reflected in building code revisions.

- Profit drive pushes all players within the construction industry to take shortcuts. The **auditing and quality control mechanisms** embedded in the legal and bureaucratic processes should be strengthened to ensure code compliance. The **legalisation of non-compliant buildings** through amnesties cannot continue.

- Building stock is primarily composed of **RC structures**, which are therefore the main cause of the casualties. We observed problems within the full life cycle of structures: design, implementation, and post-occupancy stages, which, among others, manifest in the form of poor concrete quality, inadequate detailing, short columns, failure under soft storey and post-occupancy amendment on the structural system at detriment to the seismic performance.

- Critically, despite the established technical know-how, state-of-the-art building codes and rigourous building regulations, deficiencies in RC structures were found even in the newest building stock. This demonstrates that seismic resilience is **not only a technical problem** in Türkiye but one that requires a multi-sectoral and interdisciplinary dialogue scrutinising the regulatory system, bureaucratic hierarchy, legal/political backdrop against which the construction sector operates in Türkiye, work ethics and the “social contract”, economic and professional pressures and risk perception, among others.

- Review of building stock and infrastructure is needed to review risk levels for future earthquakes; therefore **a building census** is critical. Lack of publicly available data is a big problem in Türkiye hindering not only a robust inquiry into damage and associated building characteristics, but also reliably establishing the risk profiles for future events.

- **Rapid and extensive urban expansion/densification** has been further exacerbated in the affected areas during and after the Syrian Civil War. In light of these addition pressures, proactive urban planning and urban development, responsive to seismic risk are needed to control land-use.

- **Land reclamation using liquefiable materials** was identified to be problematic by the field team.

- **Healthcare infrastructure** also requires attention. Moderately damaged healthcare facilities that could have been checked and reopened were closed due to a lack of process to inspect them in the crucial hours post-earthquake.

- The current seismic risk induced urban regeneration practices seem to rely on new builds, however we have evidence that **retrofit** can work and it should therefore be prioritised whenever possible for a lower cost/carbon footprint solution and reduce disruptions on people’s lives.

- **TOKI and in general tunnelform** buildings performed well, and the current reconstruction efforts are almost entirely characterised by TOKI new built. However, this monochromatic approach to rehousing will come at the cost of depleting the diversity and richness of living cultures, and hence a homogenisation of the built environment.

- Particularly under strain is the **vernacular/traditional civil architecture** within the affected areas, characterised by diverse use of materials and structural detailing. These are however unlisted and hence not underpinned by strong policy and legislation for their preservation, as opposed to the listed monumental heritage. They are particularly vulnerable due to the lack of guidance and practice as to the damage level thresholds that

they need to be assessed against. We noted that this category of buildings was consistently assigned higher-than-actual damage classes, and many which could be repaired will therefore be facing demolishment.

- Both urban and rural areas have a significant proportion of **complex, hard-to-categorise buildings** in them. These are often modern structures that grew in time (e.g. additional floors every few years) featuring multiple construction techniques, and not necessarily well implemented. They are therefore not only difficult to capture with data collection tools, but also to assign damage grades and therefore determine their seismic adequacy for future events.

- It is of utmost importance that future **data collection tools** that the reconnaissance teams use on site are flexible enough to capture specificities of the particular built environment and tailored to these needs for data collection.

- The affected area of this earthquake in Türkiye is home to people from many **different ethnic and religious backgrounds**. Although up-to-date information is not published by the state, there are large groups speaking Kurdish and Arabic, as well as smaller groups identifying as Circassian, Greek, Georgian, Armenian, Laz, Pomal, Bosnian, Albanian and Jewish. We observed that most of these communities drew on their larger ethnic networks to assist with relief, response and recovery, and had to rely less on the state's primacy in helping with these matters. These alternative networks of coordination and aid proved very beneficial and should be examined further.

- A centralised approach and lack of localised knowledge and strategies were quoted as barriers to risk preparedness. We propose that working groups with **multi-sectoral engagement of key stakeholders**, with representatives from local governments and affected communities are set up to allow recovery to be sustainable and reconstruction lasting.

- The earthquake sequence has further exacerbated an already **fragile and dynamic population of migrants and the need to migrate**. People who earn their lives from agriculture, orcharding, olive cultivation and animal husbandry found it particularly hard to migrate elsewhere, even temporarily, because of the need to tend to their land and the strict schedules they must follow for income.

- **Debris management and demolishment practices** have not fully recognised the potential of mid-/long-term environmental and public health implications. Our field observations and contacts in the affected communities show that they are already affected by the poor air quality.

- The **Compulsory Earthquake Insurance (CEI)** is a system that was put in place in Türkiye following the 1999 earthquakes to provide monetary reserves to fund the management of future disasters. The extent to which these funds have been used and how resources have been allocated remain unclear.

- The **reserve area system** and the more recently launched law no. 7441 on the establishment of post-disaster reconstruction funds do not give the affected communities enough confidence or better certainty about what awaits them in terms of housing. Communications on the decision-making process and implementation of post-earthquake recovery should be clear and unambiguous, ideally with local consultations.

- Resilience as a **systems problem**. The team believe we can only truly understand and learn from earthquakes through longitudinal studies of the area and in collaboration with many local and international colleagues. We are committed as professionals to be embedded with local teams to help with reconstruction and recovery, acting as advocates for their work and together coming up with strategies to incentivise good building practice.

EEFIT

CONTENTS

EEFIT

LIST OF TABLES

TABLE OF FIGURES

ACKNOWLEDGEMENTS

The team would like to thank the following organisations and individuals for their support to the mission: EPSRC (EP/P025234/1 awarded to Emily So, EP/P025951/1 awarded to Tiziana Rossetto, EP/P025641/1 awarded to Sean Wilkinson) and TUBITAK for funding, Recep Çakır (AFAD), Eray Güner & Erzin Municipality, Mayors and *Muhtar*s of the affected areas, Sevgi Harika Karakoç (AFAD), Burcu Bilir (KVKB), Gokhan Çiçek (*Vakıflar*), Filiz Diri-Akyıldız (METU), Barış Erdil (Van University), Emre Akın (Mersin University), Felat Dursun (Diyarbakır University), Katie Bitten (RedR), Filip Kirazov & Josh Macaguag (SARAID), Sebastian Kaminski (IStructE), Ahmet Yakut and the EERC (METU), METU Alumni Foundation, METU 2002 Alumni Group, METU Mountaineering and Winter Sports Club (DKSK), Deniz Demirağ, Caoimhe Butterly, Arda Özacar (METU), Erdal Şafak (KOERI, BU), Eser Çaktı (KOERI, BU), Emin Yahya Menteşe (KOERI, BU), İsra Özdemir Bostancıoğlu (İstanbul Metropolitan Municipality), Ömer Bitargil, Cem Çapar, Aren Dadiroglu, Dimyan Emektas, Ketrin Köprü an&d Anna-Maria Beylunioğlu (Nehna), Müslüm Küçük, Zilan Özcan, Kevork Özkaragöz, Abdullah Papasoğlu, Mişel Uyar, Yusuf Tabasyan, Nazan Savaş (Mustafa Kemal University), Sean Wilkinson (Newcastle University), Nima Ekhtari, Nicole Guinn (UH), Natcha Ruamsanitwong (Umbra Lab, Capella Space for SAR data acquisitions), Anıl Özdemir (Gazi University), Deniz Dalgıç & Cennet Yeşilyurt (Izmir Institute of Technology), Medine Ispir Arslan & Elif Durgut (Istanbul Technical University), İdris Bedirhanoğlu & Yavuz Dizgin (Dicle University), Baran Bozyiğit (University of Oxford, Dokuz Eylul University), Canan Yıldeniz (Diyarbakir Chamber of Architects), Bora Pulatsu (Carleton University), Alper İlki (Istanbul Technical University), Can Teymur, Ratibe Bugrahan, Alparslan Bugrahan, Aren Dadiroglu, Ahmet Cakmak, İlyas Terbiyeli, Can Sadreddin, Hanna Tere, Ahmet Saylak, Dimyan Emektas, Hasan Sen, Metin Emir, Metin Topaloglu, Nuh Uste, Abdullah Yumurta, Erdan Tunalı, Hasan Aktaş, Övgü Garbioğlu, Ceren Emir & Doğa Restaurant ve Düğün Salonları.

For providing equipment: Thomas Altinok (Screening Eagle), Shirley Underwood (Screening Eagle), Heather Viles (University of Oxford), Hong Zhang (University of Oxford).

Finally, we are indebted to the communities of the affected areas.

All pictures are EEFIT's unless otherwise stated.

1. INTRODUCTION

On February 6, 2023, a devastating earthquake sequence struck southern and central Türkiye and northern and western Syria, causing widespread damage and loss of life. The first earthquake, with a magnitude of 7.8, occurred at 04:17 TRT (01:17 UTC) near the city of Gaziantep, about 37 km west-northwest of the epicentre. The second earthquake, with a magnitude of 7.5, occurred at 13:24 TRT (10:24 UTC) about 95 km north-northeast of the first one. Both earthquakes had a shallow depth of less than 10 km and a maximum intensity reaching to “Extreme” on the Modified Mercalli scale. They were followed by thousands of aftershocks, some of which exceeded M_W 6.0, in the following months (USGS, 2023a).

The earthquake sequence resulted from the complex interaction of several major fault systems in the region, namely the East Anatolian Fault Zone, the Dead Sea Fault Zone and the Sürgü–Misis Fault Zone. The first earthquake ruptured a segment of the East Anatolian Fault, which is a right-lateral strike-slip fault that accommodates the westward motion of the Anatolian Plate relative to the Arabian Plate. The second earthquake ruptured a segment of the Sürgü–Misis Fault, which is a left-lateral strike-slip fault that branches off the East Anatolian Fault. Both earthquakes exhibited supershear rupture propagation, meaning that the rupture speed exceeded the shear wave speed in the surrounding medium, generating strong ground motions and large surface displacements (Loft, 2023; USGS, 2023b).

The earthquake sequence affected a very large area in Türkiye (11 provinces of the nation were declared as part of the disaster region) and the North of Syria, and impacted an estimated 10+ million people, or 15-20% percent of Türkiye's population. The confirmed death toll stood at 62,013: 53,537 in Türkiye and 8,476 in Syria. More than 120,000 people were injured and about 300 people are still reported missing. About 1.5 million people were left homeless or displaced, as tens of thousands of buildings collapsed or were severely damaged. The earthquake sequence also triggered landslides, liquefaction, fires, and a minor tsunami in the Mediterranean Sea. The total economic damage was estimated at more than 84.1 billion USD for Türkiye alone, making it one of the costliest disasters in history.

The earthquake sequence posed significant challenges for the humanitarian response and recovery efforts, as the affected area spanned across two countries with strained political and diplomatic relations. The Turkish government declared a state of emergency and mobilised its disaster management agencies, military, and civil society organisations to provide relief and assistance to the affected population. The Syrian government, which was still engaged in a civil war, also appealed for international aid and cooperation. Several countries and international organisations, such as the United Nations, the European Union, the Red Cross, and the World Bank, offered their support and resources to both countries. However, the coordination and delivery of humanitarian aid were hampered by security risks, logistical constraints, bureaucratic hurdles, and political sensitivities.

The purpose of this report is to provide a comprehensive and objective assessment of the situation in Türkiye after the February 2023 earthquake sequence, based on the available data and information from various sources. The report will cover the following

aspects: the seismological (Chapter 2) and geotechnical (Chapter 3) characteristics of the earthquake sequence, the extent and distribution of the physical damage in the built environment (Chapter 4) and in infrastructure (Chapter 5), remote sensing tools and methods deployed for a remote examination of the events (Chapter 6) and the immediate and long-term impacts on the social, economic, and environmental sectors, the challenges and opportunities for the humanitarian response and recovery efforts (Chapter 7), and the lessons learned and recommendations for future disaster risk reduction and resilience building (Chapter 8).

In the subsequent sections of this chapter, we will delineate the motivations for the missions, the setup of the EEFIT team, and mission planning and programme.

1.1. Motivations for an EEFIT Mission to February 2023 Türkiye-Syria Earthquake Sequence

According to data from the World Health Organization (WHO, 2023), earthquakes worldwide caused approximately 750,000 fatalities between 1998 and 2017. In this approximately 20-year period, in addition to the mentioned death toll, earthquakes affected more than 125 million people through injuries, homelessness, or evacuations. When the 2023 Türkiye earthquake sequence is added to this striking global picture, the threat posed by earthquakes to public health becomes more evident. The importance of reducing earthquake risk, shortcomings in this regard, and the necessity of multidisciplinary efforts, more pronounced. The societal impact of earthquakes in Türkiye since 1900 is illustrated in *Figure 1* (database: EM-DAT, 2023). While the effects of the 1939 Erzincan and 1999 Kocaeli earthquakes on society are noteworthy in this plot, the 2023 Türkiye earthquake sequence has left the most significant impact in this timeline. As a result of the 2023 earthquakes, the total number of fatalities in Türkiye due to earthquakes increased to 146,872, and the number of injuries rose to 209,057. Another significant finding in this plot is the total number of people affected by earthquakes in Türkiye rose from 7.7 million until the 2023 earthquakes, when there was a jump of 220%, to reach the level of 17 million.

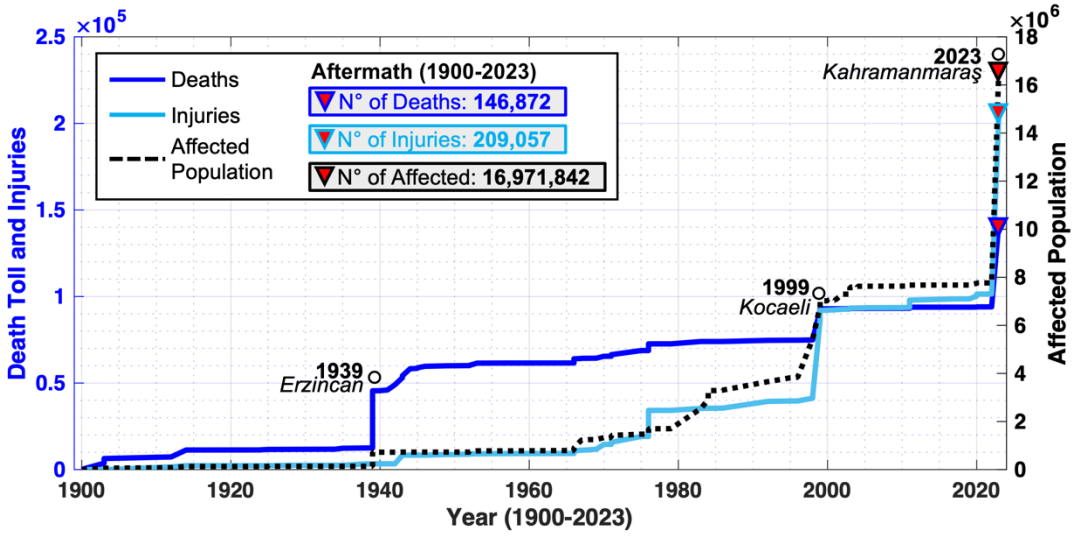

Figure 1: Earthquake-induced impact in Türkiye: Fatalities, injuries and affected population in the 20th century & early 21st century (developed by the team based on data from EM-DAT, 2023).

In addition to the very high number casualties and injuries, the sheer size of the earthquake affected areas, composed of 11 provinces (Adana, Adıyaman, Diyarbakır, Gaziantep, Elazığ, Hatay, Kahramanmaraş, Kilis, Malatya, Osmaniye, and Şanlıurfa), multiple high magnitude strong ground motions exceeding design spectra in horizontal and vertical directions in certain localities and the subsequent widespread damage in the built environment and the wider infrastructure, the relatively recent introduction of a new earthquake code in Türkiye by the time that the earthquakes hit, the diverse building stock, population profiles and rich built and non-built heritage settings in the affected area, and immediately obvious problems with the first emergency response operations prompted the EEFIT committee to make the decision to launch a mission to the events.

1.2. EEFIT Team and Planning

1.2.1. Team Composition

The team was selected and organised to cover 6 main domains in post-disaster reconnaissance: Seismotectonics and strong ground motion characteristics; Geotechnics; Structures; Infrastructure; Remote Sensing; and Relief, Response & Recover (RRR). The core team was composed of 30 individuals composed of academics (21) and industry/policy representatives (9) primarily from the UK (19), Türkiye (5), but also New Zealand (1), Hungary (1), Bulgaria (1), Greece (1) and USA (1), 12 of whom were Turkish nationals and 11 PhD students or early career researchers. Additionally, the team had two support members and has benefitted extensively from the involvement of many external contributors as shown in *Table 1*.

Table 1: Team of EEFIT Mission to 2023, Türkiye-Syria Earthquake Sequence (names in bold are theme leads)

	Remote Team	**Field Team**	**External Contributors**
Team Leaders	Emily So (University of Cambridge	Yasemin D Aktaş (UCL)	
Seismotectonics and Strong Ground Motion Characteristics	**Matthew Free** (Arup), Sarah J. Boulton (University of Plymouth), Aisling O'Kane (University of Canterbury & GNS Science), Fatma Sevil Malcioglu (KOERI, BU)	Kökcan Dönmez (UCL & KOERI, BU), Tuğçe Tetik (KOERI, BU & Tekirdağ Namık Kemal University)	
Geotecnics	**Gopal Madabushi** (University of Oxford), Ioanna Triantafyllou (National & Kapodastrian University of Athens), Joshua Jones (AECOM)	Teoman Efeoğlu (University of Bristol), Özcan Gözenoğlu (Arup), Orestis Adamidis (University of Oxford)	
Structures	Sahin Dede (UCL), Hristo Pavlov Markov (WTW), Mariana Asinari (Mott MacDonald)	**Viviana Novelli** (Cardiff University), Ahsana Parammal Vatteri (UCL), Tuğçe Tetik (KOERI & Namık Kemal University),	

		Nurullah Bektas (Szechenyi Istvan University), Eser Çabuk (Dolfen Eng & Cons), Kökcan Dönmez (UCL & KOERI), Sinan Açıkgöz (University of Oxford)	
Infrastructure	Tansu Gökçe (University of Bristol), Ji-Eun Byun (University of Glasgow)	**Anton Andonov** (Mott MacDonald), Ahsana Parammal Vatteri (UCL), Akbey Kalkan (Sellafield)	
Remote Sensing	**Pietro Millillo** (University of Houston & DLR), Joshua Nathan Jones (AECOM), Giorgia Giardina (TU-Delft), Sinan Açıkgöz (University of Oxford)		Pratyusha Gonnuru (University of Houston), Brandon Voelker (University of Houston), Amin Tavakkoli (University of Houston), Valentina Macchiarulo (TU-Delft)
Relief, Response, Recovery (RRR)	**Ali Tolga Özden** (Canakkale University), Sahin Dede (UCL)	Cassidy Johnson (UCL), Ahsana Parammal Vatteri (UCL)	Mohammed Bashein (RedR)
Data Analysis and Mapping Support	Enrica Verrucci (UCL)		

1.2.2. International Cooperation and Planning

Since 2011, academic participation in EEFIT missions has been supported by the UK's Engineering and Physical Science Research Council (EPSRC) and has deployed to most significant events around the world. Earthquakes that occurred in 2020 and 2021 during the COVID-19 pandemic challenged the disaster risk resilience community to come up with alternative ways of achieving the objectives of a reconnaissance activity. With international travel being disrupted, teams were unable to physically go to the disaster-stricken areas for a field study of damage to buildings and infrastructure. During this time EEFIT relied on a hybrid approach by exploring other and innovative means of remotely accessible information on the event and partnering up with locals to carry out the fieldwork under the coordination of the remote team.

This EEFIT mission also adopted a hybrid approach for two reasons. We believe there is much to be gained remotely prior deployment, for the team to familiarise themselves with the territory and gain a preliminary assessment of a much wider spatial coverage of the affected area. Secondly, it allows the field team to focus their time and resources more efficiently on critical regions known to have been impacted. For short time-sensitive missions, this can be invaluable to maximise what can be achieved.

For example, for the EEFIT February 2023 Kahramanmaraş Earthquake Sequence mission, the geotechnical field team was directed by the remote members to assess whether a valley-blocking landslide posed a potential dam outburst flood risk in the region. On site, the team were able to locate the large valley-blocking landslide at Değirmencik quickly and make an assessment. At the time of the visit in March 2023, there had been a lot of rain in the earthquake-affected area and a large volume of

water had filled up behind this natural dam. While on site, EEFIT members alerted the water authority (DSI) of the dangers a potential breach of the dam would pose to the village directly downstream.

Despite the advances in technology, witnessing the consequences of the event allows for a better understanding of the totality of the situation, which is hard to grasp remotely. There are also limitations of remotely sensed images (satellite, drone footage, and photographs). Buildings that from the outside and certainly at a distance look fine could have significant internal damage that is not visible. Aerial views and satellite imagery do not convey the extent of what has happened and what is visible at the time of deployment.

In all, the EEFIT team conducted four missions to the field over a period of seven months. This longitudinal study allowed the members to first gain an important overview of the consequences of the earthquake sequence, establish contacts and identify areas of interest/ concern; then with each return mission, to home in on specific questions and issues pertinent to the EEFIT team members own expertise or research interest, and investigate matters that have not been widely reported nor understood.

The team were acutely aware of the international attention of these events and the number of first response and national and international reconnaissance who were deployed or considering deployment at the early stages of the EEFIT's team planning in February 2023. We were keen not to become a hindrance to the important work our national engineering colleagues were doing, some as independents, others as directed by the ministry or prosecutors' office. Moreover, we did not want to burden the already overstretched local resources and logistical support. The team's motivation was to add value to what was being done and to provide an objective view and expertise to the global surveys. The EEFIT team therefore held back the field deployment under the advisory of AFAD and worked in data gathering mode for a month, in constant coordination with EERI and other international teams to share data and findings from our remote investigations. The team obtained permission from AFAD to visit the affected area in March 2023, and a field team of 15 were on the ground from 13-17th March 2023. Despite the team's initial plans to deploy to the affected region in Northern Syria, we encountered challenges in execution due to the complex political environment and the volatile conditions at the nation's borders.

1.2.3. Itineraries of the EEFIT Missions

The four EEFIT missions are listed in *Table 2*.

Table 2: EEFIT missions

Dates	Locations	EEFIT Team Members	External Collaborators	Notes
13-17 Mar 2023	Districts and villages in Hatay, Kahramanmaraş, Adana, Osmaniye, Gaziantep and Adıyaman	Field team of 15 delineated in *Table 1*	Mohammed Bashein (RedR) to work with the Relief, Response, Recovery (RRR) team	The main EEFIT mission with working groups on Seismotectonics and Strong Ground Motion Characteristics, Geotecnics, Structures, Infrastructure, and Relief, Response, Recovery (RRR). Stakeholder engagement.
12-20 Apr 2023	Hatay and Osmaniye	Sinan Açıkgöz and Kökcan Dönmez	Baran Bozyiğit (University of Oxford, Dokuz Eylul University), Anıl Özdemir (Gazi University), Korhan Deniz Dalgıç & Cennet Yesilyurt (Izmir Institute of Technology), Medine İspir Arslan & Elif Durgut (Istanbul Technical University), İdris Bedirhanoğlu & Yavuz Dizgin (Dicle University) , Canan Yıldeniz (Diyarbakir Chamber of Architects)	Monumental structures. Further supported by TUBITAK 2219 – Postdoctoral Research Fellowship Programme & TUBITAK 2221 - Fellowships for Visiting Scientists and Scientists on Sabbatical Leave
16-24 Jun 2023	Hatay, Kahramanmaraş and Malatya	Yasemin D Aktaş, Emily So, Cassidy Johnson, Kökcan Dönmez	Filiz Diri-Akyıldız (METU), Felat Dursun (Dicle University), Barış Erdil (Van Yüzüncü Yıl University)	Traditional/vernacular structures in. Monitoring of recovery through interviews with community members and public health professionals. Further supported by TUBITAK 2221 - Fellowships for Visiting Scientists and Scientists on Sabbatical Leave
29 Sep-4 Oct 2023	Hatay, Osmaniye, Kahramanmaraş	Yasemin D Aktaş, Kökcan Dönmez		

In addition to these, this report has benefitted from 3 additional missions with involvement from the EEFIT team members. These are detailed in *Table 3*.

Table 3: Other missions with involvement from EEFIT team members

Dates	Locations	EEFIT Team Members	Other collaborators / organisers	Notes
11-16 Feb 2023	Hatay, Kahramanmaraş, Adıyaman, Malatya	Ali Tolga Özden	Chamber of Architects Technical Committee - Structures Group: Eyüp Muhcu, Songül Üzgün, Esin Köymen, Selma Aslan, Sibel Bas & Cultural Heritage Group: Zeynep Eres, Mehmet Özdoğan, Umut Almaç, Melis Özge Gayretli	Investigation of urban and rural planning, structural damage in the housing stock and cultural assets, economic/social and socio-cultural impacts of the events. (see TMMOB Mimarlar Odası., 2023 for more details)
14-20 Feb 2023	Adıyaman city centre, Gölbaşı, Besni	Tuğçe Tetik	Expert team composed of a structural engineer (Tuğçe Tetik), an architect (Burak Enes Gülgönül), a geophysical engineer (Doğukan Durdağ) and a public prosecutor, all appointed to Adıyaman Courthouse by the Tekirdağ Office of Attorney General	Data collection from heavily damaged buildings and those responsible for casualties using datasheets at http://cbs.nabi.com.tr/Adıyaman/giris.html
16-19 Jun, 2023	Hatay, Kahramanmaraş, Adıyaman, Malatya and Gaziantep	Şahin Dede	Tiziana Rossetto (UCL), Fabio Freddi (UCL), Fernando Gutiérrez-Urzúa (UCL)	Tunnel-form buildings

1.2.4. Health and Safety

The team was given a health and safety briefing on 10 March 2023 covering general guidelines as to the personal protective equipment (PPE) and safe building damage assessment practices and packing essentials. Additionally, all field team members were given a training on asbestos related risks on site and how to minimise these by Meral Mungan Arda, Projects Coordinator on chemicals and waste at United Nations Development Programme (UNDP) in Türkiye on the morning of the 10 March 2023.

1.3. Mission Objectives

The main objectives of all EEFIT reconnaissance missions are:

- To carry out a detailed technical evaluation of the performance of structures, foundations, civil engineering works and industrial plants within the affected areas.
- To collect geological and seismographic data, including strong ground motions.
- To assess the effectiveness of earthquake protection methods, including repair and retrofit, and to make comparisons of the actual performance of structures with the expectations of designers.
- To study disaster management procedures and socio-economic effects of the earthquake, including human casualties.

More specifically to the EEFIT reconnaissance mission to the Türkiye-Syria Earthquake Sequence of February 2023, the following specific objectives were also identified as complementary to the other international reconnaissance groups' efforts and therefore were taken into the scope:

- To develop an understanding of the rural areas, both in terms of structural performance as well as the particularities of community needs and the efficacy of response and relief operations.
- To develop links with a wide-ranging local stakeholders for communication and impact.
- To develop a longitudinal understanding of recovery in the affected areas and to observe how the experience of this earthquake sequence and the devastation it caused will transpire in policy, technical guidance and overall management of the earthquake risk.

1.4. Dissemination of Results

By the time of writing this report, the following dissemination of the mission and its findings were made:

Mission blog:

https://eefitKahramanmarash.wordpress.com (accessed on 29 Jan 2023)

Mission report expanded summary in Turkish:

Aktas, Y.D., Dönmez, K., So, E., Johnson, C., Özden, A.T., Parammal Vatteri, A., O'Kane, A., Kalkan, A., Andonov, A., Verrucci. E., Çabuk, E., Opabola, E., Malcıoğlu, F.S., Marko, H.P., Giardina, G., Madabushi, G., Triantafyllou, I., Byun, J-E., Jones, J.N., Asinari, M., Free, M., Bashein, M., Bektaş, N., Adamidis, O., Gözenoğlu, O., Milillo, P., Dede, S., Boulton, S.J., Açıkgöz, S., Gökçe, T., Efeoğlu, T., Tetik, T. & Novelli, V. (2024). 2023 Türkiye Deprem Sekansı Deprem Mühendisliği Saha Çalışmaları Ekibi (EEFIT) Raporu Türkçe Genişletilmiş Özet. Available at https://www.istructe.org/resources/report/eefit-mission-report-turkey-february-2023/ DOI: 10.13140/RG.2.2.27126.16966/1

Mission lecture:

EEFIT (2023) EEFIT Mission to February 2023 Kahramanmaraş Earthquake Sequence - Preliminary Findings. Available at https://www.istructe.org/resources/case-study/eefit-mission-to-6-february-2023-Kahramanmaras-tur/ (accessed on 5 April 2023)

Journal papers:

Adamidis, O., Efeoglu, T., Gozenoglu, O., Jones, J., Madabhushi, G.S.P., Aktaş, Y.D., So, E. (2023) Technical Note: Geotechnical observations from the 2023 Kahramanmaraş EEFIT Mission; **Ground Engineering Magazine**, December 2023, pp. 24-28.

Macchiarulo V., Giardina, G., Milillo, P., Aktaş, Y.D., Whitworth, M.R.Z. (2024) Integrating post-event Very High Resolution SAR imagery and Machine Learning for building-level earthquake damage assessment, **Bulletin of Earthquake Engineering**. DOI: 10.1007/s10518-024-01877-1

Bozyigit, B., Ozdemir, A., Dönmez, K., Dalgic, D., Durgut, E., Yesilyurt, C., Dizgin, Y., Yildeniz, C., Arslan, M., Bedirhanoglu, I., Aktaş, Y.D., Acikgoz, S. (2023) Damage to monumental masonry buildings in Hatay and Osmaniye following the 2023 Turkey earthquake sequence: the role of wall geometry, construction quality and material properties, **Earthquake Spectra** (under review).

Conference papers:

Macchiarulo, V., Giardina, G., Milillo, P., Aktaş, Y.D. (2024) Assessing building damage after the 2023 Kahramanmaraş Earthquake sequence using post-disaster VHR SAR data, 2024 **IEEE International Geoscience and Remote Sensing Symposium** (IGARSS 2024), Athens, Greece

So, E., Aktaş, Y.D., Dönmez, K., Johnson, C. (2024) Learning more from earthquakes: An attempt to collect macroseismic, casualty, and early recovery data, 18th **World Conference on Earthquake Engineering** (WCEE2024), Milan, Italy.

Bozyigit, B., Ozdemir, A., Dönmez, K., Dalgic, D., Durgut, E., Yesilyurt, C., Dizgin, Y., Yildeniz, C., Ispir, M., Bedirhanoglu, I., Aktaş, Y.D., Acikgoz, S. (2024) Investigation of Stone Masonry Construction Techniques and Material Properties in Hatay and Osmaniye after the 2023 Türkiye-Syria Earthquakes, 18th **World Conference on Earthquake Engineering** (WCEE 2024), 30 June-5 July, Milan, Italy.

Jing, Y., Zhang, Z., Yang, Y., Dönmez, K., Shan, A., Acikgoz, S. (2024). Use of Reality Capture Data to Assess Masonry Buildings after the 2023 Turkey-Syria Earthquakes. 18th **World Conference on Earthquake Engineering** (WCEE 2024), 30 June-5 July, Milan, Italy.

Johnson, C., Aktaş, Y.D., So, E., Dönmez, K. (2023) The case for examining building practices in Türkiye in the wake of the 2023 earthquakes, United Kingdom **Alliance for Disaster Research (UKADR) Annual Conference** 2023 - 2030 and Beyond: Risk-informed decision making, investment and behaviour, Huddersfield, UK.

Aktaş, Y.D., So, E., Parammal Vatteri, A., Johnson, C., Cabuk, E., Malcioglu, F.S., Dönmez, K., Asinari, M., Adamidis, O. Milillio, P., Tetik, T., Novelli, V., O'Kane, A., Kalkan. A., Ozden, A.T., Andonov, A., Verrucci, E., Opabola, E., Markov, H.P., Giardina, G., Madabhushi, G., Triantahyllou, I., Byun, J-E., Jones, J.N., Free, M., Bektas, N., Gozenoglu, O., Dede, S., Acikgoz, S., Gokce, T., Efeoglu, T. (2023) Hybrid EEFIT Mission to February 223 Kahramanmaraş Earthquake Sequence. **Society for Earthquake and Civil Engineering Dynamics**, SECED 2023, 14-15 September, Cambridge, UK.

International workshops and invited talks:

Aktaş, Y.D., **Architectural Association**, School of Architecture. Symposium of **Fault Lines: (Pre)Legislation and (Post)Reconstruction** in London, UK, 16 February 2024.

Aktaş, Y.D., **Marmara Forum Deep Dive Session on Earthquake Preparedness of Istanbul** on 4-7 October 2023**.** Other speakers are Prof Mustafa Erdik (Bogazici Uni), Dr Cemil Arslan (Marmara Municipalities Union) and Emin Yahya Mentese (Bogazici Uni). All expenses covered by the Union.

Acikgoz, S. Special session on **the impact of the 2023 Turkey earthquake sequence on the historic built environment** during the 2023 Structural Analyis of Historic Constructions conference in Kyoto Japan**.** 13 September 2023. Speakers: Eleni Smyrou, Bora Pulatsu, Chiara Bertolin, Altug Erberik, Sinan Acikgoz, Yixiong Jing, Ihsan Bal.

Aktaş, Y.D., **The 2nd Joint Seminar on the 2023 Earthquake in the Southern Turkey and Syria - Current Status and Issues After 6 Months, strategy for recovery, reconstruction, BBB, and Resilient society**, on 3 August 2023, organized by IRIDeS Tohoku Univ. and IRDR UCL, METU, Istanbul Tech Univ.

So, E., **Elements of a Catastrophe**, 1st June, Hay Festival 2023, 23 May to 2 June 2023, UK.

Boulton, S.J., **Anatomy of a disaster- The East Anatolian Fault Zone and the 6 February 2023 earthquakes**, 1st on 22 March 2023, Annual Geohazards A-level Conference at University of Plymouth & 2nd on November 2023, Plymouth Atheneaum Society.

Aktaş, Y.D., **Joint Seminar on the 2023 Earthquake in Southern Turkey and Syria - Mechanism, damage and strategy for recovery, reconstruction, BBB, and Resilient society to speak on building damage**, 27 February 2023, Organized by IRIDeS, Tohoku University and IRDR, University College London & Supported by Middle East Technical University and Istanbul Technical University, Türkiye

Selected news articles:

DW (Deutsche Welle). Live on 25/09/2023 both at 1 pm and 10 pm. Topic: Poisonous Rubble: The Hidden Dangers of Asbestos after Turkey's Devastating Earthquake.

CNBC's The next earthquake: Is time running out for Europe's largest city?: https://www.cnbc.com/video/2023/08/23/the-next-earthquake-is-time-running-out-for-europes-largest-city.html

The Telegraph article on the 2023 Turkey Earthquakes: https://www.telegraph.co.uk/global-health/climate-and-people/turkey-earthquake-rebuilding-project-devastation-erdogan/

DW (Deutsche Welle). Live on 30/03/2023 on the earthquake preparedness of Istanbul

NTV (in Turkish) on 14/03/2023 on the 6 February 2023 Kahramanmaraş Earthquake.

BBC Scotland, live on 14/03/2023 on the 6 February 2023 Kahramanmaraş Earthquake. From 1:50 https://www.bbc.co.uk/sounds/play/m001k023

BBC World News, live on 14/03/2023 on the 6 February 2023 Kahramanmaraş Earthquake.

The Agenda on Dubai Eye radio news show on 19/02/2023 on the 6 February 2023 Kahramanmaraş Earthquake.

Financial Times article titled "Lessons from a disaster: building homes for an earthquake": https://www.ft.com/content/67a83b8f-fc04-4e96-88b0-c4f89c9eabbf

DW (Deutsche Welle). Live on 10&14&15/02/2023 on the 6 February 2023 Kahramanmaraş Earthquake.

BBN Panorama on 13/02/2023 on the 6 February 2023 Kahramanmaraş Earthquake: https://www.youtube.com/watch?v=cs0Xup8l928

Sanlian Lifeweek on 10/02/2023 the 6 February 2023 Kahramanmaraş Earthquake.

CNN International. Live on 10/02/2023 on the 6 February 2023 Kahramanmaraş Earthquake: https://www.youtube.com/watch?v=pogzPBPQXWs

Sky News on 09/02/2023 on the 6 February 2023 Kahramanmaraş Earthquake

Channel4 News with Fatima Manji on 08/02/2023 on the 6 February 2023 Kahramanmaraş Earthquake: https://www.channel4.com/news/engineer-explains-why-turkey-earthquake-was-so-destructive

LBS News with Chris Golds on 06/02/2023 on the 6 February 2023 Kahramanmaraş Earthquake

References

EM-DAT (2023) The OFDA/CRED International Disaster Database, CRED / UCLouvain, Brussels, Belgium. Available at www.emdat.be last accessed 12 December, 2023.

Loft, P. (2023) Earthquake in Syria and Türkiye February 2023 - The House of Commons Library. available at https://commonslibrary.parliament.uk/research-briefings/cbp-9727/ (accessed 11 Jan 2023)

TMMOB Mimarlar Odasi (2023) Mimarlar Odasi 6 Subat 2023 Depremleri Raporu – 2: Tespitler, Degerlendirmeler, Oneriler. 2 Mayis 2023, Mimarlar Odasi

USGS (2023a) M7.8 and M7.5 Kahramanmaraş Earthquake Sequence near Nurdağı, Türkiye (,Türkiye), available at https://www.usgs.gov/news/featured-story/m78-and-m75-Kahramanmaraş-earthquake-sequence-near-Nurdağı-Türkiye-,Türkiye (accessed 11 Jan 2023)

USGS (2023b) New Interactive Geonarrative Explains the 2023 Türkiye, Earthquake Sequence, available at https://www.usgs.gov/programs/earthquake-hazards/news/new-interactive-geonarrative-explains-2023-Türkiye-earthquake (accessed 11 Jan 2023)

WHO (World Health Organisation). 2023. “Earthquakes”. Available at https://www.who.int/health-topics/earthquakes#tab=tab_1 last accessed 21 November, 2023.

2. SEISMOTECTONICS AND STRONG GROUND MOTION CHARACTERISTICS

2.1. Introduction

On the 6th February 2023, two M_w 7 earthquakes occurred on the East Anatolian Fault Zone (EAFZ), and caused widespread damage across Türkiye and Syria. This chapter presents the geological background and tectonic history of the area affected by the earthquakes and offers a seismological interpretation of the events that make up the Kahramanmaraş earthquake sequence, in context with the regional and local seismic history. The main characteristics of the recorded strong ground motions from three main events are presented, and comparisons with seismic codes for Türkiye and Ground Motion Models (GMMs; formerly known as Ground Motion Prediction Equations, GMPEs) are discussed. These strong ground motion results offer insight into the engineering parameters discussed in the following geotechnical and structures chapters. In addition, a brief description of the geomorphological effects from the earthquakes are outlined, including field observations of the earthquake's surface rupturing, coastal inundation flooding, and evidence of liquefaction recorded in local harbours across Türkiye and Cyprus.

2.2. Tectonics

2.2.1. Regional Geology and Tectonics

The Eastern Mediterranean region is characterised by tectonic structures resulting from the on-going contraction of the Mediterranean Sea and the closure of the precursor ocean known as the Southern Neotethys (Robertson et al., 2016), owing to the northward motion of the Arabian and African plates relative to a stable Eurasia plate with the Anatolian microplate caught and deformed between.

Continental collision in the region is likely to have begun in the Late Cretaceous (~72 – 66 Ma) and resulted in the emplacement of ophiolites along the Bitlis-Zagros suture zone, which includes the Hatay/Kizildağ ophiolite in the Hatay province (e.g., Inwood et al., 2009). Final closure of the Southern Neotethys, which resulted in the formation of the Mediterranean Sea, is thought to have happened in the Oligocene (~35 Ma; Allen and Armstrong, 2008). This collision was initially accommodated by crustal thickening and rapid uplift of the Central and Eastern Anatolian Plateaus (Şengör et al., 2008). Collision changed to 'extrusion' in the late Miocene to early Pleistocene (Şengör et al., 1985), though the exact timing and the mechanism that caused this change in the style of deformation is debated (e.g., Schildgen et al., 2014). The extrusion of the Anatolian microplate resulted in the formation of the North Anatolian (NAFZ) and East Anatolian (EAFZ) fault zones that accommodate the westwards motion of Anatolia driven in part by the northwards propagation of Arabia pushing Anatolia but also by the roll-back of the Aegean subduction zone pulling the micro-plate to the west (*Figure 2*).

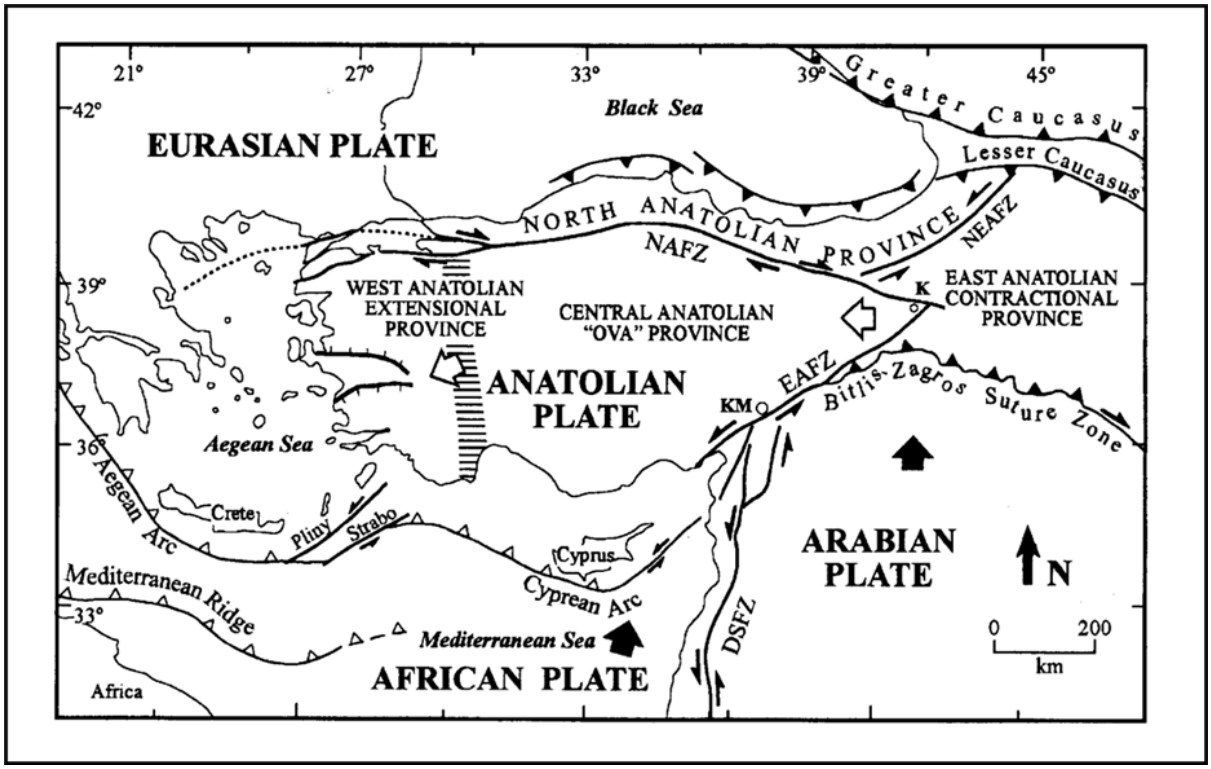

Figure 2: Present plate tectonic setting of Anatolia and the surrounding Eastern Mediterranean region (Bozkurt, 2001).

In the early Miocene (18-17 Ma), the Dead Sea Fault Zone (DSFZ) developed as a result of the difference in northward rate of motion between the African and Arabian plates. Subsequently, the DSFZ propagated northwards reaching northern Syria/southern Türkiye by the late Pliocene (~ 5 – 4 Ma; Mart et al., 2007). The other major structure of concern in the region is the Cyprus Arc (or Cyrean Arc), the inactive remnant of the subduction zone beneath Cyprus. Sea floor bathymetry suggests that the main Cyprus Arc extrapolates onshore in Latakia in northern Syria (Hardenberg and Robertson, 2007), but it is also possible that a secondary fault zone links through to the Hatay Graben/Antakya Fault Zone.

2.2.2. Event Intensity

The EAFZ is a continental sinistral (left-lateral; i.e., if you stand on one side of the fault, then the other side has moved to the left)) strike-slip fault zone trending ~NE-SW for >400 km from Karlıova in the east to the Mediterranean Sea. The fault likely initiated in the Late Pliocene (3 – 4 Ma; Şaroğlu et al., 1992; Westaway & Arger, 2001) and has an average slip rate of 7 – 9 mm/yr (e.g., Reilinger et al., 2006). In the northeast the fault is mainly characterised by a single fault strand split into a number of segments (*Figure 2* and *Figure 3*) dependent on the presence of changes in the orientation of the fault. However, towards the southwest the fault zone becomes more complex with a number of fault splays or strands. This complexity has generated a number of different schemes for defining the number of segments and different names for the same structures.

In addition, the multiple faults have also triggered debate as to the nature of the connection and the relationship between the EAFZ, the DSFZ and the Cyprus Arc.

There are three main geodynamic models for the region and the precise plate configuration remains unresolved:

1. The EAFZ has a broadly linear trend and crosses the Amanos Mountains at Türkoğlu towards İskenderun. The Amanos Fault Zone (*Figure 3*) is the northern extent of the DSFZ (e.g. Şengor and Yilmaz, 1981; Yönlü et al. 2017)

2. Similar to model 1 but the EAFZ terminates at Türkoğlu and does not extend to the southwest (e.g., Perinçek and Çemen, 1990; Yürür and Chorowicz, 1998).

3. The EAFZ extends along the Amanos Fault and meets the DSFZ at the southern end in the Amik Plain (e.g., Arpat and Şaroğlu, 1975; Şengör et al., 1985; Duman and Emre, 2013).

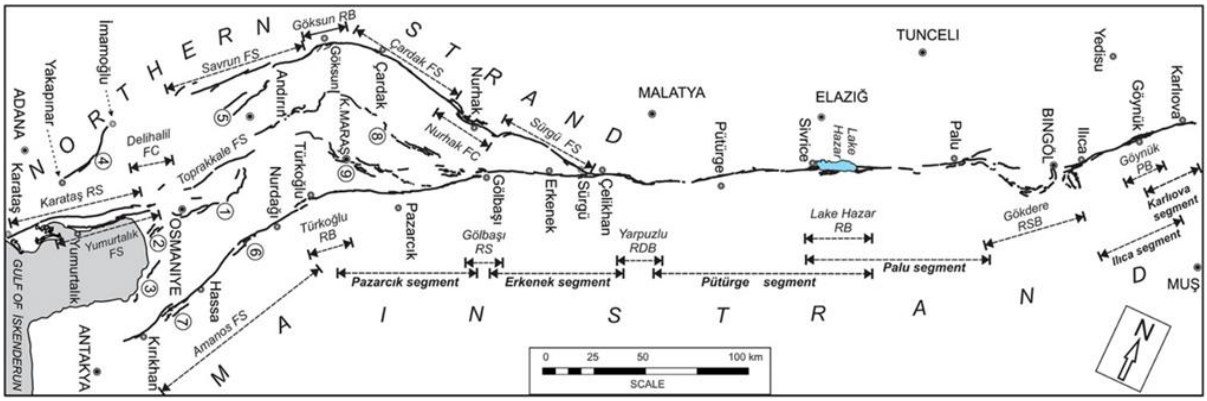

*Figure 3: Structural map of the EAFZ showing the main fault strands and segments (***Duman and Emre***, 2013). Abbreviations: FS, fault segment; RB, releasing bend; RS, releasing stepover; RDB, restraining double bend; RSB, restraining bend; PB, paired bend; (1) Düziçi–Osmaniye fault segment; (2) Erzin fault segment; (3) Payas fault segment; (4) Yakapınar fault segment; (5) Çokak fault segment; (6) Islahiye releasing bend; (7) Demrek restraining stepover; (8) Engizek fault zone; (9) Maraş fault zone. Note that this map does not show the active fault east of Antakya.*

2.2.3. Local Geology

The geological units of the region reflect the complex tectonic evolution of the plate boundary zone between Arabia and Eurasia, and can broadly be split into five main units (*Figure 4*):

1. Palaeozoic (Triassic ~200 Ma) and Mesozoic carbonates (Cretaceous ~100 – 66 Ma) comprising the Arabian Platform;
2. Various metamorphic lithologies forming the Anatolian basement;
3. Cretaceous (~100 – 66 Ma) to Miocene (~ 20 Ma) sedimentary rocks forming the cover to the Anatolian basement;
4. Ophiolites and tectonic melange emplaced on the continental margins during collision, and
5. Miocene (~23 Ma) to recent sediments and volcanics often making up basin fills.

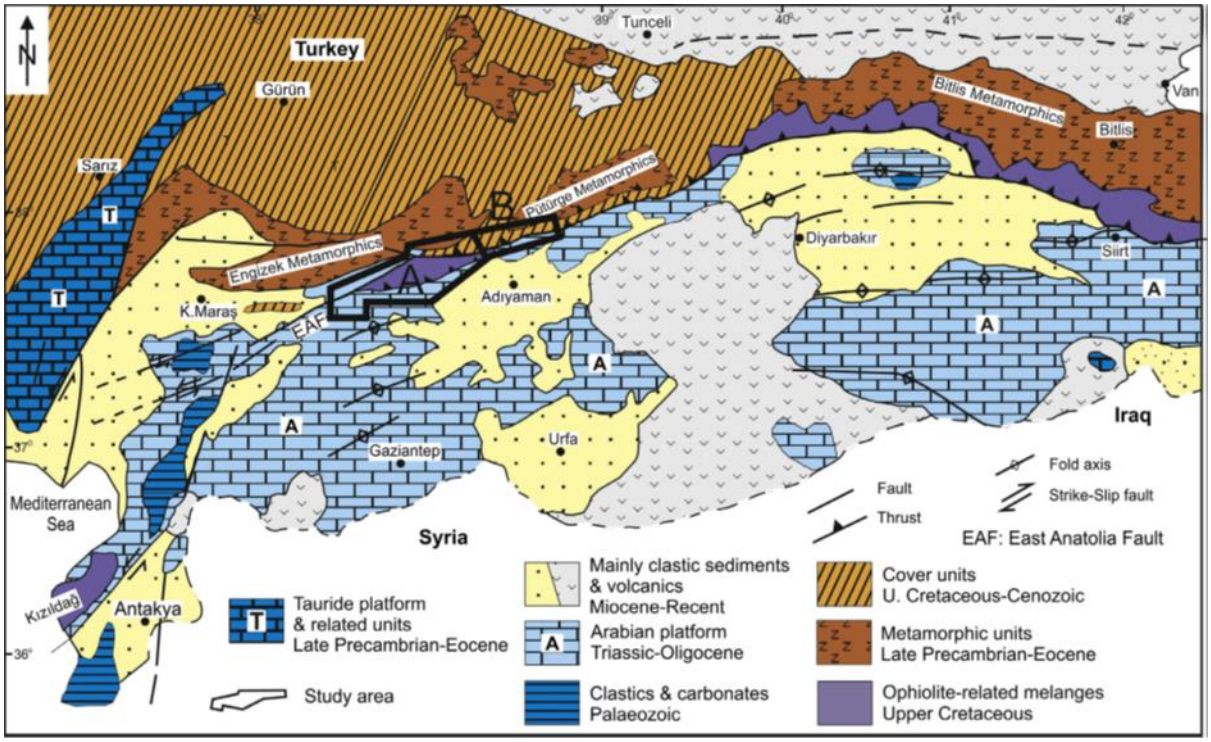

Figure 4: Geological map of the region (Robertson et al., 2016).

Five fault segments were ruptured during the earthquake sequence; these were the Narlı Fault, the Erkenek and Pazarcık fault segments of the EAFZ, the Amanos Fault zone and the Çardak Fault (*Figure 5*). These faults cross-cut all the different bedrock units, which influenced the earthquake intensity at different locations.

The Narlı Fault is a relatively unknown structure forming the eastern margin of a small basin, known as the Narlı Basin and appears to be the structure that initiated the initial M_w 7.8 Pazarcık earthquake. The fault is oblique-normal with evidence of Late Quaternary-Holocene fault activity in the form of prominent fault scarps (Duman and Emre, 2013).

Subsequently the earthquake propagated bilaterally northwards along the Pazarcık and Erkenek fault segments of the EAFZ and southwards along the Amanos Fault. The Pazarcık and Erkenek fault segments are sinistral (left-lateral) strike-slip faults of the EAFZ separated by the Gölbası basin (a pull-apart basin). The Erkenek segment is ~ 30 km in length with up to 26 km of offset, whereas the Pazarcık segment is longer at > 50 km but also has up to 25 km of offset (Duman and Emre, 2013).

To the south the rupture took place along the Amanos Fault forming the western margin of the Karasu Rift, again a sinistral strike-slip fault but with an earlier history of extension resulting in the uplift of the Amanos Mountains (Boulton, 2013). The fault has a number of sections along its ~ 125 km length with a maximum reported displacement of 700 m (Boulton, 2013) and a horizontal slip rate of ~ 3 mm/yr (Seyrek et al., 2007).

The later M_w 7.5 earthquake ruptured the Çardak Fault, which has been proposed to be a northern strand of the EAFZ (Duman and Emre, 2013). This sinistral strike-slip fault is 85 km long with a reported offset of only 135 m but a Holocene slip-rate of 2.5 mm/yr (Duman and Emre, 2013).

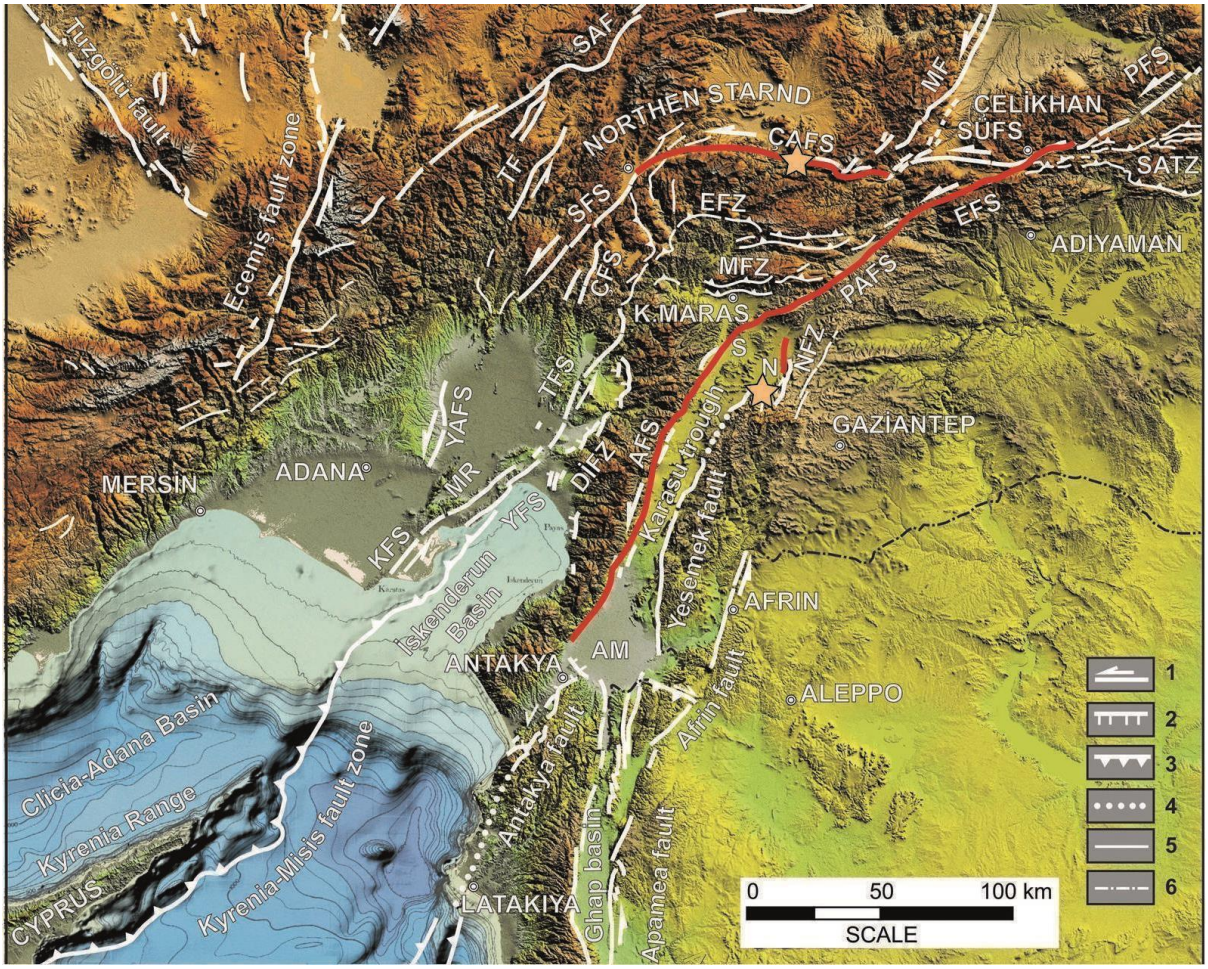

Figure 5: Active fault map of the region (modified from Duman and Emre, 2013) highlighting the faults that ruptured in the earthquake sequence (red overlay) and the position of the two main earthquakes (stars). Abbreviations: SAF, Sarız Fault; TF, Tufanbeyli Fault; SFS, Savrun Fault Segment; ÇFS, Çokak Fault Segment; ÇAFS, Çardak Fault Segment; MF, Malatya Fault; SÜFS, Sürgü Fault Segment; PFS, Pütürge Fault Segment; EFS, Erkenek Fault Segment; SATZ, Southeastern Anatolian Thrust Zone; PAF Pazarcık Fault Segment; MFZ, Maraş Fault Zone; EFZ, Engizek Fault Zone; YAFS, Yakapınar Fault Zone; DİFZ, Düziçi–İskenderun Fault Zone; TFS, Toprakkale Fault Segment; YFS, Yumurtalık Fault Segment; AFZ, Amanos Fault Segment; NFZ, Narlı Fault Zone; AM, Amik Basin; S, Sağlık Basin; N, Narlı Basin; MR, Misis Range; (1) left-lateral strike-slip fault; (2) normal fault; (3) reverse/thrust fault; (4) inferred fault; (5) secondary fault; (6) national boundary.

2.3. Geodesy

Although the regional tectonics of the affected regions has been introduced in Section 2.2.1, here we discuss the present-day relative plate motions of Anatolia, Arabia, and Nubia, relative to stable Eurasia, using the findings from many authors, who over the past 50 years used various geodetic, seismic, and plate tectonic observations to determine the plate motions of the affected regions (e.g. McKenzie,1972; Taymaz et al., 1991; Barka and Reilinger, 1997; McClusky et al, 2000; McClusky et al, 2003; Reilinger et al., 2006; Reilinger and McClusky, 2011; Nocquet, 2012; England et al. 2016).

These authors' studies concluded that Anatolia is moving anti-clockwise relative to stable Eurasia, with the centre of Türkiye behaving as a rigid block and the NAFZ and

EAFZ moving anti-clockwise towards the subduction along the Hellenic trench (*Figure 6*). Across Anatolia, the NAFZ, which extends across the entire northern margin of Türkiye (see *Figure 2*), moves at rates of 25-35 mm/yr, whilst its neighbouring, more diffuse EAFZ to the south-east, moves at approximately half that motion, at rates of 10-20 mm/yr, relative to Eurasia (Taymaz et al., 1991; Barka and Reilinger, 1997; McCluskey et al., 2000; Nocquet, 2012; England et al. 2016).

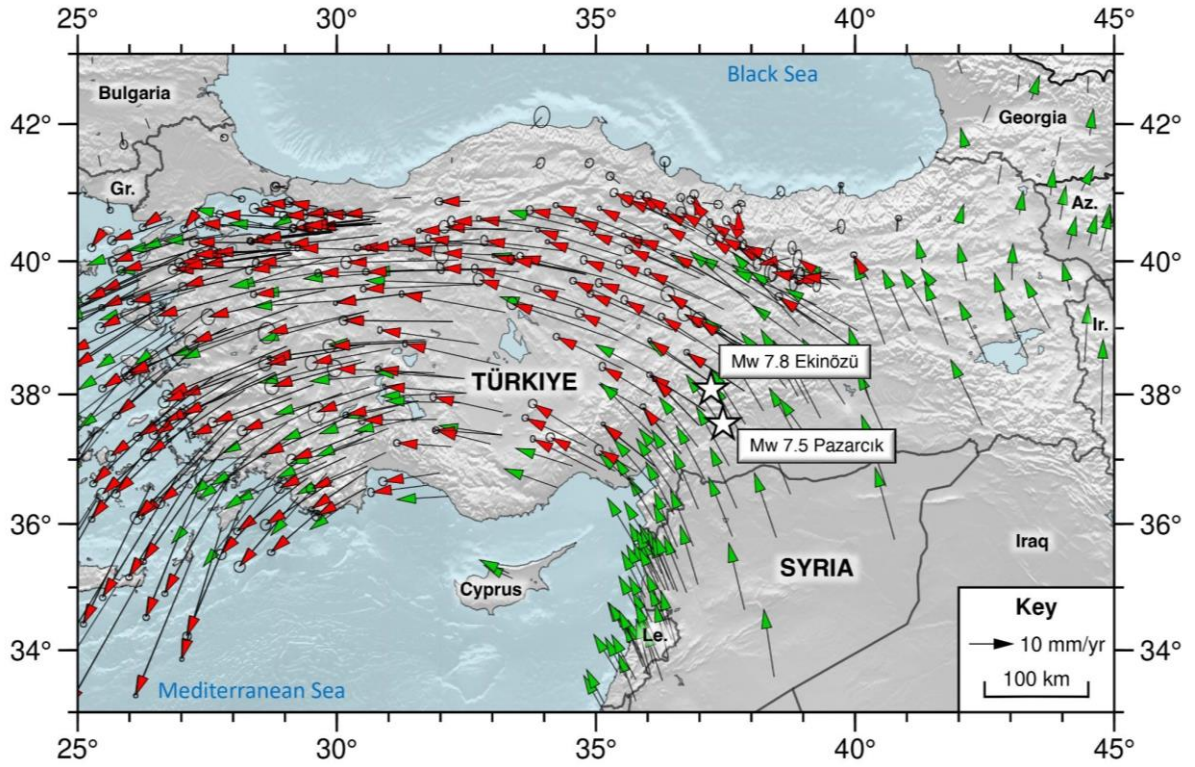

Figure 6: Velocity field for Anatolia and Arabia relative to stable Eurasia. Green and red GPS velocity vectors are from the Nocquet (2012) and England et al. (2016) catalogues, respectively.

A study conducted by Weiss et al. (2020) used Sentinel-1 InSAR and GNSS data to produce a strain rate model across Anatolia and identified the NAFZ as a high-strain-rate area, unlike the EAFZ which ruptured during the Kahramanmaraş earthquake sequence in February 2023. This is further evidence of how diffuse this EAFZ is, where the strain accumulated across the fault zone is spread amongst many active structures, rather than predominantly on one major fault (e.g., the NAFZ).

From GPS measurements in NW Syria, Alchalbi et al. (2010) provided the first observations of near-field deformation rates on the Dead Sea Fault Zone (DSFZ), that extends south from the southern end of the EAFZ (see *Figure 2*). Their relative plate motion estimates of up to 6.5 mm/yr, relative to Eurasia, are consistent with the 2-7 mm/yr rates by Reilinger et al. (2006) and Noquet (2012). The adjacent Arabian plate similarly converges northwards relative to Eurasia, at rates of 15-23 mm/yr (Barka and Reilinger, 1997; Reilinger and McClusky, 2011), with just under half the convergence taken up by the shortening across the Caucasus, and the remaining motion accommodated along the Bitlis-Zagros Suture Zone (BZSZ) (Barka and Reilinger, 1997).

2.4. Local and Regional Seismicity

The 6th February Kahramanmaraş earthquake sequence is the latest disaster to take place as a result of the seismically active Anatolian and Arabian regions. On a local scale, Eastern Anatolia is a highly seismically active region due to being a complex tectonic junction between the Arabian, African, and Anatolian plates. The seismicity is distributed across well-known structures including the Eastern Anatolian Fault Zone (EAFZ), North Anatolian Fault Zone (NAFZ), North-Eastern Anatolian Fault Zone (NEAFZ), Bitlis-Zagros Suture Zone (BZSZ), Dead Sea Fault Zone (DSFZ), and faults which extend offshore from the EAFZ at İskenderun Bay, as previously discussed in Section 2.2. Most of the seismicity in the Eastern Anatolian region is distributed across these main active structures (see *Figure 2*), however, some strain is accommodated by secondary splay faults, such as the Narlı Fault, on which the M_w 7.8 Pazarcık earthquake on 6th February originated (*Figure 5*).

On a regional scale, the NAFZ and EAFZ (as previously discussed in Sections 2.2 and 2.3) account for most of Türkiye's earthquake activity, whilst the centre is relatively aseismic. A large proportion of the country's seismicity, and the EAFZ in particular, is constrained to the upper 30 km of the crust (AFAD, 2023; Dal Zilio and Ampuero, 2023). Although Taymaz et al. (1991) demonstrate a variety of focal mechanisms for the past seismicity along the EAFZ, it is well established that the fault zone generates mainly left-lateral strike-slip faulting with earthquake slip vectors trending 063°, parallel to the strike of the fault zone. In addition, the EAFZ accommodates some shortening, consistent with the GPS velocity field illustrated in *Figure 6*. Spatially, this seismicity is represented as a wide (≈50 km) cluster of events that rupture the EAFZ and its secondary splay faults, as demonstrated in *Figure 7* below. In contrast, the earthquake release across the NAFZ tends to occur close to the fault forming a much narrower band of seismicity.

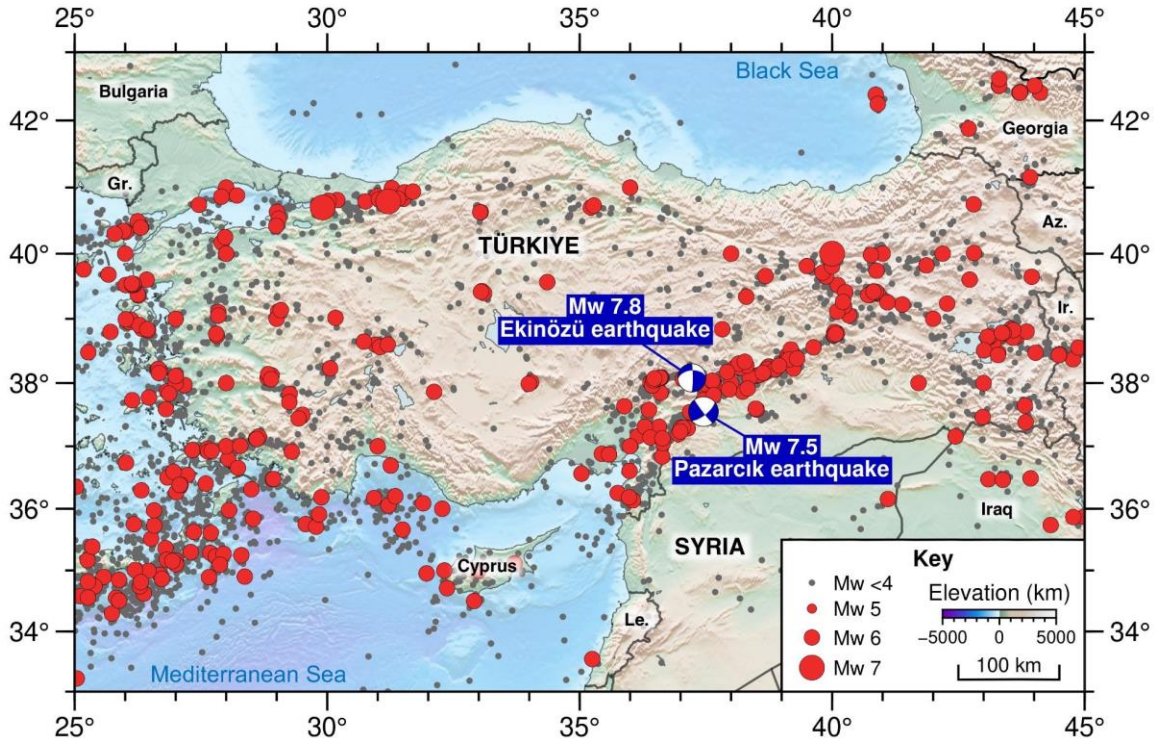

Figure 7: Historical seismicity across Türkiye and Syria. Earthquake data is sourced from the AFAD 1900-2023 earthquake catalogue (AFAD, 2023). The focal mechanisms of the 2023 February doublet events are illustrated in blue.

The instrumental record demonstrates that over 40,000 small magnitude (M_w <5) earthquakes have occurred across Türkiye and Syria since 1990 (AFAD, 2023; *Figure 7* and *Figure 8*). The catalogue reveals that over this time, there have been, on average, 10 moderate-magnitude (M_w 5) earthquakes per year, and one M_w 6 earthquake every year (*Figure 8*). The February 2023 M_w 7 earthquake sequence, which brought widespread devastation to cities across the eastern Mediterranean region, and in particular, the Kahramanmaraş area, is the first of this order of magnitude since the 2011 M_w 7.1 Van earthquake in eastern Türkiye over a decade ago.

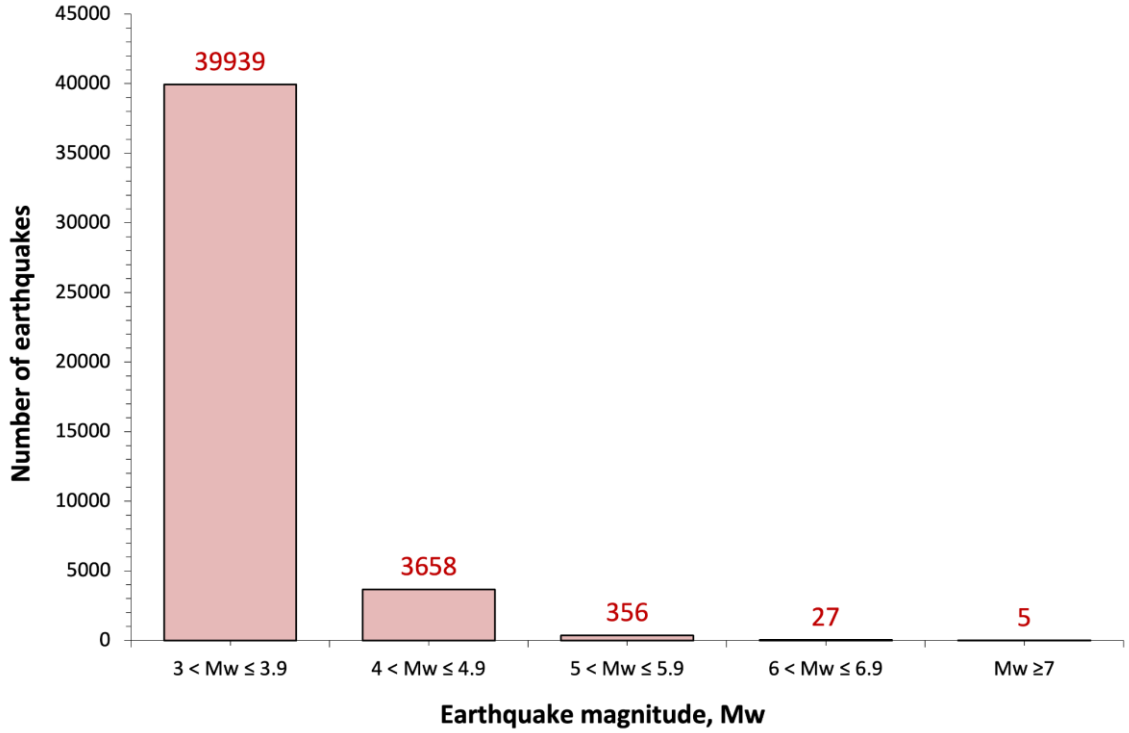

Figure 8: Earthquakes that occurred across Türkiye and Syria (within the geographical extents of Figure 7) since the advent of the AFAD instrumental catalogue in 1990 to present-day, August 2023 (AFAD, 2023).

In Türkiye, the North and Eastern Anatolian Fault Zones pose the greatest hazard to the region affected and with a history of devastating events, like the 17th August 1999 İzmit earthquake, which caused 17,000 fatalities, major infrastructure damage, and significant societal and economic losses to the regions affected. Consequently, the NAFZ and EAFZ are considered to be high seismic hazard zones, with the Karlıova triple junction regarded as the most dangerous area across the EAFZ (Bayrak et al., 2015). With a rapidly urbanising population, where hundreds of thousands of people are living within a few kilometres of the EAFZ (DalZilio and Ampuero, 2023), this means that the number of people at risk of experiencing such a disaster from earthquakes in the region is ever increasing.

While Syria is not as seismically active as its neighbour Türkiye, it has experienced a few notable earthquakes in the past which have caused significant damage and loss of life to communities along the Dead Sea Fault Zone. Sbeinati et al. (2005) conducted a study into the historical earthquakes of Syria and found that the seismicity over the past century has been moderate and a total of 181 events have occurred over the period of 1365 B.C. to 1900 A.D. Most of this seismicity was concentrated along the EAFZ and DSFZ with focal mechanisms representative of left-lateral strike-slip motion in keeping with the findings of Taymaz et al. (1991), and a minor component of the seismicity was accommodated by normal faulting, attributed to the pull-apart basins along the DSFZ (Sbeinati, 2005). Like Türkiye, the intraplate area of Syria is generally aseismic, however, there have been sporadic moderate magnitude (M_w 5.5) earthquakes recorded here, and a few also occurred along the Euphrates Fault Zone in Eastern Syria (Sbeinati, 2005).

According to the historical record, the DSFZ appears to break in moderate-to-large-sized earthquakes after long periods of seismic quiescence, and Sbeinati et al.'s

(2005) analysis indicates that the last major earthquake was over a century ago on 29th June 1896, with earthquake intensities of IV felt across Syria, Lebanon, Palestine, and Egypt. The Kahramanmaraş earthquake sequence is the deadliest present-day earthquake since the 13th August 1822 Aleppo earthquake. One such seismic gap was identified by Meghraoui et al. (2003), who found palaeo- and archaeo-seismology evidence that the northern segment of the DSFZ in Syria has not experienced a large earthquake in over 850 years (with a 6 m of potential accumulated slip), and therefore currently poses a high seismic hazard to the people of Syria and Lebanon.

2.5. Seismology of the Earthquake Sequence

2.5.1. Pazarcık and Ekinözü Mainshocks

In the early hours of the 6th of February 2023 (04:17 TRT), the first of a doublet of devastating earthquakes occurred ~35 km northwest of Gaziantep city, Türkiye, and ~60 km north of the Syrian border (AFAD, 2023). The first event, commonly referred to as the Pazarcık mainshock, was a magnitude 7.8 event that broke multiple fault segments of the EAFZ (as previously discussed in Sections 2.2 and 2.4 and illustrated by the purple line in *Figure 9*) of up to ~300-560 km in length (Karabulut et al., 2023; Mai et al., 2023; Petersen et al., 2023).

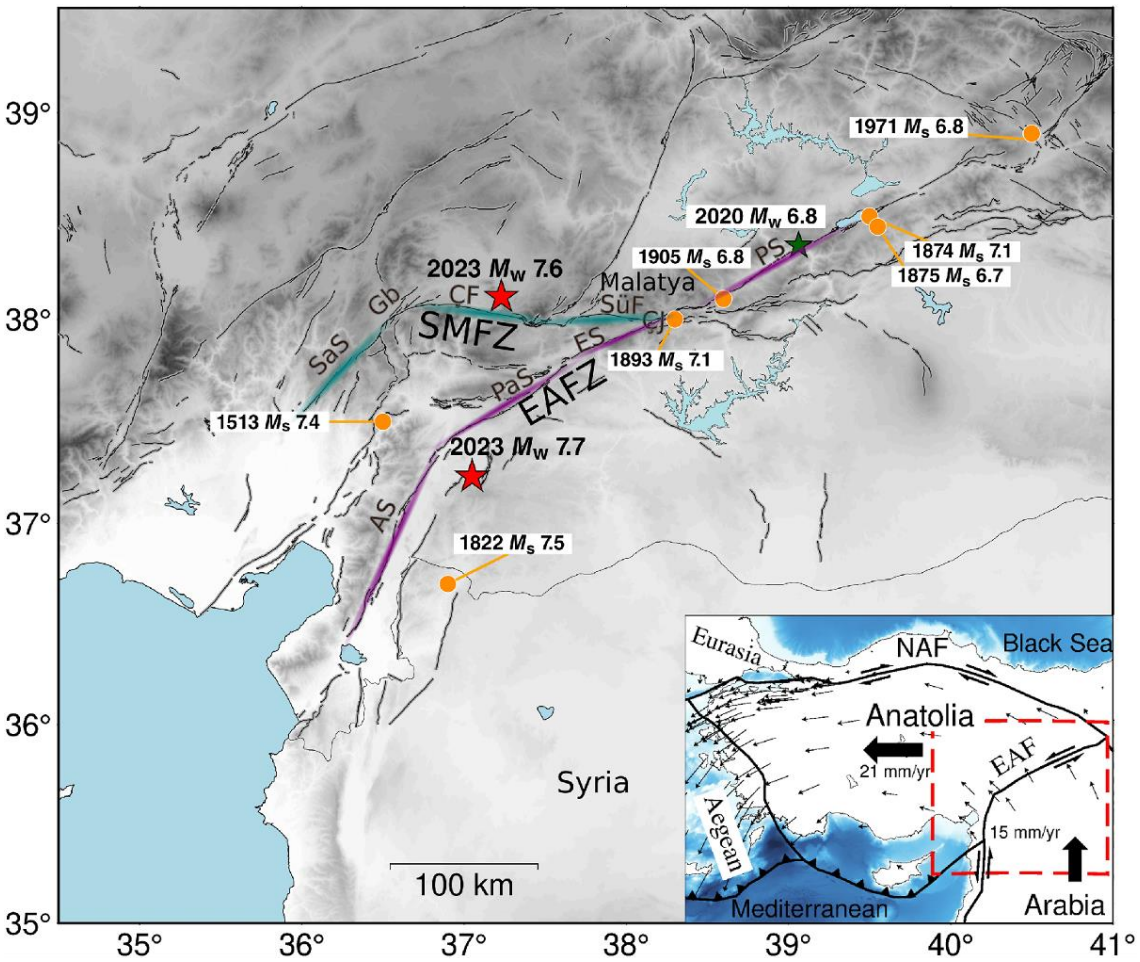

Figure 9: Map published in Petersen et al. (2023) illustrating the affected regions across Türkiye and Syria, with the annotated earthquake epicentre locations as red stars and the main fault systems which ruptured during these events: the East Anatolian fault zone (EAFZ) and the Sürgü-Misis Fault Zone (SMFZ).

The Pazarcık earthquake released left-lateral strike-slip motion at shallow depths (8.6-10.0 km) and ruptured bilaterally (meaning in two directions) from the epicentre (AFAD, 2023; Petersen et al., 2023, USGS, 2023a). The fault segments along the EAFZ broke in phases, as discussed in detail by Petersen et al. (2023). At first, it travelled north-east, and then to the south-west at speeds of up to 3.2-3.4 km/s, for a total duration of 80-117 seconds (see *Figure 10*, Karabulut et al., 2023; Melgar et al., 2023; Petersen et al., 2023). These different phases of rupture are illustrated as distinct pulses on the earthquake seismograms for the event and are later discussed in Section 2.6.

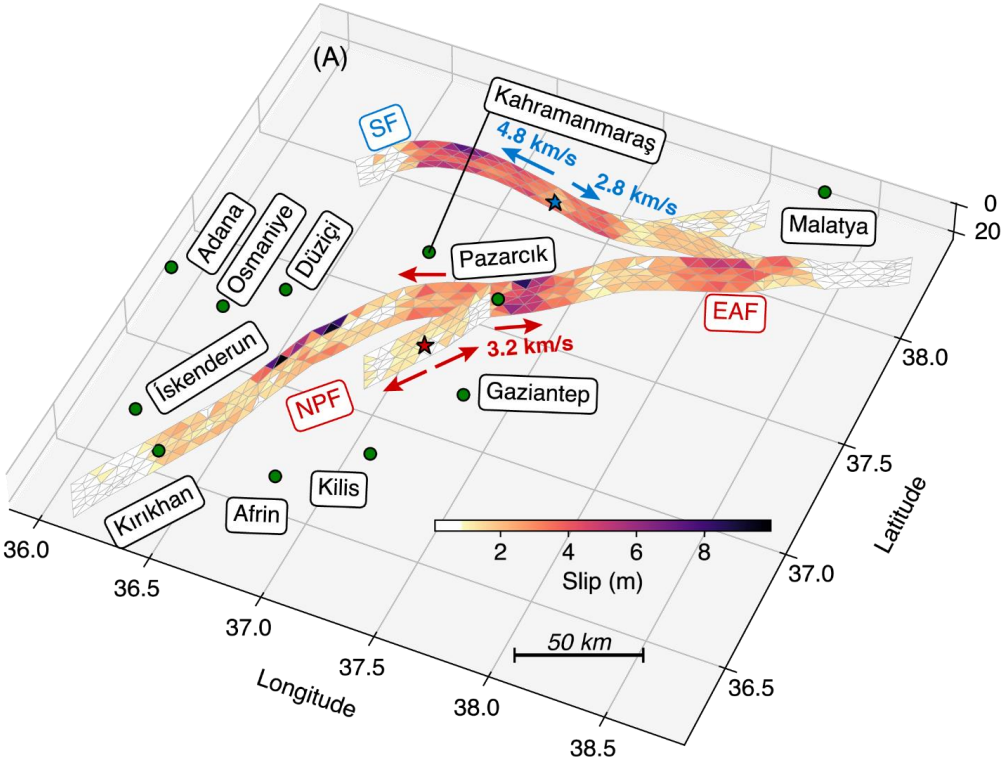

Figure 10: Melgar et al.'s (2023) best-fitting slip distributions and inverted rupture geometry for the Pazarcık and Ekinözü earthquakes.

Felzer et al. (2004) performed statistical analyses of global earthquake catalogues and found that there is a 7% chance that a mainshock will trigger a subsequent earthquake of a similar magnitude. The Kahramanmaraş earthquake sequence fell into this 7%, as 9 hours after the Pazarcık earthquake, another significantly large (M_W 7.5) earthquake ruptured 150-200 km of the Sürgü Fault (illustrated by the cyan line in *Figure 9*) at shallow depths (7.0-7.4 km, AFAD, 2023; USGS, 2023b), approximately ~100 km to the north of the mainshock's epicentre (Mai et al., 2023; Petersen et al., 2023).

This earthquake, which is later referred to as the Ekinözü mainshock, first ruptured westwards at extremely fast (super-shear) speeds of up to 5 km/s for up to 17 seconds (see *Figure 10*, Melgar et al., 2023), attributing to the higher ground motions and damage caused to cities in the southwest. Subsequently, the earthquake rupture continued to the east for a further 14 seconds at ~3 km/s, a speed that we deem normal for earthquake ruptures (sub-shear).

Several studies have conducted finite-fault rupture modelling of the Kahramanmaraş earthquakes doublet to characterise the complexity of the fault ruptures (Goldberg et al., 2023; Karabulut et al., 2023; Mai et al., 20123; Melgar et al., 2023; Petersen et al., 2023). Whether it was through the use of coseismic surface displacements and teleseismic waveforms or back projection using seismic station data, this modelling was able to help refine each of the earthquake events, from the location and geometry of the rupture to its velocity and slip amplitude. Although each inversion varies slightly, the M_w 7.8 Pazarcık earthquake was consistently reported to have occurred on 3-4 separate fault segments. The central EAFZ fault segments (EFS and PAFS on *Figure 5*) are thought to be north-east striking (053-060°) and steeply dipping (82-85°), whilst the Amanos and Narlı fault zones (AFZ and NFZ, respectively) trend more towards the North (025-028°) and have a similar dip (75° and 85°, respectively) to the central EAFZ (Mai et al., 2023; Petersen et al., 2023; USGS, 2023a). Similarly, the finite-fault modelling results for the Ekinözü mainshock suggest that the earthquake broke three segments of the SZMF. The main fault strand (CAFS in *Figure 5*) trends 276° east-west, whilst the edges of the fault strike more northeast-southwest (060°and 250°). All fault segments dip steeply at 75-85°, similar to the EAFZ (Goldberg et al., 2023; Mai et al., 20123; Petersen et al., 2023; USGS, 2023b).

The maximum slip determined on any given fault segment during the Pazarcık earthquake was estimated to be 6-8 m and largely constrained to the upper 20 km, however, Goldberg et al. (2023) did determine a slightly higher slip amplitude of 11 m, at a depth of ~28 km. Similarly, the Ekinözü event was reported to have released 6-8 m of slip. Therefore, the slip estimates from both events are in agreement with the surface displacements derived from the satellite data, as discussed in Section 2.5.2.

This devastating sequence of events was the strongest earthquake to hit Türkiye and Syria in over 80 and 100 years, respectively (Dal Zilio and Ampuero., 2023). It was widely felt across the eastern Mediterranean and western Asia, with places as far as Georgia, Armenia, Iraq, Israel and Egypt having lodged felt reports (Erdik et al., 2023). As of 04th April 2023, the IFRC (International Federation of Red Cross and Red Crescent Societies, 2023) had recorded that over 9 million people have been directly affected by the earthquake, with >100,000 people injured and almost 60,000 fatalities across Türkiye and Syria alone.

2.5.2. Aftershock Sequence

Aftershocks are a common occurrence after large earthquakes such as the 6th February 2023 doublet. The months following the deadly Kahramanmaraş earthquake sequence were filled with tens of thousands of aftershocks, which exacerbated the destruction, further weakening infrastructure and causing more deaths and displacement of communities.

In the fortnight after the 6th February earthquake sequence, nearly 7500 aftershocks were recorded (Çetin et al., 2023), and over the subsequent months, the aftershocks predominantly occurred along 350 km and 160 km segments of the EAFZ and SMFZ, respectively (Mai et al., 20123; Petersen et al., 2023). The distribution of aftershocks comprised a variety of focal mechanisms (i.e. caused by strike-slip, thrust, and normal faulting). However, the aftershocks observed in the north-eastern segments of the EAFZ and SMFZ (see *Figure 5*) were mainly a result of strike-slip motion, like the Pazarcık and Ekinözü mainshocks, and the aftershocks located along the

southwestern segments of the EAFZ and SMFZ were a result of normal-faulting (i.e. extension).

Over 350 of these events were of moderate magnitude, 5.0 < M_w < 6.0 (see *Figure 8*; AFAD, 2023) and although there were tens of M_w>6 aftershocks, a notable M_w 6.3 earthquake struck near Uzunbağ on 20th February 2023, resulting in six fatalities (Kawoosa, 2023). Some authors refer to this oblique-normal faulting event as the third mainshock event to occur in the Kahramanmaraş earthquake sequence since it caused very large peak ground motions for the magnitude of the earthquake. The reasons for this (e.g., proximity to the Antakya basin) are discussed later in Section 2.6.

2.5.3. Surface Ruptures

The Turkish earthquake resulted in a surface rupture (where the fault extends to the Earth's surface and offsets the ground) of > 300 km in length (*Figure 11*). This surface rupture has been mapped in the field by Karabacak et al. (2023) and by Kercher et al. (2023) as part of early field campaigns in the region, within 10 days after the initial earthquake. The EEFIT team also undertook some limited reconnaissance of the surface rupture as part of the field mission. These field investigations confirm observations made from a number of different remote sensing datasets that have utilised high-resolution satellite imagery, primarily from Maxar. Surface rupture maps were released by the USGS shortly after the earthquake (Reitman et al., 2023) and have been supplemented by extra mapping as part of this field mission. This includes the addition of previously unmapped faults to the USGS dataset and the validation of that dataset, resulting in the removal misidentified fault structures where these were recognized to be the result of either crop marks, such as old field boundaries, tractor marks, buried channels, forest tracks, or in some cases, the shadow of telegraph poles.

Both in the field and on remote sensing imagery, the surface rupture can be recognised through a series of features that cut and offset man-made features such as roads, buildings, railways, field boundaries, and canals, and also disrupt natural features such as rivers and the ground surface. This is because the left-lateral (sinistral) nature of the fault can be easily recognised by the lateral offset of surface features. This indicates that along the fault, there is substantial variation in the lateral displacement, with maximum displacements up to 8 m. In addition to lateral offsets, the fault can also cause small vertical offsets of around 10 to 20 cm, but in some cases, larger offsets have been observed, particularly in the north of the study area, where Karaback et al. (2023) have reported vertical offsets in the order of 1.6 m. These data compare well to information derived from satellite geodesy, such as InSAR and automated pixel tracking of satellite imagery, which show the same overall pattern and magnitude of slip offset along the fault (*Figure 12*).

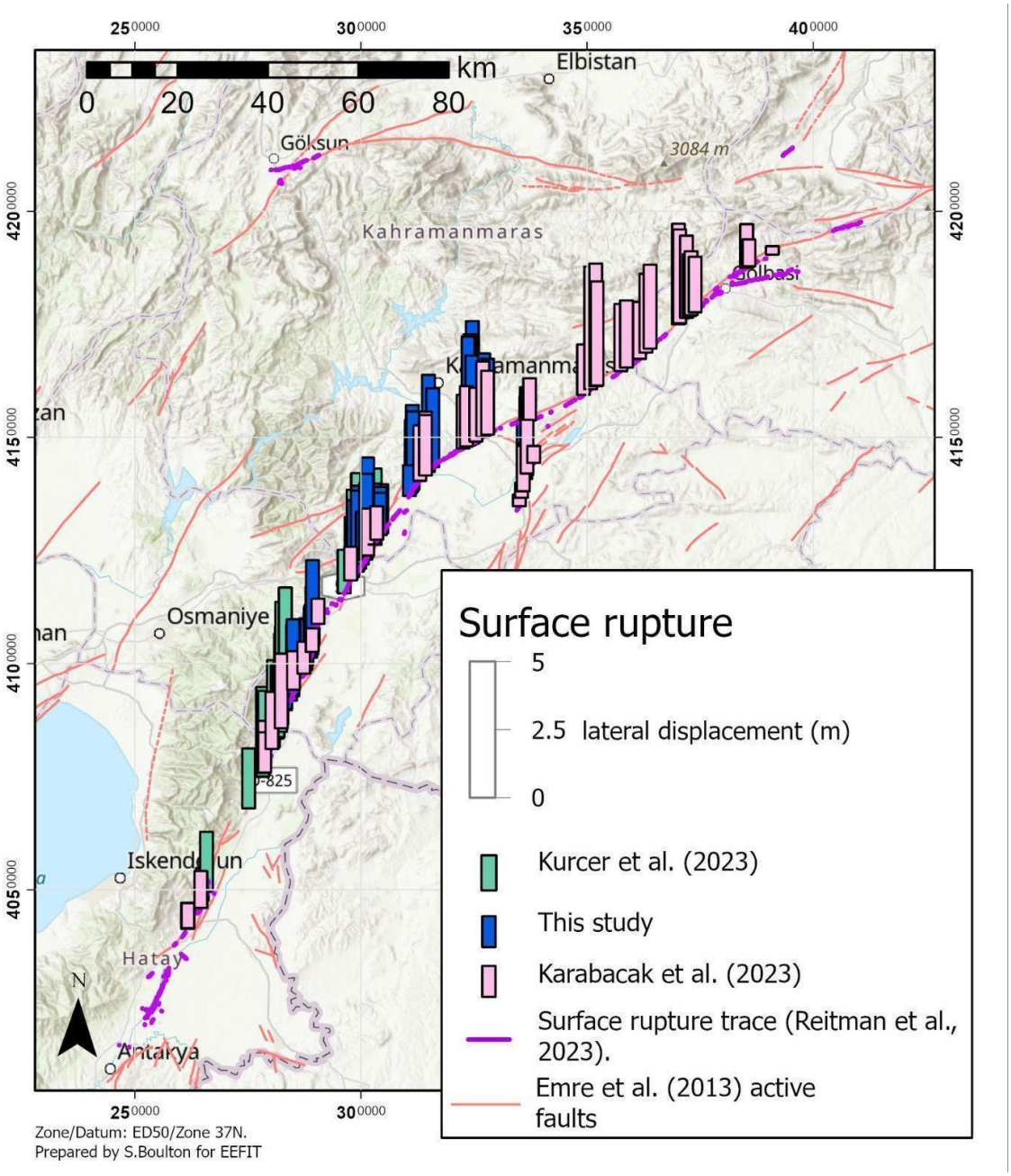

Figure 11: Map of the area showing a compilation of surface ruptures mapped from remote sensing imagery (this study, Reitman et al., 2023) and ground observations (Kurcer et al., 2023). Active fault traces are taken from Emre et al. (2018).

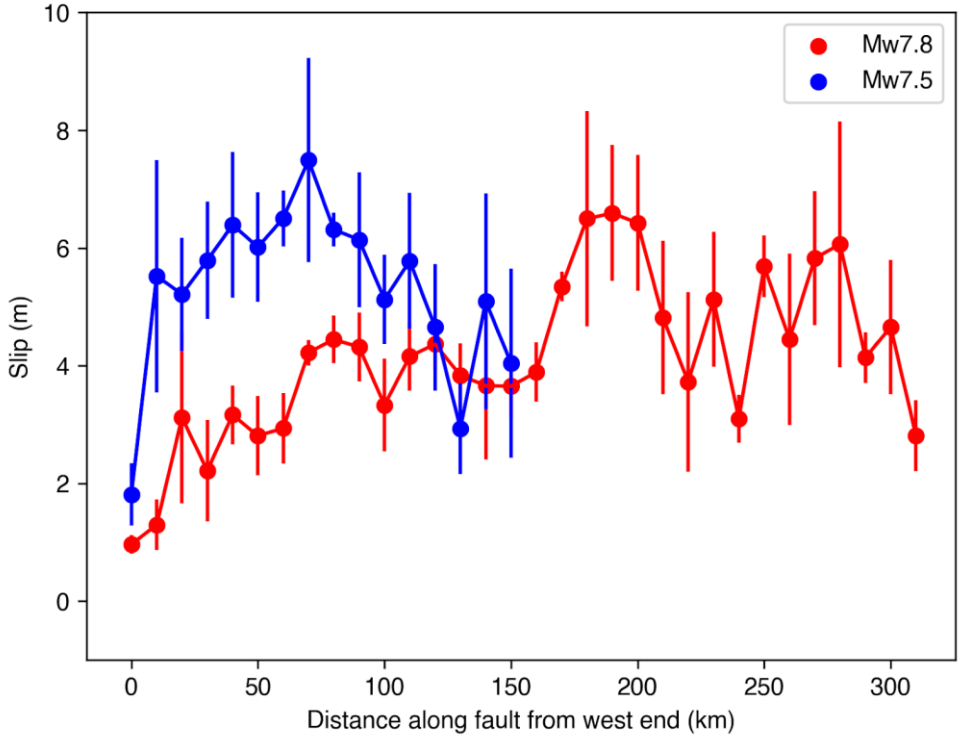

Figure 12: Graph showing variations in lateral (horizontal) slip along the strike of the main EAFZ (red) and the Cardak Fault (blue) calculated from Sentinel 1 data by COMET (Ou et al., 2023).

These data are significant for understanding the geometry and magnitude of the earthquake but also have built in environmental implications along the fault rupture, where the fault offsets and disrupts critical infrastructure. In addition to the damage seen along roads and field boundaries that have been used to map the lateral offset of the fault, the fault rupture has also been observed to cause a number of direct effects. These include where the rupture cuts the corners of buildings, collapsed buildings where the fault intersects through the building, and in the most extreme examples, ruptured gas pipelines, causing explosions and disruption to that infrastructure (*Figure 13*). These can be considered direct impacts of the fault, rather than as a result of fault shaking.

Figure 13: High-resolution Maxar satellite images of offset features caused by the surface ruptures created by the main Pazarcık earthquake. A) illustrates an offset corner of an industrial unit, B) shows collapsed domestic buildings on and adjacent to the fault rupture, C) demonstrates a gas pipeline which was cut by the fault (although the surface rupture at this location is unclear), D) is an example of the surface rupture cutting field boundaries.

2.6. Evaluation of Strong Ground Motion Recordings

2.6.1. Examination of Strong Ground Motion Stations and Field Observations

The Turkish Accelerometric Database and Analysis System (TADAS), operated by AFAD (Disaster and Emergency Management Presidency), comprises a dense strong ground motion network in the earthquake vicinity. However, there have been certain issues with the data dissemination on the TADAS website (https://tadas.afad.gov.tr/list-event). The recordings of several stations which were released immediately following the M_W 7.8 event on the website of TADAS were withdrawn later, but we detected that some of them were afterwards reloaded again (e.g., station 4614). Additionally, we were unable to access any recordings of three events in late March of 2023 since they had been taken down from the website. All

recordings were eventually uploaded again at the beginning of April. Since there was no indication on the website regarding what types of adjustments were made to which data or the reason for the modifications during all these upload and withdrawal periods of time, it was extremely challenging to analyse the ground motions. The authors emphasise that it would be helpful to clarify what modifications to the data were made during the dissemination of the publicly accessible data. It should be noted that the EEFIT lecture on March 27th comprised a presentation of the initial review of strong ground motion (SGM) recordings, which were obtained on February 9th, 2023. Due to the aforementioned issues, the data has been again retrieved on April 13 and this report incorporates the evaluation of that most recent database.

According to the TADAS website accessed on 13.04.2023, the February 6th, 2023, Pazarcık Earthquake (M_W 7.8) induced strong ground motions that were recorded at 380 TADAS stations with epicentral distances (R_{EPI}) ranging from ~13 km to 635 km, while the M_W 7.5 Ekinözü and M_W 6.3 Uzunbağ events were recorded by 386 (21 km < R_{EPI} < 628 km) and 119 (8 km < R_{EPI} < 360 km) stations, respectively. 69 stations at distances of 25 km to 995 km from the epicentre (deployed by Boğaziçi University, Kandilli Observatory and Earthquake Research Institute; KOERI)) captured strong ground motions of the M_W 7.8 event based on the Engineering Strong Motion (ESM) database, although 29 of these have been designated as “bad quality”. The ESM database has provided 22 recordings from KOERI stations (145 km <R_{EPI}< 542 km) that captured the later M_W 7.5 event, whereas the February 6 M_W 6.3 Uzunbağ event has not been included in the database. We were unable to retrieve any SGM data from Syria, the Southwestern part of which has also suffered from severe damage due to the Kahramanmaraş earthquake sequence (World Bank and GFDRR, 2023). For these reasons, explanations and assessments related to strong ground motions are concentrated mainly on observations in Türkiye.

The initial database included these aforementioned issues that emerged during a preliminary assessment by the remote team, and these prompted us to visit the SGM stations in the field. The EEFIT field team have visited six SGM stations (see Section 2.6.2) and the main observations are summarized below.

- ***Station 4614 (City: Kahramanmaraş; Date of visit: 17.03.2023)***
  Free-field station 4614 is situated in the backyard of Pazarcık Regional Boarding School in Kahramanmaraş. It has been uncovered that the location in the recording ASCII file signs around 1 km Northeast of where station 4614 is actually installed. Precise coordinates are also available in the station reports on the TADAS website. The station, which is located 37 km away from the epicentre, recorded strong peak ground accelerations (PGAs) of about 2.1g in the horizontal direction and 2g in the vertical direction during the M_W 7.8 Pazarcık event. However, these recordings were temporarily removed from the TADAS catalogue but were added back in the latest update. Although the station captured the ground motions of this event, its recordings from the M_W 7.8 Pazarcık earthquake are not included in the analyses of this report for reasons elaborated in the subsequent section. In addition, the M_W 7.5 Ekinözü event was also recorded by this station. The station was inspected in the field in order to provide a preliminary assessment of the reliability with which the recordings from the second earthquake could be utilised. According to the external inspection, the station hut does not display any indications of damage (*Figure 14*(top)). The

buildings around the station, which have relatively good underlying soil conditions (average shear wave velocity of recording sites for the top 30 m of depth, V_{S30}= 541 m/s), appear to have suffered minor damage. The minaret of the Fatih Mosque, which is located beside station 4614, has fallen in the North-South (NS) direction (*Figure 14*(top)).

- ***Station 0201 (City: Adıyaman; Date of visit: 14.02.2023)***
  Station 0201 is placed in the garden of 15 Temmuz Şehitler Secondary School in Adıyaman (*Figure 14*(bottom)). This free-field station recorded strong ground motions during the MW 7.8 Pazarcık event (REPI≈125 km) with relatively high PGAs of almost 0.5g, 0.9g, and 0.3g in the East-West (EW), NS, and Up-Down (UD) directions, respectively. The ground motion time series, on the other hand, appear to be interrupted immediately after capturing the peak value, according to our preliminary analysis of the data. Correspondingly, the EEFIT field team has documented numerous totally collapsed structures built before 2000, and out-of-plane damages surrounding the station in the EW direction.

Figure 14: External views of (top) station 4614, (bottom) station 0201 with structures nearby the stations.

- ***Station 0208 (City: Adıyaman; Date of visit: 17.02.2023)***
  The free-field station 0208 is situated in the garden of the Meteorological Station Directorate in Gölbaşı, Adıyaman (*Figure 16*). Anonymously, the ground motions at station 0208 from the M_W 7.8 event appear to have been terminated before the commencement of the S-wave. Additionally, the TADAS database does not contain any recordings of the station for the M_W 7.5 Ekinözü event. The M_W 6.3 Uzunbağ earthquake is the only one that this station appears to have accurately recorded. Moreover, this station and its directorate building exhibit no indications of damage, and the ground motion recordings of other earthquakes do not have any noticeable issues; therefore, they have been incorporated into the data set analysed in this report. Nevertheless, some of the nearby low- and mid-rise buildings (number of floors ≤7 according to classification of FEMA,1999) have shown traces of tilting and settlement.

Figure 15: External views of station 0208 with structures nearby.

- ***Station 0210 (City: Adıyaman; Date of visit: 18.02.2023)***
  Since Mevlana Secondary School was closed, inside which station 0210 is installed in Adıyaman, we were unable to perform a thorough inspection of the station. However, the outside assessment of the school does not display any signs of damage (*Figure 16*(top)). Similar to other stations in Adıyaman, the ground motions of the MW 7.8 event have been interrupted before the event ended.
- ***Station 0213 (City: Adıyaman; Date of visit: 19.02.2023)***
  Free-field station 0213, which is located in the backyard of Tut Multi-Program Anatolian High School in Adıyaman (*Figure 16*(bottom)), yields comparatively low PGAs from the Mw 7.8 Pazarcık event (0.24g in NS, 0.17g in EW, 0.3g in UD direction). However, it appears that shortly after detecting the peak ground motions, the time series is terminated as in the case of station 0201. This station does however record the entirety of the M_W 7.5 Ekinözü event. While there are no other structures in the immediate vicinity of the school, neither the high school itself nor the station hut has any visible damage. Nonetheless, it should be noted that rocks and boulders have fallen toward the NS direction from the slopes in front of the school (*Figure 16*(bottom)).

Figure 16: External views of (top) Mevlana Secondary School where station 0210 is deployed, (bottom) station 0213, and rockfalls nearby station 0213.

- ***Station 3116 (City: Hatay; Date of visit: 13.03.2023)***
  The surrounding wire fences have prevented a close-up inspection of the free-field station 3116, which is situated in a park in İskenderun/Hatay. According to TADAS, the station is on a rocky site (ophiolites) with 870 m/s of V_{S30}. The field observations support this information. The buildings surrounding this station seem to be undamaged during this earthquake sequence.

2.6.2. Generation of Final Ground Motion Database

The initial database has been compiled based on the distance and signal quality criteria. In the analyses presented in this report, the maximum R_{EPI} is restricted to 300 km for both networks. After the elimination of bad-quality recordings based on various

preliminary criteria such as interruptions in the time series, and heavy noise contamination, the number of useable stations in the final database is summarised in *Table 4*. The quality of the raw ground motion recordings can be improved by processing ground motions to eliminate undesirable noises. Firstly, baseline correction has been applied to horizontal and vertical components of the ground motion data to eliminate long-term drift. Then, the undesirable noises have been extracted from the ground motion recordings between the constant frequency range of 0.05 and 25 Hz employing 4th-order Butterworth bandpass filtering. Then, their velocity and displacement time histories have been visually inspected to ensure the selected high-pass filter frequency, and if required, ground motions undergo processing a second time.

Table 4: Number of useable stations (N) within 300 km of epicentral distance.

Event Name	N_{TADAS}	N_{KOERI}	Total
M_W 7.8 Pazarcık EQ	121	7	128
M_W 7.5 Elbistan EQ	149	5	154
M_W 6.3 Uzunbağ EQ	100	0	100

The point source approximation of the small events enables the utilisation of the epicentral (R_{EPI}) or hypocentral (R_{HYPO}) distances. However, the total energy of finite sources is not discharged at a single point, hence these distance metrics are ineffective for particularly high-magnitude events which are represented by finite sources. As a result, distance metrics that take into account the entire fault rupture, such as Joyner-Boore distance (R_{JB}) and rupture distance (R_{RUP}), are more applicable in the case of larger earthquakes, which are represented by finite sources. That's why, Joyner-Boore distance (R_{JB}), which is defined as the closest horizontal distance to the vertical projection of the rupture plane, is utilised due to the long-rupture length of both events (~350-400 km in the M_W 7.8 and ~150-200 km in Mw 7.5 earthquakes). The R_{JB}s have been empirically computed by incorporating the fault dimensions that have been computed based on Wells and Coppersmith, 1994, in the method developed by Harmsen, C. in Petersen et al., 2008 since the finite fault solution has not yet been released in the case of the M_W 6.3 Uzunbağ earthquake. Also, it should be noted that all earthquake magnitudes and epicentral coordinates in this report have been obtained from USGS solutions. In *Figure 17* it is demonstrated that the strong ground motion stations of both networks, which recorded three events, are spatially well-distributed. In particular, 16 stations are within the boundary of the surface projection of the finite fault model proposed by the USGS for the M_W7 .8 Pazarcık event (green areas in the figure). The Southern segment of the model is encircled by a dense station network, whereas the Northern segment has just a few stations in close proximity. In the case of the M_W 7.5 event, only two stations are seen on the surface projection of the USGS model (purple areas in the figure). Also, the statistical distribution of R_{EPI} and R_{JB}s in *Figure 18* verify the aforementioned judgements. Thirty percent of the stations (N=38) for the M_W 7.8 event are located at R_{JB}s in the 0 to 20 km range, yet no stations fall inside the same R_{EPI} range. The abundance of ground motions in the small R_{JB}s is particularly invaluable in comprehending near-fault characteristics of ground motions. Only five of the stations (~3%), that have been activated by the M_W

7.5 Ekinözü event appear to be within 20 kilometres from the surface projection of the fault model. The south of the M_W 6.3 Uzunbağ epicentre suffers from a lack of stations, whereas many stations are located North of the epicentre and provide many ground motion recordings of the event. The M_W 6.3 Uzunbağ event, however, has not been recorded by all Amik basin stations that recorded the significant ground vibrations in the M_W 7.8 event.

The most straightforward technique to understand the effect of the soil conditions on ground motions is the employment of the average shear wave velocity of recording sites for the top 30 m of depth (V_{S30}), mostly provided by the networks. The websites of TADAS and ESM both provide methods for determining the V_{S30} values of recording locations that are primarily based on geophysical, topographic-slope, and geological assessments. This study's V_{S30} values are compiled from 211 different stations regardless of the earthquakes. Most V_{S30}s (43%) are estimated by geophysical-based methods which can be categorised as Multi-channel Analysis of Surface Waves (MASW), Microtremor Refraction Seismic (ReMi), and Microtremor. Only MASW is utilized in the determination of V_{S30} values for 7% of recording sites while 4% of them are employed by both MASW and geotechnical drilling (Standard Penetration Test; SPT) techniques. Analysing the ground roll captured in a single shot can provide a precise dispersion curve that can be reversed to produce a reliable and consistent shear wave profile (Park et al., 1999), which is why MASW is the most preferred method for the V_{S30} identification of the sites.

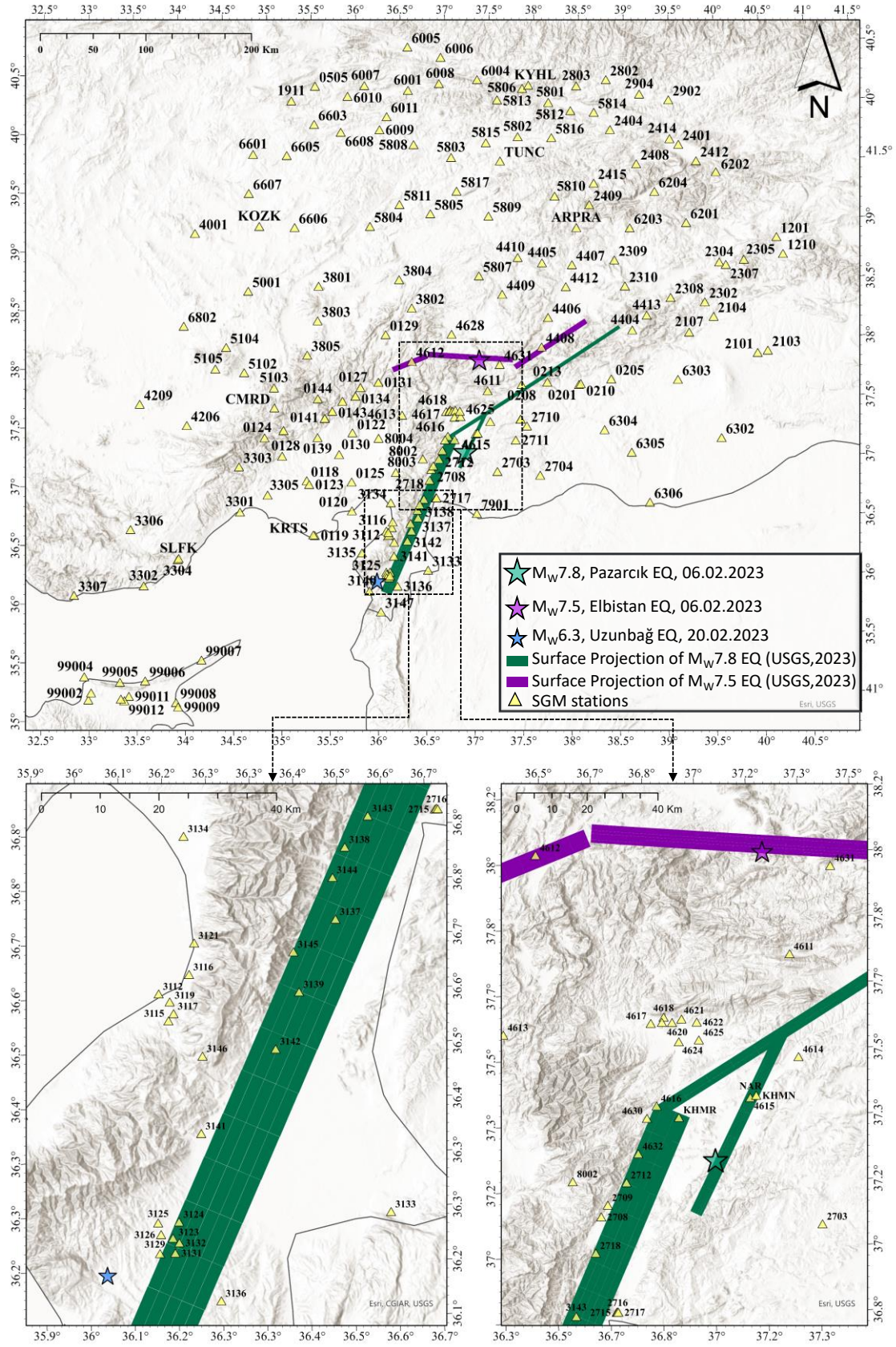

Figure 17: (top) Spatial distribution of strong ground motion stations recording the MW 7.8 Pazarcık, MW 7.5 Ekinözü and MW 6.3 Uzunbağ events, (bottom left) Closer views to stations in Antakya, (bottom right) Closer view to stations around epicentre of MW 7.8 Pazarcık and MW 7.5 Ekinözü earthquakes.

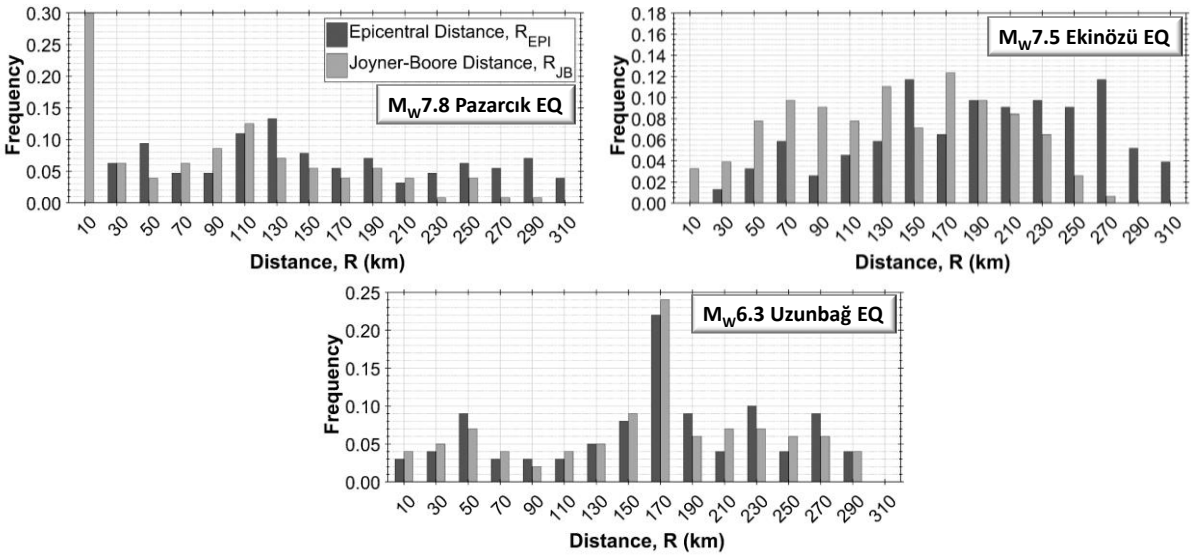

Figure 18: Statistical distribution of epicentral (REPI) and Joyner-Boore (RJB) distances of stations which recorded the MW 7.8 Pazarcık, MW 7.5 Ekinözü, and MW 6.3 Uzunbağ events.

On the other hand, the SPT only has a minor portion of site investigations despite its simplicity and widespread usage among dynamic in-situ tests. Moreover, 34% of V_{S30} values are calculated by Topographic Slope-Based methods. Since the V_{S30} of 65 stations have not been supplied on the TADAS website, their values have been extracted from a USGS topography-based V_{S30} map (Allen et al., 2007). In addition, the V_{S30} determination techniques utilized at 12% of station sites are not specified on the network websites, and therefore labelled as "unknown" in this report. *Figure 19* also contains the percentile dispersion of the V_{S30} calculating techniques regarding station amounts given in *Table 4*, to provide a more comprehensive review of the distribution of V_{S30} regarding each event. The statistical distribution of V_{S30} and soil classification according to the current seismic code of Türkiye (TBEC, 2018) is also displayed in *Figure 19*. The six main soil types in the recent seismic code of Türkiye are depicted by labels ranging from ZA to ZF, which correspond to rock and soft soils, respectively. The stations in our database are located on the recording sites that can only be characterised by three different soil types (ZB, ZC, and ZD) of the TBEC 2018 based on their VS30 values. ZB (760<VS30≤1500 m/s), ZC (360<VS30≤760 m/s), and ZD (180<VS30≤360 m/s) are described as "Slightly weathered moderately strong rocks", "very dense sand, gravel and very stiff clay or weathered, very fractured weak rocks" and "medium-dense /dense sand, gravel, or very stiff clay", respectively in the seismic code of Türkiye soil classification. A significant percentage (>60%) of recording sites pertain to the ZC soil class, as seen in *Figure 19*.

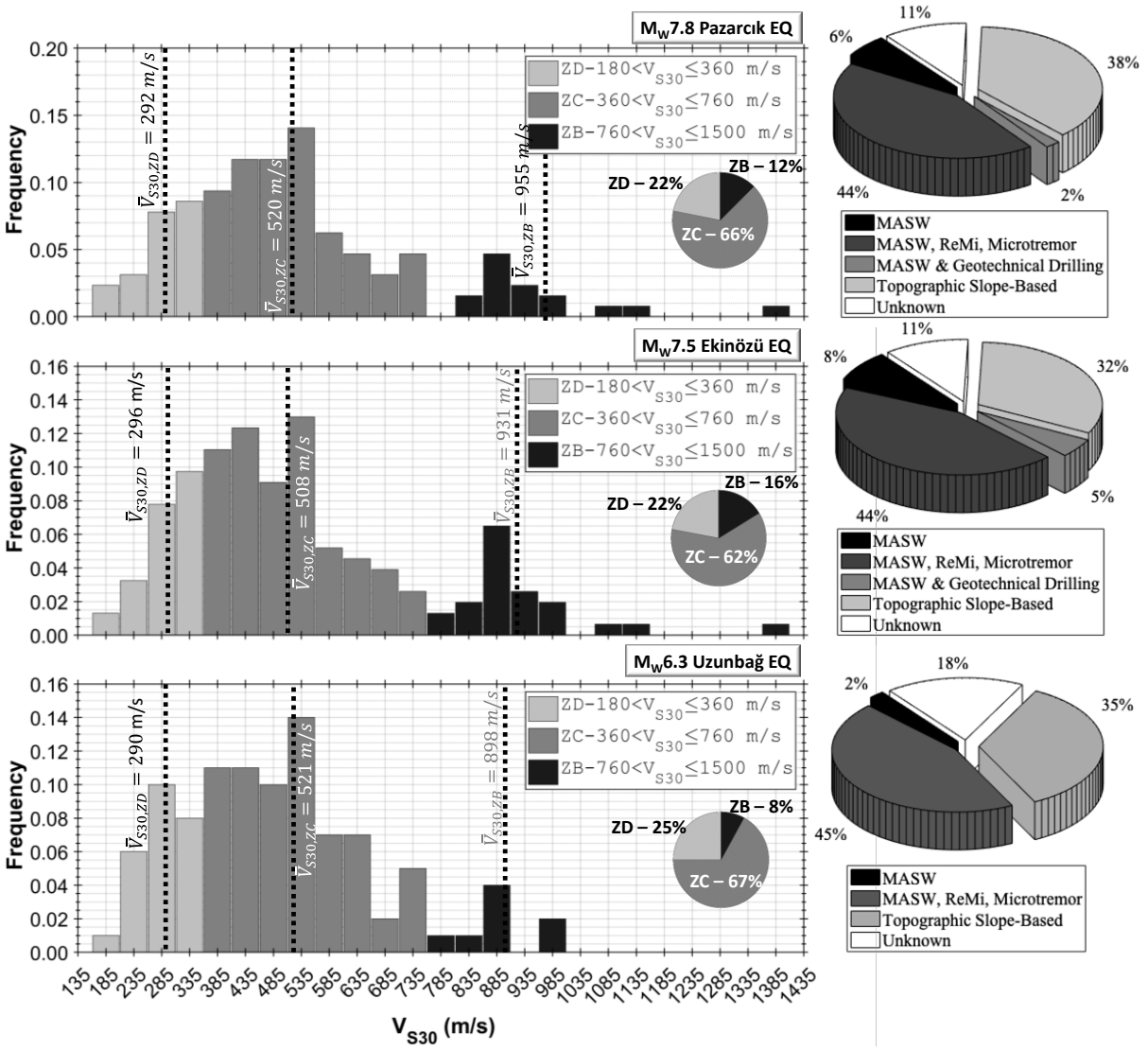

Figure 19: The distribution of the average shear wave velocities of the stations for the upper 30 m depth (VS30) and their identification methods for the MW 7.8 Pazarcık, MW 7.5 Ekinözü, and MW 6.3 Uzunbağ events.

2.6.3. Main Characteristics of Ground Motion Parameters

Peak ground acceleration (PGA) is one of the most frequently utilised indicators for a preliminary assessment of the severity of shaking. Therefore, we first dive into the ground motions releasing the highest PGAs. *Figure 20* shows the time histories of acceleration, integrated velocity, and displacement at the stations, resulted in the largest horizontal PGA for each event. The highest horizontal PGA ($PGA_{3129,NS} \approx 1379$ cm/s^2) is produced in the NS component recording of station 3129 (*Figure 20*a). In the M_W 7.5 Ekinözü earthquake, the closest station 4612 results in the highest PGA in the NS component with a value of almost 636 cm/s^2 (*Figure 20*b). The EW component of the ground motion recorded in the Antakya-basin station 3125 yields the largest PGA ($PGA_{3125,EW} \approx 769$ cm/s^2) from the M_W 6.3 Uzunbağ earthquake (*Figure 20*c). *Figure 20* additionally presents the velocity, displacement, and the vertical component

time series for the aforementioned stations. However, these do not all correspond to their highest values recorded during these events. The subsequent sections will go into further detail on this issue.

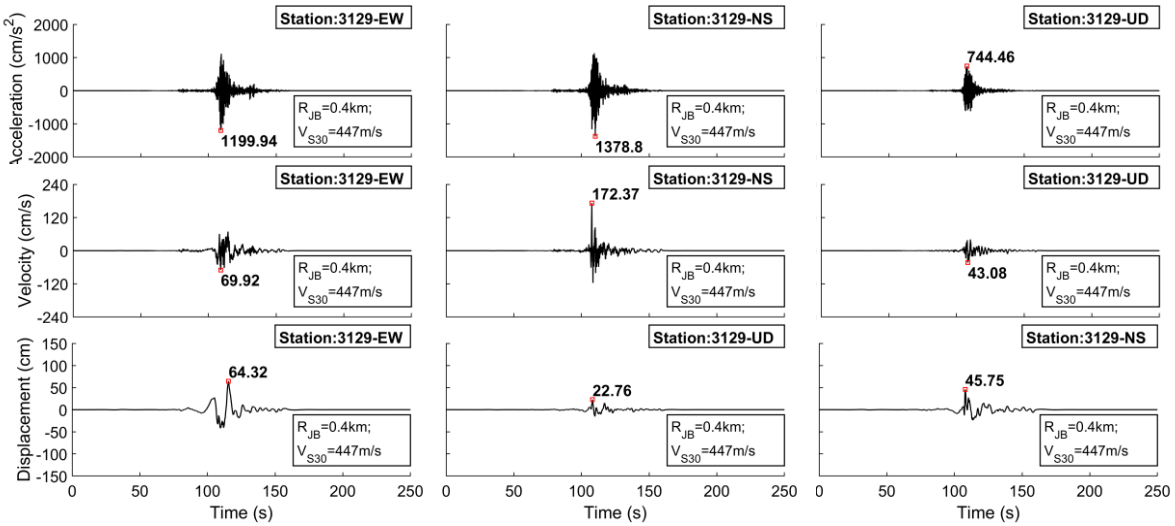

(a)

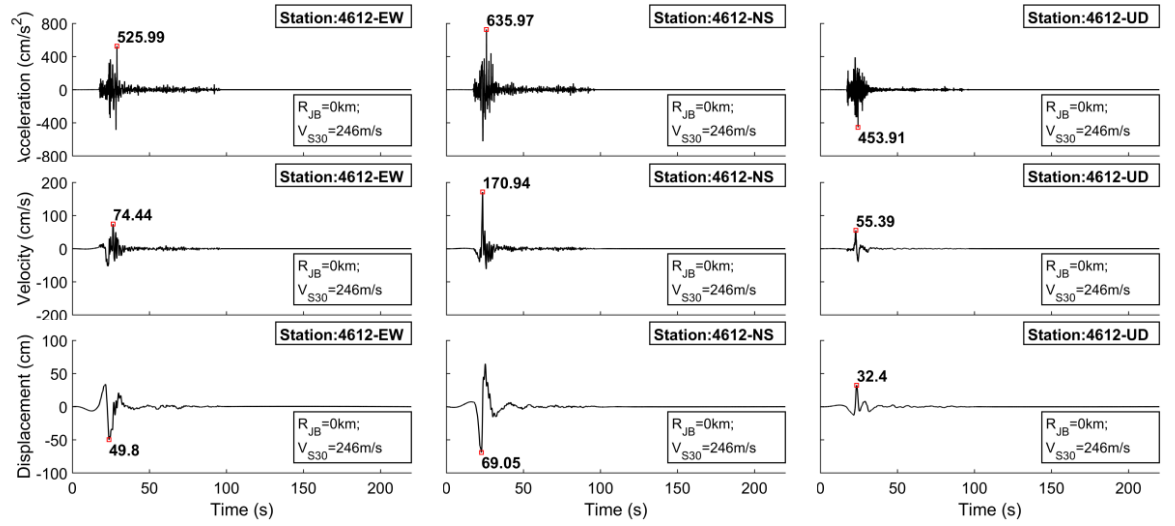

(b)

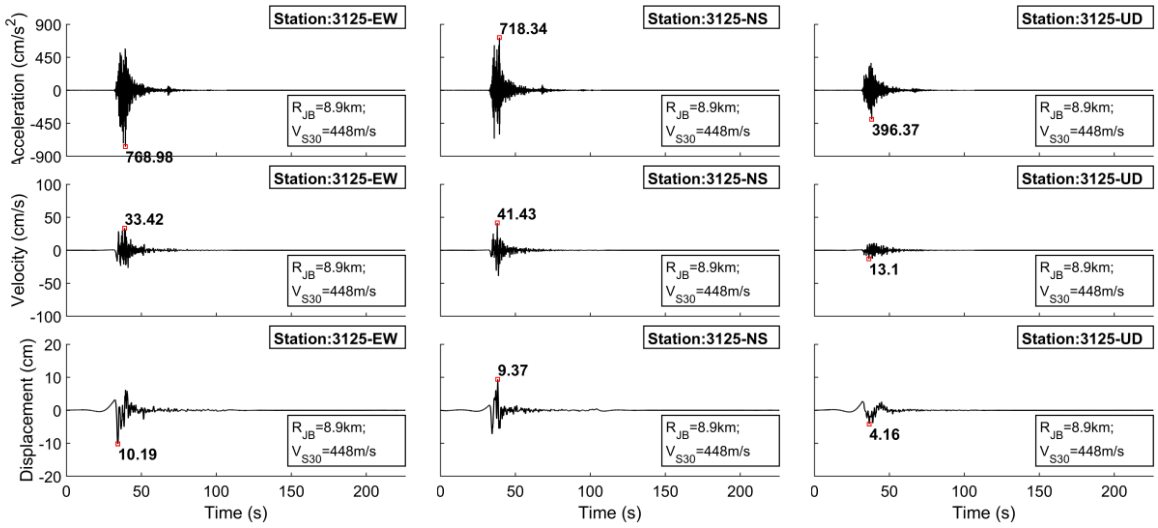

(c)

Figure 20: Acceleration, velocity, and displacement time histories for the stations which recorded the largest peak ground acceleration (PGA) for the (a) MW 7.8 Pazarcık, (b) MW 7.5 Ekinözü, and (c) MW 6.3 Uzunbağ events.

An extensive look at PGA distribution with regard to distance and soil conditions could bring about a broad understanding of the fundamental elements governing ground motion. Additionally, the spatial distribution of PGAs might enable us to get a general idea of damage spread throughout the region. *Figure 21* provides the variation of resultant PGAs, which is the absolute maximum of the acceleration time history combined by the square root of the sum of the squares of both horizontal components, with R_{JB} and V_{S30} for three events along with their spatial distribution by concentrating on the disaster region. For M_W 7.8 Pazarcık earthquake, significant PGAs are obtained in the stations with small R_{JB}s. The geographic distribution of PGAs also verifies this finding. The substantial values of PGA are provided by the stations, which are deployed in the cities of Kahramanmaraş, Gaziantep, and Hatay along the fault rupture. The stations in Adıyaman, another city situated nearby (~25 km) to the fault rupture trace were triggered by the earthquake shaking; nevertheless, their time histories could not be regarded as qualified data due to the interruptions within the ground motion times series. In Hatay, one of the most severely damaged cities due to the earthquake sequence, PGAs attain a maximum resultant value ($PGA_{3129,R} \approx 1556$ cm/s2) in station 3129 ($R_{EPI,3129} \approx 139$ km; $VS30,3129 \approx 447$ m/s) as previously stated. It should also be underlined that, despite being relatively far from the epicentre, the station is positioned on the Southwest edge of the fault rupture with an RJB of 0.4 km (*Figure 21*a). Similarly, most of the other strong ground motion stations in Hatay exhibit relatively high PGAs. In contrast to distance, it is hard to pinpoint the exact impact of VS30, one of the parameters for soil condition. If we examine the near-fault region where the RJB is nearly zero, we can see that several stations on the soil with relatively lower VS30 provide lower PGA than some of those on soils with high VS30. Nevertheless, the station's position (within the Amik Basin) might have been one of the elements contributing to the higher ground motions. The MW 7.5 Ekinözü earthquake, which took place ~90 km to the North of the epicentre of the MW 7.8 Pazarcık earthquake, has profoundly impacted the Northern parts of the region. This earthquake gives rise to the highest resultant PGAs in the stations surrounding the

fault rupture, similar to the MW 7.8 event (*Figure 21*b). However, the stations around the MW 7.5 Ekinözü earthquake's fault rupture are not as numerous as the ones that recorded the MW 7.8 earthquake. The largest resultant PGA of 678 cm/s2, is detected at station 4612, whereas station 4631, which is positioned on the lower REPI (REPI,4631 ≈ 21 km < REPI,4612 ≈ 63 km) and very slightly higher RJB (RJB,4631 ≈1.9 km > RJB,4612 ≈ 0 km), results in slightly lower PGA (PGA4631,R=463 cm/s2). The reason may also be associated with the differences in the soil conditions of both stations because station 4631 is on stiffer soil than station 4612 (VS30,4612 ≈ 246m/s < VS30,4631 ≈ 543 m/s). Contrary to the MW 7.5 event, the MW 6.3 Uzunbağ earthquake, which had the smallest magnitude but not less noteworthy among the 2023 earthquake sequence, occurred relatively far away from the epicentre of the MW 7.8 Pazarcık earthquake (147 km Southwest of the MW 7.8 event epicentre). The Hatay City, particularly Samandağ and Antakya districts, both of which are situated approximately 10 km from the epicentre, has been heavily affected by the MW 6.3 Uzunbağ earthquake, according to communication with the locals. In light of these statements, the field team reported that the extent of the damage to the built environment, which had already become vulnerable during the Mw 7.8 event, was increased substantially due to the February 20 shock. The largest resultant PGA (PGA3125,R ≈844 cm/s2 ; REPI,3125 ≈12 km ; VS30,3125 ≈ 448 m/s) is exhibited in station 3125, which is in the Amik Basin (*Figure 21*c). The highest resultant PGA of the MW 6.3 earthquake is extremely notable for being higher than that of the MW 7.5 Ekinözü event, despite the larger magnitude of the latter and smaller VS30 of its recording site. Despite its proximity to the fault rupture of MW 7.5 Ekinözü event, station 4612 is not as close to the epicentre of the event as station 3125 in the case of the MW 6.3 Uzunbağ event. Moreover, station 3125 is close to the Amik Basin and probably nearby the basin edge, and therefore the basin effects might have affected characteristics of the ground motions.

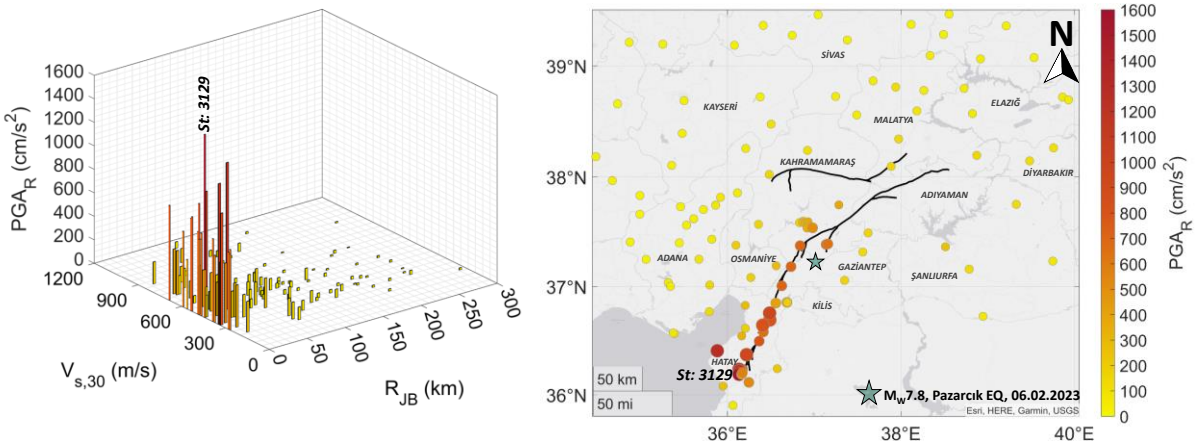

(a)

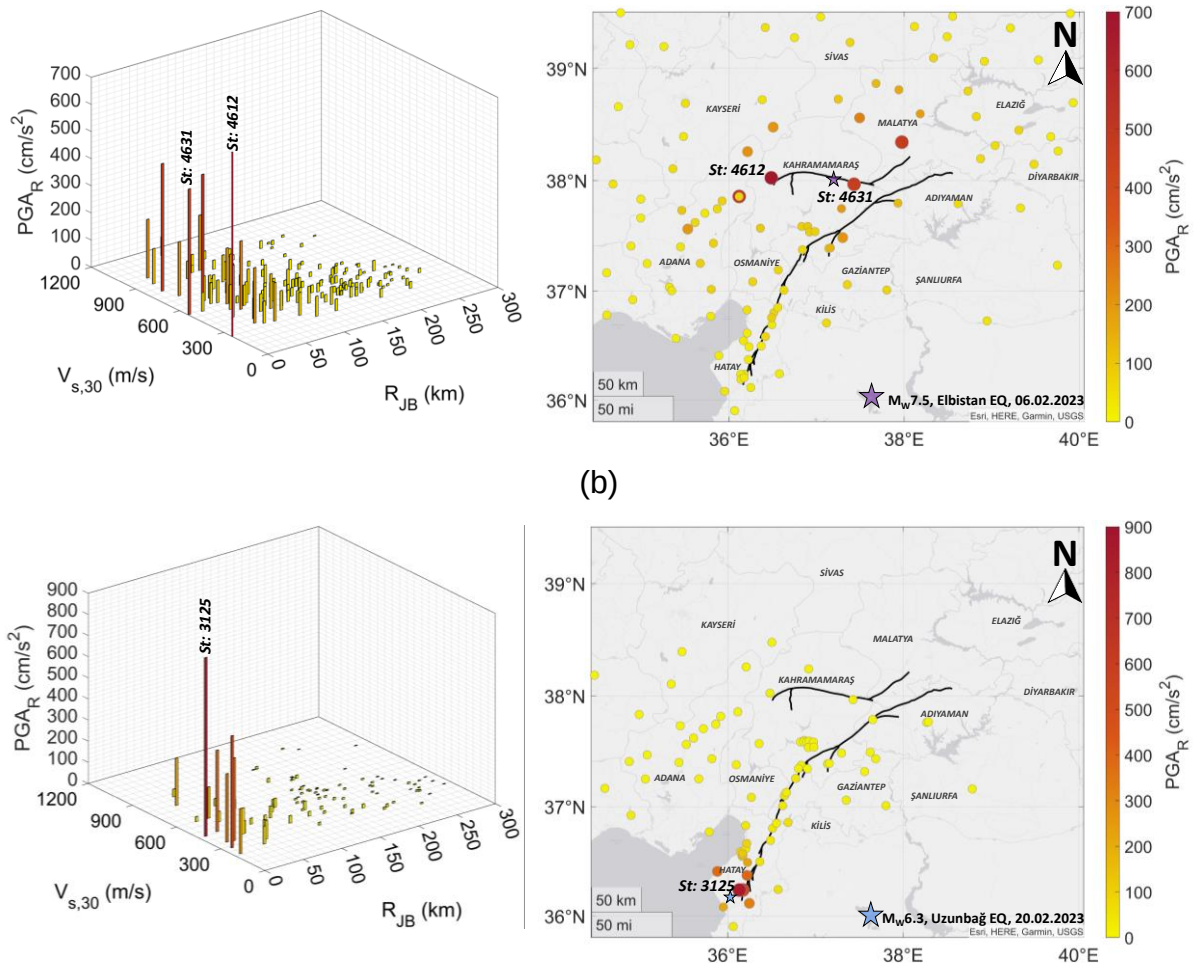

Figure 21: Spatial and statistical distribution of resultant peak ground accelerations (PGAs) with respect to RJB and VS30 for the (a) MW 7.8 Pazarcık, (b) MW 7.5 Ekinözü, and (c) MW 6.3 Uzunbağ events. Black lines on the maps are traced after the USGS published surface rupture (USGS, 2023).

Before wrapping up the section, we need to clarify the issue regarding station 4614 recordings of the MW 7.8 Pazarcık earthquake by comparing to one of the closest stations to the station 4614. Although their resultant PGVs are similar (PGVNAR,R =137 cm/s ≈ PGV4614,R=118 cm/s), Station NAR, one of the stations closest to the epicentre (REPI,NAR=22 km) and fault rupture surface projection (RJB,NAR=0 km), has produced only one-third of the PGA (PGANAR,R=894 cm/s2 << PGA4614,R=2830 cm/s2) recorded in Station 4614, despite being 15 km away and placed at a recording site with softer soil (VS30,NAR=272 m/s < VS30,4614=541 m/s). The reliability of the data seems to be controversial due to the unexpectedly large PGA of station 4614; therefore, this station's recording for the MW 7.8 Pazarcık earthquake has been omitted from study in this report.

2.6.4. Multi-Wave Patterns in Ground Motions

The ground motion recordings of the 2023 Kahramanmaraş earthquake sequence exhibit several distinctive features. Visual inspection of our database revealed that recordings of the M_W7.8 Pazarcık earthquake from 38 stations incorporate multiple wave packages that can be explicitly distinguished. In Melgar et al., 2023, kinematic inversions verify that the rupture migrates to the East Anatolian Fault (EAF) 10

seconds after the onset time following the initial cracking of the Nurdağı-Pazarcık Fault (NPF), and then proceeded bilaterally in both directions, i.e., North-easterly and South-westerly. Multiple wave packages in ground motions are probably triggered by these fault segments rupturing at shifted times. The peak ground acceleration, velocity and displacement of the first wave pattern are captured by the three stations ($R_{EPI,4615}$=21 km, $R_{EPI,NAR}$=22 km, $R_{EPI,KHMN}$= 22 km) which are the closest ones to the epicentre, whereas the recordings of other stations display peak ordinates in the second wave pattern. *Figure 22* illustrates the three-component acceleration, velocity, and displacement time series of station 4615 as an example. In light of Melgar et al., 2023, we can say that the first wave package occurs as a result of the rupture of the Pazarcık segment, whose surface rupture is very close to station 4615. Then, the rupturing of the North and South branch is seen as second and third-wave packages in the time histories. There are also some indications of multiple wave packages in the recordings of the M_W7.5 Ekinözü event, but they are not as explicitly detectable as in the case of the M_W7.8 Pazarcık earthquake. Also, given that the USGS's proposed fault rupture model for the M_W7.5 Ekinözü event appears to be divided into three segments, their ground motions might be possible to include multiple wave packages.

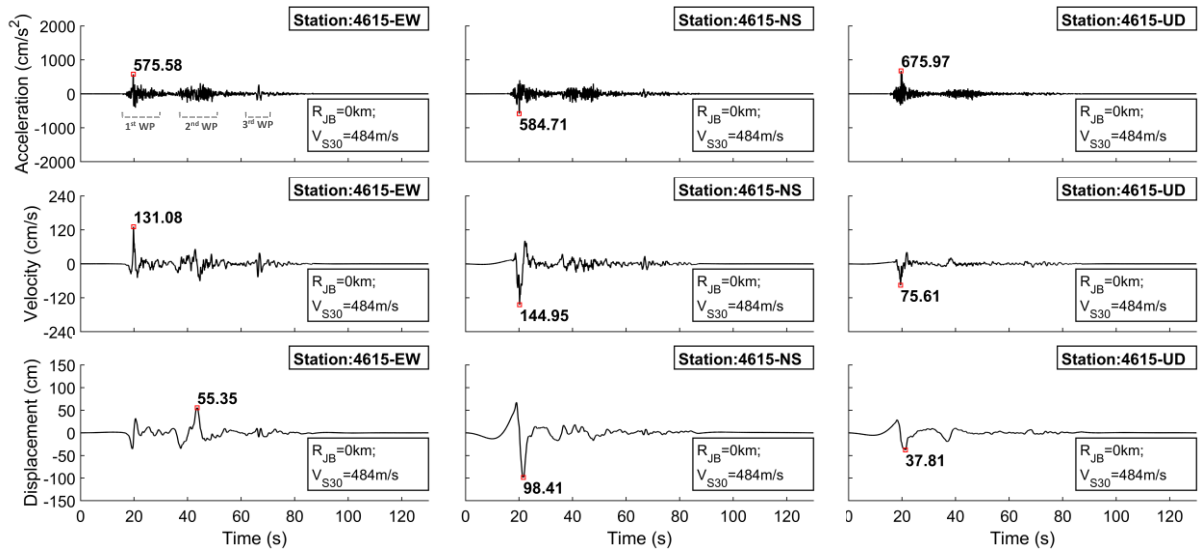

Figure 22: Multiwave patterns detected in three-component acceleration, velocity, and displacement time histories of station 4615 from MW7.8 Pazarcık earthquake (WP= Wave package).

2.6.5. Velocity Pulses

It can be recognized from the velocity traces of the 2023 Kahramanmaraş earthquakes that they possess significant PGV values, particularly in the near-fault areas. The NS component of station 3123, which resides in the Amik Basin (Antakya), has recorded the highest PGV ($PGV_{3123,NS}$=188.8 cm/s) during the M_W 7.8 Pazarcık earthquake. The EW component of another Amik basin station, station 3124, captures the highest PGV of the M_W 6.3 Uzunbağ event ($PGV_{3124,EW}$=76.5 cm/s). The same station that has recorded the highest PGA of the M_W7.5 Ekinözü event also produces the highest PGV value in its NS component ($PGV_{4612,NS}$=170.9 cm/s) (see *Figure 20* for the velocity trace of station 4612 recording). Various factors may be connected to the strong velocities. Especially, ground motions in areas close to seismic sources may possess distinctive characteristics due to the faulting mechanism, the direction of the rupture

front (forward and backward directivity) and permanent surface displacements (fling-step effects) etc. that may impact the extent to which structures perform during earthquakes thereby affecting the potential of damage. The long-period structures may be enforced by the high deformation demands in that these near-source effects give rise to high-amplitude long-period velocity pulses (Kalkan and Kunnath, 2006).

The plentiful near-field data of the Mw 7.8 Pazarcık earthquake provide an opportunity to figure out more regarding the peculiarities of near-field ground motions. Here, we have visually inspected velocity traces to make a preliminary assessment of the near-field pulses, which generate one-sided (or permanent displacement) and two-sided velocity pulses as indicators of fling-step effects and forward rupture directivity, respectively. In *Figure 23***,** velocity and displacement time histories, which have visually detected the most likely two-sided velocity pulses, of station 3143 and station 0132 are exemplified along with their velocity paths for M_W 7.8 Pazarcık and M_W 7.5 Ekinözü earthquakes.

The velocity paths of ground motions also give insights into the predominant direction of ground motion to which structures are subjected. *Figure 23* also provides the trajectories of the corresponding velocity traces. The maximum velocities, whose directions are depicted by the red dashed line, are seen in the approximately fault-normal direction for both events. It should be stated that a more comprehensive assessment of the velocity pulses may be accessed in Baltzopoulos et al. (2023).

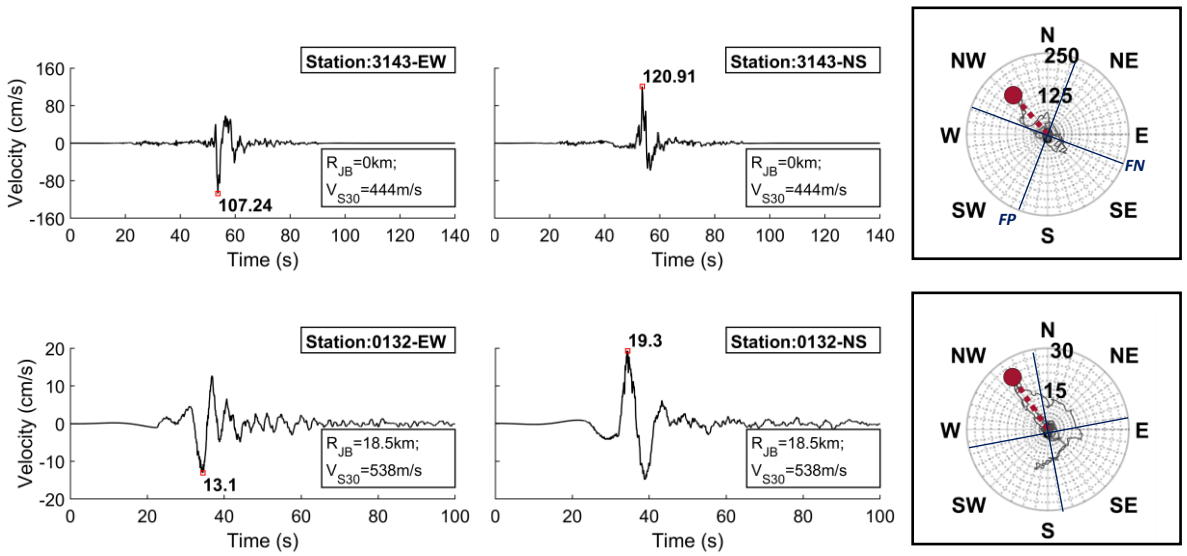

Figure 23: Pulse-like velocity waveforms along with its velocity path (within black squares on the right) for (top) station 3143 for MW7.8 Pazarcık earthquake, (bottom) station 0132 for MW7.5 Ekinözü earthquake (FN=Fault-normal; FP=Fault-parallel; Red dashed line=Predominant direction of ground motion).

2.6.6. Basin Effects

The amplitudes and frequency content of the ground motions, as well as the indirect extent of structural damage, are significantly influenced by local site conditions such as soft soils, sedimentary basins, etc. There have been various techniques to identify site amplifications from ground motions recorded at a particular site during an earthquake. One of these techniques compares the response spectra of two

recordings from neighboring stations, those of which should represent a soil site and a reference rock site (Şafak, 1997).

An outstanding example of these sorts of impacts is provided by the stations that are situated in the Amik Basin (Antakya) in both M_W 7.8 and M_W 6.3 events. Station 3124 and station 3125, which are situated 16 kilometers apart, have recorded both the M_W7.8 and M_W6.3 earthquakes. In contrast to station 3125, which is positioned on bedrock from the middle Miocene, station 3124 is placed on the soft ground of the Amik Basin, according to the geological map of Türkiye (MTA, 2011). These stations' close proximity and the relatively contrasting soil conditions of their recording sites provide an opportunity to inquire about soil amplification in the Amik Basin. The ratios of their velocity response spectra (SV_{3124}/SV_{3125}) for both the EW and NS components for the two events are presented in *Figure 24*. Spectral ratios point out about four-fold amplification, particularly in the EW component of both earthquakes around 1.0 second. However, the comparison of their resultant PGAs unveils that PGA of station 3124 (on softer soil condition) seems to be de-amplify approximately two-fold in both events ($PGA_{3124,R}$=847 cm/s^2 < $PGA_{3125,R}$=1335 cm/s^2 in M_W 7.8 event and $PGA_{3124,R}$ ≈ 603 cm/s^2 < $PGA_{3125,R}$ ≈ 1052 cm/s^2 in M_W 6.3 event). Additionally, a two-fold increase emerges between periods of 5 s and 8 s, particularly in the EW component of the M_W 7.8 earthquake. In contrast, there is not a similar prevailing raise around these periods in the M_W 6.3 earthquake. These amplifications might not be accounted for by just basin effects since there are some indications of additional critical factors, such as near-fault effects in the ground motion recordings. In order to better understand the underlying causes of amplifications, comprehensive examinations of the ground motions are essential.

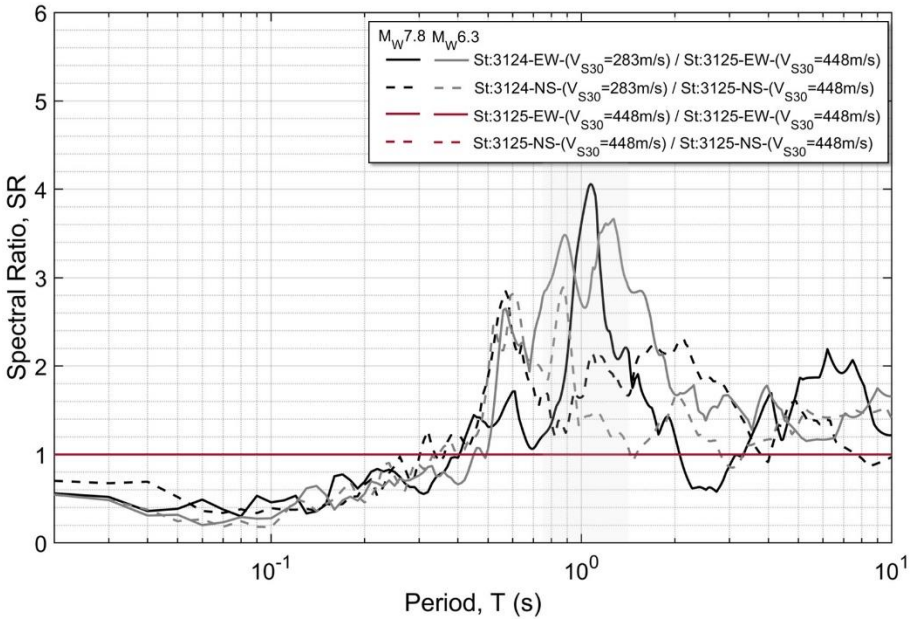

Figure 24: Spectral ratios of station 3124 to station 3125 for MW7.8 Pazarcık and MW6.3 Uzunbağ earthquakes.

2.6.7. Comparison with Earthquake Loads in Seismic Code of Türkiye

2.6.7.1. A Brief Summary for Seismic Hazard of the Region

Türkiye's earliest seismic zonation studies were conducted in the 1930s (Özmen, 2012), and they were often updated in the aftermath of Türkiye's devastating

earthquakes (MS 6.9 Erzincan earthquake in 1939, MS 6.8 Erzincan earthquake in 1992, MS 6.1 Dinar earthquake in 1995, MW 7.8 Gölcük earthquake and MW 7.5 Düzce earthquake in 1999, MW 7.2 Van earthquake in 2011). Figure 1.6.12 illustrates the overall historical evolution of the seismic zonation and hazard maps from 1945 to the present. The use of probability-based hazard maps in the recent Turkish Building Earthquake Code (TBEC, 2018) has superseded the long-used seismic zone approach in Türkiye. The 1996 earthquake zonation map proposed by Gülkan et al. (1993) totally indicates five seismic zones in terms of PGA distribution (Zone I, PGA ≥ 0.4 g; Zone II, 0.3 g ≤ PGA < 0.4 g; Zone III, 0.2 g ≤ PGA < 0.3 g; Zone IV, 0.1 g ≤ PGA < 0.2 g; Zone V, PGA < 0.1 g) based on the return period of 475 years (10% exceedance probability in 50 years). The areas close to the epicenters and surface ruptures of the three earthquakes are designated by Zone 1 on the earthquake zoning map from 1996, while Zones 2 and 3 symbolise the other regions affected by the earthquake sequence (see the map on top-right in *Figure 25*). On the other hand, the most recent hazard map enables users to pick the geo-referenced coordinates at each grid point to determine the PGA, PGV, and the 5% damped pseudo-spectral acceleration (PSA) values at T = 0.2 s and T = 1.0 s for the reference rock (VS30 = 760 m/s). Additionally, a brief report with horizontal and vertical elastic design spectra can be generated by choosing the seismic ground motion level and local soil class (ZA, ZB, ZC, ZD, ZE, ZF, from stiff to soft soils respectively) via the user-friendly web interface of the latest hazard map. However, it should be stated that users of the e-Government Gateway of Türkiye can only access this interface of the most recent hazards map. The most recent Turkish seismic code and hazard map also encompasses georeferenced-based ground motion parameters (PGA, PGV, and SAs) for four different earthquake levels (DD1, DD2, DD3, DD4) that have been specified with different probabilities (2%, 10%, 50%, 68%, respectively) of exceedance in 50 years for return periods of 2475, 475, 72, and 43 years, respectively. Standard design earthquake (SDE) corresponds to DD2 level, whilst the maximum considered earthquake (MCE) is represented by DD1 level. It should be emphasised that in the majority of residential construction projects, the DD2 level is often chosen as the seismic load level. The PGA distribution for the DD2 level earthquake is shown on the bottom-right map in Figure 1.6.12, and the PGA level rises as the hues shift from white to dark red. The intense dark red spread seen in the affected area, especially surrounding the fault rupture, signifies the considerable seismic hazard of the region.

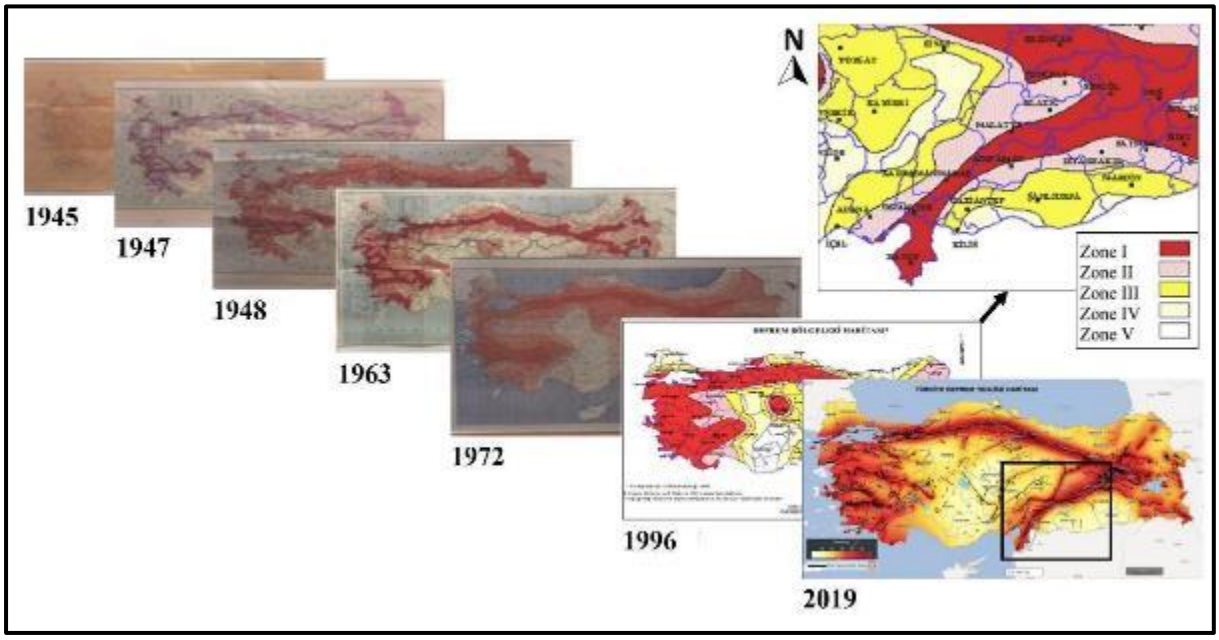

Figure 25: Historical development of Türkiye Earthquake Hazard Maps (modified from AFAD, 2018). The affected region of the 2023 Kahramanmaraş earthquake sequence is marked by a black square in the 1996 and 2018 maps.

2.6.7.2. Comparison of Ground Motion Parameters with Turkish Seismic Code

For the sake of initial comparison of actual ground motions with earthquake loads specified in the Turkish seismic code, the ratio of PGA and PGV acquired from the seismic hazard map of Türkiye for the maximum considered earthquake level (MCE or DD1 in the seismic code of Türkiye) to resultant PGA and PGV of recorded ground motions has been plotted against R_{JB} in *Figure 26*(top). The majority of the PGA and PGV ratios for all three earthquakes appear to be below 1.0, with the exception of several values in the M_W 7.8 Pazarcık earthquake. However, it should be mentioned that particularly near-field $\frac{PGA_{2475}}{PGA_{actual,R}}$ seem to be extremely close to the 1.0 and 21% of PGVs, the majority of which are recorded within 10 km or less of the R_{JB}, exhibit higher values than PGVs at the MCE level. Additionally, the PGAs and PGVs that are on the limit of or exceed the values assigned for the MCE level have mostly been recorded on soil classes C or D (ZC or ZD), as defined by the seismic code of Türkiye. This may be attributed to the inadequate data acquired on stiffer soils, particularly in the near-field areas.

The several exceedances of MCE level show that PGAs and PGVs would probably surpass the values provided by the earthquake hazard map of Türkiye for the standard design-based earthquake (SDE; 10% probability of exceedance in 50 years) level with a return period of 475 years. Therefore, it will be more explanatory to meticulously scrutinize the comparison. *Figure 26*(bottom) depicts the stations with recordings whose actual PGAs for the M_W 7.8 Pazarcık event are more than the design PGAs of DD1 (or MCE) and DD2 (or SDE) levels in the disaster zone. The majority of these exceedances are concentrated around the fault rupture as previously stated, and PGAs and PGVs of both MCE and SDE design levels are violated by ground motions recorded at the five stations (3125, 3126, 3129, 3135 and 3141), which are positioned in the vicinity of Antakya and Arsuz.

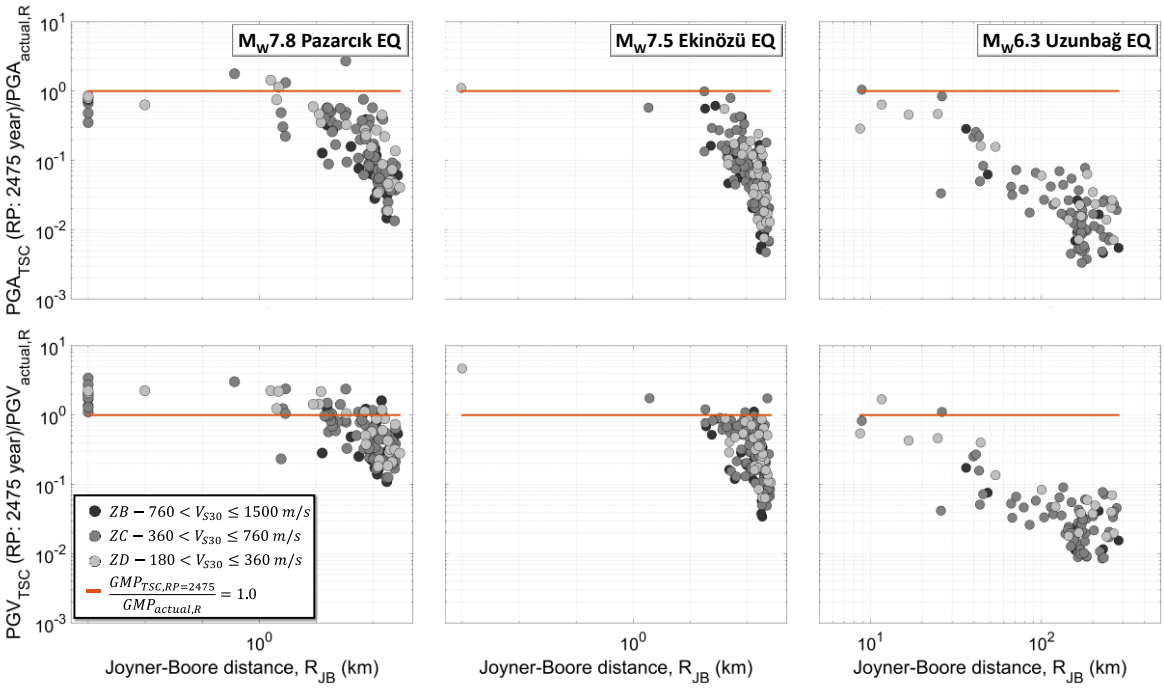

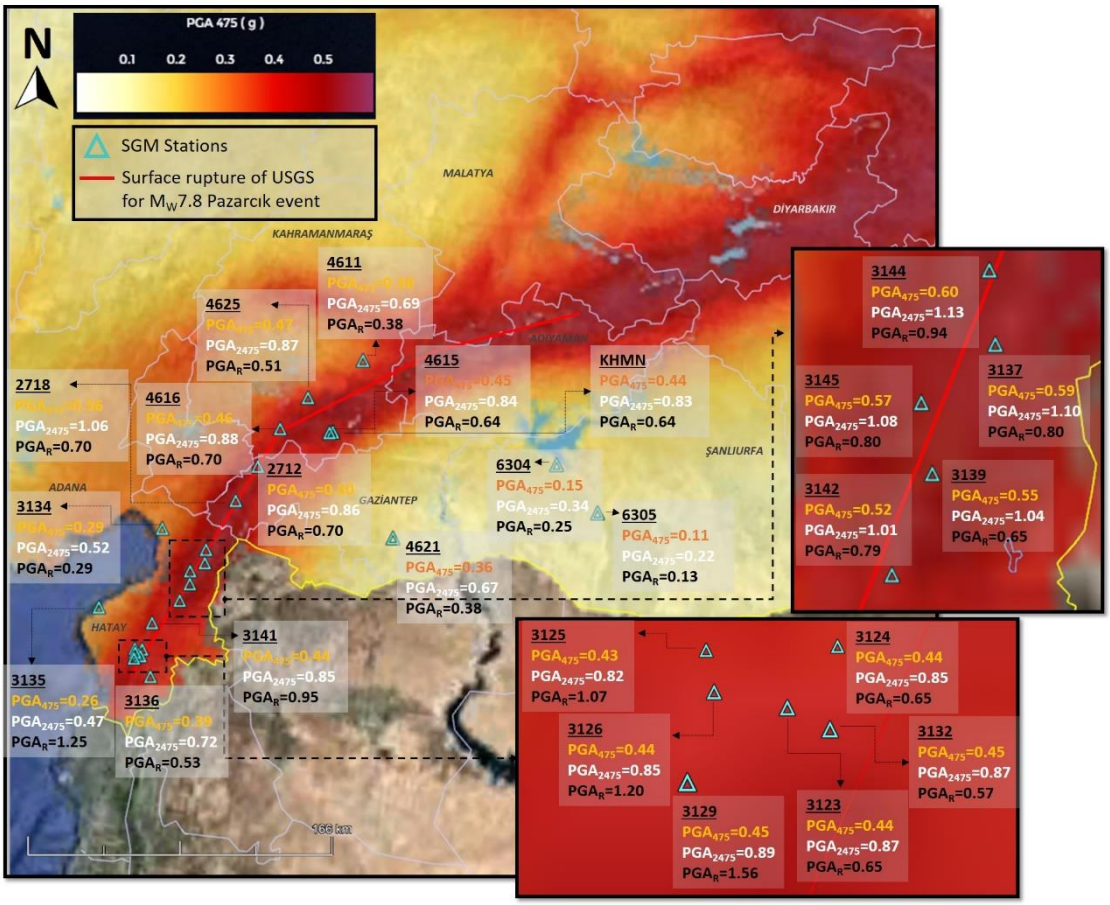

Figure 26: (top) Comparison of PGAs and PGVs of MCE (DD1) level with the resultant GMPs (GMP refers to ground motion parameter such as PGA or PGV) for the MW 7.8 Pazarcık, MW 7.5 Ekinözü, and MW 6.3 Uzunbağ events. (bottom) Earthquake hazard map of Türkiye for MW 7.8 Pazarcık earthquake illustrating the spatial distribution of exceedances of resultant PGAR to MCE (DD1) and SDE (DD2) levels.

The compliance of spectral responses of the largest horizontal acceleration ground motions for 5% damping ratios with earthquake elastic design spectra of outdated seismic code (TBEC, 2007) and MCE and SDE level acceleration spectra of the current seismic regulation (TBEC, 2018) of Türkiye is evaluated for three events in *Figure 27*. Both the EW and NS components of the spectral accelerations in the Mw 7.8 Pazarcık earthquake surpass the MCE level design spectra of the most recent seismic code of Türkiye by up to 4.0 seconds of the period, reaching about 5500 cm/s^2 of SAs at 0.25 seconds. Similarly, a mismatch between 1.0 and 4.0 seconds may also be noticed when comparing the SAs of the Mw 7.5 Ekinözü event with the corresponding MCE level design spectra. The SDE level design spectra are exceeded along a broad period range from 0.2 to 10 s. In the very short period (T<0.2 s) region, spectral accelerations seem to be higher than both design-level ordinates for the Mw 6.3 Uzunbağ earthquake. Beyond this period, the observed SAs fluctuates around spectral accelerations of the SDE level.

Since a significant amount of the structures were constructed before 2018 in the region, a critical perspective is also provided by the comparison with the design spectrum of the outdated seismic code for Türkiye (TBEC, 2007). The largest spectral accelerations acquired from both the Mw 7.8 Pazarcık and Mw 7.5 Ekinözü earthquakes generally surpass the acceleration design spectra recommended in the outdated seismic code for site classes B and C. In the smallest magnitude event (Mw 6.3), spectral accelerations exceed the TBEC design spectra in the short period region (up to ~0.5 s), whereas the design conditions of outdated spectra seem to be met by the observed spectral accelerations.

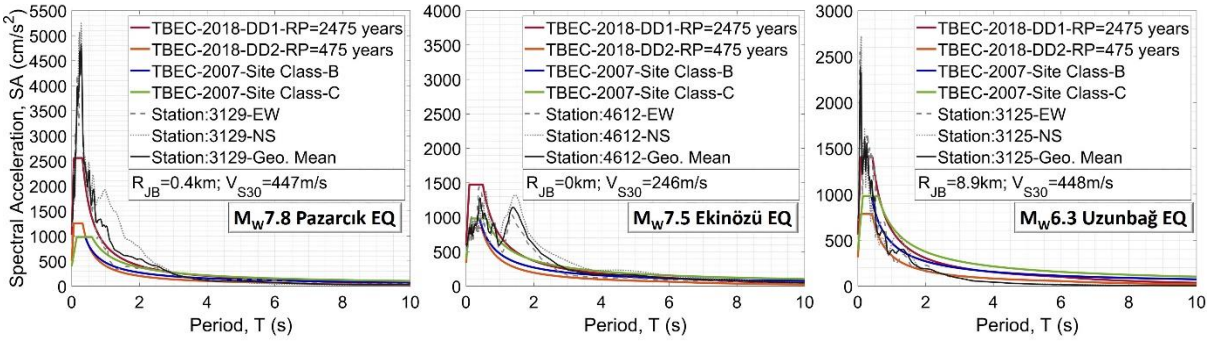

Figure 27: Comparison of largest horizontal acceleration response spectra with design spectra of 2007 and 2019 Türkiye building earthquake code for MW7.8 Pazarcık, MW7.5 Ekinözü, and MW6.3 Uzunbağ events.

The vertical components of ground motions have also produced significant values throughout the Kahramanmaraş earthquake sequence in 2023, particularly in the Mw 7.8 Pazarcık earthquake. The field team has reported that many residents (especially in many districts of Hatay) made remarks about the considerable vertical movement during the earthquake and the severity of vertical movement is evident in many cases, such as rocking/overturning failures of slender structures (particularly minarets), large permanent drifts of the RC frames, and stripping of the longitudinal reinforcement rebars at the foundation level. The structural impact of these were investigated during the field deployment, and related figures and discussions are presented in the further sections of this report.

From the SGM viewpoint, typically, vertical PGA values are expected to be roughly equivalent to 2/3 of horizontal PGA values (Bozorgnia and Campbell, 2003). Several recordings of the Kahramanmaraş earthquake sequence, though, deviate from this conventional ratio. For comparative purposes, both the horizontal and vertical directions of the acceleration time series featuring the largest vertical PGAs are portrayed in *Figure 28*(top) in both horizontal and vertical directions for the M_W 7.8 Pazarcık, M_W 7.5 Ekinözü and M_W 6.3 Uzunbağ events. At station 3126, the M_W 7.8 earthquake has caused extremely high vertical PGAs ($PGA_{3126,UD}$=1066 cm/s^2) that are at the same level with its horizontal PGA values and almost greater than gravity. Furthermore, one of the near-fault recordings from the M_W 7.5 Ekinözü event results in PGA that is greater in the vertical direction than those in the horizontal direction. ($PGA_{4631,UD}$=490 cm/s^2 > $PGA_{4631,EW}$=380 cm/s^2). In contrast to these events, the largest vertical PGA constitutes approximately 50% of its horizontal PGA in the recordings of station 3125 for the M_W 6.3 Uzunbağ event. *Figure 28*(bottom) compares the acceleration response spectra of the aforementioned vertical component time series with the vertical design spectra for both MCE (or DD1) and SDE (or DD2) earthquake levels suggested by TBEC 2018. The largest vertical acceleration response spectrum of the M_W 7.8 event surpasses the MCE level throughout a broad period range, while the MCE level design spectrum is underneath the actual vertical responses of station 4631 only between 0.5 and 1.6 s and an impulsive bump in the short period region for the M_W 7.5 Ekinözü event. In the M_W 6.3 event, the rapid exceeding of MCE level design SAs is also noticeable at T=0.05 s, but at other periods, SAs seems to be around MCE level.

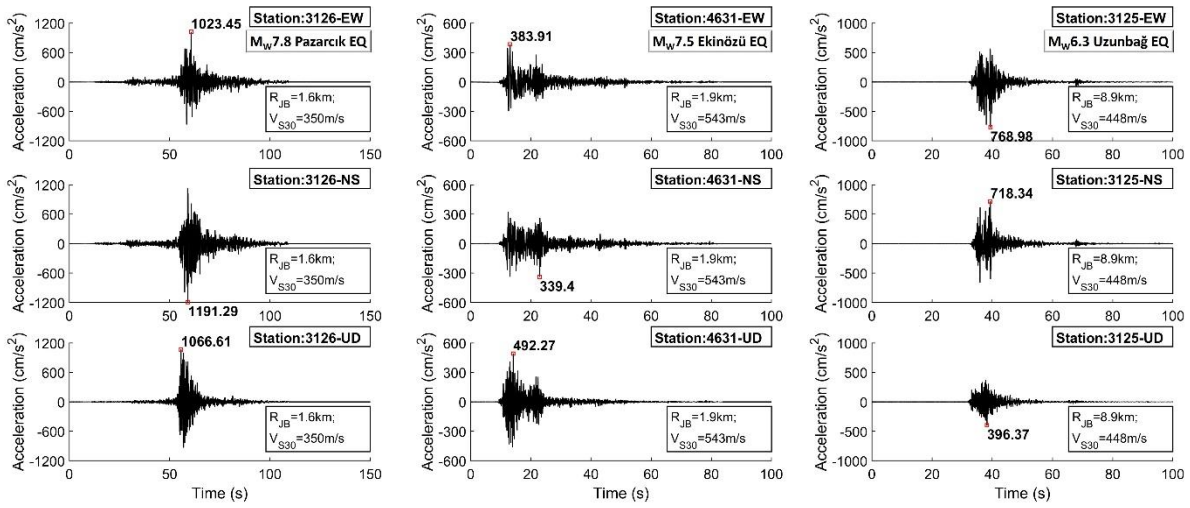

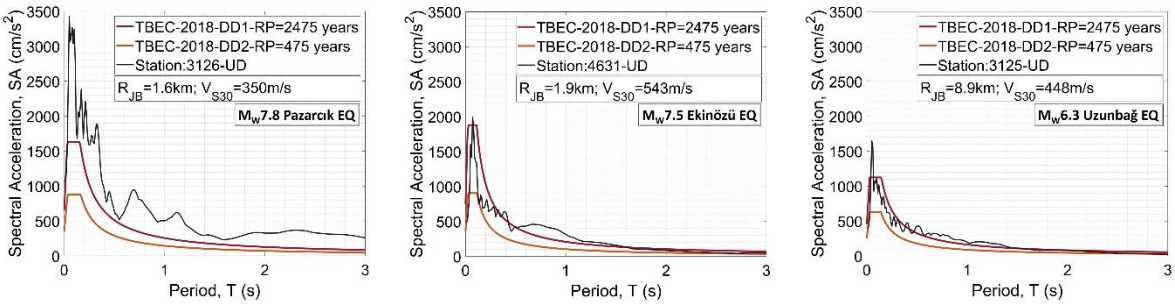

Figure 28: (top) Three-component acceleration time series with the largest vertical PGAs. (bottom) Comparison of largest vertical acceleration response spectra with the 2018 Türkiye design spectra for the MW 7.8 Pazarcık, MW 7.5 Ekinözü and MW 6.3 Uzunbağ events.

2.6.8. Comparison with Ground Motion Prediction Equations

The PGAs, PGVs, and SAs with 5% damping ratio at T=0.8 s of only the M_W 7.8 Pazarcık earthquake have been compared with the estimates of the ground motion prediction equation generated by Kale et al., 2015, which will be called as KAAH15 in the section, in order to better grasp the attenuation aspects of the data with respect to the R_{JB} and soil conditions. The mean V_{S30} values of each soil class (292 m/s for ZD, 520 m/s for ZC and 955 m/s ZB), which are thoroughly explained in the Section 1.6.3, are taken into account in the construction of the attenuation lines of KAAH15 in order to reflect the variations in the soil conditions under recording sites. Additionally, the strike-slip faulting and Türkiye, which is suggested as a regional alternative in KAAH15, has been chosen in the derivation of GMPE curves. As shown in *Figure 29*, the comparisons have been conducted for the median, median±σ, and median±2σ estimations of KAAH15. Actual PGAs seem to be within the median±2σ range for all soil classes. It should be noted that data with a zero R_{JB} has been assigned at R_{JB}=0.1 km in order to visualize the plot logarithmically. In the case of soil types C and D, near-fault PGAs do not exceed the median±σ limit values, whereas the stiffest soil class (Soil class B) suffers from a scarcity of very near-fault data (R_{JB}<10 km). Additionally, the relatively good agreement of actual near-fault PGAs with estimations of KAAH15 could not be attained for near-fault PGV and SA (T=0.8 s). The greater distances showcase faster attenuation tendencies for all ground motion parameters (PGA, PGV, and SA(T=0.8 s)), as evidenced by earlier earthquakes that occurred in Türkiye, such as the M_W 5.7 Silivri earthquake in 2019 (Malcioglu et al., 2022a) and the M_W 6.9 Aegean Sea earthquake in 2020 (Malcioglu et al., 2022b) even if the majority of data falls into the median±2σ band.

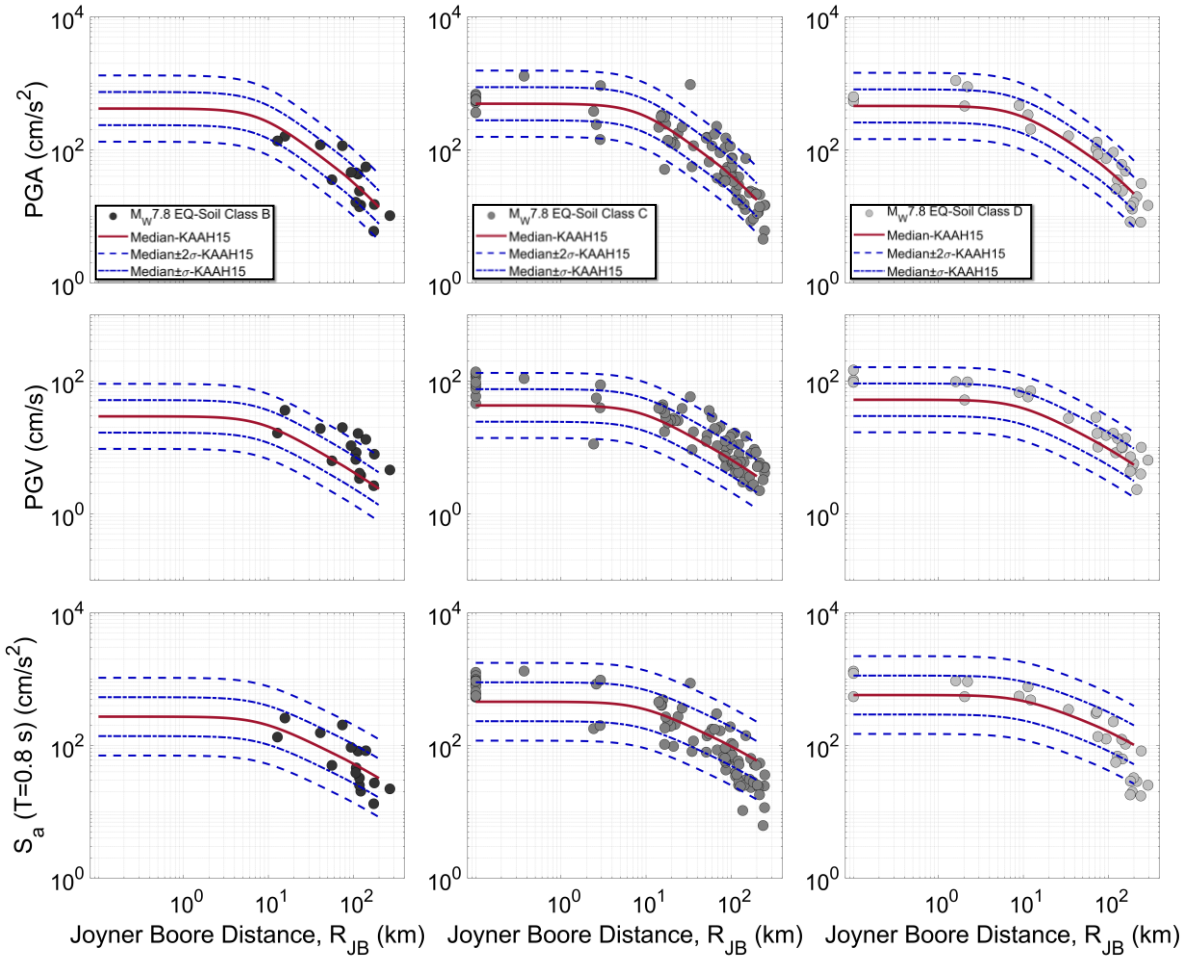

Figure 29: Comparison of the geometric mean of PGA, PGV, and SA (T=0.8 s; ξ=5%) with ground motion prediction equation of Kale et al., 2015 (KAAH15) for the MW 7.8 Pazarcık earthquake.

The authors recommend conducting a comparison with different GMPEs in order to get the best estimate of ground motion parameters for potential future studies. The research report for the Kahramanmaraş earthquakes of Çetin et al., 2023 from the collaboration of NSF, EERI, GEER, and METU involves a more comprehensive comparison of ground motion parameters with ground motion estimation models.

2.7. Tsunami

Although the M_W 7.8 Pazarcık earthquake was almost 100 km inland from the coast, the Intergovernmental Oceanographic Commission - United Nations Educational, Scientific and Cultural Organization (IOC-UNESCO) for the Northeast Atlantic, Mediterranean, and connected seas Tsunami Warning System (NEAMTWS) responded promptly offering critical tsunami advice to the public.

The Italian tsunami service provider (TSP) for the NEAMTWS, Centro Allerta Tsunami (CAT) of Istituto Nazionale di Geofisica e Vulcanologia (INGV) issued a basin-watch tsunami warning for both the south and east coasts of Italy just 8 minutes after the mainshock (CAT-INGV, 2023). A basin-watch (red-level) tsunami warning indicates the potential for a tidal wave of >0.5 m in deep ocean or a run-up of more than 1 m,

therefore posing the risk of inundation to coastal communities that are topographically 1 m or less from sea level. Additionally, KOERI, the Turkish TSP for the NEAMTWS, issued a land threat within 15 minutes of the initial Pazarcık earthquake as tsunami amplitudes of 0.5 m were estimated along the southern coast of Türkiye (Cetin et al., 2023). In other regions of Türkiye and Greece, an orange-level advisory warning was issued, and other countries, including Cyprus, Albania, Montenegro, Croatia, and Malta were placed on tsunami watch.

Small amplitude tsunami waves were recorded at four tide gauges in the Eastern Mediterranean within 30 minutes of the M_W 7.8 Pazarcık earthquake (*Figure 30*). The highest tsunami amplitudes were measured on the eastern coast of Cyprus, at Fumagusta station, where wave heights of 17 cm were recorded (Cetin et al., 2023). Additionally,13-14 cm high waves were measured along the north coast of Cyprus (Girne station) and the south-east coast of Türkiye at the Arsuz and Erdemli tidal gauges (Cetin et al., 2023).

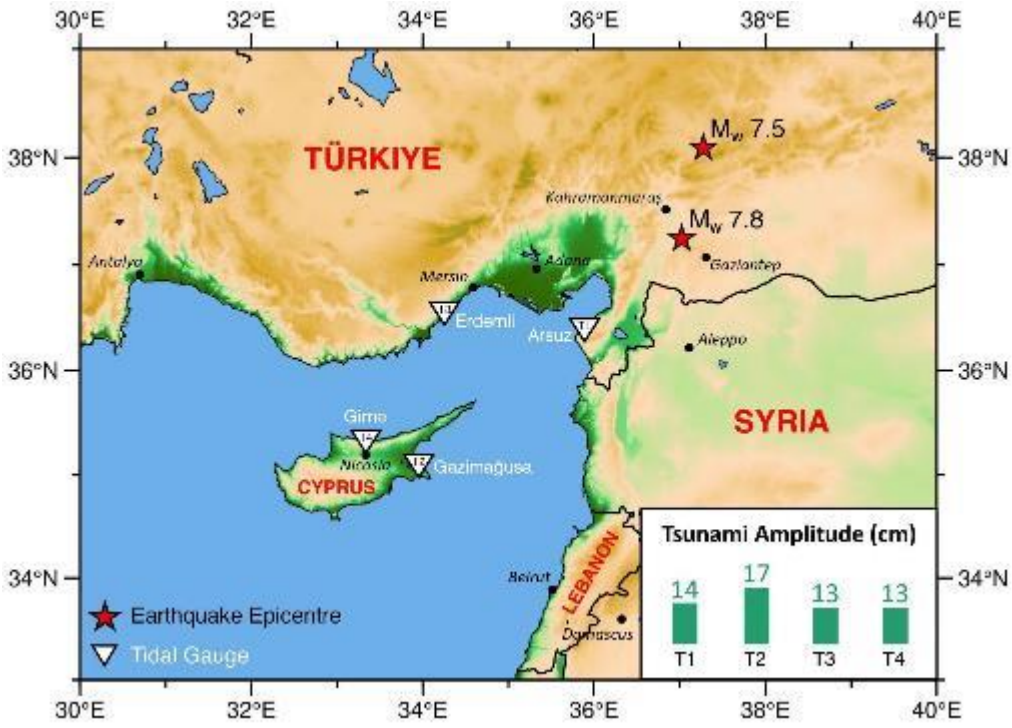

Figure 30: Map of the eastern Mediterranean illustrating where small tsunamis with <0.2 m amplitudes were recorded at Arsuz, Erdemli, Girne and Gazimagusa tidal gauge stations across south-east Türkiye and north-east Cyprus (Cetin et al., 2023).

In the days following the 6th February Kahramanmaraş earthquake sequence, significant water inundation was observed across Türkiyeand Cyprus, in small Fishery ports where the small tsunamis were recorded. The worst affected was the port of İskenderun (approximately 30 km north-east of Arsuz in *Figure 30*), mainly due to a combination of liquefaction and lateral spreading, further discussed by Cetin et al. (2023) and Taftsoglou et al. (2023).

The rapid warning responses from both TSPs, KOERI and INGV, demonstrate the effectiveness of an established tsunami early warning system since its establishment

in 2012 (Necmioğlu et al., 2021), even if the warning was later removed as the threat was analysed and reduced.

2.8. Conclusions

In February 2023, a sequence of large-magnitude earthquakes hit South-eastern Türkiye and North-western Syria. From the SGM perspective, the report had to focus on the national seismic networks of Türkiye, due to the absence of recordings from any networks in Syria. Strong ground motion recordings supplied by TADAS and KOERI networks have been examined for the M_W 7.8 Pazarcık ($N_{STATION}$=128), M_W 7.5 Ekinözü ($N_{STATION}$=150), and M_W 6.3 Uzunbağ ($N_{STATION}$=100) earthquakes. The progression of the analysis has been challenging due to issues with data transmission. Visual inspection of the six stations in the field confirms that there is no exterior damage on the huts. The Joyner-Boore distance (R_{JB}), which takes into account the entire fault rupture, has been preferred in the analyses due to the significant rupture length (~350-400 km in the M_W 7.8 and ~150-200 km in Mw 7.5 earthquakes). The segmental rupture characteristics of particularly the M_W 7.8 Pazarcık event are witnessed with the multiple wave patterns in the strong ground motion time series. The Amik basin (Antakya/Hatay), which is situated on the Southeast end of the fault rupture of the M_W 7.8 Pazarcık event and is an average of 10 km from the epicentre of the M_W 6.3 Uzunbağ earthquake, is where the strongest ground motions are detected. Ground motions in this area are probably amplified by not only the near-fault phenomenon but also the basin effects, especially in the fault-normal direction. The M_W 7.5 Ekinözü ground motions, however, are more pronounced in the Northern part of the earthquake disaster region, such as North of Kahramanmaraş, Northeast of Adana, and South of Malatya. The 5%-damped response spectra surpass the SDE level (return period: 475 years) design spectra of TBEC2018, which are typically employed in the design of conventional residential buildings and also the design spectra defined in outdated earthquake building code, TBEC2007. The MCE level (return period: 2475 years) design spectra of TBEC2018 also mostly fail to encompass the 5%-damped spectral accelerations of particularly near-field ground motions. Moreover, strong vertical ground motions (with occasionally >1000 cm/s^2 PGAs) result in the TBEC2018 vertical design spectrum being violated. The impacts of basin sediments and being close to the fault should be taken into consideration in the earthquake loads specified in the prospective building design codes, and regulations should be prepared for buildings to be constructed in these areas. Even though KAAH15 estimations seem to be relatively consistent with actual PGAs, PGVs and SAs (T=0.8 s) tend to be overestimated in distant R_{JB}s and underestimated in distances close to faults. A thorough comparison of ground motion parameters with GMPE predictions is required in order to achieve more reliable coordinate-based estimations, notably utilised in the construction of fragility functions and other hazard and risk studies of the area. Moreover, the comprehensive analyses of ground motions, particularly regarding their frequency contents and durations, will provide useful information on correlating ground motions with damage rates in the region.

References

AFAD (Disaster and Emergency Management Authority). (2023) 1900 – 2023 Earthquake Catalog (M >= 4.0), https://deprem.afad.gov.tr/depremkatalogu/.

AFAD (2018). *Earthquake Hazard Map of Türkiye*. Republic of Türkiye Ministry of Interior Disaster and Emergency Management Presidency. Retrieved May, 2023, from https://tdth.afad.gov.tr

Allen, T.I. & Wald, D.J. (2007). *Topographic slope as a proxy for global seismic site conditions (Vs30) and amplification around the globe*. Open-File Report 2007–1357. Reston, Virginia, USA: U.S. Geological Survey

Alchalbi, A., Daoud, M., Gomez, F., McClusky, S., Reilinger, R., Romeyeh, M. A., ... & Barazangi, M. (2010). Crustal deformation in n`orthwestern Arabia from GPS measurements in Syria: Slow slip rate along the northern Dead Sea Fault. Geophysical Journal International, 180(1), 125-135.

Allen, M.B. & Armstrong, H.A., (2008). Arabia–Eurasia collision and the forcing of mid-Cenozoic global cooling. *Palaeogeography, Palaeoclimatology, Palaeoecology*, *265*(1-2), pp.52-58.

Arpat, E. & Şaroğlu, F. (1972). The East Anatolian Fault System; thoughts on its development. *Bulletin of the Mineral Research and Exploration Institute of Türkiye*, **78**, 33-39.

Baltzopoulos, G., R. Baraschino, E. Chioccarelli, P. Cito, I. & Iervolino (2023). *Preliminary Engineering Report on Ground Moton Data of the Feb. 2023 Türkiye Seismic Sequence*. Consortium of Italian Universites. https://doi.org/10.13140/RG.2.2.13103.82080/9

Bozorgnia, Y., & Campbell, K. W. (2004). The vertical-to-horizontal response spectral ratio and tentative procedures for developing simplified V/H and vertical design spectra. *Journal of Earthquake Engineering*, 8(2), 175–207. https://doi.org/10.1080/13632460409350486

Barka, A., Reilinger, R. (1997). Active tectonics of the Eastern Mediterranean region: deduced from GPS, neotectonic and seismicity data.

Bayrak, E., Yılmaz, Ş., Softa, M., Türker, T., & Bayrak, Y. (2015). Earthquake hazard analysis for East Anatolian fault zone, Türkiye. *Natural Hazards*, *76*, 1063-1077.

Boulton, S.J., (2013). Tectonic development of the southern Karasu Valley, Türkiye: successive structural events during basin formation. *Geological Society, London, Special Publications*, *372*(1), pp.531-546.

Bozkurt, E., (2001). Neotectonics of Türkiye–a synthesis. *Geodinamica acta*, *14*(1-3), pp.3-30.

CAT-INGV (2023). 06.02.2023 - Türkiye and Syria (updating), WATCH tsunami warning for M 7.9 earthquake. Centro Allerta Tsunami, Istituto Nazionale di Geofisica e Vulcanologia. Available online: https://cat.ingv.it/en/media-and-documents/news-en/381-06-02-2023-Türkiye-and-syria-updating-watch-tsunami-warning-for-m-7-9-earthquake. (accessed on 10 April 2023).

Çetin, K.Ö., Ilgaç, M., Can, G., Çakır, E. (2023). Preliminary Reconnaissance Report on February 6, 2023, Pazarcık Mw = 7.7 and Elbistan Mw = 7.6, Kahramanmaraş-Türkiye Earthquakes. Middle East Technical University, Earthquake Engineering Research Center, Report No: METU/EERC 2023-01, Ankara, Türkiye.

Dal Zilio, L., & Ampuero, J. P. (2023). Earthquake doublet in Türkiye and Syria. *Communications Earth & Environment*, *4*(1), 71.

Duman, T.Y. & Emre, Ö., (2013). The East Anatolian Fault: geometry, segmentation and jog characteristics. *Geological Society, London, Special Publications*, *372*(1), pp.495-529.

Emre, Ö., Duman, T. Y., Özalp, S., Şaroğlu, F., Olgun, Ş., Elmacı, H., & Çan, T. (2018). Active fault database of Türkiye. *Bulletin of Earthquake Engineering*, *16*(8), 3229-3275.

England, P., Houseman, G., & Nocquet, J. M. (2016). Constraints from GPS measurements on the dynamics of deformation in Anatolia and the Aegean. Journal of Geophysical Research: Solid Earth, 121(12), 8888-8916.

Erdik, M., Tümsa, M. B. D., Pınar, A., Altunel, E., & Zülfikar, A. C. A Preliminary Report on the February 6, 2023 Earthquakes in Türkiye; Temblor 2023. Available at: https://temblor.net/temblor/preliminary-report-2023-Türkiye-earthquakes-15027/.

ESM (2023). Engineering Strong Motion Database (ESM). https://esm-db.eu/

FEMA (1999). HAZUS99 user and technical manuals. Federal Emergency Management Agency Report: HAZUS 1999, Washington D.C., USA

Felzer, K. R., R. E. Abercrombie, and G. Ekström (2004). A common origin for aftershocks, foreshocks, and multiplets, Bull. Seismol. Soc. Am. 94, no. 1, 88–98, doi: 10.1785/0120030069.

Goldberg, D. E., Taymaz, T., Reitman, N. G., Hatem, A. E., Yolsal-Çevikbilen, S., Barnhart, W. D., ... & Altuntaş, C. (2023). Rapid Characterization of the February 2023 Kahramanmaraş, Türkiye, Earthquake Sequence. The Seismic Record, 3(2), 156-167.

Gülkan, P., Koçyiğit, A., Yücemen, M. S., Doyuran, V., & Başöz, N. (1993). En son verilere göre hazırlanan Türkiye deprem bölgeleri haritası. *Rapor no: METU/EERC*, *93*(01).

Hardenberg, M. F., & Robertson, A. H. F., (2007). Sedimentology of the NW margin of the Arabian plate and the SW–NE trending Nahr El-Kabir half-graben in northern Syria during the latest Cretaceous and Cenozoic. *Sedimentary Geology,* **201**, 231-266.

IFRC (21 April 2023). "Türkiye - Earthquakes Operation Update #2 - Emergency Appeal № MDRTR004 (21/04/2023)". ReliefWeb. Retrieved 23 April 2023.

Inwood, J., Anderson, M.W., Morris, A., Robertson, A. H. F., (2009). Successive structural events in the Hatay Ophiolite of southeast Türkiye: Distinguishing oceanic, emplacement and post-emplacement phases of faulting. *Tectonophysics*, **473**, 208-222.

Kale, Z., Akkar, S., Ansari, A., & Hamzehloo, H. (2015). A Ground-Motion Predictive Model for Iran and Türkiye for Horizontal PGA, PGV, and 5% Damped Response Spectrum: Investigation of Possible Regional Effects. *Bulletin of the Seismological Society of America*, 105(2A), 963–980. https://doi.org/10.1785/0120140134

Kalkan, E., & Kunnath, S. K. (2006). Effects of Fling Step and Forward Directivity on Seismic Response of Buildings. *Earthquake Spectra*, 22(2), 367–390. https://doi.org/10.1193/1.2192560

Karabacak, V., Ozkaymak, C., Sozbilir, H., Tatar, O., Aktug, B., Ozdag, O. C., Cakir, R., Aksoy, E., Kocbulut, F., Softa, M., Akgun, E., Demir, A., Arslan, G., (2023) The 2023 Pazarcık (Kahramanmaras, Türkiye) Earthquake (Mw 7.7): Implications for surface rupture dynamics along the East Anatolian Fault Zone. In review/pre-print.

Karabulut, H., Güvercin, S. E., Hollingsworth, J., & Konca, A. Ö. (2023). Long silence on the East Anatolian Fault Zone (Southern Türkiye) ends with devastating double earthquakes (6 February 2023) over a seismic gap: implications for the seismic potential in the Eastern Mediterranean region. Journal of the Geological Society, 180(3).

Kawoosa, V. M. (2023, March 01) 10,000 tremors: How Türkiye has been rattled by aftershocks since the Feb. 6 earthquake. Reuters, Retreived from https://www.reuters.com/graphics/TÜRKIYE-QUAKE/AFTERSHOCKS/dwpkdzklevm/

Kurcer, A., Elmaci, H., Ozdemir, E., Given, C., Guler, T., Avcu, I., Ozalp, S., (2023). 06 ŞUBAT 2023 PAZARCIK (KAHRAMANMARAŞ) DEPREMİ (Mw 7,7) SAHA GÖZLEM RAPORLARI SERİSİ 1-AMANOS SEGMENTİ. MTA Report 14121.

Mai, P. M., Aspiotis, T., Aquib, T. A., Cano, E. V., Castro-Cruz, D., Espindola-Carmona, A., ... & Jónsson, S. (2023). The Destructive Earthquake Doublet of 6 February 2023 in South-Central Türkiye and Northwestern Syria: Initial Observations and Analyses. The Seismic Record, 3(2), 105-115.

Malcioglu, F. S., Süleyman, H., & Çaktı, E. (2022). Seismological and engineering characteristics of strong motion data from 24 and 26 September 2019 Marmara Sea earthquakes. *Bulletin of Earthquake Engineering*, 20(11), 5567–5599. https://doi.org/10.1007/s10518-022-01422-y.

Malcioglu, F. S., O'Kane, A., Dönmez, K., & Aktaş, Y. D. (2022). Characteristics of Strong Ground Motions in the 30 October 2020, M_W6.9 Aegean Sea Earthquake. *Frontiers in Built Environment*, 8. https://doi.org/10.3389/fbuil.2022.870279.

Mart, Y., Ryan, W. B., & Lunina, O. V. (2005). Review of the tectonics of the Levant Rift system: the structural significance of oblique continental breakup. Tectonophysics, 395(3-4), 209-232.

MTA, General Directorate of Mineral Research and Exploration (2011) 1/250,000 scale geological maps of Türkiye.

Meghraoui, M., Gomez, F., Sbeinati, R., Van der Woerd, J., Mouty, M., Darkal, A. N., ... & Barazangi, M. (2003). Evidence for 830 years of seismic quiescence from palaeoseismology, archaeoseismology and historical seismicity along the Dead Sea fault in Syria. *Earth and Planetary Science Letters*, *210*(1-2), 35-52.

Melgar, D., Taymaz, T., Ganas, A., Crowell, B. W., Öcalan, T., Kahraman, M., ... & Altuntaş, C. (2023). Sub-and super-shear ruptures during the 2023 Mw 7.8 and Mw 7.6 earthquake doublet in SE Türkiye.

McClusky, S., Balassanian, S., Barka, A., Demir, C., Ergintav, S., Georgiev, I., ... & Kastens, K. (2000). Global Positioning System constraints on plate kinematics and dynamics in the eastern Mediterranean and Caucasus. Journal of Geophysical Research: Solid Earth, 105(B3), 5695-5719.

McClusky, S., Reilinger, R., Mahmoud, S., Ben Sari, D., & Tealeb, A. (2003). GPS constraints on Africa (Nubia) and Arabia plate motions. Geophysical Journal International, 155(1), 126-138.

McKenzie, D. (1972). Active tectonics of the Mediterranean region. Geophysical Journal International, 30(2), 109-185.

Melgar, D., Taymaz, T., Ganas, A., Crowell, B., Öcalan, T., Kahraman, M., Tsironi, V., Yolsal-Çevikbilen, S., Valkaniotis, S., Irmak, T. S., Eken, T., Erman, C., Özkan, B., Dogan, A. H., & Altuntaş, C. (2023). Sub- and super-shear ruptures during the 2023 Mw 7.8 and Mw 7.6 earthquake doublet in SE Türkiye. *Seismica*, 2(3). https://doi.org/10.26443/seismica.v2i3.387

Necmioğlu, Ö., Turhan, F., Özer Sözdinler, C., Yılmazer, M., Güneş, Y., Cambaz, M. D., ... & Özener, H. (2021). KOERI's tsunami warning system in the eastern mediterranean and its connected seas: a decade of achievements and challenges. *Applied Sciences*, *11*(23), 11247.

Nocquet, J. M. (2012). Present-day kinematics of the Mediterranean: A comprehensive overview of GPS results. Tectonophysics, 579, 220-242.

Ou, Q.; Lazecky, M.; Watson, C.S.; Maghsoudi, Y.; Wright, T. (2023): 3D Displacements and Strain from the 2023 February Türkiye Earthquakes, version 1. NERC EDS Centre for Environmental Data Analysis. doi:10.5285/df93e92a3adc46b9a5c4bd3a547cd242.

Park, C. B., Miller, R. D., & Xia, J. (1999). Multichannel analysis of surface waves. *Geophysics*, 64(3), 800–808. https://doi.org/10.1190/1.1444590

Perinçek, D. & Çemen, İ. (1990). The structural relationship between the East Anatolian and Dead Sea fault zones in Southeastern Türkiye. Tectonophysics, 172, 331-340.

Petersen, G. M., Büyükakpinar, P., Vera Sanhueza, F. O., Metz, M., Cesca, S., Akbayram, K., ... & Dahm, T. (2023). The 2023 Southeast Türkiye Seismic Sequence: Rupture of a Complex Fault Network. The Seismic Record, 3(2), 134-143.

Petersen, M.D., Frankel, A.D., Harmsen, S.C., Mueller, C.S., Haller, K.M., Wheeler, R.L., Wesson, R.L., Zeng, Y., Boyd, O.S., Perkins, D.M., Luco, N., Field, E.H., Wills, C.J., and Rukstales, K.S. (2008). *Documentation for the 2008 Update of the United States National Seismic Hazard Maps*. Reston, Virginia: U.S. Geological Survey. Open-File Report 2008–1128, 61 p. https://doi.org/10.3133/ofr20081128

Reilinger, R., McClusky, S. (2011). Nubia–Arabia–Eurasia plate motions and the dynamics of Mediterranean and Middle East tectonics. Geophysical Journal International, 186(3), 971-979.

Reilinger, R., McClusky, S., Vernant, P., Lawrence, S., Ergintav, S., Cakmak, R., Ozener, H., Kadirov, F., Guliev, I., Stepanyan, R., Nadariya, M., Hahubia, G., Mahmoud, S., Sakr, K., ArRajehi, A., Paradissis, D., Al-Aydrus, A., Prilepin, M., Guseva, T., Evren, E., Dmitrotsa, A., Filikov, S.V., Gomez, F., Al-Ghazzi, R. & Karam, G., (2006). GPS constraints on continental deformation in the Africa-Arabia-Eurasia continental collision zone and implications for the dynamics of plate interactions. *Journal of Geophysical Research*, **111** (B5), B054011, doi:10.1029/2005JB004051.

Reitman, N. G., Briggs, R.W., Barnhart, W.D.,Thompson Jobe, J.A., DuRoss, C.B., Hatem, A.E., Gold, R.D., and Mejstrik, J.D. (2023) Preliminary fault rupture mapping of the 2023 M7.8 and M7.5 Türkiye Earthquakes. DOI: https://doi.org/10.5066/P985I7U2

Robertson, A., Boulton, S.J., Taslı, K., Yıldırım, N., İnan, N., Yıldız, A. and Parlak, O., (2016). Late Cretaceous–Miocene sedimentary development of the Arabian continental margin in SE Türkiye (Adıyaman region): Implications for regional palaeogeography and the closure history of southern Neotethys. *Journal of Asian Earth Sciences*, *115*, pp.571-616.

Safak, E. (1997). Models and Methods to Characterize Site Amplification from a Pair of Records. *Earthquake Spectra*, 13(1), 97–129. https://doi.org/10.1193/1.1585934

Saroglu, F., (1992). The east Anatolian fault zone of Türkiye. Ann. Tectonicae, pp.99-125.

Sbeinati, M. R., Darawcheh, R., & Mouty, M. (2005). The historical earthquakes of Syria: an analysis of large and moderate earthquakes from 1365 BC to 1900 AD. *Annals of Geophysics*.

Schildgen, T.F., Yıldırım, C., Cosentino, D. & Strecker, M.R., (2014). Linking slab break-off, Hellenic trench retreat, and uplift of the Central and Eastern Anatolian plateaus. *Earth-Science Reviews*, *128*, pp.147-168.

Şengör, A.C. and Yilmaz, Y., (1981). Tethyan evolution of Türkiye: a plate tectonic approach. *Tectonophysics*, *75*(3-4), pp.181-241.

Şengör, A.M.C., Görür, N. & Şaroğlu, F., (1985). Strike-slip faulting and related basin formation in zones of tectonic escape: Türkiye as a case study. *Society of Economic Palaeontology and Mineralogy Special Publication*, **37**, 227-264.

Şengör, A.C., Özeren, M.S., Keskin, M., Sakınç, M., Özbakır, A.D. and Kayan, I., (2008). Eastern Turkish high plateau as a small Turkic-type orogen: Implications for post-collisional crust-forming processes in Turkic-type orogens. *Earth-Science Reviews*, *90*(1-2), pp.1-48.

Seyrek A., Demir T., Pringle M. S., Yurtmen S., Westaway R. W. C., Beck A., Rowbotham G., Cunningham W. D., Mann P. (2007). Kinematics of the Amanos Fault, southern Türkiye, from Ar/Ar dating of offset Pleistocene basalt flows: transpression between the African and Arabian plates In: *Tectonics of Strike-Slip Restraining and releasing Bends 290* 255-284 Geological Society London Special Publications

*TADAS-AFAD (*2023). Republic of Türkiye Prime Ministry Disaster & Emergency Management Authority (AFAD). tadas.afad.gov.tr.

Taftsoglou, M., Valkaniotis, S., Karantanellis, E., Goula, E., Papathanassiou, G. (2023). Preliminary Mapping of Liquefaction Phenomena Triggered by the February 6, 2023, M7.7 Earthquake, Türkiye/Syria, Based on Remote Sensing Data. Available online: https://zenodo.org/record/7668401.

Taymaz, T., Jackson, J., & McKenzie, D. (1991). Active tectonics of the north and central Aegean Sea. Geophysical Journal International, 106(2), 433-490.

TBEC (2007). Specification for structures to be built in disaster areas. Ministry of Public Works and Settlement, Government of Republic of Türkiye, Ankara, TR: Official Gazette No.26454.

TBEC (2018). Specification for structures to be built in seismic areas. Ministry of Public Works and Settlement, Government of Republic of Türkiye, Ankara, TR: Official Gazette No. 30364

USGS (2023). Earthquake Hazards Program | U.S. Geological Survey. https://earthquake.usgs.gov

Wells, D.L. & Coppersmith K.J. (1994). New Empirical Relationships among Magnitude, Rupture Length, Rupture width, Rupture Area, and Surface Displacement. *Bulletin of the Seismological Society of America, 84(4), 974-1002.* https://doi.org/10.1785/BSSA0840040974.

USGS. (2023a). M 7.8 - Pazarcık earthquake, Kahramanmaraş earthquake sequence, https://earthquake.usgs.gov/earthquakes/eventpage/us6000jllz/finite-fault.

USGS. (2023b). M 7.5 - Elbistan earthquake, Kahramanmaraş earthquake sequence, https://earthquake.usgs.gov/earthquakes/eventpage/us6000jlqa/finite-fault.

Weiss, J. R., Walters, R. J., Morishita, Y., Wright, T. J., Lazecky, M., Wang, H., ... & Yu, C. (2020). High-resolution surface velocities and strain for Anatolia from Sentinel-1 InSAR and GNSS data. Geophysical Research Letters, 47(17), e2020GL087376.

Westaway, R. & Arger, J.A.N., (2001). Kinematics of the Malatya–Ovacik fault zone. *Geodinamica Acta*, *14*(1-3), pp.103-131.

World Bank Gpurl D-RAS Team. (2023). *Global Rapid Post-Disaster Damage Estimation (GRADE) Report M_w 7.8 Türkiye-Syria Earthquake –Assessment of the Impact on Syria: (Results as of February 20, 2023)*. -World Bank and Global Facility for Disaster Reduction and Recovery (GFDRR). *https://openknowledge.worldbank.org/server/api/core/bitstreams/abd7967f-fa5c-4e01-baf6-63372a3c1a1b/content*.

Yönlü, Ö., Altunel, E. & Karabacak, V., (2017). Geological and geomorphological evidence for the southwestern extension of the East Anatolian Fault Zone, Türkiye. *Earth and Planetary Science Letters*, *469*, pp.1-14.

Yürür, T. & Chorowicz, J., (1998). Recent volcanism, tectonics and plate kinematics near the junction of the African, Arabian and Anatolian plates in the Eastern Mediterranean. *Journal of Volcanology and Geothermal research*, **85**, 1-15.

3. GEOTECHNICAL ASPECTS OF THE 2023 KAHRAMANMARAŞ EARTHQUAKE

This section describes the geotechnical observations made as part of the EEFIT Kahramanmaraş 2023 mission. It includes observations made by both the virtual and field reconnaissance teams. The 6th of February 2023 sequence of events (major events based on USGS: M 7.8 - Pazarcık earthquake, M 7.5 - Elbistan earthquake) affected a large area. As part of the EEFIT mission, the geotechnical team covered a large area, including Antakya and the Orontes River, İskenderun, Islahiye, Çöçelli, and Gölbaşı. Areas of particular interest in Hatay and around Islahiye were identified by the virtual reconnaissance team ahead of the field mission. Within the areas visited, a multitude of observations of geotechnical interest were made. These are categorised here in five broad sections: landslides and rockfall, surface rupture and interaction with buildings, liquefaction and subsidence, bridge foundations and approach structures, and retaining structures. Within each category, major findings are presented, and a brief discussion is provided. Soil amplification and basin effects were particularly important in this earthquake sequence and some relevant discussion can be found in the seismotectonics section, using the recorded motions. However, information about stratification and further analysis is required to discuss amplification effects from a geotechnical perspective, which is beyond the scope of this report that aims to present the findings of the reconnaissance mission.

3.1. Lanslides and Rockfall

Landslides and rockfalls were identified in the area around Islahiye ahead of the field mission, using satellite data. The area highlighted A in *Figure 31* was visited by the field team. Station 2718 in close proximity recorded an EW PGA of 0.67g and a NS PGA of 0.69g. In Area A, a large landslide had taken place. The horizontal distance from the crown of the landslide to the end of the runout on the opposing slope of the valley was about 510m. The width of the landslide varied from about 180m at the crown to about 280m at the foot (*Figure 32*).

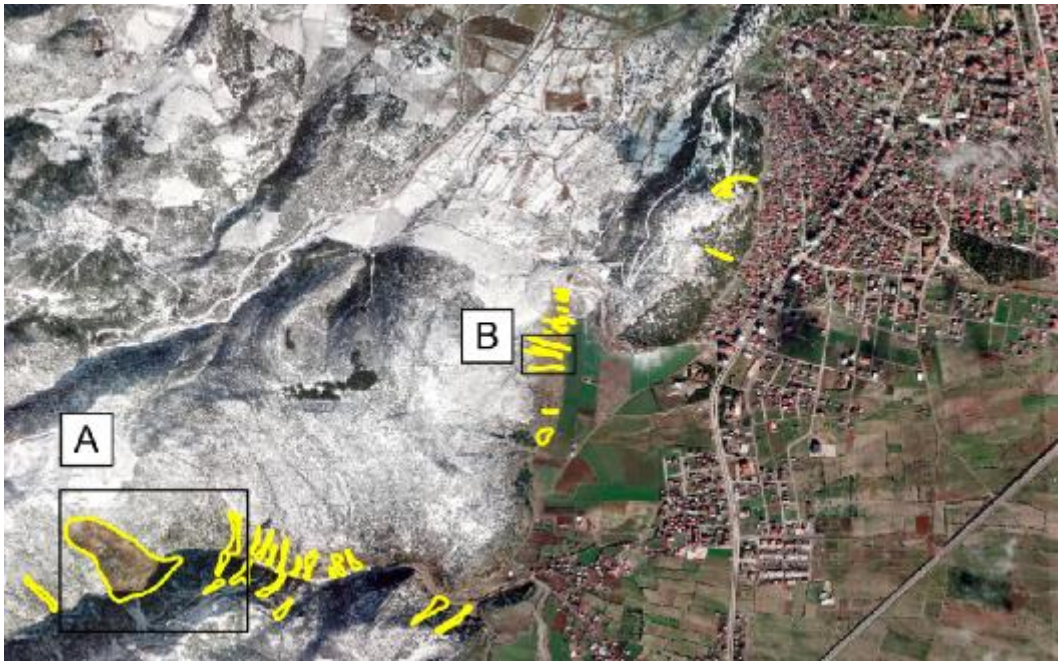

Figure 31: Landslides and rockfalls identified virtually in the area around Islahiye.

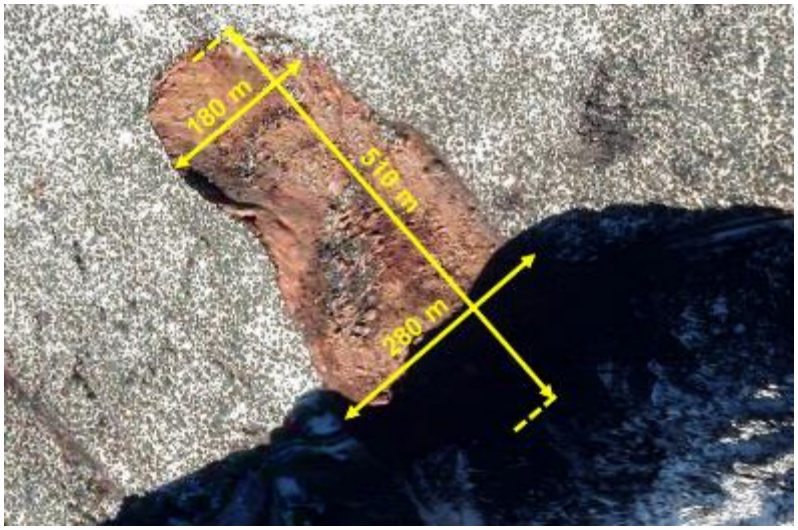

Figure 32: Dimensions for the landslide of area A, 37.001253, 36.591395 (image CNES/Airbus).

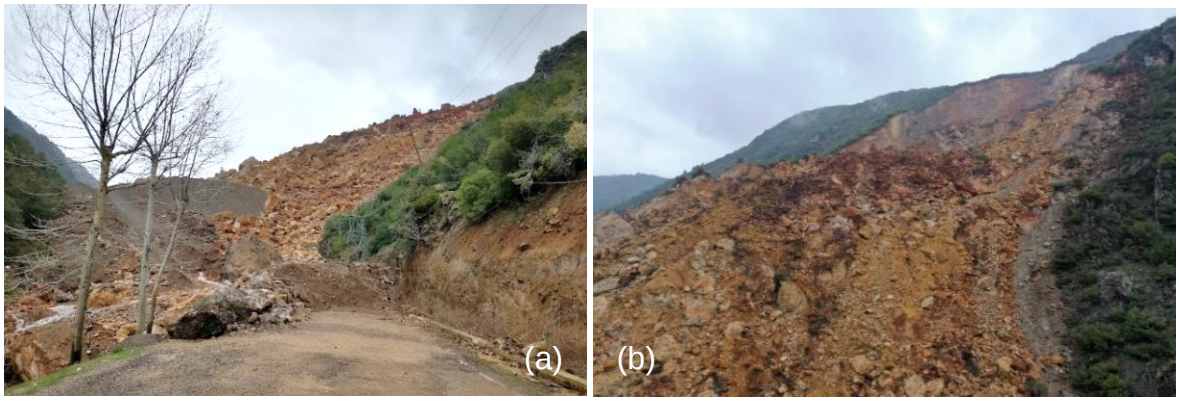

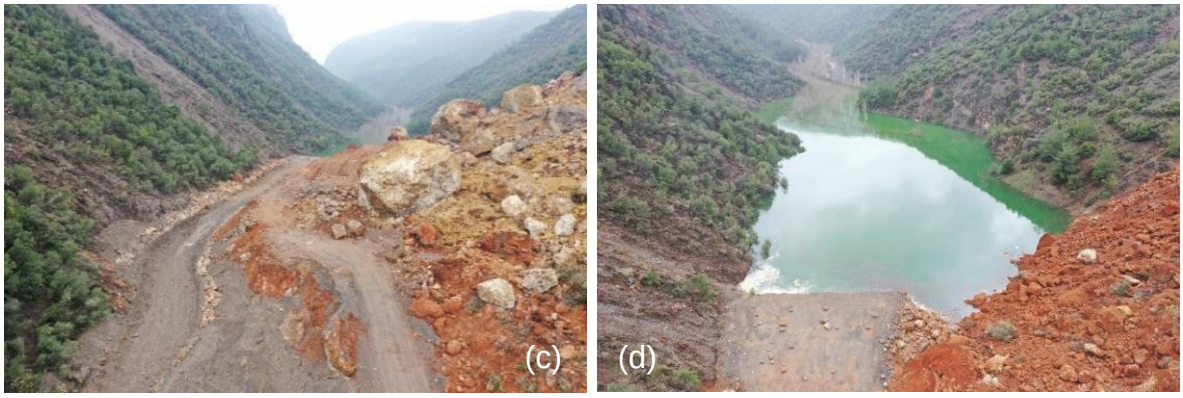

Figure 33: The large landslide of area A, upstream of at Değirmencik (37.001253, 36.591395). (a) Landslide view from the road. Note the water coming through on the bottom left of the photograph. (b) The crown of the landslide (c) Heavy vehicles appear to have accessed the area and (d) The reservoir formed behind the landslide

The landslide in Area A had blocked the local road from Değirmencik (*Figure 33*a) as well as a stream that passed through the valley. The material from the slide appeared well-graded and included multiple boulders, visible towards the foot of the landslide (*Figure 33*b&c). A secondary grey granular material was visible at the foot of the landslide and adjacent to the opposing slope of the valley (*Figure 33*a). Vegetation in the opposing slope of the landslide was disturbed along a band opposite the landslide (*Figure 33*c) and so it is possible that part of the material visible originated from that slope. Traces from heavy machinery were visible on the foot of the landslide (*Figure 33*c); as a result, we could not exclude the possibility of the grey material being brought in. A large reservoir had formed behind the landslide (*Figure 33*d), which acted as a natural dam for the stream that ran across the valley. The size of the reservoir was impressive given the amount of time elapsed between the earthquake and the inspection, of just over a month. Water emerging through the natural dam was visible (*Figure 33*a, bottom left), indicating internal erosion and piping. Given the location of the landslide upstream of the village of Değirmencik, the volume of water in the formed reservoir, the observation of ongoing piping, and the weather prediction for significant rainfall in the coming days, the local authorities were alerted to the possibility of failure of the natural dam, which could have significant consequences for the downstream population. At the time of contact, they appeared unaware of the existence of the landslide and reservoir.

The neighbouring area shown highlighted in *Figure 34*, between Fevzipasa and Türkbahçe was also visited by the field team. Multiple features of interest were observed.

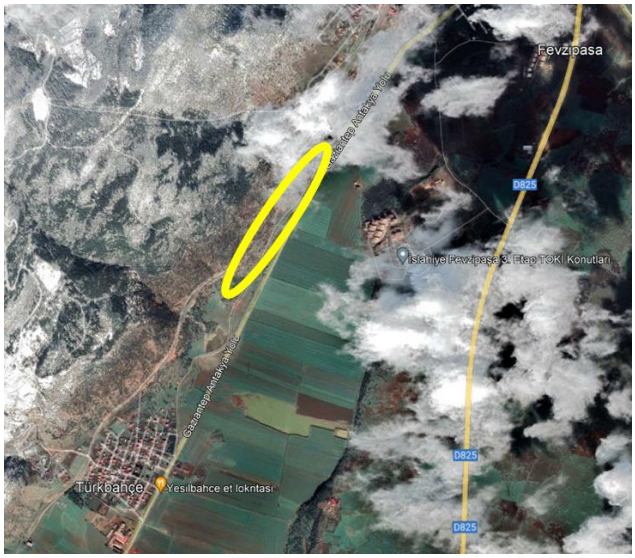

Figure 34: Area of landslides and rockfalls inspected, between Fevzipasa and Türkbahçe (image CNES/Airbus).

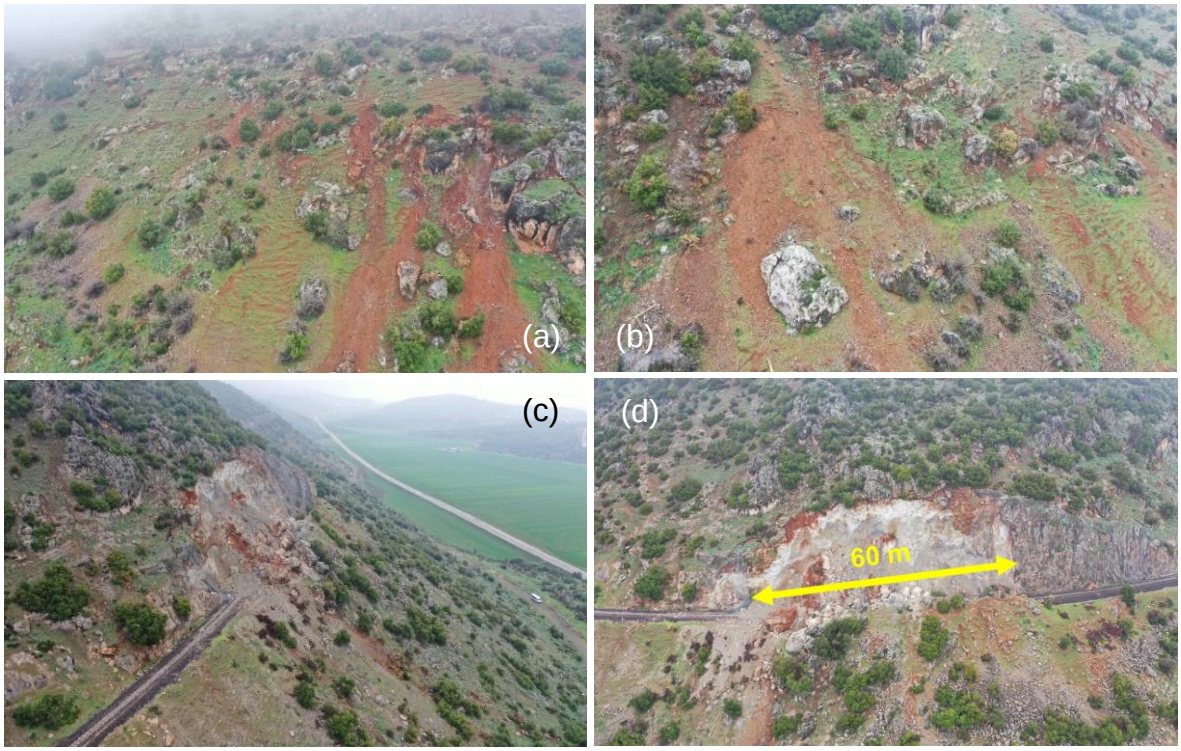

Figure 35: Landslides in the Fevzipasa – Türkbahçe area (a) Shallow, extensive landslide, (b) Continuation of the shallow landslide, (c) Landslide blocking the rail line (37.084009, 36.627685) and (d) Length of the rail line covered by slide (37.084009, 36.627685)

An extensive but shallow slide mechanism was activated within the soil throughout most of the area (*Figure 35*a&b). The mobilised material was a mixture that included gravel and fine-grained soil. Hand-held shear vane tests at the surface gave an average peak shear strength of 107 kPa and an average residual strength of 8 kPa. Closer to Türkbahçe, a landslide had initiated on a rock cut made along the rail line and had blocked approximately 60m along the line (Figure 35c&d).

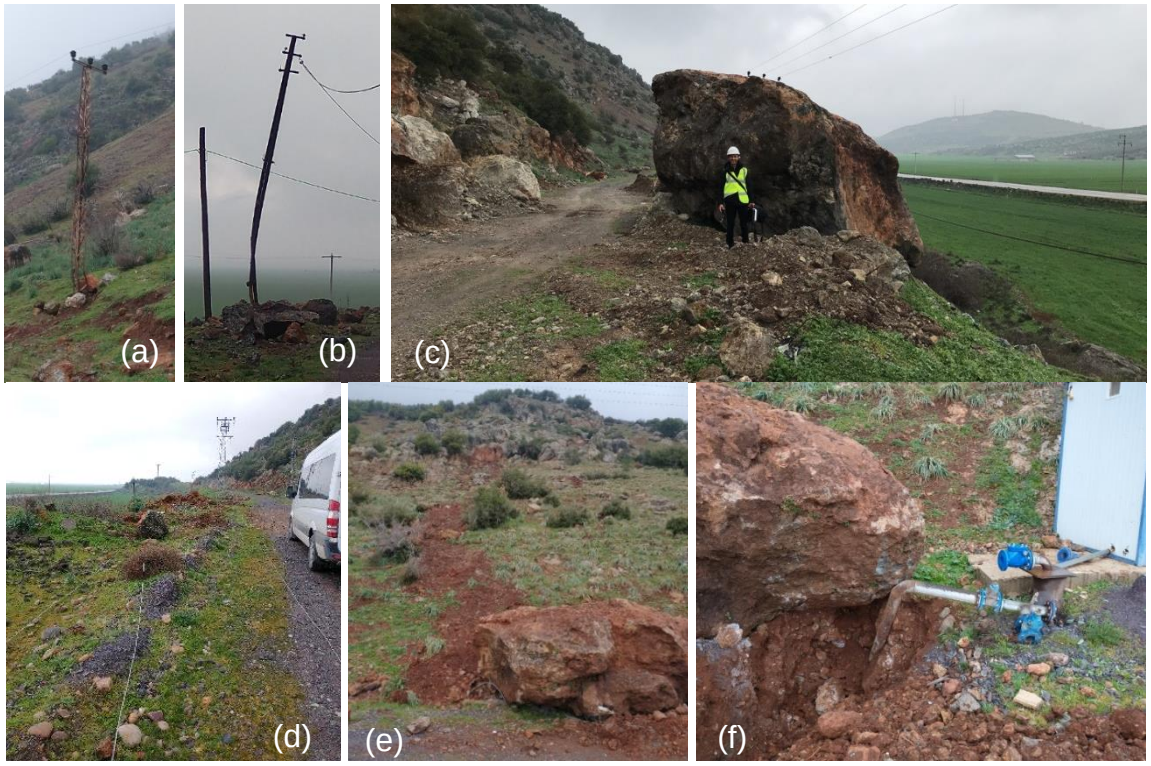

Figure 36: Rockfalls in the Fevzipasa – Türkbahçe area. (a, b) Electricity and phone line poles hit by rocks, (c) Rockfall of a boulder with dimensions 6x5.5x4 m, (d) Electricity wires on the road, (e, f) Rockfall hitting a water line. Dimensions of rock 2.2x6x4 m

In the same area, multiple rockfalls were observed. Some characteristic cases are presented in *Figure 36*, selected to demonstrate the vulnerability of lifelines to rockfalls. Electricity and communication lines were disrupted with several poles being hit (*Figure 36*a&b). A large boulder with dimensions 6x5.5x4m had partially blocked the road (*Figure 36*c). Electrical wires were lying on the ground in multiple locations (*Figure 36*d). Locals informed us of disruption to electricity supply for about two weeks after the earthquakes. Another boulder with dimensions 2.2x6x4m hit a water line after travelling a distance of about 60m down the slope (*Figure 36*e&f), which would have caused a water leak after the earthquake.

3.2. Surface Rupture and Interaction with Structures

The fault surface rupture was mapped by the virtual reconnaissance team over a length of about 300km. Surface rupture was investigated by the field team at two locations around Islahiye and also in the area of Gölbaşi, Adıyaman.

3.2.1. Islahiye

Two locations close to Islahiye were visited by the field team to inspect the surficial features, as indicated in *Figure 37*a. The surface rupture observed in area A was part of the main rupture mapped across almost 300km from satellite data. In the location visited, a vertical offset was at times pronounced.

Figure 37: Observations of surface rupture in locations around Islahiye. (a) Areas where the surface rupture was inspected by the field team, (b) Surface rupture manifesting along a slope in area A. Notice the toppled electricity tranmission tower and the lateral displacement along the canal. (c) Fault surface rupture in area A. (d) Rupture in the plains of area B. (e-g) Surface rupture on a hill in area B. Multiple fissures were visible, which were deeper and wider than the rupture observed in the fields.

Distortion of linear features, such as the canal of *Figure 37*b indicated localised lateral displacement between the two sides of the surface rupture, indicative of a strike slip fault. The rupture in area A (*Figure 37*c) was running along a row of electricity transmission towers. A toppled tower whose foundation interacted with the surface rupture is shown in *Figure 37*b.

In area B, the surface rupture feature was observed through fields, though it was only visible as a crack without being accompanied by an easily discernible vertical or horizontal offset (*Figure 37*d). Though the feature appeared continuous on the satellite data, upon closer inspection it was made up of a continuation of parallel linear segments with an offset from one to the next (*Figure 37*d). This stepping pattern in surface cracks is characteristic of strike-slip faults. Based on indications of local residents, the filed team visited a hill adjacent to the previously observed surface

feature, where more rupture features were observed (*Figure 37*e-g). These were not individually equally long to the rupture features in the fields below. Instead, they were wider and deeper, with widths of up to 0.5m and depths of up to 1.4m measured. Moreover, these features were diffuse, with multiple fissures observed in the same area, rather than a single continuation of ruptures, as observed in the fields. The appearance of these scattered cracks on the hill indicates that the stiffer material of the hill could have caused a wider shear deformation zone to form, leading to multiple fissures appearing on the surface.

3.2.2. Gölbaşı

Further surface rupture observations were made in the area of Gölbaşı, within the Adıyaman prefecture. Gölbaşı is a town that suffered multiple failures of geotechnical interest. A significant part of it was affected by earthquake-induced liquefaction, as will be discussed in the following chapter. *Figure 38*, created by ForM@Ter, depicts east-west displacement in the area affected by the earthquakes, based on satellite data. Gölbaşı is indicated on this figure and lies within a zone between eastwards and westwards displacement. At the town of Gölbaşı, the exact boundary between eastwards and westwards displacement is not as clear as at other locations. Indeed, two fault segments are identified in *Figure 38*, with the town located between them.

This observation matches the depiction of fault segments by Yönlü et al. (2013), shown in *Figure 39*. There, two fault segments are identified, Gölbaşı – Türkoğlu and Çelikhan – Erkenek, in close proximity to the town of Gölbaşı. In *Figure 38* from ForM@Ter, overstepping between the fault segments is depicted. In *Figure 40*, possible linkage patterns between two strike-slip fault segments are demonstrated by Brogi (2011). Though more research is required into the specific patterns developed in Gölbaşı, it is reasonable to expect that a zone of intense shearing developed between the two main fault segments, with multiple parallel cracks forming at the soil surface.

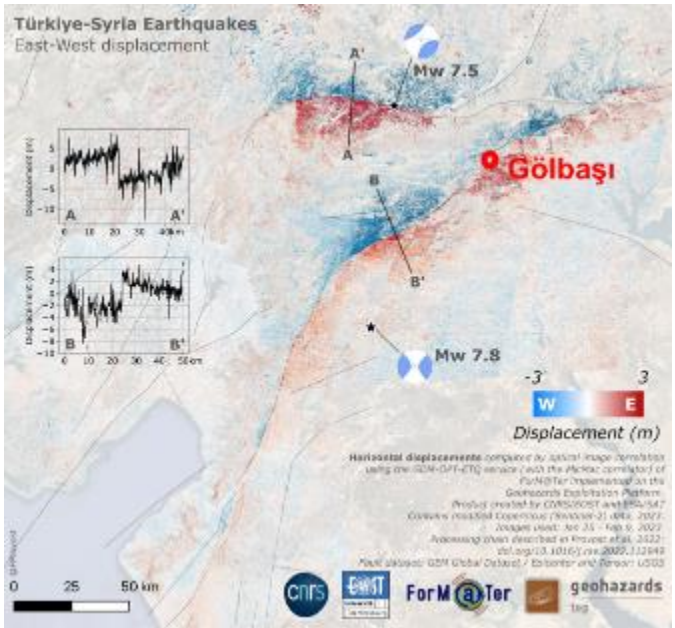

Figure 38: East-west horizontal displacement in the affected area. Image reproduced from ForM@Ter (methodology described by Provost et al. (2022)). The location of Gölbaşi is highlighted.

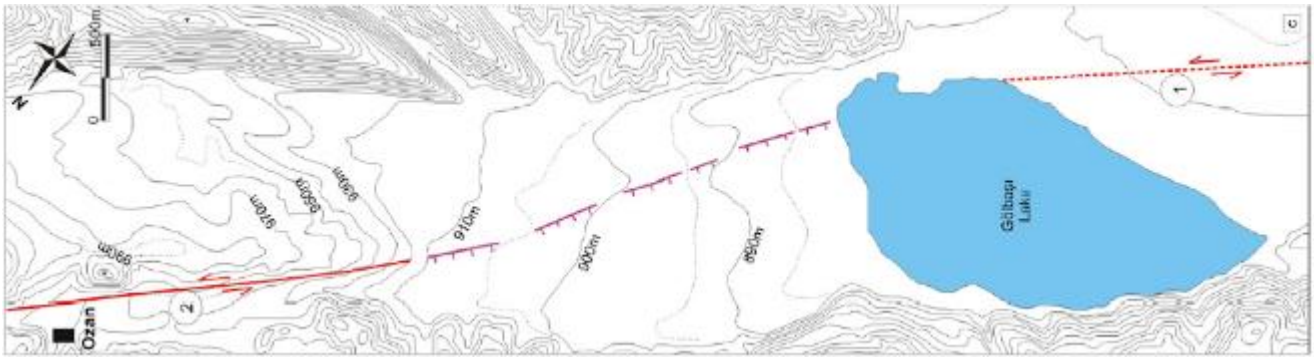

Figure 39: Topographic map of the Gölbaşı basin, including two fault segments 1: Gölbaşı – Türkoğlu, 2: Çelikhan – Erkenek. The purple dashed lines represent the morphological scarp between the Gölbaşı Lake and Ozan Village. Reproduced from Yönlü et al. (2013).

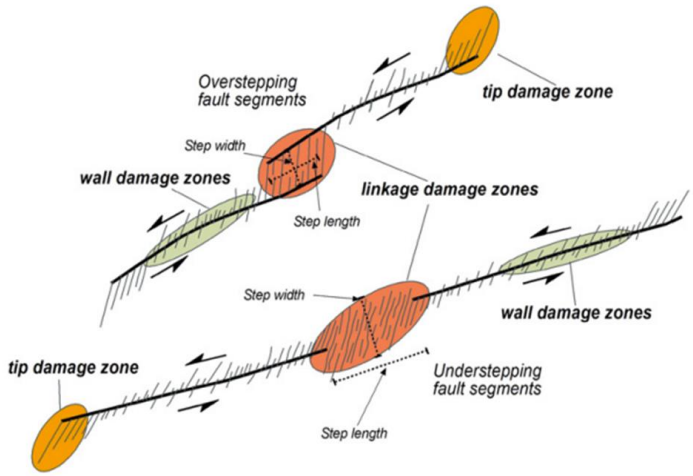

Figure 40: Linkage patterns between two strike-slip fault segments. Reproduced from Brogi (2011).

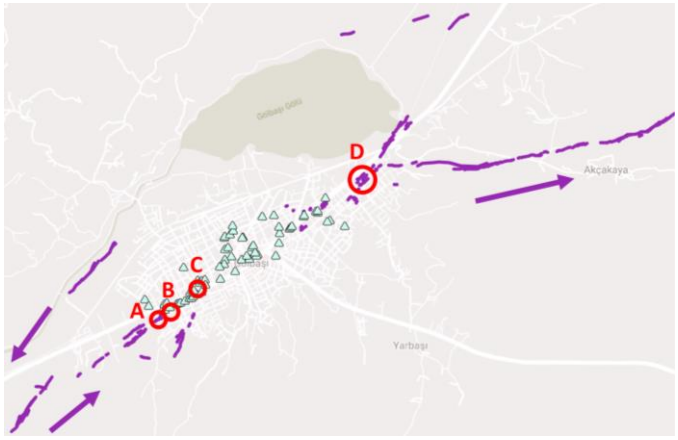

Figure 41: Surface cracks identified from virtual and field reconnaissance. The triangular markers indicate collapsed buildings.

In *Figure 41*, the surface cracks identified in Gölbaşı by both the virtual and field reconnaissance teams are depicted. These confirm that the main fault segment to the southwest of Gölbaşı and the next fault segment to the northeast of Gölbaşı did not connect. Instead, multiple cracks were visible, as shown in *Figure 41*. In addition, a

secondary surface rupture feature towards the east was observed, which coincides with large eastwards displacements identified from the satellite data of *Figure 38*.

The southwest of Gölbaşı main fault segment continued in an interrupted fashion towards the town. Lateral displacements consistent with a strike slip fault were observed in locations A, B, and C of *Figure 41*, depicted in greater detail in *Figure 42*, which shows satellite images before and after the earthquake sequence. In *Figure 42*, the lateral displacement along linear features due to the surface rupture is visible (e.g. roads or backyard walls). Lateral displacements observed in these locations were of magnitude of about 2m. The triangular markers of *Figure 41* depict collapsed buildings. On the western part of Gölbaşı, a line of collapsed buildings is observed in continuation to the surface rupture, which indicates that further research is required regarding the potential for interaction of the surface rupture with these buildings.

On the eastern side of town, multiple parallel cracks were observed, at a steep angle to the secondary surface rupture that was formed towards the east, which might be associated with a tip damage zone, as shown in *Figure 40*. Buildings in this area, labelled as location D in *Figure 41*, were inspected in detail by the field team.

Two parallel cracks in location D of *Figure 41* are analysed in more detail using the pictures of *Figure 43*. Based on privately provided boreholes, the first 20m from the surface at that location are made up of a mixture of gravelly sandy clay. Based on handheld shear vane measurements, the peak shear strength of the material at the surface was 59kPa and the residual strength was 10kPa. The photos in *Figure 43*a-d correspond to the northern crack while those in *Figure 43*e-h correspond to the southern one. The northern crack began as shown in *Figure 43*a, passing through a shallow canal and causing damage to the pavement of the adjacent road. It then passed between the two neighbouring structures shown in *Figure 43*b, which were touching before the earthquakes. Post-earthquake, a gap of 0.67m opened between the two structures. The crack then continued in photo *Figure 43*c, again passing next to the foundations of buildings. *Figure 43*d shows how the crack was diverted, wrapping around the corner of a foundation before continuing. All buildings along this crack appeared to have stiff raft foundations. The southern crack begins at *Figure 43*e, where it was visible on the soil surface. It then continued towards a two-storey structure, in *Figure 43*f. Instead of being diverted around the foundation, as happened for all buildings along the northern crack, it went through the building. The resulting displacement and partial collapse on the western side, is shown in *Figure 43*f, while the gap opened due to the crack on the eastern side is shown in *Figure 43*g. The crack continued into the adjacent park, which was used as a container camp (*Figure 43*h).

Figure 42: Satellite images before and after the earthquake sequence at locations A, B, C along the surface rupture (locations shown in map of Figure 41. (a) Location A before the earthquake (10/2022 Maxar Technologies) (b) Location A after the earthquake. Lateral displacement along a road and a rotated structure are visible, along with a surface rupture (3/2023 Airbus) (c) Location B before the earthquake (10/2022 Maxar Technologies) (d) Location B after the earthquake. Lateral displacement along the backyards and a road is visible. Structures collapsed along the surface rupture (3/2023 Airbus) (e) Location C before the earthquake (10/2022 Maxar Technologies) (f) Location C after the earthquake. Lateral displacement along a road is visible. Structures collapsed along the surface rupture (3/2023 Airbus)

Figure 43: Interaction of surface cracks with buildings in location D of the map of Figure 41 – buildings are shown in the satellite image at the top. Notice the multiple parallel cracks visible on the soil surface. The letters correspond to the locations of the field reconnaissance photos included here.

The difference in response of structures with respect to the interaction with the surface crack, can be attributed primarily to the quality of their foundation. The structure along the southern crack (photos *Figure 43*e-h) was a multi-occupancy building of poorer quality than the single-family houses along the northern crack. We anticipate that the stiffness and strength of the foundation of the southern building was lower than for the buildings along the northern crack. It is anticipated that the kinematic constraint imposed by the stiff foundations along the northern crack forced the surface feature to divert around the buildings. On the contrary, in the absence of a stiff and sufficiently strong foundation for the southern building, the crack was able to pass through it, causing damage along the way. We expect that the kinematic

constraint imposed by the different foundation typologies was the controlling factor, rather than the bearing pressure imposed by the structures, since bearing pressure was comparable for the examined cases, with all buildings in area D having between one and three storeys. This hypothesis is supported by the findings of Agalianos et al. (2023), who used centrifuge testing and Finite Element Modelling to study the interaction of shallow foundations with a strike-slip fault rupture. As shown in *Figure 44*, the diversion of a surface crack around a shallow foundation is primarily controlled by the kinematic constraint that the foundation imposes. The bearing pressure alone appears to be less significant in diverting a crack, as seen in *Figure 44*a, and in agreement with our observations in Gölbaşı.

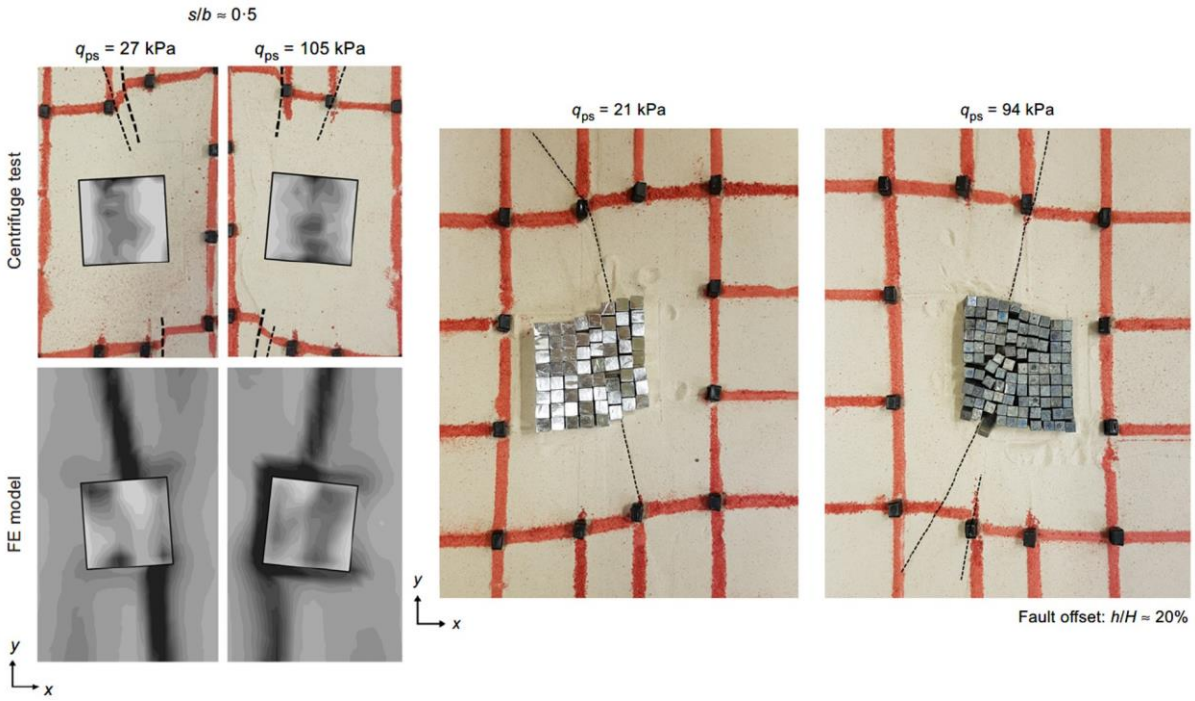

Figure 44: Centrifuge testing and FEM analysis for the response of shallow foundations on strike-slip faults. The diversion of a surface crack is primarily controlled by the kinematic constraint imposed by the foundation. Reproduced from Agalianos et al. (2023). (a) Centrifuge testing and FEM results for shallow foundations along a strike-slip fault rupture (b) Centrifuge testing for a shallow foundation along a strike-slip fault rupture, using elements that apply the required bearing pressure but do not offer a kinematic constraint.

The final case of surface rupture and structure interaction presented in this report is that of a house in the village of Ozan, to the north-east of Gölbaşı. The house was on the surface rupture identified through satellite data (*Figure 45*a), which is at the edge of the Çelikhan – Erkenek main fault segment depicted in *Figure 39*. As such, it was a clearer case of fault-imposed displacement, as one might expect along a strike-slip fault rupture. The house had a stiff raft foundation, typical of structures in the area. It had practically displaced as a rigid block, with the surface rupture wrapping around it, being diverted by the kinematic constraint imposed by the foundation. *Figure 45* depicts the measured offset of the structure from its patio: 80 cm along the vertical direction and 160cm along the horizontal direction, parallel to the surface rupture.

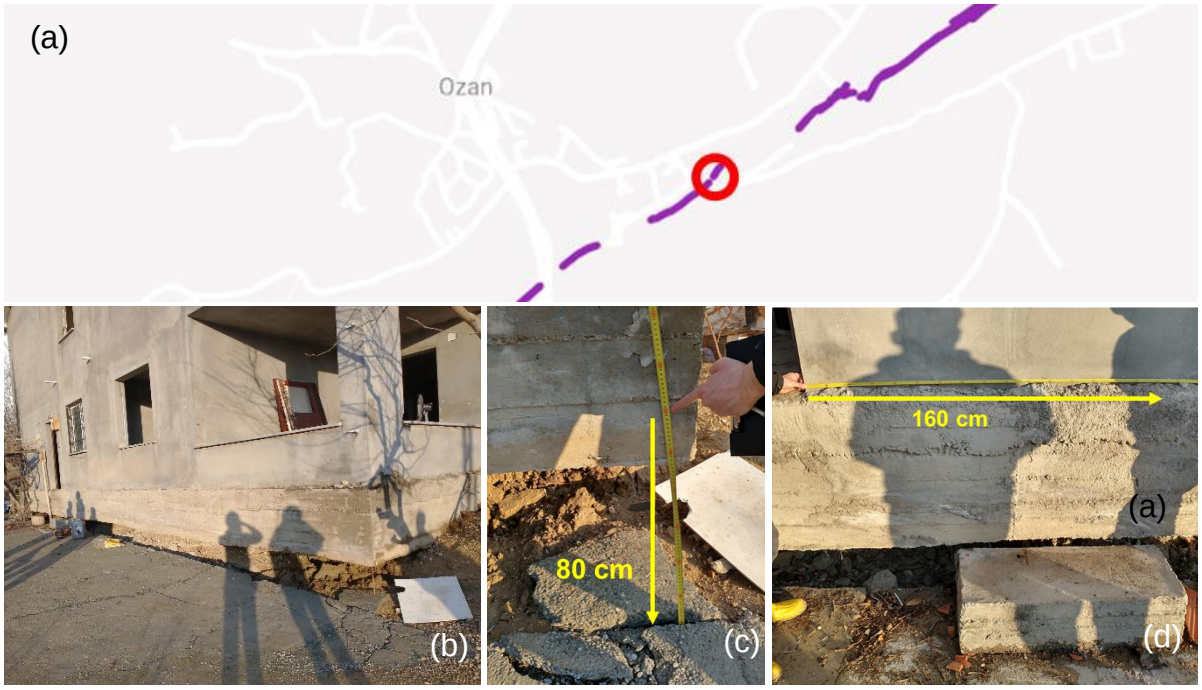

Figure 45: Surface rupture and structure interaction in Ozan, Adıyaman. (a) Map highlighting the location of the structure examined in Ozan (37.820418, 37.685387). (b) Gap between the structure and its patio (c) Vertical offset of 80 cm and (d) Horizontal offset of 160 cm

3.3. Liquefaction and Subsidence

Liquefaction was identified at three of the main locations visited: the seafront of İskenderun, the Orontes River in Hatay, and the town of Gölbaşı (*Figure 46*).

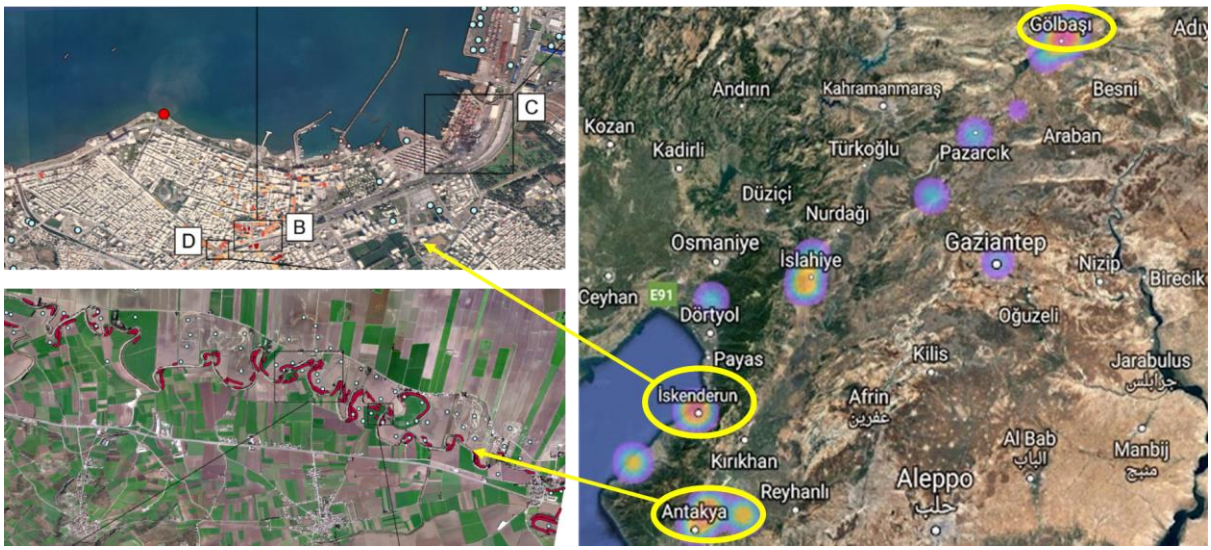

Figure 46: The yellow ellipses show the areas where liquefaction was observed. Satellite images with liquefaction features identified by virtual reconnaissance are included.

For İskenderun and the Orontes River, virtual reconnaissance had identified points of interest, as highlighted in *Figure 46*. Observations from the three locations visited are presented in more detail below, after a brief introduction to the phenomenon of earthquake-induced liquefaction. Though multiple locations of liquefaction were

virtually identified along the Orontes River, the cases presented here are only those in close proximity to the village of Demirköprü.

3.3.1. Earthquake-Induced Liquefaction

Water-saturated granular soils, primarily sands but also silts and gravel, can experience liquefaction during an earthquake. Liquefaction is a phenomenon during which soil loses most of its shear strength and behaves in a way reminiscent of a heavy liquid. Liquefaction most typically manifests in soils that are loosely packed and hence have the tendency to contract and rearrange into a denser packing when subjected to shearing. During an earthquake, for a liquefiable soil under the water table to contract, water must be expulsed from within the porous network between soil particles. Due to the rapidity of earthquake loading, there is not sufficient time for water to fully drain from within the porous space. The consequence is an increase in the pore water pressure, u. At a given element, the total stress, σ, is practically constant, and equal to the weight of soil and water above the element divided by the area of the element. As the pore water pressure u increases, the effective stress, σ'=σ-u, which indicates the stress taken up only by the soil particle skeleton, decreases.

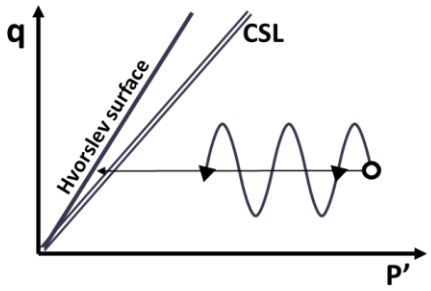

Figure 47: Schematic effective stress evolution during an earthquake, leading to liquefaction. The axes represent p', which is the mean effective stress, and q, which is the deviator stress.

Both the strength and the stiffness of soil are functions of the effective stress, σ', hence both diminish as pore pressure increases. Under strong seismic shaking, the pore water pressure may increase sufficiently to annul the effective stress, leading to a state of full liquefaction. If the stress path of a soil element reaches Hvorslev's fracture surface (*Figure 47*), brittle failure can take place, manifested as piping, boiling, or sand volcanoes. Engineering structures, including foundations, embankments, and retaining walls, depend on the soil's shear strength for their stability and could suffer failure due to earthquake-induced liquefaction. The process of pore water pressure build-up with successive cycles of loading was first studied systematically in the 80s using an undrained condition, i.e. assuming that no water can escape from within the porous network between particles and using cycles of a given shear stress amplitude (Luong and Sidaner, 1981; Ishihara, 1985). Dobry et al. (1982) focused on the amplitude of shear strain instead and showed that using it can achieve meaningful normalisations. Their results reveal that partial liquefaction, where some effective stress is maintained, can still allow large deformations to take place. More recently, the undrained assumption for liquefaction has come into scrutiny, with partial drainage considered more as a more realistic condition (e.g., Adamidis and Madabhushi, 2018a), an observation that could be impactful, especially for the liquefaction of layered deposits (e.g., Cubrinovski et al., 2019).

Much of the liquefaction damage observed has to do with structures. The majority of the structures inspected were founded on shallow raft foundations. For such structures founded on liquefiable soils, large settlement and residual rotation can be expected at the end of an earthquake. The intensity of the earthquake, the density of the liquefiable layer, the thickness of the soil that liquefied as compared to the width of the foundation, the aspect ratio of the structure, the weight of the structure, the existence of static shear stress and the effects of drainage can all affect performance (Dashti et al., 2010, Bullock et al, 2019a). The mechanisms that drive displacements for such structures were experimentally depicted through centrifuge testing by Adamidis & Madabhushi (2018b), with some results reproduced in *Figure 48*. While the soil layer liquefies, a bulb of non-liquefied material is maintained under the structure, due to the increased pressure imposed by it. In deep layers where the liquefied soil is deeper than the width of the foundation, this bulb does not reach the base of the liquefied layer. Settlement is accumulated as the foundation along with the non-liquefied bulb gradually displace the surrounding liquefied material. The accelerations that reach the foundation in this case are significantly diminished. However, if the depth of the liquefied soil is less than a foundation width, a more localised mechanism takes hold. In this case, the bulb of non-liquefied soil reaches the base of the liquefied layer and transmits higher accelerations to the structure. Depending on its aspect ratio, the structure is likely to respond by rocking. Maximum displacements are now observed under the edges of the rocking foundation, where the neighbouring liquefied soil can easily be displaced.

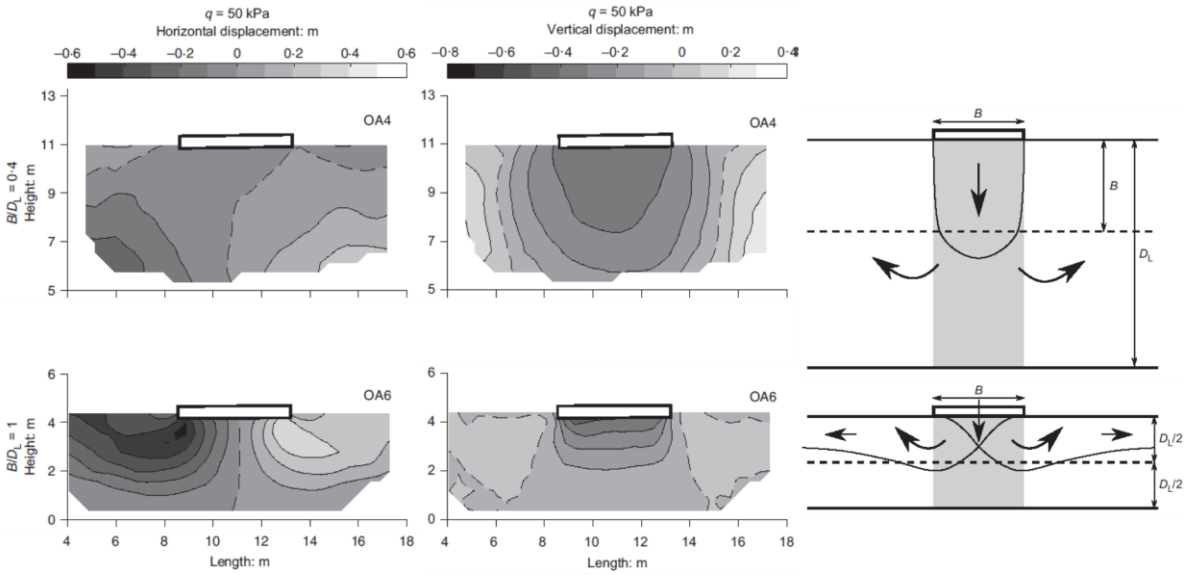

Figure 48: Experimentally observed displacement contours under a structure with a shallow foundation and applied bearing pressure of 50kPa for different depths of liquefied soil. Sketches of simplified deformation mechanisms for different ratios of foundation width are included.

Simplified methods exist in literature for the estimation of settlement (e.g., Bertalot et al., 2013; Bullock et al, 2019a) or residual rotation (e.g. Bullock et al., 2019b, Adamidis & Madabhushi, 2022). These will not be described here as they are beyond the scope of this report. It should however be noted that these methods are derived for structures in isolation, not considering the existence of close neighbours. This assumption has to be considered with care when examining structures in an urban setting, where simplified methods can lead to unconservative results, especially regarding rotation (Qi & Knappett, 2021; Kassas et al., 2022).

3.3.2. İskenderun

İskenderun was particularly affected by the earthquake sequence, with many failures being of geotechnical interest. Station 3115 (36.54634, 36.16458) to the south of İskenderun recorded an EW-PGA of 0.23g and a NS-PGA of 0.29g. Station 3116 (36.61618, 36.20661) to the northeast of İskenderun recorded an EW-PGA of 0.17g and a NS-PGA of 0.16g.

The soil surface around the seafront of İskenderun, along Atatürk Boulevard, from İskenderun lunapark all the way to İskenderun Nihal Atakaş Camii, displayed several signs of liquefaction, including ejected sandy material, lateral spreading cracks, and subsidence (*Figure 49*). The boulder seawall moved towards the sea, settlement was observed behind it, with parts of the ground behind the wall being at sea level, and at some locations ejected sandy material was visible in close proximity (*Figure 49*a). The park along Atatürk Boulevard was reclaimed with its surficial material appearing to be fine-grained. Multiple cases of localised sand ejecta were visible in the park, indicating that the surface layer could have acted as a non-liquefiable crust that facilitated their creation (*Figure 49*b, c). Cracks related to lateral spreading were visible all along the inspected waterfront (*Figure 49*d, e). Cumulative displacements of more than 40cm towards the sea were measured at multiple locations. The crack on Atatürk Boulevard shown in *Figure 49*f, was caused by liquefaction and lateral spreading but is also related to the existence of a water line below it (notice the manhole in the photo). Extensive subsidence was observed along Atatürk Boulevard in the districts of Yenişehir and Çay (e.g., *Figure 49*g), large parts of which were under water at the time of inspection. The surface of the İskenderun Anıt Meydanı square was also under water, indicating significant subsidence (*Figure 49*). Finally, manholes were observed to “float” relative to their surrounding pavement, which had subsided. (*Figure 49*i).

A single-storey water management building close to the seafront in Çay district was inspected, which had suffered significant liquefaction-related settlement (*Figure 50*). The structure was square in plan, with each side 9.8m in length. Its walls were made of concrete and had a thickness of 25cm. It housed a wide well that took most of the inner area and according to the officers on duty was deep. The surface of the well was assumed to not have settled significantly. Taking measurements relative to the well, the surrounding structure had settled by 47cm on its south side and by 41cm on its north side. It was tilted towards the west by 1.5^{o} and no tilting was measured in the NS direction. Local damage was observed in the wall at a point where metal pipes were entering the building and connecting to the well, as the pipes had caused a hole elongation failure in the wall.

Figure 49: Characteristic surface features of liquefaction in İskenderun. (a) Sea wall movement (b-c) Ejected material (d-e) Lateral spreading crack, Yenişehir district C Boulevard, Pirireis district. (g) Subsidence along Atatürk Boulevard, Yenişehir district. (h) İskenderun Anıt Meydanı square subsidence. (i) Manhole in Atatürk Boulevard, Yenişehir district.

Figure 50: Liquefaction at a water management building close to the seafront (36.590891, 36.175676).

Liquefaction-related settlement of structures was also observed to the south of Atatürk Boulevard in the Çay district. An example is shown in *Figure 51*, focusing on a 6-storey reinforced concrete building with a basement. The neighbouring structures of the block are also depicted in *Figure 50*: a single-storey structure to the west, and another 6-storey reinforced concrete structure to the north. Based on borehole data that cannot be fully shared due to commercial reasons, an anticipated soil profile at that location is included in *Figure 51*. A layer of silty sand relatively close to the surface is expected to be the critical for liquefaction. Given the existence of a basement for the examined structure, it is anticipated that the structure is founded very close to the liquefiable layer. In addition, the water table at the examined location is expected to be close to the surface, due to the proximity to the sea front. The water level within the water drainage system was measured at 103cm from the surface through a manhole in very close proximity to the structure. Given the damage and cracking of this network along the neighbouring Atatürk Boulevard, which was partially underwater, it is reasonable to assume that the water level within the drainage network is representative of the water table. Ejected sand was observed along the periphery of the building. The basement was covered with water, with a pump in constant operation to keep it from fully flooding. Water was coming into the basement from small cracks along the concrete walls, which is consistent with our measurement of the height of the water table. Structural damage within the whole building was limited, with some cracks visible in non-load bearing elements and finishes. Variable settlement was measured along the periphery of the building, with a maximum settlement of 14cm at the location furthest away from the neighbouring buildings. This pattern of settlement and rotation can be qualitatively justified based on findings on Structure-Soil-Structure Interaction (SSSI) for buildings on liquefiable layers (Qi & Knappett, 2021; Kassas et al., 2022). In the case of two adjacent structures with strip foundations founded on a thin liquefiable layer, where the layer depth is less than the width of the foundations, a shallow displacement mechanism takes hold (*Figure 52*). Soil wedges under the edges of foundations are formed, with minimal displacement between the two structures. These findings are qualitatively consistent with the measured settlements. The length of the examined building is greater than its width by a factor of almost three, hence its response can be simplified to that of a strip foundation for the purpose of a simplified understanding of response. The depth of the liquefiable layer (~9m) is lower than the width of the foundation (~13m), hence a shallow mechanism is expected. Indeed, the settlement measured at the boundary of the examined structure with its single storey neighbour was zero and the measured settlement values were maximised when the transverse distance from that same neighbour was maximised. It should be noted that the developed mechanism would be different for a thicker liquefiable layer, with the formation of bigger wedges that cause maximum settlement between the two structures (*Figure 52*).

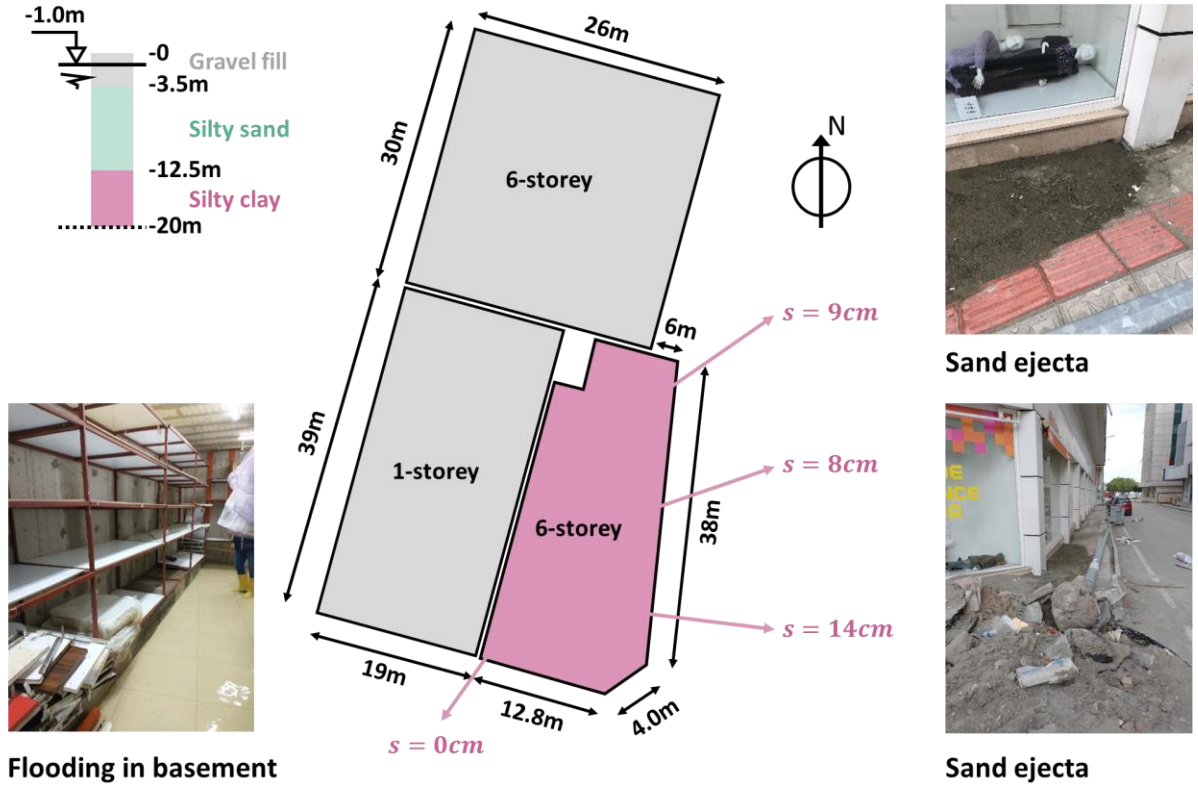

Figure 51: Liquefaction-related settlement for a 6-storey reinforced concrete building with a basement in the Çay district (36.589935, 36.173527).

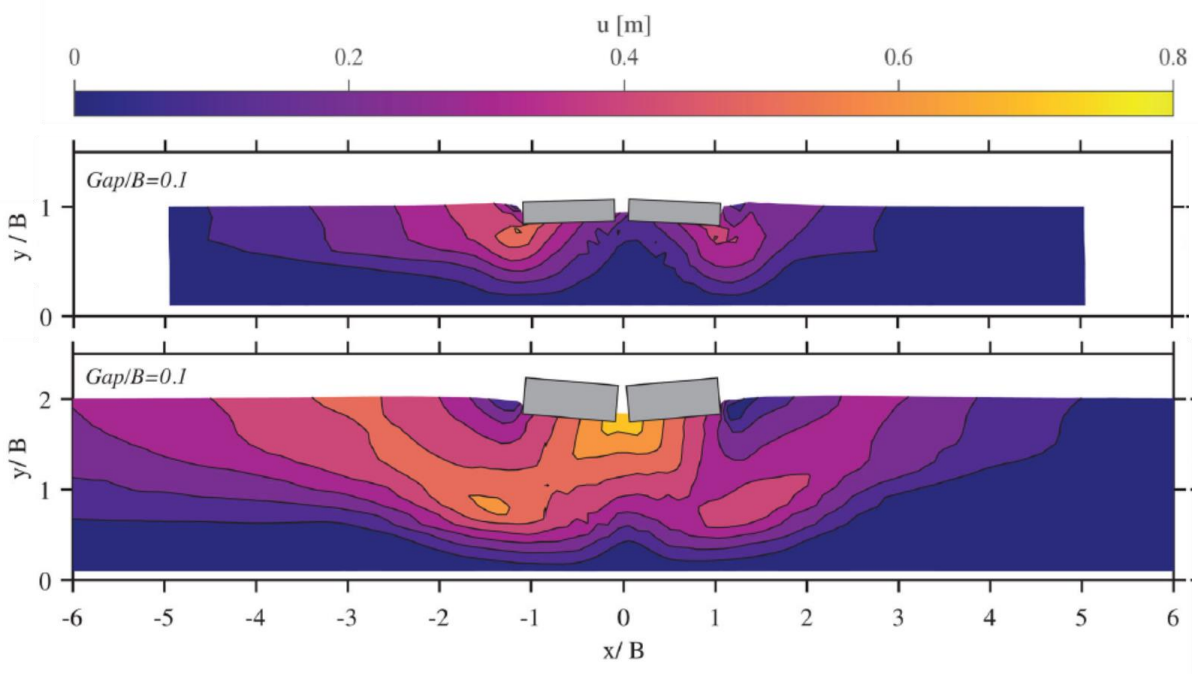

Figure 52: Displacement mechanism under two adjacent neighbouring structures on a liquefiable layer of depth equal to one foundation width (B) or two foundation widths (2B), reproduced from Kassas et al. (2022).

3.3.3. Demirköprü and Orontes River

Multiple locations of liquefaction manifestation were identified through virtual reconnaissance along the Orontes River. The field team visited the location of bridges, reported separately in the next section, and some locations of liquefaction and lateral spreading in close proximity to the village of Demirköprü, reported here.

Figure 53: Liquefaction-related failures in Demirköprü.(a) The masonry bridge of Demirköprü did not suffer major damage (36.248750, 36.354769), (b) Lateral spreading cracks in close proximity to the masonry bridge, (c) Lateral spreading at the school of Demirköprü (36.250107, 36.352776), (d) Lateral spreading towards the river , (e-f) Shallow founded structures in the zone of spreading next to the school of Demirköprü

The historic masonry bridge of Demirköprü (36.248750, 36.354769) suffered relatively little significant damage, though the wall above the road level had collapsed at multiple locations and the bridge was out of use for vehicles (*Figure 53*a). Directly to the east of the bridge, significant signs of lateral spreading towards the river were visible, with large cracks running parallel to the river (*Figure 53*b). The next location visited was the school of Demirköprü (36.250107, 36.352776). Lateral spreading towards the river was again visible, having distorted the cobblestone school yard (*Figure 53*c, d).

According to the locals, a neighbouring building with shallow foundations had moved significantly towards the river. At the time of our visit, the building was already demolished, with little evidence of the related damage remaining. However, the field team managed to obtain some photos of these buildings from the aftermath of the earthquakes from locals (*Figure 53*e, f). These reveal a collapsed reinforced concrete structure (right structure in *Figure 53*e), and the aforementioned shallow founded structure that had moved laterally towards the river and suffered significant tilting along the way.

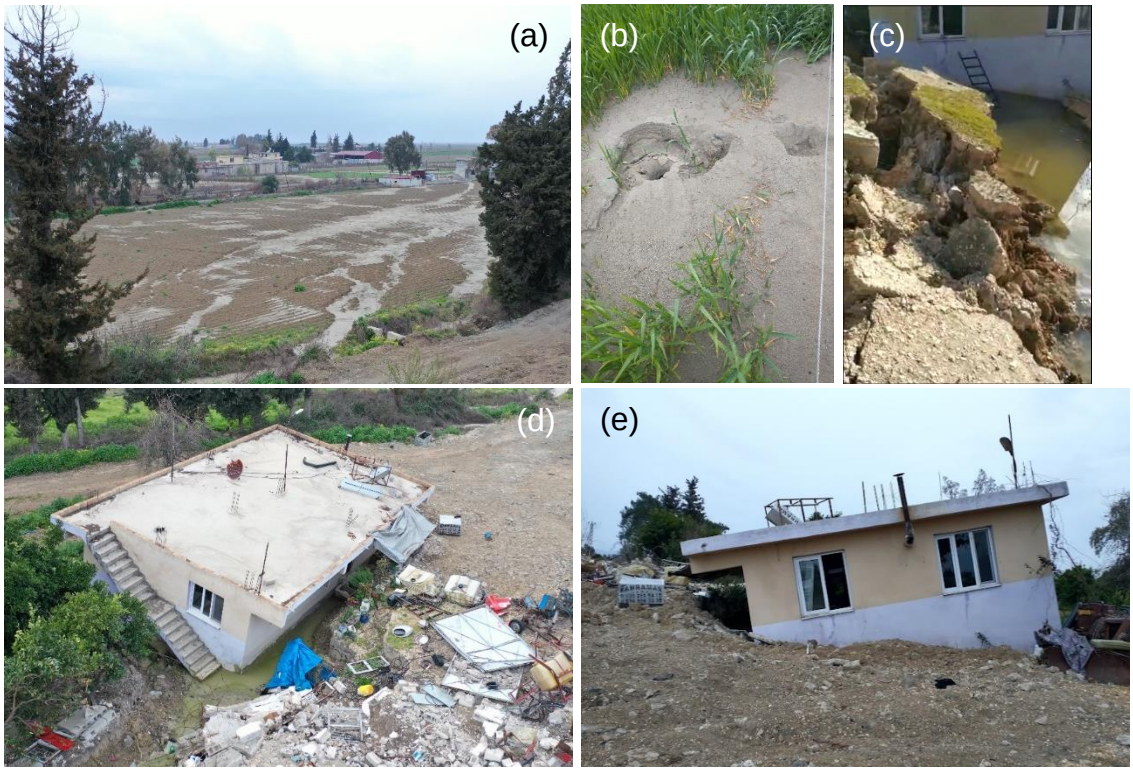

Figure 54: Liquefaction-related damage along the Orontes River. (a) Large features of surface sand boiling (b) Ejected sand (c) Photo directly after the earthquake (d) Drone view of a shallow-founded structure at an area of liquefaction and spreading (36.253701, 36.347800) (e) Excessive settlement and tilting

A similar case of a shallow-founded structure in a laterally spreading zone was identified to the west of Demirköprü, along the Orontes River (36.253701, 36.347800). Surface signs of liquefaction, including sand boils and lateral spreading cracks were visible in the area (*Figure 54*a&b). A photo of the structure directly after the earthquake sequence (*Figure 54*c) reveals a large spreading crack opening under the edge of the building that experienced most settlement. The studied structure experienced very significant settlement and rotation (*Figure 54*d&e). Discussion with the owner indicated that a reinforced concrete raft foundation was used in the building, of a thickness of about 0.6m. Indeed, the building seemed to have moved like a rigid block, which would be the expected behaviour for a strong raft foundation (*Figure 55*). The structure rotated in its transverse direction. No rotation was recorded along its longitudinal plane. The side of the structure away from the river settled more, indicating a deep scoop mechanism that encompasses all of the foundation. Such a mechanism requires a deep layer of liquefied material, so that the deformation scoop does not significantly interact with any non-liquefiable sub-stratum. A thinner liquefiable layer could have forced a shallower mechanism with settlement mostly under the edge of

the foundation closer to the river to take hold. The scoop mechanisms of *Figure 52* offer a qualitative indication for the different deformation mechanisms that take hold depending on the depth of the liquefiable layer.

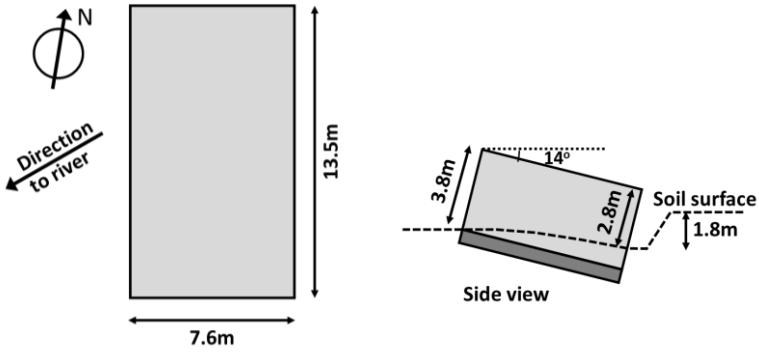

Figure 55: Sketch of single-storey structure in liquefaction zone next to the Orontes River (36.253701, 36.347800).

3.3.4. Gölbaşı

A plethora of liquefaction-related damage was identified in the town of Gölbaşı. The areas adjacent to the lake experienced lateral spreading, with a particularly affected area being that of a park shown in *Figure 56*. Significant settlement and lateral displacement had caused some structures of the park to be partly under water. Based on satellite data, the lateral displacement of the structures was estimated at 12m.

Figure 56: Lateral spreading in a lake-side park in Gölbaşı (37.794157, 37.649400).

A large part of the town to the north of the D360 main road and to the south of the train lines, experienced liquefaction-related damage to structures. Some examples of these geotechnical failures are presented in *Figure 57*. Geolocations are provided for the photos of *Figure 57*, which are all within a small radius of about 300m from the intersection of Gazi Caddesi with 511. Sk. Data from a borehole from the reveal that the first 17m from the surface consist of clayey sand, below which silty and sandy gravel was identified. The water table was measured at about 2.5m below the surface.

Figure 57: Liquefaction-related damage of buildings in Gölbaşı. (a) Building with a shallow foundation (37.789275, 37.645262) (b) Building founded on piles (37.787486, 37.642252) (c) Settlement of residential building (37.788127, 37.642037) (d) Series of buildings affected by liquefaction (37.787687, 37.642644) (e) Series of buildings affected by liquefaction (37.787367, 37.642858) (f) Large settlement of structure with shallow foundation (37.787958, 37.643190) (g) Significant tilting (37.787730, 37.643366)

Given the response of buildings seen in *Figure 57* and the observation of ejected material at the surface and around foundations its highly likely that the layer of clayey sand of the first 17m liquefied, at least to some extent. The majority of the affected structures were founded on stiff raft foundations. Structural damage was generally limited for the structures founded on soil that liquefied, indicating more of a rigid-body-

like response, facilitated by the raft foundations and the relatively large depth of the liquefiable layer. Many structures experienced more than 1m of settlement. For structures with a high aspect ratio (height of structure over width of the foundation's narrowest dimension), tilting was also observed (e.g., *Figure 57*a&g). Structures with a lower aspect ratio settled but exhibited limited tilting (e.g., *Figure 57*c). According to locals, one of the inspected structures was founded on piles (*Figure 57*b). This structure suffered excessive settlement of 180cm and accumulated rotation of 3.5°, indicating that at least partly, the piles were dependent on friction within the liquefiable layer for their capacity. Another point of interest in Gölbaşı was that liquefaction affected structures in an urban setting. As such, liquefaction-related damage was observed for multiple adjacent structures (e.g., *Figure 57*d), for which the effects of Structure-Soil-Structure Interaction cannot be neglected. These observations indicate that further research is required to offer guidance on both the design of new structures in liquefaction-prone areas and on the mitigation of liquefaction hazard for existing structures.

3.4. Bridge Foundations and Approach Structures

In this section observations made on bridge foundations in Hatay are presented, as well as the failure of an approach structure in Pazarcık/Kahramanmaraş.

Figure 58: Hatay state hospital bridge (a) the old bridge (b) the new bridge behind the old one (c) slope failure at the connection point of the deck with the ground (d) slope failure next to the bridge (e) slope failure at the connection point of the deck with the ground.

In Hatay, a bridge whose deck was made up of five segments, simply supported on piers (*Figure 58*a), collapsed right next to a new bridge (*Figure 58*b) that remained practically intact. It was on the Karasu River (36.272115, 36.207783), close to the Hatay State Hospital. Slope failures were seen at the bridge entry on both sides of the river (*Figure 58*c-e). There was no structural damage to the piers. Instead, settlement and tilting of the foundations resulted in the collapse of the decks. The new bridge was

undamaged and still in operation; the bridge's structural design and the used bearings allowed relative movement of the piers and deck during the events.

Figure 59: Hatay stadium bridge geotechnical features. (a) general view of the bridge, (b) spread-related movement on the east slope, (c) spread-related movement on the east slope, (d) spread-related movement on the east slope, (e) spread-related movement on the west slope, (f) slope stability failure on the eastern bank, (g) spreading along the eastern riverbank further away from the bridge, (h) spread along the riverbank: an inclined electricity tower far from the bridge

Figure 60: Hatay stadium bridge structural features. (a) movement and tilting of the east abutment, (b-c) deck compression crack, (d) plastic hinging at pillars on west bank (e) plastic hinging at pillars, (f) falling bearings on west bank, (g) shear key failure, (h-i) damaged girder

The Hatay Stadium Bridge (36.254532, 36.203347), which provides the Hatay state hospital road crossing over the Karasu River, is shown in *Figure 59*a. It is a pair of 5-double bridges, with each span approximately 27m. Although it was still standing, it was closed to traffic due to heavy damage. Spreading cracks of about 40cm width were observed along the surface on both sides of the river (*Figure 59*c-h). These formed part of spreading cracks along the riverbanks continuing even far from the bridge (*Figure 59*g&h). No ejected material was visible in situ and the top layer appeared to be include fine-grained and plastic material along with a proportion of gravel. Due to the soil movement towards the river on the western bank, there were some local failures around the abutment (*Figure 60*a) though the rotation recorded at the vertical wall of the abutment was negligible (<0.5°). The first raw of pillars was still practically vertical. The rows of pillars further towards the river were rotated by up to 3.5°, as their foundations moved towards the river but the supporting beam on top of them did not move due to the presence of the deck. As a result of this imposed rotation,

many pillars on the west bank formed plastic hinges at their connections with the foundation (*Figure 60*d&e). On the eastern bank, which had a steeper slope, a slope stability failure was observed, with large quantities of soil moving down the slope and "shadowing" observed behind the piers of the bridge, that opposed this movement (*Figure 59*f). Due to this slope stability failure and the forces applied by the displacing soil, the piers on the eastern bank rotated towards their river, with their foundations moving less than the beam at the top of the piers. The outcome of these geotechnical failures on both the east and the west bank of the river was that the deck was subjected to compression. Indeed, a compression-related crack and vertical offset was observed at the centre of the deck (*Figure 60*c). Large displacements and rotation of the beams supporting the deck caused multiple bearings to fall on the ground (*Figure 60*f). Additionally, exterior shear keys were broken due to large transverse displacements and girders were damaged in proximity to the abutments (*Figure 60*g&h), indicating possible impact with the abutment wall.

Figure 61: Lateral spreading-related damage of bridge in Demirköprü (36.245878, 36.357019). (a) damage of pavement to the east of bridge (b) View of the bridge from the west side (c) Rotation of piers and visible spreading of soil (d) Rotation of abutment due to spreading.

Figure 61 depicts lateral spreading-related damage of bridge in Demirköprü (36.245878, 36.357019), which was out of operation at the time of our visit. This bridge was crossing the Orontes River, all along which signs of liquefaction and lateral spreading were visible. To the east of the bridge, significant settlement-induced damaged to the pavement was visible, consistent with a mechanism of lateral spreading towards the river (*Figure 61*). To the east of the river, laterally spreading soil was also observed and a significant rotation of the abutment was visible. The behaviour of this bridge is reminiscent of damage observed in the 2011 Christchurch earthquakes for bridges in areas of lateral spreading. Haskell et al. (2013) studying these bridges proposed failure mechanisms (*Figure 62*) that seem to qualitatively fit

our observations for this bridge. The base of the abutment moved along with the laterally spreading soil towards the river while the top of the abutment was held in place by the deck, leading to the observed rotation.

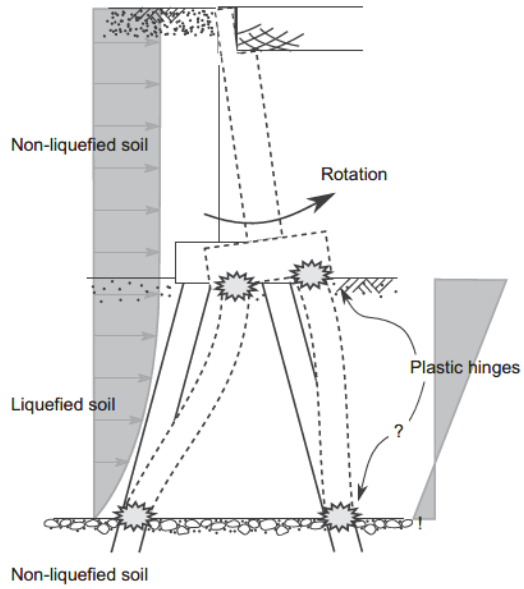

Figure 62: Rotational mechanism of abutment in laterally-spreading soil. Reproduced from Haskell et al. (2013).

*Figure 63*a shows an approach embankment leading to an overpass bridge between Evri and Çöçelli in Pazarcık/Kahramanmaraş (37.283880, 37.113587). Surface cracks were found in flat areas around the approach embankments on both sides of the overpass bridge (*Figure 63*b-e). They indicate a weak foundation soil that likely failed during the earthquake leading to a slope-stability failure of the embankment, with a shear surface passing through the foundation soil. No indications of liquefaction such as ejected material or sand boils were visible on the surface and the surface material appeared to be plastic. Hand-held shear vane measurements on the surface layer showed that it was of very low strength, with and average 14kPa peak shear strength and 3.5kPa residual shear strength. The failure of the embankment is likely a slope stability case, with a large shear surface forming and passing through the weak foundation soil. The embankment along with some of the foundation soil have moved towards a neighbouring waterway, whose presence introduced asymmetry and facilitated the formation of a shear mechanism. This mechanism can be observed in the drone pictures *Figure 63*f&g, where the soil movement and the resulting narrowing of the water channel is visible.

Figure 63: Embankment between the villages of Evri and Çöçelli (37.283724, 37.113888). (a) general view of embankment failure, (b-e) surface crack, (f-g) water channel-related failure

3.5. Retaining Structures

Slope stability problems were detected on both sides of the Orontes River in central Antakya. One of the most striking examples is illustrated in *Figure 64*a, Bekir Karabacak Bridge (36.215443, 36.162129). Retaining wall failures were observed on both sides of the bridge. The walls were structured independently; no connection was seen between them. The ones that freely stood collapsed, and an active wedge formed behind them (*Figure 64*b-e). Significant displacement, depicted in Figure 34e, was observed closer to the bridge; however, as the bridge acted like a prop, it prevented the retaining wall from collapsing at that location. Slope instability-related big cracks reaching up to 90 cm were measured around the surface (*Figure 64*f&g). Vertical displacement was observed at the conjunction point of the bridge deck and the approach road (*Figure 64*h).

Figure 64: Bekir Karabacak Bridge / Retaining wall failure (36.215443, 36.162129). (a-e) retaining wall failure, (f-g) slope instability related cracks (h) vertical displacement.

3.6. Limiting Distances for Ground Effects

In this section, limiting distances for ground effects are considered. Ground effects are categorized in three main types: (1) soil liquefaction and subsidence, (2) landslides and (3) rockfalls. The field observations collected have been documented in a series of about 1500 photos. These observations are geographically concentrated in six main areas as shown in *Table 5*. Soil liquefaction and subsidence was observed in four out of six areas. Landslides and rockfalls were documented in one area.

Geographic coordinates of each observation point were extracted from the geo-location of each photo. However, due to the short time interval between the M_w7.8 and M_w7.6 earthquake occurrences it has not been possible to discriminate between the ground effects caused by each one of the two earthquakes. Therefore, the distance of each point was calculated only from the epicenter of the M_w7.8 earthquake.

Table 5: Ground failures observed by the EEFIT field team after the 6 February 2023 earthquakes.

	Place	Liquefaction	Landslide	Rockfall
1.	Adıyaman	X		
2.	İskenderun	X		
3.	Gölbaşı	X		
4.	Antakya	X		
5.	Pazarcık	X		
6.	İslahiye		X	X

The occurrence of an earthquake-induced ground effect in a given observation point depends on two main factors. The first is the ground susceptibility to a particular type of ground effect while the second is the distance, R_e, of the observation point from the earthquake epicenter. From the examination of several cases of ground effects around the world it has been found that distance R_e increases with the increase of the earthquake magnitude, M. Empirical relationships between M and maximum R_e have been proposed by several authors.

For soil liquefaction and subsidence, such M/R_e relationships have been found for Japan as well as for other parts of the world (e.g., see references in Ambraseys, 1988). One problem, however, associated with older data is the indiscriminate use of earthquake magnitudes derived from different scales. Ambraseys (1988) added new data, used uniform earthquake magnitudes and proposed new empirical relationships. As a follow-up, Papadopoulos and Lefkopoulos (1993) collected more liquefaction cases from Greece, western Türkiye and from other seismogenic places of the world and published revised world M/R_e relationship:

$$M_w = -0.44 + 3 \times 10^{-3} R_e + 0.98 \log R_e \quad (R_e \text{ in cm}) \qquad (a)$$

Similar relationship was proposed by Papathanassiou et al. (2005).

By following a similar procedure M/R_e relationships for earthquake-induced landslides have been proposed (e.g., Keefer, 1984). Later, Papadopoulos and Plessa (2000) used an enriched data set from Greece and worldwide and proposed the next relationship:

$$\log R_e = -2.98 + 0.75 M_s \qquad (b)$$

Curves representing formulae (a) and (b) are plotted in *Figure 65* along with the maximum distances R_e of areas where ground effects were observed after the 6 February M_w7.8 earthquake. *Figure 65* clearly shows that all the observation areas fall well within the envelope shaped by the empirical relationships (a) and (b), which means that ground effects were not observed at anomalously large epicentral distances.

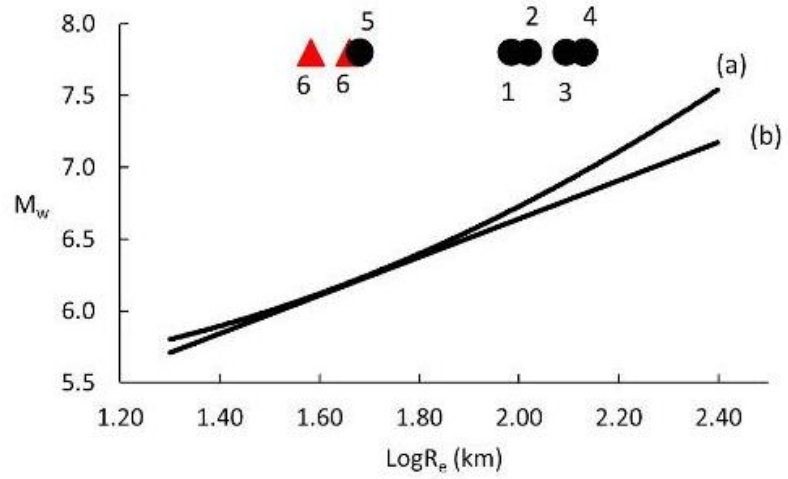

Figure 65: Maximum epicentral distance, Re, of sites with ground effects. Key for data: solid circle=liquefaction and subsidence, solid triangle=landslides and rockfalls. Numbers from (1) to (6) correspond to numbering of areas listed in Table 1. Curves (a) and (b) correspond to formulae (a) and (b) (see text above the figure).

3.7. Summary

In this section, the geotechnical aspects of the 2023 Kahramanmaraş earthquake sequence were presented. A multitude of observations were made, within a large area that covered Antakya and the Orontes River, İskenderun, Islahiye, Çöçelli, and Gölbaşı. The observations presented were made both through virtual reconnaissance and by the field team. Five broad sections are included in the section: landslides and rockfall, surface rupture and interaction with buildings, liquefaction and subsidence, bridge foundations and approach structures, and retaining structures.

Soil amplification and basin effects, though important in this earthquake sequence, are not discussed here as they require analysis beyond the scope of this report. Some information based on recorded motions can be found in the seismotectonics section. Observations on structural damage, in particular in cities like Antakya that are adjacent to mountain formations, can act as a qualitative way to verify future simulations of wave propagation investigating soil amplification and topographical effects.

The landslides and rockfalls observed provide useful examples for the possible disruption they can cause to lifelines (electricity, communications, water) and as such the importance of cascading hazards. Moreover, they highlight the need for rapid response and remediation works, both to restore lifelines and to address the accumulation of large quantities of water behind landslides. Virtual reconnaissance is a particularly useful tool in identifying areas that need to be prioritised.

The surface fault rupture was observed over great length. At points, the surface rupture was observed to damage electricity lines and water canals. Many cases of interaction of the surface rupture with buildings were observed in the town of Gölbaşı, which lies in a transition zone between main fault segments. The response of shallow founded structures when interacting with surficial rupture was found to depend on the stiffness and strength of their foundation. When the foundation was able to impose a kinematic constraint to the movement of the soil, the rupture was diverted and wrapped around the foundation before continuing. More research is needed, both to verify the nature of the surface cracks observed in Gölbaşı, and to study the response of structures in interaction with surface cracks.

Liquefaction, lateral spreading, and related subsidence was observed in multiple locations visited and was a primary contributor to geotechnical-related damage. It was particularly prominent around the Orontes River before its approach to Antakya, with a multitude of locations of spreading identified virtually, using satellite data. The field team observed such cases of lateral spreading and also recorded the very high residual rotation and settlement of shallow-founded structures within these zones. A number of bridges along the river were also visited by the field team. In cases of lateral spreading, rotation of abutments and movement of pier foundations was observed, where the foundation moved towards the river and the deck of the bridge acted as a prop. More work is needed to quantify the hazard from lateral spreading when it comes to bridges and to give guidelines for design. In İskenderun, liquefaction was prominent along the seafront part of which was reclaimed. Observations included the displacement of seawalls, lateral spreading along the seafront, significant subsidence, cones of ejected material, and settlement and rotation of buildings within the zone that liquefied. In Gölbaşı, liquefaction caused very significant settlement and rotation of structures. In addition, lateral spreading was also observed in proximity to the lake of Gölbaşı. The vast majority of the buildings observed in Gölbaşı were shallow-founded. Those with a high aspect ratio suffered large permanent rotations, in addition to settlement. The interaction of neighbouring structures in a liquefiable zone is a potentially important aspect for the response of buildings in Gölbaşı which has not received enough attention in literature.

References

Adamidis, O. & Madabhushi, S. P. G. (2018a). Experimental investigation of drainage during earthquake-induced liquefaction. Géotechnique 68, No. 8, 655–665, https://doi.org/10.1680/jgeot.16.P.090

Adamidis, O., & Madabhushi, S. P. G. (2018b). Deformation mechanisms under shallow foundations on liquefiable layers of varying thickness. Géotechnique, 68(7), 602–613. https://doi.org/10.1680/jgeot.17.P.067

Adamidis, O., & Madabhushi, S. P. G. (2022). Rocking response of structures with shallow foundations on thin liquefiable layers. Géotechnique, 72(2), 127–145. https://doi.org/10.1680/jgeot.19.P.077

Ambraseys N.N. (1988). Engineering seismology, Int. J. Earthquake Eng. Struct. Dyn., 17, 1-105.

Agalianos, A., Korre, E., Abdoun, T., & Anastasopoulos, I. (2023). Surface foundation subjected to strike-slip faulting on dense sand: centrifuge testing versus numerical analysis. Geotechnique, 73(2), 165–182. https://doi.org/10.1680/jgeot.21.00083

Bertalot, D., Brennan, A. J., & Villalobos, F. A. (2013). Influence of bearing pressure on liquefaction-induced settlement of shallow foundations. Géotechnique, 63(5), 391–399. https://doi.org/10.1680/geot.11.P.040

Brogi, A. (2011). Variation in fracture patterns in damage zones related to strike-slip faults interfering with pre-existing fractures in sandstone (Calcione area, southern Tuscany, Italy). Journal of Structural Geology, 33(4), 644–661. https://doi.org/10.1016/j.jsg.2010.12.008

Bullock, Z., Karimi, Z., Dashti, S., Porter, K., Liel, A. B., & Franke, K. W. (2019a). A physics-informed semi-empirical probabilistic model for the settlement of shallow-founded structures on liquefiable ground. Géotechnique, 69(5), 406–419. https://doi.org/10.1680/jgeot.17.P.174

Bullock, Z., Dashti, S., Karimi, Z., Liel, A., Porter, K., & Franke, K. (2019b). Probabilistic Models for Residual and Peak Transient Tilt of Mat-Founded Structures on Liquefiable Soils. Journal of Geotechnical and Geoenvironmental Engineering, 145(2), 04018108. https://doi.org/10.1061/(ASCE)GT.1943-5606.0002002

Cubrinovski, M., Rhodes, A., Ntritsos, N. & Van Ballegooy, S. (2019). System response of liquefiable deposits. Soil Dyn.Earthq. Engng 124, 212–229, https://doi.org/10.1016/j.soildyn.2018.05.013

Dashti, S., Bray, J. D., Pestana, J. M., Riemer, M., & Wilson, D. (2010). Mechanisms of Seismically Induced Settlement of Buildings with Shallow Foundations on Liquefiable Soil. Journal of Geotechnical and Geoenvironmental Engineering, 136(1), 151–164. https://doi.org/10.1061/(ASCE)GT.1943-5606.0000179

Dobry, R., Ladd, R. S., Yokel, F. Y., Chung, R. M., and Powell, D. (1982). Prediction of pore water pressure buildup and liquefaction ofsands during earthquakes by the cyclic strain method. Building science series, National Bureau of Standards, Washington, DC.

ForM@Ter image: https://www.poleterresolide.fr/seismes-en-turquie-les-implications-de-formter/

Haskell, J. J. M., Madabhushi, S. P. G., Cubrinovski, M., & Winkley, A. (2013). Lateral spreading-induced abutment rotation in the 2011 Christchurch earthquake: observations and analysis. Géotechnique, 63(15), 1310–1327. https://doi.org/10.1680/geot.12.P.174

Ishihara, K. (1985). Stability of natural deposits during earthquakes. Proc. 11th international conference on soil mechanics and foundation engineering, San Francisco, August 1985. Vol. 1, (Balkema), pages 321–376.

Kassas, K., Adamidis, O., & Anastasopoulos, I. (2022). Structure–soil–structure interaction (SSSI) of adjacent buildings with shallow foundations on liquefiable soil. Earthquake Engineering & Structural Dynamics, May 2021, 1–20. https://doi.org/10.1002/eqe.3665

Keefer, D.K. (1984). Landslides caused by earthquakes. Geol. Soc. Am. 95, 406–421.

Luong, M. and Sidaner, J. (1981). Undrained behaviour of cohesionless soils under cyclic and transient loading. In 1st International Conference on recent advances in geotechnical earthquake engineering and soil dynamics, pages 215–220, University of Missouri-Rolla, St. Louis, USA.

Mai, P.M., Aspiotis, T., Aquib, T.A., Cano, E.V., Castro-Cruz, D., Espindola-Carmona, A., et. al. (2023). The Destructive Earthquake Doublet of 6 February 2023 in South-Central Türkiye and Northwestern Syria: Initial Observations and Analyses. The Seismic Record, 3 (2): 105–115. https://doi.org/10.1785/0320230007.

Papadopoulos G. & Lefkopoulos, G. (1993). Magnitude – distance relation for liquefaction in soil from earthquakes, Bull. Seism. Soc. Am, 83(3), 925-938.

Papadopoulos, G.A. & Plessa, A. (2000). Magnitude–distance relations for earthquake-induced landslides in Greece. Eng. Geol. 2000, 58, 377–386.

Papathanassiou, G., Pavlides, S., Christaras, B., & Pitilakis, K. (2005). Liquefaction case 847 histories and empirical relations of earthquake magnitude versus distance from the 848 broader Aegean region. Journal of Geodynamics, 40(2–3), 257–78.

Provost, F., Michéa, D., Malet, J. P., Boissier, E., Pointal, E., Stumpf, A., Pacini, F., Doin, M. P., Lacroix, P., Proy, C., & Bally, P. (2022). Terrain deformation measurements from optical satellite imagery: The MPIC-OPT processing services for geohazards monitoring. Remote Sensing of Environment, 274(June 2021). https://doi.org/10.1016/j.rse.2022.112949

Qi, S., & Knappett, J. A. (2021). Effect of soil permeability on soil–structure and structure–soil–structure interaction of low-rise structures. Géotechnique, Ca V, 1–16. https://doi.org/10.1680/jgeot.20.p.109

Yönlü, Ö., Altunel, E., Karabacak, V., & Akyüz, H. S. (2013). Evolution of the Gölbaşi basin and its implications for the long-term offset on the East Anatolian Fault Zone, Türkiye. Journal of Geodynamics, 65, 272–281. https://doi.org/10.1016/j.jog.2012.04.013

4. STRUCTURES

4.1. Evolution of the Turkish Building Codes

4.1.1. Development of Building Seismic Codes in Türkiye

The Kahramanmaraş earthquake sequence caused significant loss of life and widespread damage in several cities, including Kahramanmaraş, Hatay, Gaziantep, Osmaniye, Malatya, Adıyaman, Adana, Diyarbakır, Kilis, Şanlıurfa, Elazığ, Sivas (Gürün district) (TBMM, 2023), Bingöl, Kayseri, Mardin, Tunceli, Niğde, and Batman (AFAD, 2023). The performance of structures in these areas played a crucial role in determining the scale of the destruction. Building regulations in Türkiye (*Figure 66*) have undergone continuous updates since the 1940s to mitigate the adverse effects of seismic factors.

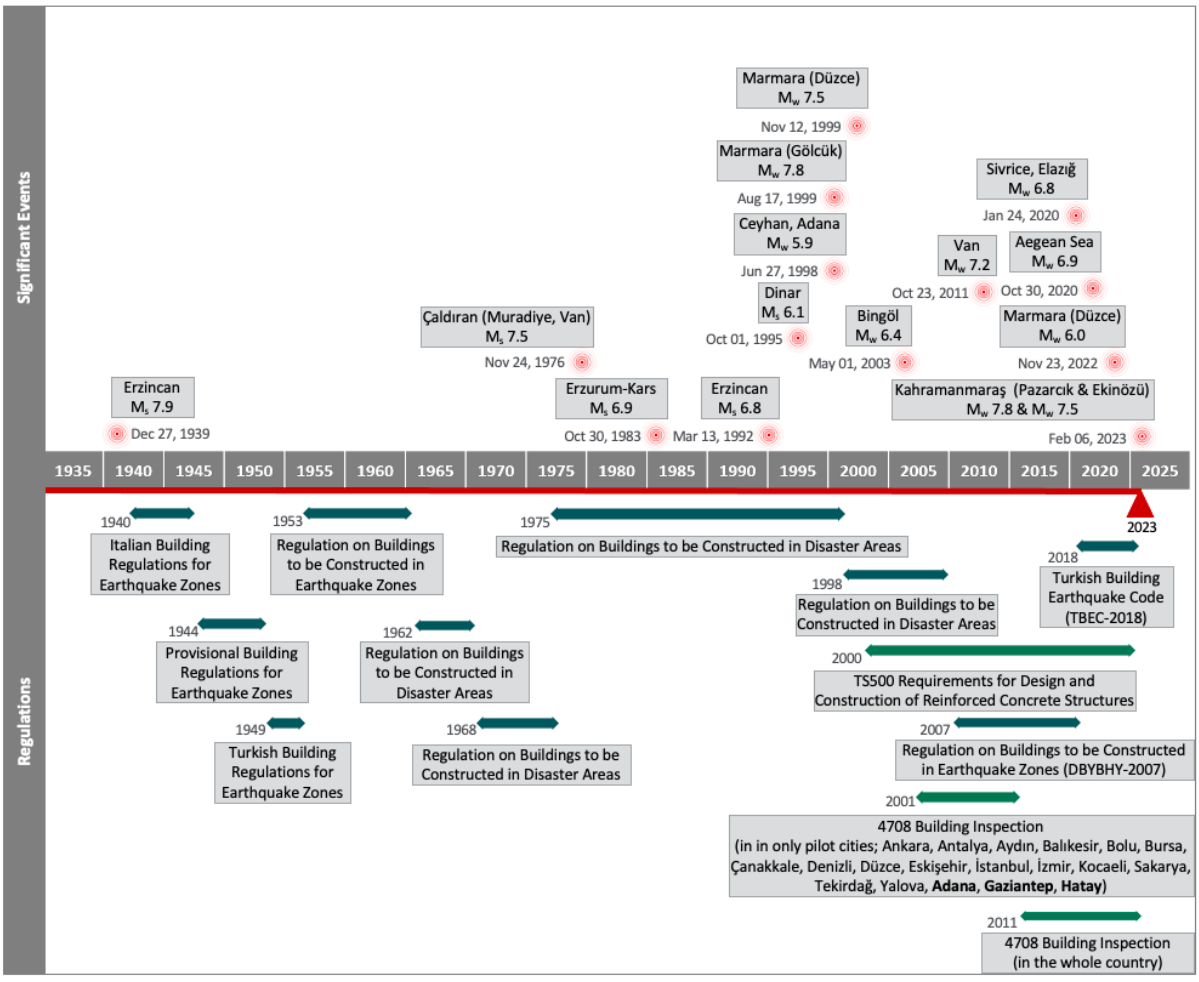

Figure 66: Significant historical events and development of Turkish building regulations.

Additional measures, as further detailed in Section 4.1.2, were introduced in response to devastating earthquakes in the past. Post-earthquake observations, assessments, evaluations of the seismic performance of existing buildings, soil investigations, and risk and hazard studies have all played roles in guiding the development of these building codes. *Figure 66* illustrates a timeline that correlates destructive earthquakes in Türkiye with the corresponding revisions in building codes. Unfortunately, the regulations implemented after the 1939 Erzincan Earthquake were unable to prevent

casualties and property damage. To enhance future safety, subsequent revisions incorporated advanced fault line research, updated geological surveys, modern structural modelling, material types, risk analysis, and post-earthquake observations. During the 1940s and 1950s, a better understanding of building periods and their influence on structural seismic design led to changes in the building codes. Between the 1960s and 1970s, concepts such as ductility and allowable stress levels were developed. Subsequently, bearing capacity methods became prominent in design. By the 2000s, performance-based analysis became the recommended approach for earthquake-resistant building design projects. In addition to these regulations, following two catastrophic events in 1999, Türkiye issued further regulations related to construction details in 2000 (Section 4.1.2.1) and building inspections (Section 4.1.2.2).

The TBEC (Turkish Building Earthquake Code) of 2018 is the latest regulation that introduces specific guidelines for the design of various types of buildings in Türkiye. The guideline cover a wide range of construction materials and methods, including cast in-situ and prefabricated reinforced concrete (RC), structural steel and cold-formed steel, masonry, timber, high-rise structures, and seismically isolated buildings, and includes provisions regarding soil-foundation-structure interaction, evaluation and reinforcement design of existing buildings, design principles for non-structural building elements, and analysis requirements for force-based and displacement-based design of buildings. Moreover, Türkiye has updated the hazard map based on risk and hazard studies. Section 2.6.7.1 provides a brief overview of the historical development of Türkiye's earthquake hazard map and earthquake design levels. However, assessing the success of the most recent regulation remains uncertain due to the prevalence of existing buildings in the earthquake zone constructed according to the 1975, 1998, and 2007 regulations (see section 4.2.1 for a breakdown of building stocks by percentage in the region).

In addition to the points mentioned above, the following list briefly summarizes some key differences between the two most recent regulations (DBYBHY 2007 and TBEC 2018):

- In contrast to TBEC 2018, DBYBHY 2007 lacks a vertical design response spectrum accounting for vertical earthquake effects on structural elements (refer to *Figure 97* in Section 3.3.1)
- DBYBHY 2007 classifies soil groups into four categories: A, B, C, and D, with decreasing soil bearing capacity from Group A to Group D. Additionally, the standard categorizes soils into four different soil classes: Z1, Z2, Z3, and Z4. In contrast, TBEC 2018 combines soil groups and classes, referring to them as local soil classes (ZA, ZB, ZC, ZD, ZE, and ZF, denoting stiff to soft soils, respectively).
- DBYBHY 2007 assigns four values to the Building Importance Factor (I) as 1.0, 1.2, 1.4, and 1.5. While TBEC 2018 retains the term Building Importance Factor (I), it uses three different values: 1.0, 1.2, and 1.5. The prior code applied a value of 1.4 to buildings with long-term occupancy and buildings storing valuable assets, but TBEC 2018 combines this value with the previous value of 1.5 in the new earthquake code. TBEC 2018 also introduces the Building Usage Class (BKS) indicating occupancy of buildings, as a factor in calculating I. Structures with building importance coefficients of 1.5, 1.2, 1.0, respectively, are defined as 1st (buildings that need to be used after an earthquake, such as hospitals, educational buildings, museums where people stay

for long periods of time), 2nd (buildings where people stay for short periods of time, such as shopping malls, sports facilities, cinemas, theatres, concert halls) and 3rd (residential buildings) class.

- DBYBHY 2007 lacks information on building heights, whereas TBEC 2018 classifies buildings into eight distinct height classes.
- The new regulation in TBEC 2018 includes a definition of the over-strength factor.

4.1.2. Supplementary Regulations

This section includes two specific sections related to the requirements for design, construction, and inspection of reinforced concrete structures.

4.1.2.1. TS500 Requirements for Design and Construction of Reinforced Concrete Structures

TS500 provides critical guidelines for the design and construction of reinforced concrete buildings (*TS500 Betonarme Yapıların Tasarım ve Yapım Kuralları*, 2000).. Initially implemented in 1969, it was influenced by the German Concrete Reinforcement Regulation DIN 1045. In 1984, an update was made to incorporate international standards for symbols and introduce a load-bearing capacity method for cross-section calculation, shifting from a deterministic to a semi-probabilistic approach for structural safety. The 1984 update also involved reorganising the calculation of second-order moments for columns and addressing issues related to shear, torsion, and adhesion using new methods and approaches.

In 2000, significant changes were introduced to TS500. Allowable stresses were removed from cross-section calculations, and the emphasis was placed on the use of load-bearing capacity as the primary method. Concrete classifications were reorganised, and the use of ready-mixed concrete became mandatory. Minimum reinforcement requirements and reinforcement hook details were modified. The approximate method for calculating the second-order moment was updated in line with international regulations, considering research findings on short cantilevers and high beam heights. The calculation of shear-friction reinforcement was also introduced. The sections concerning RC foundations and slabs were expanded, and significant revisions were made to the part addressing deflection and crack width. Section 3.3.1 displays pictures of buildings built according to the pre-2000 practices that were in use before the year 2000. These updates and revisions in TS500 reflect advancements in understanding and techniques for reinforced concrete design and construction, incorporating international standards and research findings to enhance structural safety and performance.

4.1.2.2. 4708 Building Inspection

Building inspections are critical to ensuring the structural health and safety of buildings. It involves a thorough examination of the whole structure, from the foundation to the roof. Professionals check for structural fragility, potential hazards and compliance with building codes and regulations. In this context, the purpose of the 4708 Building Inspection law is to provide for the supervision of projects and constructions to ensure the safety of life and property, as well as the construction of quality structures in accordance with the development plan, scientific practices, and standards of health and art. It also outlines the principles and procedures for

construction supervision. The law was initially enacted in 2001. However, the implementation of the law was gradual and took some time to be fully enforced in the whole country (in 2011). In 2001, it was applied in only pilot cities such as Ankara, Antalya, Aydın, Balıkesir, Bolu, Bursa, Çanakkale, Denizli, Düzce, Eskişehir, İstanbul, İzmir, Kocaeli, Sakarya, Tekirdağ, Yalova, and also Adana, Gaziantep, Hatay which are located in disaster-area.

Taking into account the supplementary regulations, the performance of RC buildings can be evaluated in two separate groups: before and after 2000.

4.2. Building Stock and Damage Assessment

4.2.1. Description of Building Stocks

In this section, the building stock in the affected area is categorised based on the structural system and year of construction, as shown in *Figure 67*. The “Load-Bearing Systems of Buildings” classification (*Figure 67*a) illustrates the breakdown of different construction systems used as the primary structural support in buildings. The values presented indicate the percentage distribution of each system within the overall building stock. Reinforced concrete (RC) comprises the majority, accounting for 87% of the load-bearing systems. Prefabricated systems make up 4% of the load-bearing systems. Masonry, including materials like brick or stone, accounts for 3% of the load-bearing systems. Steel represents a relatively small portion at 2% of the load-bearing systems. Lastly, the category labelled "Other" comprises 4% of the load-bearing systems and may include alternative, traditional or otherwise less commonly used construction methods that are not specifically listed in the breakdown. This classification provides insight into the composition of the building stock, highlighting the prevalence of reinforced concrete and the presence of other construction systems. Understanding the distribution of these systems is crucial for assessing the vulnerability and potential damage during seismic events and for formulating appropriate mitigation and retrofitting strategies.

The "Building Construction Year" classification (*Figure 67*b) provides a breakdown of buildings based on the year of their construction. The values given indicate the percentage distribution of buildings within different time periods. Approximately 13% of the buildings were constructed in 1980 or earlier using "1975 Regulation on Buildings to be Constructed in Disaster Areas" aforementioned in *Figure 66*. These structures may be potentially lacking adequate seismic resistance due to lack of code imposed seismic measures, or older, less robust standards used back then, as well as age and cumulative damage. Around 31% of the buildings were constructed between the years 1981 and 2000 via "1975 and 1998 Regulations on Buildings to be Constructed in Disaster Areas" as stated in *Figure 66*. This time period represents a significant portion of the building stock and encompasses structures built during a period of evolving construction practices and regulations. While these buildings may have improved seismic design compared to older structures, they may still benefit from retrofitting or reinforcement measures. The majority, accounting for 47% of the buildings, were constructed in 2001 or later considering 1998 and 2007 regulations, and TS500 requirements, as presented in *Figure 66*. This indicates a construction boom in the area in the last two decades with buildings more likely to comply with modern construction standards, benefitting from advancements in building technology and seismic design practices. The category labelled "unknown" represents 9% of the

buildings, indicating that the construction year of these structures is not known or documented. This could be due to various reasons, such as lack of available records or incomplete data.

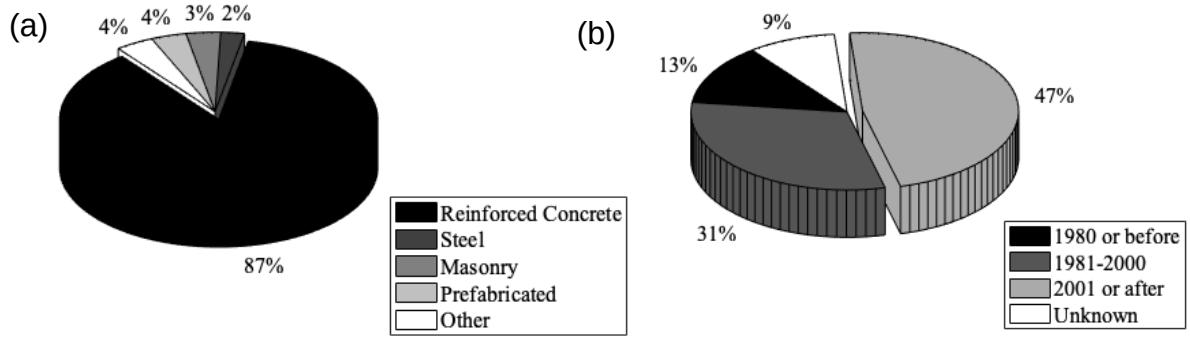

Figure 67: Breakdown of (a) Load-Bearing Systems of Buildings (%) and (b) Building Construction Year (%) in the earthquake-affected region (Numbers are taken from PSB, 2023).

4.2.2. Mission Itinerary and Approach for Damage Assessment

Prior to the field mission, the EEFIT team utilised two main sources of data to gather preliminary information and plan their site visits. The first source was the Türkiye's Ministry of Environment, Urbanisation and Climate Change (TMoEUCC), which played a pivotal role in coordinating the field work for assessing the earthquake damage – the results of this activity can be seen at the hasartespit.csb.gov.tr website. This source, where the results are summarised in Section 4.2.3, offers an overview of the areas that have been investigated and the extent of damage in the primary regions affected by the earthquakes. These results provide valuable insights into these regions, giving to the EEFIT team an understanding of what has been examined and highlighting areas that require further investigation. The second source of data was derived from social media platforms, as demonstrated in Section 4.2.4. These platforms, including social media outlets like Facebook, Twitter, and Instagram, proved to be instrumental in gathering relevant information regarding regions, building typologies most affected, and the extent of damage spread.

In the subsequent sections, the different resources and outcomes of these data collection efforts will be discussed. The criteria used to define the itinerary for the site visits will be explained, and the analysis of the data gathered from various sources will be presented. This comprehensive approach will provide a detailed understanding of the assessment process and the factors that influenced the team's decision-making during their site visits.

4.2.3. Damage Database by the Türkiye's Ministry of Environment, Urbanisation, and Climate Change (TMoEUCC)

The EEFIT team assessed an extensive dataset taken from the public TMoEUCC website, which played a pivotal role in coordinating fieldwork to assess earthquake damage. This data resulted from nationwide data collection efforts promptly organized by the ministry following the initial seismic events. It involved a substantial team of over 7,000 experts, including technical staff from the ministry, engineers from vocational chambers, and academics from national universities. Their collective

expertise and diverse backgrounds contributed to a comprehensive analysis of the earthquake's impact and distribution of damage in 11 provinces of Türkiye that were declared as part of the disaster region. These provinces included Adana, Adıyaman, Diyarbakır, Gaziantep, Elazığ, Hatay, Kahramanmaraş, Kilis, Malatya, Osmaniye, and Şanlıurfa. To access the TMoEUCC 's dataset, the EEFIT team utilized the hasartespit.csb.gov.tr website, which provided address-based information about the inspected buildings and their damage levels. *Figure 68* has been produced based on the data taken from the TMoEUCC 's dataset and provides the damage breakdown for each of the 11 provinces, encompassing a total of over 1.28 million buildings. Hatay, Kahramanmaraş, Adıyaman, and Malatya are seen to be the most severely affected by the earthquake. This observation aligns with the seismotectonic characteristics of the earthquake sequence, suggesting that the structural damage was concentrated within or around the fault ruptures of the two MW7+ events (see *Figure 17*).

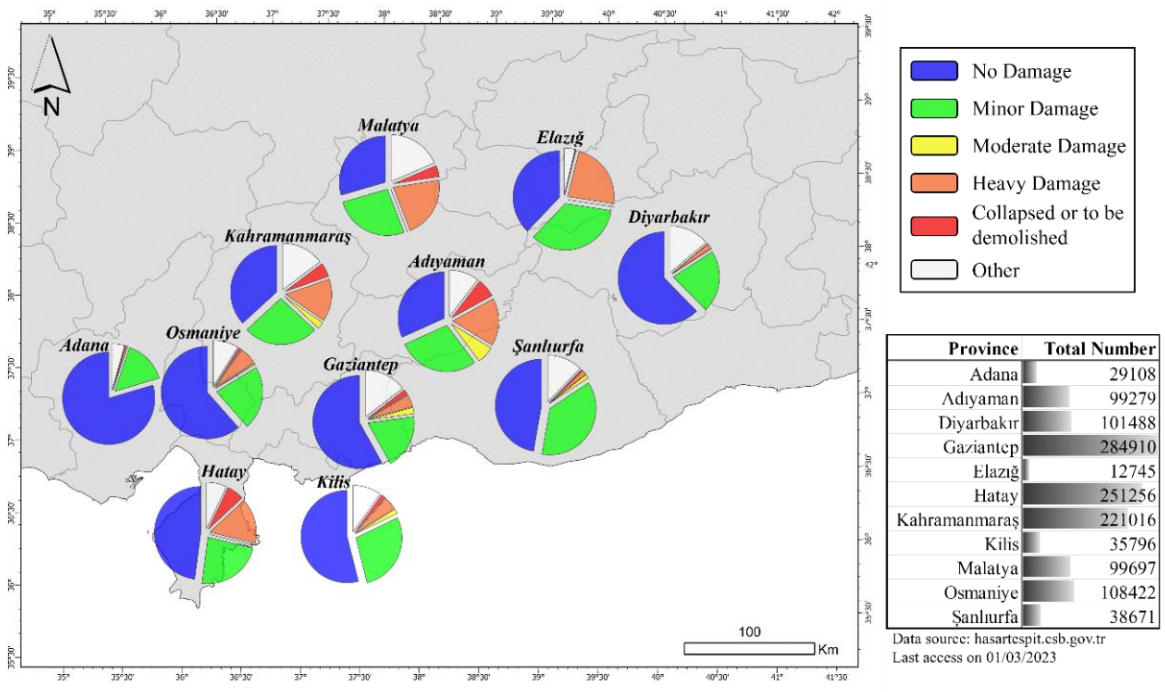

Figure 68: Distribution of the building damage in the eleven provinces declared as disaster region by the Turkish government.

4.2.4. Preliminary Remote Assessment

As part of the preliminary remote assessment component various social media platforms were systematically scanned to gather relevant data.

The preliminary remote assessment study had several primary objectives:

- Tracking the earthquake damage from the first day: Due to various limitations, logistical challenges or safety and public health concerns as well as not to obstruct the ongoing critical search and rescue operations, it was not preferred to travel to the affected areas immediately after the earthquake. Therefore, the remote assessment study aimed to monitor and document the extent of damage remotely from the first day of the earthquake event.
- Identifying key preliminary findings for fieldwork planning: The initial findings obtained through remote assessment were used to identify specific locations or areas

that required further investigation. These findings helped in prioritising and planning field visits to gather more detailed data and assess the situation on the ground.

- Broadening data sources for comprehensive understanding: Remote assessment allowed for the collection of data from diverse sources, including news outlets, social media platforms, web-based tools, and remote sensing technologies.

By incorporating these various data sources, the study aimed to achieve a more comprehensive understanding of the specificities of the events under examination here, as well as of the viable data sources for post disaster reconnaissance work, their strengths and limitations and how they can be tailored for their extended use by the post-disaster engineering communities in different contexts (see Aktaş and So, 2022 for further discussion).

Starting from the 6th of February, the following platforms were explored:

- LinkedIn
- Facebook
- YouTube
- Instagram
- Twitter and other news outlets

By actively monitoring and analysing posts and content shared on these platforms, the remote assessment team aimed to gather information about the affected areas and assess the extent of damage caused by the earthquake. Social media platforms can provide valuable real-time information and user-generated content that can aid in understanding the immediate impact of the disaster (Contreras et al., 2022).

4.2.4.1. Social Media Platforms: Insights from Preliminary Data Analysis

The remote assessment team conducted an analysis of over 217 posts, categorised as follows: 104 LinkedIn, 15 Facebook, 3 YouTube, 60 Instagram, 20 Twitter, and 15 sourced from various online platforms like news outlets. Figure 69 illustrates the initial distribution of posts gathered and accessed from each of these sources.

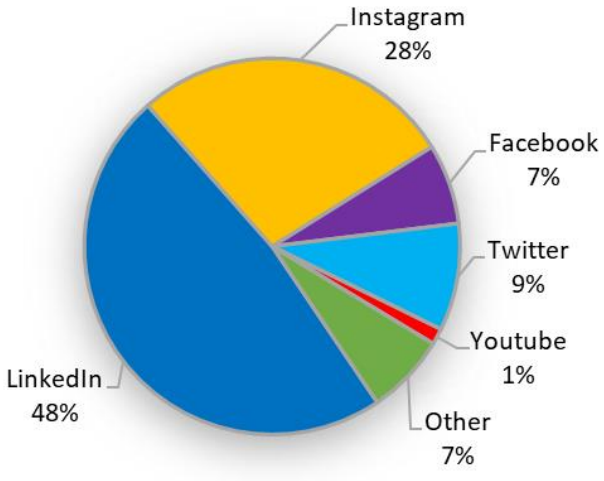

Figure 69: Distribution of social media platforms used.

Among the various social media platforms in *Figure 69*, it was evident that LinkedIn, in contrast to others, is the platform that is predominantly used for this preliminary assessment and consistently provides more comprehensive information. This includes geolocation data in the majority of the posts, often accompanied by relevant images and description of the building type and damage.

Figure 70 illustrates a typical LinkedIn post showcasing and discussing the performance of the Chamber of Civil Engineers in Kahramanmaraş. With geolocation data, it was possible to pinpoint the exact location using Google Search and Google Maps (N 37.57645°, E 36.92232°). This allowed comparing the images from Google Maps and LinkedIn, both before and after the earthquake. The comparison clearly indicates that the building itself did not sustain any damage, despite the evident failures in the surrounding buildings.

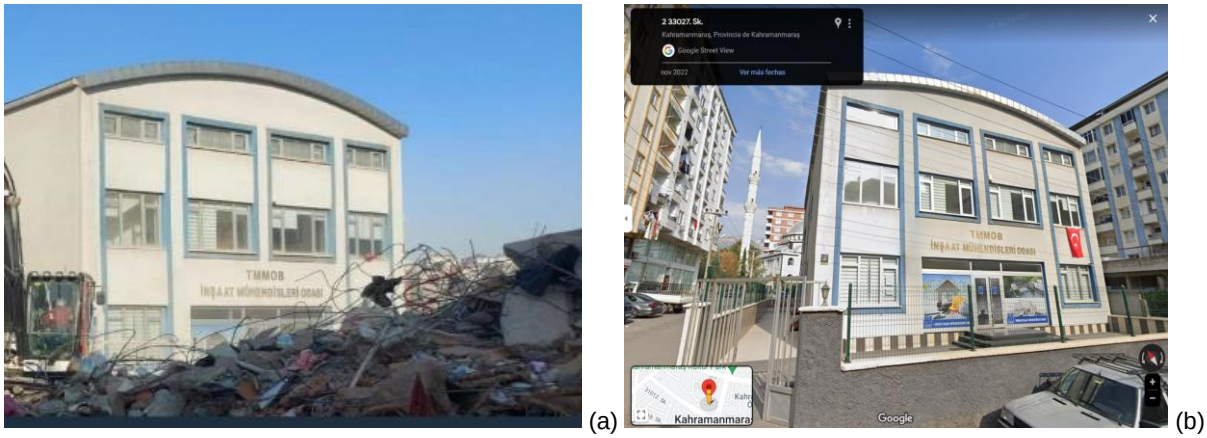

(a) (b)

Figure 70: Building used as the Chamber of Civil Engineers in Kahramanmaraş a) after the earthquake taken from Image the American Society of Civil Engineers (ASCE)'s LinkedIn post (https://www.linkedin.com/feed/update/urn:li:activity:7030213933072277504) b) before the earthquake taken from Google Street view

Figure 71 presents a further example of a LinkedIn post, featuring in a) a list of inspected building types with their respective geolocations and, in b) building photos. In particular, *Figure 71*(b) shows a photograph depicting the masonry church, known as Alexandretta or İskenderun Cathedral, which regrettably was destroyed by the earthquake.

- We investigated a masonry church located at N 36.59149°- E 036.16813°. 1st and 2nd pictures were taken next to it.
- We investigated a masonry mosque located at N 37.49333°- E 037.30141°. 3rd and 4th pictures were taken next to it.
- We investigated towers for asphalt machine located at N 37.77218°- E 037.61297°. 5th, 6th, and 7th pictures were taken next to it.
- We investigated a house split into two parts located at N 37.79262°- E 037.65730°. 8th and 9th pictures were taken next to it.

(a)

(b)

Figure 71: a) list of inspected building types with their respective geolocations b) Alexandretta or İskenderun Cathedral destroyed by the earthquake. Source: LinkedIn post https://www.linkedin.com/posts/tunc-deniz-uludag-6657a3115_earthquake-Türkiye-Türkiyeearthquake-activity-7035255419258228736

4.2.4.2. Data Organization and Challenges: Navigating Complexities in Remote Assessment

This data was organised into a dataset with the following information:

- Social media source
- Link to the post for future reference
- Date of publication
- Location (Address or Longitude/Latitude) of the assessed building
- Photo/description
- Primary structural system
- Building use
- Number of storeys
- Damage grade according to the EMS-98 scale

Nonetheless, as is customary with any data collection method, various challenges and issues were encountered. Unfortunately, it was not always feasible to acquire all the requisite information for a clear damage assessment. Some data consisted of plain videos or photos devoid of georeferencing. In response, the EEFIT team exerted extra effort, particularly when dealing with online images that lacked geolocation. They adeptly discerned location details such as the province and street by scrutinising landmarks visible in the photos and employed Google Maps to allocate longitude and latitude coordinates to these posts.

In other scenarios, social media posts predominantly comprised rudimentary news updates, which, regrettably, did not significantly enrich the database. This was chiefly attributable to the challenges encountered in collating the specific information necessary for the assessments. These news posts often lacked the comprehensive data essential for evaluating damage, building typologies, or affected regions effectively. Despite the team's efforts, the limited information available in these posts presented difficulties in their integration into the analysis.

4.2.4.3. Temporal Analysis of Social Media Engagement Post-Earthquake

Figure 72 presents a holistic view of the distribution of publication dates for posts across multiple digital sources. The observation exhibited a pronounced concentration 15 days subsequent to the seismic events of February 6th offering a compelling temporal insight. This temporal gap indicates a noteworthy shift in how social media discussions evolved after the earthquake occurrences. Possible factors contributing to this peak could encompass delayed reactions, a heightened awareness of the earthquake's consequences, or an increased focus on discussions related to recovery and response endeavours. Subsequently, the decline in post frequency following this zenith may imply a waning of immediate public response or interest in the post-earthquake scenario. This decline likely reflects the natural fluctuations inherent in social media discourse, influenced by evolving priorities and shifts in topical concerns. In summary, this temporal analysis of social media posts offers a pertinent perspective on the fluctuating dynamics of social media engagement in the aftermath of seismic events. It underscores the significance of accounting for temporal dimensions when scrutinizing social media dynamics in similar contexts.

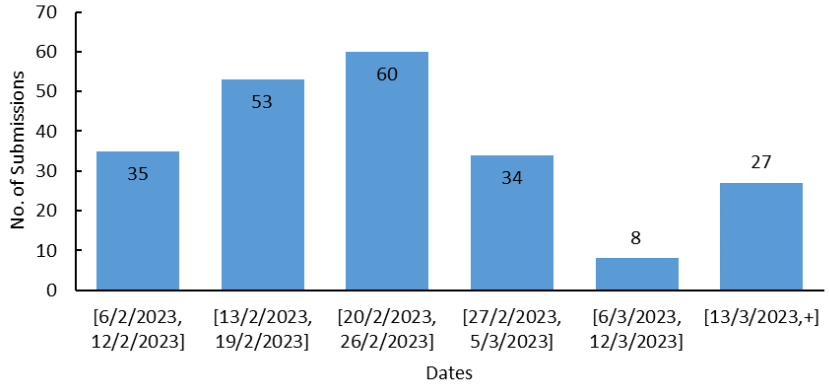

Figure 72: Distribution of remote data by publication dates.

The findings presented in *Figure 73*a, provides a comprehensive view of the locations mentioned in these posts and, *Figure 73*b a map view displaying the geographical distribution of buildings with exhibited damage. Notably, a substantial 30% of the posts were dedicated to showcasing photographs illustrating structural damage, primarily centred around the Hatay region. This concentration suggests a heightened level of concern or focus on the structural impact within this geographical area. Furthermore, the observation that the Kahramanmaraş region accounted for the second-highest percentage of posts featuring structural damage highlights the geographical distribution of social media content related to earthquake effects. Such insights are invaluable for understanding the regional variations in public discourse and perceptions following seismic events. These results offer valuable contextual information for further investigation and analysis within the study's scope.

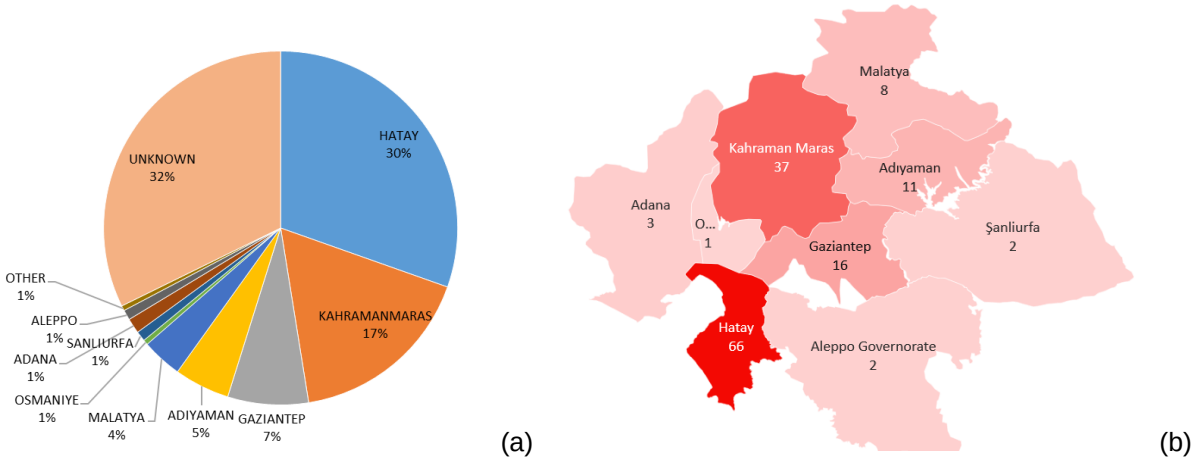

Figure 73: (a) Distribution of remote data by published locations. (b) Map distribution of remote data.

4.2.4.4. Effectiveness of Preliminary Remote Building Classification

The analysis reveals that 82% of the collected social media posts were found to be useful for conducting a preliminary remote damage assessment. These posts offer clear information regarding the location and include photos facilitating the determination of the primary structural system; building use; number of storeys and damage grade according to EMS-98 (Grünthal, 1998). As an example, *Figure 74* illustrates how informative the information collected using media could be. The picture taken from Instagram indicates that the photo was taken in Kahramanmaraş. The 4-

storey building is in reinforced concrete (RC), serves as a residential building with commercial activity on the ground level, and has Damage Grade 4 (DG4) due to a soft storey at the first level.

Figure 74: Picture taken from https://www.instagram.com/p/CpVWSV_sjx1/?igsh=cWZxbjQzNGV5a2U4

*Figure 75*a illustrates that the primary structural system predominantly aligned with reinforced concrete (RC) buildings. It was followed by masonry, timber, steel, and other structural types. Notably, no posts indicated the presence of earth or timber structural systems. While the high prevalence of RC systems aligns with the findings described in Section 4.2.1, the percentages do exhibit variations. This divergence could be attributed to potential misinterpretations or the lack of clarity in some images. Nevertheless, this underscores the importance of conducting a more comprehensive and detailed investigation in the subsequent stages of the on-site inspection.

*Figure 75*b indicates that the main use of the structures described in the posts was residential followed by industrial occupancy. The distribution for the remaining building use, hospital, commercial, and religious, remains approximately the same. This can be due to the preference of the different contributors to post the performance of residential and industrial buildings.

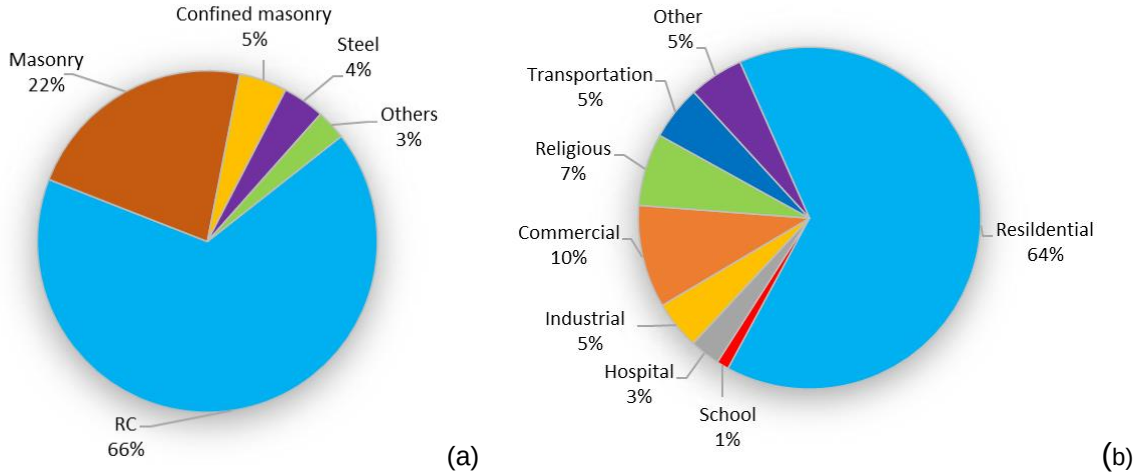

Figure 75: Distribution of remote data by (a) primary structural system and (b) building use.

4.2.4.5. Preliminary Damage Assessment Analysis: Unveiling Seismic Impact on Structures

In terms of the damage assessment, *Figure 76* illustrates a higher percentage of the assessed buildings falling into Damage Grade 4 (DG4) and Damage Grade 5 (DG5) categories. This indicates that a significant number of the buildings featured in the analysed posts suffered severe damage or complete collapse due to the earthquake. However, it is important to note that this representation may not necessarily reflect the overall scenario accurately. Social media tends to predominantly feature buildings with substantial damage or complete failure, while those with minimal damage or those remaining unscathed are less likely to be posted. This emphasizes the necessity for a more comprehensive and diverse investigation that covers various regions and sheds light not only on the most severely affected buildings but also on those that sustained minimal or no damage. Analysing such cases can offer valuable insights into the construction of resilient structures and a deeper understanding of the factors contributing to a building's ability to withstand seismic events.

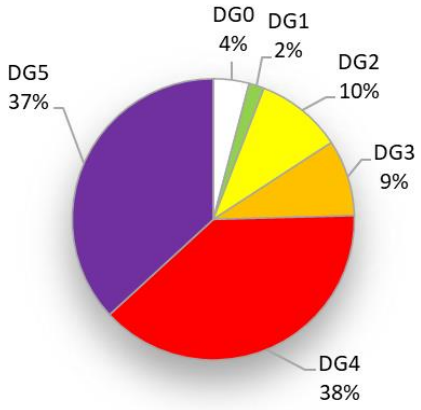

Figure 76: Distribution of remote data by damage grade (EMS-98) classification.

4.2.4.6. Preliminary Damage Assessment Insights: Factors Influencing Damage Grades

Figure 77(a) provides a compelling glimpse into how the remote damage assessment has shed light on the evaluation of different primary structural systems. Notably, Reinforced Concrete emerges as the predominant choice for construction in the assessed submissions. However, a particularly intriguing observation arises when we delve into the Damage Grade (DG) distribution.

It becomes evident that there is a notable preponderance of submissions with DG4 and DG5 ratings. This skew towards higher damage grades piques our curiosity. To decipher this phenomenon, we turn to *Figure 77*(b), which unveils that social media platforms tend to accentuate the most severe destruction. LinkedIn stands out as the most informative in this context, providing a unique perspective by showcasing resilient structures that withstood the earthquakes impact, as evidenced by a higher proportion of DG0 to DG2 structures.

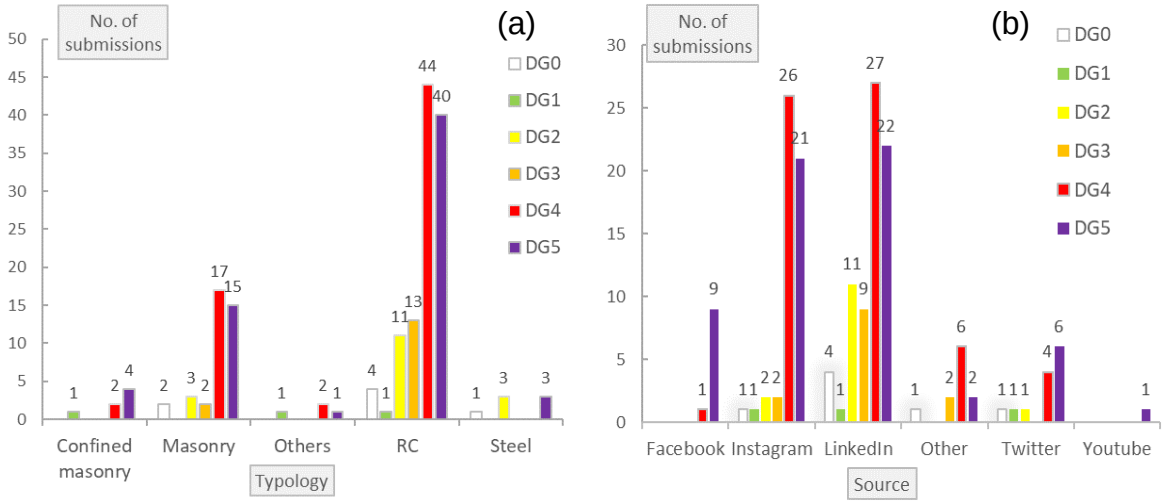

Figure 77: Remote collected data (Remote) - (a) Distribution of Damage Grade (DG) based on primary structural system. (b) Distribution of Damage Grade (DG) based on data source.

*Figure 78*a unveils the Damage Grade (DG) based on the number of floors. It's evident that most of the buildings in the collected data are medium (3 to 5 floors) and high-rise (greater than 5), while fewer are in low-rise (1 and 2 floors). Clearly, the damage grade is spread throughout, with medium and high-rise structures appearing to be the most damaged. *Figure 78*b shows the damage grade per province. The most damaged province is Hatay, which is also the most populated and inspected. This is followed, as expected, by Kahramanmaraş.

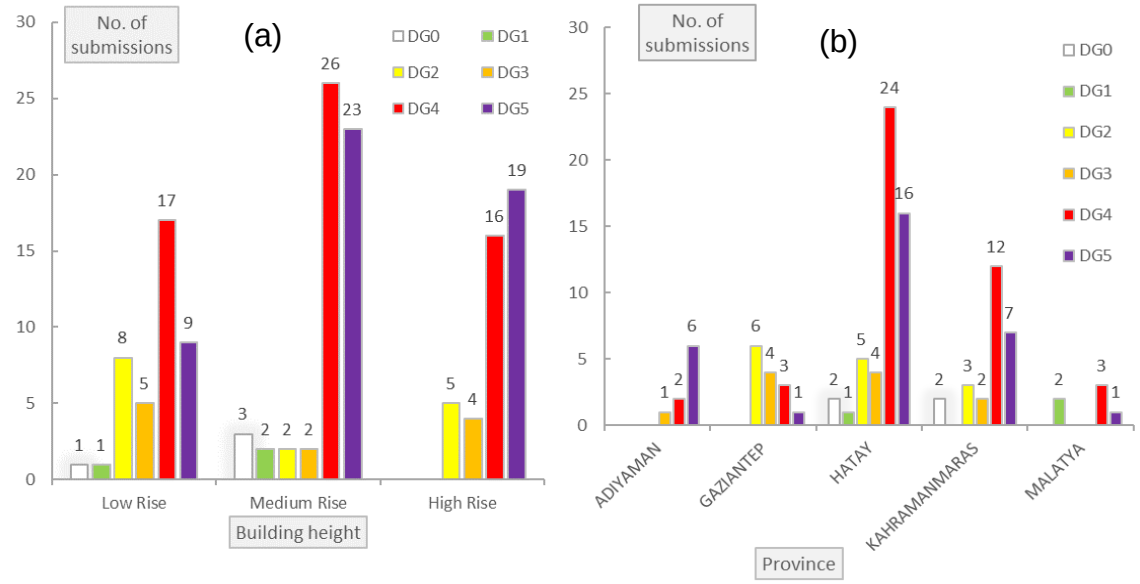

Figure 78: Remote collected data (Remote) – (a) Distribution of Damage Grade (DG) based on number of floors. (b) Distribution of Damage Grade (DG) based on location of source.

4.2.5. EEFIT Fieldwork Itineraries

Based on the gathered information and analysis of the dataset, the EEFIT team designed an itinerary that served as a roadmap for their assessment activities on 13-17 March 2023. The itinerary covered the highlighted areas on the map (*Figure 79*), ensuring that the field crew composed of 15 team members could scan through the large, affected area to develop a well-rounded understanding of the level and distribution of damage, as well as of the affected building stocks. The team visited İskenderun and Antakya the first two days. These cities were deemed essential to visit due to the high levels of damage they received, their rich building stock characteristics (both in terms of primary structural system/material and age), cascading hazards due to road closures and other infrastructure failure, and the subsequent critical delays in response, as well as because they offered a wide range of soil conditions, allowing a cross-disciplinary evaluation of building performance.

One of the primary objectives of the EEFIT March mission in relation to building performance was to collect damage assessment data for the buildings in the rural localities within the affected area. The previous reconnaissance missions and preliminary reports released by that point focussed largely on city centres and peri-urban areas, and therefore the EEFIT team identified this as a priority and one of the core scopes of their mission. Based on this, the team from 3rd day of the mission onwards split to cover the rural areas. While one team covered a wide arch starting from Osmaniye through villages north of Kahramanmaraş and into the city centre for two days, another team drew a shorter arch further south, covering east of Osmaniye and down north to Kırıkhan. The last day the teams reunited to visit the peri-urban and rural area south of Antakya, in Samandağ region (*Figure 79* and *Figure 80*).

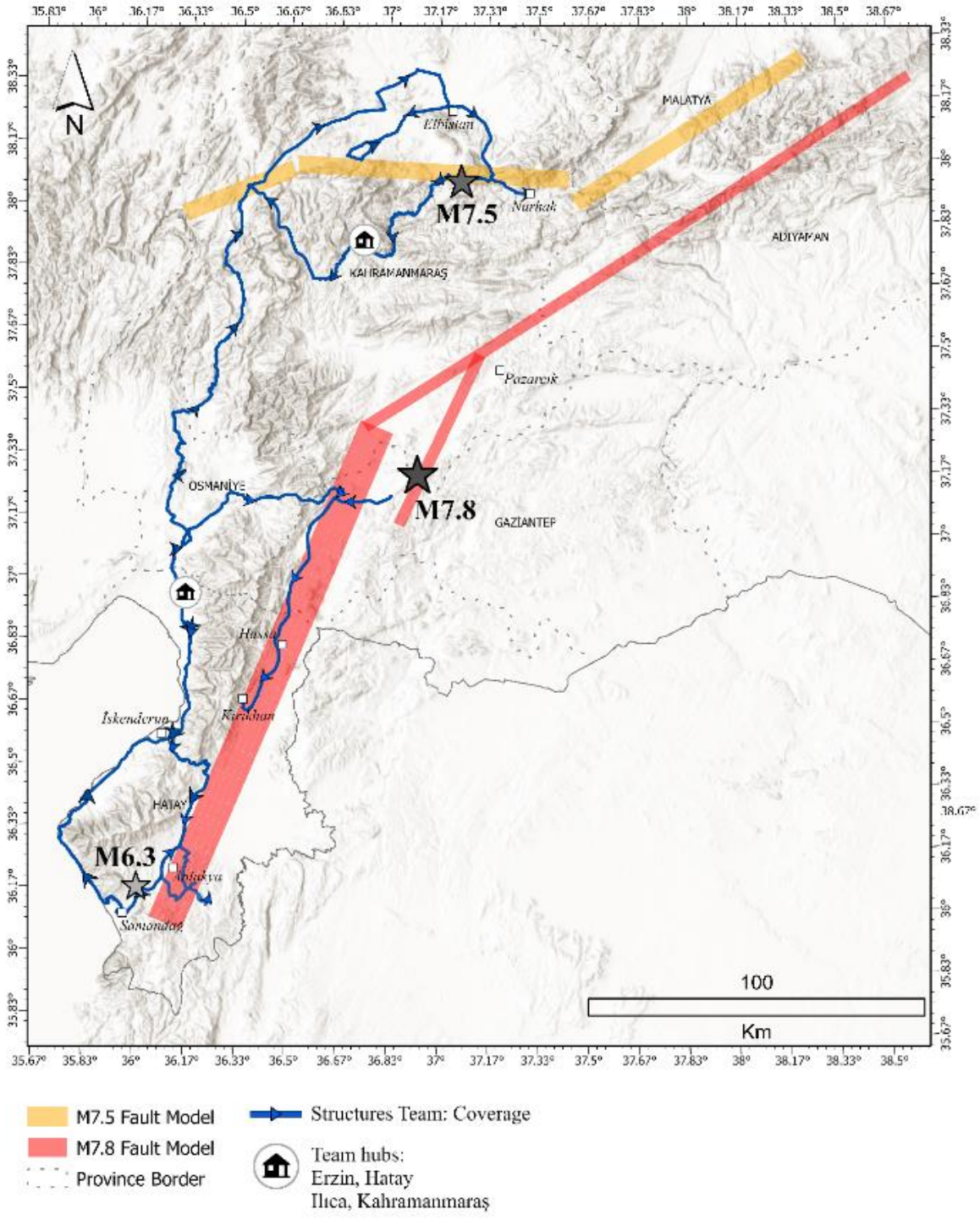

Figure 79: EEFIT March Fieldwork Itinerary

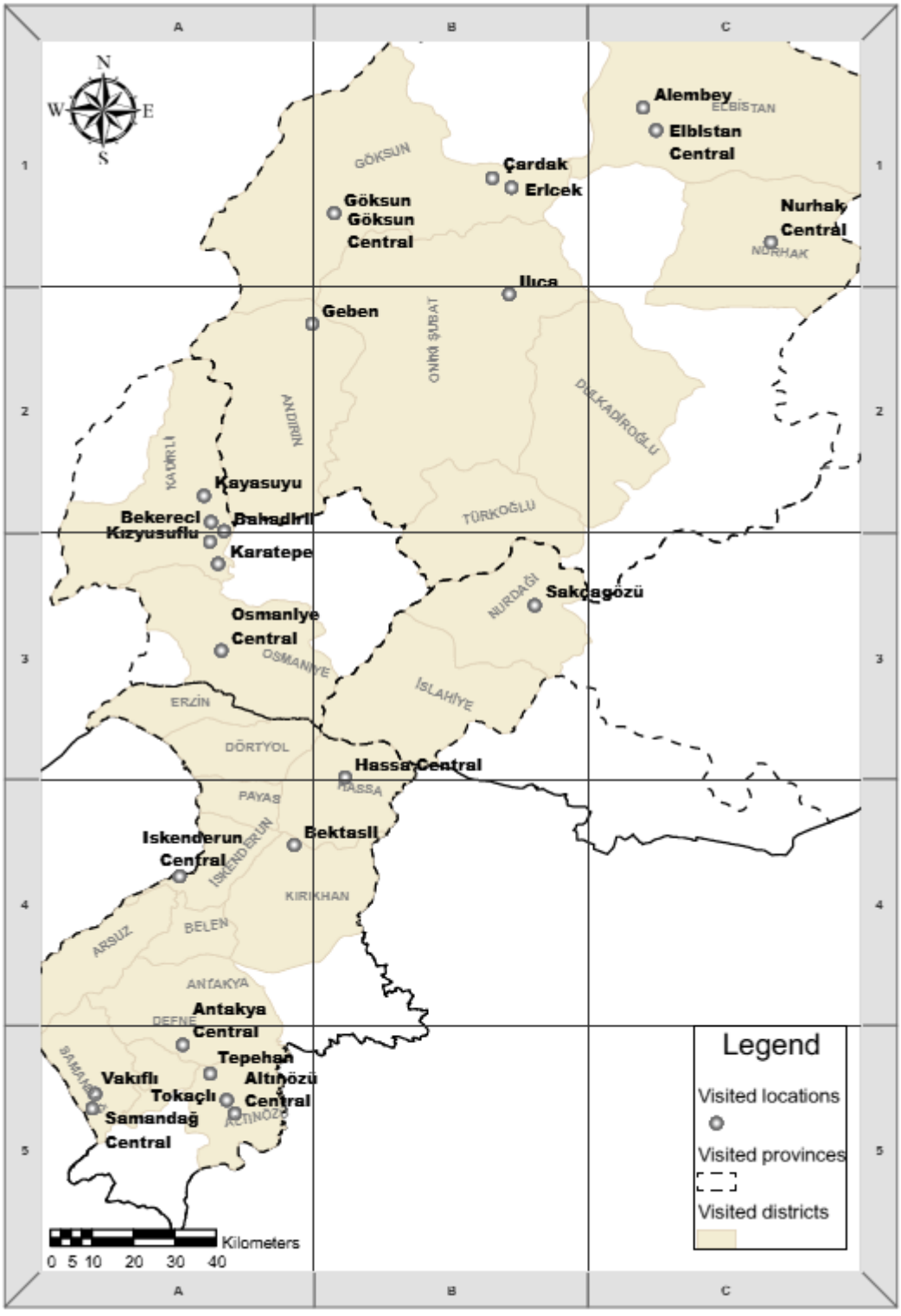

Figure 80 Visited Locations during EEFIT March Fieldwork

In addition to the March mission, the affected areas were visited for another three times by various subsets of the EEFIT team. These are as follows:

- 12-20 April 2023: Hatay and Osmaniye, with focus on monumental structures
- 16-24 June 2023: Hatay, Kahramanmaraş and Malatya, with focus on traditional/vernacular buildings, and monitoring of the recovery.

- 29 September-4 October 2023: Hatay, Osmaniye and Kahramanmaraş, with focus on traditional/vernacular buildings.

More information about the setup and outcomes of these missions can be found in Section 1.2.3 and Section 4.3, respectively.

4.2.6. Field Data Collection Tools and Methods for Damage Assessment

4.2.6.1. The Tools: *Fulcrum*, *Device Magic and Survey123*

During the first onsite mission for damage assessment, the Structure team utilised two web-based tools: Fulcrum and Device Magic (DM) data collection apps. These apps hosted the Steer and LfE data collection forms, respectively. Both apps share a similar architecture as no-code form builders, enabling users to select and customise data attributes and types (e.g., text, photo). Metadata is collected automatically. In terms of outputs, both apps compile submissions into tabular datasets (e.g., csv, xls). Fulcrum also allows downloading data directly in a GIS-ready format, storing media files separately. While Fulcrum enables the collection of photos, videos, and audio, the DM setup is limited to photo capture. In addition to that, ArcGIS-based Survey123 was utilised during the latest two field investigations on traditional typologies. Survey123 allows users to design their own surveys taking the field work requirements/needs into account with photos, audio. Possible data outcomes are csv- or xls-based tabulated formats as well as geo databases that can be opened and analysed in any GIS software.

All apps can operate offline, with submissions reaching cloud-based storage when connectivity is established—a critical feature in disaster-stricken areas. Data retrieval requires connectivity via central portals or, for DM, through a chosen destination (e.g., Google Drive).

Detailed documentation on app design and data collection forms is available here for Fulcrum and here for LfE.

4.2.6.2. The Hosted Forms and Modes

Both Steer and LfE forms follow a similar approach to data collection, starting with essential information and adding detail progressively. The LfE form includes a multi-tier workflow with two collection modes—'Driving' (Tier 0) and 'Walking' (Tier 1-5), representing time-dependent tiers. The 'Driving' mode rapidly collects basic information, while the 'Walking' mode, with five tiers, facilitates more comprehensive and detailed analysis (Aktaş et al., 2022a). In Fulcrum Steer, data was exclusively collected using the 'Walking' mode, as it is the only available option. On the other hand, designed Survey123 and for traditional typologies forms did not follow a tiered mode for data collection and aimed at collecting/documenting detailed structural features and damage types/mechanisms from each surveyed building.

4.2.6.3. Field Collected Data: Analysis and Discussion

With the Device Magic/LfE data collection form, a team of two members of the EEFIT team collected a total of 330 data, of which 120 submissions were in the ‘Driving’ mode and 210 submissions were in the ‘Walking’ mode. The Fulcrum Steer, utilised by an additional five members of the EEFIT team, collected 322 submissions. The data collected using both tools were meticulously consolidated to construct a comprehensive distribution profile. This profile identifies construction materials

indicative of the primary structural system (PSS) within a building, building use (BU), and damage grade (DG). Survey123 was used to develop and host a detailed form consisting of 80+ fields to collect data from 189 traditional buildings on construction materials, PSS and construction technology details, BU and occupancy, geometry, level of maintenance, among others. A brief summary of the mentioned Survey123 data set, related field investigations and breakdown of the data can be found in subsection 4.3.2.3.c.

a) Primary structural systems and building use

Figure 81a shows that the surveyed buildings have the following PSS:

1. Reinforced Concrete (RC): The presence of reinforced concrete elements, such as columns and beams, suggests a reinforced concrete frame system. This system is widely used in various building types, including residential, commercial, and industrial buildings.
2. Masonry: The use of masonry materials, such as brick, stone, or earth, can indicate a load-bearing masonry structural system. In this system, the walls themselves bear the vertical and lateral loads of the building.
3. Confined (masonry): It combines masonry walls with RC columns and beams to enhance the seismic performance and structural integrity of a building. In confined masonry construction, the load-bearing walls, typically made of brick or concrete or rarely earth masonry, are surrounded or "confined" by RC elements.
4. Mixed: Typically refers to traditional houses constructed with both masonry and timber elements used to strengthen the masonry walls, categorised as hybrids (*hımış* or other masonry-timber composites).
5. Prefabricated: Components or entire structures are manufactured in a controlled factory environment before being transported to the construction site for assembly. These prefabricated components are designed and built to fit together seamlessly, allowing for quicker and more efficient construction compared to traditional on-site building methods.
6. Steel: The use of steel as a primary construction material often implies a steel frame structural system. Steel frames are commonly used in high-rise buildings and industrial structures due to their strength and flexibility.
7. Other: It refers to components, materials, or aspects of a building that do not fit into specific predefined categories. It serves as a catch-all category for elements that are not explicitly mentioned but are still relevant to the discussion or description.

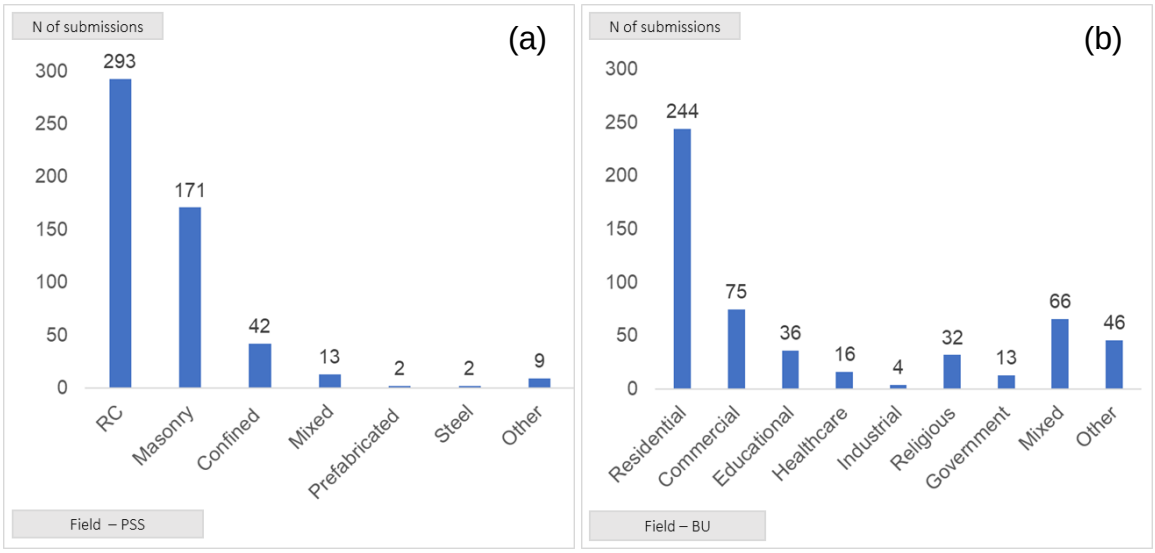

Figure 81: Field-collected data (Field) – (a) Distribution of Primary Structural System (PSS) and (b) Distribution of Building Use (BU)

The analysis in *Figure 81*a shows that the predominant structural typology is RC, constituting 45% of the total, followed by masonry at 26%. When compared to *Figure 67*, these percentages validate the prevalence of RC structures. However, the percentages for RC (87%) and masonry structures (3%) in *Figure 67* significantly differ from the on-site observations. It is essential to acknowledge that although the EEFIT team conducted a rapid assessment, they may have scrutinised these buildings with a more discerning eye, potentially identifying features that facilitated their classification into distinct structural system categories. Furthermore, the use of assessment tools (e.g., Fulcrum and DM) may have assisted surveyors in examining specific characteristics that aided in identifying the PSS. This is further substantiated by the number of buildings classified as confined masonry (6%) and mixed (2%), two PSS which were not included in *Figure 67*. These systems might have been omitted due to the challenges or ambiguity involved in classifying buildings into confined masonry or mixed structural systems, or because they are less common and were excluded to simplify the presentation. Prefabricated, steel, and "other" PPSs are represented in smaller numbers, as shown in *Figure 67*.

In *Figure 81*b, the data indicates that the predominant BU is residential, followed by commercial and mixed-use buildings. The latter category encompasses structures with dual residential and commercial functions. With "other" BU refers to BUs that do not fit into specific predefined categories.

b) Spatial Damage Grade Distribution and Profiles

Maps shown in *Figure 82* highlight the spatial extent of the damage survey and the distribution of damage states within and between the locations visited, at varying regional scales. While *Figure 82*a shows the DG distribution in the entire area covered during the field mission, *Figure 82*b zooms into one of the most affected provinces. *Figure 82*c&d further detail the distribution at district level.

Figure 83a presents the distribution of seismic DG observed during onsite inspections. This is classified from 1 to 5 (negligible, moderate, substantial to heavy, very heavy damage, and destruction) according to EMS 98 (Grünthal, 1998). To these classes,

DG0 (no damage) is also considered to consider the cases of buildings with no damage. The majority of buildings are categorized as DG1 (27%), signifying minor damage or potential habitability with minor repairs, while DG0 (10%) suggests no damage and immediate habitability. This indicates that many buildings can be occupied immediately, which is a positive outcome for the affected communities. However, the presence of DG4 (15%) and DG5 (17%) categories indicates a significant number of severely damaged or collapsed structures, underscoring the urgent need for reconstruction efforts. Interestingly, DG2 (17%) and DG3 (14%) exhibit nearly equal distributions, surpassing the 'moderate' levels depicted in *Figure 68*. This highlights the importance of separately assessing these categories, as they may have distinct implications for building safety and retrofitting strategies in vulnerable regions. Consequently, conducting further investigations into these cases could yield valuable insights for enhancing earthquake resilience measures.

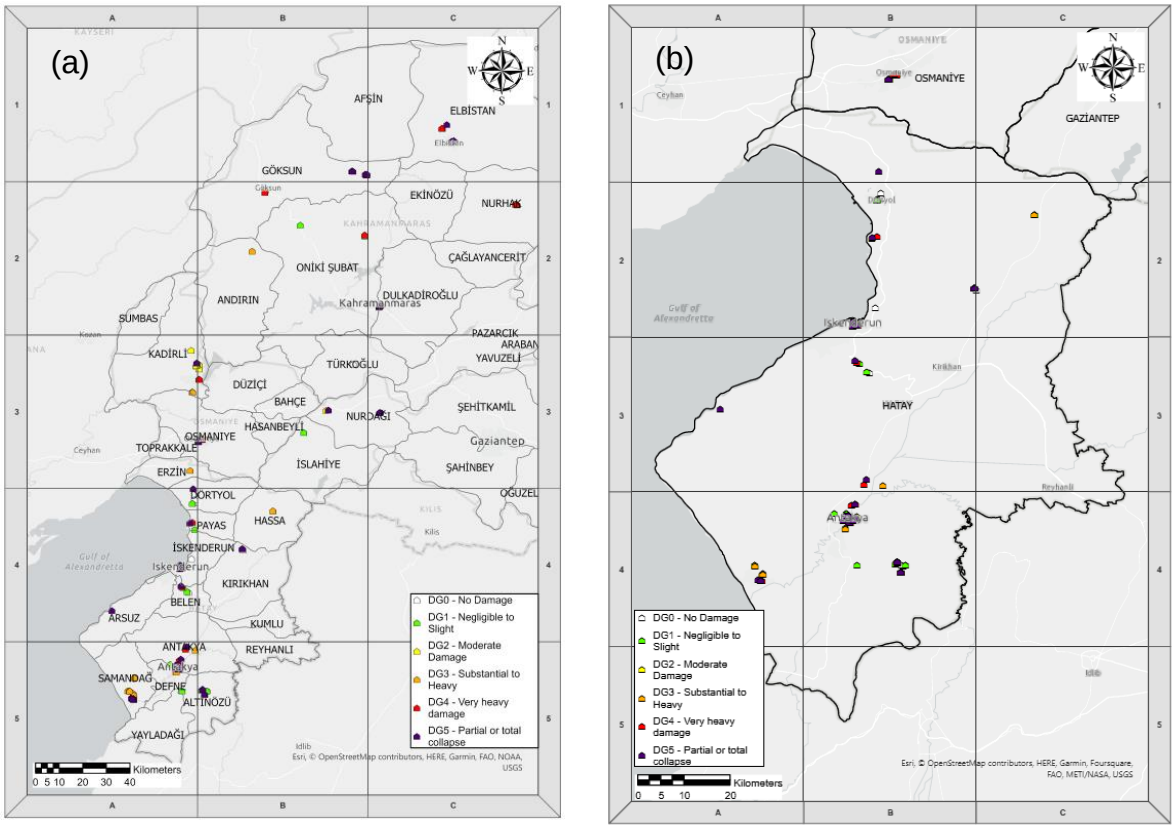

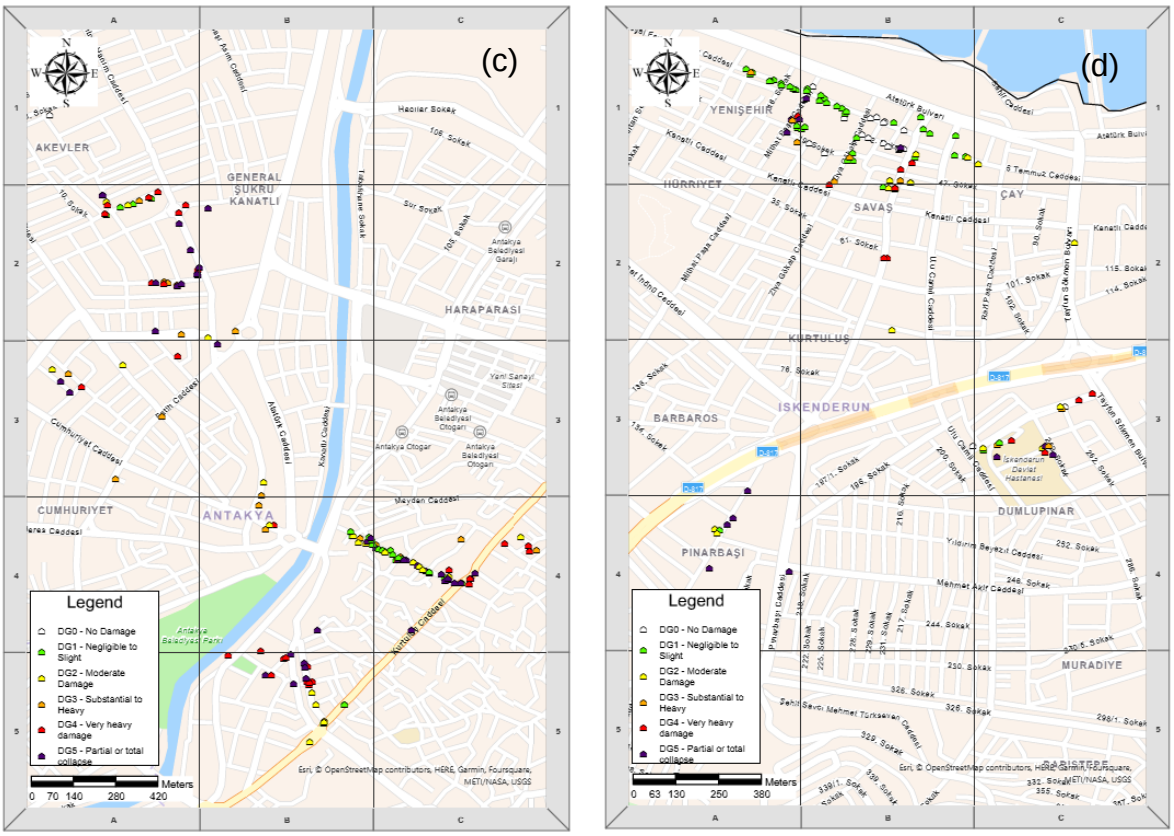

Figure 82 Field-collected data (Field)- Distribution of Damage Grade (DG) in: a) all visited locations, b) Hatay province, c) Antakya, and d) İskenderun

*Figure 83*b represents the primary assessment results based on different floor ranges and damage grades. It's interesting to note that low-rise buildings (1-2 floors) have a higher count in DG1 and DG2 compared to medium-rise (3-5 floors) and high-rise buildings (> 5 floors). Additionally, high-rise buildings seem to have a relatively lower count in the lower DG (e.g., 0 and 1) compared to the other categories. This data may suggest potential patterns related to building height and earthquake damage, which could be explored further for insights into structural vulnerabilities.

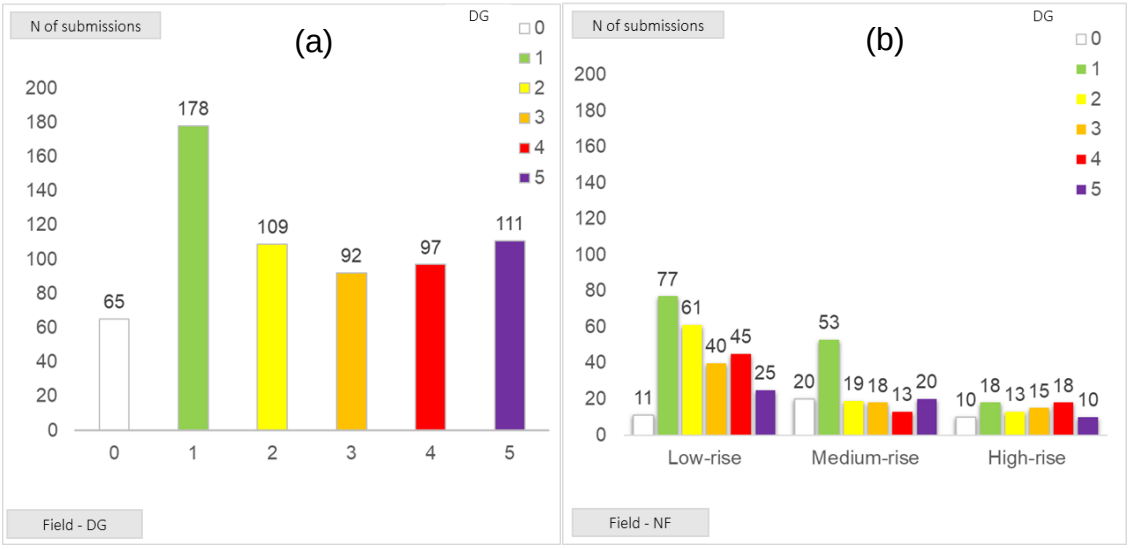

Figure 83: Field-collected data (Field) - a) Distribution of Damage Grade (DG) and b) Distribution of Damage Grade (DG) based on Number of Floors (NF)

Figure 84 illustrates the distribution of primary structural systems (PSS) by DGs. It is apparent that RC structures are prevalent across all damage grades, with a higher count in DG1 and DG5. Masonry structures show a substantial presence in DG1 and DG2, indicating their vulnerability. The confined masonry category exhibits fewer instances but is mostly observed in DG1 and 2, suggesting the need for improved resilience in such structures. The other PSSs, such as mixed, prefabricated, steel, and other, show limited representation in the data, but they do provide insights into the distribution of DGs across different structural systems.

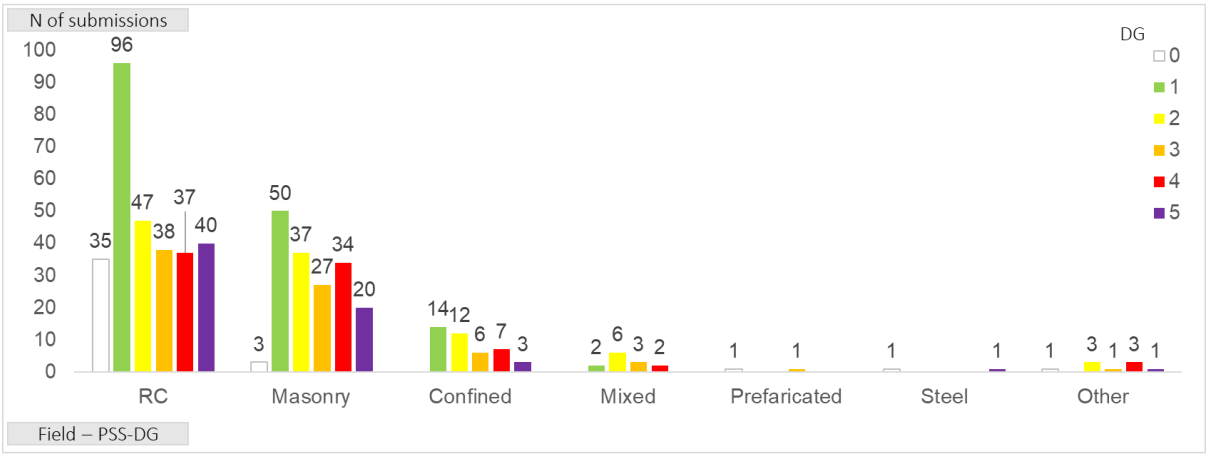

Figure 84: Field-collected data (Field) - Distribution of Damage Grade (DG) based on Primary Structural System (PSS)

Figure 85 provides insight into the distribution of occupancy types by DGs. Residential buildings show the highest count across all damage grades, indicating their vulnerability during the earthquake. On the other hand, commercial buildings have a significant number of lower DGs (e.g., 0 and 1), which could imply a relatively better performance during the seismic event. It's also notable that mixed-use buildings exhibit a diverse distribution across DGs, suggesting varying levels of structural resilience within this category.

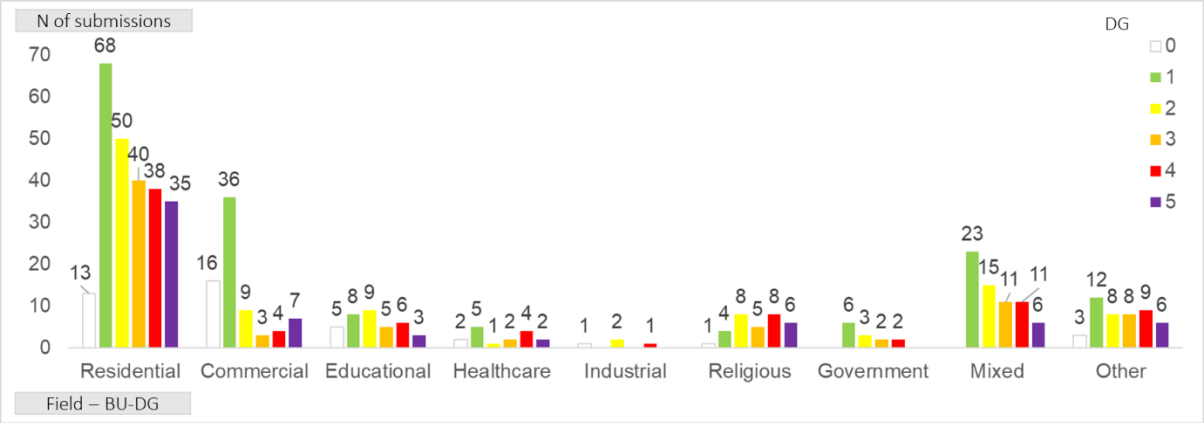

Figure 85: Field-collected data (Field) - Distribution of Damage Grade (DG) based on Building Use (BU)

4.2.7. Re-Assessment of Field-Collected Data: *Fulcrum*, *Device Magic* and Insights from Secondary Assessment

The following sections provide insight into the step-by-step procedure followed to perform the secondary assessment (Re-assessment of field-collected data), which includes:

- Description of the type of data;
- Data review: cleansing and harmonising;
- Data redistribution to the secondary assessors;
- Reconciling and analysis of the secondary assessment and comparison with the field-collected data.

4.2.7.1. Description of the Type of Data

For Device Magic the data were retrieved using the previously set up Google Drive destination, bypassing the main portal. The photos of each submission were pre-sorted by the app into a data archive accessible in Google Drive and sorted using the Device Username, the date of collection, and the submission id. For Fulcrum, the data were retrieved from the cloud-hosted portal, and the photos were sorted into a data archive on Google Drive, creating as many folders as the number of submissions using a custom Python scripting.

4.2.7.2. Data Review: Cleansing and Harmonising

When collecting data with multiple forms, it has to be expected that the data schema and attributes of the data collected will overlap only in part, with differences in the taxonomy (e.g., the same information being associated with fields with different names) and in the semantic of the data attribute (e.g., the same type of information being recorded in data formats that are different, or follow different standards). These differences need to be reviewed and considered before any data analysis and/or enhancement can take place. To this end, firstly, the data were cleansed of any partial/non-usable submissions. These include submissions lacking a geo-stamp and/or a damage grade. This process was done semi-automatically by building data cleansing pipelines in Excel. The cleansed data was then harmonised to ensure that the field containing the same type of information had the same field name and same

legend. The data collected in tabular format were cleansed and exported to create a simplified data schema containing the key information for the secondary assessment.

These included:

- a set of key metadata to identify the submission to be analysed and by whom.
- the primary assessment data, which included the primary structural type and the material, the occupancy, the damage grade, and a free text field for any notes on the damage observed.

4.2.7.3. Data Redistribution to the Secondary Assessors

Once the harmonisation is complete, a twin set of fields for the secondary assessment created to be populated by the secondary assessors. Then, the harmonised dataset was split amongst the secondary assessors. Instructions were provided to direct the secondary assessors to the Fulcrum or Device Magic data archive, both hosted on Google Drive and accessible remotely. With the aim of minimising systematic misclassification errors and encouraging discussion regarding load bearing systems and damage mechanisms of the rather complex building stocks we observed, the field-collected damage assessment data was shared among different team members for a re-assessment, or “secondary assessment”.

This step is deemed critical also because one of the aims of this mission was to test the viability of remote damage assessment for the building stocks specific to the affected areas. The ability and inability of the remote team to complete a given secondary assessment task using a specific set of visual material with a reasonable level of confidence in alignment with the field team is therefore an essential marker for how far we can go with the hybrid post-disaster reconnaissance model.

To this end, each secondary assessor was provided with a spreadsheet listing the Submission Ids/Building IDs of the buildings assigned to them and were asked to assess the primary structural system, material, occupancy, and the EMS-98 damage grade (as well as optional notes) by looking solely at the pictures associated with each building and without any prior knowledge of the primary assessment determinations. It is acknowledged that the type of information that primary and secondary assessors has access to is different and therefore their final determination of damage can also differ. In particular, the primary assessor has a more complete understanding of the overall level of damage in an area, and by comparing a building with its surroundings can also ascertain the general level of maintenance of the buildings. The determination of the damage grade should account for the relatively different positions of primary and secondary assessors, play an important role, especially for the lower degrees of damage which cannot be read as easily from photographs as in the field or when it comes to passing judgement as to the damage existing prior to the event. The secondary assessor evaluates the damage in more absolute terms by looking at a single building at the time. When available, it can also use bird-eye view datasets and pre-disaster data (such as Google acquisition, Copernico date and Google Streetview data) to attain more comprehensive information about the distribution of damage from above, thus accessing information that is not necessarily available to the primary assessor at the time of the assessment.

4.2.7.4. Reconciling and Analysis of the Secondary Assessment and Comparison with the Field-Collected Data

In the upcoming sections, the analysis will present a comparative examination of the results obtained from both primary and secondary assessments.

The data presented in *Figure 86*a indicates the distribution of DGs as assessed by the secondary evaluation. It is notable that DG1 has the highest number of submissions, followed by DG5 and DG2. However, the submission count decreases progressively for higher DGs, with DG4 having the lowest number of submissions.

To assess the alignment between the two evaluations, *Figure 86*b illustrates the distribution of DG discrepancies between the secondary and primary assessments. It's worth noting that the majority of submissions (325) show no discrepancies, meaning that the secondary assessment largely agreed with the primary assessment in assigning damage grades. However, there are cases with negative values, indicating that the primary assessment assigned a higher damage grade than the secondary assessment. This occurs less frequently, with only a few submissions in the negative range. On the positive side, there are more instances of the secondary assessment assigning a higher damage grade than the primary assessment, particularly in the range of +1 and +2.

The presence of these discrepancies highlights the potential challenges and subjectivity in assessing earthquake damage, which can depend on factors such as data collection methods, assessment criteria, or the level of expertise of assessors. Analysing these discrepancies can be valuable for refining assessment protocols and improving the accuracy of damage assessments in the future.

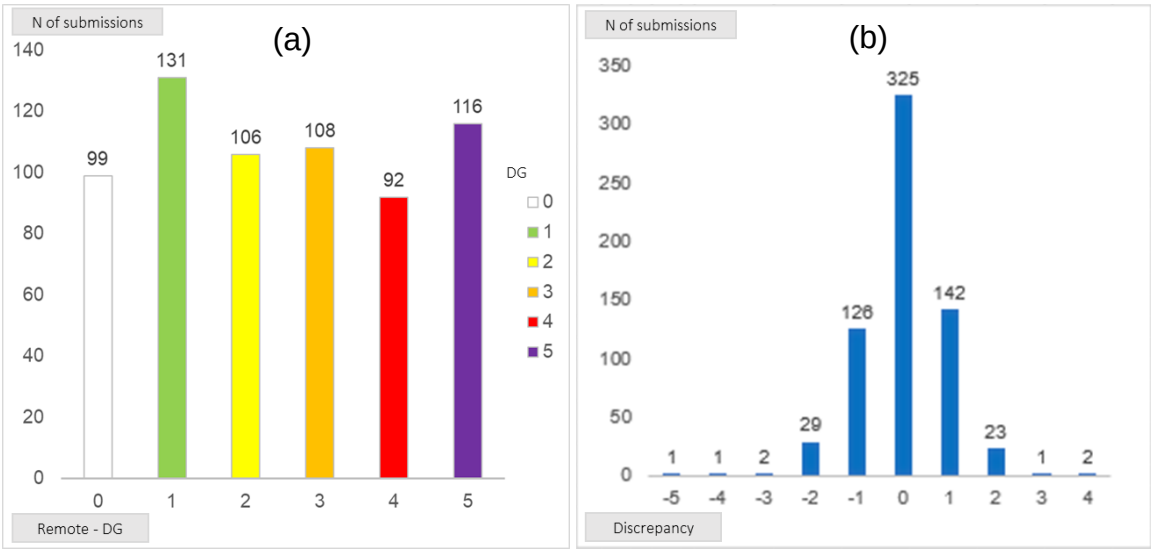

Figure 86: a) Secondary assessment (Remote) Damage Grade (DG) and b) Discrepancy between Field-collected data and secondary assessment.

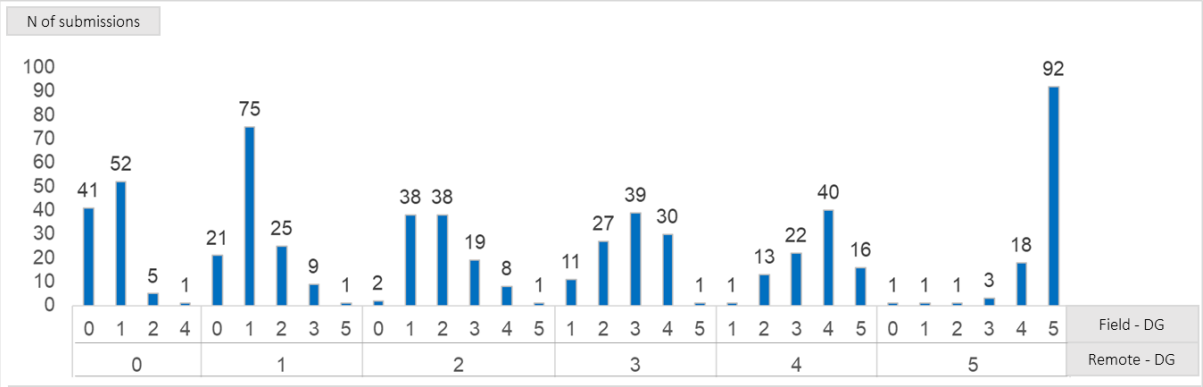

Figure 87: Damage Grade (DG) - Comparison between Field-Collected Data (Field) and Secondary Assessment (Remote) Distributions

In *Figure 87* the comparison between primary and secondary assessments of DGs reveals several noteworthy observations. It is significant to note a substantial alignment in DG1 of the secondary assessment, where a high level of correspondence with DG1 in the primary assessment is evident, totalling 75 submissions. This consistent pattern, where the peak within each DG of the secondary assessment harmoniously corresponds with the DG in the primary assessment, underscores the reliability and robustness of the remote assessment process. Recognising this congruence between the primary and secondary assessments, where the maximum number of submissions within each DG meticulously aligns with the corresponding DG in the primary assessment, yields valuable insights into the dependability and efficacy of the assessment methodology.

Furthermore, a dynamic process of re-evaluation or re-assessment for these submissions becomes evident when examining the secondary assessment. In this context, submissions classified as DG3 in the secondary assessment are found to fall within the range of DG2 to DG4 in the primary assessment. This pattern of reclassification also extends to DG4 in the secondary assessment, encompassing the range from DG3 to DG5 in the primary assessment. Likewise, DG2 in the secondary assessment corresponds to the range from DG1 to DG3 in the primary assessment. Furthermore, it is notable that DG0 in the secondary assessment aligns with DG0 and DG1 in the primary assessment, and DG5 in the secondary assessment corresponds to DG4 and DG5 in the primary assessment.

It is also important to note that the secondary assessment results in higher DGs compared to the primary assessment. For instance, buildings initially assessed as DG0 (total number: 65) in the primary assessment are sometimes upgraded to DG1 (total number: 21) and DG2 (total number: 2) or even DG5 (total number: 1) in the secondary assessment. This discrepancy may arise due to variations in data collection methods, unclear pictures, assessment criteria, or the interpretation of damage severity.

These variations underline the significance of both primary and secondary assessments, as they offer complementary insights into the extent of damage and help refine assessment methodologies. A more detailed investigation of the data could shed light on why there is a mismatch between the assessments and how this could be improved through refined assessment methods and adequate training.

4.3. Prevalent Building Typologies and Observed Seismic Performance

During the mission, the EEFIT team focused on identifying and documenting the associated strengths and deficiencies of the various building typologies found in the affected regions, shedding light on areas that require improvement in terms of seismic resilience and construction practices. The assessment encompassed a wide range of building typologies, including reinforced concrete structures, traditional masonry buildings, traditional timber-masonry composite typologies, monumental structures, and modern non-engineered buildings. Each typology presented unique challenges and vulnerabilities, and the team examined their performance to gain a comprehensive understanding of the observed damage and its causes. Of particular interest to the team were retrofitted buildings, as they provided insights into the effectiveness of different retrofit strategies. In the following sections, information about various building typologies will be provided, along with a discussion of their observed performance and notes on their future seismic resilience.

4.3.1. Reinforced Concrete (RC) Buildings

Reinforced concrete (RC) buildings have the highest proportion of load-bearing system available in the affected area with almost 87% of all buildings, as mentioned in Section 4.2.1 (PSB, 2023). Most of the RC buildings that collapsed were built before 2000 with poor concrete quality and inadequate reinforcement arrangement. Section 4.1 summarised the differences between pre-and post-2000 construction in the light of the Turkish Building Codes and supplementary regulations. In this part of the report, general design issues causing damage to RC buildings have been considered, disregarding unauthorized construction, additional floors, and zoning amnesty matters.

Figure 88 shows the most common problems we observe in RC structure. These include plain round rebars, inadequate hook details and lack of tension zone lengths (for stirrups) associated with reinforcement details on structural members. Many buildings that failed to resist the shear forces were observed to have short overlap extensions at the junction of columns. Additionally, inappropriate granulometry in concrete, such as the use of unscreened/uncleaned river gravel, absence of crushed stone and abnormal aggregate particle-size distributions were observed, resulting in low concrete strength (*Figure 89*). Therefore, the use of poor-quality concrete and insufficient rebar detailing in insufficient adhesion with the concrete were identified as among the most prominent issues in the RC structures which led to severe damages.

In addition to design failures of RC components, corrosion defects were observed in almost all the reinforcements in the buildings due to the moisture problems due to exposure or other reasons e.g. high ground moisture which manifest through rising damp and exacerbated by the voids in the concrete. Insufficient drainage in and waterproofing of basements and flooding through sewerage or other water pipelines can be the main causes of corrosion defects, even in cases where use of ready-mixed concrete with adequate concrete cover was observed. Secondly, cracking and falling of infill walls were commonly observed (*Figure 90*) due to their low deformation capacity.

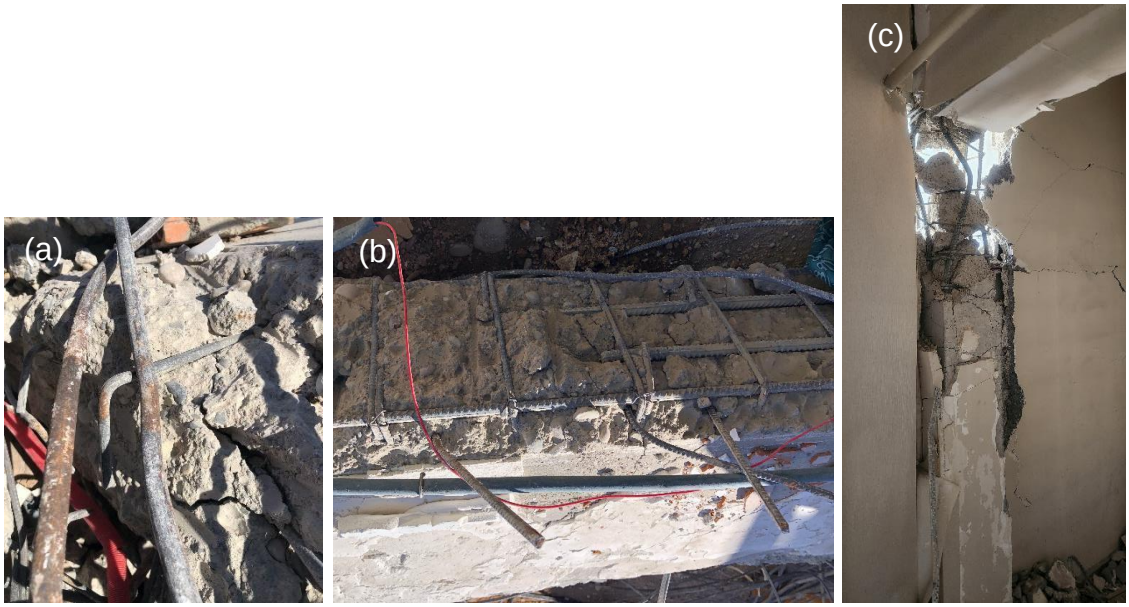

Figure 88: Reinforcing steel details which must be capable of withstanding tensile stresses. (a) Plain round rebars; (b) 90° hooks at the end of stirrups; (c) Stirrup tightening zone.

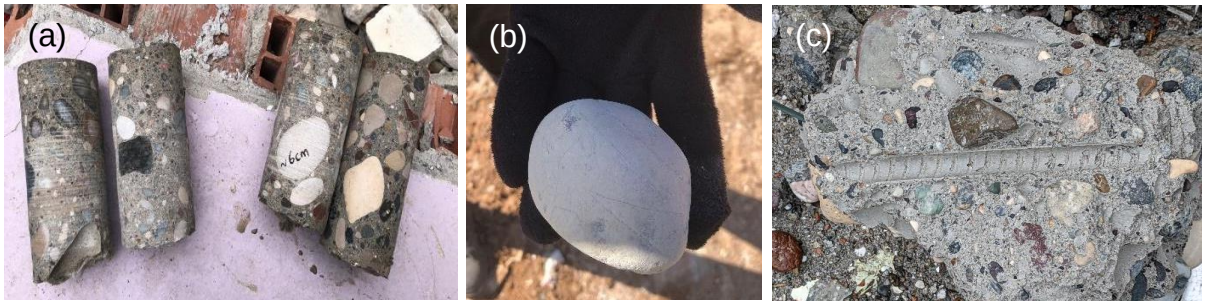

Figure 89: Poor concrete quality and non-adherence. (a) Core sample; (b) Aggregate sample; (c) Trace of removing rebar.

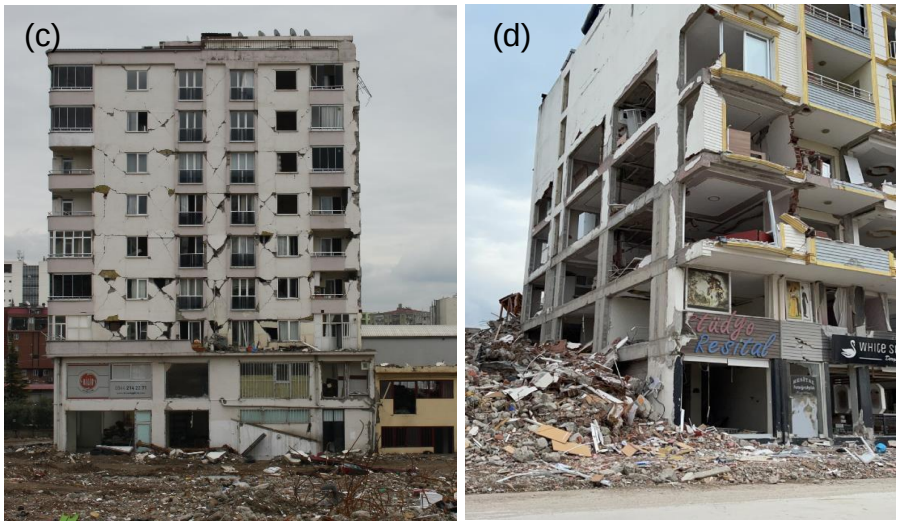

Figure 90: Cracking and fallings of infill walls in (a&c) Kahramanmaraş, (b&d) Samandağ/Hatay).

In addition, problems in relation to the dimensions of the structural components, the layout of the load-bearing system, and plan and elevation irregularities were observed. *Figure 91*, for example, shows column-to-column ribbon windows which lead to the short column effect, which is common especially if there are not enough crushable fill materials of the sides of the, and if there are insufficient lateral reinforcements on the columns. In this case ground shaking led to brittle and diagonal fractures of the columns, along with diagonal failure on shear walls as previously exemplified in *Figure 92*, because of increased shear forces on the lower floors of buildings.

Figure 91: Diagonal cracks in the columns and short column effects (Payas/Hatay).

Figure 92: Shear wall damages (Belen/Hatay).

The damaged floors in *Figure 93* indicate a significantly lower strength (weak storey), and lower stiffness (soft storey) than the other flats due to vertical irregularities. While the weak storey is formed by the elimination or reduction of the number of rigid non-structural walls (used as a workplace/general store of the floor) in the floors, the soft storey is characterised by variable floor heights and moment of inertia of the members. In this case, the moment of the column-ends reaches the maximum capacity under ground shaking, and the floor with inadequate shear resistance, or ductility fails to resist the earthquake-induced stresses as shown in the examples. *Figure 94* pinpoints another soft storey effect by hollow-tile floor slabs. This floor system is usually preferred for the appearance of a flat ceiling without beams, and for heat and sound insulation, but the infill material makes the slab heavier, causing the structure to behave like a strong beam-weak column case.

Figure 93: Soft&weak story in (a) Gölbaşı/Adıyaman, (b) Antakya/Hatay, (c) İskenderun/Hatay.

Figure 94: Hollow-tile floor slabs and their strong beam-weaker column effect (City Center/Adıyaman).

Torsional damage (*Figure 95*) was observed in buildings with plan irregularities, including column replacement errors (lateral strength asymmetry) and problematic reinforcement arrangements. By way of illustration, *Figure 95*a shows knife-cut damage to columns; *Figure 95*b shows the collapsed structure closing 6 metres to the neighbouring building due to torsion.

Figure 95: Torsional damage (a) Knife-cut damage in Gölbaşı/Adıyaman; (b) Torsional collapse in Center/Adıyaman.

Finally, earthquake-induced pounding damage (*Figure 96*) was observed in adjacent buildings of different heights with insufficient dilatation gaps between structures with varying dynamic parameters such as periods, resonant frequencies, and mode shapes.

Figure 96: Pounding effects in (a) City Center/Adıyaman; (b) Gölbaşı/Adıyaman.

As pointed out in seismotectonic chapter of this report, in these events the spectral accelerations were very high in both horizontal and vertical directions, mainly because of the Antakya Basin. By exceeding the earthquake design levels, column damages occurred as a result of the excessive increase in axial pressure force, especially in the ground floor columns of the building, as shown in *Figure 97*.

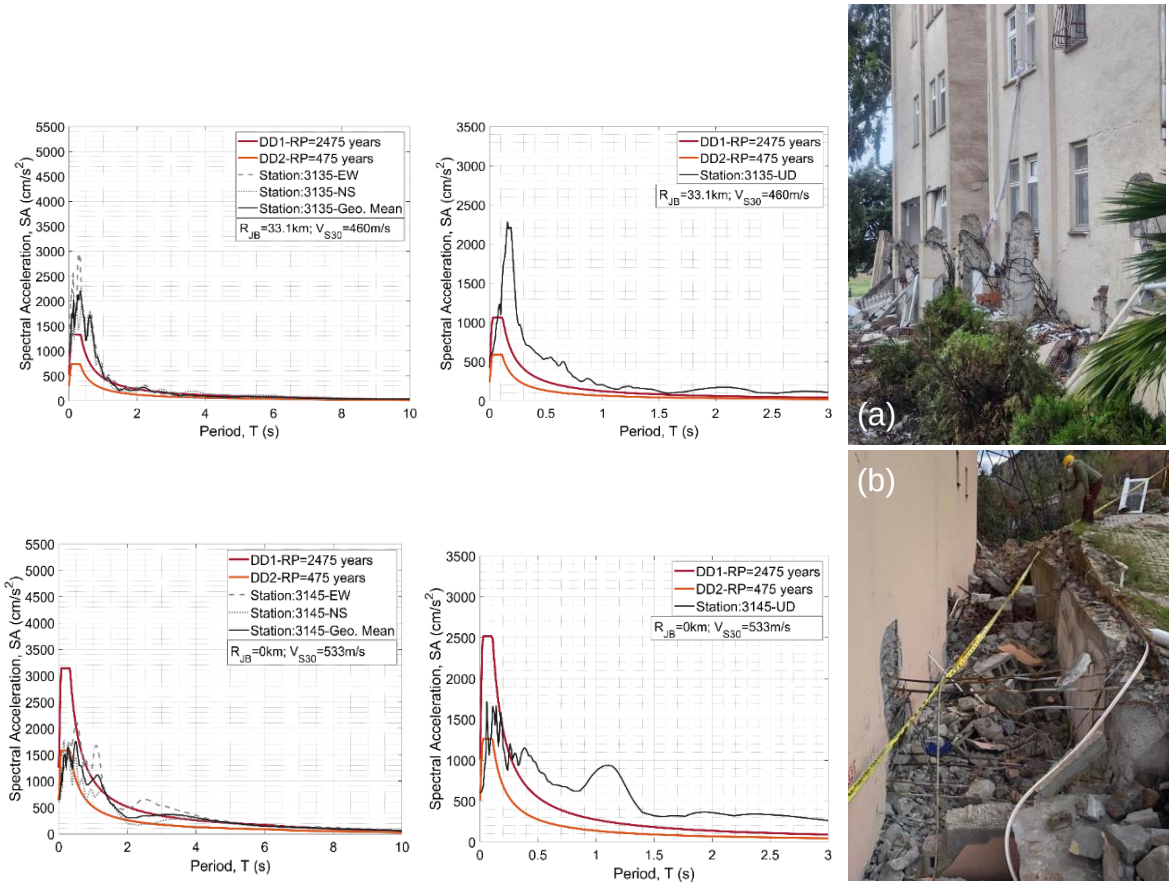

Figure 97: Exceeding the earthquake design levels in the horizontal and vertical directions in (a) Arsuz/Hatay, (b) Bektaşlı/Hatay accompanied by a damage example in these locations.

Additionally, settlement and overturning damages were concentrated in Gölbaşı/Adıyaman (*Figure 98*) due to the liquefaction and landslide as the soil deposits lost their strength. A more detailed explanation for these phenomena can be found in Sections 3.2.2 and 3.3.4.

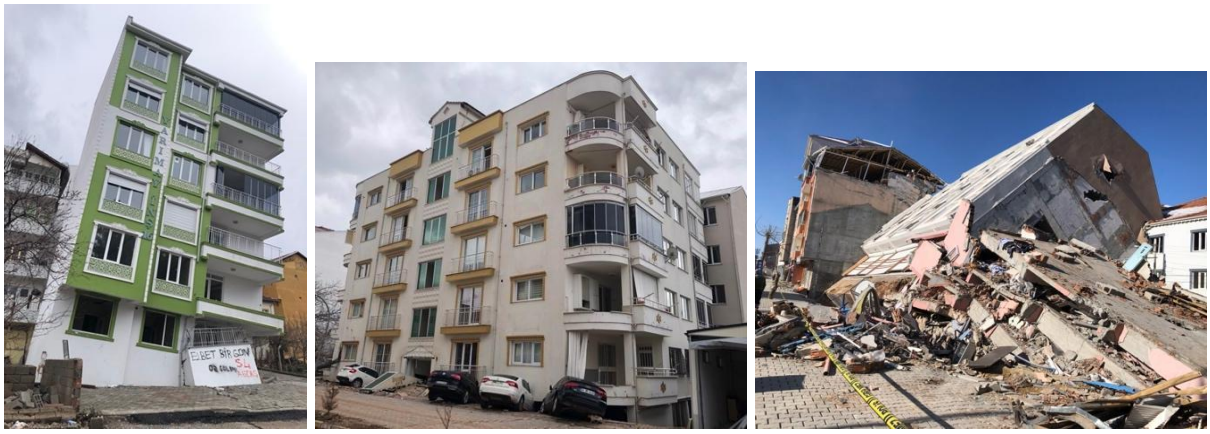

Figure 98: Settlement and liquefaction (Gölbaşı/Adıyaman).

One of the most common and critical damages suffered in the affected region, as depicted in *Figure 99*, is the total collapse mode of the poorly constructed buildings.

Choosing a “strong beam-weak column” approach can be disastrous for a structure, as the columns not being able to support the weight of the building can lead to an unexpected collapse and a life-threatening situation for occupants. “Strong column-weak beam” principle is to ensure that in the event of overload, the beams will fail before the columns, which reduces the risk of a pancake collapse. The failure of the beams would allow for horizontal displacement, but the building would remain standing. This gives occupants a better chance of evacuating the premises safely during an emergency. In addition to these, the use of quality materials has a significant impact on the strength and durability of the building to prevent a collapse.

Figure 99: Total collapse and pancake (Besni/Adıyaman).

This section has attempted to provide a brief summary of the damage patterns associated with RC buildings considering the reconnaissance, and the following comments on the next steps are extracted:

- The existing building stock urgently needs to be assessed, and the level of “Life Safety” performance should be provided.
- In terms of durability, it is essential to avoid high levels of concrete admixtures and to ensure that the minimum cement dosage is strictly adhered to.
- The inspection of ready-mixed concrete companies needs to be increased.
- Recording and controlling the moisture content of the concrete after pouring is essential to protect the concrete at the construction site.
- It is necessary to put forward and inspect the minimum requirements and construction rules by issuing a regulation on waterproofing in basement floors to prevent corrosion defects that reduce the seismic performance of the RC frame.
- It is necessary to design the structural system to provide sufficient strength, rigidity, and ductility. The structures should be as regular and symmetrical as possible, and irregularities should be best avoided. The design of ground floors to be used as workplaces/general stores should receive extra care, if these functions are a must.
- To avoid construction on liquefaction susceptible soil, or to build liquefaction resistant structures using appropriate foundation types and depths, it is essential to improve the soil strata beneath the foundations.

4.3.2. Traditional Buildings

Traditional houses in the Antakya, Osmaniye, Kahramanmaraş and Malatya regions underwent comprehensive inspections at all EEFIT field surveys. The scope of this

endeavour encompassed both urban areas and villages, with the overarching aim of identifying prevalent building typologies and discerning discernible disparities in construction techniques, material compositions, and their respective seismic performance characteristics.

4.3.2.1. Construction Materials

The traditional masonry houses eloquently embody a harmonious fusion of architectural styles deeply influenced by diverse civilizations, most notably the Ottoman, Byzantine, and Arab influences, as underscored by the research of Akboy-Ilk and Akboy-İlk (2023). In the Antakya region, square or rounded stones prevail as the primary construction materials of choice, while the Kahramanmaraş area (e.g. Malatya and Maras) predominantly employs irregular stone, dry stones, and adobe in its traditional constructions (*Figure 100* and *Figure 101*). Significantly, lime cement prevails as the primary construction material in the urban centres of Antakya. In contrast, villages in Kahramanmaraş frequently employ mud mortar, or in certain cases, opt for the use of dry stones (e.g., without mortar).

A tangible disparity emerges when transitioning from the urban centres to the villages, specifically from the Antakya to Kahramanmaraş regions, conspicuously evident in the quality of construction materials employed. In the context of village construction, when compared to houses inspected in urban areas, traditional houses in rural areas often exhibit more pronounced weaknesses. More specifically, there is a prevalence of stone with mud mortar and adobe houses in villages, and these structures frequently lack the necessary robust binding properties essential for preserving the structural integrity of the construction materials. This phenomenon is further exacerbated in villages by the chronic lack of adequate maintenance, leading to accelerated material degradation and the subsequent deterioration of the overall structure. Furthermore, it is worth highlighting that a notable proportion of buildings in the villages were vacant, and in a significant number of instances, the observed structural damage had already occurred before the earthquake event took place. This raises questions about the ongoing maintenance and structural integrity of these unoccupied structures, emphasising the need for comprehensive assessment and potential rehabilitation efforts.

Figure 100: a) Rounded stones with lime mortar, and b) square stones with mortar loss on the surface.

Figure 101: (a) Irregular stones, (b) dry stones and (c) earth blocks (adobe)

However, it has also been observed that despite the poor materials identified in the villages, masonry constructions in Kahramanmaraş, more so than in Antakya, traditionally incorporate timber elements such as lintels, tie-beams (*hatıl*), or vertical posts (*Figure 102*). These elements are thoughtfully integrated to strengthen structural robustness and effectively mitigate crack propagation within the masonry load-bearing walls. The selection of construction materials and methods in these regions reflects a unique regional tradition and locally acquired knowledge, which has evolved over time to accommodate the available resources and building techniques. The incorporation of both masonry and timber elements stands as a testament to the pragmatic wisdom of the local communities. This blend of timber and masonry not only serves practical purposes but also demonstrates resilience in traditional architectural design. They have demonstrated their better response during past earthquakes, as well as during this earthquake, compared to houses made solely of masonry without any reinforcement elements.

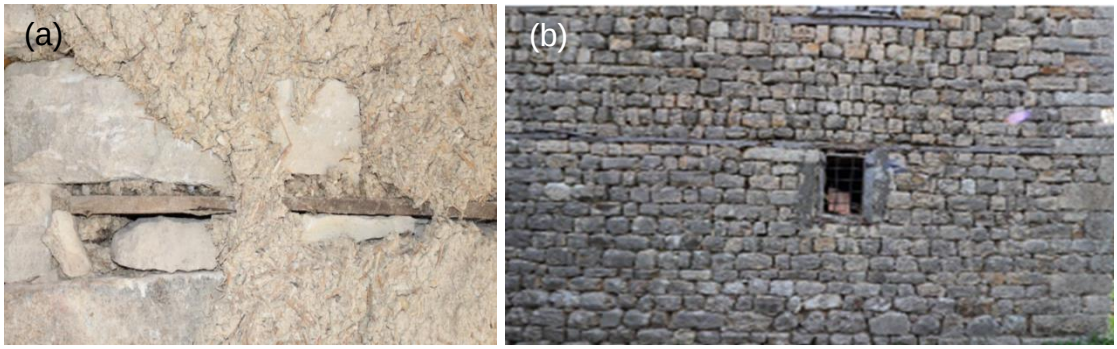

Figure 102: a) Stone with lime mortar reinforced with timber elements b) presence of timber tie-beams serving as lintels and running across openings.

4.3.2.2. Floor Systems

Traditional buildings in the Antakya region exhibit a wide range of flooring options, as documented by several researchers (Şakar & Güçhan, 2018; Polat, 2017; Topbaş & Arslan, 2017). These options encompass timber flooring (*Figure 103*a), vaults with their distinctive arched construction providing structural strength under gravity loading (*Figure 103*b), and, in certain cases, reinforced concrete (RC) slabs (*Figure 103*c). Notably, RC slabs may be supported by steel I-beams (*Figure 103*d). The diverse typologies of traditional structures highlight the richness of the area's traditional living culture. Additionally, many of these structures, particularly those with RC flooring, which deviate from traditional timber floors, have undoubtedly undergone alterations and modifications over time. These changes have not only altered the original design

of these houses but have also added more mass to the structures, thereby increasing their vulnerability to seismic events.

In villages within the Kahramanmaraş area, more traditional flooring systems are observed. These floors typically exhibit flexibility and are constructed using timber joists and rafters (*Figure 104a*), occasionally covered with straw (*Figure 104b*). For some of them, the timber flooring system is covered with metal sheets (*Figure 104c*), typically added in a second stage.

Figure 103: (a) Timber roof, (b) Vaults; (c) RC slabs; and (d) RC slabs supported by steel I beam.

Figure 104: a) Timber roof, b) timber roof with straw and c) timber roof with metal sheets.

4.3.2.3. Building Typologies

Traditional houses in the assessed regions can be classified into three main typologies based on their construction materials and floors/roof systems:

- Unreinforced Masonry (URM)
- Masonry Reinforced with timber elements
- *Hımış* (hybrid typologies)

a) Unreinforced Masonry (URM)

This typology (*Figure 105*) involves the construction of buildings using bearing walls. The walls are load bearing and carry the weight of the structure and lateral loads (e.g., wind and seismic loads). URM buildings are characterised by their masonry walls,

which provide strength and stability. The types of masonry and floors observed should be referred to in Sections 4.3.2.1 and 4.3.2.2.

Figure 105: (a) URM made of regular stones with lime mortar, (b) URM made of irregular stones with mud mortar and (c) URM made of earth blocks (adobe)

One of the primary factors contributing to failures observed in this building typology pertains to the construction method employed for masonry walls. These walls are constructed by arranging irregular, small-sized, and rounded stones or rubble to fill the gap between the wall leaves. As outlined by Giuffrè (1993), this construction approach introduces significant vulnerabilities, as the filled materials may not be compact and aligned perfectly with the wall leaves, leaving gaps and irregularities that compromise the overall stability of the wall. When subjected to lateral forces such as those generated by earthquakes, these inherent weaknesses can result in significant structural failures of the walls. Furthermore, this issue becomes even more critical when combined with the use of inadequate mortar characterised by weak binding properties. Consequently, the combination of irregular stones and inadequate mortar makes these walls even more prone to separation and fragmentation (*Figure 106*).

These issues can lead to various types of failures which include roof collapse (*Figure 107* a), localised out-of-plane (OOP) failure of individual spandrels and piers (*Figure 107* b), global OOP failure of entire façade (*Figure 107c*), failure at corners, separation of quoins that are unable to strengthen the connections between walls (*Figure 108a*) and failure of the gable (*Figure 108b*).

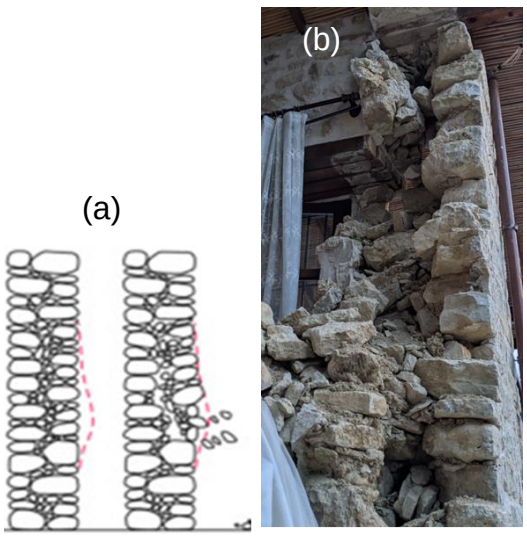

Figure 106: a) Giuffrè, A. (1993) and b) Rubble leaf separation in Vakıflı, Samandağ

Figure 107: a) Roof failure and severe damage due to leaf separation, b) OOP of localised piers/spandrels; and c) OOP of façade due to lack of connections.

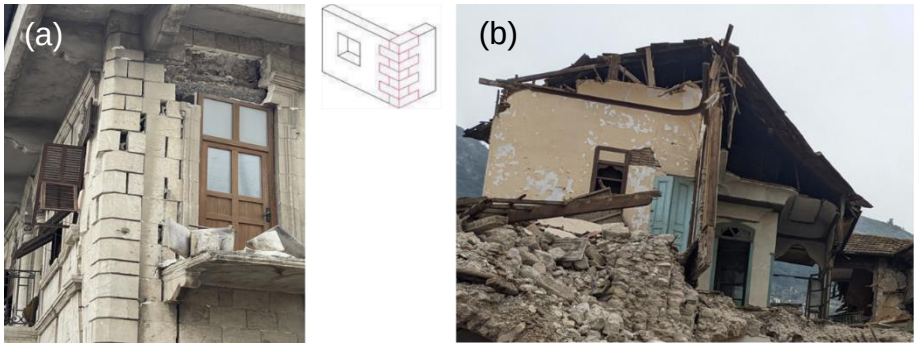

Figure 108: a) Corner failure due to the lack of connections in the quoin induce OOP of the facade, b) OOP failure of the gable.

These buildings become even more vulnerable to seismic events when constructed not only with poor materials but also lacking proper connections between load-bearing walls and floors/roof (Martins, Vasconcelos, & Costa, 2017). One notable failure due to this issue is the global OOP failure of an entire wall, as it completely detaches from the adjacent wall due to overturning (*Figure 109a*). The absence of connections between external and internal load-bearing walls can also trigger global OOP failure of entire load-bearing walls (*Figure 109b*). The lack of connections for load-bearing walls on one side (*Figure 109c*) contributes to OOP failures and poses a risk to the overall integrity of the structure. Gable failure due to OOP (*Figure 109d*) also highlights the vulnerability of this specific structural component due to inadequate connections between the gable and the adjacent walls and between the gable and the roof. These failures underscore the critical importance of robust connections to ensure the stability of the structure under seismic loads (Novelli et al. 2021). This emphasises the need for proper integration and support between different macroelements (e.g., load-bearing walls and floors/roof) of the building to enhance the building's response to seismic events.

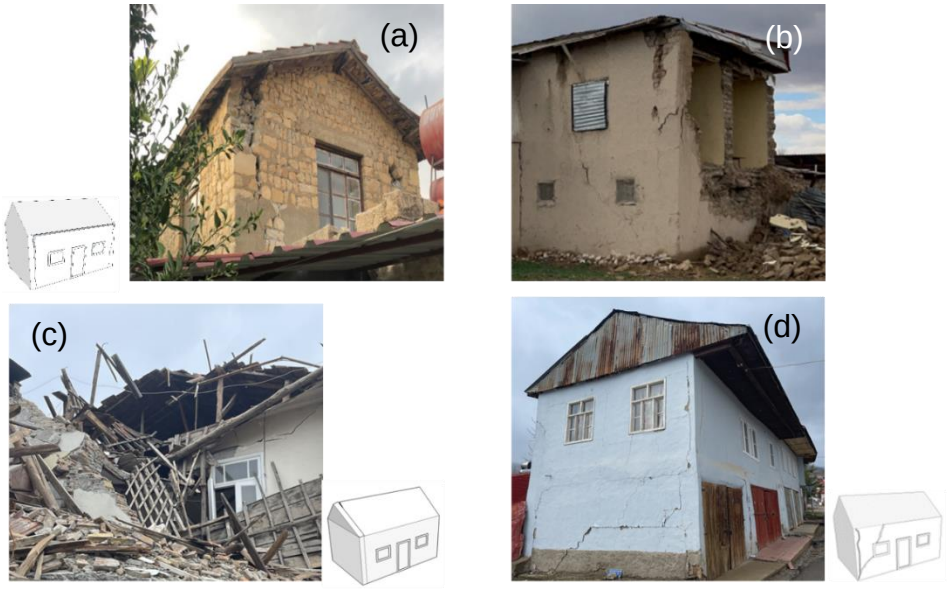

Figure 109: (a) OOP failure due to the absence of connections between external bearing walls; (b) OOP failure due to the lack of connections between external and internal walls; (c) Gable collapse resulting from OOP failures; (d) OOP failure due to the absence of connections on one side of the load-bearing walls. Sketches adapted from Novelli et al. (2021).

Another common failure observed in URM structures is arch failures at the roof level. This failure can be attributed to a combination of factors, including the use of irregular, small-sized, and rounded stones or rubble within the wall leaf, the inadequacy of strong mortars, and the absence of connections between the roof and the rest of the structure. These failures are often attributed to the lateral forces exerted by earthquakes on the rafters, which apply pressure on the bearing walls in a direction parallel to the motion of the earthquake (*Figure 110*).

Figure 110: Adobe building failures: (a) Arch failure of the walls due to poor mortar properties; (b) Presence of irregular, small-sized, and round stones or rubble within the wall leaf and a lack of connection between the wall and the roof.

Another significant factor contributing to failures should be linked not only to the original construction methods but also to the subsequent alterations these buildings have undergone. These alterations have had a substantial impact on their overall structural integrity and their ability to withstand seismic forces, as evidenced by on-site observations. Alterations, such as the construction of additional floors or veranda built on the original building (*Figure 111a*), replacement of original floors with heavier RC slabs (*Figure 111b*), and the absence of connections bearing walls and party walls built latterly in a second stage (Figure 111c), can jeopardize the building's seismic resilience (Vettore et al., 2022).

Figure 111: (a) Failure of the veranda built on the original building, (b) Failure of the RC flooring built to replace the original floor, (c) Lack of connections within party walls and bearing walls, and (d) Failure due to pounding.

Although these modifications may improve functionality or accommodate new purposes, they introduce vulnerabilities if not executed with proper consideration and implementation. Furthermore, carrying out modifications without sufficient engineering guidance can result in imbalanced structural systems and compromised load paths. This considerably increases the vulnerability of the structure, ultimately leading to the partial or total failure of floors, roofs, or even entire buildings, as observed on-site. It is most essential to recognise that alterations should be carefully planned and executed, considering the original design principles, and ensuring that necessary engineering considerations are met. This includes consulting with structural engineers and, whenever possible, following building codes and guidelines to minimise vulnerabilities and preserve the historical and cultural significance of these structures (Novelli et al. 2015).

This would also prevent the failures observed on-site, such as the detrimental effects of pounding between buildings constructed too closely or with different structural systems and materials (*Figure 111d*). The alterations observed in traditional constructions are not the sole cause of pounding failures, as it has been frequently

observed during EEFIT missions. Hammering between buildings is commonly observed in structures with varying heights, constructed using different structural systems, and at different times. These differences in building characteristics, including vibration periods, stiffness, and frequencies, can indeed contribute to the types of failures observed during assessments that are attributed to pounding effects. It is crucial to recognise and consider these factors, along with their potential impact on structural integrity, when evaluating and addressing the risks associated with pounding.

b) Masonry Reinforced with Timber Elements

This typology (*Figure 112*) pertains to a construction technique in which timber elements (*Figure 113* and *Figure 114*), such as lintels, tie-beams (*hatıl*) and vertical posts, are integrated into a masonry structure with the aim of increasing the strength, stability, and structural integrity of the load-bearing walls (Öztank, 2010). This combination of masonry and timber elements leverages the advantages of both materials: masonry provides stability and load-bearing capacity, while timber elements offer flexibility (Vasconcelos et al., 2015). These construction techniques are a tangible evidence of Türkiye's enduring history with severe earthquakes exhibiting a rich architectural heritage that incorporates a diverse range of earthquake-resistant techniques.

Notably, tie-beams are not always continuous throughout the entire building; this means that they are not always connected to tie-beams running perpendicularly, and as a result, they do not constitute ring beams. In some buildings, the tie-beams are added at floor level (*Figure 112*) or run at the top of the openings (*Figure 114*), functioning not only as beams but also as lintels. The best example of tie beams (or ring beam) where we can really claim the seismically resistant property is when they are repeated every 50-100 cm and are continuous across the plan. When detailed properly these prevent in-plane failures, support the structure, and mitigate damage propagation and crack development.

Figure 112: Masonry reinforced with timber elements.

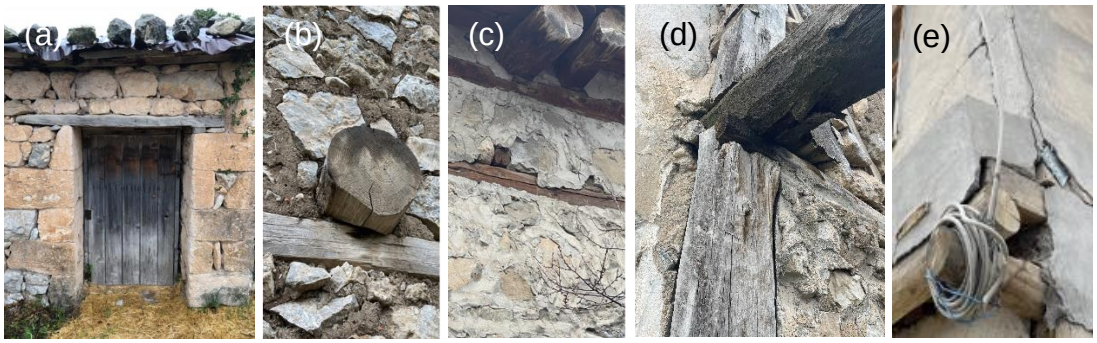

Figure 113: a) Timber lintel support, b) Joist resting on the wall plate, c) Tie-beams running along the wall at the floor level, d) Inadequate joint between vertical post and tie-beam, e) Lack of connection between perpendicular tie-beams.

Figure 114: Timber (vertical and horizontal) elements filled with earth blocks (adobe)

Figure 115: Timber beams on the top of the openings.

However, when diagonal bracing is inserted at corners, this help to enhance the connections between the load-bearing walls, making them more resistant to seismic forces and preventing corner failures caused by overturning. The incorporation of bracing within the timber frames (*Figure 116a*) offers increased flexibility and optimal load distribution, while the insertion of timber bands within partition walls (*Figure 102*b) enhances their stability.

Figure 116: (a) Bracing in the timber frames; (b) Partition wall with timber band.

The observed failures in these structures have demonstrated a relatively better performance compared to URM constructions. As illustrated in *Figure 112*, the presence of timber elements has been found to effectively restrain crack propagation, preventing significant damage. Notably, houses with corner bracing (*Figure 116a*) tend to exhibit minimal damage. Upon closer inspection, it has been observed that partition walls often develop horizontal cracks on the plaster in areas where timber elements are located (*Figure 116b*). While in some cases, these cracks may appear more pronounced, it is important to highlight that the majority of these damages may not necessarily be attributed to the combination of masonry and timber construction systems. Rather, they often result from a lack of adequate maintenance, which clearly indicates material degradation and poor wall conditions that have been exacerbated by seismic events.

Figure 117: Localised arch failure.

The primary failure mode observed in these structures is arch failure (*Figure 117*), which shares similarities with the phenomenon observed in URM constructions (*Figure 110*). However, unlike URM buildings where arch failures often lead to the collapse of entire walls and roofs, in these timber-reinforced masonry structures, the failures tend to be localised. This localised failure is primarily attributed to a loss of materials, primarily caused by the fact that the wall leaves are filled with small stones and rubble, similar to the construction method used for URM buildings (*Figure 106*). These materials, due to their lack of compactness and weak binding with the wall leaves, became loose under the impact of seismic lateral loads. It is important to note that

these types of damage can be easily repaired, facilitating the reoccupation of these buildings.

These observed techniques, present in the building typologies located within villages, have undergone continuous refinement and consistently demonstrated their effectiveness in withstanding earthquakes, even when constructed using materials of relatively weaker strength (Ortega et al. 2017). Gaining a comprehensive understanding of these techniques serves as a valuable resource for informing modern seismic design practices. A synergy between traditional and modern engineering exemplifies the enduring value of local knowledge. It not only holds the potential to preserve lives during seismic events but also plays a pivotal role in safeguarding the cultural heritage deeply embedded within these construction methods. These time-honoured techniques encapsulate the narratives and identities of local communities, serving as a profound link between people and their constructed environment. By embracing and integrating this invaluable heritage into modern construction guidelines and practices, building safety and resilience can be significantly enhanced, along with the reinforcement of a sense of identity and continuity within these communities (Yadav et al. 2023). The principles of Local Seismic Culture, informed by generations of experience, underscore the significance of context-aware design and sustainable construction methods. As society progresses, preserving traditional techniques and integrating them into modern engineering lays the foundation for the establishment of sustainable and resilient communities that are not only physically robust but also culturally enriched.

Failing to adhere to traditional construction techniques can result in potentially catastrophic scenarios, as exemplified in *Figure 115*. This figure depicts a building that exemplifies substandard workmanship carried out without the involvement of any engineering design. The initial level of the structure was originally constructed using traditional methods, specifically relying on masonry reinforced with timber elements such as tie-beams and vertical posts.

Conversely, the second level of the building was erected using concrete blocks, with an additional reinforced concrete (RC) floor placed atop the pre-existing timber floor. It's noteworthy that the original timber floor served as the roof when the house was initially built as a single-story structure. Unfortunately, the second floor has suffered a complete collapse, primarily due to the substantial increase in structural load. This catastrophic event has also inflicted severe damage upon the floor of the first level.

The visual representation in *Figure 115* serves as a stark reminder of the potential hazards associated with deviating from established construction norms in earthquake-prone areas. Neglecting or disregarding traditional construction wisdom in seismic regions can have devastating consequences. This serves as a powerful illustration of the critical importance of gaining a profound understanding of local building practices and the imperative to integrate proven techniques for bolstering structural integrity and earthquake resilience.

c) *Hımış*

Hımış is the building typology that characterises traditional built environment in Türkiye and are also common in Greece and the Balkans (Aktaş et al., 2022b). This typology (*Figure 118*) can be categorised as a hybrid system due to its integration of two distinct structural systems within a single building (Aktaş, 2017). Typically, the ground level

comprises load-bearing masonry walls (URM), while the second level incorporates timber elements to reinforce either masonry walls or timber frames filled with masonry. In cases where frames are employed on the second level, the infill panels may consist of materials such as stone, adobe, or wooden cladding (*bağdadi*). This cladding technique involves the use of timber laths and plaster to enclose the structure.

Figure 118: Hımış a) Detail of the wooden (bağdadi) cladding; b) timber frame filled with masonry.

Interestingly, similar types of failures have also been observed in traditional buildings with timber frames and masonry infills. However, these buildings have exhibited a superior response to earthquakes compared to URM constructions, which is in line with previous observational (Aktaş, 2017), analytical (Aktaş and Turer, 2016) and experimental evidence (Aktaş et al., 2014). While they may have experienced some damage, they have managed to meet life-safety requirements, demonstrating a higher level of resilience. The incorporation of seismic-resistant elements in traditional buildings, such as timber tie beams that provide additional stability, lintels that distribute loads effectively, frames that offer structural strength, and carefully crafted corner joints that enhance connections, has proven beneficial. These features contribute to the overall performance of the buildings during seismic events, allowing them to withstand the forces generated by earthquakes to a greater extent.

The data and observations presented here are based on three missions deployed on four affected provinces (Kahramanmaraş, Hatay, Malatya and Osmaniye), the latter two of which are specifically focussed on *hımış* structures (see Section 0 and Section 4.2.5 for more details). Accurate vulnerability assessment of *hımış* is critical in order to develop a reliable estimation of the expected performance of a considerable traditional civil architecture stock in Türkiye and beyond under the threat of earthquakes. During these two deployments, a detailed survey generated in ArcGIS-based Survey123 was utilised. The design of the survey aimed to collect and included some key components: geometry; structural materials and details; construction techniques; restoration, interventions, and originality; first damage assessments; environmental exposure on timber frame; damage mechanisms and failure modes. The earthquake damage assessments, conducted on 189 structures in four provinces

(*Figure 119*), utilised the EMS-98 scale approach for the on-site initial evaluations due to the absence of a *hımış*-specific damage scale. The focus of the assessment included performance of masonry infill and that of timber frames, and their structural integrity, formulated specifically around the repairability and importance of damage in terms of the overall structural safety. Preliminary analysis of the collected data revealed that 31% of the assessed buildings, totalling 59 structures, were assigned a damage grade of DG4+, associated with out-of-plane (OOP) failure and in-plane (IP) degradation of infill walls, along with connection and stability issues in timber posts. The approach adopted here accounted for the hybrid nature of the load bearing system of *hımış* at different floor levels.

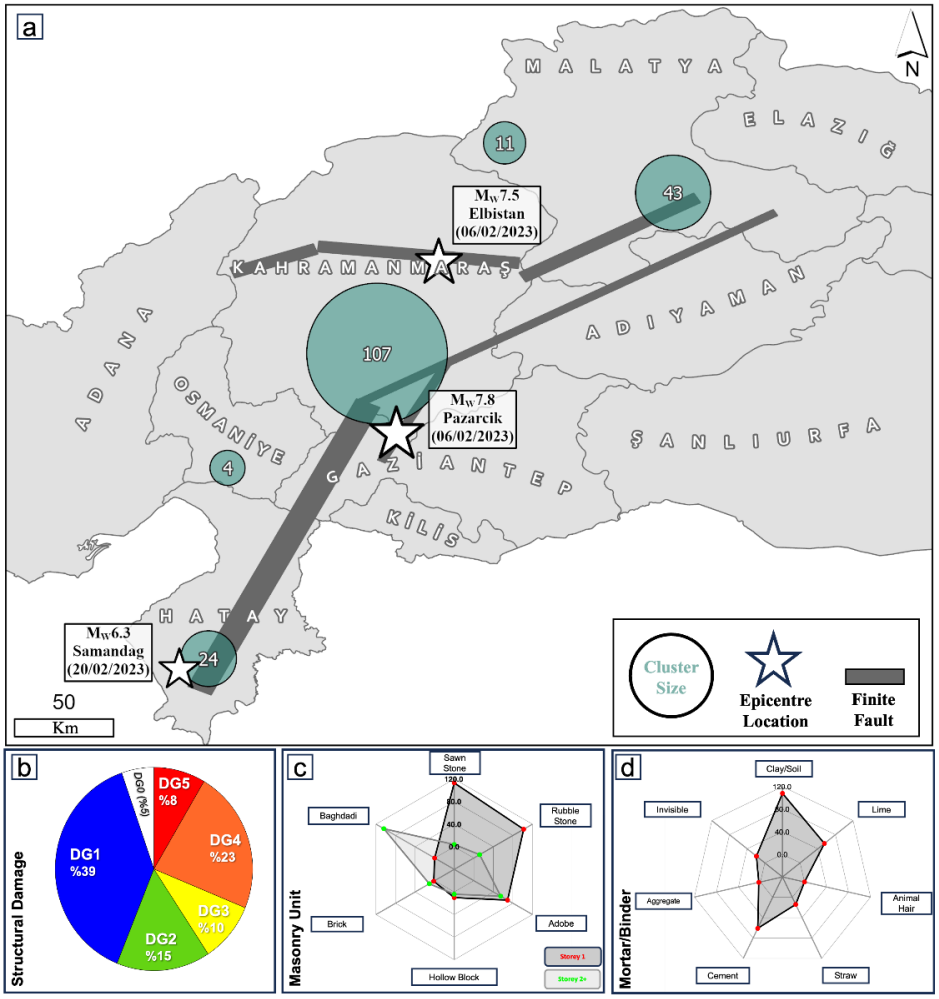

Figure 119: Breakdown of the data collected in June and September\October missions: (a) February 6 earthquakes (MW7.8 and MW7.5), MW6.3 earthquake on February 20, and geographic distribution of hımış clusters (N=189); (b) Initial on-site damage assessments; and masonry materials: (c) masonry units per floor and (d) observed binders.

Data analysis by the team towards entangling the seismic vulnerability of different *hımış* sub-typologies is continuing. However, preliminary key messages are as follows:

- That a high proportion of our surveyed *hımış* buildings received limited damage is in broad agreement with the existing experimental and analytical evidence and post-disaster observations as to the seismic reliability of these structures. Further, most of the highly damaged buildings were observed to have had fallen into disuse and hence be suffering from significant material and

component degradation, and/or built on a masonry ground floor with poor seismic resistance (for example, one with rubble stone masonry with poor quality binder and/or without and tie-beams) which failed and acted as a trigger for damage elsewhere.

- Due to the lack of a ***hımış*** specific damage categorisation system, and also because damage assessment personnel/volunteers do not have training or experience in damage assessing this typology, the buildings surveyed by our team were almost exclusively tagged with overestimated damage levels. Unless objected by the resident (which is a rare incident) this means that many ***hımış*** buildings will be demolished despite the fact that the damage is for example limited to the infill in timber framed upper storeys and can be easily repaired (e.g. *Figure 120*).

Figure 120: A hımış building in Kahramanmaraş officially categorised as heavily damaged and will therefore be demolished despite the fact that the damage is limited to out-of-place failure of the infill on one portion of one façade.

4.3.3. Monumental Buildings

4.3.3.1. Geographic Focus

The eleven Turkish provinces affected by the 2023 Türkiye-Syria Earthquake Sequence feature historic cities which are home to numerous monumental structures. To choose an area of focus for the EEFIT fieldwork, the shortest distance from various historic centres to the surface projection of the rupture plane of the 6 February Earthquake is investigated in *Figure 121*. Some districts with historic built environment in the province of Hatay (Antakya, İskenderun, Samandağ and Altınözü) are close to the ruptured fault plane. The epicentre of the destructive aftershock on the 20th of February, was also in this region. This proximity and the reports of widespread damage in the province led team members to focus their attention on monumental structures in Hatay. Although structures in all parts of the Hatay province were examined remotely, the focus of the field team was on the districts of Antakya, İskenderun, Samandağ and Altınözü. A small number of monumental structures were also surveyed in the neighbouring province of Osmaniye, particularly in the centre of Osmaniye and the districts of Bahçe and Kadirli.

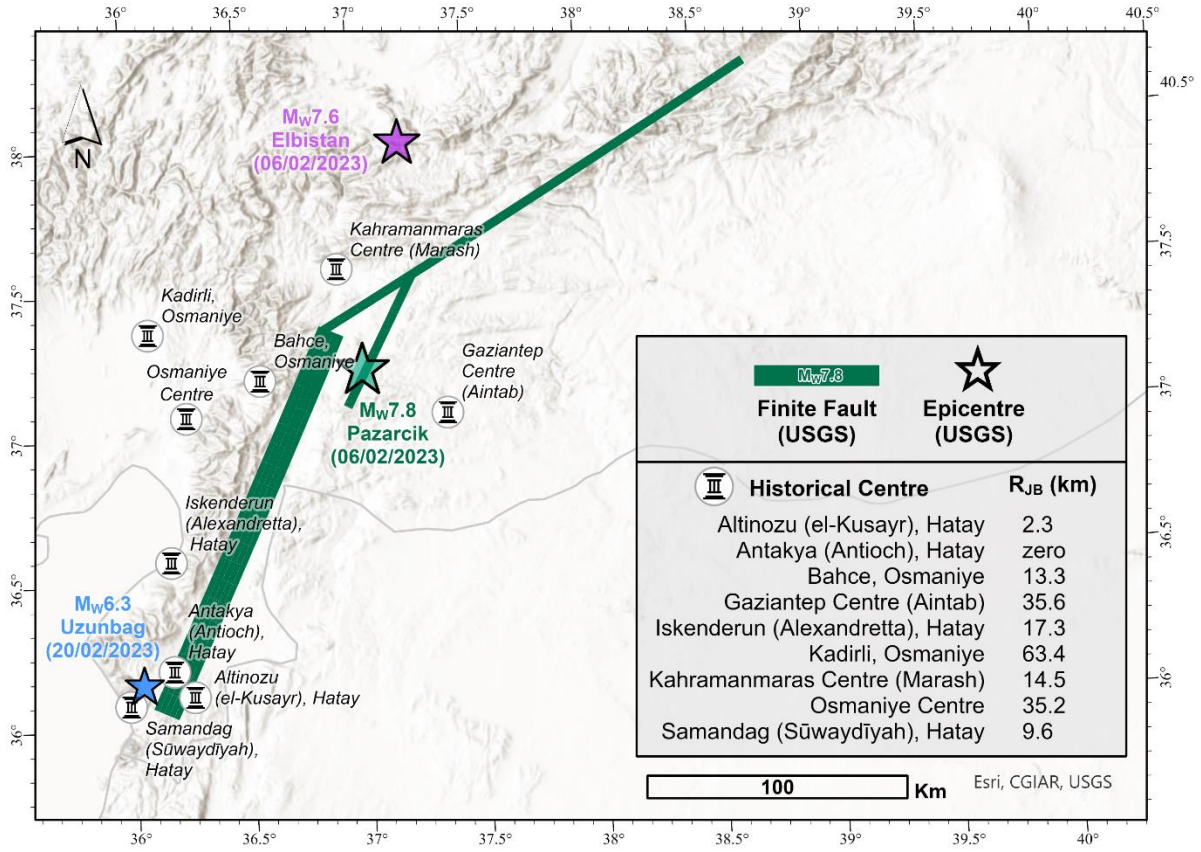

Figure 121: Joyner-Boore Distance (RJB) of historic urban centres in provinces affected by earthquakes. The map highlights the surface projection of rupture plane for the MW7.8 mainshock on February 6, 2023.

4.3.3.2. History of the Region

Hatay has been "an important confluence of states, faiths and peoples from its earliest times" (Abrahamczyk et al., 2017). The earliest human settlements in the Hatay region date back to 40,000 BC or earlier. Before the Hellenic Period, Hatay was ruled by the Hittites, the Urartians, the Assyrians and the Persians. Alexandre the Great conquered the area around 333 BC, following the battle of Issus. In the year 64 BC, Antakya became a part of the Roman Empire. During the 2nd and 3rd century, it was the third most populous metropolis in the Roman Empire. The area passed over to Byzantine rule following the division of the Roman Empire. Later, it was conquered by the Islamic army in 638 and was ruled by the Umayyad and Abbasid kingdoms. The province, which again joined the territory of the Byzantine Empire in 969, also played an important role during the Crusades. Antakya was taken from the Crusaders by the Mamluks. In 1516, Yavuz Sultan Selim conquered a large area including Hatay and the Ottoman Period began. The region was taken over by French forces after the First World War. Hatay remained under the French mandate for 18 years before the establishment of the independent Hatay State. Hatay State was annexed to the Republic of Türkiye in 1939.

4.3.3.3. The Historic Built Environment

Historical records, spanning more than 2000 years, describe frequent major earthquakes in Hatay (Över et al., 2011). For this reason, only a small number of pre-

Ottoman monumental structures survive today (*Figure 122*). In particular, the most recent major earthquakes during the 19th century are known to have caused significant loss of life and destruction.

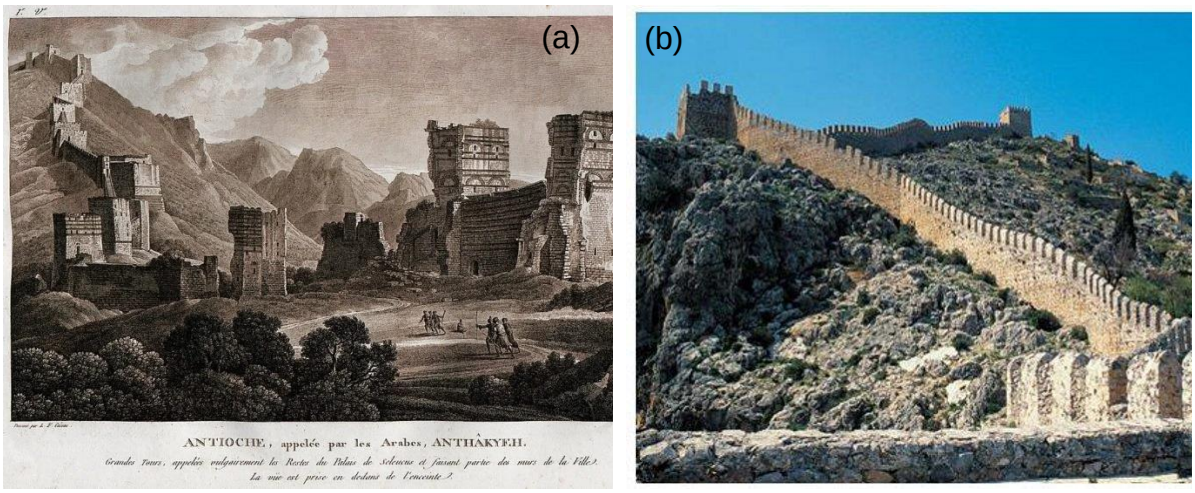

Figure 122: (a) Louis Francois Cassas' 19th century engraving of the ruins of the Seleucid palace in Antioch (known today as Antioch castle), which was damaged during the 526 earthquake. (b) A contemporary photograph of the walls and the towers of the palace. Credit: (a) https://greekreporter.com/2022/12/03/history-hellenistic-city-antioch/, (b) https://secreTürkiye.com/surlari-ile-meshur-antakya-kalesi.html

Ottoman-era buildings that are mostly encountered in Hatay today are religious buildings, particularly mosques and tombs. Churches and a small number of synagogues can also be found in historic urban centres. Ottoman public buildings, such as markets, madrasahs, and baths, are also encountered. The Westernisation of the Ottoman Empire during the late 19th century started a transformation in the built environment. Besides the traditional Ottoman structures, buildings for schools, hospitals, banks, museums and new administrative units started to be constructed (Garbioglu, 2017). A notable number of public monumental buildings which were constructed during the French mandate survive today.

Monumental residential structures also form an important part of the built environment. Traditional Antakya houses are 1-2 storey mixed masonry-timber constructions built around an open courtyard (Demir, 2014). Remaining structures mostly date from the 18th and 19th century. The traditional stone houses of Samandağ are clustered in the villages of Vakıflı, Kapısuyu, Hıdırbey, Eriklikuyu and Batıayaz. These buildings are thought to date from the 19th and early 20th century, where a significant Armenian population lived in the area (Surmeli, 2019). Although most of these buildings are 1-2 storey vernacular constructions, several of them have larger proportions and are listed. They will also be discussed in this section.

4.3.3.4. Management of Monumental Historic Buildings

Many traditional Ottoman structures in Türkiye, including religious (e.g., mosques and tombs) and public (e.g., madrasahs and baths) buildings, are owned by the Directorate General of Foundations (*Vakıflar Genel Müdürlüğü*). The Directorate manages around 18,500 historical buildings (VGM, 2007), this corresponds to approximately 15% of all immovable cultural property that is under the care of the Ministry of Culture and Tourism (TC Kültür ve Turizm Bakanlığı, 2022). Approximately 100 historic buildings managed by the Directorate are in the provinces of Hatay and Osmaniye. Besides

Ottoman structures, the Directorate owns other religious (e.g., churches), public (e.g., shops) and residential buildings of historic value. The Directorate has the responsibility to manage and restore its historic estate. Aside from the Directorate General of Foundations, various other state organisations own and manage historic estates. For instance, the Directorate of Religious Affairs (*Diyanet İşleri*) is responsible for running a number of historic mosques, while the Ministries of National Education and Health (*Milli Eğitim Bakanlığı* and *Sağlık Bakanlığı*, respectively) manage historic school and hospital buildings, which continue to be used today. Foundations representing minority groups may have ownership of their religious buildings. Some historic structures are privately owned and the responsibility to maintain these structures lies with the owner.

Specialised local government organisations (known as Protection, Application and Inspection Offices, *Koruma Uygulama ve Denetim Büroları, KUDEB*) are responsible for assessing the compliance of routine maintenance and minor repair projects carried out on listed historic buildings. More extensive construction activities, which may involve strengthening, are managed by the Ministry of Culture and Tourism via regional conservation boards (known as *Kültür Varlıklarını Koruma Bölge Kurulu*). Members of these boards are typically conservation professionals, architects, art historians and archaeologists. While seismologists, geotechnical and structural engineers may occasionally serve in these committees, their representation in these committees is not required. Projects relating to listed historic buildings in Hatay and Osmaniye provinces are managed by the Hatay Conservation Board.

This section demonstrates that there is a complex ownership structure for monumental buildings. Different state organisations own historic buildings, while private ownership is also common when it comes to cultural assets of minority communities. The responsibility to maintain and manage these buildings lie with the owners although intervention projects are overseen by either local governmental structures or committees elected by the Ministry of Culture and Tourism.

4.3.3.5. State of Monumental Historic Buildings Before the Earthquakes

There is limited information on the construction details and earthquake vulnerability of monumental masonry buildings in the Hatay region. Although several studies investigated the architectonic characteristics of monumental buildings in Hatay, engineering investigations on materials, construction details and earthquake vulnerability lack in the scientific literature. A joint research project funded by Turkish and German governments provides useful preliminary information on masonry buildings in Antakya (Erberik et al., 2013), although the focus of this study is on vernacular buildings.

The EEFIT fieldwork (to be discussed next in 4.3.3.6) indicated that the investigated monumental structures in Hatay and Osmaniye were well-maintained in general, with a few exceptions. Many buildings showed signs of recent maintenance and repair activities. Some of the investigated buildings were reported to have been restored or restituted recently; generally, these restoration projects do not appear to have involved strengthening. The most common significant alteration to buildings during restoration and restitution projects appeared to be the replacement of floor structures.

4.3.3.6. Description of the EEFIT Field Study

Monumental structures that were examined during the EEFIT fieldwork were identified with a prior desk study. Information on the internet and advice from local contacts were used to choose the most affected structures that will be investigated on site.

The primary goal of the field study was to quantify the damage in monumental historic structures following the earthquake sequence. The methodology and results of the preliminary damage assessment is discussed in Section 4.3.3.7. Some key observations, derived from the evaluation of construction practices and damage patterns, is discussed in Section 4.3.3.8.

In addition to the above, to evaluate the geometry and material properties of monumental structures, data was collected on site. A second field study was conducted for this purpose between the dates 11 and 19 April. Laser scanning and photogrammetry were used to record geometry (*Figure 123a*) while non-destructive testing techniques (such as rebound hammer, mortar penetrometer and Ultrasonic Pulse Velocity measurements, *Figure 123d*), were used to quantify material properties. The data is currently being processed and will not be discussed in this report. However, the data will be made available to the research community once processed.

Figure 123: Views towards the northern nave wall of Latin Catholic Church in İskenderun; (a) point cloud of the structure obtained from terrestrial laser scanning. (b) the nave, aisles, colonnade system as photographed in November 2019 (Credit: Google Maps; Adrian E. Loza). (c) the damage observed in April 2023, with the total collapse of the cross vaults of western aisle and the nave, and (d) Ultrasonic Pulse Velocity measurements.

4.3.3.7. Damage Assessment Results

Shortly after the earthquakes, the Ministry of Environment, Urbanisation and Climate Change tasked engineers to rapidly evaluate damage in buildings. These included monumental buildings, most of which are of masonry construction. The procedure that was used to assess damage relies on a staged evaluation (Ilki et al., 2020). During the first stage, the exterior of the building is evaluated. If there is total or partial collapse, or residual floor drifts more than 1% or wall tilts greater than 3°, damage is classified with the letter 'D' corresponding to 'Very heavy damage'. If the damage in the building is not classified as heavy and deemed safe to enter, a new classification is proposed depending on crack width observations. For instance, buildings with cracks smaller than 1mm width are classified with the letter A (corresponding to 'Light' damage) and cracks greater than 10mm are classified with the letter 'C' or 'D', corresponding to 'Heavy' or 'Very Heavy' damage.

The classification method adopted by the Turkish state requires direct measurement of cracks which was often infeasible. Due to this limitation and the wish to relate the results of this field study with prior studies, widely adopted European Macroseismic

Scale 1998 (EMS-98) damage assessment approach was used (Grünthal, 1998). In this method, a graphical abaqus (mainly considering criteria such as wall/roof failures, and pattern/spreading/frequency of cracks) is used to evaluate the global structural damage. This enables a rapid preliminary evaluation of damage. During the EEFIT fieldwork, monumental structures were uniformly evaluated through assigning a damage grade (DG; 0 to 5) to each asset. Most of the structures in the figures were visited by the EEFIT team. However, a small minority of these structures were either evaluated using publicly available photographs or satellite imagery from the internet or from collaborators and local contacts (e.g., Ulu Mosque and Yeni Mosque in Antakya). Efforts are under way to expand the list and make the photographs and the associated damage assessment results publicly available. All of the examined structures are masonry constructions. Nearly all buildings are constructed of stone masonry (see Section 4.3.3.8 for further details).

The monumental structures have been divided into five geographical clusters (based on districts), the name and location of each cluster is shown in *Figure 124*. As displayed in the same figure, the focus of this research has been the historic centres surrounding the 160 km long southern segment of the ruptured fault during the Pazarcık earthquake. The majority of monumental structures in our dataset are located in Hatay; these structures have also been impacted by the M_W 6.3 Uzunbağ aftershock on February 20. According to those interviewed during the field deployment, the Uzunbağ event, which occurred at the intersection of Antakya and Samandağ, significantly increased the extent of the damage in Samandağ, Altınözü and Antakya.

Figure 125 summarises the earthquake damage to structural types, covering the entire monumental building dataset (N=33). The most striking observation in this set is that almost half of the mosques and the majority of churches were classified at DG4 (*very heavy damage*), meaning that their structural integrity was severely compromised as they suffered partial/total collapses of primary structural components. Further details are reported on a cluster basis. The content between *Figure 126* and *Figure 130* reports the names, locations and types of monumental structures alongside their EMS-98 global damage criteria.

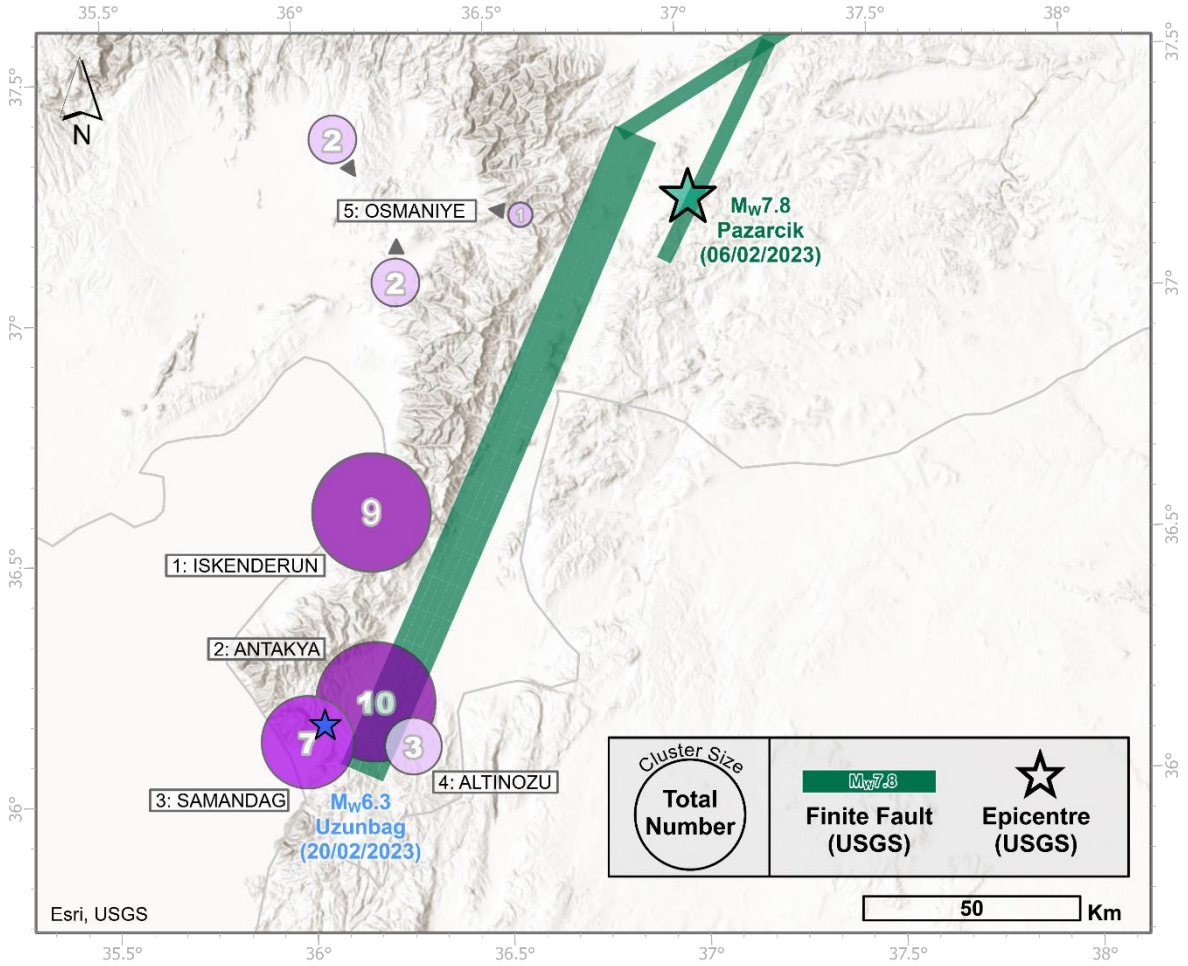

Figure 124: The distribution of monumental structures within the five clusters that have been the geographical focus of field deployments in provinces of Hatay (N=29; Antakya, Altınözü, İskenderun and Samandağ districts) and Osmaniye (N=5; the city centre, Bahçe and Kadirli).

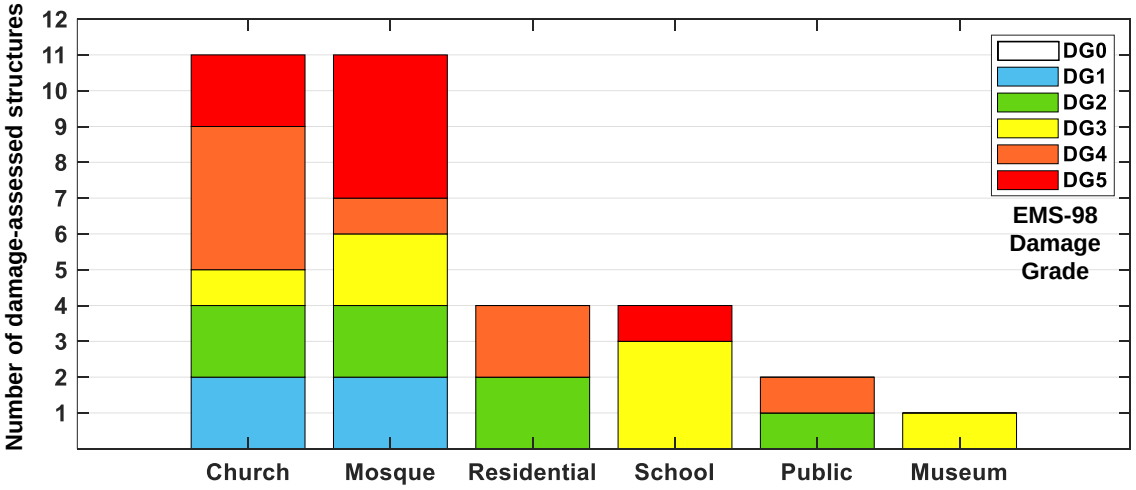

Figure 125: The breakdown of the damage induced by earthquake sequence per asset type.

Cluster-wise, the statistical interpretation of damage assessments is shown *Figure 131* depicting the median damage grade, extent and quartiles (25% & %75) of damage suffered. Combining damage criteria with the SGM characteristics of the Pazarcık event, each cluster is represented by a single resultant PGA value from stations

nearby. Their IDs, distances to their cluster, resultant PGAs, and horizontal XY trajectories of displacement are given *Table 6*. The trajectories show that the ground displacements were predominantly in the East-Westerly or North-Westerly directions, corresponding to the Fault-Normal direction.

DG4, as a median, was observed in both Antakya (#2, *Figure 127*) and Altınözü (#4, *Figure 129*) clusters, where the PGA values exceeded 500 cm/s^2 on average. Among all, these two were nearest to the ruptured fault. While almost the entire Antakya historic centre was located within the surface projection boundaries of the rupture, the Altınözü cluster was at an approximate normal distance of 3 km from the fault. In addition to the increased performance demand due to near fault effects, both extensive vertical shaking and poor local site conditions in Antakya may have been other agents of damage.

Cluster 1 in İskenderun, features churches and school buildings and has a median damage grade of DG3 (*Figure 126*). Structures with DG4 or DG5 experienced global out of plane collapse. The failure directions generally corresponded to weak axes of these structures, where lateral supporting systems are weaker. DG4 was limited to (partial) failures in a single façade.

Monumental structures in Samandağ Central and its rural areas built on the southern end of the Nur Mountain range (comprises the Cluster 3. These were classified with a median damage of DG3. When all the structures are grouped based on their R_{JB}s (varying between 8.2 and 11.7 km) and local site conditions (C or D, based on the classification of NEHRP), see *Figure 132*, the median damage grade reduces to the DG2 in the group of structures located on the mountain range. As mentioned previously, another highlight for the cluster 3 (and partially Cluster 2) is that it was also exposed to the 20 February M_W6.3 earthquake (with the mean R_{EPI} of 5.50 km); this aspect was not accounted for in the simple comparisons above which utilised seismological parameters from Pazarcık event only. Witness reports suggest that the significant damage levels in Samandağ Central may be largely attributed to the 20 February earthquake.

Cluster 5, Osmaniye, has the lowest median damage value, DG2. Three subclusters with varying R_{JB} properties (between 13.0 and 63.0 km, *Figure 132*) are displayed in *Figure 130*. In central Osmaniye, failure of the outer leaf and wide in-plane cracks in numerous wall segments were evident in structures coded by C5.1 and C5.2, which were classified in DG3. On the other hand, DG1 was assigned to structures coded by C5.4 and C5.5 in Kadirli, where the R_{JB}>60 km.

The suffered damage was displayed in *Figure 132* in relation to both the rupture proximity and local site conditions. Firstly, this representation shows the role of local site conditions in clusters of C2 (Antakya) and C3 (Samandağ); the damage grade increased by poorer site characteristics, i.e., reduced V_{S30} values. Secondly, another result gained is that the damage suffered by these monumental structures is the most significant in near-fault, which is evident among clusters by an increase with decreasing fault proximity, i.e., R_{JB} distances.

This section summarises the extent of damage to the historic built environment, mostly in Hatay and partially in Osmaniye, by interpreting its correlation to seismological parameters. To quantify damage, the EMS-98 criteria is used, which enables rapid damage classification. However, the use of a single scalar measure to quantify

damage in masonry buildings with various structural components is not always satisfactory. It is often necessary to evaluate damage levels in different components (e.g. different floors or components) to deliver a more nuanced interpretation of damage and determine appropriate short-term countermeasures. In the future, the use of more detailed damage assessment forms (such as the AeDes form, see (Baggio et al., 2007)) will be explored in lieu of the EMS-98. This will enable quantitative exploration of the links between construction characteristics (collected as a part of the forms) and more detailed evaluation of the damage sustained during the earthquakes. Furthermore, the use of alternative damage quantification techniques for churches (Lagomarsino & Podestà, 2004) and the adoption of these techniques for mosque and tomb structures will be explored. Future investigations will also examine seismological parameters from the other earthquakes in the sequence, to evaluate their impact.

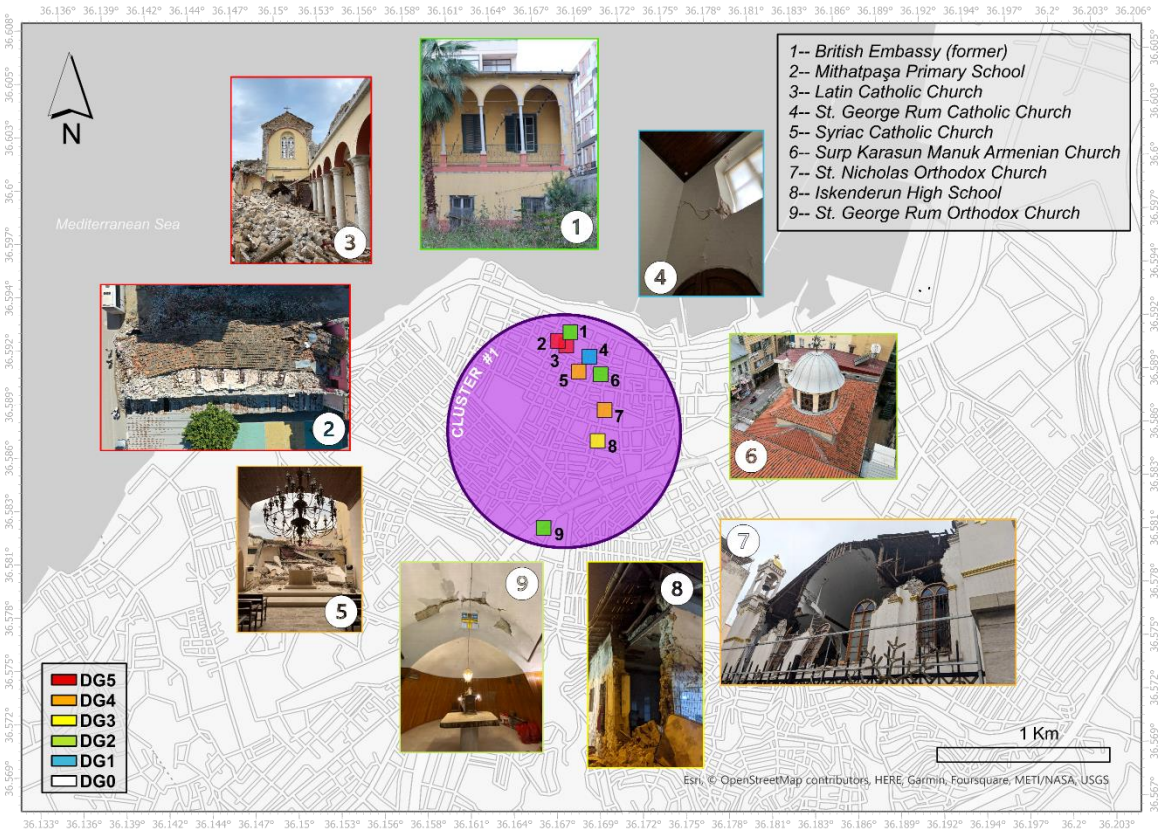

Figure 126: Cluster 1: Historic urban centre of İskenderun.

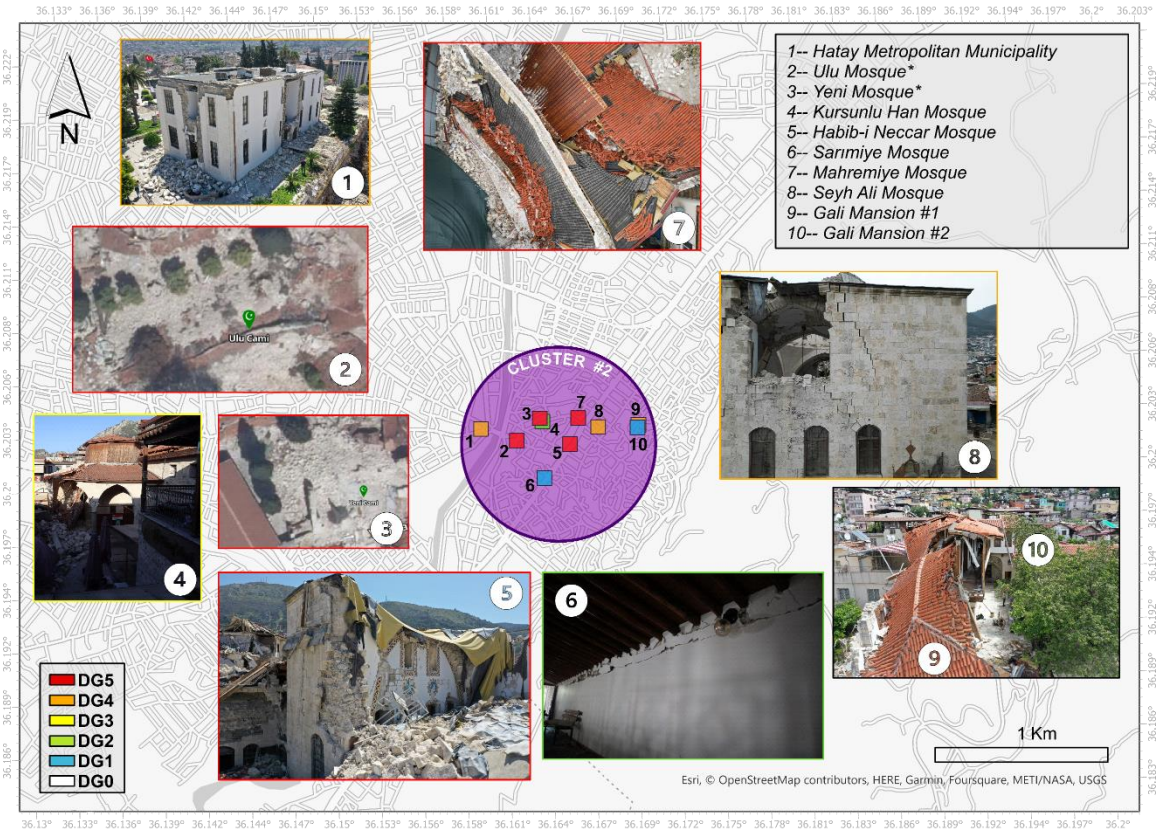

Figure 127: Cluster 2: Historic urban centre of Antakya (*satellite imagery from atlas.harita.gov.tr).

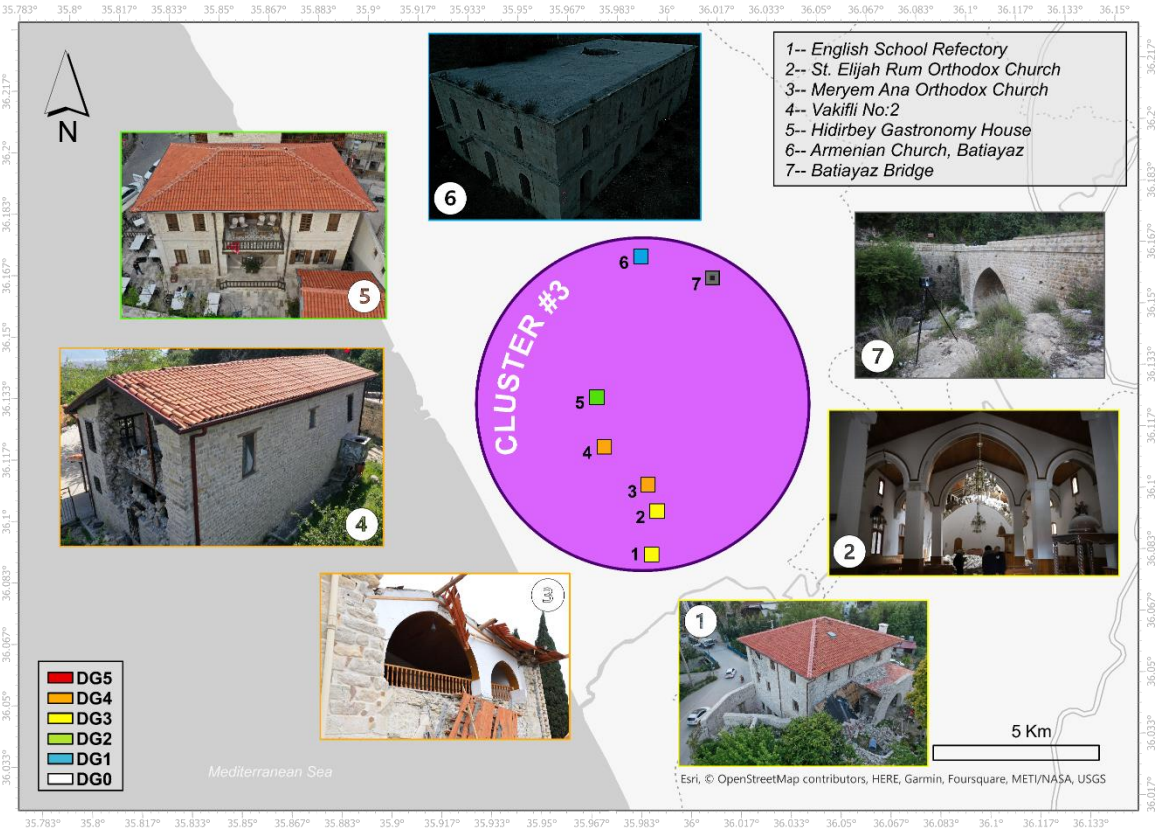

Figure 128: Cluster 3: Monumental assets in Samandağ as well as its rural settlements.

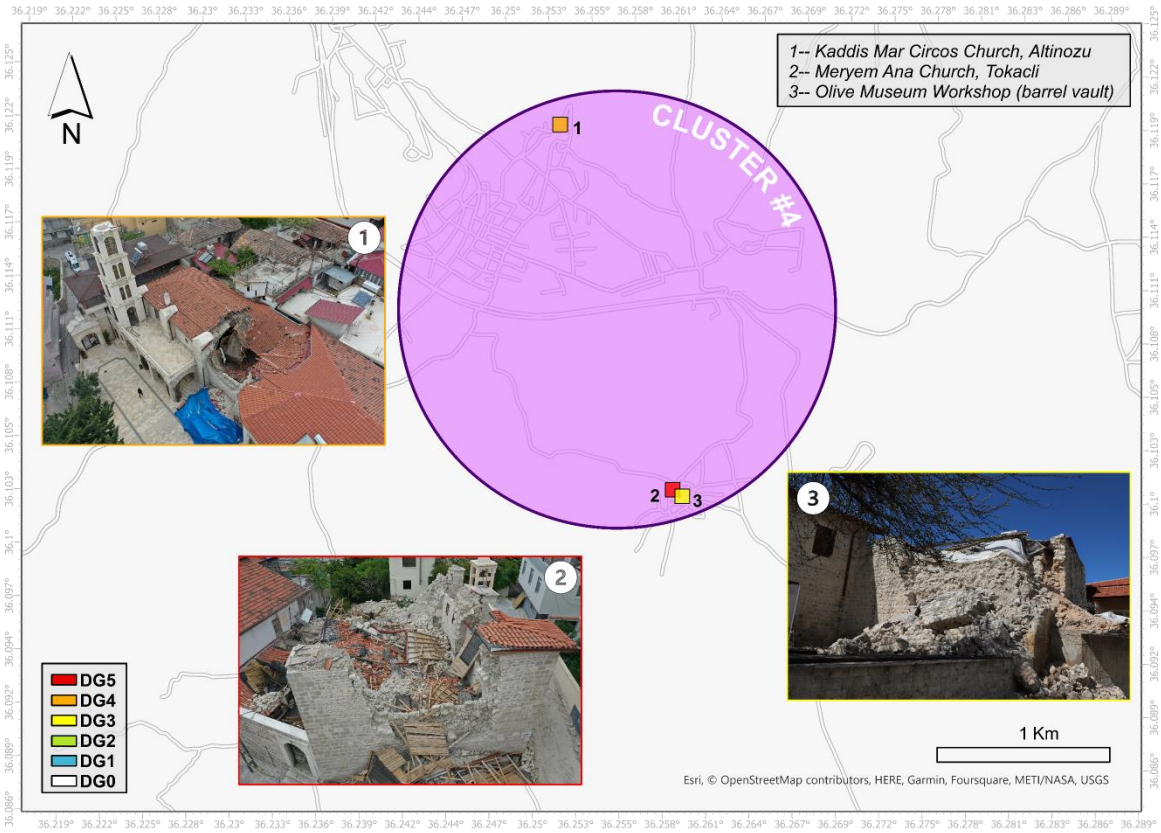

Figure 129: Cluster 4: Altınözü and Tokacli.

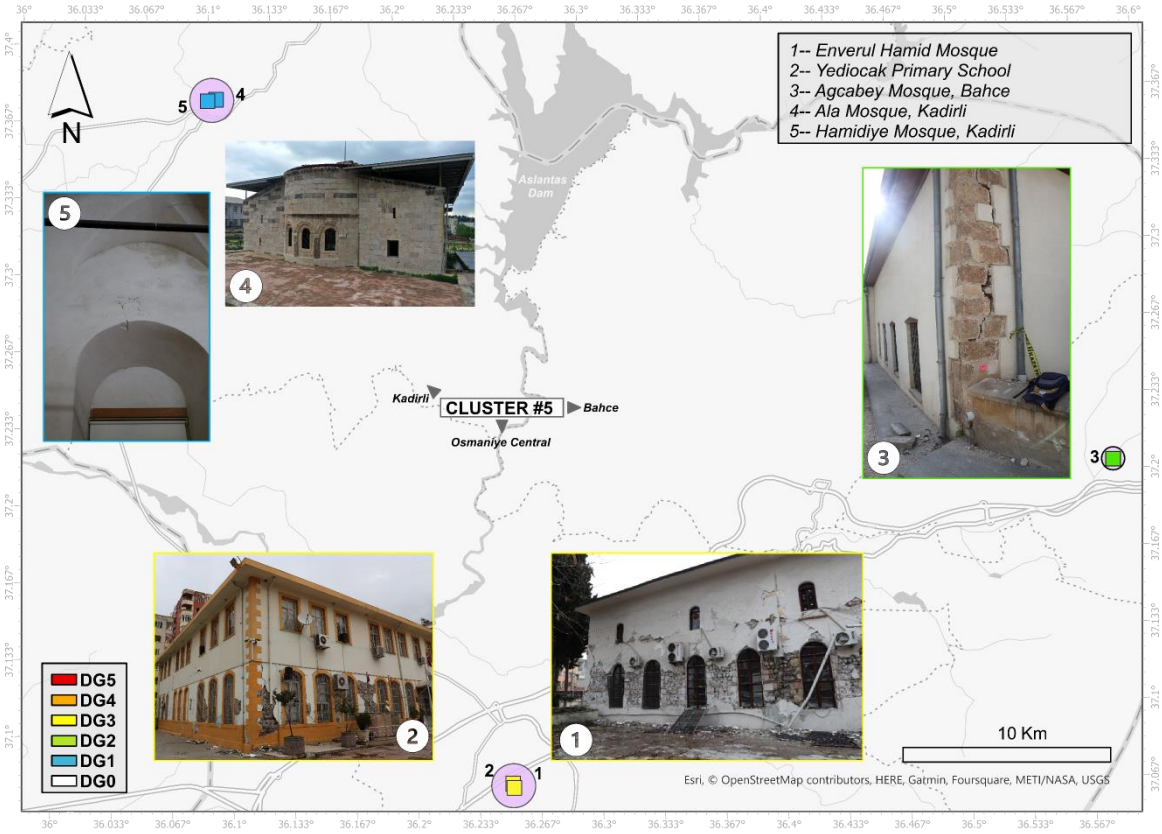

Figure 130: Cluster 5: Monumental structures in Osmaniye central and its districts Bahçe and Kadirli.

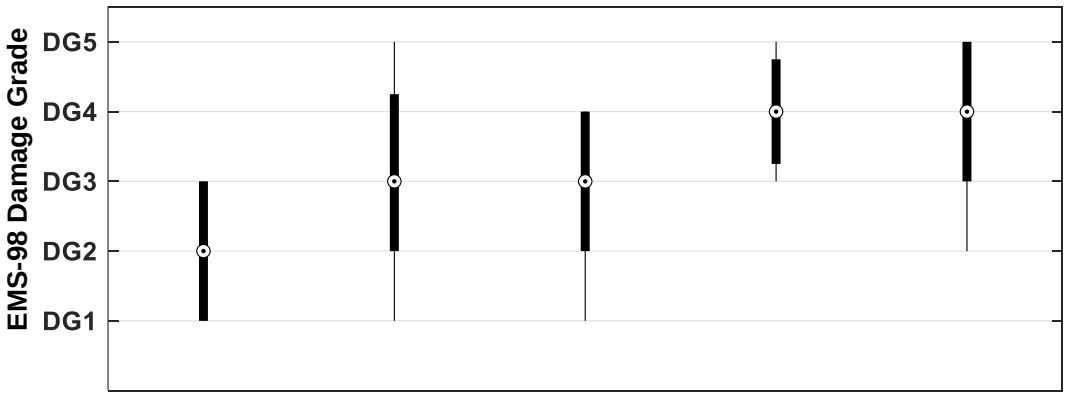

Geographical Cluster	Osmaniye (n=5)	Iskenderun (n=9)	Samandag (n=6)	Altinozu (n=3)	Antakya (n=10)
PGA_R (cm/s^2)	218	247	259	530	537

Figure 131: Statistical box plots summarising the main properties of the damage to monumental structures in each cluster, which ordered based on the resultant Peak Ground Acceleration levels from the Pazarcık event. Geometric means were taken for those clusters represented by more than one SGM station (İskenderun, Antakya and Osmaniye).

Table 6: Summary of the nearby SGM station(s) selected in each cluster: Station code, its distance to clusters, resultant horizontal peak ground acceleration recorded during the Pazarcık event, and azimuth of the horizontal maxima of peak ground displacement (blue: fault-normal direction, red: fault-parallel direction).

Cluster	Station ID	Distance to Cluster Centres (km)	V_{S30} (m/s)	Resultant PGA (cm/s^2)	Particle Motion (cm)
1: İskenderun	3115*	4.4	424	328.60	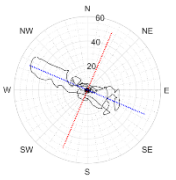
	3116	4.6	870	185.66	
2: Antakya	3123	1.4	470	651.00	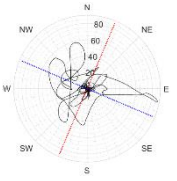
	3131	1.2	567	417.63	
	3132	0.8	377	569.59	
3: Samandağ	3140	6.0	210	259.85	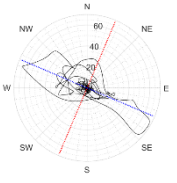

4: Altınözü	3136	1.0	344	530.87	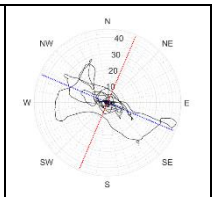
5: Osmaniye	8002	2.3	430	283.77	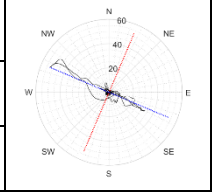
	8003	2.0	350	190.51	
	8004	0.8	426	193.47	

Figure 132: 3D scatter plot of cluster-based damage variation with VS,30 (Okay, 2022) and distances to the finite fault of the Pazarcık event, RJB. Structures are also grouped based on their local site conditions (based on NEHRP) and RJB (CX.Y; where X is cluster number, Y indicates the structure number as depicted in cluster damage figures.

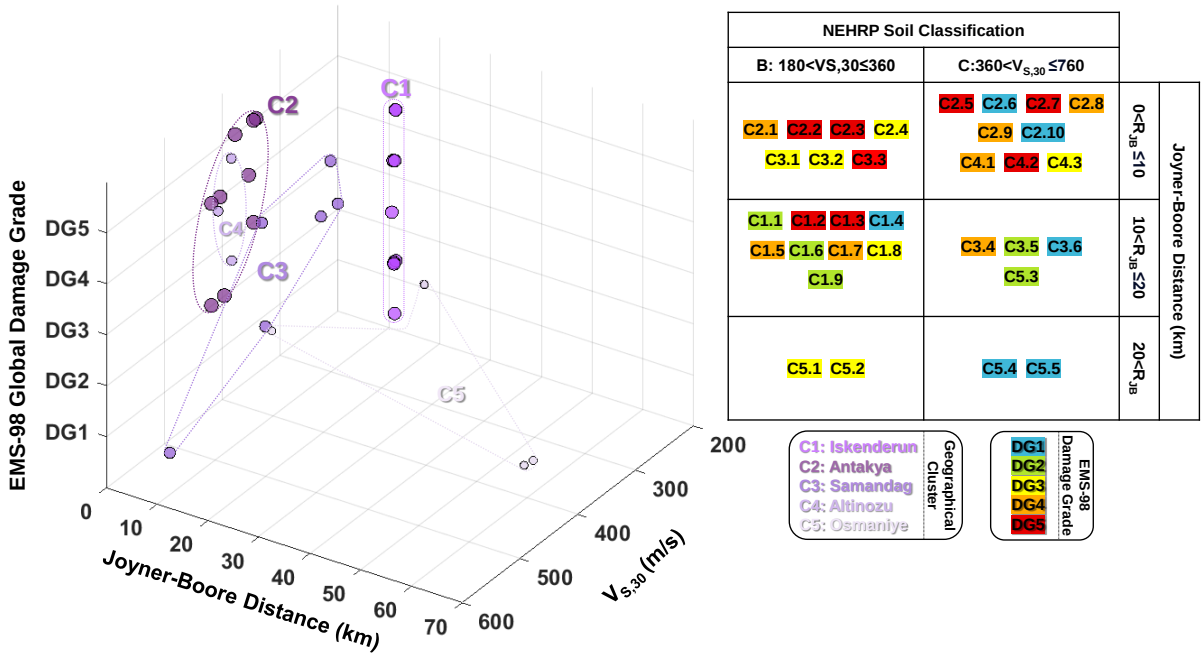

4.3.3.8. Key Observations

This section discusses the key observations from the EEFT field investigation. Some of these observations relate to the construction details of structural components, such as walls, floors and roofs. Although each monumental structure is unique, there are similarities between the construction details adopted in different structures. These details have a significant influence on earthquake response of structural components. This section aims to identify the key details that make structural components more susceptible to damage.

a) Bearing walls

Due to the local availability of stone, most of the historic monumental structures in Hatay are constructed of stone masonry. Mortar is typically present and is used to bond stone units to one another. While detailed information on the constituents of

mortar used in Ottoman buildings in Hatay is not available, previous related studies refer to the use of 'lime' and 'mud' mortars (Erberik et al., 2013). Walls are generally thick and multi-leaf wall construction is commonly adopted.

In multi-leaf stone wall construction, the space between the outer leaves of stonework is infilled with rubble. In some monumental structures, the outer leaves are constructed from ashlar masonry. Ashlar masonry is characterised by finely cut and regularly arranged stone courses. Alternatively, outer leaves can be constructed from rubble masonry. Stones in rubble walls are irregular; they are either uncut or roughly cut. It is not uncommon to use stones salvaged from other structures (*spolia*) or collected from riverbeds. As such, stone shapes, sizes and arrangements vary significantly in rubble walls. To facilitate construction and enable interlocking between stones in rubble walls, a large amount of mortar is needed. For this reason, the mechanical properties of mortar play a more significant role in the behaviour of rubble stone walls than in ashlar masonry.

The use of metal and timber reinforcing elements in masonry structures dates back to Antiquity. Metal cramps and pins, or timber tie-beams may be used to tie stone walls together. They are commonly used in Ottoman architecture from the 16th century onwards (Tanyeli, 1990). Use of metal and timber reinforcing elements was not commonly observed in Hatay and Osmaniye. There were two noteworthy exceptions to this. In the ruins of several minarets, including the minaret of Habibi Neccar Mosque, metal clamps were found. The Enverul Hamid Mosque in Osmaniye, was the only monumental building surveyed, whose walls featured timber tie-beams.

A scientific evaluation of the quality of multi-leaf masonry wall construction in Hatay was not available in the scientific literature surveyed for this study. While a comprehensive evaluation requires field and laboratory tests on masonry constituents and components, a qualitative evaluation can be carried out using the Masonry Quality Index (MQI) (see Borri et al., 2015). MQI evaluates the quality of masonry wall constructions by evaluating the presence, partial presence, or the absence of certain good construction practices. For instance, it is considered that a well-maintained wall constructed with large ashlar blocks arranged in an interlocking pattern with good mortar will result in high quality masonry that will have high resistance against earthquakes. To quantify this observation, parameters were proposed to evaluate the conservation state, stone dimensions, stone shapes, wall leaf connections, bonding patterns, and mortar properties. Each parameter is evaluated and graded according to the classes F (fulfilled), PF (partially fulfilled) and NF (not fulfilled). MQI is then calculated using a simple formula which weighs parameters according to their importance. For instance, if the out of plane resistance of walls is of interest, then the parameter describing the quality of wall-leaf connections (denoted by WC) is weighed the most. In the following discussion, MQI is characterised to evaluate the out of plane resistance of the load bearing walls of several monumental structures, see *Table 7*.

Table 7: Masonry Quality Index (MQI) for the load bearing walls of three monuments (F = Fulfilled, PF = Partially Fulfilled, NF = Not Fulfilled).

Indicator:	SM, Conservation State	SD, Stone Dimension	SS, Stone Shape	WC, Wall-leaf connection	HJ, Bed joint horizontality	VJ, Vertical joint stagger	MM, Mortar properties	Masonry Quality Index
Weight:	1	1	2	3	2	1	1	
İskenderun High School	PF	PF	PF	NF	F	PF	PF	3.9
Habibi Neccar Mosque	F	F	F	NF	F	F	PF	6.5
Enverul Hamit Mosque	F	PF	NF	NF	NF	PF	PF	1.5

Figure 133 shows the İskenderun High School building (R_{JB}=17.2 km). Historical and architectural information on this early 20th century building can be found in Garbioglu (2017). Today, the building is disused and is in a poor state of repair. Water staining and associated stone and mortar degradation is evident. The outer leaf of the multi-leaf load bearing wall of this building is constructed from sawn stones and rubble. The southeastern corner of this building collapsed out of plane during the 6 February Pazarcık earthquake, which revealed a vertical cross-section of the eastern external wall of the building. This cross-section indicates that header stones which penetrate the thickness of the wall were not used. This enables the formation of vertical cracks which may lead to wall disintegration and out of plane collapse. Due to this poor wall-leaf connection, the critical WC parameter in MQI is rated as not fulfilled (NF). The MQI of this wall 3.9, which indicates poor construction quality.

Figure 133: İskenderun High School, photographs of (a) the west façade, (b) the collapsed south-eastern corner, (c) a multi-leaf wall cross-section from the collapsed southeast corner of the building.

Figure 134 shows the Habib-i Neccar Mosque in Antakya (R_{JB}=0 km, i.e., within the surface projection of the fault ruptured). Historical and architectural information on this

landmark monument can be found in Sanci (2006). The monument is thought to date back to the 13th century, with significant repair works completed during the 19th century. The ashlar external walls of this building are constructed using large and regularly laid stones. The northern wall of this mosque collapsed out of plane during the 6 February Pazarcık earthquake, which revealed a wall cross-section. Similar to *Figure 133*c, this cross-section in *Figure 134*c indicates that header stones which penetrate the thickness of the wall were not used. This poor detailing may have contributed to the out of plane collapse of the north wall. The critical WC parameter in MQI is rated as not fulfilled (NF) whereas all the other parameters are fulfilled (F). The MQI of this wall is 6.5, which indicates decent construction quality. However, regardless of overall quality, the damage sustained by the wall highlights that the connection between the wall leaves is critical.

Figure 135 shows the Enverul Hamit Mosque (R_{JB}=34.8 km) in Osmaniye, which is thought to date from early 20th century. The mosque has been heavily altered from its original construction during the building works in the 1970s; a reinforced concrete mezzanine floor and a reinforced concrete roof was added to the structure, along with supporting column and beam structures. The load-bearing walls of the mosque are constructed using rubble masonry. Round stones of varying sizes are used. Around the window openings large sawn stones and interlocking corner detailing can be observed. Three levels of timber tie-beams are also visible in the piers. The timber elements appear to be less than 5 cm high and 10 cm wide; interestingly, these are significantly smaller than the timber tie-beam elements of Ottoman structures surveyed in (Demir, 2012). The critical WC parameter in MQI is rated as not fulfilled (NF). Due to its poor rubble construction, the MQI of this wall is obtained as 1.5. Interestingly, despite its poor quality, the wall did not suffer out of plane collapse during the earthquakes and only experienced in-plane shear damage. However, signs of disaggregation were evident. The avoidance of out of plane failures despite poor wall quality should not be entirely attributed to the presence of timber tie-beams; while they may have improved the inter-leaf interactions, the presence of a well-connected rigid diaphragm appears to have allowed the structure to demonstrate ‘box behaviour’. A building with similar geometric characteristics, rubble wall construction and reinforced concrete floors in Osmaniye (the Yediocak school, see *Figure 130*) also demonstrated ‘box behaviour’ although it did not have timber tie-beams.

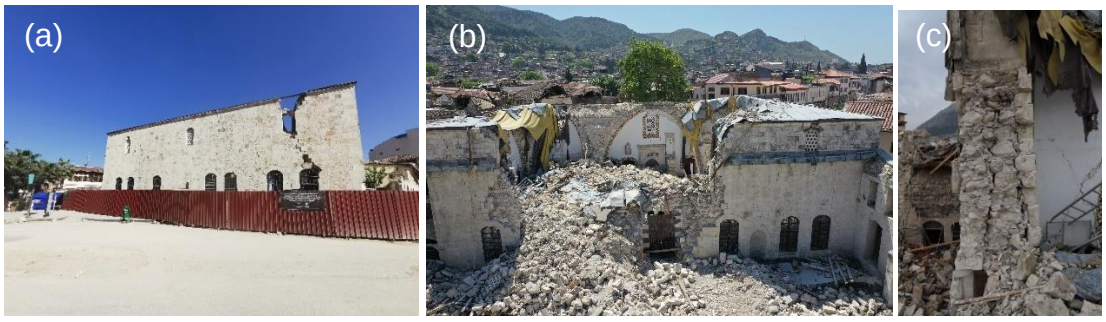

Figure 134: Habibi Neccar Mosque, photographs of (a) the south façade, (b) the collapsed north façade, (c) a multi-leaf wall cross-section from the collapsed north wall of the building.

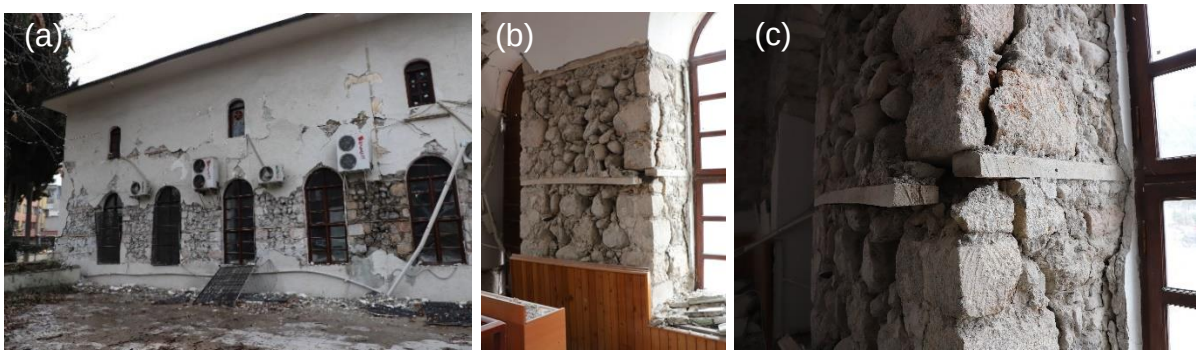

Figure 135: Enverul Hamit Mosque, photographs of (a) the east façade, (b) a rubble pier in the east façade, (c) a large crack around the poorly connected tie-beams in the east façade.

To summarise, the examples demonstrate that multi-leaf stone wall construction quality varies significantly amongst the examined monumental structures, from irregular rubble walls to regular finely cut ashlar walls. However, many of the examined walls appear to have poor inter-leaf connection. This may explain the significant amount of out of plane damage observed in these structures.

b) Floor structures

Floor structures are typically categorised as flexible, semi-rigid and rigid (Baggio et al., 2007). Within this context, flexibility refers to the flexibility of the floor structures in their own plane. Floors belonging to all three categories were observed in the monumental structures surveyed in Hatay and Osmaniye. Specific examples are given below.

Figure 136: Photographs of two buildings with timber floors (a) east façade of the Vakıflı No.2 house and (b) the north and east facades and (c) damage detail around stone quoins of the Hıdırbey Gastronomy House in Samandağ.

Figure 137: Photographs of damage in two buildings with floor structures spanning in a single direction: (a) a building in İskenderun with a timber floor and (b) the west façade of the early 20th century Liwan Hotel building in Antakya with a retrofitted steel-concrete floor.

Floors supported by timber beams and joists spanning in one or two directions are considered as ***flexible*** or ***semi-rigid***. The joists are typically overlain by timber planks. The connections of these overlying elements to the walls are important to generate diaphragm action. If the diaphragm action is generated, the floor structure may be considered as semi-rigid. The two-way spanning timber floor structure of a Vakıflı village stone house became visible following the partial collapse of one of its supporting masonry walls. *Figure 136*a shows the connections between the beams and the internal leaf of the wall, as well as the joist and decking layout. The out of plane damage on the wall spans the storeys and indicates lack of sufficient connection between the floor and the failed wall. *Figure 136*b shows a similar building from the nearby village of Hıdırbey. In this case, it appears that diaphragm action enabled the seismic force to be transferred to the transversal walls and prevented out of plane failure. However, cracks are observed around the stone quoins in the corners of the Hıdırbey Gastronomy House building, *Figure 136*c, indicating the initiation of an out of plane mechanism in one of the facades.

While the floor structures in *Figure 136* featured beams and joists spanning in two directions, floor structures may also span in a single direction. In this case, façade walls which are parallel to the floor spanning direction do not carry floor loads and act independently from the floor. This lack of connection promotes out of plane failure. *Figure 137*a and b provide examples of two buildings where out of plane failures have occurred. In both cases lack of connection led to the formation of out of plane mechanisms which involve almost the full height of the façade. It is noteworthy that the building in *Figure 137*b features a nominally rigid reinforced concrete-steel composite floor. However, due to poor detailing, diaphragm action was not generated.

Figure 138: Photographs of damage in two buildings with barrel vaulted floors: (a) south façade of the 16th century Kursunlu Han building in Antakya and (b) the north and west facades of the Shahut hotel building in Antakya.

Figure 139: Photographs of: (a) south façade of the early 20th century Hatay Metropolitan Municipality building and (b) the interior of the building during restoration works.

Stone vaulted floors may be classified as ***flexible*** or ***semi-rigid***. They are considerably heavier than timber floors and depending on the geometry and thickness may exert unbalanced lateral thrusts that make walls more vulnerable to out-of-plane damage. Similar to the cases presented in *Figure 137*, wall structures on the façade are susceptible to out of plane actions due to the independence of the floor structure and façade walls. *Figure 138* shows this type of damage for two historic structures with barrel stone vaults.

Reinforced concrete floors are typically introduced to historic buildings during renovation works. They are classified as ***rigid*** floor structures. Experimental evidence suggests that with the correct detailing they can be effective in providing diaphragm action and preventing out of plane failure (Senaldi et al., 2014). However, they also increase the overall building weight which may result in higher seismic loads and lead to uneven distribution of stiffness changing the overall vibrational characteristics of the building as a system. *Figure 139* shows the Antakya Metropolitan Municipality building, which has a reinforced concrete beam and slab floor system. It appears that the rigid floors have enabled diaphragm action and encouraged in-plane deformations in the masonry. The damage in the building appears to have remained local (e.g. parapet failure at roof level and out of plane failures in poorly connected north, west and south facades of the building, see *Figure 127*).

Observations from monumental structures indicate that floor structures which ensured diaphragm action helped control the propagation of damage. Examples presented

above and the published scientific literature demonstrate that flexible, semi-rigid or rigid floor systems may all achieve diaphragm action if designed properly.

c) Roof structures

Flat roof systems are structurally similar to floor systems and will not be discussed further. The focus of this section will instead be on non-flat roof systems. Timber roofs, stone vaults and domes are the most common roof types in monumental buildings in Hatay.

Timber roofs are typically light and flexible. They do not exert significant thrust on supporting walls. *Figure 140* shows two timber truss examples. The example in *Figure 140*a shows how the timber truss was not connected to the west façade of the Syriac Catholic Church in İskenderun, which collapsed in the out of plane direction during the 6 February Pazarcık earthquake. The example in *Figure 140*b shows how the large conference hall in second storey of the Mithatpasa Primary School collapsed. The first floor of this structure appears to be a jack arch overlain with a concrete slab while the roof is of timber truss construction. The floor structure appears to have redistributed seismic load and prevented collapse of the whole façade. However, the lack of internal walls and an effective roof-level load distribution mechanism appear to have led to overturning collapse above the first storey.

Propped timber roofs are common in historic churches and mosques of Hatay. *Figure 141*a shows the timber roof of Nakip Mosque, where timber joists meet at the apex of the roof. A series of masonry arches extending in the longitudinal direction at mid-width of the plan props up the timber roof at its apex. The presence of the prop likely reduces the lateral thrust exerted by the roof on the side walls. The presence of a strong ridge beam at the apex is indicated by *Figure 141*b; the collapse of series of arches during the earthquakes does not appear to have led to collapse. However, there are large distortions in the ridge beam and church walls. In an alternative arrangement adopted in Meryem Ana Samandağ Church, the series of masonry arches is placed parallel to the span of the timber roof. In this case, the role of the arched framing is to provide stiffness to the church structure in the transverse direction to the nave and carry some of the roof loads. The damage sustained by church wall is shown in *Figure 141*d. The concentration of damage in this location may be due to increased thrust following the damage in the arched frame closest to the apse (*Figure 141*c).

Figure 140: Photographs of damage in structures with roof timber trusses: (a) the Assyrian Catholic Church in İskenderun and (b) the Mithatpasa Primary School in İskenderun.

Figure 141: Photographs of the propped roof timber systems and the damage they experienced during the earthquakes: (a-b) Nakip Mosque in Antakya and (c-d) Meryem Ana Church in Samandağ.

There are several monuments which employ stone vaulted roof structures. Stone vaults are typically used internally, and they are covered by a light external waterproofing roof structure. Cross vaults are the most commonly used vault form in Hatay. *Figure 142*a and c show the interior of the Meryem Ana Tokacli and Kaddis Mar Circos churches. In *Figure 142*d, the vault appears to be backfilled to the level of the crown with granular material to provide lateral stability. *Figure 142*b and d show aerial views of the churches after the earthquakes. In both cases, it is interesting to note that some of the buttresses remain standing although they show signs of disaggretation and are out of plumb in the church nave transverse direction. This may suggest that the vault collapses may have arisen due to large lateral movements of the buttress and wall structures supporting the vaults.

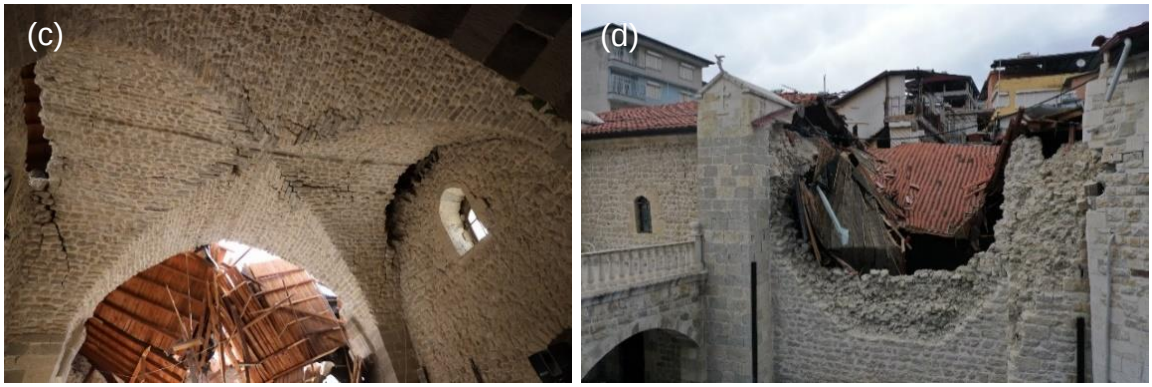

Figure 142: Photographs of the cross-vaulted Meryem Ana Church in Tokacli (a) before (from Wikipedia) and (b) after the 6 February Pazarcık Earthquake. Photographs of the cross-vaulted Kaddis Mar Circos Church: (c) vault, (d) external walls.

According to (Sanci, 2006), most of the mosques in Antakya are covered by a propped timber roof. Only three major mosques of the city are covered by a central dome, flanked by vaults. Photos from two of these mosques (Habib-i Neccar and Seyh Ali) are provided in *Figure 143*. It is noteworthy that the structural arrangement for these closely situated mosques are strikingly similar. The earthquake response also shows some similarities. In both structures, the minaret and the porch collapsed. Minarets are slender structural components, and the porch structure is supported by freestanding slender columns. The propensity of minarets to experience overturning failure has been recognised in the scientific literature (Oliveira et al., 2012).

However, there are also some important differences between the collapse mechanisms observed in the two mosques. The full collapse of the dome and the cross-vaults of Habib-i Neccar appear to be related to the partial collapse of the north wall of the mosque (see *Figure 134*b). In contrast, in the Seyh Ali mosque, the walls and cross-vaults have been damaged but remain standing (*Figure 143*b). The dome of Seyh Ali mosque has partially collapsed above its drum. The remaining portions show brick tile construction of the dome above the drum level. This observation is consistent with the contemporary 16th century Ottoman practice (Ahunbay, 1988). Discontinuity of materials may have played a role in the collapse of the dome structure although further investigations are needed to evaluate this hypothesis. Furthermore, the vaults and the supporting East and West walls appear to be leaning outwards (*Figure 143*c) – this also indicates that the dome failure may have been influenced by movements of the supporting structures.

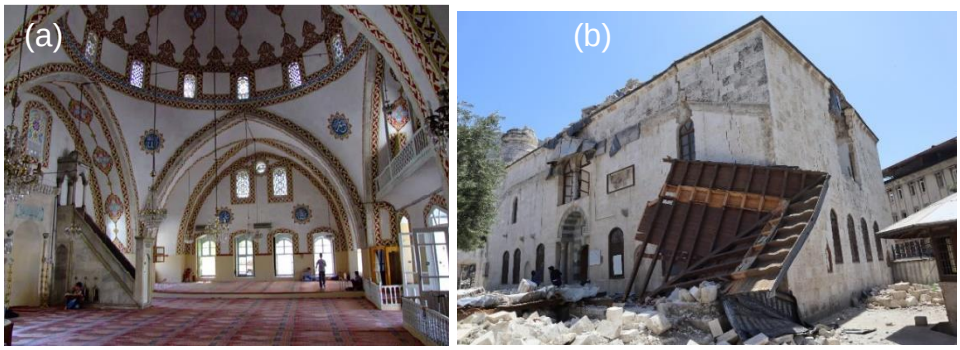

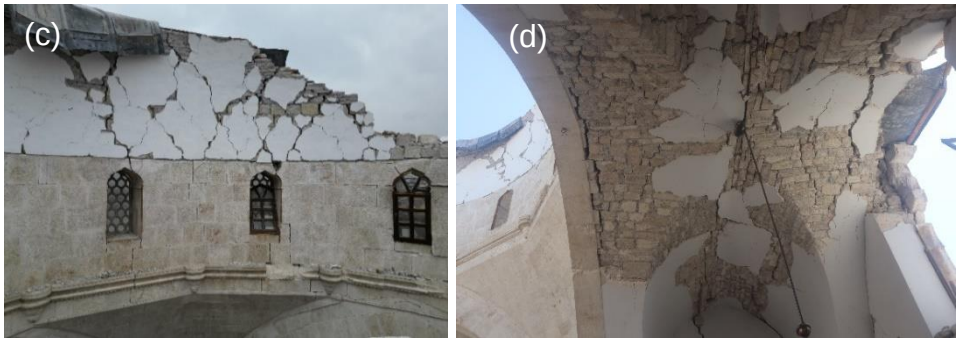

Figure 143: Photographs of (a) Habibi Neccar mosque interior before the earthquakes (Sanci, 2006) (b) Seyh Ali Mosque north and west facades, (c) dome and (d) east vault after the earthquakes.

4.3.3.9. Conclusions

This section described preliminary results from a damage survey of monumental historic structures in the provinces of Hatay and Osmaniye in the aftermath of 2023 Türkiye-Syria earthquakes. 33 monumental structures were investigated by assigning a global damage class to each structure and exploring correlations between the damage class and site-specific seismological parameters. The results showed the expected relationship between local earthquake intensity and damage; monuments located in cities where local earthquake intensity was the highest due to their proximity to the fault or ground amplification, were observed to experience more significant damage.

Structural components common to all historic buildings, namely load-bearing walls, floor and roof structures were examined. The poor inter-leaf connection in multi-leaf walls and the use of small, rounded stones without any/sufficient transverse tying using *hatıl*s which have been demonstrated to improve the performance of masonry (Spense and Coburn, 1992; Vintzileou, 2008) was highlighted as the potential cause of many failures. The importance of diaphragm action in floor structures was highlighted. The superior performance of buildings with retrofitted concrete floor structures was explained with the diaphragm action, although it was noted that with proper detailing, timber floor structures could also achieve load transfer and good performance. Observations on roof systems highlighted the damage vulnerability caused by insufficient stiffness and large lateral thrusts.

Brief indications on the overall management and earthquake damage assessment of historic structures in Türkiye were also presented. While the monumental structures were well-maintained, there appeared to be limited consideration for potential earthquake influence on these structures. Many recently restored or restituted monuments featured structural deficiencies which the earthquakes exposed. These deficiencies were either not spotted or acted upon during recent works. A lack of qualified engineers and seismologists in committees overseeing restoration and strengthening works may have contributed to this omission. Separately, various building owners noted that their monumental structures did not have detailed construction drawings. This will cause difficulties during the restoration and restitution activities that will follow. 3D models generated during this study were shared with building owners where possible, to aid stabilisation, repair and reconstruction work.

The post-earthquake inspection and remedial actions regarding monumental structures appeared to indicate a lack of earthquake preparedness. The rapid assessment techniques used in the field have been effective for initial assessments but they need to be complemented with more detailed assessment activities. These are needed to determine suitable short-term countermeasures to prevent collapse in historic buildings. There is a need to develop detailed assessment forms to support these activities and sufficiently customise them for structural typologies in Türkiye. The presence of such detailed assessment forms could have facilitated the rapid implementation of countermeasures, which may have been sufficient to prevent the unnecessary collapse of some historic structures during the aftershocks (especially the destructive 20 February aftershock). During the field investigations in April 2023, the EEFIT team observed several structures, such as the ones in *Figure 141*, which are on the brink of collapse. Future efforts should concentrate on the procedures required to rapidly determine and implement short-term countermeasures to ensure stability of monuments following earthquakes. It is recognised that the complex ownership structures and permit procedures may present an impediment towards the adoption of these rapid countermeasures. Therefore, necessary legal frameworks may need to be developed to enable rapid post-earthquake interventions.

4.3.4. Non-Engineered Modern Buildings

Non-engineered buildings are structures constructed without direct involvement from engineers or architects in their design and construction processes. Non-engineered buildings are characterised by a notable absence of the thorough structural analysis, meticulous planning, and strict adherence to contemporary engineering standards that are typically associated with engineered or professionally designed structures. Instead, they frequently depend on local construction techniques, or are erected by individuals lacking formal engineering training. While traditional/vernacular structural forms are also typically considered to be non-engineered, under this title we focus on more recent buildings exhibiting a conglomeration of modern (and occasionally non-modern) structural systems and materials.

Non-engineered buildings exhibit varying levels of structural integrity, not only because they are built in the absence of engineering oversight, but also because they often undergo alterations and modifications over time. These alterations may involve a transition from traditional to more modern construction techniques, including different primary structural systems and materials, which can introduce various irregularities in plan and elevation. For example, there may be a shift from load-bearing masonry walls to RC frame systems. Additionally, alterations in floor types may occur, transitioning from flexible timber constructions to rigid structures, often implemented as RC slabs. Other changes, such as the closure of openings, construction of new floors, and building additions, can also contribute to the complexity and irregularity of these structures.

During the field inspections conducted for this study, numerous examples of non-engineered modern buildings were encountered in both rural villages and, to a lesser extent, urban areas. These instances provide valuable insights into the diverse nature of such constructions and the various building practices and employed materials. Below, a comprehensive analysis is conducted on several noteworthy examples, each offering distinct insights into non-engineered construction techniques.

*Figure 144*a illustrates a typical non-engineered construction that utilises a single primary structural system while employing various types of construction materials. The building is constructed with load-bearing walls, which consist of clay bricks, adobe, and stone, all within the same structure.

In many instances, buildings showcase distinct primary structural systems coexisting within a single structure. As depicted in *Figure 144*b, this construction incorporates RC frames for the first level, while the second level is comprised of bearing walls with rigid concrete diaphragms.

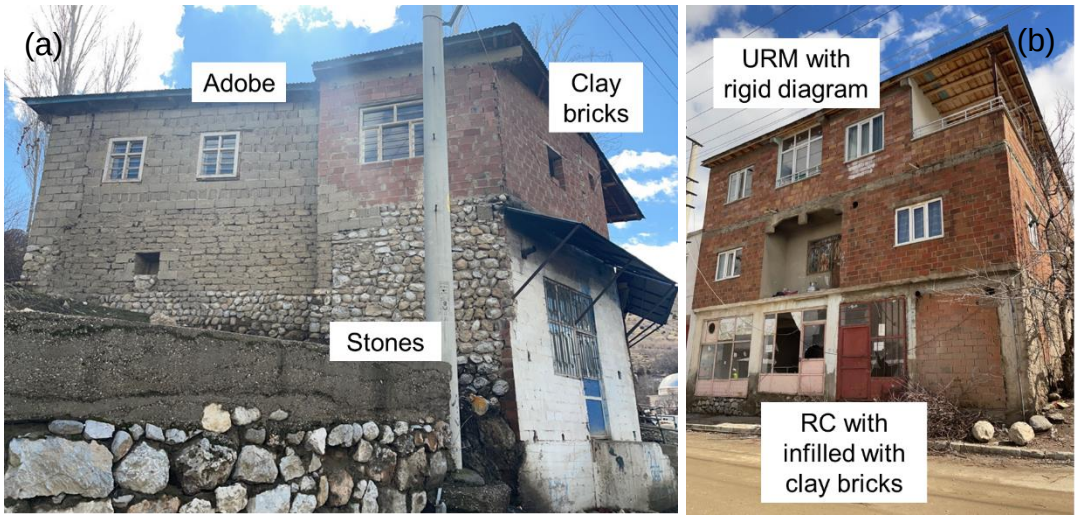

Figure 144: Hybrid buildings with (a) bearing walls made of adobe, clay bricks and stone; (b) a first level made of RC frames and a second level with bearing walls with rigid concrete diaphragms.

In *Figure 145* presents another example of a non-engineered construction, specifically a confined masonry structure, which is one of the less common systems observed on-site. A confined masonry structure is a type of building construction that combines masonry walls with additional reinforcement elements (e.g., column and beams) to enhance its earthquake resistance. In a confined masonry structure, the masonry walls are enclosed or "confined" within reinforced concrete columns and beams. This confinement with reinforced concrete provides added strength and ductility to the masonry walls, making the building more resilient to seismic forces. However, in this specific case, the masonry is made of stone, and this construction features a lightweight and flexible floor system supported by timber elements and covered with a metallic sheet. This deviates from the typical confined masonry construction, which generally incorporates an RC flooring system to provide rigidity and act under seismic loads as a box behaviour for the building. It is important to note that the absence of a ring beam at the top of the wall indicates a lack of constraint between the walls and the lightweight floor system.

Figure 145: Confined masonry building.

Figure 146: Hybrid building with beams and columns which are not continuous.

Another emblematic example highlighting the autonomy and lack of control during on-site construction is illustrated in *Figure 146*. In this case, the building is constructed as an RC frame with brick panels. However, it is evident that the front portion of the building has been extended using a construction technique that defies classification and contradicts engineering design principles. Beams and columns in this building are not only unconnected but also discontinuous.

The irregularities in materials, structural systems, and the arrangement of structural elements observed on-site can significantly impact the overall structural integrity and seismic performance (Korkmaz et al., 2010; Celep et al., 2011). The complexity

observed in these irregularities poses challenges when attempting to comprehend their structural behavior, as it is difficult to ensure that loads are properly distributed and that the structures can resist seismic forces effectively. Understanding their performance and identifying their strengths and weaknesses can be quite challenging.

Figure 147: a) OOP failures; b) failed infilled panel and c) Non-Engineered Interventions on a Building with a Vulnerable Soft Storey Due to Large Ground-Floor Openings for Commercial Activities.

In regions where these buildings were inspected, they are typically located in areas where many buildings had completely collapsed, making it impossible to observe the cause of failure as only rubble was visible. However, it was still feasible to examine the ones still standing, which had experienced varying degrees of damage, ranging from light to significant (*Figure 147*). Damage in these structures typically results from a combination of various failure types discussed in previous sections. Their performance is influenced by deficiencies arising from the integration of different systems and materials. For instance, load-bearing walls (URM) may experience OOP failures, soft stories in RC frames can lead to pancake failures, and these structures often display heavily cracked panels or overturning as they detach from the entire structural system.

It is essential to note that assessing these buildings is challenging not only after earthquakes have occurred but also beforehand, as understanding the complexity of these systems is not always straightforward (Kayaalp et al., 2021). The current building codes are inadequate in effectively evaluating these hybrid structures, making it difficult to assess their deficiencies related to earthquake resistance. To address these issues, it is imperative to develop a comprehensive understanding of how these deficiencies affect the buildings' response to earthquakes and establish appropriate assessment methods tailored to their unique characteristics.

4.3.5. Retrofitted Buildings

Enhancing the resilience of buildings through appropriate retrofitting measures is crucial for mitigating the devastating impacts of earthquakes. By reinforcing structures to withstand ground motion and shaking, their vulnerability to earthquake-related damage is significantly reduced. This not only minimises property loss but also plays a vital role in safeguarding human lives, reducing the risk of injuries or fatalities. Additionally, robust buildings can effectively mitigate the economic consequences of

seismic events. Prior to the occurrence of the Kahramanmaraş and Hatay earthquakes, several buildings underwent reinforcement measures. These retrofitted structures exhibited distinct behaviour compared to their unmodified counterparts, highlighting the paramount importance of strengthening buildings to withstand earthquakes. In the subsequent sections, specific examples of retrofitted buildings will be discussed to explore the methods employed to enhance their seismic resilience. The post-earthquake performance of retrofitted buildings provides compelling evidence of the effectiveness of these strengthening techniques, demonstrating that the proper implementation of retrofit measures can significantly enhance the structural performance of buildings. Moreover, by meeting the required life safety standards, residents can safely evacuate these buildings during seismic events.

4.3.5.1. Antakya Municipality Residentials

During the earthquake sequence in Hatay, Türkiye, three reinforced concrete building blocks, constructed almost 50 years ago in accordance with the 1974 earthquake management regulations. *Figure 148*a provides a pre-earthquake street view of these structures. These buildings, which shared an identical construction typology and a net floor area of 415 m², displayed different responses during the earthquake event. One of the buildings, known as A2 block which is the closest in *Figure 148* b, has a height of nearly 30 m and consists of ten floors. The building was originally constructed with reinforced concrete frames and lacked shear walls. It exhibited plan irregularities and was subsequently strengthened as part of an M.Sc. level academic study conducted by Mustafa Tan in 2009 (Tan, 2009). The objective of the study was to evaluate the building's seismic performance and address its non-compliance with the earthquake code regulations of 2007. The strengthening process involved the use of carbon-fibre reinforced polymer (CFRP) on internal masonry walls (*Figure 149*a) and columns (*Figure 149*b). The CFRP on the masonry walls were also anchored to the concrete frames to enhance their earthquake response. During the site observation, the EEFIT team also noted that the ground level of the building had a comparatively greater story height than the other floors, resulting in a soft story irregularity. The second building, known as the A1 block and situated on the right side of *Figure 148*b, was a ten-floor structure that underwent a retrofitting process similar to that of the A2 block. However, in the case of the A1 block, the CFRP were specifically applied on structural elements at the entrance of the ground level. In this area, regular masonry infill walls (shear walls) were added to external frames (*Figure 150*) increasing the lateral rigidity for the building. In contrast, the A3 block, located behind the Block A2 in *Figure 148*b, remained in its original state and did not undergo any strengthening measures.

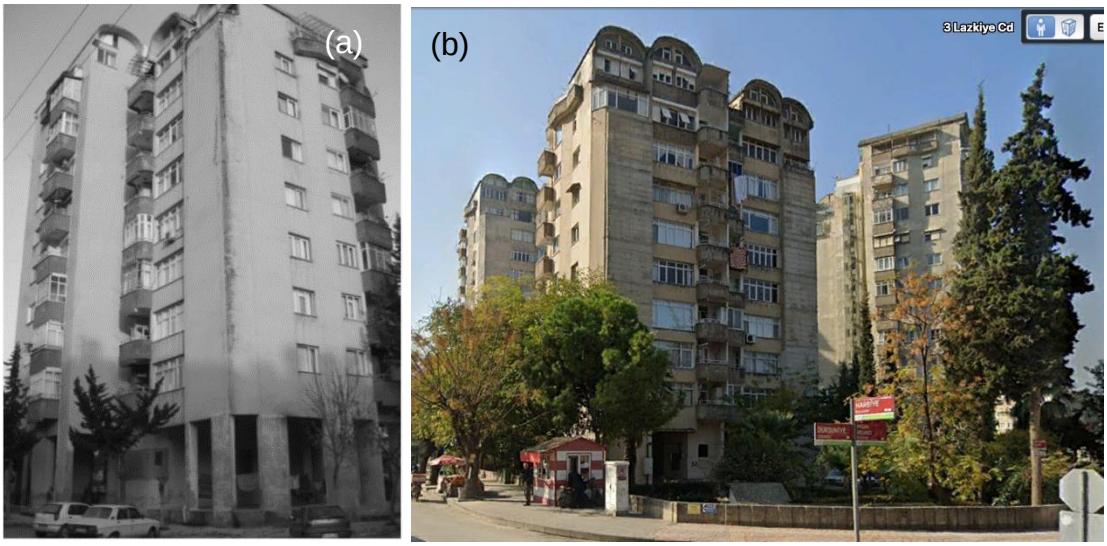

Figure 148: (a) Building before the retrofit interventions (Tan, 2009) and (b) Google Maps view of the three blocks before the earthquakes, additional shear walls can be seen on the facade.

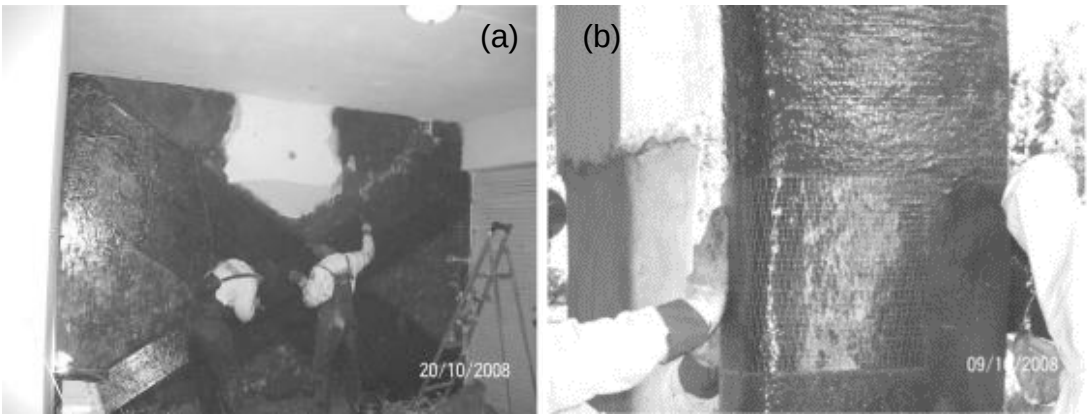

Figure 149: CFRP application to the masonry infill walls (a) and columns (b) (Tan, 2009).

Figure 150: Post earthquake condition of an external shear wall.

The performance of these buildings during the earthquake displayed significant variation, as illustrated in *Figure 151*. The two buildings that underwent retrofitting using the mentioned techniques experienced critical damage because of the earthquake. However, despite the damage, they exhibited a life safety performance level, enabling the residents to evacuate safely. In contrast, the building that was not strengthened collapsed during the first earthquake. This stark contrast between the two performances highlights the crucial importance of retrofitting measures in enhancing the resilience of buildings.

Figure 151: Aerial drone footage of remaining two blocks after the earthquake.

4.3.5.2. Fevzipasa Station Buildings

In Fevzipasa district of Gaziantep, there are historical masonry station buildings that are nearly a century old and are owned by the Turkish State Railways (*Figure 152*). These buildings serve both as administrative spaces and residential quarters for the station personnel.

Figure 152: Google Earth view of Fevzipaşa Train Station before the earthquakes.

As these are listed buildings, only non-invasive retrofitting interventions were permitted, which required expertise and skill. Only non-structural renewal works were carried out to preserve most of these buildings. Unfortunately, some of these buildings collapsed during the earthquake due to their lack of lateral rigidity, out-of-plane instability of the gable walls, and absence of seismic detailing. *Figure 153* depicts a partially collapsed building during the event.

Figure 153: Collapsed building at the Fevzipaşa Train Station [https://sendikalmucadele.org/btsden-deprem-raporu-demiryollarinda-hasar-fazla/].

Out of all the buildings mentioned, two of them underwent retrofitting through the application of CFRP on the masonry structural walls. Remarkably, these retrofitted buildings not only withstood the series of earthquakes but also sustained minimal

damage. As a testament to their resilience, the residents were able to remain in the buildings even after the earthquakes occurred.

Figure 154 displays one of the buildings that survived the earthquake and remained intact. It stands as a testament to the effectiveness of the retrofitting measures implemented. Additionally, *Figure 155* illustrates the non-structural crack formation resulting from the earthquake, highlighting the impact on elements other than the main structural components.

Figure 154: Standing masonry building at Fevzipaşa Train Station.

Figure 155: Non-structural crack through the beam-wall connection observed in one of the buildings at Fevzipaşa Train Station.

In addition to the examples, similar instances of retrofit techniques proving effective can be observed in Pazarcık train station in Kahramanmaraş province and, Doğanşehir, and Kapıdere train stations in Malatya provinces. The buildings that underwent strengthening measures in these stations demonstrated significantly improved performance during the earthquakes compared to those that were not retrofitted. Conversely, unreinforced buildings in these locations experienced severe damage or even collapse. Further information can be found in a news article in Turkish (Sendikal Mücadele, 2023).

4.3.6. TOKİ and Tunnel-Form Buildings

The Toplu Konut İdaresi Başkanlığı (TOKİ) is a government agency in Türkiye that is primarily involved in the development of mass housing projects. TOKİ is responsible for a wide range of construction initiatives, including the establishment of model settlements, social housing projects, and reconstruction activities. The primary aim of TOKİ is to provide affordable housing options for individuals with lower incomes. While TOKİ undertakes the construction of buildings for various purposes, this particular section focuses on residential buildings and the construction techniques employed in their development. *Figure 156* showcases two examples of residential complexes constructed by TOKİ.

Figure 156: Some examples of TOKİ buildings (Gündoğmuş, 2023).

TOKİ buildings constitute a significant portion, approximately 2-5%, of the building stock in earthquake-affected regions. These buildings are primarily constructed using tunnel formwork techniques, resulting in a higher percentage of shear walls compared to other construction methods, as further discussed below. The EEFIT fieldteamvisited various TOKİ housing complexes in Altınözü and Antakya districts in during the March visit. Additionally, another field trip to specifically to investigate the response of tunnel-form buildings to the 2023 Türkiye earthquakes took place between June 16-19, 2023 (see Section 1.2 for the details and team composition for this fieldtrip). This latter trip focused on the five most affected provinces: Hatay, Kahramanmaraş, Adıyaman,

Malatya, and Gaziantep. The primary objectives of the field trip were to evaluate the seismic response of mid- and high-rise tunnel-form buildings, investigate the prominent damage patterns, and observe the post-earthquake reconstruction achieved through tunnel-form building mass housing projects.

Most of the existing tunnel-form buildings and almost all of the new mass housing projects in the region are the premises of TOKİ. Contrary to conventional construction methods, tunnel-form buildings are constructed by specific formworks that allow the casting of walls and slabs in a single pour. This construction process results in a cellular structure with the main, in most cases only, vertical load-bearing member being shear walls. The most salient property of this typology is the high density of shear walls, resulting in relatively stiffer systems with limited flexibility compared to frame structures.

In the locations visited during the field trip, the superior performance of tunnel-form buildings compared to other building typologies was clearly observed. However, tunnel-form buildings in many areas were still found to exhibit varying levels of structural and non-structural damage. Due to their specific construction method, the structural system of tunnel-form buildings is composed of shear walls, slabs, beams and coupling beams. The high density of shear walls leads to a stiffer system than frame buildings. Moreover, this stiff structural mechanism limits the contribution of infill walls in seismic response, as was observed during the field trip. *Figure 157*a is an example of non-structural damage frequently encountered in the field. It has been observed that the infill walls are often separated from the load-bearing system at the ground floor level in these buildings. Depending on the ground motion level, these separations ranged from very fine cracks to significant separations reaching up to 1 centimetre. In cases where the damage was not limited to the non-structural elements, crushing of cover concrete was observed at the boundaries of structural walls. *Figure 157*b provides an example of cover concrete crush accompanied by the separation of infill walls at the ground level. *Figure 157*c, d shows corrosion and concrete cover spalling. *Figure 158*, on the other hand, is an example of widespread non-structural damage in a high-rise tunnel-formwork building. Diagonal cracks around the opening in infill walls were observed in many high-rise tunnel-formwork buildings in different locations. However, these non-structural damages remained very limited compared to their counterparts in RC frames. This situation is attributed to the fact that tunnel-form buildings are stiffer and exhibit less deformation. In addition to the infill damage, roof tile and chimney damage were frequently observed at the roof level of tunnel-formwork buildings, as shown in *Figure 158*.

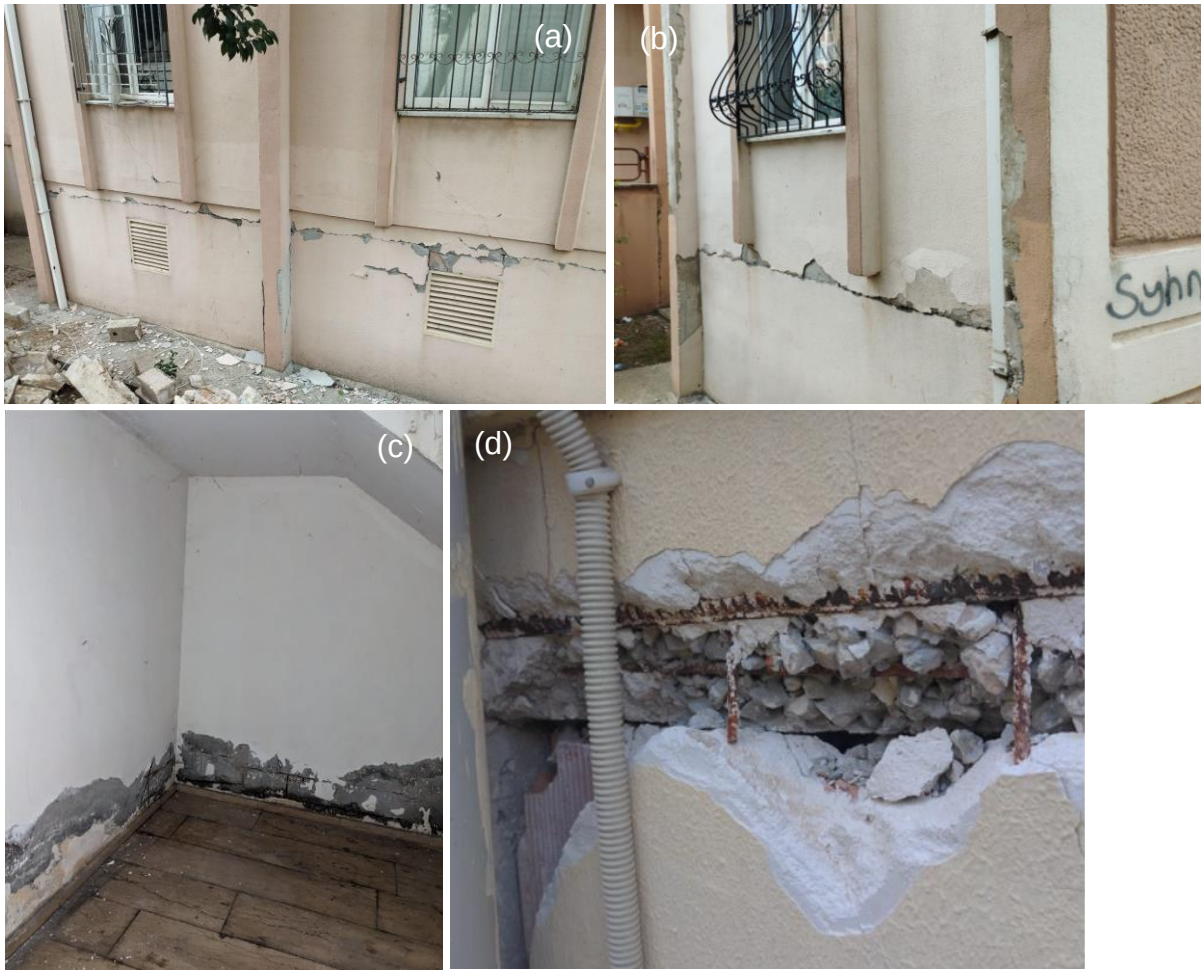

Figure 157: Damage observed in TOKI housing: (a) Separation of infill walls at the ground story and (b) Initiation of cover spalling and separation of infill walls at the ground story; (c) Corrosion of reinforcement on basement floor; (d) Concrete cover spalling and infill wall damage.

Figure 158: Widespread diagonal cracks in the infills around the window openings.

The extensive coverage of the field trip also provided a means to compare the performance of tunnel-form buildings to the neighbouring reinforced concrete (RC) frames. *Figure 159* exhibits a good comparison of RC tunnel-form buildings and frame buildings in Antakya, representing the general situation where tunnel-form buildings performed better than frame buildings with regard to structural and non-structural damage. It is important to emphasise that the tunnel-form buildings in the region were constructed mainly by TOKİ and had strict construction inspections to comply with the requirements of seismic codes. It is known that similar inspections failed to succeed in the projects of private enterprises.

Figure 159: Comparison of a tunnel-form building with a frame building in Antakya.

In more severe damage cases, it has been observed that the loss in the cover concrete propagates along the wall section and spreads to the concrete in the boundary zones. In high-rise tunnel-formwork buildings, concrete crushing and reinforcement buckling were encountered (*Figure 160*a). Furthermore, in several cases, the damage was propagated beyond the boundary regions, followed by the concrete crushing and reinforcement buckling at the web, resulting in exposed mesh reinforcements (*Figure 160*b). This damage pattern was also accompanied by reinforcement fracture at the extremities of the wall.

Figure 160: Shear wall damage.

As mentioned previously, shear walls form a stiff structure where coupling beams are left as the primary source of seismic energy dissipation. During the field investigation, it was observed that coupling beams played an important role in absorbing seismic energy by undergoing significant levels of damage (*Figure 161*).

Figure 161: Coupling beam damage.

References

Abrahamczyk, L., Langhammer, T., & Schwarz, J. (2017). Vulnerability Assessment of Large Building Stocks – Lessons from the SERAMAR project. *Proceedings of the 16th World Conference on Earthquake Engineering*. http://seramar.edac.biz

AFAD (2023) Genel Hayata Etkili Afet Bölgesi Hk. AFAD. https://www.afad.gov.tr/genel-hayata-etkili-afet-bolgesi-hk. (Last accessed: 2023, Apr 03).

Ahunbay, Z. (1988). *Mimar Sinan Yapılarında Kullanılan Yapım Teknikleri ve Malzeme*. in: Mimarbaşı Koca Sinan Yaşadığı Çağ ve Eserleri. Cilt 1, T.C. Başbakanlık Vakıflar Genel Müdürlüğü

Akboy-Ilk, S., & Akboy-İlk, S. (2023). The Architectural Pedigree of İznik's 14th-Century Green Mosque in Türkiye. Architectural Histories, 11(1).

Aktaş, Y. D., & So, E. (2022). Disaster Reconnaissance Missions: Is a Hybrid Approach the Way Forward? *Frontiers in Built Environment*, *8*. doi: 10.3389/fbuil.2022.954571

Aktaş, Y.D., et al. (2022a) Hybrid Reconnaissance Mission to 30 October 2020 Aegean Sea Earthquake and Tsunami: Description of Data Collection Methods and Damage, *Frontiers in Built Environment*, doi: 10.3389/fbuil.2022.840192

Aktaş, Y.D., Ioannou, I, Malcioglu, F S, Parammal Vatteri, A., Kontoe, M., Dönmez, K., Black, J., Kazantzidou-Firtinidou, D., Dermanis, P, Diri, F (2022b) Traditional structures in Türkiye and Greece in 30 October 2020 Aegean Sea Earthquake: Field observations and empirical fragility assessment, Frontiers in Built Environment – Earthquake Engineering, doi: 10.3389/fbuil.2022.840159

Aktaş, Y. D. (2017). Seismic resistance of traditional timber-frame hımış structures in Türkiye: A brief overview. *International Wood Products Journal*, *8*(sup1), 21-28.

Aktaş, Y.D., Türer, A. (2016) Seismic Performance Evaluation of Traditional Timber *Hımış* Frames: Capacity Spectrum Method Based Assessment, Bulletin of Earthquake Engineering 14(11), pp. 3175-3194, doi: 10.1007/s10518-016-9943-2.

Aktaş, Y.D., Akyüz, U., Türer, A., Erdil, B., Şahin Güçhan, N. (2014) Seismic Resistance Evaluation of Traditional Ottoman Timber-Frame Hımış Houses: Frame Loadings and Material Tests, Earthquake Spectra 30(4), pp. 1711-1732, doi: 10.1193/011412EQS011M

Baggio, C., Bernardini, A., Colozza, R., Pinto, A. V, & Taucer, F. (2007). *Field Manual for post-earthquake damage and safety assessment and short-term countermeasures (AeDES)*. http://ipsc.jrc.ec.europa.eu

Bassal, C., Rabea, M., & Felix, M. (2023). A Comparative Study of Mediterranean Courtyard Houses and the Bioclimate Impact on Their Design from Four Axes: Historical, Environmental, Social and Geometry. Green Building & Construction Economics, 123-137.

Borri, A., Corradi, M., Castori, G., & De Maria, A. (2015). A method for the analysis and classification of historic masonry. *Bulletin of Earthquake Engineering*, *13*(9), 2647–2665. https://doi.org/10.1007/s10518-015-9731-4

Celep, Z., Erken, A., Taskin, B., & Ilki, A. (2011). Failures of masonry and concrete buildings during the March 8, 2010, Kovancılar and Palu (Elazığ) earthquakes in Türkiye. Engineering Failure Analysis, 18(3), 868-889.

Contreras, D., Wilkinson, S., Aktaş, Y D, Fallou, L., Bossu, R., Landes, M (2022) Intensity-based sentiment and topic analysis. The case of the 2020 Aegean earthquake, Frontiers in Built Environment – Earthquake Engineering 8:839770, doi: 10.3389/fbuil.2022.839770

Demir, A. (2014). The urban pattern of Antakya: streets and houses. *Topoi. Orient-Occident, 5*(1). https://www.persee.fr/doc/topoi_1764-0733_2004_act_5_1_2898

Demir, C. (2012). *SEISMIC BEHAVIOUR OF HISTORICAL STONE MASONRY MULTI-LEAF WALLS*.

Erberik, M. A., Yakut, A., Geneş, M. C., Abrahamczyk, L., Bikçe, M., Kaçın, S., Langhammer, T., Gulkan, P., & Schwarz, J. (2013). Characteristics of unreinforced masonry buildings in Antakya through filed survey. *2nd Turkish Conference on Earthquake Engineering and Seismology*.

Ersoy, U. (2000). TS500-2000. *Türkiye Mühendislik Haberleri*, 406–407.

Garbioglu, O. (2017). *Tanzimant'tan Cumhuriyet'e Hatay'daki kamu yapilari*.

Giuffrè, A. (1993). Restauro strutturale. Il rilievo quale indispensabile preliminare dell'analisi meccanica.

Grünthal, G. (1998). *European macroseismic scale 1998: EMS-98*. European Seismological Commission (ESC), Subcommission on Engineering Seismology, Working Group Macroseismic scales.

Gündoğmuş, Y. N. (2023). TOKİ'nin deprem bölgesindeki 134 bin konutu, depreme dayanıklı sistemler sayesinde zarar görmedi. *Anadolu Agency*. https://www.aa.com.tr/tr/asrin-felaketi/tokinin-deprem-bolgesindeki-134-bin-konutu-depreme-dayanikli-sistemler-sayesinde-zarar-gormedi/2816762

Ilki, A., Demir, C., Cömert, M., & Halici, O. F. (2020). *Betonarme ve Yığma Binalarda Deprem Kaynaklı Hasarlar ve Hasar Tespiti*.

Kayaalp, F. B., Yurdakul, Ö., & Routil, L. (2021). Stochastic assessment of concrete core strength in fire exposed specimens simulating non-engineered RC structures in Türkiye. Construction and Building Materials, 289, 123133.

Korkmaz, H. H., Korkmaz, S. Z., & Donduren, M. S. (2010). Earthquake hazard and damage on traditional rural structures in Türkiye. Natural Hazards and Earth System Sciences, 10(3), 605-622.

Lagomarsino, S., & Podestà, S. (2004). Seismic vulnerability of ancient churches: I. Damage assessment and emergency planning. *Earthquake Spectra*, *20*(2), 377–394. https://doi.org/10.1193/1.1737735

Martins, A., Vasconcelos, G., & Costa, A. C. (2017). Brick masonry veneer walls: An overview. *Journal of Building Engineering, 9, 29-41*.

Mihçioğlu Bilgi, E., & Uluca Tümer, E. (2020). Building Typologies in Between the Vernacular and the Modern: Antakya (Antioch) in the Early 20th Century. SAGE Open, 10(2). https://doi.org/10.1177/2158244020933318

Novelli, V. I., De Risi, R., Ngoma, I., Kafodya, I., Kloukinas, P., Macdonald, J., & Goda, K. (2021). Fragility curves for non-engineered masonry buildings in developing countries derived from real data based on structural surveys and laboratory tests. *Soft Computing*, *25*, 6113-6138.

Novelli, V. I., D'Ayala, D., Makhloufi, N., Benouar, D., & Zekagh, A. (2015). A procedure for the identification of the seismic vulnerability at territorial scale. Application to the Casbah of Algiers. Bulletin of Earthquake Engineering, 13, 177-202.

NTV. (2023) Depremden Etkilenen 10 İli Kapsayan Ohal Tezkeresi TBMM Genel Kurulu'nda Kabul Edildi. *https://www.ntv.com.tr/,Türkiye/depremden-etkilenen-10-ili-kapsayan-ohal-tezkeresimecliste-kabul-edildi,EbzF1W1AvU6xeab1jT-KwQ.* (Last accessed: 2023, Feb 09)

Oliveira, C. S., Çakti, E., Stengel, D., & Branco, M. (2012). Minaret behavior under earthquake loading: The case of historical Istanbul. *Earthquake Engineering and Structural Dynamics*, *41*(1), 19–39. https://doi.org/10.1002/eqe.1115

Ortega, J., Vasconcelos, G., Rodrigues, H., Correia, M., & Lourenço, P. B. (2017). Traditional earthquake resistant techniques for vernacular architecture and local seismic cultures: A literature review. *Journal of Cultural Heritage*, *27*, 181-196.

Över, S., Büyüksaraç, A., Bekta, Ö., & Filazi, A. (2011). Assessment of potential seismic hazard and site effect in Antakya (Hatay Province), SE Türkiye. *Environmental Earth Sciences*, *62*(2), 313–326. https://doi.org/10.1007/s12665-010-0525-3

Öztank, N. (2010). An investigation of traditional Turkish wooden houses. Journal of Asian Architecture and Building Engineering, 9(2), 267-274.

Polat, H. I. (2017). A Classification Study on the Development Stages of Construction Technologies in Türkiye. Engineering, Technology & Applied Science Research, 7(5), 1909-1913.

PSB, Presidency of Strategy and Budget, Presidency of Republic of Türkiye. (2023). Türkiye earthquakes recovery and reconstruction assessment report. Available at: https://www.sbb.gov.tr/wp-content/uploads/2023/03/,Türkiye-Recovery-and-Reconstruction-Assessment.pdf

Regulation on Buildings to be Constructed in Earthquake Zones (DBYBHY) (2007), *Official Journal* 26454, 06 March.

Republic of Turkey Ministry of Environment and Urbanization. (2023). Türkiye earthquakes recovery and reconstruction assessment. https://www.sbb.gov.tr/wp-content/uploads/2023/03/,Türkiye-Recovery-and-Reconstruction-Assessment.pdf

Şakar, F. S., & Güçhan, N. Ş. (2018). Building System Characterization of Traditional Architecture in Cappadocia, Türkiye. Adalya, (21), 375-410.

Sanci, F. (2006). *HATAY İLİNDE TÜRK MİMARİSİ I*.

Senaldi, I., Magenes, G., Penna, A., Galasco, A., & Rota, M. (2014). The effect of stiffened floor and roof diaphragms on the experimental seismic response of a full-scale unreinforced stone masonry building. *Journal of Earthquake Engineering*, *18*(3), 407–443. https://doi.org/10.1080/13632469.2013.876946

Sendikal Mücadele (2023). BTS'den Deprem Raporu; Demiryolları'nda Hasar Fazla. *https://sendikalmucadele.org/btsden-deprem-raporu-demiryollarinda-hasar-fazla/*

Spense, R. and Coburn, A. (1992) Strengthening Buildings of Stone Masonry to Resist Earthquakes, Meccanica 27: 213-221

Surmeli, B. S. (2019). *Hatay Musa Dağı Kirsal Yerleşimlerİ Ve Geleneksel Konutlarin Korunmasi İÇİN Öneriler*.

Tan, M. T. (2009). Seismic strengthening of a mid-rise reinforced concrete frame using CFRPs: an application from real life. MS Thesis, Middle East Technical University.

Tanyeli, G. (1990). *Osmanlı Mimarlığında Demirin Strüktürel Kullanımı (15-18. yy)*.

Tayla, H. (2007). *Geleneksel Türk Mimarisinde Yapı Sistem ve Elemanları*. Tac Vakfi Yayinlari.

TC Kultur ve Turizm Bakanligi. (2022). *Türkiye Geneli Korunması Gerekli Taşınmaz Kültür Varlığı İstatistiği, https://kvmgm.ktb.gov.tr/TR-44798/,Türkiye-geneli-korunmasi-gerekli-tasinmaz-kultur-varligi-istatistigi.html*

Toker, Ç. (2023). Deprem ihaleleri 150 milyar lirayı aştı. [online] T24. Available at: https://t24.com.tr/yazarlar/cigdem-toker/deprem-ihaleleri-150-milyar-lirayi-asti,39563 (Accessed 18 Aug. 2023)

Topbas, A., & Arslan, D. (2017). Seismic Design, Detailing and Construction of the First Flat-Laid Vault and Domes of Istanbul. In Proceedings of IASS Annual Symposia (Vol. 2017, No. 20, pp. 1-9). International Association for Shell and Spatial Structures (IASS).

TS500 Betonarme Yapıların Tasarım ve Yapım Kuralları. (2000). Bayındırlık ve İskan Bakanlığı.

Turkish Building Earthquake Code (TBEC) (2018), *Official Journal* 30364, 18 March.

Uysal Urey, Z. C. (2023). Creation of a New Vernacular Architecture and the Attainment of Sustainability: The Case of Akyaka Town Development. Sustainability, 15(3), 2643.

Vasconcelos, G., Lourenço, P. B., & Poletti, E. (2015). An overview on the seismic behaviour of timber frame structures. Historical earthquake-resistant timber frames in the mediterranean area, 119-132.

Vettore, M., Saretta, Y., Sbrogiò, L., & Valluzzi, M. R. (2022). A new methodology for the survey and evaluation of seismic damage and vulnerability entailed by structural interventions on masonry buildings: Validation on the Town of Castelsantangelo Sul Nera (MC), Italy. International Journal of Architectural Heritage, 16(2), 182-207.

Vakıflar G. M., VGM. (2007). Vakıf Medeniyeti çevre Yılı ve Vakıflar Haftası Etkinlikleri Kitabı. *Ankara, 2007.*

Vintzileou, E. (2008). Effect of timber ties on the behavior of historic masonry. *Journal of Structural Engineering*, *134*(6), 961-972.

Yadav, S., Sieffert, Y., Vieux-Champagne, F., Malecot, Y., Hajmirbaba, M., Arléo, L., Crété, E. and Garnier, P. (2023). Shake table tests on 1: 2 reduced scale masonry house with the application of horizontal seismic bands. *Engineering Structures*, *283*, 115897.

5. REMOTE SENSING

Remote sensing (RS) plays a critical role in all phases of the emergency management cycle and it has been extensively and effectively used for almost two decades for post-earthquake reconnaissance missions and recovery assessments (Yun et al., 2015, Milillo et al., 2016, Wania et al., 2016, Salamon et al., 2021) The technology and the numerous techniques (e.g., classification, change detection, masking and filtering) which have stemmed from it take advantage of the two key characteristics associated with the bird-eye viewpoint: the synoptic view, which allows for the rapid and efficient collection of data over a wide area, and the ability to revisit the same area with multi-temporal acquisitions. These characteristics are useful in supporting the assessment of the damage caused by an earthquake, especially when used alongside geolocated vector data (e.g., administrative boundaries, critical infrastructures and the natural, perilous environment) for the production of actionable descriptive maps. In the immediate aftermath of the event - when media information is numerous but coarse and repetitive and the official reports are still unavailable, the data collected through remote sensing provide information to ground-based teams, helping them to prioritize their efforts on the most affected areas. Remote sensing also helps improve situational awareness of what occurred in the most remote areas that media and response teams may have difficulty accessing and reporting on. As such, the use of RS in post-earthquake reconnaissance missions is important because it can allow for a rapid, comprehensive, and better-informed response to the disaster. This is crucial in a rapidly changing environment, when time is of the essence, and ground-based teams do not have the capacity to timely cover the entire affected area.

The EEFIT team has applied RS to post-earthquake reconnaissance missions since the early 2000s. The interest in this topic has grown with time and it is becoming progressively more formalized, especially in recognition of the changing needs of the group and of its now-established hybrid mission mode of operation, which sees remote and field teams cooperating and exchanging information throughout the mission. EEFIT's 2021 Haiti Mission and 2022 Nepal Return Mission were the first occasions in which a Remote Sensing working group was officially formed to provide remote support to the field team during the mission planning and to follow the step-by-step acquisition and processing of the data collected.

This report summarises the activities carried out by the Remote Sensing team before and during the post-earthquake reconnaissance mission conducted in March 2023. These have been grouped under two overarching goals:

- To assist ground-based teams in selecting the most relevant areas of interest (AOIs) to conduct field surveys, based on damage, impact intensities, and characteristics of the urban environment.
- To develop a replicable framework to identify, apply, and validate suitable RS approaches, methodologies, and datasets to assist post-earthquake reconnaissance missions, both for this mission and in the future.

To fulfil these objectives, the RS team has:

1. Collated and reviewed the data sources, maps, and models produced by authoritative scientists and institutions that could assist in the determination of the damage distribution and its intensity;
2. Collated, and reviewed data sources to characterize the urban fabric of the affected areas and produced actionable descriptive outputs based on information such as building count, built-up area, and average building height per district;
3. Produced preliminary maps showing geotechnical and geological impacts including fault surface ruptures, landslides, and areas that underwent liquefaction and lateral spreading;
4. Data processing and selection of areas of interest suitable for a field deployment;
5. Identified optical, lidar, and radar sensors that had collected or were due to acquire datasets over identified AOIs;
6. Connected with satellite vendors to acquire data while the ground-based mission was ongoing, to assist with ground-truthing.

Amongst the available datasets, optical and radar data were identified as the most suitable to map the extent of damage to buildings, infrastructure, and the natural environment, and to identify potential continuing hazards such as landslides, landslide outburst floods, or ground movement due to ongoing liquefaction and lateral spreading effects.

Six **high-priority areas,** located near the cities of Hatay/Antakya, Islahiye, Kahramanmaraş, Nurdağı, Bahçe, and Osmaniye, were identified (*Figure 162*).

To aid the assessment of the damage across the whole building stock, the high-priority AOIs include areas where a suitable variety of building typologies – with diverse heights, building ages, and damage grades, were located. Additionally, the team selected **six low-priority AOIs** which presented a lower diversity of damage and building characteristics but were geographically close to the high-priority ones, to allow the ground-based team to increase the volume of data collected, should time allow.

PROVIDED ACTIONABLE PRODUCTS

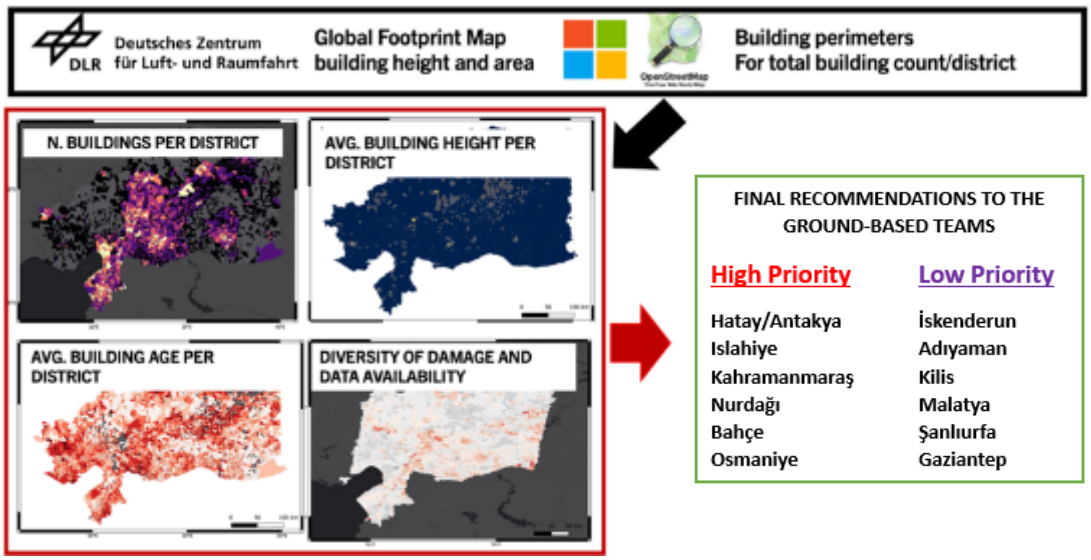

Figure 162: Examples of the outputs generated for delineating the AOIs for the EEFIT Türkiye remote sensing mission.

5.1. Workflow for the Selection of AOIs for the Ground-Based Surveys.

5.1.1. Step 1 – Collation and Review of the Data Sources, Maps, and Models for the Determination of the Damage Distribution and its Intensity

The RS team collated and reviewed the available damage data sources, including raw data, as well as maps and models, produced by authoritative scientists and institutions and made available to the whole scientific community in an analysis-ready and open-source format. The review also included commercial products made available by the providers free-of-charge. The findings of this review are organized in Table 1, which provides the dataset name, the Author/Institution, the website or link for its retrieval, a short description of each dataset, and its format.

The purpose of the table is to facilitate access to the most relevant datasets available for this mission and to provide a starting point for building an expandable reference list for the main data providers to be reviewed and enriched during the following missions, as new remotely sensed data and products become available.

The datasets listed in *Table 8* were gathered from various online sources and repositories, including GitHub, AWS, Google, and other relevant websites. Considerable time and effort were spent browsing through these sources and identifying suitable data among the available ones. The main challenge to this task was posed by the scattered and unstandardized format of the data and the need to ensure that the data were relevant and up to date. This process required the team to verify each source and check for updates on the most dated datasets. To aid the data dissemination, the verified datasets were categorized and made available to team members on a repository accessible online. Data were organized on a timeline, so as

to analyse pre- and post-earthquake sources and news articles related to the earthquake sequentially, as they became available.

While time-consuming, collating, cataloguing, and providing a narrative on the available datasets is an essential and necessary task to perform before all reconnaissance missions, as many reliable resources of open source remotely sensed data are nowadays made available by the international scientific and engineering community. Organizing the data before the mission facilitates the streamlining of information and data management processes, enabling the team to make informed decisions that guide reconnaissance efforts while informing future response efforts. Mission planning is a rigorous and meticulous procedure that necessitates a principled reliance on empirical data, in contrast to historical practices which have primarily drawn from media sources. During our mission it was evident that media-derived information remains a relevant component of the planning process; nonetheless, when remote sensing data become accessible, they should be accorded elevated precedence due to their enhanced reliability and superior georeferencing attributes compared to media-derived datasets.

Table 8: List of the open-access remote sensing products made available by commercial providers and scientific institutions within 1.5 months of the earthquake, as well as commercial product made available for this mission free of charge. For all acronyms related to SAR technology we refer the reader to the NISAR Manual (https://nisar.jpl.nasa.gov/mission/get-to-know-sar/overview/)

Dataset	Dataset Author	Link	Description
MAXAR	Maxar Technologies Inc.	Kahramanmaraş-Türkiye-earthquake-23	Commercial optical data but provided in an open-source repository.
Sentinel-1	ESA	L1 Single Look Complex (SLC)	C-band open-source SAR data in single & dual polarizations -VV or HH, VV+VH or HH+HV for SM, IW, EW modes. The revisit time is 6 or 12 days.
Capella	Capella Space	gaziantep-Türkiye-earthquake	AWS-provided x-band SAR data; resolution varies by mode: up to 0.5m for Spotlight, 0.5-1m for Stripmap, and 3-20m for Scan SAR. Revisit time is 12hours.
ALOS-2	JAXA	Advanced Land Observing Satellite	L-band SAR with revisit time of 14 days showed a comparison of backscatter intensity difference and colour composite images (HH Polarization).
EMSR648	Copernicus Emergency Management Service	Earthquake in East Anatolian Fault Zone, Gaziantep province	Rapid Response damage maps from very- high resolution (under 1 meter) optical data over 20 AOIs near the EQ epicentres.
ALOS2/Sentinel-1	NASA/JPL/Caltech/ ARIA product	Türkiye_EQ/Displacements	The PALSAR-2 Data showed the area close to epicentre of the Mw 7.8 earthquake that moved towards east and up.

Sentinel-1	Geohazards-tep	geohazards-tep.eu	Generated the surface motion map of Türkiye–Syria earthquake for the pre-seismic period by the SNAPPING PSI.
EOS-RS	Earth Obsevatory of Singapore – Remote Sensing (EOS-RS) & Advanced Rapid Imaging and Analysis Singapore (ARIA-SG)	202302_,Türkiye_Syria_Earthquake	Tracked changes and identified damaged areas comparing the February 8 data to observations made by the same satellite before the earthquake (on April 7, 2021, and April 6, 2022)
MAXAR / Planet Labs	Microsoft	Türkiye-Earthquake-Report-2_MS.pdf	High resolution optical imagery was used to classify damaged buildings with convolutional neural networks.
Planet Labs	Planet Labs	Central Kahramanmaraş bbc.com/news/world-europe-	Showed building-by-building damage maps; complete/ partial damage of buildings destroyed around the stadium.
Sentinel-1	Remote Sensing Lab University of Tabriz	Kahramanmaraş Türkiye EQ	Coherence damage proxy maps, were produced in the initial damage map of the settlements in Türkiye and Syria.
RADARSAT -2	Natural Resources Canada, Canadian Space Agency	nrcan_Products_Türkiye	C-band RADARSAT-2 showed more than 3m displacement along the fault line.
Sentinel-1	NERC Comet	nceo_geohazards/interferograms	The pixel offset map from Sentinel-1 shows the two ruptures.
Planet Labs	Published by Chris Milliner on Twitter 2023/02/08	Geo_GIF/status	Pixel tracking of satellite images showed fault rupture. Displacement varies from 2-4 m.
Sentinel-1	SatSense COMET	www.bbc.com	Used InSAR to measure deformation and mapped fault lines.
Sentinel-1	CES Kaust Research Group	Destructive-Earthquake-Doublet-of-6-February	Mapped co-seismic surface displacements and horizontal 3D surface displacements and their spatial pattern left-lateral motion across the two main faults.
Sentinel-1	USGS	usgs.maps earthscope.org/geophysical-event	A first estimate of surface rupture length– over 300 km (~185 mi) and simple fault lines from both Earthquakes.
Sentinel-2	European Space Agency Zenodo	Kahramanmaraş EQ	Generated EW and NS displacement maps from single-pair feature tracking of the 25 Jan 2023 and 9 Feb 2023 Sentinel-2 optical images.

5.1.2. Step 2 – Collation and Review of Data to Describe the Characteristics of the Urban Fabric and Production of Actionable, Descriptive Maps

Once the damage data sources were identified, the team proceeded in a similar fashion to identify, review, and analyse datasets that could be useful to characterize the urban fabric and extract descriptive analytics. The following paragraphs describe the dataset used during the decisional process and their application for the undertaken analyses.

5.1.2.1. Microsoft Building Maps

The Microsoft building maps were used to estimate the building count, area, and height per province and district. Subsequent to the seismic events the Microsoft research team (Robinson et al., 2023) initiated the application of artificial intelligence (AI) methodologies in conjunction with high-resolution satellite imagery to undertake a comprehensive assessment of the structural damage incurred by buildings within the afflicted region. Their collaborative effort was focused on the provisioning of granular, building-level damage estimations spanning four municipalities situated in the southeastern region of Türkiye, utilizing satellite imagery captured within the initial three days subsequent to the disaster event. The resultant analysis revealed a cumulative estimate of 3,849 buildings experiencing varying degrees of damage or destruction across the four aforementioned municipalities. Notably, the city of Kahramanmaraş emerged as the most severely impacted among the assessed localities, with approximately 7.44% of its building infrastructure exhibiting discernible signs of damage as discerned through satellite imagery.

5.1.2.2. Türkiye Administrative Boundaries

The administrative boundaries at the district level were sourced via the Humanitarian Data Exchange (HDX) portal. This repository, managed by the United Nations Office for the Coordination of Humanitarian Affairs, provides direct access to an ample collection of humanitarian data, and typically also contains the vector files of the administrative boundaries of all countries in the World, in a GIS-ready format. Administrative data are provided as a collection of layers, each representing a different geographical extent (from national - Level 0 to Districts - Level 3).

The district data layer was used to define the geographic scale to which all the other variables analysed to assess the damage were reconciled. This type of analysis is known as zonal statistics and was used to obtain the per district distribution of urban footprints, building geometry, building age, and building damage. Statistics such as mean, count, or standard deviation were calculated for the datasets described here below.

5.1.2.3. Global Urban Footprints

The Global Urban Footprints (GU 2020) dataset (*Figure 163*) was created by the German Aerospace Center (DLR) and consists of building footprints for urban areas around the world. The dataset describes the global spatial distribution of human settlements. A total of 180,000 TerraSAR-X and TanDEM-X scenes were used with the Urban Footprint Processor (UFP) operational processing chain to delineate urban

areas with global coverage at a spatial resolution of ~12 meters. The data was downloaded in 5 degrees by 5 degrees tiles, which were merged over the study area. Additional reference data sources such as Open Street Map, US National Land Cover NLCD, wetlands and water from GlobeLand 30 Land Cover, and SRTM DEM roughness were integrated to confirm or exclude indicated GUF areas.

The DLR Global Footprint maps were used to estimate the population density per district.

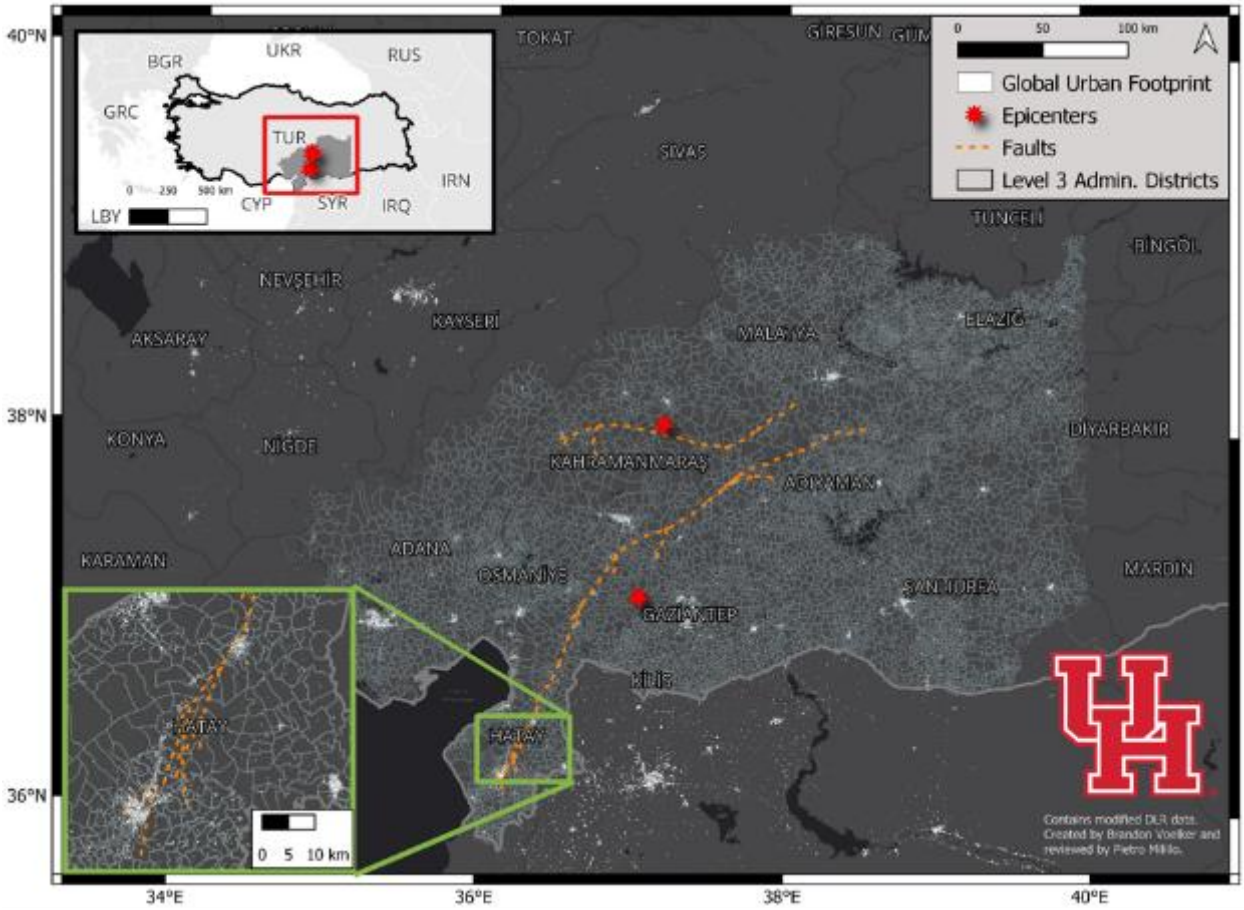

Figure 163: Administrative boundaries map. The white clusters of pixels represent urban areas. The study area is covered by over 9000 districts. The districts' administrative boundaries are displayed as polygons outlined in grey, the faults are represented as dashed orange lines, and the red stars are the locations of the epicentres of the earthquake sequence.

5.1.2.4. World Settlement Footprint 3D

The World Settlement Footprint (WSF 2019) 3D dataset from the DLR includes detailed information on total area, average height, total volume, and fraction of buildings for a global grid with 90 m cell size, covering every settlement on the planet. The WSF 3D data was created from Sentinel-1 and Sentinel-2 satellite imagery at 10 m resolution with 3D vertical structuring from TanDEM-X digital elevation models at 12 m resolution. The information on building size and distribution from this dataset was used to quantify district with the greatest density of buildings. *Figure 164* shows the distribution WSF 3D and WSF Evolution data over Gaziantep, Türkiye.

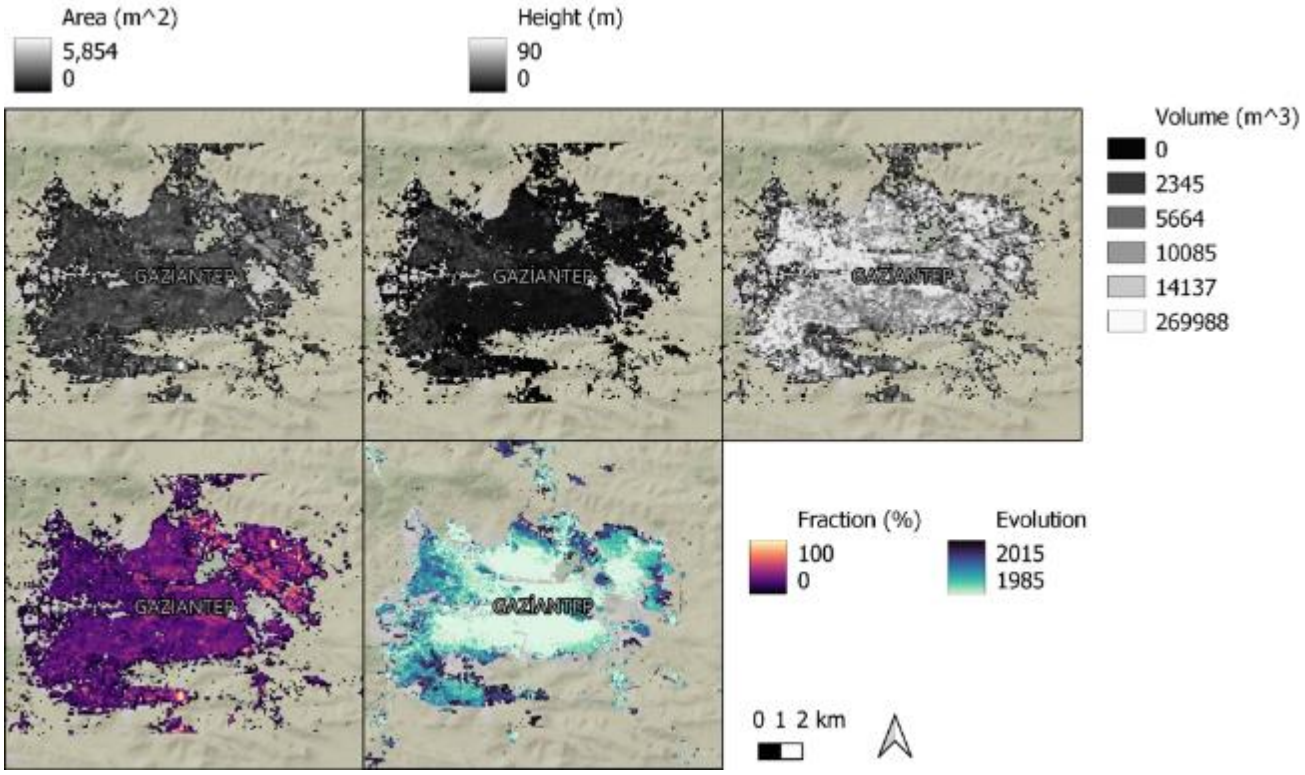

Figure 164: DLR WSF 3D and Evolution data around Gaziantep, Türkiye. Area, height, and volume characterize the dimensions of the buildings inside a 90m pixel, while fraction describes the percentage of each pixel that contains buildings, and the Evolution dataset displays the average building age in each pixel.

5.1.2.5. World Settlement Footprint Evolution

The World Settlement Footprint Evolution dataset (WSFE 2020) is a 30m resolution dataset from the DLR outlining global settlement extent on a yearly basis from 1985 to 2015. All available Landsat-5 and Landsat-7 scenes within a given area are acquired and key temporal (i.e., temporal mean, minimum, maximum, etc.) are extracted for different spectral indices, such as normalized difference built-up index (NDBI), normalized difference vegetation index (NDVI) and modified normalized difference water index (MNDWI). For each year, these features are then trained on settlement and non-settlement samples from the WSF 2015 data, and the pixels within the target year are classified. This dataset was used to compare the distribution of building age across districts; older buildings were expected to be constructed under different building codes.

5.1.2.6. OpenStreetMap Buildings

The building footprint dataset was obtained from the Humanitarian OpenStreetMap Team (HOT), hosted by the Humanitarian Data Exchange. When a natural disaster occurs, the HOT team comes together with thousands of volunteers online and on the ground to create open-source disaster-response data. After the February 2023 earthquake, the HOT team generated crowd-sourced building footprints to aid the relief efforts. This data was compared to the earliest official damage maps to understand which regions had the greatest need for further surveys still existed. Some

inconsistencies were found across the two datasets in terms of missing building footprints.

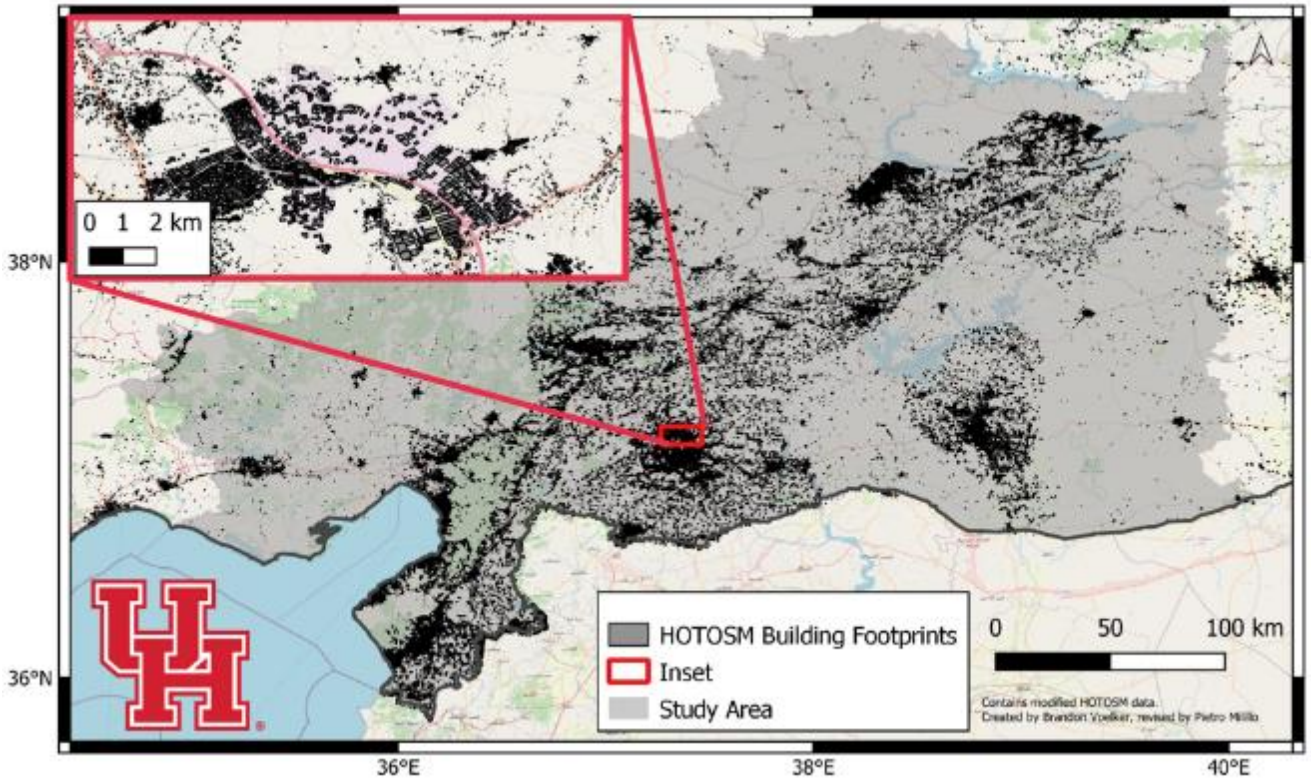

Figure 165: Building footprints in southeast Türkiye from the Humanitarian OpenStreetMap Team, over a basemap of other OpenStreetMap features.

5.1.3. Step 3 – Data Processing and Selection of Areas of Interest

Using the data collected in the steps described above, the Remote Sensing team assisted the ground-based teams in choosing areas of interest (AOIs) to conduct field surveys. The selection process was based on the concurrent analysis of the available remote sensing datasets describing urban fabric and damage distribution, and the location of critical infrastructure. A detailed framework was developed to characterize and validate the remote sensing approaches, methodologies, and datasets to assist post-earthquake reconnaissance missions.

In the immediate aftermath of the earthquake, numerous groups created damage proxy maps from several satellite sources to provide insight into the extent and severity of damage caused by the earthquake (*Table 8*). The team used damage maps used obtained from the NASA – ARIA laboratory, Copernicus EMS, the European CMCC, and Microsoft/MAXAR maps. The list below provides more details about the origin of these dataset:

- C-band Sentinel-1 SAR imagery, processed by the NASA Advanced Rapid Imaging and Analysis (ARIA) laboratory.

- Copernicus Emergency Management Service (EMS) activation EMSR648, which used very high resolution (< 1m) optical satellite imagery to classify damage for 20 cities in southeast Türkiye near the earthquake epicentre.
- SAOCOM L-band SAR data: SAOCOM results were provided by the Euro Mediterranean Center for Climate Change (CMCC). The processing methodology is described in the following section.
- MAXAR optical data processed by Microsoft using machine learning techniques over 4 cities. Imagery from Planet Labs and Maxar Technologies, at spatial resolutions of 50cm and 30cm, respectively, were used with convolutional neural networks (CNNs) to classify the imagery as part of a damaged building, part of an undamaged building, or neither. Finally, the percentage of pixels within each building footprint from either the Microsoft Building footprint dataset or from OpenStreetMap that was classified by the CNN as "part of a damaged building" was calculated.

From each map, the standard deviation of the damage values within each administrative district was calculated. The standard deviation was used as an indicator to pinpoint to the ground team the locations in which the greatest variety of building damage grades could be surveyed. For instance, a district where all buildings are destroyed, and a district where all buildings are intact would both a low standard deviation. High standard deviation within a district therefore indicated districts that contain varying levels of damage.

These processed standard deviation maps were corroborated and verified using official maps provided by local official or by other authoritative institutions. These include the official damage maps from Turkish government which were obtained from the hasar.cbs.gov.tr website. These maps provide information on the extent and severity of building damage caused by the earthquake. They were processed by Gece Yazılım (http://www.geceyazilim.com.tr/) for address information and visualized by Yer Çizenler (https://yercizenler.org/en/home/) to produce maps available on https://hasar.6subatdepremi.org. Every building in the dataset was classified by the observed damage grade. A bespoke damage scale was used, with 4 grades of damage: "Slightly damaged", "Heavily damaged", "Needs demolition", and "Collapsed" as opposed to the 5-tier damage categorisation system that the Turkish Ministry of Environment, Urbanisation and Climate Change (MoEUCC) which was primary governmental organisation leading on damage assessment (see Section 4.2.3).

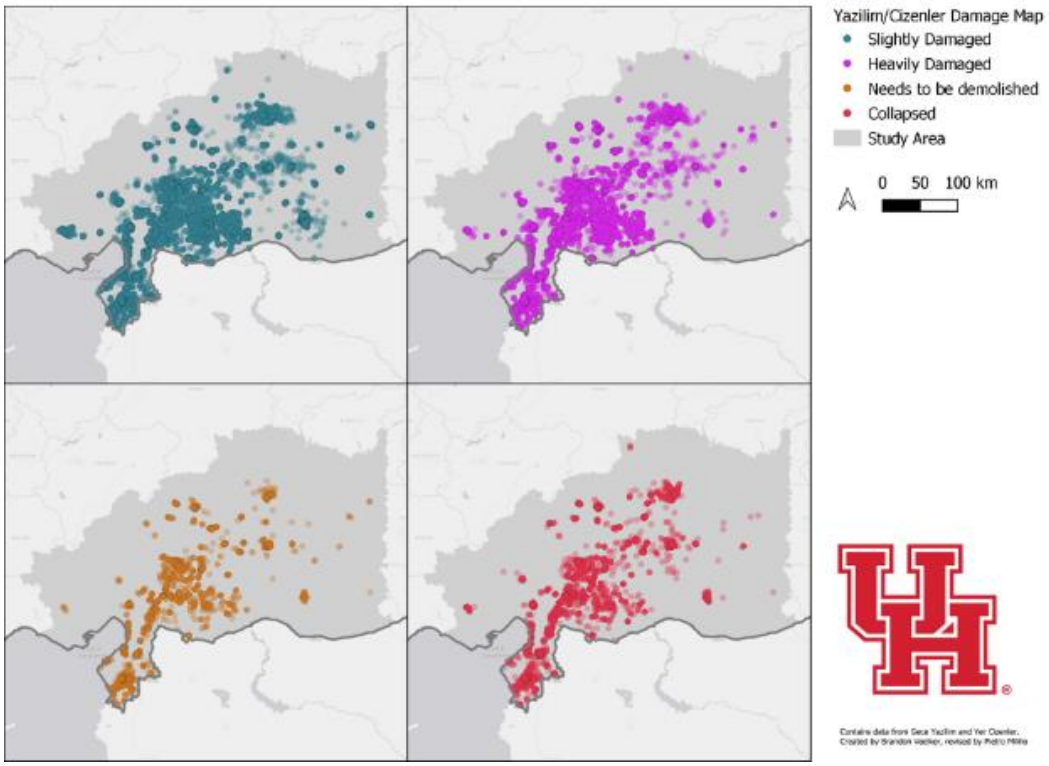

Figure 166: Density plots representing Damage maps from Turkish government reports. Each point represents a building that was classified as slightly damaged, heavily damaged, in need of demolition, and collapsed. Solid colours are used in this map to represent areas where most damaged buildings are located. Faded colours represent areas where fewer buildings (up to 10% of the buildings in the resolution cell) have been characterized by damage.

This framework facilitated the selection of the top 6 areas of interest for ground-based surveys (*Figure 167*).

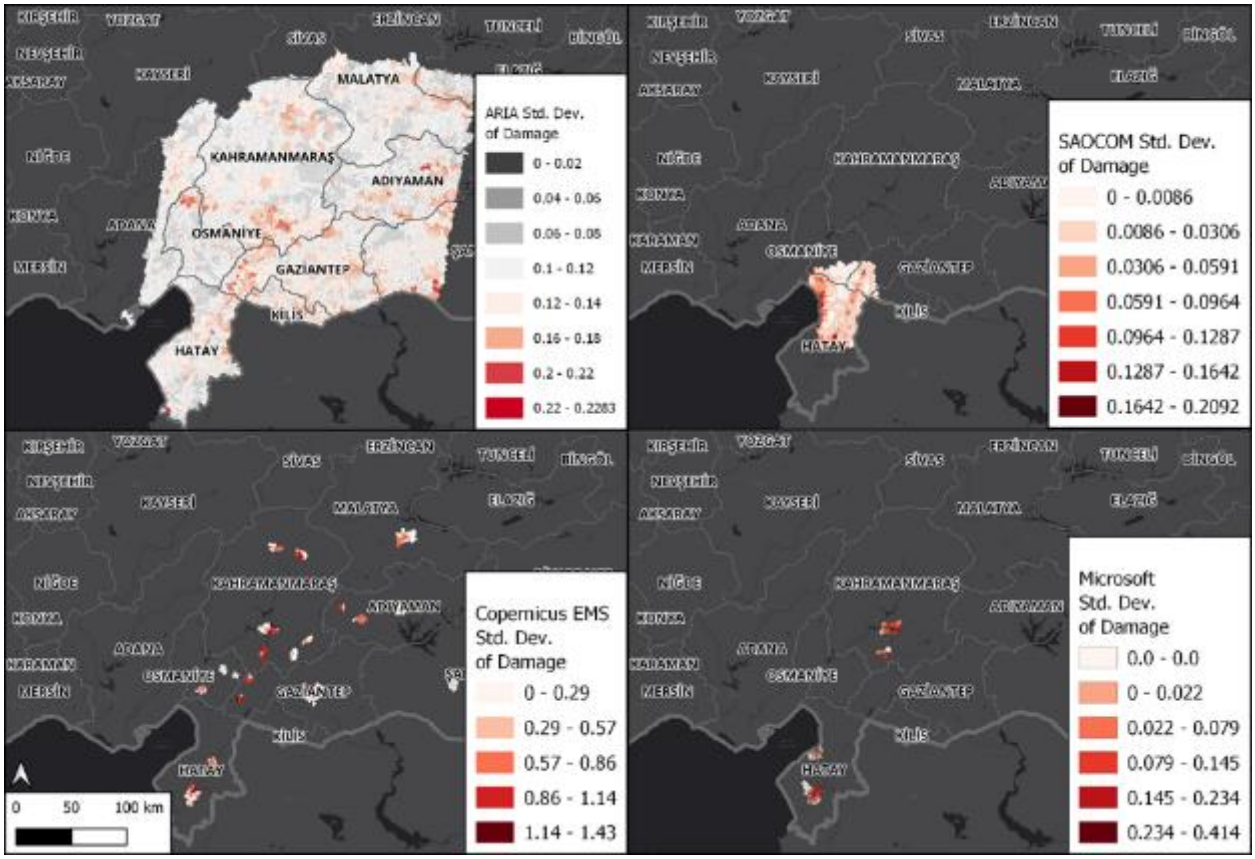

Figure 167: Standard deviation of the available damage proxy maps derived from optical and radar data in the southern part of the study area.

5.1.4. Step 4 and 5 – Contacting Commercial Vendors: Mission Support on Behalf of Umbra and Capella

The Remote Sensing team also connected with commercial satellite vendors Umbra and Capella to acquire data while the ground-based mission was ongoing. This provided real-time access to satellite imagery and improved the accuracy and timeliness of the assessment of the damage. The data acquired from Umbra and Capella was integrated with the existing datasets to refine the selection of areas of interest and prioritize ground-based surveys. A methodology developed by Giardina et al. (2013) and already deployed for the EEFIT HAITI remote mission was applied to generate damage neighbourhood maps based on SAR amplitude entropy.

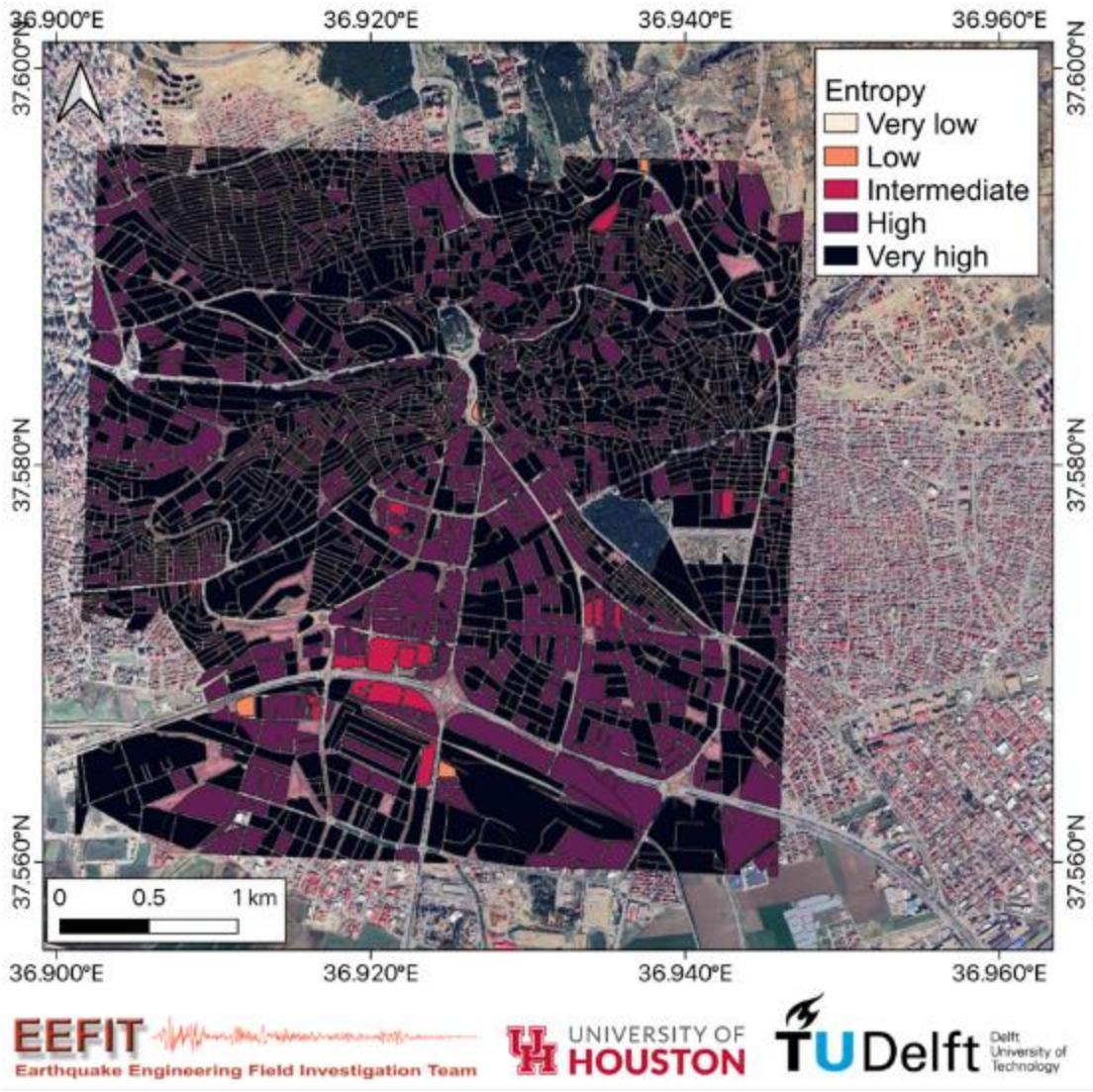

Figure 168: Example of Damage Product generated using Umbra Space satellite data.

5.2. Conclusion

The Remote Sensing team played a crucial role in supporting the EEFIT post-earthquake reconnaissance mission in Türkiye in February 2023. We created a database of damage products, identified existing satellites that acquired relevant datasets, and connected with private satellite vendors to acquire real-time data. Our activities facilitated the selection of areas of interest for ground-based surveys and improved the accuracy and timeliness of the assessment of the damage.

The activities undertaken on this report provide proof of the large variety of RS data available and techniques applicable to a reconnaissance mission and how these can be standardized into a replicable, standardized framework. The growing availability of remotely sensed data reinforces the interest towards their inclusion into every phase of a reconnaissance mission, from early planning to final reporting and dissemination. Building on the positive outcomes of this mission, future research and efforts in this

direction will be dedicated to reconciling and validating different remote sensing-based damage with ground truth datasets.

In order to generate damage proxy maps for Türkiye earthquake we adopt a methodology described by Yun et al. (2015).

5.3. Dataset

SAR sensors operate on different wavelengths such as C-band and L-band. The longer the wavelength, the higher the penetration depth is (Sharma, Hajnsek et al. 2012). Consequently, interferometric phases are expected to remain coherent for a longer temporal baseline compared to the C-band. Most L-band spaceborne operating sensors are commercial such as SAOCOM. SAOCOM is the Argentinian's spaceborne twin L-band polarimetric SAR sensors. Argentinian space agency lunched SAOCOM-1A and SAOCOM-1B on 07 October 2018 and 30 August 2020, respectively with the design life of five years(CONAE October 2018)

SAOCOM available image frames over the impacted area consist in: three SLC hh-polarized descending images, covering Islahiye and acquired in 2022-07-11, 2023-02-20 and 2023-02-28.

5.4. Methodology

To do DInSAR with the purpose of measuring the deformation, the ideal condition is when the interferometric phase quality is high. Coherence, also known as correlation, a measure of phase quality, shows how correlated the back scattered signal remains between two images. According to equation below, it can be determined using complex values of corresponding pixels in those images (Zebker and Villasenor 1992, Hanssen 2001).

$$\gamma = \frac{\sum_{i=1}^{N}\sum_{j=1}^{M} P_{ij} \times S_{ij}^{*}}{\sqrt{\sum_{i=1}^{N}|P_i|^2} \times \sqrt{\sum_{j=1}^{N}|S_j|^2}}$$

where P and S are the primary and secondary images, respectively. N and M are the size of the coherence window and * stands for complex conjugate. Even though the higher the size is, the lower would be the coherence bias, the spatial resolution will be coarser. So, a balance should be struck between these two factors. Here, a 7x7 square window is used for coherence estimation. Decorrelation can be considered as the multiplication of 4 terms, i.e., geometrical, volume, thermal and temporal. Geometrical decorrelation happens because of spatial separation of two sensors, to be compensated using the common band filtering. Volume decorrelation occurs due to the volumetric scattering and depends on the scatterer characteristic. The thermal depends on the signal to noise ratio (SNR) and can be reduced by filtering the data. Temporal decorrelation is due to the temporal separation of acquired images, as is the case in repeat-pass interferometry.

In urban areas, the coherence value between two acquisitions is generally expected to remain high unless there is damage. Based on that, in a post-seismic pair the coherence is going to be higher compared to the co-seismic one. Equation (1)

indicates that the coherence values are scaled from 0 to 1. Unlike the deformation monitoring approaches, damage proxy maps (DPM) look for changes in coherence values. Such maps can be generated by subtracting the post- and co-seismic coherence maps. Positive values in the DPM depict damaged areas, with higher values indicating more significant damage. Negative values are mostly due to the temporal decorrelation not the earthquake damage. Thus, they cannot be interpreted as damaged areas.

The coherence index is calculable for each pixel in an image, but it can only be accurately interpreted at a coarser resolution due to the spatial sampling of image pixels involved in the estimation process.

When analyzing damage maps for planning and response purposes, it may be more beneficial to evaluate damages based on predefined regions such as administrative boundaries, building codes, or urban infrastructure instead of solely relying on the image geometry of an imaging system. To this end, the World Settlement Footprint is used to mask out nonresidential areas.

5.5. Results

The Euro Mediterranean Center for Climate Change (CMCC) generate DPM over Islahiye using co-seismic images, acquired on 2022-07-11 and 2023-02-20. Post-seismic coherence maps have been using images acquired on 2023-02-20 and 2023-02-28. Since both co- and post-seismic pairs are characterized by large differences in the temporal baseline, we expect this DPM to be characterized by an elevated number of false positives that will be assessed at a later time. In order to have a square pixel size, the multi-looking factor along the azimuth should be two times bigger than the range factor. In the light of the argument mentioned above, the multi looking factor is considered as 10 by 20 in range and azimuth direction. It corresponds to a 100 by 100 square meter resolution on the ground. *Figure 169* shows the post-, co-seismic coherency maps and their DPM. Coherence maps are displayed from black to yellow, representing 0 and 1, respectively.

Dark areas in *Figure 169*a can be interpreted as both damaged areas as well as the temporal decorrelation due to the almost a 7-month temporal baseline. In the post-seismic pair, the coherence values are higher as shown in *Figure 169*b. To focus only on residential damaged areas, non-residential areas are masked out from DPM (*Figure 169*c). Moreover, negative values are cancelled out from the DPM since they cannot be interpreted as damaged areas. Therefore, the remaining values range from 0 to 1, with highly damaged areas represented in red.

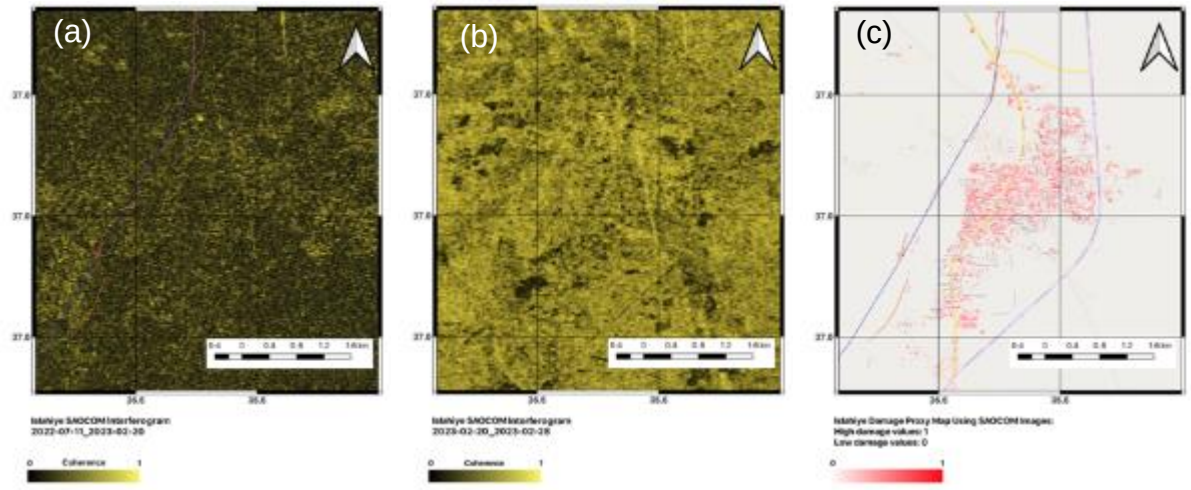

Figure 169: Islahiye SAOCOM coherency and DPM. a) Co-seismic coherency map. b) Post-seismic coherency map. c) DPM masked using the World Settlement Footprint map. Red areas depict highly damaged regions.

References

CONAE (October 2018). "Successful launch of the SAOCOM 1A Satellite — The first steps of SAOCOM 1A in Space." from Https://www.argentina.gob.ar/noticias/exitoso-lanzamiento-del-satelite-saocom-1a.

Giardina, G., Macchiarulo, V., Foroughnia, F., Jones, J. N., Whitworth, M. R., Voelker, B., ... & Kijewski-Correa, T. (2023). Combining remote sensing techniques and field surveys for post-earthquake reconnaissance missions. *Bulletin of Earthquake Engineering*, 1-25.

DLR (2020) Global Urban Footprint. available at https://www.dlr.de/eoc/en/desktopdefault.aspx/tabid-9628/16557_read-40454/ (Last accessed December 5th 2023)

DLR (2019) World Settlement Footprint. available at https://geoservice.dlr.de/web/maps/eoc:wsf2019 (Last accessed December 5th 2023)

Hanssen, R. F. (2001). Radar interferometry: data interpretation and error analysis, Springer Science & Business Media.

Robinson, C., Gupta, R., Nsutezo, S.F., Pound, E., Ortiz, A., Rosa, M., White, K., Dodhia, R., Zolli, A., Birge, C., Ferres, J.L. (2023) Türkiye Building Damage Assessment, available at: https://www.microsoft.com/en-us/research/uploads/prod/2023/02/Türkiye-Earthquake-Report-2_MS.pdf (last accessed December 5th 2023)

Salamon, P., Mctlormick, N., Reimer, C., Clarke, T., Bauer-Marschallinger, B., Wagner, W., ... & Walli, A. (2021, July). The new, systematic global flood monitoring product of the copernicus emergency management service. In *2021 IEEE International Geoscience and Remote Sensing Symposium IGARSS* (pp. 1053-1056). IEEE.

Sharma, J. J., et al. (2012). "Estimation of glacier ice extinction using long-wavelength airborne Pol-InSAR." IEEE Transactions on Geoscience and Remote Sensing **51**(6): 3715-3732.

Wania, A., Broglia, M., Kucera, J., Spruyt, P., Rossi, M., Spinoni, J., ... & Louvrier, C. (2016, March). 2016 User Workshop of the Copernicus Emergency Management Service–Summary Report. In *Workshop held on* (Vol. 15, p. 16).

DLR (2019) World Settlement Footprint (WSF). available at https://geoservice.dlr.de/web/maps/eoc:wsf2019 (Last accessed December 5th 2023)

DLR (2020) World Settlement Footprint Evolution (WSFE) available at https://geoservice.dlr.de/web/maps/eoc:wsfevolution (Last accessed December 5th 2023)

Yun, S.-H., et al. (2015). "Rapid damage mapping for the 2015 M w 7.8 Gorkha earthquake using synthetic aperture radar data from COSMO–SkyMed and ALOS-2 Satellites." Seismological Research Letters **86**(6): 1549-1556.

Zebker, H. A. and J. Villasenor (1992). "Decorrelation in interferometric radar echoes." IEEE Transactions on Geoscience and Remote Sensing **30**(5): 950-959.

6. INFRASTRUCTURE

During the remote and field components of the mission the EEFIT team focused mainly on critical infrastructure that is most needed and most difficult to substitute for efficient relief, response and recovery. In particular, the team focused its efforts on healthcare facilities, fire-brigade buildings, schools and large power generating plants. The types of infrastructure covered in this section of the report are listed below:

- Healthcare infrastructure
- Education infrastructure
- Emergency Response infrastructure
- Transportation infrastructure
- Energy infrastructure
- Industry infrastructure
- Water and Wastewater infrastructure
- Dams and reservoirs
- Communication infrastructure

In addition, the report makes an attempt to identify and highlight the interdependencies between the different types of infrastructure and to trace cascading effects.

6.1. Healthcare Infrastructure

6.1.1. Design and Construction Regulations Related to Hospitals and Other Healthcare Facilities in Türkiye

After the 1939 M7.9 Erzincan earthquake, the first seismic building regulations were issued. Since then, the construction codes in Türkiye have been updated several times in line with the knowledge at the time and enhancement of earthquake engineering research. The seismic code in 1975 introduced the equivalent static force concept, through a seismic coefficient C_0, structural coefficient K, and spectral coefficient S. An importance factor of 1.5 was incorporated for all government buildings, emergency buildings and buildings of high occupancy. The 1997 Seismic code incorporated the lessons learned from the Erzincan earthquakes in 1992. The code was very similar to the EN 1998 in that the capacity design principles were adopted, and the ductile design principles were explicitly introduced. The 2007 building code was issued after the devastating M 7.9 earthquakes in Izmit and Kocaeli, where the performance-based design was introduced.

12 hospital buildings (26% of out of the 47 hospitals) were damaged beyond repair after the 1999 Kocaeli (Mw 7.4) and Düzce (Mw 7.2) earthquakes (Erdik, 2001). Similarly, several hospitals were damaged (structural, non-structural and equipment) in the cities of Van and Ercis in the 2011 Van earthquake, (Erdik, 2001; Di Sarno et al., 2013). These heavy damages and interruptions of health services due to the earthquakes in the last decades in Türkiye have led Turkish Ministry of Health (MoH) to release a regulation and technical specifications in 2013 to enforce that “Hospital Buildings, located in seismic zones 1 and 2 with number of bed capacity over 100 should be constructed with base-isolation” (Ministry of Health, Construction Repair

Department, 2012). The MoH also prepared a technical specification for the seismic isolation design for hospital buildings (General Directorate of Health Investments, (2013) which can be summarised as follows:

- Structural systems should be designed considering the ground motion levels having a 475-year return period (10 percent probability of exceedance in 50 years).
- The system below the isolation layer should remain primarily elastic, with a response modification factor of 1.0. The system above the isolation layer shall be designed with a maximum response modification factor of 1.5.
- The displacement capacity of the isolation system should be determined for the ground motion level with a 2475-year return period (2% probability of exceedance in 50 years). The displacement values of the isolation system shall be increased by a minimum of 10% to consider torsional effects.
- The story drift values above the isolation layer must not exceed 0.50%.
- The average horizontal acceleration at each story level should be limited to 0.30 g.
- The non-structural elements (i.e. heating, ventilating, and air conditioning, plumbing, electro-mechanic systems) should be designed to accommodate the isolation system displacement and to continue its function after an earthquake.

In 2018, the design requirements for seismically isolated structures were outlined in a section called "Special Rules for the Seismic Design of Isolated Structures" within the latest version of the Turkish Earthquake Resistant Design Code (TBEC, 2018). The seismic isolation design utilizes ground motion levels corresponding to a 475-year Design Basis Earthquake (DBE) and a 2475-year Maximum Considered Earthquake (MCE).

The TBEC (2018) is a thorough update of the 2007 building codes. There are several new sections, including those dedicated to high rise buildings, seismic isolation, cold formed steel, and wooden buildings. The 2018 Turkish Earthquake Code includes a short chapter on the design of nonbuilding structures and the anchorage of mechanical and electrical equipment. Prior to the adoption of the 2018 code, the engineering design of these systems was not emphasised. However, these services are not provided by the Engineer of Record for the building, and it is not clear how they will be enforced.

Further, the 2018 seismic code introduced changes in the seismic hazard map from 1996. Both maps are based on Mean Return Period (MRP) 475 years and are for rock soils. However, the TBEC 2018 map (e-Devlet Kapısı: ,Türkiye.gov.tr) is a contour map, and the hazard is expressed as spectral acceleration, unlike the hazard map from TEC 2007 which has 5 zones, and the action is expressed in PGA.

6.1.2. Healthcare Infrastructure in the Affected Area

In the affected 11 provinces there are 116 hospitals (12.5% of all hospitals in Türkiye) with a total capacity of almost 24,000 hospital beds (14% of capacity in Türkiye). Of the 118,675 medical specialists and general practitioners serving in the hospitals under the MoH, 19,616 work in the affected 11 provinces (PSB, 2023). A breakdown of the healthcare facilities, hospitals, physicians and other healthcare staff and hospital beds per province is provided in *Table 9* below (PSB, 2023).

Table 9: Healthcare sector capacity in the earthquake-affected region (PSB, 2023).

Province	Number of primary level healthcare facilities	Number of hospitals	Number of physicians	Other healthcare staff	Hospital beds per 10,000 people
Adana	291	14	3,686	10,082	34.3
Adıyaman	125	10	883	4,040	22
Diyarbakir	264	18	2,723	8,145	28
Elazığ	135	8	1,047	3,709	54
Gaziantep	302	12	2,626	8,124	32
Hatay	350	12	2,373	7,443	27
Kahramanmaraş	329	10	1,579	5,846	27
Kilis	52	2	285	1,453	44
Malatya	226	12	1,540	5,163	44
Osmaniye	133	5	563	3,024	23
Şanlıurfa	247	13	2,311	8,300	20
Region total	2,454	116	19,616	65,329	32.3
Türkiye total	14,031	927	118,675	421,377	31.3

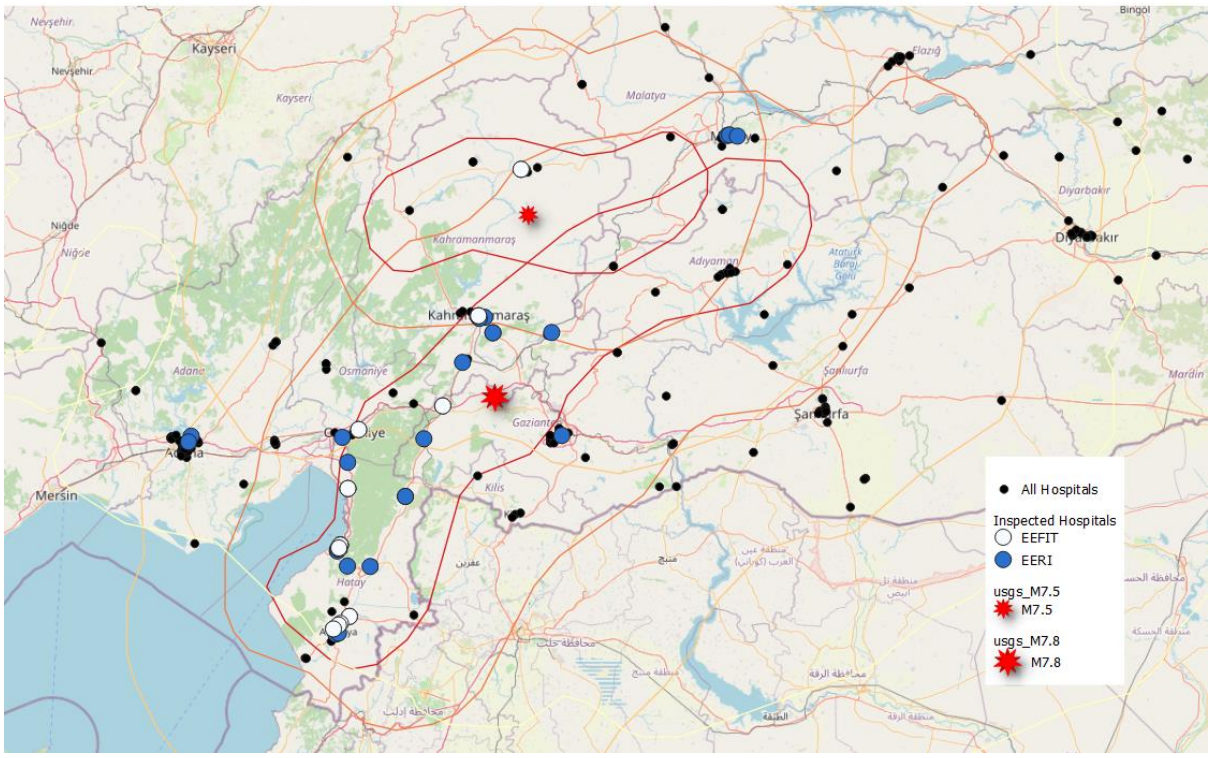

Figure 170: Hospitals visited by EEFIT team [white] and EERI team [blue] (EERI, 2023)

Hospitals visited by the EEFIT team and separately by the EERI team are shown in *Figure 170*. Most of the hospital buildings in the area are reinforced concrete structures built after 2000, with 2 to 10 storeys. The common structural types are reinforced concrete frame or reinforced concrete wall system, with unreinforced masonry partition walls and masonry façade infills. The hospitals constructed after 2013 with more than 100 beds should be built on base isolation. As for the smaller facilities and the ones designed before 2013, the most common foundation type is slab foundation. Most hospital buildings are regular in elevation and have simple plan shapes. Buildings designed on multiple levels and buildings with more complicated plan schemes are separated with seismic joints such that individual the separate parts meet the regularity criteria in plan and elevation. Facades with heavy exterior cladding are commonly observed.

The description above is based on our team's desk study and on-site visual inspection, not on official building documentation.

6.1.3. Overall Impact on the Healthcare Infrastructure

The 6 February earthquake sequence from 6th of February in Southern Türkiye affected an area of nearly 350,000 km^2 inhabited by over 15 million people. The damages among the transport infrastructure, emergency and health infrastructure, facility lines and the winter storms additionally hampered the rescue and relief effort. The earthquake caused 108,000 injuries and had a confirmed death toll of 62,013: 53,537 in Türkiye and 8,476 in Syria.

According to the initial assessment made by the Turkish Ministry of Health (MoH) and the World Health Organisation (WHO), a quarter of the hospitals in the 11 affected provinces were severely or moderately damaged, while 15% of primary health care facilities (236 facilities in total) were left inoperable by the earthquakes. In the most affected districts of the four provinces (Hatay, Adıyaman, Kahramanmaraş and Malatya) more than 40% of district Health Directorates, more than 70% of family health centres, and 50% of migrant health centres were damaged. The operation of some of the hospitals was temporarily interrupted because of the disruptions in the utility lines, the lack of running water or electricity. The Disaster and Emergency Management (AFAD) and the Medical Emergency Coordination Centre, mobilised National Medical Rescue Teams (UMKEs) from across the country, with 1,253 ambulances, 14 air ambulances, 245 vehicles and a total of 12,749 UMKE and 112 medical staff, together with 26,353 physicians and medical personnel deployed at the healthcare facilities in the earthquake-affected region. The shortcomings of the hospitals that were undamaged or that were lightly damaged but could not operate due to lack of energy, etc., were quickly corrected and these hospitals started service delivery.

As per the damage assessment performed by the Government (PSB, 2023) a total of 42 hospital buildings in the region (27 owned by the MoH, 6 owned by universities and 9 privately owned) suffered severe and moderate damage and 94 hospital buildings were lightly damaged (75 owned by MoH, 12 university hospitals and 7 privately owned). Damage distribution along the healthcare sector is provided along with the type of ownership is presented in *Figure 171*. This means that approximately 30% of the building stock in the health care sector in the affected region was damaged beyond repair and put out of service for a long term. The total losses across the healthcare sector were estimated to be 80.9 billion TRY (2.7 billion GBP) Government (PSB,

2023). Majority of the damage was concentrated in the hospitals owned by MoH, with a total cost amounting to 72.3 billion TRY (2.4 billion GBP). The losses associated with the private hospitals were reported to be 6.9 billion TRY (230 million GBP). The repair costs and disaster-induced machinery-equipment needs of the 8 university hospitals in the region was valued at 1.7 billion TRY (56 million GBP).

Besides the EEFIT mission, other teams have studied the performance of the hospitals in the affected region as well. Team of the Chinese Earthquake Administration visited twelve hospitals and published their findings in a paper, where they report that the operation of the newly built hospitals with seismic base isolation was not interrupted and some of the older hospital buildings with fixed foundations managed to maintain structurally stability despite the intense shaking beyond the levels considered for above their design basis (Qu et al., 2023). According to the EERI report (EERI, 2023), the prevalence of cracks in walls degraded the patient-s and medical personnel confidence regarding the building safety and was among the reasons why buildings and floors were closed. There is no information as to how many of the hospitals were evacuated in the early hours after the disaster and how many of them re-opened once the buildings were confirmed to be safe and the repair works have finished. The observed non-structural damages concentrated most commonly on non-load bearing masonry walls, claddings, and partitions, suspended ceilings, mechanical electrical equipment, utility distribution lines, and medical equipment. Façade systems with heavy cladding were seriously damaged. Failure of systems like unanchored electrical generators, AHU machines and large medical equipment often occurs before failure of the building, rendering the infrastructure and its services unusable even when the structure is undamaged.

EEFIT teams visited on-site 14 hospital buildings, 9 of which were closed. Three buildings collapsed: the oldest building within the complex of Iskenderun State Hospital, constructed in 1968; the Education and Research Centre in Hatay, constructed in 2001; and the Antakya Private Akademi Hospital (Ozel Antakya Akademi Hastanesi), constructed in 2011. By the time the team visited the sites, works to remove the debris had already started and the failure mechanisms for these buildings were not fully identifiable.

A summary of the collected information by the EEFIT team and EERI teams (EERI, 2023) on the structural losses at hospital buildings and their operational status is presented on the maps shown in *Figure 172-Figure 174*. Out of the 39 hospitals that were inspected by the EEFIT and EERI teams, 14 were closed by the time of their visits. The distribution of structural damages among the closed hospitals was various: 3 of them have collapsed, 1 experienced moderate damage, and the other 10 experienced minor or no damages.

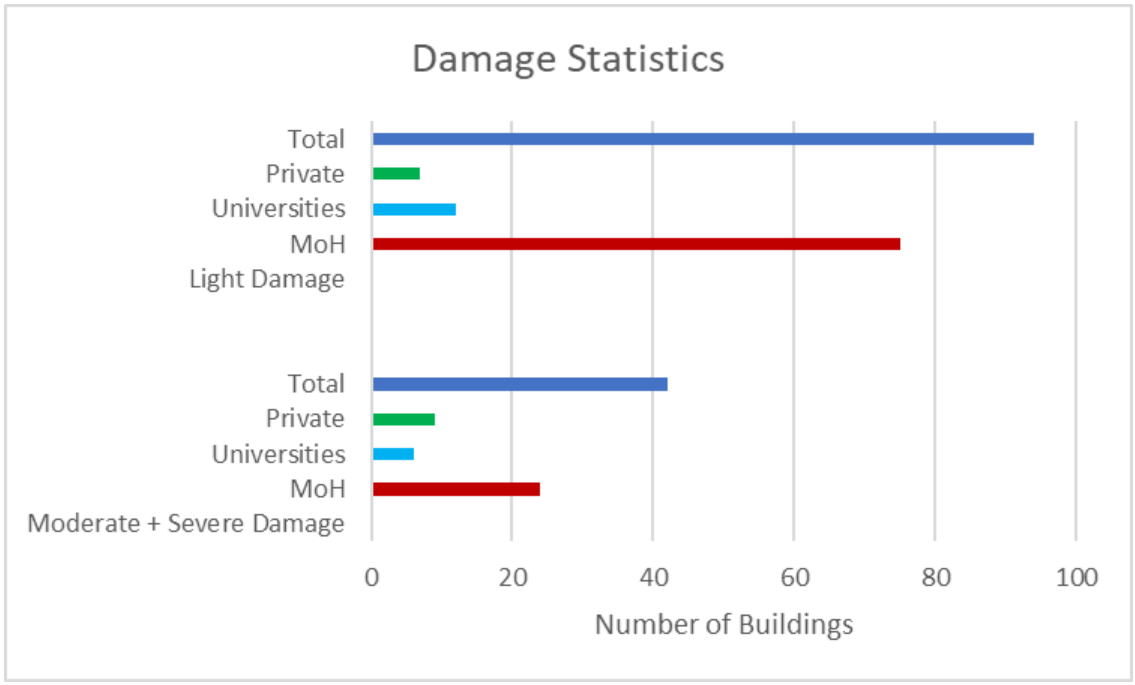

Figure 171: Damage distribution along the healthcare sector.

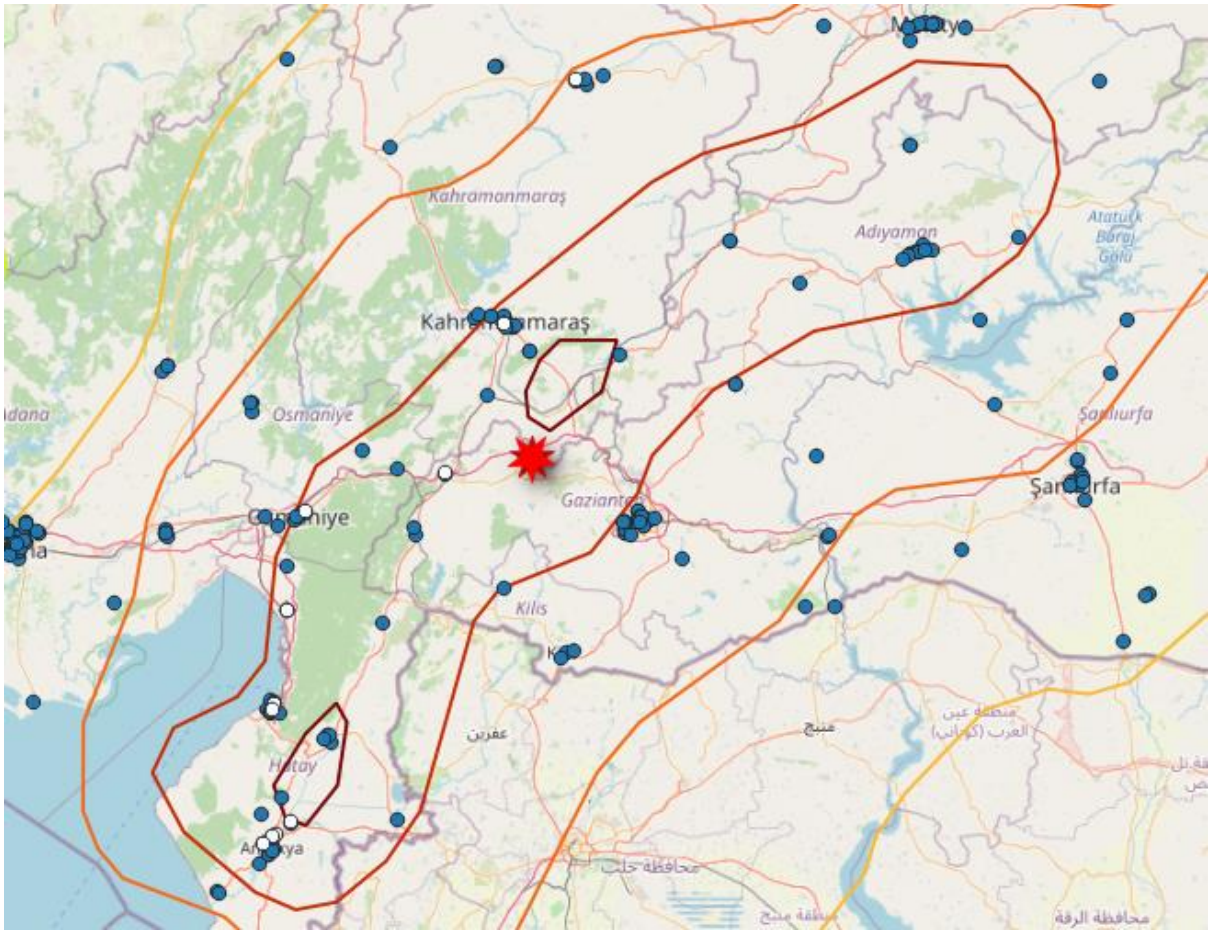

Figure 172: Hospitals visited by EEFIT team.

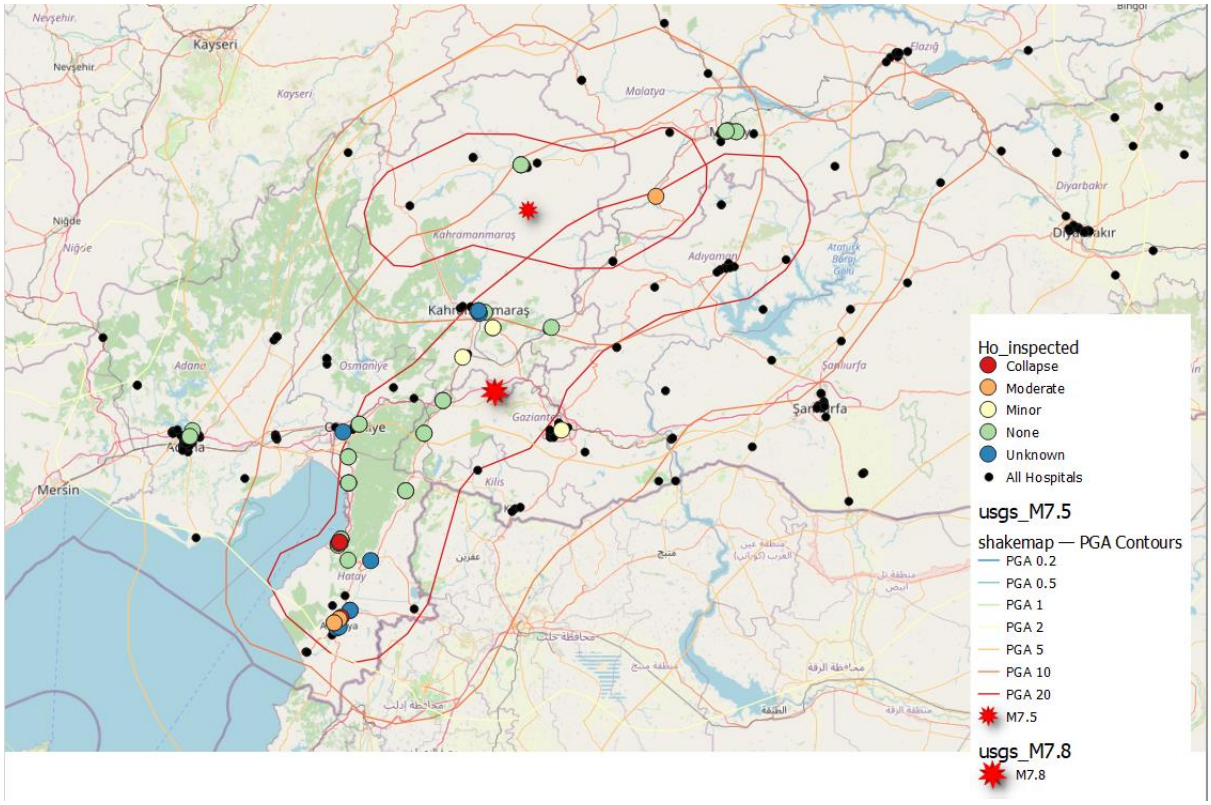

Figure 173: Damage states of the hospitals visited by the EEFIT and EERI (EERI, 2023) missions.

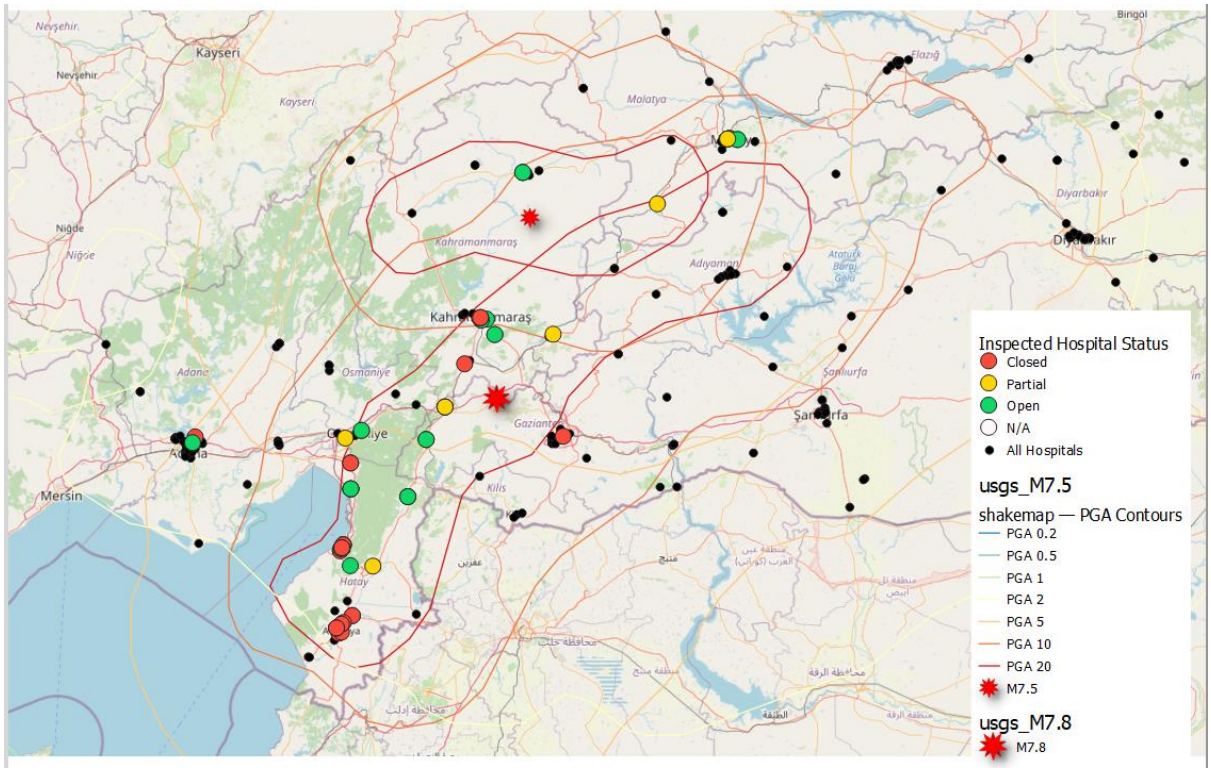

Figure 174: Operational status (closed, open, partially open, unknown) of the hospitals as observed six weeks after the earthquake from the EEFIT and EERI (EERI, 2023) teams/missions.

6.1.4. Case Studies

Table 10 below summarises the hospitals visited by the EEFIT field mission.

Table 10: Hospitals visited by the EEFIT team during the field mission.

Hospital Name	Capacity	Year	No. Floors	Str. system	PGA [g]	Structural damage	Operational status (after 6 weeks)	Comment
Dörtyol State Hospital (new)	250	2022	10	RC	0.24	None	Open	Base isolation.
Dörtyol State Hospital (old)	unknown	1983	unknown	RC	0.24	None	N/A	Not in use as a hospital. Used as a storage space.
Iskenderun State Hospital (old)	670	1968	2.5	RC	0.28	Collapse	Closed	
		2005	6	RC		Minor	Closed	
		2020	6	RC		unknown	Closed	
Iskenderun State Hospital (new)	N/A	N/A	N/A	RC	0.28	None	Closed	Temporarily replaced by a field hospital
Hatay State Hospital	1130	N/A	5, 8	RC	0.62	unknown	Closed	Serviced delivered via field hospital
Antakya Private Akademi Hospital	unknown	unknown	9, 10	RC	0.62	Collapse	Closed	
Defne Private Hospital	245	2008	9	RC	0.62	Moderate	Closed	
Hatay Education and Research Hospital	150	2001	7	RC	1.2	Collapse	Closed	SGM station 3126 @ 500m North
Elbistan State Hospital	355	2017	3, 4, 8	RC	N/A	None	Open	Base Isolation
Nurdağı State Hospital	25	2016	2	RC	0.32	None	Closed	Significant non-structural damage

Vatan Private Hospital	Unknown	2008	7	RC	0.36	Unknown	Closed	Severe non-structural damage
Osmaniye State Hospital	420	2023	7	RC	0.18	None	Open	

6.1.4.1. Severe Damage and Collapses

The team visited three of the hospitals that were reported as collapsed after the earthquake, namely the Iskenderun State Hospital, the Hatay Education and Research Hospital and the Antakya Private Akademi Hospital. Demolishing works to remove heavily damaged structures were completed on all three sites before the team visited them and direct observations about the possible reasons for their collapses were not possible.

The Iskenderun State Hospital occupied multiple buildings constructed at different times with the two main blocks built respectively in 1968 and 2005. The building constructed in 1968 collapsed due to the earthquake, while the one constructed in 2005 stood up however was nonetheless evacuated and due to the extent of non-structural damage by the time of our team's visit could not be reoccupied (*Figure 175* and *Figure 176*). Based on the observed debris, the structural system of the 1968 building seems to be RC Moment Resisting Frame (MRF) like the one in the 2005 building. The reason for the collapse is unknown. The maximum PGA recorded in the nearest strong ground motion (SGM) station (4.3km south from the site) is 0.28 g with maximum spectral acceleration 0.6 g in the short period range and 0.48 g in the long period range. Another SGM station at a similar distance (4.75 km NE) from the site reveals significantly lower strong ground motion parameters. See *Table 1Table 11* for more information.

Figure 175: Iskenderun State Hospital: a) satellite view (blue arrows show the location and direction of the taken photographs) and b) as observed on 13 of March 2023

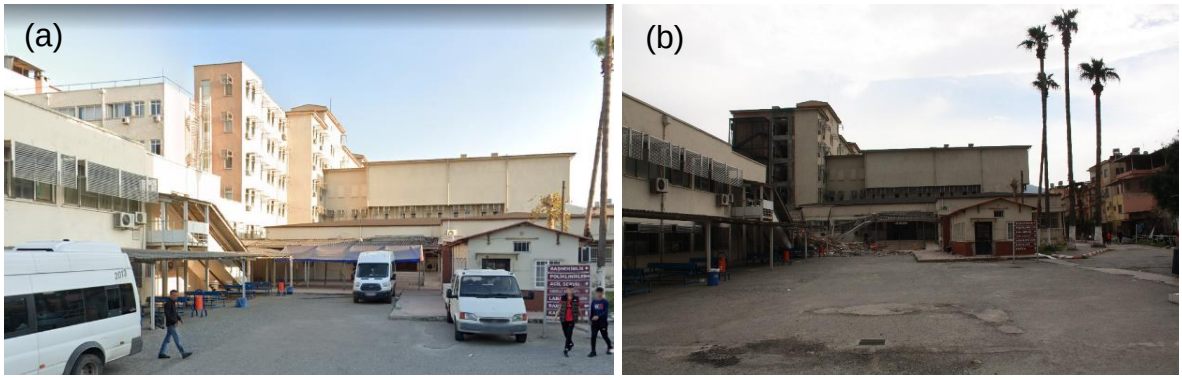

Figure 176: Iskenderun State Hospital: a) before (Google Maps Street view) and b) after the earthquake (as observed on 13 of March 2023)

Table 11: Strong Ground Motion parameters in the nearest SGM station to Iskenderun State Hospital

SGM Station 3116 / SGM Station 3115			
Earthquake	Mw 7.8 Pazarcık (1st event)		
Vs30 [m/s]	870 / 424		
Distance from the site [km]	4.75 NE / 4.3 S		
SGM Parameter	EW	NS	Vertical
PGA [g]	0.16 / 0.23	0.16 / 0.28	0.16 / 0.22
PGV [cm/sec]	35 / 48	38 / 40	19 / 20
Sa @ T=0.2s [g]		0.47 / 0.62	
Sa @ T=0.4s [g]	0.34 / 0.40		0.15 / 0.24
Sa @ T=1.2s [g]	0.19 / 0.48	0.26 / 0.31	0.14 / 0.22
Sa @ T=2.0s [g]	0.16 / 0.3	0.14 / 0.27	0.07 / 0.08

The Antakya Private Akademi Hospital is a multipurpose hospital with capacity of 101 beds (Türkiye Kamu ve Ozel Saglik Kurumlari Rehberi, 2023). The hospital building is of two 10 storeys high sections with an RC structural system and total gross area of 11,500 m2sq. m. gross area. At the time of writing this report, the year of construction is unknown nor was it built originally as a hospital or they adapted the building.

One of the two sections collapsed after the earthquake but as at the time the team was visiting the site there were interventions on the structure with construction equipment to remove partially damaged elements it was difficult to trace back the reason for structural failure. Comparing photographs before and after the earthquakes, (see *Figure 177-Figure 179*), it seems the first three storeys were weaker and collapsed under the tremor with the upper seven floors falling on top of them. A video showing the damaged hospital soon after the earthquake can be seen at https://www.youtube.com/watch?v=HBp8os1dv98. The nearest SGM station is less

than a kilometre away and the recorded PGA is 0.6 g with spectral accelerations exceeding 1.2 g in both, the short and long periods (*Table 12*).

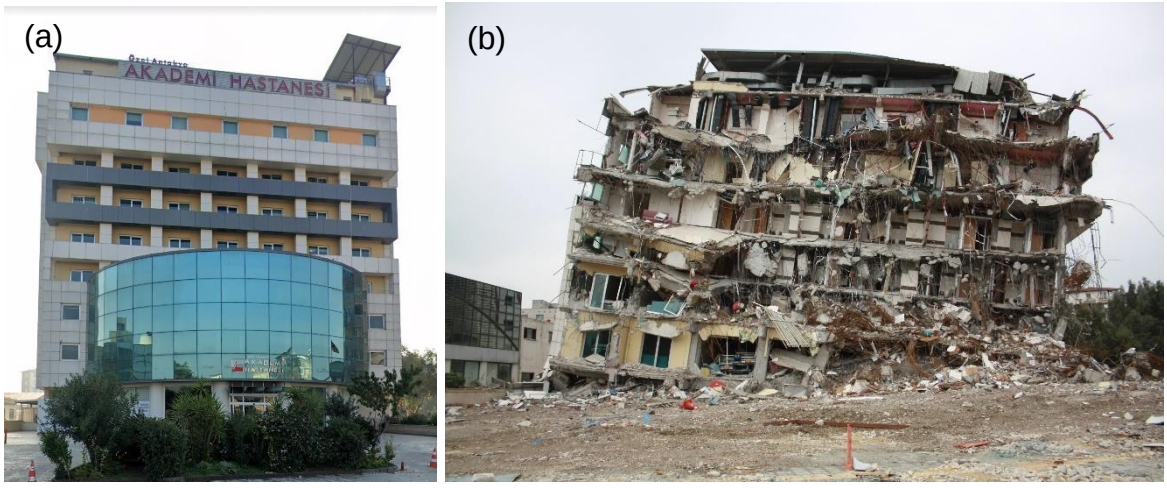

Figure 177: Antakya Private Akademi Hospital: a) before (Google Maps Street view) and b) after the earthquake (as observed on 14 of March 2023)

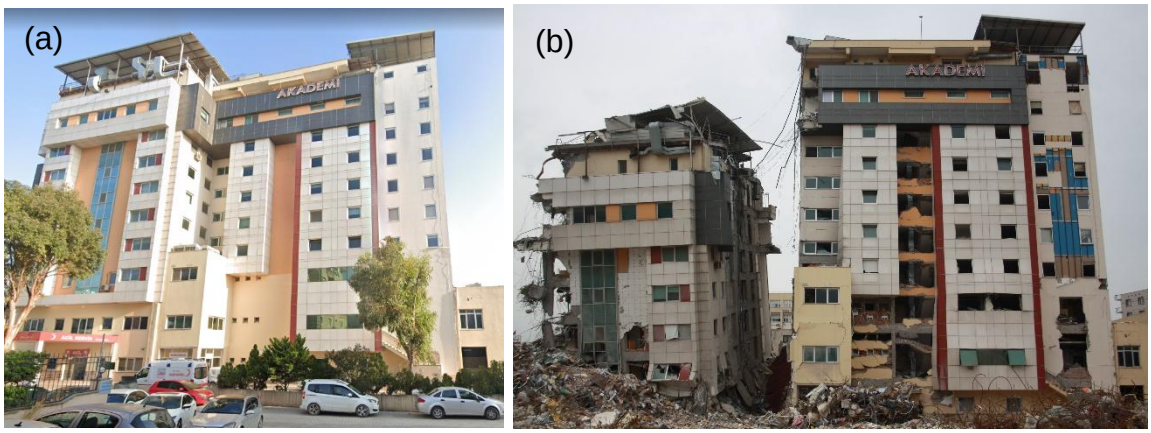

Figure 178: Antakya Private Akademi Hospital: a) before (Google Maps Street view) and b) after the earthquake (as observed on 14 of March 2023)

Figure 179: Antakya Private Akademi Hospital: a) before (Google Maps Street view) and b) after the earthquake (as observed on 14 of March 2023)

Table 12: Strong Ground Motion parameters in the nearest SGM station to Antakya Private Akademi Hospital

SGM Station 3124			
Earthquake No	Mw 7.8 Pazarcık (1st event)		
Vs30 [m/s]	230		
Distance from the site [km]	0.75		
SGM Parameter	EW	NS	Vertical
PGA [g]	0.62	0.57	0.58
PGV [cm/sec]	95.80	112.18	43
Sa @ T=0.2s [g]		1.16	
Sa @ T=0.4s [g]	1.26		0.88
Sa @ T=1.2s [g]	1.37	1.02	0.28
Sa @ T=2.0s [g]	0.52	0.81	0.24

6.1.4.2. Moderate and Low Damage

The Vatan Private Hospital is located near the stadium in Kahramanmaraş which is one of the most damaged areas in the city. It is a seven floors high RC building built in 2008. The satellite view on *Figure 180* shows the Vatan Private Hospital to be one of the very few buildings in this land plot to stand after the earthquake. However, the building sustained significant non-structural damages, some of which manifested in damaged façade walls as shown in *Figure 181-Figure 183*. It is not clear if was the building was originally designed/constructed as a hospital or an existing building was adapted to serve as a hospital. The building was subjected to a strong ground motion with a PGA of about 0.36 g (*Table 13*).

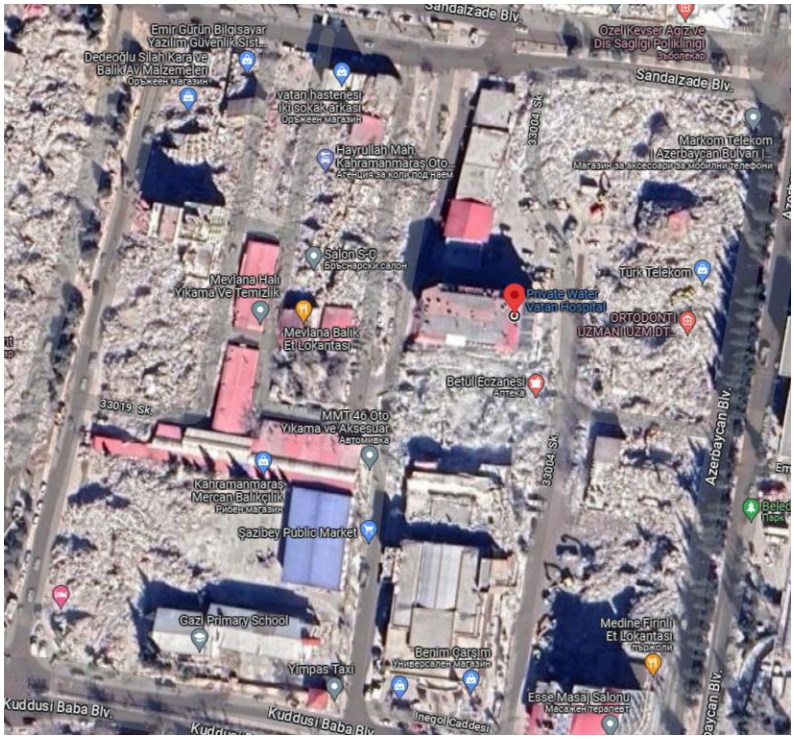

Figure 180: Vatan Private Hospital (Kahramanmaraş): satellite view showing the extent of damage in neighbouring buildings.

Figure 181: Vatan Private Hospital (Kahramanmaraş), north façade: a) before (Google Maps Street view) and b) after the earthquake (as observed on 16 of March 2023)

Figure 182: Vatan Private Hospital (Kahramanmaraş), west façade: a) before (Google Maps Street view) and b) after the earthquake (as observed on 16 of March 2023)

Figure 183: Vatan Private Hospital (Kahramanmaraş), south façade after the earthquake (as observed on 16 of March 2023)

Table 13: Strong Ground Motion parameters in the nearest SGM station to Vatan Private Hospital

SGM Station 4620 / SGM Station 4624			
Earthquake No	Mw 7.8 Pazarcık (1st event)		
Vs30 [m/s]	484 / 280		
Distance from the site [km]	2.5 / 4.6		
SGM Parameter	EW	NS	Vertical
PGA [g]	0.33 / 0.32	0.30 / 0.36	0.17 / 0.16

PGV [cm/sec]	35 / 56	31 / 59	15 / 35
Sa @ T=0.2s [g]		0.55 / 0.71	
Sa @ T=0.4s [g]	0.55 / 0.77		0.28 / 0.28
Sa @ T=1.2s [g]	0.13 / 0.55	0.16 / 0.56	0.08 / 0.23
Sa @ T=2.0s [g]	0.13 / 0.24	0.11 / 0.25	0.07 / 0.15

The state hospital in Nurdağı is a small two-storeys high RC building with a and has capacity of 25 beds. The team inspected the hospital only from outside and could not identify any evidence of structural damage. However, the hospital was evacuated and put out of service due reportedly to non-structural damage which we cannot confirm independently. At the time of our visit approximately six weeks after the two main earthquakes, the hospital was still non-functioning and providing only emergency services in two tents in its courtyard. Evidence of non-structural damage of the façade claddings is shown in *Figure 184*.

The nearest SGM station is located 400 m away from the hospital and had registered peak ground accelerations of about 0.6 g and spectral accelerations in the short period zone in the range of 1.3 - 1.7 g (*Table 14*). This is just about or slightly above the values used in the design of this buildings and the building's observed performance confirms its code compliance it seems it had code compliant behaviour. The hospital is situated in the hilly part of the town and likely sits on stiff soil.

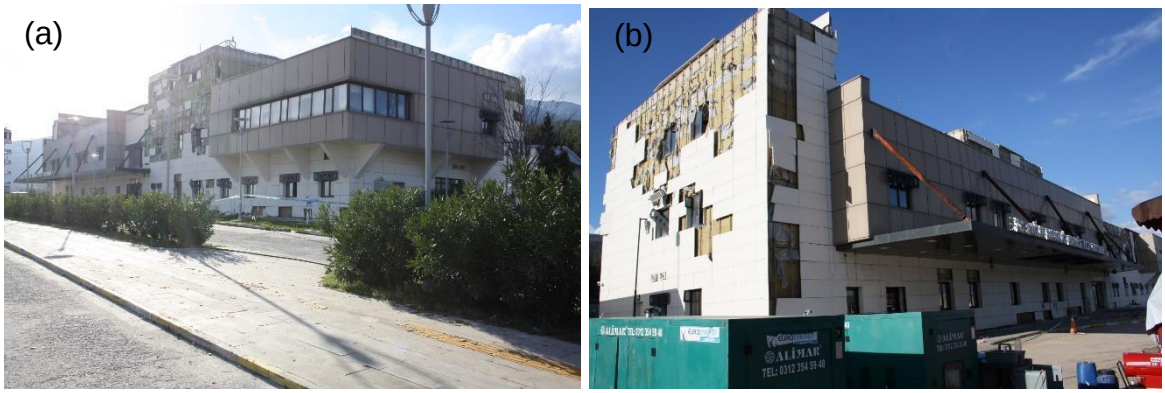

Figure 184: Nurdağı State Hospital (as observed on 15 of March 2023)

Table 14: Strong Ground Motion parameters in the nearest SGM station to Nurdağı State Hospital

SGM Station 2712			
Earthquake No	Mw 7.8 Pazarcık (1st event)		
Vs30 [m/s]	0/unknown		
Distance from the site [km]	0.4		
SGM Parameter	EW	NS	Vertical

PGA [g]	0.60	0.56	0.3
PGV [cm/sec]	111	75	26
Sa @ T=0.2s [g]		1.26	
Sa @ T=0.4s [g]	1.73		0.39
Sa @ T=1.2s [g]	0.91	0.42	0.18
Sa @ T=2.0s [g]	0.47	0.3	0.18

Hatay State Hospital is a large multipurpose hospital with a capacity of 1300 beds. It is a recently built eight floors high RC building on a fixed base. At the time of our visit approximately six weeks after the earthquake the building was closed for use and the hospital was providing its medical services via a large external tent camp organised by an international NGO. The team did not have access to the indoors interiors to observe the sustained structural and non-structural damage. The inspection from outside showed cracking and complete damage of exterior walls and opened seismic gaps, (*Figure 185*-*Figure 186*). The medical staff in the field hospital communicated verbally that they were hearing “sounds of cracking” from the hospital and were observing spontaneous opening of façade windows. This is likely to be due to continuous increase accumulation in the of residual displacements in the structure.

The nearest SGM station is located approximately. 5 m away from the hospital and has registered PGAs in the scale of 0.6 g and spectral accelerations in the short period range of about 1.2 g and about 1.0 to 1.4 g in the long period range (*Table 15*). However, another SGM station about 11 km away in the opposite direction has registered PGAs of 0.9 g and short period spectral accelerations exceeding 2 g. It is very likely the design-based values of the seismic loading were exceeded by the seismic loading.

Figure 185: Hatay State Hospital (as observed on 14 of March 2023)

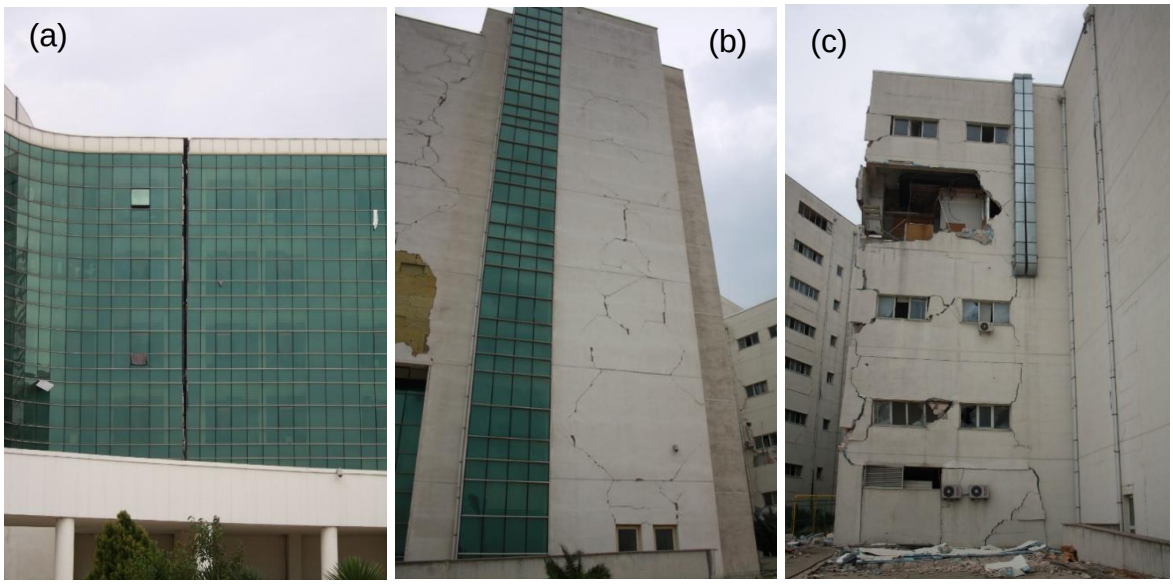

Figure 186: Hatay State Hospital (as observed on 14 of March 2023): a) opened seismic gap between two blocks, b) cracks in exterior walls and c) cracks and complete damage of exterior walls.

Table 15: Strong Ground Motion parameters in the nearest SGM station to Hatay State Hospital

SGM Station 3124 / SGM Station 3141			
Earthquake No	Mw 7.8 Pazarcık (1st event)		
Vs30 [m/s]	283 / 338		
Distance from the site [km]	5.5 / 11.3		
SGM Parameter	EW	NS	Vertical
PGA [g]	0.62 / 0.85	0.57 / 0.93	0.58 / 0.62
PGV [cm/sec]	96 / 123	112 / 77	43 / 40
Sa @ T=0.2s [g]		1.26 / 2.21	
Sa @ T=0.4s [g]	1.16 / 2.13		0.88 / 0.54
Sa @ T=1.2s [g]	1.37 / 0.79	1.02 / 0.94	0.28 / 0.38
Sa @ T=2.0s [g]	0.52 / 0.70	0.81 / 0.34	0.24 / 0.15

6.1.4.3. No Damage and Functional

Since 2013 all hospitals with more than 100 beds must be constructed with the use of base isolation and so far over 50 base isolated hospitals were built in Türkiye, eleven of which in the affected region. The EEFIT team visited four of them, these in Dörtyol, Osmaniye, Malatiya and Elbistan. All base isolated hospitals were reported to have that remained fully functional after the earthquakes and the team witnessed that this is the case in the four visited hospitals. The operability functioning of these hospitals was extremely critical after the earthquake as they were needed in order to cover a

huge gap in the hospital sector capacity due to the large number of non-functional hospitals after the earthquake. In its extreme this was seen in the Hatay province, where the Dörtyol State Hospital, shown in *Figure 187*, was one of the very few functioning medical facilities. It was verbally reported by from the local staff that, initially, a high huge number of masses of people from the area evacuated their homes and, scared of from aftershocks, occupied the common spaces in the hospital, using it as a shelter from the tremors and the cold outside. The figures mentioned was in the range of 20,000 people but the EEFIT team cannot validate this numbers. The number of surgeries within the first week after the earthquake was reported to have increased dramatically. The nearest SGM station is located at about 1 km from the hospital and the registered PGAs are about 0.2 g (*Table 16*), and much below the design levels values in the recent code.

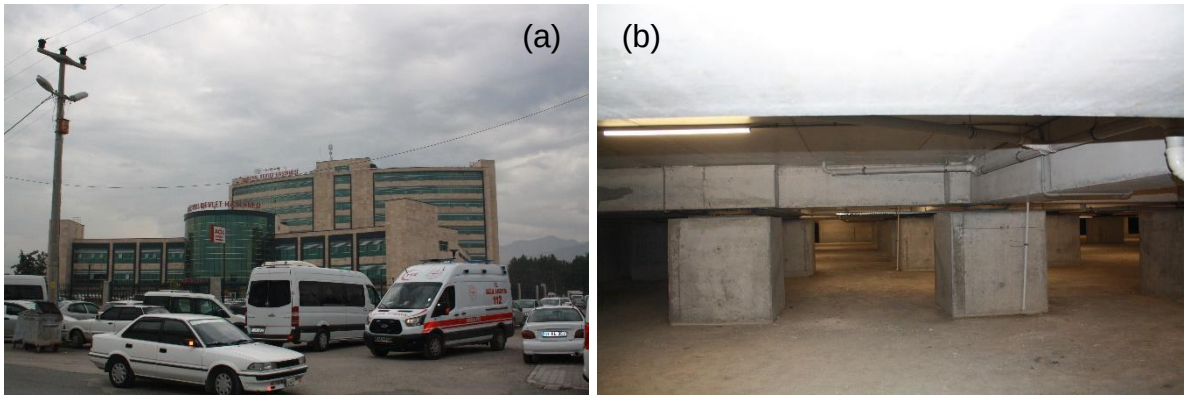

Figure 187: Dörtyol State Hospital (as observed on 13 of March 2023): a) overall view and b) view of the base isolators in the basement.

Table 16: Strong Ground Motion parameters in the nearest SGM station to Dörtyol State Hospital

SGM Station 3134			
Earthquake No	Mw 7.8 Pazarcık (1st event)		
Vs30 [m/s]	374		
Distance from the site [km]	0.9		
SGM Parameter	EW	NS	Vertical
PGA [g]	0.2	0.24	0.12
PGV [cm/sec]	39	39	19
Sa @ T=0.2s [g]		0.53	
Sa @ T=0.4s [g]	0.39		0.17
Sa @ T=1.2s [g]	0.31	0.19	0.11
Sa @ T=2.0s [g]	0.14	0.21	0.06

6.2. Educational Infrastructure

In Türkiye, the state finances primary and secondary education, which is therefore and free of charge in public schools, for age groups 6-19. As per the records in 2019, 97% of the eligible age group has enrolled in primary schools (The Global Economy (2022).

6.2.1. Design and Construction Regulations Related to Schools in Türkiye

The Ministry of Public Works and Settlement (MPWS) is responsible for all construction, maintenance and repair of public buildings, including schools. It has three divisions namely, General Directorate (GD) of (Public Building) Construction Affairs (GDCA), GD of Disaster Affairs, GD of Technical Research. GDCA is responsible for planning new school facilities and maintaining existing ones as per the requirements of the Ministry of National Education (MoNE). Changes in the education law in 1998 created a sudden increase in need for education facilities, increasing the workload of GDCA to create new designs and construct new buildings. Hence, the Division of Investments and Facilities (DIF) under the MoNE was tasked with feasibility analysis, planning, designing and contracting services. They ended building several boarding schools (YIBO) in rural areas and Pension-type primary schools (PIO) for areas in the periphery of urban settlements. (OECD, 2004). 81 provinces in Türkiye are administered by governors, who are responsible for the administration of GDCA in the province, with the assistance of local MPWS officers.

6.2.1.1. Past Earthquake Performance of Schools in Türkiye

820 schools were affected by the Kocaeli earthquake in Istanbul, in 1999, of which 689 were only slightly damaged and easily repairable. Of the remaining 131 schools, 13 were where heavily damaged, hence replaced with seismically safer schools, 59 were repaired, 37 were strengthened and 22 were demolished and reconstructed due to high heavy cost of foundation repairs. Boarding schools and provinces in highest risk zones were prioritised. In the 2003 Bingöl earthquake, several schools were damaged: 3 new schools collapsed and the collapse of a dormitory killed many children. A subsequent survey verified that most buildings were not compliant to 1998 Turkish Seismic Code, despite the legislation in April 2000 to enforce mandatory design checks and supervision, following the 1998 earthquake.

In the design of school buildings, the design level earthquake loads are increased by 50% according to TBEC (2018). The seismic performance target required by the code regarding school structures is immediate occupancy (IO) for earthquake level with probability of exceedance of 10% in 50 years (return period 475-year) and maintaining only the life safety (LS) level for earthquakes with a probability of exceedance of 2% in 50 years (return period 2475-year). From the recent and past earthquakes, it has been observed that school buildings performed much better than the general building stock. The main reason behind this is the 50% increase in earthquake design loads for these buildings (i.e. importance factor=1.5) and simple symmetric structural layout with no soft/weak stories (Erdik, 1999; Cetin et al. 2023).

6.2.1.2. Educational Infrastructure in the Affected Area

Currently, there are about 56,000 educational institutions under the MoNE in the 11 provinces affected by the earthquakes. 11,699 (21%) of these are schools are in the 11 provinces affected by the earthquakes, including kindergartens (1168), primary schools (5298), secondary schools (3221), high schools (1494), teachers' guest

houses (101), public education centres (132), vocational education centres (47) and special education schools (244). Provinces of Adana, Diyarbakir, Gaziantep, Hatay and Şanlıurfa have recorded student population of more than 500,000, while others have 50,000 to 350,000 students in the schools. Additionally, there are 5024 private schools and 16 universities in the affected region, catering to about 556,000 and 380,000 students, respectively (PSB, 2023).

6.2.2. Overall Impact on the Educational Infrastructure

Damage assessment was completed by the authorities for about 40% of the MoNE schools by March 2023, with 8162 buildings in total, out of which 4725 buildings did not have any damage. The distribution of damage in the remaining inspected buildings is shown in *Figure 188* which affected more than 38,820 classrooms in various degrees of damage. 2.5% of the private schools and all the universities in the region were also inspected and found to suffer varying levels of damage (*Figure 188*). At least 41 private schools and 120 university buildings were either collapsed or severely damaged, while the remaining inspected buildings were moderately or lightly damaged (PSB, 2023).

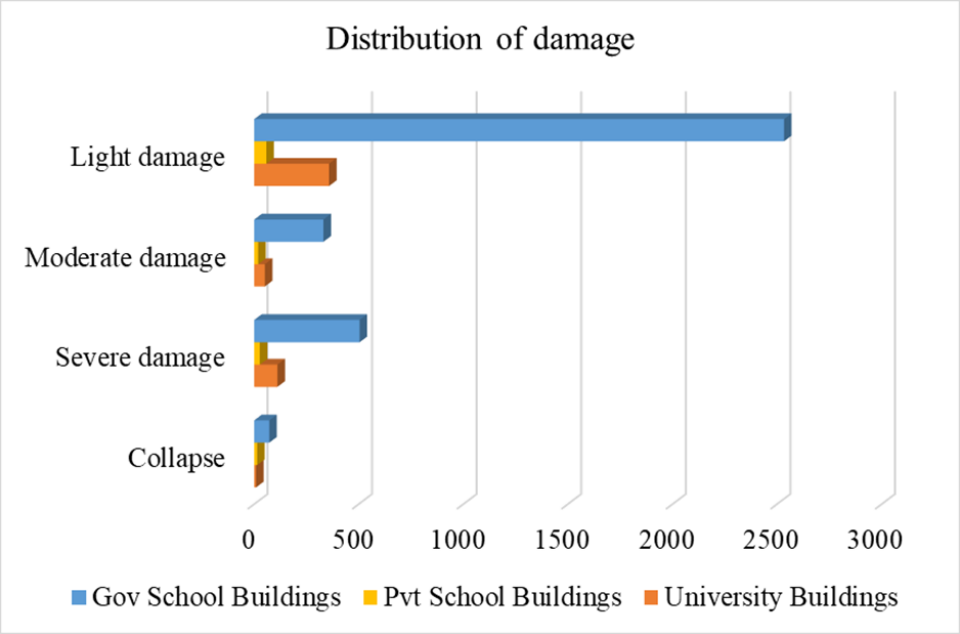

Figure 188: Damage distribution of public schools, private schools and universities.

6.2.3. Case Studies

The school buildings built with reinforced concrete structural systems performed exceptionally well in most places, with limited, mild damage to non-structural infill walls, even in areas with catastrophic damage to residential buildings. This includes 24 schools built by the MoNE within the affected areas since 2017, with the support from the World Bank, to be safer and more resilient to disasters. All these schools survived the earthquake with no damage, and 4 of them were used as temporary shelters in Kahramanmaraş (The World Bank, 2023).

There were however cases of mild, moderate and extensive damage cases among in old masonry school buildings, mostly built using stone. A brief description of the pPerformances of some of the school buildings observed during the field mission is

given below. Additionally, more detailed account of the performance of some monumental structures used as schools are elaborated under Section 4.3.3 of the Structures Chapter.

In *Figure 189* are photos of some the well-performed schools (i.e. remained functional or achieved immediate occupancy) visited during the field mission. On the other hand, *Figure 190* shows RC schools visited during the mission and were found to suffer from slight to moderate damage, which were visited during the field mission. Damage was often limited to non-structural elements such as infill walls and finishes. These were found to be empty and not in use for schooling or other purposes at the time of the field mission. Finally, *Figure 191* shows schools observed by the field mission to be severely damaged, collapsed or designated for demolition.

Figure 189: Well-performed schools observed during the field mission: a) Anadolu Imam Hatip Lisesi (Campus 1), Altinozu, Hatay, b) Anadolu Imam Hatip Lisesi (Campus 2), Altinozu, Hatay–The main building is being used a distribution hub of relief material, (c) Fikret Kocak Ilkokulu, Iskenderun, Hatay, and d) School from Hatay, being used as a government office

Figure 190: Schools with faced slight to moderate damage, observed during the field mission. a) Vilayetler Hizmet Birligi Anakolu, Defne, Hatay and b) Sehit Sirin Diril Cok Programli Anadolu Lisesi, Nurdağıgi, Gaziantep (RC buildings undergoing slight damage, not in use)

Figure 191: Schools observed to be severely damaged, collapsed or designated for demolition. a) Mithatpasa Ilkokulu, Iskenderun, Hatay– Top floor of one building in stone masonry collapsed, while the remaining buildings were not visibly damaged, b) Inonu Ortaokulu, Antakya, Hatay–RC building. Two other buildings in this compound were demolished and removed and c) Bektasli Ilkokulu, Kirikhan, Hatay– Stone masonry building heavily damaged, while adjacent RC building remained undamaged.

6.2.4. Education Recovery

An estimated 40 billion TRY (1.3 billion GBP) is considered to be needed estimated for reopening all the schools in the region (PSB, 2023). Considering the limited damage in the majority of the school buildings, the recovery of educational infrastructure could be quicker than the other sectors. However, schools were not operational in most of the region even after a month from the earthquake. The reopening of schools was delayed due to various factors, such as:

- Schools used as temporary shelters
- School buildings used as government offices, police check posts and temporary offices
- Schools used as distribution hubs for relief material.
- School grounds are reportedly being used for temporary tent accommodation

The reopening plan of schools within the affected areas is shown in *Figure 192*.

As temporary measures, some educational and training activities are resumed in limited capacity. About 2000 tents, containers and prefabricated classes were set up in the disaster area in the first two months to resume educational and training activities in limited capacity. MonE timeline indicates that face-to-faceeducation resumed in suitable districts of all affected provinces by 27 March (Özer, Şensoy and Suna 2023).

104 hospital classrooms and boarding facilities were also arranged for displaced students in these months from the events. Classes 8 and 12 were given priority due to the public board examinations at these levels (PSB, 2023). More than 166,000 students were transferred to less affected provinces by the end of February and this number increased to 252,829 by end of March. However, by then the MoNE started transferring students back to the highly affected areas, and about 32,600 students were brought back by April 2023 (Özer, Şensoy and Suna 2023). Universities were advised to switch to online learning for the Spring semester 2023 and were to remain closed until Summer 2023. They are encouraged to twin with universities in other provinces. News articles suggest that about 30% of the affected households had no access to education when the new academic year started in September 2023 (Save the Children 2023).

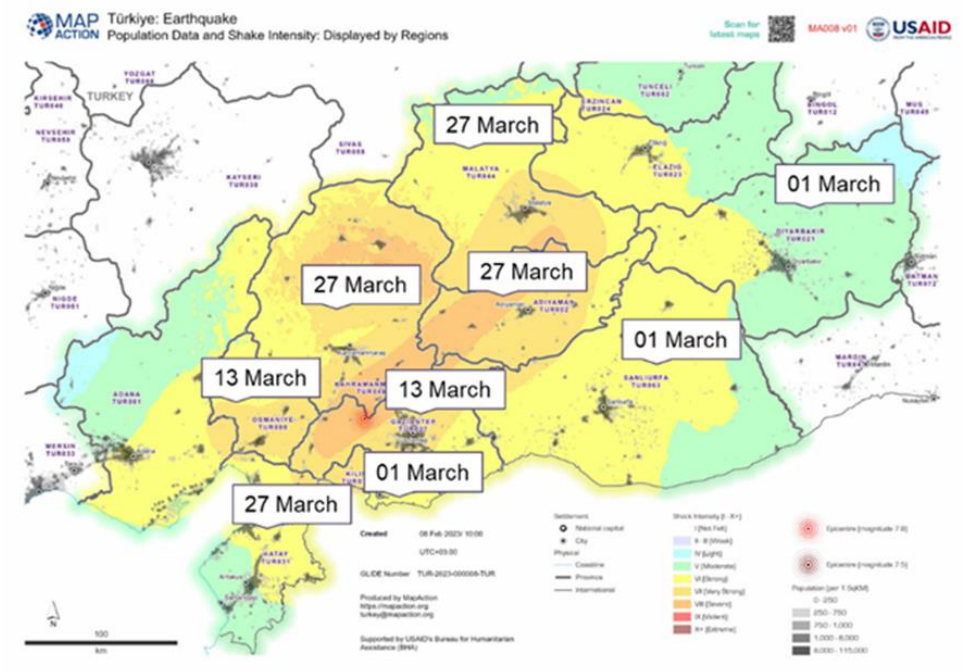

Figure 192: Opening of schools after the earthquake sequence

6.3. Emergency Response Infrastructure

For the purpose of this report, the buildings considered as an emergency response infrastructure are fire-brigade buildings and AFAD (Disaster and Emergency Management Agency) facilities.

6.3.1. Design and Construction Regulations Related to Fire-Brigade Buildings, Police Stations and AFAD Buildings in Türkiye

Fire-brigade buildings & facilities, police stations and AFAD buildings are classified as “Buildings required to be utilised after the earthquake” in the Turkish Earthquake Resistant Design Code 2018 (TBEC, 2018) and the building importance factor is defined as I=1.5 for structural design which means design level earthquake loads are topped up by 50%. The seismic performance target required by the code regarding school structures is immediate occupancy (IO) for earthquake level with probability of exceedance of 10% in 50 years (return period 475-year) and maintaining only the life

safety (LS) level for earthquakes with a probability of exceedance of 2% in 50 years (return period 2475-year).

Among these structures, the most vulnerable to damage is the firefighting buildings because generally, the ground floor heights of these facilities are higher than the other floors in order to allow vehicle entry. Similarly, there are usually no infill walls on one façade to allow vehicle entrances, while infill can be found on the other three façades of the building. All these irregularities made in the design for operational reasons of the fire facilities may allow the formation of weak storey.

6.3.2. Emergency Response Infrastructure in the Affected Area

The disaster management in Türkiye is the responsibility of the Disaster and Emergency Management Agency (AFAD), which since 2018 is affiliated with the Ministry of Interior (MoI). AFAD has been the central organisation managing Provincial Directorates of Disaster and Emergency (İl Afet ve Acil Durum Müdürlükleri), which are directly linked to related with the governors of the provinces. AFAD's responsibilities include the organisation and coordination of public institutions and organisations, universities, local administration, Turkish Red Crescent, NGOs, private sector, and international organisations in emergency situations.

The Ministry of Environment, Urbanisation and Climate Change (MoEUCC) also has responsibilities in the emergency planning and response. The MoEUCC's duties include drafting legislation for settlement and land development, building inspections, damage assessment, demolition of damaged buildings, debris removal and its following processing, and safe debris disposal.

The emergency services and law enforcement in Türkiye, and the roles of fire departments and, police services, and how search and rescue services are handled are detailed organised on municipal level.

6.3.3. Overall Impact on the Emergency Response and Law Enforcement Infrastructure

At the time of writing this report the team could not find a detailed breakdown of damage within fire-brigade buildings and AFAD buildings. During the field site mission, the team visited the regional AFAD facilities in Hatay and Kahramanmaraş. In both locations the buildings seemed to be fully functional. In the AFAD facilities in Hatay, the team observed non-structural damage of the light-weight external façade panels (see *Figure 193*) at of an auxiliary building functioning as a call-centre on the ground floor and a dormitory on the upper floor. At the time of the EEFIT visit approximately six weeks after the earthquake the call-centre on the ground floor was operational functioning and there were ongoing debris removal and repair works on the upper floor.

Figure 193: An auxiliary building in the AFAD regional centre for Hatay province as observed on 14 March 2023

In the official damage evaluation of the Government (PSB, 2023), there is an information about the extent of damage within buildings housing the built environment related to municipal services of with a breakdown per different categories (based on gross floor area in *Table 17*). These are One of these categories is “municipal service buildings;, fire department service buildings;, municipal police buildings; and other municipal service buildings”. The information about the extent of damage (based on gross floor area) is provided in *Table 17* and *Figure 194*.

Table 17: Damage distribution aincross sub-category: municipal service buildings, fire department service buildings, municipal police buildings and other municipal service buildings (PSB, 2023)

Damage level	Area, m^2	% Distribution
Collapsed	17700	10%
Severely damaged	22085	13%
Moderately damaged	49676	29%
Lightly damaged	84688	49%

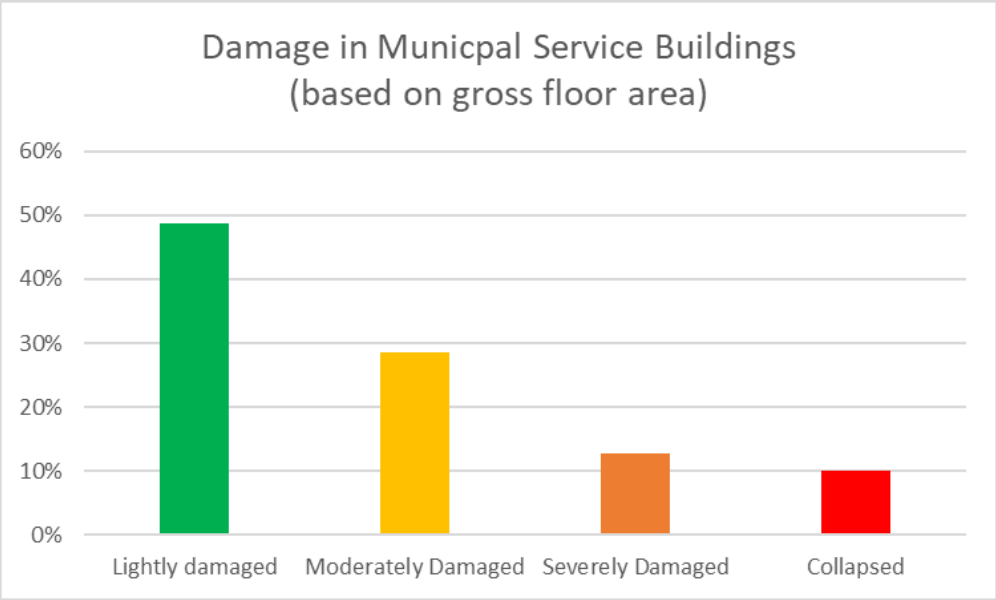

Figure 194: Damage distribution across sub-category: municipal service buildings, fire department service buildings, municipal police buildings and other municipal service buildings (PSB, 2023)

Within the collapsed buildings, there is at least one fire-brigade building, namely the Central Fire Station of Antakya (see Section 6.3.4.1). At the time of the field mission the team had not been informed of for other collapsed fire station buildings, nor we identified any such at the time of writing this report. However, the collapse of the main fire station of Antakya inevitably affected the search and rescue activities in the first two days after the earthquake when the province needed to rely predominantly on its own capacity. The collapse of the fire station building led to the complete damage of two fire trucks, three SAR vehicles and five sets of SAR equipment with an estimated total cost of £1.4M (PSB, 2023). More detailed information is provided in Section 6.3.4.

6.3.4. Case Studies

During the field mission between 13 and 18 of March the team visited five fire stations. These were namely the central fire stations in Iskenderun, Antakya and Kahramanmaraş and two smaller fire stations in Samandag and in the suburbs of Iskenderun.

6.3.4.1. Severe Damage and Collapses

During the preparation for the field mission, the team identified that the main buildings of Hatay Fire Department had have collapsed which they and visited the site on the 2nd day of the main field mission (14 March) approximately six weeks after the first two main shocks. By the time of our visit the debris was removed, and the team could not make any observation related to the failure mode and the reasons for failure.

The main building consists of a couple of two-storey high sections connected with an entrance and internal staircase. One of the two sections houses the dormitories located on the upper floor above the garage for fire trucks and the other section has two floors with office spaces. The building seems to be an RC moment-resistant frame (MRF) structure with a façade and partition walls made of Unreinforced Masonry (URM). The construction year is unknown, but it seems to be built before 2000 and hence prior to the introduction of the new seismic design codes in Türkiye.

The section with garages collapsed due to soft first storey on the ground floor – see *Figure 195*. By the time of writing this report the team could not find any identify information and photographs to help identify for the extent and form of damage of the other section and the reason for collapse therefore of the other section remains unknown. The two nearest SGM stations are located within a radius of 1.2km from the fire department and have registered PGAs from in the range of 0.6 to 1.2g, and short period spectral accelerations in the range of 1.2 to 2.0g and long period spectral accelerations of 0.6 to 1.6g, as detailed. Detailed information is provided in

able 18.

The collapse of the main building led to complete loss of two fire trucks and three SAR vehicles together with five sets of SAR equipment affecting the capability of Hatay fire department to perform its duties after the earthquake, although our interviews with the fire brigade officers in June 2023 revealed substantial individual effort from many to compensate for the unavailability of systematic contribution from the department to search and rescue operations (see Section 7.6 of the Relief, Response, Recovery Chapter). Six weeks after the earthquake, the Hatay Fire Department was mainly functioning within a tent, which was still the case in June 2023.

Figure 195: The main building of Hatay Fire Department photographed immediately after the earthquake (Hafiza, 2023)

able 18: Strong Ground Motion parameters in the nearest SGM station to the Hatay Fire Department

SGM Station 3126 / SGM Station 3123			
Earthquake No	Mw 7.8 Pazarcık (1st event)		
Vs30 [m/s]	350 / 470		
Distance from the site [km]	1.0 / 1.15		
SGM Parameter	EW	NS	Vertical
PGA [g]	1.02 / 0.59	1.19 / 0.65	1.07 / 0.85
PGV [cm/sec]	87 / 97	111 / 189	81 / 57
Sa @ T=0.2s [g]		1.77 / 1.18	
Sa @ T=0.4s [g]	1.97 / 1.20		0.94 / 0.58
Sa @ T=1.2s [g]	0.63 / 1.25	0.82 / 1.64	0.47 / 0.52
	0.28 / 0.51	0.71 / 1.07	0.33 / 0.37

6.3.4.2. Moderate and Low Damage

On the 13th of March the team visited the Iskenderun Fire Department. The main building is shown on *Figure 196*. It is a RC structure with masonry infill walls, with a high open ground floor that serves as a with parking space for fire trucks, and two upper storeys with dormitories and administrative space on top of that. The building was built in the 2000s. The team could not identify evidence for structural damage, but observed non-structural damage on the exterior walls on the ground floor and the upper floors, see *Figure 197*. The building was evacuated after the earthquake and was not put back in service by the time of the field mission (six weeks after the earthquake). Instead, the operations were delivered through a tent camp.

The nearest SGM stations are located at approximately 4km from the site and have registered PGAs from 0.16 to 0.28g, short period spectral accelerations from 0.34 to 0.6g and long period spectral acceleration from 0.19 to 0.48g (*Table 19*), which are all below the design thresholds.

Figure 196: The main building of Iskenderun Fire Department as observed on 13 March 2023

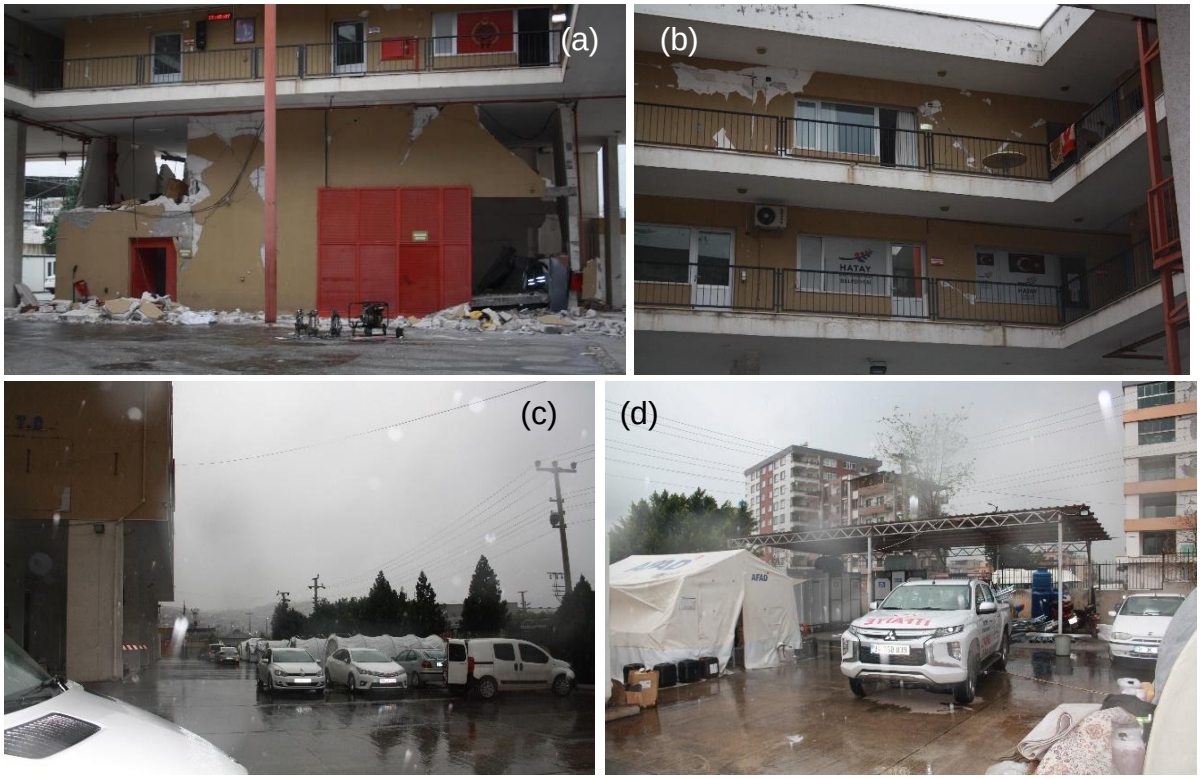

Figure 197: The main building of Iskenderun Fire Department as observed on 13 March 2023: a) damaged exterior walls on the ground floor, b) cracked infill walls on the upper two floors, c) tents used for dormitories for the firefighters on duty and d) tent used for command/dispatcher room.

Table 19: Strong Ground Motion parameters in the nearest SGM station to the Iskenderun Fire Department

SGM Station 3116 / SGM Station 3115			
Earthquake	Mw 7.8 Pazarcık (1st event)		
Vs30 [m/s]	870 / 424		
Distance from the site [km]	4.5 / 4.15		
SGM Parameter	EW	NS	Vertical
PGA [g]	0.16 / 0.23	0.16 / 0.28	0.16 / 0.22
PGV [cm/sec]	35 / 48	38 / 40	19 / 20
Sa @ T=0.2s [g]		0.47 / 0.62	
Sa @ T=0.4s [g]	0.34 / 0.40		0.15 / 0.24
Sa @ T=1.2s [g]	0.19 / 0.48	0.26 / 0.31	0.14 / 0.22
Sa @ T=2.0s [g]	0.16 / 0.3	0.14 / 0.27	0.07 / 0.08

The regional centre of AFAD for Hatay province was visited on the 14th of March. Like other regional AFAD centres, it consists of a command centre and several auxiliary facilities with different functions. Based on the SGM station located at about 900m from the site, the experienced ground motion was much above the design values – the registered PGAs are about 0.9g with short period spectral accelerations exceeding 2.0g and long period spectral accelerations in the range of 0.8-0.9g. The command centre seemed to be a robust two-storeys high building and at the time of our visit the building was fully functional. Based on the external inspections there were no visible signs of any structural and non-structural damage but there were signs of soil settlement around the building. The only damaged building at the site seen from the team was the auxiliary building that hosts the AFAD call centre on its ground floor and a dormitory on the upper levels (*Figure 193*). This is a steel frame structure with light-weight façade and partition panels, and the damage was concentrated only to these non-structural elements.

Table 20: Strong Ground Motion parameters in the nearest SGM station to the AFAD centre for Hatay province

SGM Station 3141			
Earthquake No	Mw 7.8 Pazarcık (1st event)		
Vs30 [m/s]	338		
Distance from the site [km]	0.9		
SGM Parameter	EW	NS	Vertical
PGA [g]	0.85	0.93	0.62

PGV [cm/sec]	123	77	40
Sa @ T=0.2s [g]		2.21	
Sa @ T=0.4s [g]	2.13		0.54
Sa @ T=1.2s [g]	0.79	0.94	0.38
Sa @ T=2.0s [g]	0.70	0.34	0.15

6.3.4.3. No Damage and Functional

The Kahramanmaraş Fire Department was visited on 16th of March (*Figure 198*). This is the main fire station for the Kahramanmaraş. The building has two sections with offices/operational space connected through with an 8-bay garage for fire trucks. The garage roof is covered by full span steel trusses supported by steel columns. The third (top) storeys of the two sections with administrative/operational spaces are also made of steel structure and the structural system of the lower two storeys is either steel or RC MRF with infill walls. Based on the records from the three nearest SGM stations, during the first earthquake, the building experienced PGAs from in the range of 0.3g to 0.45g and short period spectral accelerations from the range of 0.55g to 1.06g (see *Table 21*). The fire station remained fully functional after the earthquake and without any structural damage. The extent of non-structural damage is unclear as the team inspected the buildings only externally.

Figure 198: Kahramanmaraş Fire Department as observed on 16 March 2023

Table 21: Strong Ground Motion parameters in the nearest SGM stations to the Kahramanmaraş Fire Department building.

SGM Station 4620 / SGM Station 4624			
Earthquake No	Mw 7.8 Pazarcık (1st event)		
Vs30 [m/s]	484 / 280		
Distance from the site [km]	4.1 / 4.6		
SGM Parameter	EW	NS	Vertical

PGA [g]	0.33 / 0.32	0.30 / 0.36	0.17 / 0.16
PGV [cm/sec]	35 / 56	31 / 59	15 / 35
Sa @ T=0.2s [g]		0.55 / 0.71	
Sa @ T=0.4s [g]	0.55 / 0.77		0.28 / 0.28
Sa @ T=1.2s [g]	0.13 / 0.55	0.16 / 0.56	0.08 / 0.23
Sa @ T=2.0s [g]	0.13 / 0.24	0.11 / 0.25	0.07 0.15

6.4. Transportation Infrastructure

6.4.1. Design and Construction Regulations Related to Transportation Infrastructure in Türkiye

In addition to the Turkish building earthquake code (TBEC, 2018), the regulations named "Principles for the Design of Highway and Railway Tunnels and Other Ground Structures Under Seismic Load" (Ministry of Transport and Infrastructure, 2020) and “Principles for the Design of Highway and Railway Bridges and Viaducts under the Influence of Earthquakes” (Ministry of Transport and Infrastructure, 2020) also govern the seismic design of highways and railways structures. According to these regulations, the design of such structures should be informed by 3D analyses in the time history domain. Considering the relatively long length of highways and railway structures, longitudinal ground movement differentials are accounted for, and local ground conditions are used to determine design-based earthquake ground movements. Before these regulations, the AASHTO (2002) regulation was in place for seismic design of highway bridges.

The required seismic performance level of highway and railway tunnels and other ground structures is immediate occupancy (IO) for earthquakes with probability of exceedance of 10% in 50 years (return period 475-year) and life safety (LS) for earthquakes with a probability of exceedance of 2% in 50 years (return period 2475-year). In other words, it is required to be fully operational in an earthquake with a return period of 475 years and to be in a Damage Control (DC) zone for the earthquake level with a return period of 2475 years.

6.4.2. Transportation Infrastructure in the Affected Area

The affected area contains the 12% of the total length of the national motorway network and the 14% of the total length of the provincial motorway network. Those roadway infrastructures carry 15% of the total vehicle-km, 15% of the passenger-km and 20% of the tonne-km on Turkish motorways. As of railway, 9% of the national railway is located in the disaster region. There are two important tracks, one carrying freight and passengers transport along Adana-Hatay-Osmaniye-Gaziantep-Kahramanmaraş-Malatya route and one carrying freight transport especially of exported goods and mines along Sivas-Çetinkaya-Malatya-Narlı-Iskenderun. Airports are located in Adana, Elazığ, Hatay, Adıyaman, Şanlıurfa, Diyarbakır, Malatya, Gaziantep and Kahramanmaraş, which account for 6% of the total number of passengers of the country (PSB, 2023). Regarding water transport, there are 13 ports

within the affected area, which manage 135.9 million tonnes of shipment within the region.

6.4.3. Overall Impact on Transportation Infrastructure

Structural performance of the motorways following the earthquakes was found desirable. Only around 2.6% of length of the motorways is reported to have been damaged. The total damage of related infrastructures (i.e. roadways, tunnels, viaducts, bridges, signal facilities and tolling facilities) is estimated to cost 12.2 billion TRY (537 million GBP) (PSB, 2023). According to the General Directorate of Highways (Karayolları Genel Müdürlüğü, KGM)'s tweet twitter on 8 February (i.e. the third day of the earthquake), there was no route closed to traffic due to earthquakes: "All of the main arteries (main road with heavy traffic) in our road network in Türkiye are open for transportation. We do not have a route that is closed to traffic due to the earthquake. Highways Teams continue to work 7/24 all over the country." However, the road network to allow access to Antakya and Samandag is known to be closed, making it very difficult for the response and aid to arrive the first days following the earthquakes (Kenez, 2023).

Meanwhile, motorways were also affected by the floods that took place in Şanlıurfa and Adıyaman on 15 March 2023. Some roadways were inundated completely, being unable to deliver any traffic flows.

As of railways, the (PSB, 2023) estimates damage for some 1,204 km long rail route as 1.2 billion TRY (52.9 million GBP). During the first few days, Fevzipaşa-Narlı, Narlı-Gaziantep, and Narlı-Matalya railway lines were closed, and Malatya-Cetinkaya and Malatya-Yolçatı lines were open for emergencies only.

Hatay Airport was most severely affected and completely closed until 11 February, while flights from other cities to Hatay were suspended until 20 September (Ilk Kursun, 2023). The runway formed a large crack in the middle because of soil and foundation problems. Such damage is attributed to its location on the Amik Plain. The airport's closure resulted in disruptions in emergency activities. Adana Sakirpaşa Airport was completely closed until 10 February, because of a damaged terminal. Meanwhile, Gaziantep Airport experienced only minor damages and was never completely closed. However, to facilitate emergency activities, it was opened only for rescue teams and relief supplies and not for civilian flights, serving as the main airport for international rescue service aircrafts. Şanlıurfa Airport and Kahramanmaraş Airport did not experience notable damage, and they were never completely closed, but kept operational only for rescue teams and relief supplies.

Seaways were put in operation from the second day of the earthquake. On the other hand, the earthquake caused a massive fire in İskenderun port. The fire started on the evening of 6 February in a single container, and until the next day, the fire was not subdued and was spread to other containers. Services at the port started to be resumed only in early March.

There are testimonies that emergency activities were hampered by lack of coordination between transport modes as a unified system. For example, the Chamber of Mining (2023) testifies that on the day of the earthquake, they had difficulties in using highways because of adverse weather conditions and damaged roadways, and that while airways and seaways were implemented with a delay, they did not perform

efficiently enough to compensate for the degraded functionality of roadways. They estimate that such lack of coordination resulted in 15-20 hours delay of arrival of the rescue force, which was critical to save people alive buried alive under debris. For example, Samandağ was one of the settlements for which help arrived late because of a delayed deployment of sea transport as the area faces a coast to the Mediterranean but has a limited road access.

Another noteworthy difficulty was the unsuccessful communication of the latest status of transport availability to the public and professional and community groups trying to access the site. While some highways were closed during the first week after the earthquake occurrence, there was no guidance on alternative routes that rescue teams had to resort to trials and errors. For example, the Chamber of Architects (2023) testifies that “Phone calls came to inform us that, there was a great destruction in Afşin and Elbistan and. Information came that the Afşin Municipality building was demolished. We went back to Afşin again. Alternative roads were closed and there were reports of collapses in the tunnels. Traffic was congested. We were able to reach Afşin hours later.” Similar situations were also reported by the Chamber of Mining (2023). We note that although all motorways were in service only after three days (as aforementioned), their dysfunctionality during the first two days had notable impacts as initials periods are critical for search and rescue activities.

Not only structural facilities but also transport vehicles proved to be important. For example, as the Chamber of Mining (2023) reported, no vehicles were provided for their rescue works and that the teams they had to hitchhike from site to site, which unnecessarily consumed their energy and time.

6.4.4. Case Studies

6.4.4.1. Collapsed Bridges

The field mission team visited two bridges, one of which was located in Hatay crossing the Karasu river and was collapsed. *Figure 199* and *Figure 200* show the two bridges located next to each other, which showed very different damage levels. However, it was reported that the collapsed one was out of service prior to the earthquakes.

Figure 199: A collapsed bridge crossing the Karasu çayı river (location: Lon 36.2720, Lat 36.2073)

Figure 200: An intact bridge crossing the Karasu çayı river (location: Lon 36.2724, Lat 36.2074)

6.4.4.2. Paved Roadways

Both remote and field investigations observed that damaged paved roads reduce traffic capacity by reducing vehicle speed. As shown in *Figure 201-Figure 203* most of such damage is attributed to fault lines, which we observed also were the primary cause of damage to both pedestrian pavements and roads alike.

Figure 201: Cracked roadways due to fault lines – photos taken during the field mission (location: a) Lat 37.2836 Lon 37.1141; b) Lat 37.7886 Lon 37.6470

Figure 202: Reduced road capacity by cracked pavement – retrieved from https://www.instagram.com/reel/CpxR_U9ouLT/?ugsgud=YzAyMDM1MGJkZA%3D%3D

Figure 203: Damaged pedestrian roads – photos taken during the field mission (location: a) Lon 36.5895 Lat 36.1754; b) Lat 37.7887 Lon 37.6482)

6.4.4.3. Indirect Impacts by Damage in Adjacent Buildings

As for reduction in traffic capacity caused by damage and collapse in adjacent buildings, we observed two mechanisms: (1) structures overturning to roads (*Figure 204* and *Figure 205*) and (2) debris spilled from collapsed buildings (*Figure 206*). *Figure 205* depicts some dangerous moments at a roadside where a building suddenly collapsed onto cars passing by. On the other hand, we observed the second mechanism more often than the first one. The debris-heaped areas are particularly disadvantaged for rescue works, prohibiting access of heavy equipment and delaying arrival of rescue forces. Meanwhile, after rescue activities, such reduced traffic capacity often became less troublesome since traffic demands also decreased for there are no facilities left to visit.

Figure 204: A roadway blocked by an overturned structure – retrieved from https://www.instagram.com/p/Cra0IgPIaM9/?utm_source=ig_web_copy_link&igshid=MzRlODBiNWFlZA%3D%3D

Figure 205: Sudden collapse of building with cars running nearby– retrieved from https://www.instagram.com/reel/CpaaaCFIya5/?utm_source=ig_web_copy_link

Figure 206: Blocked roadways by debris (location: a) Disrupted roadway by debris; b) Disrupted transport network by collapsed buildings) – a) retrieved from https://www.instagram.com/reel/CoXoeO0Kx4F/?utm_source=ig_web_copy_link and b) from https://www.instagram.com/reel/CoaYzjWK2J4/?utm_source=ig_web_copy_link&igshid=MzRlODBiNWFlZA%3D%3D

1.5.4.4. Inundation of Roadways

From the field investigation, we observed prevalence of inundated roadways during the flooding in Iskenderun (*Figure 207*). The roadways were unusable, and detours had to be made.

Figure 207: Inundated roadways in Iskenderun – observed during the field mission.

6.4.4.4. Potential Mitigation Measures

While structural performance of transport infrastructure constructions iswas deemed broadly positively evaluated, the notable limitation was observed on transport operations of the transport system was that it failed to operate as a unified system. This was particularly critical for emergency activities during the first week after the earthquake occurrence. First of all, closer coordination is required between different transport modes (e.g. motorway, airway, seaway and railway). Backup plans through other transport modes need to be arranged to mitigate direct and indirect impacts of some transport modes going out of service. In addition, the observation that the closure of the Hatay airport still caused disruptions despite the other airports in service underlines the lack of a coordination system between transport locales. This could have been mitigated by pre-identifying possible supply points for each of the destination points.

A communication system needs to be arranged to disseminate information of current availability status of airports/stations, routes and ports, and this information must be accompanied by alternative route suggestions. This would require an interdisciplinary collaboration between transport authorities and telecommunication authorities.

It is also imperative to secure plans and provisions of enough vehicles and equipment to facilitate emergency activities. This requires quantifying the expected extent of damage in each neighbourhood in a pre-disaster stage.

We note that in the aftermath of a very intense earthquake, traffic flows for ordinary activities decrease significantly even long after the earthquake and, thus, are of less concern. This is because there are no social functionalities left to demand such travels.

On the other hand, quick and efficient response in the first couple of days isare pivotal as this is when lives can be saved. Therefore, to prepare against an earthquake with a high intensity, implementation of the aforementioned measures should aim for being initiated within the first couple of hours after an earthquake.

6.5. Energy Infrastructure

6.5.1. Design and Construction Regulations Related to Energy Infrastructure in Türkiye

In the past, seismic damages on electricity transmission lines and substations caused interruption of electric distribution in Türkiye. 9 substations were damaged in the 1999 Kocaeli earthquake which resulted in interruption of electricity transmission of several cities in the Marmara region between 1 to 7 days (MCEER, 2000). There was no significant substation damage in the 2011 Van earthquake, however electric transmission interrupted due to the downed power lines in the city (EERI, 2011).

As a reaction to the past earthquakes-induced disruption on the energy infrastructure, “Türkiye Electricity Transmission Systems and Communication Facilities Earthquake Regulation” (Republic of Türkiye Ministry of Energy and Natural Resources, 2020a) was published by the Ministry of Energy and Natural Resources of Türkiye in 2020, based on the rules defined in IEEE-693 (IEEE Recommended Practice for Seismic Design of Substations). However, the enforcement date of this regulation is 2024. For this reason, most of the existing systems were designed in accordance with IEEE 693 and IEC (International Electrotechnical Commission) guidance.

6.5.2. Overall Impact on Energy Infrastructure

6.5.2.1. Electricity

There are a total of 125 high voltage substations, including 154 kV and 400 kV, in operation in the earthquake-affected region, and 25 of these substations were damaged in the first earthquake at 04.17 am on 06.02.2023. Additionally, 11 of the 32,183 Electricity Transmission Line poles have also been damaged by the first earthquake (TEIAS, 2023).

To demonstrate the impact of the earthquake on the electricity infrastructure, the night satellite images of Antakya city centre and its surroundings before and after the earthquake are given in *Figure 208*. The satellite images show that after the earthquakes, much of the region lost electric power.

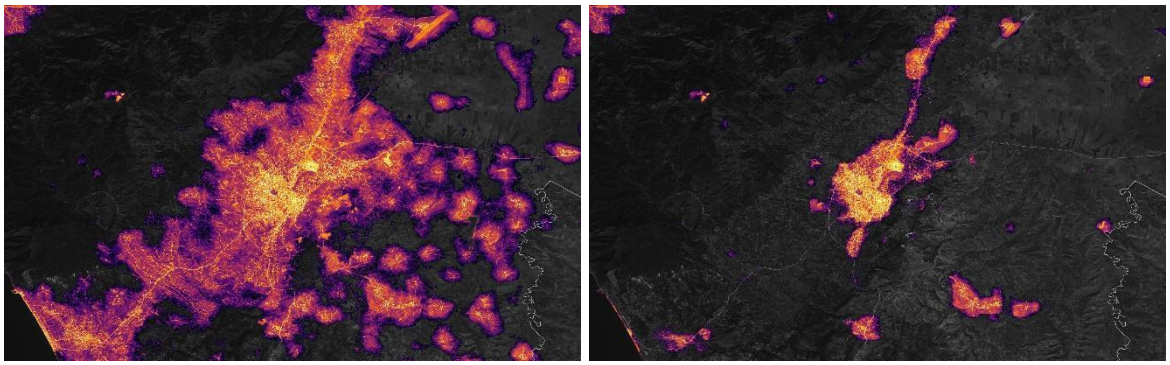

Figure 208: Night satellite image of Antakya before and after the earthquakes: (a) satellite image on the 4th of Feb.2023 and (b) satellite image on the 8th of Feb. 2023 (photos retrieved from NASA – The Black Marble Project, 2023 and NASA – Earth at Night, 2023)

After the Pazarcık/Kahramanmaraş earthquake on 6th February 2023 at 4:17 am, electricity power could not be supplied to a total of 1,041,926 electricity subscribers in Adana, Gaziantep, Hatay, and Osmaniye provinces. The distribution of households without electricity transmission according to cities is given in *Table 22* (Caliskan, 2023). After the Mw 6.8 Defne/Hatay earthquake on February 20, 2023 at 20:04, although there was no significant damage in other provinces, serious damages occurred in the networks in Hatay Province and the number of subscribers without electricity in Hatay region increased from 187,665 to 296,808.

Table 22: The interruption of electric transmission to the subscribers (Caliskan, 2023)

City	Subscribers without electricity supply	
	6th Feb. 2023	20th Feb.2023
ADANA	31.415	12.713
GAZİANTEP	62.407	59.282
HATAY	770.504	187.665
OSMANİYE	177.600	17.689
TOTAL	**1.041.926**	**277.349**

Hourly electricity consumption data from Toroslar Elektrik Dagitim A.S. (Toroslar EDAS) which provides electricity power to Adana, Gaziantep, Mersin, Hatay, Osmaniye, and Kilis provinces, before and after the earthquake, is presented in *Figure 209.* The data shows that even one month after the earthquake, the electricity consumption is about two-thirds of the pre-earthquake period.

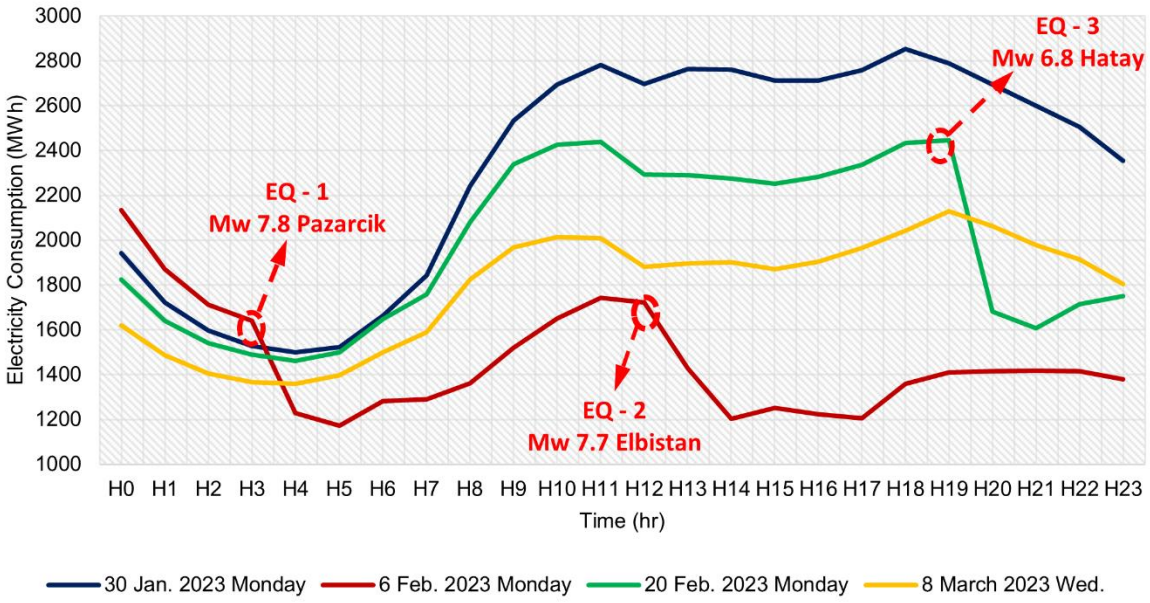

Figure 209: Electric consumption data of Toroslar EDAS before and after the earthquakes (Caliskan, 2023).

Hourly electricity consumption data for Hatay province, before and after the earthquake, is presented *in Figure 210.* The electricity distribution was heavily affected by the earthquakes Mw 7.8 on 06 Feb. 2023 and Mw 6.8 on 20 Feb. 2023. The electric consumption one month after the first earthquake is about half of the pre-earthquake period.

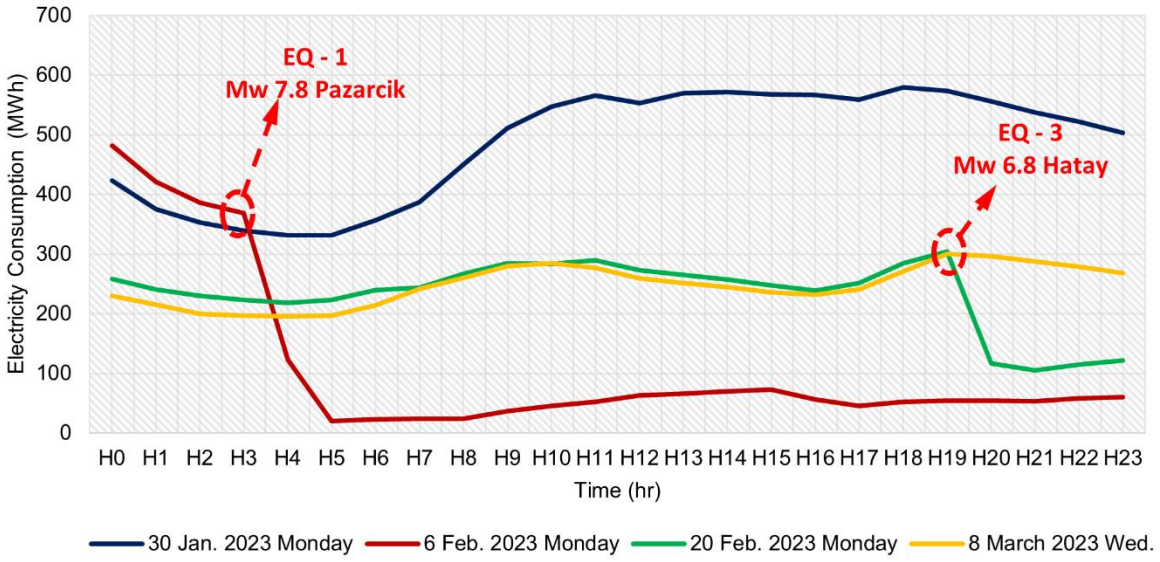

Figure 210: Electric consumption data of Hatay province before and after the earthquakes (Caliskan, 2023).

The electricity distribution lines and substations in the region, and particularly those in Hatay, Gaziantep, Kahramanmaraş and Adıyaman, were significantly damaged. According to the results of the post-earthquake preliminary studies, it is estimated that there is a total damage of 31 million GBP to the electricity transmission facilities owned by TEIAS, and 335 million GBP to the private electricity distribution facilities in the affected 11 provinces (PSB, 2023).

6.5.2.2. Oil and Gas

There was damage to two sections of gas transmission lines in Hatay. Their failure led to a halt in gas flows to Gaziantep, Hatay and Kahramanmaraş provinces. It was confirmed that “the main gas transmission line in Turkoğlu district of Kahramanmaraş, near the epicenter, was damaged the most” (Novinite, 2023). The pipelines gradually resumed their operation as of 11 February.

As for oil pipelines, “there was no damage to the Kirkuk-Ceyhan pipeline, which carries oil from Iraq to Türkiye, nor to the Baku-Tbilisi-Ceyhan (BTD) pipeline, an energy sector official told Reuters.” However, right after the earthquakes, oil imports from Iraq and Azerbaijan through the Turkish port of Ceyhan have been suspended for safety concerns. “The Kurdish region normally exports about 450,000 barrels of oil per day through Türkiye” (Novinite, 2023). Import from Iraq was resumed on the second day of the earthquake (7 Feb) and that from Azerbaijan the week after (12 Feb).

6.5.3. Case Studies

High-voltage substations performed exceptionally well in most places. There is a number of damages reported mostly due to the poor fixing of transformers to their foundations by anchor bolts or rail supports (*Figure 211*). These damages in the high-voltage substations were repaired within a few days after the earthquake, and electricity transmission to the earthquake-affected zone was restored.

Figure 211: Damaged High Voltage transformers, poor fixing to the rail or foundation: a) Transformer damage, Gaziantep (source : https://www.instagram.com/yuksek_gerilim_ariza/) and b) Transformer damage, Hatay (source : https://www.linkedin.com/posts/rehasen_deprem-trafo-reee-activity-7028409428567560192-kcvY/?utm_source=share&utm_medium=member_desktop

However, it was observed that most of the medium and low voltage substations located in the city centres are heavily damaged (*Figure 212*). Most of the damages were observed to be the collapse of the infill walls on the transformers, poor fixing of transformers on rails or their foundation, or the collapse of surrounding buildings on substations.

Figure 212: Heavily damaged Low- Medium Voltage transformers observed in Hatay on 17th March.

6.6. Industry Infrastructure

Approximately 18.5% of the population of Türkiye (including Syrians under temporary protection) lives in the 11 earthquake affected provinces. The contribution of the industry and manufacturing in the region to the overall GDP is around 11% (Turkstat, 2023). Gaziantep accounts for 36% of this contribution, Adana 19%, Kahramanmaraş 12% and Hatay 11%.

Significant industrial sectors in the region are chemistry, textile and food in Adana, chemistry, food and fresh fruit, textile, machinery and furniture in Gaziantep, iron-steel, and fresh fruit in Hatay and Osmaniye, and textile-clothing in Kahramanmaraş.

Textiles is a strong sector and accounts for 1/3 of all textile exports of Türkiye (PSB, 2023). The conglomeration of the steel industry around the Iskenderun Steelworks which itself is one of in the top 5 of industrial companies is nationally significant.

Manufacturing industry is generally concentrated in the 38 industrial centres throughout the region employing half a million people. The region is home to 11 of the top 100 industrial companies.

The region is a net contributor to in electrical energy generation with 23.5% of the installed capacity and 20.5% of the production in January 2023 (EPDK, 2023). Nationally significant power plants Afşin-Elbistan A and B, ISKEN Sugozu and Iskenderun Atlas with a total capacity of 5.4 GW are located in the region.

Kirkuk–Ceyhan and Baku–Tbilisi–Ceyhan Oil Pipelines both cross the region and terminate in Ceyhan, Adana. Dörtyol Gas Terminal in Hatay performs as a storage and regasification plant.

Locations of major power plants in the affected area are mapped in *Figure 213*.

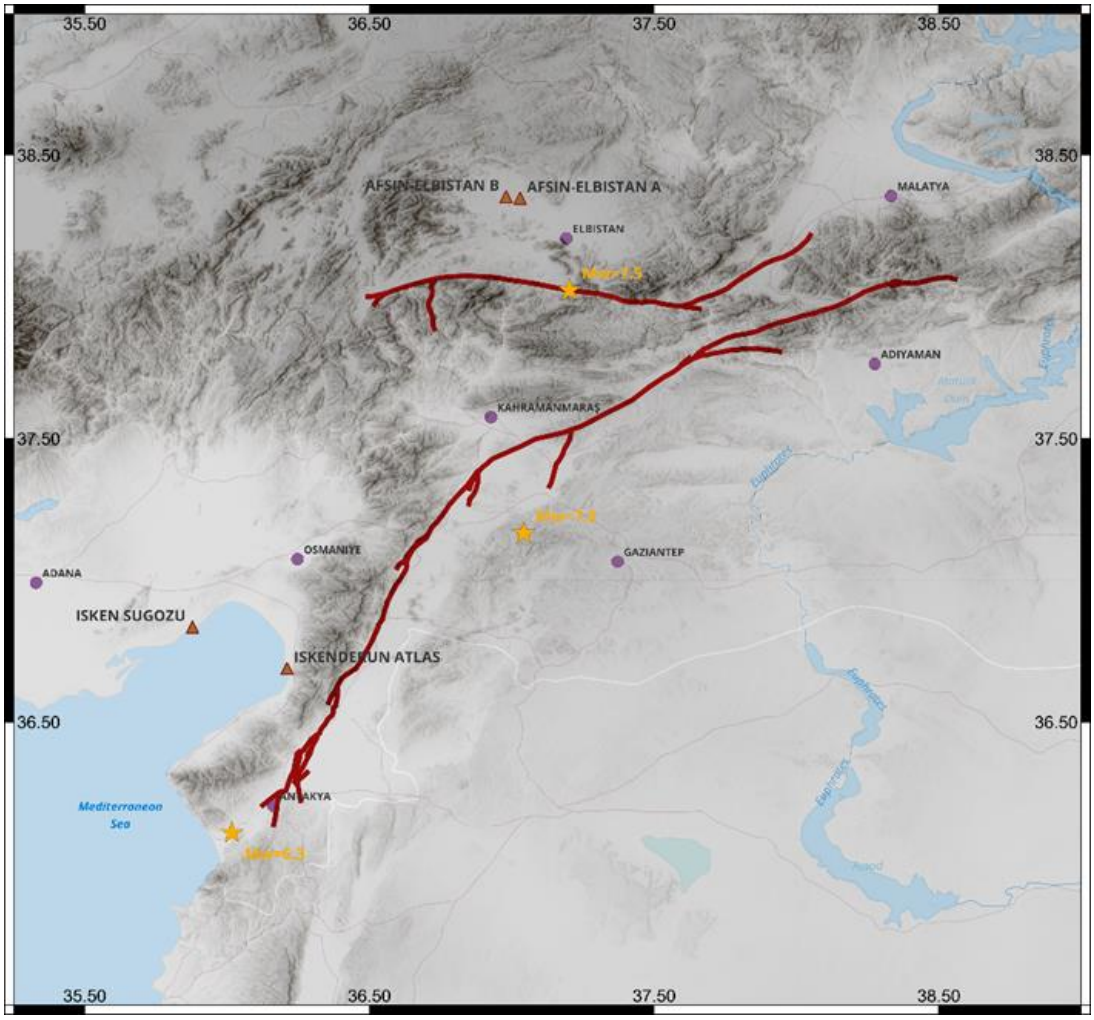

Figure 213: Location of Major Power Plants

6.6.1. Design and Construction Regulations Related to Industrial Buildings in Türkiye

The seismic design of industrial buildings in Türkiye is carried out in accordance with the Turkish Building Earthquake Regulation (TBECTERDC, 2018). There are no special regulations for such structures. The design level earthquake load is increased for the energy facilities with generation or transmission duties. Similarly, it is increased for structures where toxic, explosive, flammable, etc. materials are stored.

6.6.2. Overall Impact on Industry

Industrial facilities are intrinsically major investments receiving high quality engineering and construction services, and therefore they generally withstand earthquakes with no significant damage. Mid-scale industry is somewhat more affected but still expected to recover in a reasonable time frame.

The workforce, and the entire population in the region, are significantly affected by the earthquakes and together with the disruption in energy, telecommunications and transport, industrial production is expected to reduce. For comparison, following the 1999 Kocaeli Earthquake the GDP contracted by 3.3% but the affected region was the industrial heartland of Türkiye and hence had a far greater contribution of output.

6.6.3. Case Studies

6.6.3.1. Afşin-Elbistan B

There are two adjacent power stations in Afşin-Elbistan denoted as A and B. They use locally sourced low calorific value lignite and their combined generating capacity of 2.79 GW in 8-units is the highest of any station in Türkiye, and corresponding to 2.6% of installed electric energy capacity.

Construction of Afşin-Elbistan A and B power plants was completed in 1987 and 2006 respectively by multinational consortiums with local partners (*Figure 214*).

Figure 214: Afşin-Elbistan B Thermal Power Plant

EEFIT Field Team visited Afşin-Elbistan B power station on 16 March 2023. The seismic design parameters of the Afşin-Elbistan B power station are unknown however

according to the latest Türkiye Earthquake Map it has peak ground accelerations of 0.2 and 0.4g for 475 year and 2475-year return periods, respectively.

The power station building is a well-designed steelwork structure (*Figure 215*). It has four parallel units housing 110 m high boilers top-hung from a chevron and cross-braced steel frame with substantial fabricated rectangular hollow sections. All pipework and mechanical systems are base isolated by bearings and cable supports.

Figure 215: Construction Photo of Afşin-Elbistan B

After the first Pazarcık event, control systems initiated shutdown and plant-wide inspection process commenced. During the ongoing inspection, the second Elbistan event occurred, which was felt strongly both in the power station itself, and at in the personnel and family accommodation some 30 km away. Electric power supply and communications were interrupted, and the personnel had to leave the station to look after their own families, mostly living in accommodation blocks which were also damaged. Outside temperature was as low as -28°C and lack of personnel caused freezing of some pipework within the station and increased the extent of damage.

Loss of accommodation prevented personnel redeployment and detailed damage assessment. Plant management relocated the personnel and families to other residential units and prefabricated temporary housing. Manning levels improved slowly and at the time of EEFIT visit damage assessment was largely complete with and some minor repair works having commenced.

No damage was observed in the substantial steelwork frame except in a pair of chevron bracing at +100 m level (*Figure 216*). Gusset plates connecting the chevron bracings to the horizontal beam buckled and the welds forming the rectangular hollow

section failed. This failure was observed only in one of 4 units and can be attributed to an originally defective weld at this location.

Figure 216: Chevron bracing connection.

Displacements in various base isolated mechanical systems were beyond the maximum travel requiring repairs, further delaying restart of plant operations. In addition, coal feeding systems, vapour and air pipes, ash and coal filters were damaged but considered to be repairable by the in-house maintenance teams (*Figure 217* and *Figure 218*).

Figure 217: Secondary coal feeding system fallen off the support.

Figure 218: Displacement of secondary coal feed system.

A circular hollow section cross bracing of circular portal structure covering the reinforced concrete fuel tank also failed (*Figure 219*).

Figure 219: Bracing failure of diesel silo canopy.

In general, the seismic damage in the structural framing system of the power station was limited and the performance was satisfactory. However, seismic travel in many mechanical systems was beyond the capability of the base isolation and as a result, the plant was out-of-operation. The financial impact of loss of production in both power stations corresponding to 2.6% of overall generation capacity is significant. The plant has resumed limited operation in around May 2023.

6.6.3.2. Grain Silos

The region contributes about 15% of the total agricultural production in Türkiye and the share of the agriculture in the economy is higher than the Türkiye average (PSB, 2023).

Grain production of the region is generally stored in steel silos as they are easier to construct and operate compared to the traditional reinforced concrete silos. Two types are commonly used: Flat bottom and elevated hopper silos. Hopper silos are more practical to unload and used when frequent loading/unloading is required whereas flat bottom silos are for long term storage.

Silos are supplied by both international and local companies. A prominent local manufacturer uses ANSI/ASAE EP433 “Loads Exerted by Free-Flowing Grain on Bins” for the definition of grain loading and indicates that design for wind, snow and seismic loads to customer requirements and to Eurocodes is optional.

Large scale grain storage organisations are licenced by the Ministry of Agriculture and their specifications require seismic design but without any reference to design parameters and codes [TMO-TOBB LIDAS, 2020].

As grain production of US is mainly concentrated in the non-seismic Midwest, ANSI/ASAE EP433 covers flow patterns and loads exerted on the silo skin but does not reference seismic loads. ASCE 7-22 provides guidance on “Ground-Supported Storage Tanks for Granular Materials”, but it is not referenced in the manufacturer’s literature. Turkish Seismic Code does not have any provisions for non-building structures. EN 1998-4: Silos, tanks and pipelines has the most extensive provisions for seismic design of silos. This code considers an elastic analysis with an effective mass corresponding to 80% of the silo contents and associated rotary inertia applied at the centre of mass moving in unison with the silo wall.

The mass of the silo itself is low compared to the ensiled contents and the seismic behaviour is governed by the frictional properties of the product and its interaction with the thin corrugated steel silo wall (Mansour et al., 2022). The behaviour is highly nonlinear and the seismic code provisions are approximate and conservative.

Steel silos are typically fabricated from S450 corrugated and galvanised steel. Vertical posts provide the required strength and stiffness for seismic loading. Manufacturers generally use grade 10.9 fasteners with limited ductility.

Immediately after the earthquake, satellite imagery revealed the failure revealed failure of many steel grain silos in the region. Two locations were visited in the field, one in Hatay and the other in Nurdağı, Gaziantep. The facility in Hatay is a flour factory and the one in Nurdağı is only for storage (*Figure 220*).

Figure 220: Satellite images of grain silo failures.

The facility in Hatay has elevated reinforced concrete bases and vertical stiffeners. Elephant foot failure and failure of bolted connection of stiffeners to the silo skin were observed (*Figure 221*). The grain was contained but the emptying mechanism was damaged.

Figure 221: "Elephant foot" failure of silo wall and vertical stiffeners.

The facility in Nurdağı has both elevated hopper and flat bottom types. Holding down arrangements of 16No elevated hopper silos in this facility failed. Empty silos were also damaged with buckling of tie-bracing and horizontal beams. Only one of the flat bottom silos types failed completely but the emptying mechanisms for the remaining five were also damaged and the steel skin had to be cut to retrieve the contents (*Figure 222*).

Figure 222: Satellite image of Nurdağı Grain Silos, before (a) and after (b)

Figure 223: Failure of holding down arrangement and bracing.

Flat bottom steel silos performed better as they do not rely on holding-down arrangements, columns, and bracing. The effective mass of the ensiled content is also lower in height compared to hopper silos where overturning moments are critical. Notwithstanding this, all flat bottom silos were also out-of-service after the event and the skin had to be locally removed to retrieve the ensiled content.

The performance of the steel grain silos in the earthquake region Is unsatisfactory. They either failed completely or were out-of-service. The storage capacity for this year's harvest is lost which will put further strain on the agricultural sector in the region. Regulation by the Ministry of Agriculture and seismic design rules applicable to Türkiye to protect the contents in major seismic events should be considered to prevent future failures.

6.6.3.3. Prefabricated Industrial Buildings

Despite a noticeable increase in use of steel, precast concrete is still commonly used in light industrial warehouse construction in Türkiye.

As they are fabricated in a shop environment under supervision, material quality of precast concrete structures is well controlled. The main columns in typical precast industrial building construction comprises of columns inserted in a socket prepared in the ground and therefore moment resisting at the base. The connection of this vertical cantilever column with the floor beams and roof rafters is generally not moment resisting, however. In the out-of-plane direction the stability relies on the connections and on the infill walls and floor/roof decking. During construction, these structures lack the stability provided by the walls and decking and are more vulnerable to earthquakes.

Tying of various structural elements of precast concrete construction is critical, especially the pin connection between the column and the beams. This is recognised in the Turkish Seismic Code TDY-2007 and the connections are required to be designed for 1.5 times the calculated seismic force which should include both in-plane and out-of-plane directions. Rules on Precast Reinforced Concrete Buildings are further expanded in TDY-2018 and some standard details are given with detailed rules to calculate capacity of critical connections.

In the first revision of the TDY-1997 the response modification factor, R for this type of inverted pendulum precast structures were given as 5. In the subsequent revisions and in the new versions of the code, the R factor is reduced to 3. In general, this type

of construction is flexible and responds with significant seismic displacements reducing stability.

In industrial areas along the highway connecting Kahramanmaraş to the main motorway between Adana and Gaziantep many precast concrete industrial structures under construction collapsed. A typical precast light industrial building collapsed during construction is in Turkoglu, Kahramanmaraş. This building has moment resisting connections at the first-floor level (but most likely incomplete at the time of earthquake) and a simple hinged connection at the top of the column to the roof rafters (*Figure 224*a). This building has two reinforcing bars that connects the beams to the main column (*Figure 224*b).

Figure 224: Lightweight precast building (a) Failure of roof beams and cladding (b) Dowels connecting the beams to the column.

In addition to collapse due to lack of stability, concrete spalling is observed both in the corbels and in the column base (*Figure 225*). The spalling in the corbel is considered to be from the impact of the beams but in the column, it is an indication of a plastic hinge.

Figure 225: Spalled concrete (a) at the corbel (b) at the column base due to plastic hinge.

The adjacent completed industrial units of similar construction performed better. Some infill wall damage is observed but not significant enough to prevent continued occupation (*Figure 226*).

Figure 226: Cracking of infill walls completed unit.

Performance of prefabricated industrial buildings were unsatisfactory in the previous major earthquakes in Türkiye including 1998 Adana and 1999 Kocaeli. Turkish Seismic Code of 1999, 2007 and 2018 have progressively extended the design rules for precast concrete construction. This type of construction is practical and economical, but failures are still common due to inherent weaknesses. It is expected that adaptation of new rules and guidance of TDY-2018 by the precast reinforced concrete manufacturers and contractors would reduce future failures.

6.7. Water and Wastewater (WWT) Infrastructure

6.7.1. Design and Construction Regulations Related to WWT Infrastructure in Türkiye

The regulation named “Principles for the Design of Pipeline Systems Under the Impact of Earthquakes” (Republic of Türkiye Ministry of Energy and Natural Resources, 2020b) was published by the Ministry of Energy and Natural Resources which will be enforcedenteredenter into force in 2023. The design of existing pipeline systems has been carried out in accordance with TS EN 1295 “Structural design of buried pipelines under various conditions of loading” (Turkish Standard, 1999) and ALA 2001 “Guidelines For The Design Of Buried Steel Pipe” (ALA, 2001).

6.7.2. WWT Infrastructure in the Affected Area

Municipal water is supplied to Hatay province from the wells sunk into the aquifers of Amik Plain. There are 593 wells supplying municipal water (Hatsu, 2021) and 2500 wells for agricultural irrigation (AA, 2023).

There is widespread damage to the water supply network. Following reports of contamination in one of the water sources, Municipality of Hatay and subsequently the Government advised against drinking tap water where it remained available. Hatay Municipality is continuing to install community fountains and provides and wastewater collection to tent camps (YetkinReport, 2023).

Throughout Hatay, bottled water for drinking was being supplied through distribution centres which is a huge logistical challenge for both the authorities and the public (*Figure 227*) (see Section 7.10.1 for a more comprehensive discussion as to the relief operations).

Figure 227: Bottled water supply.

Local farmers of the Amik Plain reported that 75% of the 2500 wells used for agricultural irrigation were damaged which would affect this year's harvest and the livelihood of farmer households (AA, 2023).

Similar to Hatay, there were public warnings against drinking municipal water in Kahramanmaraş. But about two months after the earthquake, the municipality announced a return to normal as a result of ongoing laboratory tests (Marasgundem, 2023).

There is no significant visible damage to wastewater treatment plants in Hatay and Kahramanmaraş from the satellite imagery. However, sewage systems are expected to be damaged in both provinces and therefore the demand on wastewater treatment is expected to significantly reduce, especially in Antakya.

The earthquake sequence demonstrated that deployment of mobile water treatment equipment using existing groundwater supply is essential to reduce inconvenience to survivors.

6.8. Dams and reservoirs

Majority of dam design and construction in Türkiye is carried out or licenced by the DSI (State Hydraulics Works). Seismic design of dams generally follows ICOLD (International Commission of Large Dams) guidelines.

DSI geotechnical investigation specification considers two levels of earthquake, operating basis and maximum design with 144-year and 475-year return periods. For some major projects DSI may also specify a greater return period of up to 10000-year (DSI, 2016).

As an example, probabilistic seismic hazard assessment for the Hatay-Büyükkaraçay Dam considered 144-year and 475-year return periods with corresponding peak ground accelerations of 0.20 and 0.31g (Yunatci and Cetin, 2007).

There are 7 dams with more than 1 million m^3 of dam volume in the region (*Figure 228*), whose damage levels are given in *Table 23*.

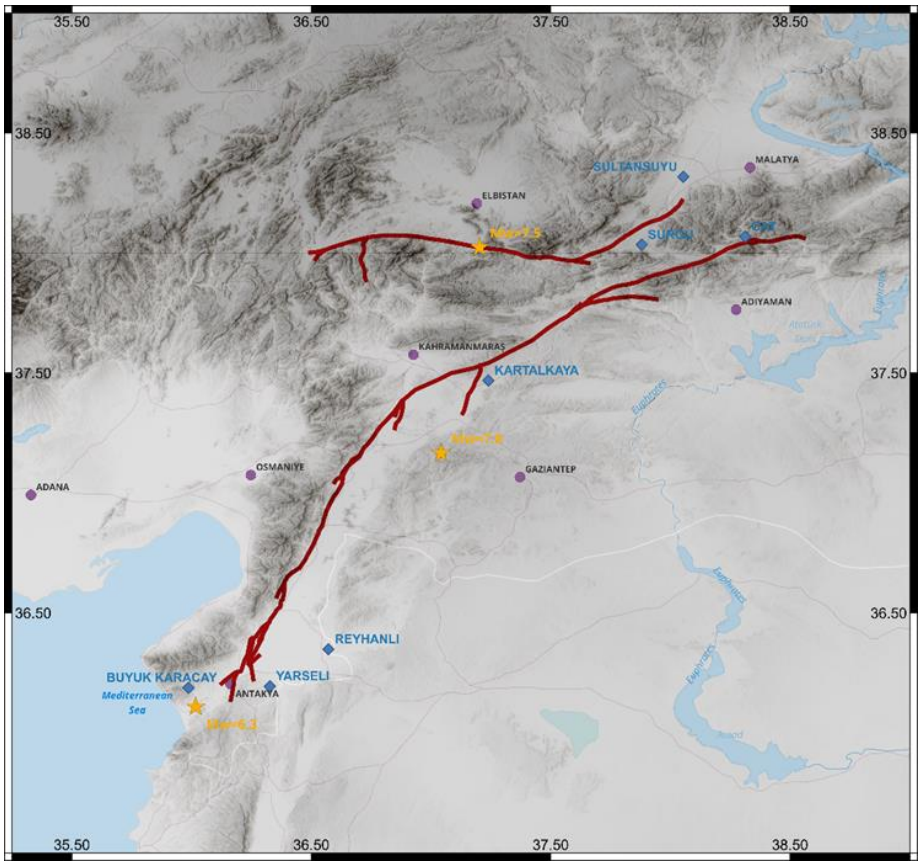

Figure 228: Major dams of the region.

Table 23: List of Damaged Dams

Dam	Structure Volume	Damage
Hatay-Reyhanlı Dam	20,730,055	Moderate
Malatya-Sultansuyu Dam	3,205,000	Severe
Kahramanmaraş-Kartalkaya Dam	1,452,000	Moderate
Malatya-Sürgü Dam	1,220,000	Moderate
Hatay-Yarseli Dam	3,000,000	Light
Hatay-Büyükkaraçay Dam	2,500,000	Light
Malatya-Çat Dam	2,500,000	Light

Malatya Sultansuyu (*Figure 229* and *Figure 230*) is the only severely damaged dam with cracks in the 60 m high crest and was emptied immediately after the earthquake (Turkish Society on Dam Safety, 2023).

Figure 229: Dam Safety Society – Sultansuyu Dam

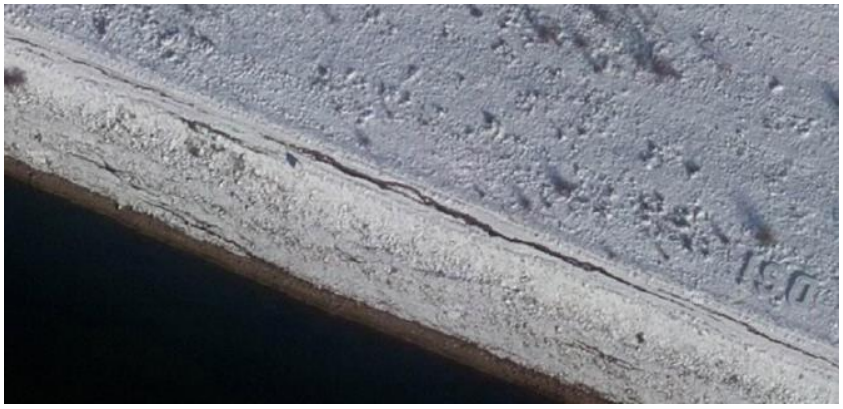

Figure 230: Visible Cracks in Crest – Sultansuyu Dam – Harita Genel Mudurlugu

Al-Rastan Dam in Syria was also emptied as a precaution, and this caused flooding, landslides and ground movement along River Asi where it enters the Turkish soil (PSB, 2023).

Ataturk Dam, third largest dam in the world, is between Adıyaman and Şanlıurfa and is 119 km away from Pazarcık. It was surveyed on multiple occasions by the DSI, and no damage was reported (AA, 2023).

6.9. Communication Networks

6.9.1. Overview, Design, and Construction of Base Stations

The main mobile network operators in the affected regions are Vodafone, Turk Telekom, and Turkcell. Prior to the disaster, there were over 11 million mobile phone subscribers supplied by 8900 base stations in the affected region (Haberturk, 2023). *Figure 231* shows the distribution of mobile phone subscribers across the affected region. Of the total number of subscribers, Turkcell and Vodafone had over 6.5 million and 3.7 million subscribers, respectively (Lipscombe, 2023; Vodafone, 2023). Turkcell subscribers were supplied by about 3,300 base stations. On the other hand, Vodafone customers in the affected regions were connected to the network through over 3000

base stations. According to Vodafone (Vodafone, 2023), about half of their base stations are located on buildings across the cities. *Figure 232* shows a base station at the rooftop of a building.

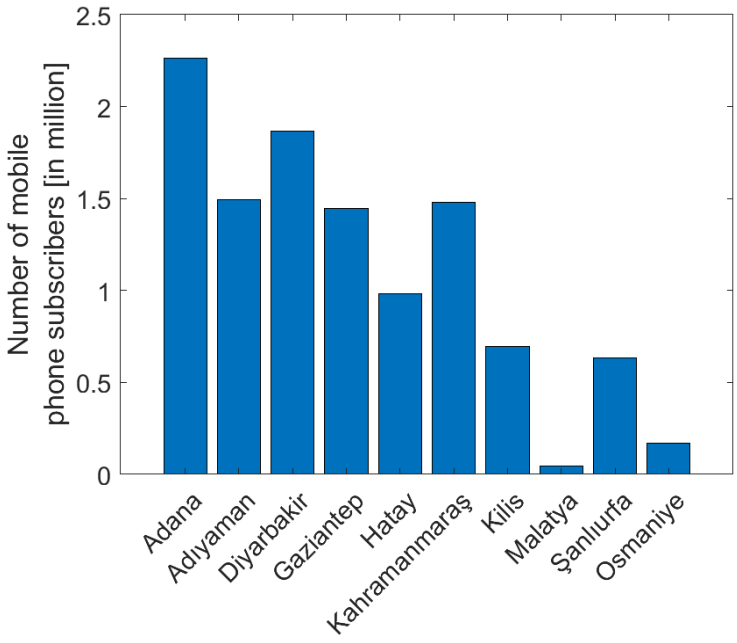

Figure 231: Distribution of mobile phone subscribers across the affected region (Data source: BTK)

Figure 232: A base station on the rooftop a building.

According to Electronic Communications Law No. 5809 (Government of Türkiye, 2008), the Information Technologies and Communications Authority (BTK) is the regulatory body for base station installation in Türkiye. Amongst other obligations, Law No. 5089 mandates mobile operators to (a) take appropriate measures to prevent exposure of the general public to electromagnetic fields from electronic communication networks, (b) maintain the integrity of electronic communications network, and (c) take necessary measures for maintaining uninterrupted communication under major disaster situations. All mobile operators are issued a security certificate for every base station that is established and operating in accordance with the regulations.

According to BTK (https://tuketici.btk.gov.tr/baz-istasyonlari), base stations are installed in places where coverage and capacity increase are required, provided that

the electromagnetic field intensity emanating from the electronic communication devices is within the international standard stipulated exposure limit values. The regulation does not provide any recommendations on the seismic vulnerability of the host buildings for mobile base stations. Hence, it is possible that mobile operators did not consider the seismic vulnerability of host buildings during the location selection process.

6.9.2. Impact

Following the disaster, about 50% of Turkcell's base stations were out of service due to power outage and/or damage (Lipscombe, 2023). According to Turkcell, only one tower and about 150 base stations were damaged by the earthquake. Hence, the majoritymajority of the service loss was attributed to power outage. Similarly, 1700 base stations belonging to Vodafone were also out of service due to power outage and/or damage (Vodafone, 2023). However, most of the base stations were destroyed due to significant damage to the host buildings. *Figure 233* shows an example of a destroyed base station due to building collapse. Overall, 2451 base stations (about 28% of total base stations) were reported to have suffered significant damage (Haberturk, 2023).

Figure 233: Photo of a collapsed building with a base station (Source: Manset61.com)

In general, the post-disaster functionality of a significant proportion of telecommunication network was dependent on (a) seismic fragility of the components of the base station, (b) availability and post-disaster functionality of power back-up system at the base station, (c) the resilience of the electric power network, and (d) post-disaster damage state of the host building for base stations. *Figure 234* provides an overview of the initial post-disaster network connectivity in the affected areas. As shown in the figure, telecommunication systems were mostly affected in Adıyaman, Hatay, Kahramanmaraş, and Osmaniye.

Following the earthquake, citizens were mandated only to make essential calls, to avoid overloading the communication channels. Citizens were encouraged to communicate using the internet or via SMS (Haberturk, 2023).

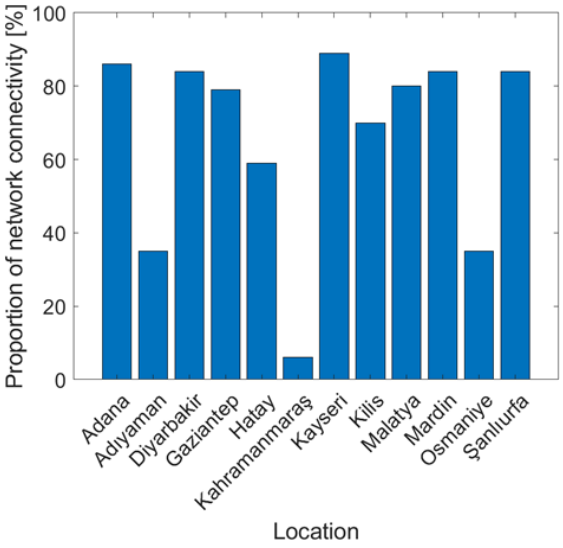

Figure 234: Initial post-disaster network connectivity in the affected areas (Source: netblocks.org).

The widespread post-earthquake communication disruption clearly showed that the mobile operators could not fulfil their obligations, as stated in Law No. 5089. Following the earthquake, an investigation was launched against Turkcell, Vodafon, and Turk Telekom for their failure to provide uninterrupted communication and internet access in the affected region.

6.9.3. Post-Disaster Recovery

Each of the three mobile operators reportedly acted swiftly in restoring connectivity in the affected region. Turkcell deployed over 1400 power generators and 250 mobile base stations to the affected region. Restoration efforts were carried out by over 1200 Turkcell personnel (Lipscombe, 2023). Similarly, Vodafone deployed over 1000 power generators and 100 mobile base stations to bolster the network (Vodafone, 2023). According to Vodafone, restoration efforts were being carried out by over 450 personnel daily. An example of a deployed mobile base station is shown in *Figure 235*.

Figure 235: Deployed mobile base station following the earthquake (Kilinc, 2023)

Figure 236 presents the restoration trajectory of network connectivity across 11 affected provinces. As shown, several provinces were still experiencing communication disruptions over two days after the disaster.

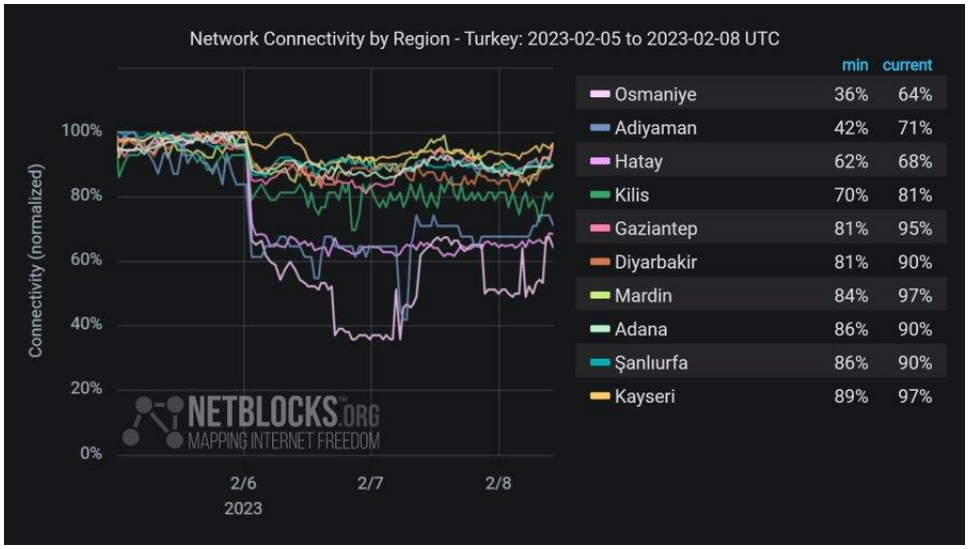

Figure 236: Restoration trajectory in the affected areas (Source: netblocks.org)

One of the biggest challenges of the intervention process is the fuel supply logistics to distributed power generating sets. According to one of the operators, some of the generators ran out of fuel after 3-4 hours and enormous logistics had to be put in place to ensure continued functionality through constant refuelling (Haberturk, 2023).

6.9.4. Potential Mitigation Measures

Appropriate investments are needed to improve the seismic resilience of existing base stations. Furthermore, there is a need to identify and promote the adoption of other alternatives to existing earthquake-vulnerable stations.

The robustness of electronic communication systems can be improved by installing back-up power systems that can ensure continued functionality for long hours following disaster-induced municipal power loss. Renewable energy sources (e.g., solar panels) are more sustainable alternatives to fuel-powered generating plants.

Mobile operators should avoid installing base stations on buildings. However, in cases where this cannot be avoided, mobile operators need to consider the disaster resilience of host buildings as one of the critical criteria for selecting the location of mobile stations. Ideally, host buildings should have a high probability of being functional following design-level events.

Efficient regional action plans are needed to improve the preparedness level of mobile operators. Such plans must be developed through engagement (e.g, focus group discussions and workshops) with mobile operators and other relevant stakeholders.

6.10. Interdependencies and Cascading Effects

This section highlights the reported/observed interdependence of infrastructure systems in the affected areas. We focus on the electric power network, gas pipelines, transportation infrastructure, water and wastewater system, telecommunications, and hospitals. *Table 24* provides an overview of the impact of failures in different infrastructures on other infrastructure types.

Table 24: Reported/observed interdependence of infrastructure systems in the affected area.

		Reported Impact on:					
		Electric power network	Gas pipelines	Transportation	Water & Wastewater	Telecommunications	Hospitals
Damage to:	Electric power network			Y		Y	Y
	Gas pipelines						Y
	Transportation					Y	Y
	Water & Wastewater						Y
	Telecommunications						Y
	Hospitals						

Electricity, water, and gas supplies significantly impacted hospital functionality in the affected regions (Cooper, 2023; HOPE, 2023). Hospitals with backup power sources for buildings (e.g., generators) and medical equipment (e.g., batteries in medical devices) were able to maintain some functionality. Hospitals without access to the communal power grid and backup power sources could not provide services to disaster victims, even raising arguments that in some hospitals, power outage resulted in casualties (Turkish Minute, 2023). Furthermore, due to the cold weather conditions, constant heating was needed for the habitability of the hospital rooms. Only hospitals with electricity and electric heaters could provide heating to hospital rooms.

Transportation logistics issues impeded hospitals' capability to refill depleted medical resources (OCHA, 2023). The combination of power loss and telecommunication failure also impacted hospital service delivery. For example, hospital staff could not coordinate activities, identify injured patients, document admission, transfer, and referrals, follow up with patients, etc.

As previously highlighted in Section 6.9, one of the main reasons for telecommunication failure was power outage. Over 2000 base stations belonging to Turkcell and Vodafone were out of service due to power outage and/or damage. The three main telecommunication companies quickly deployed personnel to restore connectivity in the affected areas. However, poor accessibility (as a result of damaged roads) to some areas restricted swift deployment of mobile base stations and generators.

Transportation networks were also impacted by the power outage. It was reported that electrical energy was not supplied to a number of railway lines due to 10 non-operational substations (Railtech, 2023). Moreover, a lack of communication means hampered the travels of the rescue teams as they could not effectively obtain information on road closures and detour routes.

6.11. Summary and Conclusions

The healthcare infrastructure performance was in par with the residential building stock and below the expectations for this critical infrastructure sector. The total losses across the healthcare sector were estimated to be 80.9 billion TRY (2.7 billion GBP). Approximately 30% of the building stock in the health care sector in the affected region was damaged beyond repair and put out of service for a long term. Many hospitals

that were lightly damaged were out of operation for several weeks after the earthquake due to lack of clear guidance about post-earthquake inspections and action plans. The situation was most critical in Hatay province where three big hospitals collapsed, and many were unusable either due to structural and non-structural damage or evacuated due to safety concerns. That left the entire province to rely mainly on the state hospital in Dörtyol which was built on base-isolation and remained fully functional after the earthquake. Türkiye is a pioneering country in the construction of base-isolated hospitals. Since 2013 there is a requirement for all hospitals with capacity of more than 100 beds and located in 1st and 2nd seismic zone to be base-isolated. So far over 50 base-isolated hospitals were built in Türkiye, eleven of which in the affected region. The EEFIT team visited four of them, these in Dörtyol, Osmaniye, Malatya and Elbistan. All base isolated hospitals were reported that remained fully functional after the earthquakes, which was critically important as they needed to cover a huge gap in the hospital sector capacity due to the large number of non-functional hospitals after the earthquake.

The education infrastructure performance was clearly better than the residential building stock even in the areas of heavy destruction. This could be the result of the importance and priority given to the safe construction of schools. However, the disruption to education is found to be extensive and lengthy, due to various reasons. Even the undamaged schools didn't resume schooling more than a month after the event, as they were also used as relief distribution hubs and shelters.

It is difficult to draw any conclusions about the overall performance of emergency response infrastructure due to the limited information available and limited observations during the mission. The AFAD facilities in Kahramanmaraş and Hatay, the two most affected provinces, were visited and were seen fully functional after the earthquakes. This is likely the case with AFAD buildings in the other nine provinces. The performance of fire brigade buildings was not to that level. The main fire brigade building in Antakya has collapsed which led to the complete loss of two fire trucks and the very needed at the exact moment three SAR vehicles together with five sets of SAR equipment, thus affecting the capability of Hatay fire department to perform its duties after the earthquake. The team observed two fire stations in the Iskenderun area, one of which is the main fire station, to be evacuated for safety reasons and to be operated through external tent camps.

A total of 25 high-voltage substations and 11 electricity transmission line poles were damaged in the first earthquake, causing a significant power outage in the affected region. The damages on the high-voltage substations and transmission lines were repaired within a few days. However, the medium and low-voltage substations in city centres suffered heavy damage primarily due to the collapse of the substation buildings, the collapse of the infill walls of the substation buildings onto equipment, and poor fixing of transformers. As well as, the surrounding residential buildings collapsed onto substations, transmission lines and poles which completely destroyed the electric transmission in the city centres. The total estimated cost of the damage on the electricity infrastructure is 31 million GBP for TEIAS-owned facilities and 335 million GBP for private distribution facilities in the earthquake-affected area.

From the perspective of structural performance, transport infrastructures performed satisfactorily as they underwent relatively minor damages. Meanwhile, their performance in terms of the operational perspective manifested many limitations. The

significant intensity of the earthquakes made their performance during the first two days, when emergency activities took place, all the more critical. On the other hand, in the long term, their importance became less important than with low- or medium-intensity earthquakes since traffic flows arising from normal activities have been significantly reduced owing to massive destructions in the community.

Roughly 50% of Turkcell's base stations were out of service. Likewise, 1700 base stations belonging to Vodafone were also out of service. Majority of the communication service loss was attributed to power outages and damage to host buildings. The three main telecommunication companies quickly deployed personnel to restore connectivity in the affected areas. However, restricted road access to some areas inhibited the swift deployment of mobile base stations and generators. Another big challenge was the fuel supply logistics to backup power generating sets for base stations. Some of the generators ran out of fuel after 3-4 hours, and enormous logistics had to be put in place to ensure continued functionality through constant refuelling. Several locations were still without internet connectivity several days after the disaster.

References

AA. (2023). Earthquakes also hit the water wells in the Amik Plain, published 10 March 2023. https://www.aa.com.tr/tr/asrin-felaketi/depremler-amik-ovasindaki-su-kuyularini-da-vurdu/2841856 (Accessed 19 June 2023)

AA. (2023). The condition of the dams in the earthquake zone is closely monitored, published 14 February 2023. https://www.aa.com.tr/tr/asrin-felaketi/deprem-bolgesindeki-barajlarin-durumu-yakindan-izleniyor/2818818 (Accessed 19 June 2023)

AASHTO. (2002). Standard Specifications for Highway Bridges. American Association of State Highway and Transport Officials.

American Lifelines Alliance (ALA). (2001). Guidelines for the design of buried steel Pipe (with addenda through 2005).

Caliskan, O. N. (2023). 06 February 2023 Kahramanmaraş 20 February 2023 Hatay earthquake and their effects on the distribution network, Electromechanical Industrialist Association, Ankara, Türkiye. https://www.emsad.org.tr/panel-sunumlari/8.pdf (Accessed May 5, 2023)

Chamber of Architects, (2023). Kahramanmaraş Branch Earthquake Report. Available at: https://www.kmarasmimod.org/Dosyalar/20230227193852863.pdf (Accessed May 5, 2023)

Chamber of Mining, (2023). 6 February 2023 Earthquakes Report. Available at: https://api.maden.org.tr/uploads/contents/2023-02-5-11-59-50-697933.pdf (Accessed May 5, 2023)

Cetin, KO, JD Bray, JD Frost, A Hortacsu, RES Moss, & JP Stewart. (2023). February 6, 2023,Türkiye Earthquakes: Report on Geoscience and Engineering Impacts, Report GEER-082, GEER Association, 382 pages.

Cooper, L. (2023). Essential Medications Prepped for Earthquake-Ravaged Areas of Syria, Türkiye, Direct Relief. Available at: https://www.directrelief.org/2023/02/essential-medications-prepped-for-earthquake-ravaged-areas-of-syria-Türkiye/ (Accessed: 10 February 2023).

Di Sarno L, Yenidogan C, & Erdik M. (2013). Field evidence and numerical investigation of the Mw7.1 October 23 van, Tabanli and the Mw5.7 November earthquakes of 2011. *Bulletin of Earthquake Engineering*, 2013(11), 313–46.

DSI (2016), Specification for Geotechnical Investigation

EERI. (2021). *EERI Report – Learning from Earthquakes: The Mw 7.1 Erciş-Van, Türkiye Earthquake of October 23, 2011.*

EERI. (2023). *EERI Report – February 6, 2023 Türkiye Earthquakes: Report on Geoscience and Engineering Impacts, May 6, 2023*

EPDK (2023), Energy Market Sectoral Report

Erdik M. (2001). Report on 1999 Kocaeli and Düzce (Türkiye) earthquakes, in Structural Control for Civil and Infrastructure Engineering, 149–86.

Erdik M, Kamer Y, Demircioglu M, & Sesetyan K. (2012). 23 October 2011 Van (Türkiye) Earthquake. *Natural Hazards* 2012, 64, 651–65.

Government of Türkiye. (2008). Law Number 5809: Electronic Communications Law. https://www.mevzuat.gov.tr/mevzuat?MevzuatNo=5809&MevzuatTur=1&MevzuatTertip=5 (Accessed 1 May 2023)

Haberturk. (2023). GSM operators collapsed in the earthquake that destroyed 10 provinces. https://www.haberturk.com/operatorler-yine-sinifta-kaldi-3564007-teknoloji (Accessed 1 March 2023)

Hafiza, R. (2023). Tweeter post: https://twitter.com/ResimliHafiza/status/1624459993394081793 (Accessed 18 June 2023)

Hatsu (2021), Activity Report

HOPE. (2023). 2023 Türkiye & Syria Earthquakes Response: Situation Report #3, February 8, 2023. Available at: https://reliefweb.int/report/,Türkiye/2023-,Türkiye-syria-earthquakes-response-situation-report-3-february-8-2023 (Accessed 19 June 2023)

Ilk Kursun (2023) Hatay Havalimani Acildi. Available at: https://ilkkursungazetesi.org/haber/hatay_havalimani_acildi-27986.html (Accessed 31 Jan 2024)

Kenez, L (2023) Failure to deliver aid and send rescue teams to quake disaster area is turning into anger against Erdoğan. Available at https://nordicmonitor.com/2023/02/failure-to-deliver-aid-and-rescue-teams-to-disaster-areas-turns-into-anger-against-erdogan-government/ (Accessed 31 Jan 2024)

Kilinc, U. (2023). Statement from BTK on Communication Collapse in Earthquake Zone: Base Stations, Small Part of the Problem. https://www.webtekno.com/btk-baz-istasyonlari-sorunun-kucuk-kismi-h133349.html (Accessed 1 May 2023)

Lipscombe, P. (2023). Turkcell outlines response to last month's devastating earthquakes. https://www.datacenterdynamics.com/en/news/turkcell-outlines-response-to-last-months-devastating-earthquakes (Accessed 4 April 2023)

Mansour S, Pieraccini L, Palermo M, Foti D, Gasparini G, Trombetti T and Silvestri S (2022) Comprehensive Review on the Dynamic and Seismic Behavior of Flat-Bottom Cylindrical Silos Filled with Granular Material. Front. Built Environ. 7:805014. doi: 10.3389/fbuil.2021.805014

Marasgundem. (2023). Description about drinking water in Kahramanmaraş. published 8 April 2023. https://www.marasgundem.com.tr/Kahramanmaraş/Kahramanmaraşta-icme-suyu-hakkinda-aciklama-1509182h (Accessed 19 June 2023)

Ministry of Health of Türkiye, General Directorate of Health Investments. (2013). The standards to be applied in the projects and construction works of the buildings to be constructed as seismically isolated, 2013. Circular No. 2013/3.

MCEER. (2000). The Marmara Türkiye Earthquake of August 17, 1999: Reconnaissance Report. Rep. No. MCEER 00-0001, Ed: Scawthorn C. Multidisciplinary Center for Earthquake Engineering Research, Buffalo, New York, USA, 2000.

Ministry of Transport and Infrastructure. (2020) Principles for the Design of Highway and railway Tunnels and Other Ground Structures Under Seismic Load. Ministry of Transport and Infrastructure, Republic of Türkiye, Ankara.

NASA. (2023). The Black Marble Project. (Accessed 5 May 2023)

NASA Earth Observatory. (2023). Earth at Night. (Accessed 5 May 2023)

Novinite. (2023). “Türkiye's Energy Infrastructure after the Earthquakes: Huge Fire, Stopped Gas and Oil Pipelines”, published 7 Feb 2023. https://www.novinite.com/articles/218748/Türkiye%27s+Energy+Infrastructure+after+the+Earthquakes%3A+Huge+Fire%2C+Stopped+Gas+and+Oil+Pipelines (Accessed 8 May 2023)

OCHA. (2023). Earthquake: Türkiye and north-west Syria Flash Update No. 5 As of 10 February 2023. Available at: https://reliefweb.int/report/,Türkiye/earthquake-,Türkiye-and-north-west-syria-flash-update-no-5-10-february-2023 (Accessed 19 June 2023)

PSB, Presidency of Strategy and Budget, Presidency of Republic of Türkiye. (2023). Türkiye earthquakes recovery and reconstruction assessment report. Available at: https://www.sbb.gov.tr/wp-content/uploads/2023/03/,Türkiye-Recovery-and-Reconstruction-Assessment.pdf

Railtech. (2023). Railway services suspended following earthquake in Türkiye and Syria. Turkish press agency AA reports. Available at: https://www.railtech.com/infrastructure/2023/02/07/railway-services-suspended-following-earthquake-in-Türkiye-and-syria/#:~:text=In. (Accessed 4 April 2023)

Republic of Türkiye Ministry of Energy and Natural Resources. (2020a). Electric Transmission Systems and Communication Facilities Earthquake Regulation, Ankara.

Republic of Türkiye Ministry of Energy and Natural Resources. (2020b). Principles for the Design of Pipeline Systems Under the Impact of Earthquakes, Ankara.

TBECTERDC. (2018). Turkish Earthquake Resistant Design Code. The Disaster and Emergency Management Presidency of Türkiye. Ankaras.

TMO-TOBB LIDAS (2020), Technical Specification for Design, Construction and Commissioning of Corum 20000 tonne Capacity Steel Silo and Grain Storage Units

Turkish Standard. (1999). TS EN 1295: Structural design of buried pipelines under various conditions of loading. The Institution of Turkish Standards, Ankara, Türkiye.

Turkish Electricity Transmission Corporation (TEIAS). (2023). February 2023 TEIAS activities after the earthquake in Kahramanmaraş, Electromechanical Industrialist Association, Ankara, Türkiye. https://www.emsad.org.tr/panel-sunumlari/5.pdf (Accessed May 5, 2023)

Turkish Minute. (2023). Opposition MP claims patients died due to power outage at hospital following earthquakes, published 1 March 2023. https://www.turkishminute.com/2023/03/01/opposition-mp-claim-patient-died-due-to-power-outage-at-hospital-following-earthquakes/ (Accessed 8 May 2023)

Turkish Society on Dam Safety (2023), Impact on Dams in the Region and Possible Problems in the Future

TR Ministry of Health, Construction Repair Department. (2012). Issues to be complied with at the project stage for the health facility to be built within the scope of the health transformation project. Circular No. 2012/6, Ministry of Health of Türkiye, Construction Repair Department.

Türkiye Kamu ve Ozel Saglik Kurumlari Rehberi. (2023). Private Antakya Academy Hospital. https://www.trhastane.com/ozel-antakya-akademi-hastanesi-476.html (Accessed 18 June 2023)

Turkstat (2023), Turkish Statistical Institute (TURKSTAT) (tuik.gov.tr)

Qu, Z., Wang, F., Chen, X., Wang, X., & Zhou, Z. (2023). Rapid report of seismic damage to hospitals in the 2023 Türkiye earthquake sequences. *Earthquake Research Advances*, 100234.

Vodafone. (2023). Vodafone’s Humanitarian Response in support of Türkiye and Syria. https://www.vodafone.com/news/inclusion/vodafone-humanitarian-response-support-Türkiye-syria (Accessed 4 April 2023)

YetkinReport. (2023). "Drinking water problem grows in Hatay", published 4 March 2023. https://yetkinreport.com/2023/03/04/hatayda-icme-suyu-problemi-buyuyor/ (Accesssed 19 June 2023)

Yunatci and Cetin (2007), Büyük Karaçay Barajı ve HES için olasılıksal sismik tehlike analizi, 1. Ulusal Baraj Güvenliği Sempozyumu ve Sergisi

7. RELIEF, RECOVERY AND RECONSTRUCTION

7.1. Methods and Sources of Information

This section concerns the relief, response and recovery (RRR) operations in a large area affected by the February 2023 Kahramanmaraş Earthquake sequence through the lens of the human and economic aftermath. To this end the RRR sub-team conducted a series of interviews to understand the first-hand experience of residents of the affected areas, professionals involved in RRR operations and other stakeholders. Other critical sources of information included field visits and observations made to the disaster area between March and end of June 2023 by the different team members, press releases, AFAD reports and documents, many academic and institutional reports, Relief Web, and government and NGO reports.

The interviewees include government officials, educational and medical staff, volunteers and members of NGOs, residents living in the disaster region (see *Table 25* for a non-exhaustive list). Interviewees provided 'on-the-ground' perspectives of stresses, challenges, and successes. This included the impact of success of the response and recovery actions, emergency and temporary housing, debris removal and dumping actions. Some interviews were more formally organised, and names are provided here, and others were more spontaneous field conversations with affected families, and staff members and therefore their names are not provided here.

The fact that the impact area of the disaster is very wide (11 provinces and affiliated settlements), its high severity, and the extent of the destruction means that the recovery and reconstruction processes in the disaster area will be a long-term process. For this reason, it is also considered that the RRR team will carry out longer-term studies in the region.

Table 25: List of interviews for the report

Informant	Location	Date
Filip Kirazov and Josh Macaguag, SARAID	online	21&24.02.2023
Step Haiseldon, Care International	Online	09.03.2023
Katie Bitten and Mohammed Bashein, RedR	online	09.03.2023
Dörtyol hospital employee	In person	13.03.2023
Fire station, İskenderun	In person	13.03.2023
Lütfü Savaş, Hatay Metropolitan Municipality Mayor	In person	14.03.2023 & 20.06.2023
Nazan Savaş, Professor of Public Health, Mustafa Kemal University	In person	14.03.2023
Kadirli Belediye Muhtar and local residents	In person	15.03.2023
Family in tents at Göksun municipality grounds	In person	15.03.2023
Çardak Village Community Leader	In person	16.03.2023

Residents in Ericek	In person	16.03.2023
Residents in Samandağ	In person	17.03.2023
Caoimhe Butterly, Volunteer therapist from Ireland	In person	17.03.2023
Volunteer chef at soup kitchen	In person	17.03.2023
Canan Küçük, volunteering doctor working at the Italian Field Hospital, Antakya	In person	17.03.2023
Oğuzhan Karayiğit, Mersin District Municipality, Private Secretary of Mayor	Telephone	17.03.2023
Metin Açik, Hatay Municipality, Deputy Secretary General	Telephone	21.03.2023
Soner Büyükatalay, METU Mountaineering and Winter Sports Club (DKSK)	phone	24.03.2023
Deniz Demirag, Researcher from Gaziantep	Online	30.03.2023
Tacettin İnandı, Professor of Public Health, Mustafa Kemal University	In person	20.06.2023
Antakya KUDEB staff	In person	20.06.2023
Traditional home dwellers in Maras and Malatya	In person	16-19.06.2023
*Muhtar*s in Maras and Malatya	In person	16-19.06.2023
Family living near dump site area in Antakya	In person	23.06.2023
Elif Okşan Çalıkoğlu, Professor of Public Health, Gaziantep University	In person	28.09.2023

7.2. Development Context of the Region Before the Earthquakes

7.2.1. Earthquake Risks of the Region in Past Publications

In the past, many studies and publications have been produced on the seismicity and earthquake risks of the region, which can be considered as warnings. In this sense, a quick review of the studies conducted for Hatay province and Antakya town has been made as an example, and the diversity of publications on the subject has been tried to be summarized in a table. It is aimed to examine of the studies that were carried out on the earthquake risks in Antakya and its close vicinity before the February 6 earthquakes and to understand which of them have the quality of warning.

The other aim of this section is to understand that the disaster that occurred was not a surprise and to get a general idea of the recommendations and determinations made before the February 6 disaster. The studies were found by using the keywords (*Hatay, Antakya, Earthquake, Disaster, Disaster Risk, Urban Growth*) through the academic publication research platform of Google Scholar (*Table 26*).

Table 26: A list of selected publications on earthquake hazards and vulnerability in the area affected by 6 February earthquakes.

#	Name of Publication	Science/Research Area	Publication Year	Notes	Reference
1	Earthquakes in Anatolia during the Period of Seljuks	Social Sciences / History	1992	Article	Arik, F.Ş. (1992)
2	Physical and Demographic Structure of Antakya in the Ottoman Period 1709-1860	Social Sciences / History	1994	Article	Özdemir, R. (1994)
3	The Seismic Activity of Antioch from Past to Present and the Assessment of the Actions to be Taken in the Light of an International Conference	Science / Engineering	2003	Conference Paper	Beyen, K., et al. (2003)
4	Ecological Anthropology: Antakya	Social Sciences / Social Environmental Theory	2005	Thesis	Aygün, B. (2005)
5	Korkmaz, H. (2006). The Relationship Between Soil Properties and Earthquake Effects in Antakya. Journal of Geographical Sciences, 4(2), pp. 49-66	Social Sciences / Geography	2006	Article	Korkmaz, H. (2006)
6	1822 Halep-Antakya Earthquake and Its Impact on the Region	Social Sciences / History	2007	Article	Ekin, Ü. (2007)
7	Büyük Karaçay Baraji ve Probabilistic Seismic Hazard Analysis for Great Karaçay Dam and Hydroelectric Power Plant	Science / Engineering	2007	Conference paper	Yunatçi, A.A., Çetin, K.Ö. (2007)
8	Research and Development of Economical Seismic Isolation and Strengthening Methods of Masonry Structures Against Earthquakes	Science / Engineering	2007	Research Project	Özen, Ö., et al. (2007)
9	Traces Of Historical Earthquakes in The Ancient City Life At The Mediterranean Region	Social Sciences / History-Archaeology	2007	Article	Erel, T.L., Adatepe, F., Erel, T.L. (2007)
10	Crusader tate of Antioch	Social Sciences / History	2008	Thesis	Özonur, Ş. (2008)
11	A look at natural disasters and epidemics that occurred in Antakya in the Middle Ages	Social Sciences / History	2009	Article	Kaya, S., Kıyılı, E. (2009)
12	Evaluation of Hatay Site Selection in Antakya in terms of Geomorphological Features and Natural Risk	Social Sciences / Geography	2010	Article	Özşahin, E. (2010)

13	A Geographical Approach at Natural Environment Problems In The Asi (Orontes) River Delta (Hatay/Turkey)	Social Sciences / Geography	2010	Article	Özşahin, E. (2010)
14	Assessment of Hatay Airport in terms of Geomorphological Features and Natural Risk	Social Sciences / Geography	2010	Article	Özşahin, E. (2010)
15	Investigation of Damage and Seismic Characteristics of Reinforced Concrete Framed Structures Based on the Mixed Approach of Combining Instrumental and Numerical Data	Science / Engineering	2010	Research Project	Bikçe, M., et al. (2010)
16	Investigation and mapping of active faults in Antakya and its surroundings	Science / Eurasian Institute of Earth Sciences	2011	Thesis	Lom, N. (2011)
17	Temporal Change of the Relationship between Antakya City and Geomorphological Units (Hatay)	Social Sciences / Geography	2011	Article	Özşahin, E., Özder, A. (2011)
18	Investigation of Neotectonic Period Structures between Hatay (Antakya)-Samandağ	Science / Eurasian Institute of Earth Sciences	2011	Thesis	Tekeşin, Ö., (2011)
19	Determination of Damage Vulnerability of Residential Multi-storey Reinforced Concrete Structures by Combining Instrumental and Numerical Data and Static Thrust Analysis	Science / Engineering	2011	Article	Genes, M., et al. (2011)
20	Preparation of earthquake scenarios of Hatay province and its surroundings by using GIS analysis techniques and comparison of these scenarios with historical earthquakes	Science / Eurasian Institute of Earth Sciences	2012	Thesis	Üsküplü, S. (2012)
21	Geographic Distribution of Earthquakes Causing Death in Türkiye (500 AD-2011)	Social Sciences / Geography	2012	Conference paper	Ceyran, S., Elibüyük, M. (2012)
22	An Example for the Evaluation of Disaster Culture: Antakya City	Social Sciences / Geography	2013	Article	Özşahin, E., Kaymaz, Ç.K. (2013)
23	Analytical Evaluation of the Properties of Masonry Buildings in Antakya in Terms of Earthquake Performance	Science / Engineering	2013	Conference paper	Demirel, İ.O., et al. (2013)
24	Eastern Anatolia Fault System Earthquake Activity, Future Earthquake Potential	Science / Engineering	2013	Article	Demirtaş, R., Erkmen, C. (2019)

25	Estimation of Earthquake Hazard for Antakya and its Neighbourhood by Stochastic Methods	Science / Engineering	2013	Conference paper	Topkara, N., et al. (2019)
26	Investigation of the Behaviour of Hatay Government House under Earthquake Loads	Science / Engineering	2013	Conference paper	Kiliç, İ., Çoşkun, H., Uslu, H. (2013)
27	The Formation of Christianity In Antioch and Habib-i Neccar	Social Sciences / Social Life-History-Religion-Geography	2013	Article	Bahadir, G. (2013)
28	Modeling Of Seismic Hazard Risk Analysis in Antakya (Hatay, South Turkey) By Using GIS	Social Sciences / Geography	2013	Article	Özşahin, E., Değerliyurt, M. (2013)
29	Geomorphological Observations on Active Tectonics in the Antakya-Kahramanmaraş Graben	Social Sciences / Geography	2014	Article	Ege, İ. (2014)
30	Estimating Shear Wave Velocity Using Acceleration Data in Antakya (Turkey)	Science / Engineering	2014	Article	Büyüksaraç, A., et al. (2019)
31	Sürdürülebilir Kentsel Determination of Areas Suitable for Settlement for Sustainable Urban Development: The Case of Iskenderun City	Social Sciences / Geography	2014	Conference paper	Değerliyurt, M., Çabuk, S.N., Aksu, R. (2014)
32	Natural Disasters That Occurred in Anatolia in the 11th Century	Social Sciences / History	2015	Article	Subaşi, Ö. (2015)
33	Evaluation based on calculation and device data under the earthquake impact of masonry type buildings	Science / Engineering	2015	Thesis	Yücel, S.S. (2016)
34	Examination of historical urban fabric of Antakya in terms of urban design and a case study	Science / Landscape Architecture	2016	Thesis	Kocaoğlu, S.E. (2016)
35	Hatay Studies -II	Social Sciences / Social Life-History-Religion	2016	Book	Gunduz, A., Kaya, S. (2016)
36	Accessibility of Fire Brigades in Antakya (Hatay) in Emergency Situations	Social Sciences / Geography	2018	Article	Geçen, R., Ölmez, İ., (2018)
37	Observations of Natural Phenomena and Earth Sciences in the Chronicle of Theophanes	Social Sciences / History	2018	Article	Maden, N., Beker, Y., Nazir, B. (2018)
38	The History of Disaster as Time-Space Expansion	Social Sciences / History	2018	Article	Sert, Ö. (2018)
39	Determination Of 3-D Crustal Seismic Velocity Structure	Science / Engineering	2019	Article	Ozer, C. (2019)

	Beneath Hatay And Surroundings				
40	Investigation of Soil Properties Based on Accelerometer Stations Using Earthquake Recording: The Case Study Of Hatay, Turkey	Science / Engineering	2019	Article	Perk, S., Ozer, C. (2019)
41	A Spatial Evaluation for the Protection of Cultural Heritage: Functional Change of Old (Traditional) Antakya Houses	Social Sciences / Geography	2019	Article	Sargin, S., Dinç, Y. (2017)
42	The City of Antakya through the Eyes of Travelers (Between the 10th and 19th Centuries)	Social Sciences / History	2020	Article	İstek, E. (2020)
43	The City in the Shadow of Earthquakes (6th Century)	Social Sciences / Art History	2021	Article	Bakir, M. (2021)
44	Natural Disasters and Epidemic Diseases During the Turkish Seljuk State Period (From Its Establishment to Its Collapse)	Social Sciences / History	2022	Thesis	Akarsu, E. (2022)

For example, a paper (given as number 24 within the table above) which is titled as "Hatay Hükümet Konağının Deprem Yükleri Etkisinde Davranışının İncelenmesi" (Investigation of The Behavior of Hatay Government House Against Earthquake Loads) studied the earthquake performance of this building in the year 2013. According to the research results of this study, building was determined as very weak against earthquake and needed to be retrofitted. Indeed, the picture of Hatay Government House taken during the site visit shows the structural damages of the building following The Kahramanmaraş Earthquakes of 6 Feburary 2023 (*Figure 237*).

Figure 237: Hatay Government House, April 2023

It is possible to multiply such examples and studies drawing attention to the earthquake hazards of the region. At this point, the issue that needs to be discussed should be why scientific/academic studies cannot be taken as a reference in

implementation processes and efforts to increase urban resilience. The fact that such scientific studies are predominantly discussed on academic platforms and remain in the literature as produced publications shows that there is a significant gap between theory and practice, science and policies.

7.2.2. Construction Processes

Following the devastating 1999 Kocaeli and Düzce earthquakes in the Marmara region, efforts have been made to improve the building processes there has been an updated building code (covered in the Chapter 4 of this report focussed on structures), and a Law on Construction Inspection (Law 4708) was passed on 13 July 2001. This law aimed to develop more effective inspection activities by means of private building inspection firms and a creating a building inspection system governed by the Ministry of Environment and Urbanization (Ozden and Erkilic, 2015). Additionally, a law on "Transformations of Areas Under Disaster Risk" (Law 6306) was passed in 2012 to redevelop informally-built areas that are high risk of earthquakes, however this law has been criticised for displacing low-income families in prime development areas and at the same time failing to substantially reduce the number of buildings at risk of earthquakes (TMMOB Mimarlar Odasi, 2023). A dominant framework of capital accumulation (Yesilbag, 2016) through the construction sector has prevailed over the years since 1999, and many areas have been opened for illegal and unplanned construction.

The findings from the 2023 earthquakes report of the Union of Chambers of Turkish Engineers and Architects(TMMOB Mimarlar Odasi, 2023) succinctly outline the main reasons behind the high level of damage from the earthquakes in relation to urban planning and construction supervision processes. These three points are discussed in more detail below:

- Zoning plans and urban planning decisions are made without accounting for disaster risk data, this has led to construction on agricultural lands and soft soils that have low load bearing capacity.
- Encouraging illegal construction through zoning amnesty, projects and practices contrary to zoning rules.
- Lack of qualified architecture, engineering and planning services in the building production and inspection process, including a lack of highly qualified technical expertise and lack of supervision.

In relation to the first point above, local governments have legal and governance bases where they can use and reproduce data on disaster risk and risk mitigation including Strategic Plan Implementations, KENTGES, Smart City Implementations, planning studies prepared for 5-year periods such as the 11th Development Plan, and Urban Transformation Laws and Implementations. There are also specially prepared studies such as ISMEP, which covers a city (Istanbul). However, despite these, urban planning is not well integrated into everyday decision-making about development in most urban areas; the plans are often prepared by outside firms or universities to meet the legal requirements and are not adopted in practice by municipalities due to lack of expertise and understanding of how the planning might be relevant for their work (Guler and Karanuh, 2018). Local governments may have access to data, but there is a lack of training of local governments to use this information, and sometimes the data is not good quality (Ozden, 2023). In relation to the second point above, construction or

zoning amnesties have been implemented 13 times since 1984, including eight times since the 1999 earthquakes (Tercan, 2018). The amnesties enable building owners who had constructed a building prior to the date of the amnesty to apply for a permit post-construction or post-occupancy and pay a fee that enables them to legalise the structures, a system that is supported informally by many municipalities throughout the country (Polat, 2019). For example, with Law 7143, which came into effect on 18.05.2018 a construction registration certificate can be issued for buildings in rural and urban areas which are constructed before 31.12.2017 but had not been previously licensed nor registered. Applications must be made through an "e-government" portal and fees are 3% for houses and 5% for commercial properties of the total approximate cost of the building and property value. Once the building is declared legal, it is the owner's responsibility owner to be compliant with earthquake resistance.

This system arguably incentivises illegal construction, and many argued this has paved the way for creating built environments that are at high risk of earthquakes and ultimately what has happened in 2023. This is because it paves the way for the realistic possibility of legalising illegal and non-compliant buildings in the future, and therefore builders can get away with using lower-quality materials, hire fewer professionals to oversee projects and adhere less to regulations or guidelines, which is arguably increasing the earthquake risks.

However, at the same time, this amnesty system, in the 1980s and 1990s enabled access to low-cost housing for people who might not otherwise be able to access the housing market and enabled families to build capital through legalisation of their informal housing. Most cities in Türkiye have been built up with this system of informal building production and subsequent legalisation.

7.2.3. Inspection of Building Processes

The Law on Construction Inspection (Law 4708) is particularly important as it should govern the process that the building industry follows, and ensure checks are made at relevant times and that ultimately buildings are safe for inhabitation. The law was heavily criticised for being less effective than it could have been, as it did away with the private indemnity function of the inspectors (Gulkan, 2000). After being passed in 2001 and active as a pilot law in 19 provinces, it was expanded to all provinces in 2011. In 2018, the law was updated, to make improvements that would reduce corruption, including (Bakirci et al., 2019): 1) rather than choose their own, building owners are required to appoint construction audit companies chosen by the Ministry based an electronic grading system; 2) the service fee amount would be equal to a flat 1.5% of estimated construction costs and such fee would no longer be adjusted afterwards; 3) that audit services agreements could only be terminated on certain grounds to be determined by the Ministry (Bakirci et al., 2019).

As of the 2018 updates, the system is meant to work as follows (according to Erol and Dede, 2022):

- Inspection activities are performed by the inspectors employed by the building inspection companies. These companies are authorized by the Ministry of Environment and Urbanization. As mentioned above, the company is appointed by the Ministry through an electronic system;
- A service contract is signed between the project owner and the building inspection company;

- The inspectors examine the drawings and technical documents prepared by the designer. If approved, it will also be reviewed by the relevant local authority (municipality or special provincial administration [*il ozel idare*]). If deemed appropriate by both entities, then the project is licenced;
- Once a construction contract is signed between the contractor and project owner, the site operations are carried out under the supervision of a construction manager who is appointed by the contractor. The inspectors from the building inspection company are responsible for the examination of the construction process;
- The building inspection company must also ensure that the required experiments are performed by the test laboratories authorized by the Ministry. Concrete samples must be taken at the construction site and pressure tests must be carried out in laboratories authorized by the Ministry of Environment and Urbanization. Temperature control and slump test (the consistency of fresh concrete) must also be done on-site. The samples taken are evaluated according to 7- and 28-day concrete curing results.
- When the building inspection company approves that the construction has been completed in accordance with the standards, a building occupancy permit is issued by the local authority.
- There are sanctions stipulated in Law 4708 for the stakeholders who do not fulfil their responsibilities outlined above.

There are some differences between urban and rural practices and regulations, however as we found in rural areas there are standardised designs to choose from to simplify the design process. As an example to the latter: During our fieldwork, we enquired about the inspection process of a simple reinforced concrete house structure (see *Figure 238*), built in the rural districts of Kadirli Municipality, which is about 40km north of Osmaniye. The process was explained to us by the local government representative (*muhtar*) and the building owner as follows:

- There is a catalogue of architectural plans available at all *muhtar* offices, and a person who wishes to have a house built can choose from this catalogue (or have a bespoke design prepared themselves). Each entry within the catalogue is very prescriptive and detailed extensively in terms of geometry, material and detailing, among others. The person is then responsible to buy the materials and hire a contractor.
- As reported by the *muhtar* and the building owner in Kadirli, the system of inspection, in this case, worked as follows:
    - A first inspection was done to check the plot and the location of the building to ensure it met the regulations
    - A second inspection checked the completed foundations of the building
    - A third inspection was undertaken when the reinforcement was completed
    - A fourth inspection happened when the concrete was poured and a sample of the concrete was taken for analysing the lab.
    - The *muhtar* and building owner explained that this was the system for ‘projects’ but that simple outbuildings on a property not used for the inhabitation of people, but as storage would not go through this inspection process.

The EEFIT team remarked that the building did not appear seismically resistant due to the lack of infill walls on the ground floor and the comparatively heavy first floor. There did not seem to be a check on the final infill walls, or finishing, as the building had been signed off for inhabitation despite the lower infill walls not being completed.

Figure 238: Reinforced concrete house in Kadirli Municipality (Source: EEFIT Team)

There have been several studies that look at how well Law 4708 is implemented in practice, and where the problems remain (for some studies looking at the efficacy of the building inspection law see for example: Atabey and Bozdoğan, 2012; Bayram et al., 2018; Çelik and Ünal, 2017; Erol and Dede, 2022; Erdiş and Gerek, 2012; Hacıbaloğlu, 2003, Kuraland, Ünal, 2015; Ömürbek et al., 2016; Ozden and Erkilic, 2015; Pala and Demir, 2017). These studies conclude that the building inspection system in Türkiye is not functioning properly due to several inter-related factors, which are partially summarised below:

- Poor performance of contractors and construction managers. The research (cited above) attributes this partly due to a lack of sanctions or punitive measures for poor performance, and lack of a public grading system which rates the performance of contractors, records publicly the corruptive practices between contractors and inspectors.
- Lack of capable inspectors, which is related to low pay of the inspectors, poor quality engineering education, and inadequate specialised training for the job. Inspection is not considered as a desirable job and is not professionalised with high quality training and commiserate pay.
- The need for standardisation of inspection procedures to minimise subjectivity, and ensure accuracy and reliability. The system is lacking standardised objectives, checklists, detailed guidelines, and standard codes of practice to guide all inspection efforts (Erol and Dede, 2022).
- Lack of monitoring of inspection firms' work and ineffective inspection efforts from municipal officials due to lack or insufficient number of competent professionals to undertake the work. There is a need for regular monitoring of building inspection firms through examinations and evaluations by relevant institutions and organizations (Government of Turkey, 2023).

- We also found through informal discussions with engineers that there are short-cuts that are made on the testing, for example the on-site experiments of temperature control and slump testing is not always being performed. Also, if there are flags raised about the quality at the 7-day test point, production of concrete should be stopped, however this is not economical, so conversion factors are used to decide if the strength is strong enough without waiting until the 28th day. There are critical issues with the testing that require greater scrutiny for understanding better the practices in reality.

7.2.4. Spatial Development of the Urban Regions, Urban History, Demographics and Socio-Economics

There are 11 provinces (AFAD, 2023) that have been affected by the earthquake (*Table 27*) with a total of 14,013,196 Turkish citizens, which represents 16.43% of the total population in Türkiye (Sağıroğlu et al., 2023). In addition, there were 1,738,035 Syrian people under temporary protection status living in the earthquake region, which represents almost half (49.6%) of the Syrian people under temporary protection in Türkiye, plus 33,159 people with temporary residence permits in the earthquake region (many of whom are Syrian), which represents 2.45% of all people with temporary residents permit in Türkiye (*Table 28*). Thus overall, it is estimated that there were 15,784,390 people affected by the earthquakes, representing 17.51% of the known human presence in Türkiye (Sağıroğlu et al., 2023).

Table 27: Population of the Earthquake-affected provinces (Source: www.tuik.gov.tr)

Province	Pop. of Province 2022	Pop. of Province 2012	Pop. change in 10 years	Pop. growth rate over 10 years	Ratio to Türkiye's pop. in 2022	Household Size 2022
Adana	2,274,106	2,125,635	148,471	0.70	2.67%	3.4
Adıyaman	635,169	595,261	39,908	0.67	0.74%	3.9
Diyarbakır	1,804,880	1,592,167	212,713	1.34	2.12%	42
Elazığ	591,497	562,703	28,794	0.51	0.69%	31
Gaziantep	2,154,051	1,799,558	354,493	1.97	2.53%	3.9
Hatay	1,686,043	1,483,674	202,369	1.36	1.98%	3.5
Kahramanmaraş	1,177,436	1,063,174	114,262	1.07	1.38%	3.6
Kilis	147,919	124,320	23,599	1.90	0.17%	3.4
Malatya	812,580	762,366	50,214	0.66	0.95%	33
Osmaniye	559,405	492,135	67,270	1.37	0.66%	3.4
Sanlıurfa	2,170,110	1,762,075	408,035	2.32	2.54%	4.8

Total/Average across affected provinces	**14,013,196**	**12,363,068**	**1,650,128**	**1.33**	**16.43%**	**3.5**
Total in Türkiye	**85,279,553**	**75,627,384**	**9,652,169**	**1.28**	**100.00%**	**3.2**

Table 28: Foreign Population in the Earthquake (Source: Reproduced from AYBU-GPM report. Original is from compiled data from TUIK and from GIB - Directorate of Migration Management, all from 27 February 2023.)

Province	Turkish citizens	Foreign Nationals, 2023			Grand Total
		Temporary Protection	Residence Permit	Total	
Adana	2,274,106	250,711	6,359	257,070	2,531,176
Adıyaman	635,169	21,688	450	22,138	657,307
Diyarbakır	1,804,880	21,672	1,270	22,942	1,827,822
Elazığ	591,497	12,188	801	12,989	604,486
Gaziantep	2,154,051	460,150	11,767	471,917	2,625,968
Hatay	1,686,043	354,648	2,903	357,551	2,043,594
Kahramanmaraş	1,177,436	91,640	2,137	93,777	1,271,213
Kilis	147,919	87,409	1,388	88,797	236,716
Malatya	812,580	31,421	1,339	32,760	845,340
Osmaniye	559,405	38,285	647	38,932	598,337
Şanlıurfa	2,170,110	368,223	4,098	372,321	2,542,431
Total in affected provinces	**14,013,196**	**1,738,035**	**33,159**	**1,771,194**	**15,784,390**
Total in Country	**85,279,553**	**3,500,964**	**1,354,707**	**4,855,671**	**90,135,224**

Over the ten years prior to the earthquakes the provinces of Diyarbakır, Gaziantep, Hatay, Kilis, Osmaniye and Şanlıurfa have grown at a faster rate than the median annual population growth rate of Türkiye (*Table 27*). Especially, Şanlıurfa and Gaziantep have had much higher population growth rates than the national average. Most Syrian people have settled in Gaziantep, Şanlıurfa and Hatay (*Table 28*). Cities

across the earthquake-affected region have seen significant spatial expansion and densification over the past decades.

Economic activities in the region increased between 2011 and 2021 in conjunction with the population increase and refugee influx. The provinces represent 9.8% of GDP in 2021, up from 9.4% in 2011 (*Table 29*). The trends also show diversification of economic activity over the period, especially with increases in industry and manufacturing industry. Agriculture, Industry, Manufacturing industry and Construction as well as Public administration, education, health, social work represent the biggest industries.

Table 29: Share of the 11 earthquake-affected provinces in National Income 2011-2022 (reproduced from TERRA report [Government of Türkiye, 2023])

Year	Agriculture, forestry, and fishery	Industry	Manufacturing industry	Construction	Services	Information and communication	Financial and insurance activities	Real estate activites	Professional, administrative & support service activites	Public adminisration, education, human health, and social work activites	Other service activities	GDP
2011	16.2	9.1	8.8	9.5	7.3	4.0	4.9	8.8	5.8	13.3	8.3	9.4
2012	15.4	9.3	9.0	9.7	7.5	3.4	4.9	8.9	6.3	13.3	8.2	9.4
2013	15.7	9.7	9.4	10.5	7.6	3.1	5.0	9.1	6.4	13.3	8.1	9.5
2014	14.4	9.6	9.4	9.9	7.6	2.8	5.4	9.3	6.6	13.3	8.0	9.4
2015	15.8	9.7	9.4	9.5	7.7	2.7	5.5	9.8	6.8	13.4	7.7	9.5
2016	15.5	9.9	9.8	8.7	7.9	2.6	5.3	9.8	7.3	13.5	8.0	9.6
2017	15.6	10.3	10.3	9.3	7.5	2.3	5.5	9.7	7.0	13.6	7.8	9.5
2018	16.7	10.4	10.2	8.5	7.0	2.2	5.2	9.7	6.3	13.5	7.7	9.4
2019	15.1	10.4	9.9	8.3	7.0	2.2	4.8	9.5	6.2	13.9	7.4	9.4
2020	15.2	10.7	10.5	9.5	7.7	2.2	4.8	9.6	6.8	14.0	6.9	9.8
2021	15.1	11.4	11.5	10.0	7.4	2.2	4.6	9.7	6.3	14.1	5.6	9.8

Table 30 shows an interesting picture of the share of industry in sub-sectors in each province – they vary by province, but one can note that Agriculture is particularly important in the provinces of Şanlıurfa, Adana, and Diyarbakir; Industry and manufacturing industry are important in Gaziantep and Adana; Public Adminstration/education/health/social work in Adana and Diyarbakir. Adana shows a well-diversified economy across all sectors. Hatay is also strong across a wide range of sectors including Industry, Manufacturing Industry and Public Adminstration/Education/Health/Social work. It is also worth noting that Agriculture, Industry and Manufacturing Industry are quite developed in Kahramanmaraş. These statistics point to important elements for the recovery, because they outline the dependence of the economy on specific sectors and therefore indicate priorities for economic recovery.

Table 30: Share of earthquake-affected provinces GDP and subsectors (From TERRA report [Government of Türkiye, 2023], p19).

Sector / Province	Agriculture, forestry, and fishery	Industry	Manufacturing industry	Construction	Services	Information and communication	Financial and insurance activities	Real estate activites	Professional, administrative and support service activites	Public adminisration, education, human health, and social work activites	Other service activities	GDP
Adana	2.5	2.2	2.1	1.7	1.9	0.7	1.5	1.6	1.6	2.3	1.5	2.0
Hatay	1.3	1.8	1.9	1.0	1.4	0.1	0.5	1.3	0.8	1.6	0.6	1.4
Kahramanmaraş	1.4	1.4	1.3	0.8	0.4	0.1	0.3	0.8	0.4	1.1	0.3	0.9
Osmaniye	0.6	0.7	0.7	0.3	0.2	0.0	0.1	0.5	0.1	0.6	0.2	0.4
Malatya	0.9	0.5	0.5	0.7	0.3	0.1	0.3	0.8	0.3	1.1	0.4	0.5
Gaziantep	1.3	3.6	4.0	1.7	1.5	0.2	0.8	1.6	1.1	1.8	0.7	2.0
Adıyaman	0.8	0.3	0.2	0.3	0.2	0.0	0.2	0.5	0.2	0.7	0.2	0.3
Kilis	0.2	0.1	0.1	0.1	0.1	0.0	0.0	0.1	0.0	0.2	0.0	0.1
Şanlıurfa	3.0	0.4	0.3	0.8	0.5	0.1	0.3	0.8	0.6	1.7	0.8	0.8
Diyarbakır	2.2	0.4	0.2	1.2	0.5	0.6	0.4	1.1	0.7	2.2	0.6	0.9
Elazığ	0.8	0.2	0.2	1.3	0.3	0.1	0.2	0.5	0.4	1.0	0.4	0.5
Total	15.1	11.4	11.5	10.0	7.4	2.2	4.6	9.7	6.3	14.1	5.6	9.8

7.2.5. Languages and Ethnic Groups

The earthquake affected region is heterogeneous in terms of ethnic and religious groups and identities. However, up to date statistics on ethnic groups are not readily available in the public domain as these could be seen to run counter to the homogeneity proclaimed by the State (The Open Society Institute, 2003). The last census that tabulated language use in Türkiye was in 1965. Several studies exist that analyse language distribution at that point in time (Zeyneloglu et al., 2016). Table *31* gives a breakdown of different languages spoken across the earthquake-affected region in 1965, and shows a high concentration of Kurdish spoken in Adıyaman, Diyarbakir and Sanilurfa and high concentration of Arabic in Hatay and to a lesser extent in Şanlıurfa. Other languages, such as Zazaki, Circassian, Greek Georgian, Armenian, Laz, Pomal, Bosnian, Albanian and Jewish are also found in small pockets across the region. Hatay has the greatest range of different languages. In some contexts, the existence of different ethnic groups is published in publicly available information, such as that published by the Göksun People's Association website (Goksunlular.com, 2024), which gives information about the ethnic groups in different settlements of its region and population estimates.

During the short time of our field visit, we interacted with representatives of at least eight different ethnic groups in the region engaged in supporting recovery from the earthquake of their members, advocating for rights, and a prevalence of community-led groups focusing on women's rights. We found that these ethic and gender identities were important for activating solidarity networks to support relief and recovery, as

people from these groups, and their supporters and prominent figures, who lived outside of the earthquake zones assisted affected people with goods, accommodation, technical expertise, monetary and other donations, among other things. This created different networks of distribution, assistance and solidarity that exist outside of the formal government systems.

Table 31: Number of people speaking different languages across the affected provinces, based on 1965 Census (Source: reproduced from https://en.wikipedia.org/wiki/Languages_of_Türkiye#cite_note-18)

Province /Language	Adana (inc. Osmaniye)	Adıyaman	Diyarbakır	Elazığ	Gaziantep	Hatay	Malatya	Kahraman maraş	Şanlıurfa	Total
Turkish	866,316	143,054	178,644	244,016	490,046	350,080	374,449	386,010	207,652	3,240,267
Kurdish	7,581	117,325	236,113	47,446	18,954	5,695	77,794	46,548	175,100	732,556
Arabic	22,356	7	2,536	17	885	127,072	33	21	51,090	204,017
Zazaki	332	6,705	57,693	30,921	1	7	10	0	14,554	110223
Circassian	51	0	1	0	4	780	14	4,185	3	5,038
Greek	51	0	1	2	6	767	5	0	0	**832**
Georgian	0	0	3	0	0	11	7	0	5	**26**
Armenian	28	84	134	2	4	376	148	13	2	**791**
Laz	9	4	3	30	3	6	5	3	4	**67**
Pomak	0	0	48	12	0	2	4	0	0	**66**
Bosnian	312	0	1	3	1	8	0	0	2	**327**
Albanian	483	0	5	2	11	44	3	9	0	**557**
Jewish	29	0	0	0	0	1	0	0	0	**30**

7.3. Economic Aftermath

The financial burden of the earthquake sequence is investigated through several sources, including the Strategy and Budget Presidency of Türkiye (PSB, 2023), Worldbank, and traditional media with first-hand observations from the field mission.

According to the Global Rapid Post-Disaster Damage Estimation (GRADE) Report of World Bank, it is estimated that the earthquake sequence caused US$34.2 billion worth of direct damage to residential and non-residential buildings and infrastructure. 53% of these direct damages are attributed to financial costs due to the damages to residential buildings. The contribution of non-residential buildings and infrastructure in this direct damage estimation was 28% and 19%, respectively. Their report states that this calculation does not include indirect or secondary impacts, and so the total losses are lower than the government's TERRA report (World Bank and Global Facility for Disaster Reduction and Recovery, 2023).

Considering the extent and intensity of the February earthquakes, the interpretation of the economic impact contains high uncertainty as the secondary impacts on the economy accumulate until the area returns to its pre-earthquake normal. Each day in the recovery phase prolongs the recession in trade and production of small and medium-sized enterprises (SMEs) as well as industry, the decline in tourism revenue, and the loss of employment. This situation will inevitably have an impact on Türkiye's GDP. Furthermore, the presidential election in the country also occupied a significant portion of the agenda and budget, further prolonging the recovery process and its

economic effects. Considering all these factors, indirect effects accumulate, and the estimation of financial loss becomes increasingly challenging. The data on the electricity consumption of industrial zones in earthquake-hit regions shared by the Organized Industrial Zones Supreme Board (OSBUK) in late February is a good indicator of the possible secondary effects (Albayrak, 2023). Table 32presents the most significant drops in electricity consumption in February 2023 compared to that of February 2022, according to data provided by OSBUK.

Table 32: Drops in electricity consumption of organized industrial zones in February 2023 compared to that of February 2022

Organized industrial zone (OSB)	Drop in electricity consumption (%)
İskenderun OSB (Hatay)	88.57
Adıyaman OSB	78.96
Kahramanmaraş OSB	77.86
Malatya 1st OSB	73.48
Şanlıurfa OSB	73.03

The report of Strategy and Budget Presidency of Türkiye (TERRA, 2023; PSB, 2023]) provide an idea about the possible impact. The recovery and reconstruction assessment report of TERRA, released in early March 2023, provides detailed estimations of financial loss and includes direct and indirect economic implications of the February earthquakes. TERRA estimates US$56.9 billion worth of housing damage based on the buildings that are collapsed, severely damaged, and in need of urgent demolition. Damage to public sector accounts and private sector accounts for US$12.9 and US$11.8 billion, respectively. The financial burden due to the secondary impacts of the earthquake, e.g., load on the insurance sector, revenue losses of tradespersons, and macroeconomic effects, are estimated at US$22 billion. In total, TERRA reveals US$103.6 worth of financial burden, equivalent to 9% of Türkiye's forecast GDP in 2023. Turkish Statistical Institute's (TUIK) data as well presents that 11 provinces in the earthquake hit region significantly contributes to Türkiye's GDP. According to TUIK, total share of these provinces in country's GDP in 2021 was 9.8% (Table 32). Their contribution to the country's export was 15.3% of total in 2022. Looking at the provided data, disruptions in production and supply chain will have strong consequences on country's economy along with the direct losses.

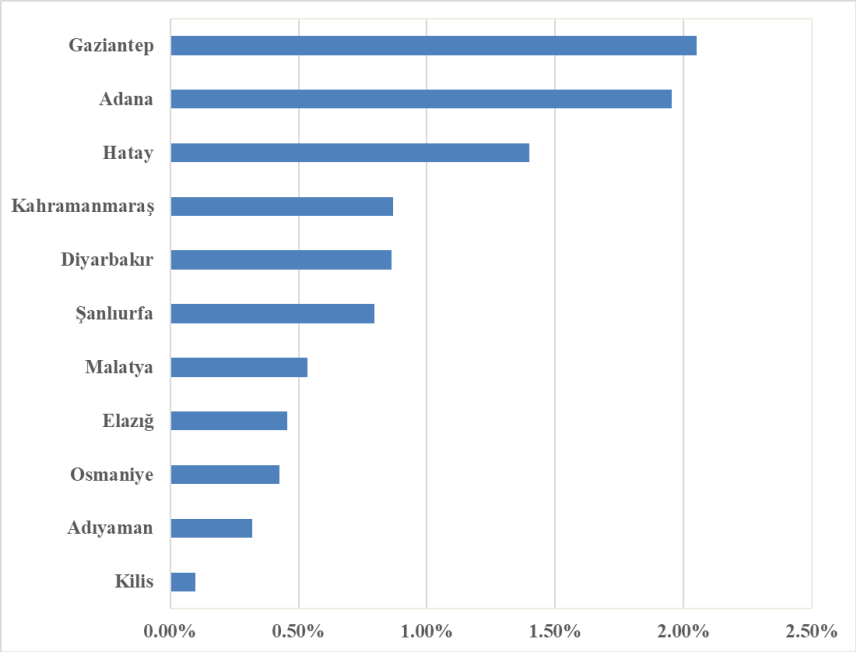

Figure 239: Disaster region's share of GDP in 2021 as percentage of Türkiye's total GDP

Based on the aforementioned reports and field observations presented in the previous chapters of this report, most of the financial loss emerges from the damage in Hatay, Kahramanmaraş, Gaziantep, Malatya and Adıyaman provinces. GDP share data of these five provinces since 2004 show that Gaziantep and Hatay increased their share in the last years, whereas the rest had a steady trend (see *Figure 240*). Next year's data will better reveal the earthquake's ramification on the region's economy.

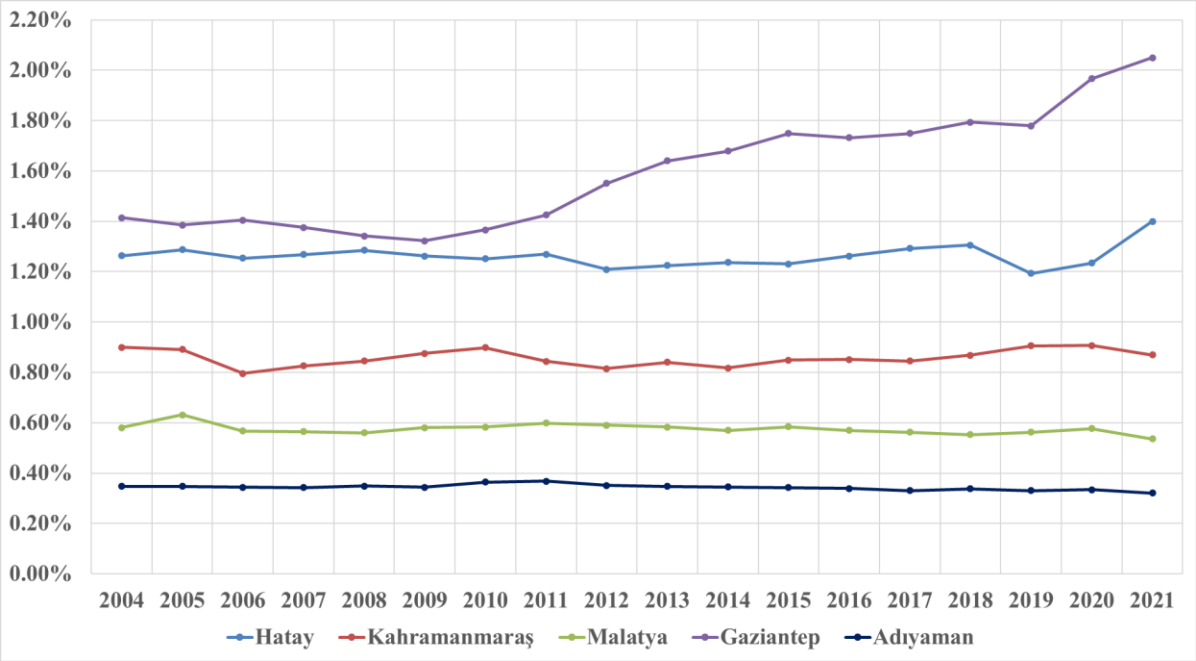

Figure 240: GDP share trend of most severely affected cities in the last eighteen years (taken from TERRA repprt)

In the aftermath of the first earthquakes, a crisis in the rental market in the region sparked as profiteers wanted to take the benefit of increased demand for undamaged apartments (Soylu, 2023). In several cases, survivors stated that rent prices rocketed and almost doubled following the earthquakes. These statements were also supported by estate agents in the region declaring that rent prices have spiked. This surge was also evident in nearby cities because of the profiteers wanting to benefit from many people relocating. Mersin, one of the nearby metropolises that the survivors relocated to, is an example of this case, as increases of up to 100% were observed. The situation was not any better for the survivors who went to the metropoles in the west of Türkiye, as the rents there were already higher than in the disaster region. The rental market issue expanded quickly and became a weighted issue that the minister of the interior acknowledged the crisis and declared that the government was working to resolve the problem (Gündoğan, 2023). These issues are also discussed in the sections on migration and rental support in Section 7.8.

7.4. Risk Transfer Mechanism

Following the 1999 Kocaeli and Duzce earthquakes, the Turkish public and lawmakers were faced with the need for more serious steps to tackle the earthquake risk and its possible outcomes. The Compulsory Earthquake Insurance (CEI) System introduced in 2000 is one of the steps taken within this period. For the acquisition, implementation, and management of CEI, the Turkish Catastrophe Insurance Pool (TCIP) has been established as a public institution with a legal identity (see the details about the scheme at DASK, 2023). In compliance with the Catastrophe Insurance Law No. 6305, TCIP is managed by technical operators for 5-year periods. The current technical operator of TCIP is TürkReasürans, established in 2019 by the Ministry of Treasury and Finance's capital only.

Table 33 shows the number of buildings and insured buildings in Türkiye and the earthquake-hit cities covered by state of emergency enforcement. The total number of buildings in those cities accounts for almost 11% of ,Türkiye's building stock, and they have a 53.0% of average insurance rate (DASK, 2023), which is lower than the country's average insurance rate, 59.1%. Among other cities, Hatay, which suffered the most damage, draws attention as it has the second lowest insurance rate amongst 11 provinces.

Table 33: Insurance rate in the earthquake-hit cities

City	Total Building	Current Policy	Insurance Rate
Adana	479,000	257,190	53.7%
Gaziantep	339,000	237,380	70.0%
Hatay	315,000	126,699	40.2%
Diyarbakır	231,000	88,287	38.2%
Kahramanmaraş	210,000	116,047	55.3%
Şanlıurfa	198,000	106,534	53.8%

Malatya	188,000	107,550	57.2%
Osmaniye	101,000	51,693	51.2%
Elazığ	135,000	92,060	68.2%
Adıyaman	89,000	39,169	44.0%
Kilis	25,000	16,713	66.9%
,Türkiye	20,032,000	11,837,071	59.1%

The recovery and reconstruction assessment report of TERRA estimated TRY 36.4 billion (~USD 1.2 billion) of insurance compensation based on the total claims and damage in the region. As of May 22, total insurance compensation has reached up to TRY 24.6 billion (~USD 1.2 billion) for 314,894 cases (*Table 34*). Based on these values, an average of TRY 78,240 was paid back for each application. It is also essential to state that shared data also contains a significant number of incomplete applications, and thereof the table may be subject to change.

Table 34: Insurance compensations by damage state

Damage State	Number of Paid Cases	Paid Amount (Billion, TRY)
Heavy/Collapse	87,745	16.19
Moderate	27,691	2.07
Light	199,458	6.38
Total	314,894	24.64

To receive the compensation, policyholders should make an official application to DASK. Following that application, given that there is no missing documentation, a loss adjuster conducts a damage assessment to determine the total amount of compensation. The maximum amount of compensation is limited to TRY 640,000 by DASK as of November 25, 2022. Any financial loss above this capping value can be covered only if the policyholder has an additional insurance from a private company. Furthermore, the law, which came into force on November 25, 2022, also set a fixed amount of TRY 3,016 and TRY 2,080 per meter square as the unit cost for calculating the capping value for reinforced concrete and any other buildings, respectively. However, CEI does not cover the following subsets of buildings:

- Buildings used as public service buildings,
- Buildings built in and around the village settlements and in the hamlets by the permanent residents of the village, registered with the village population,
- Buildings solely used for commercial or industrial purposes,
- Buildings without a project and any prior engineering service,
- Buildings modified or weakened the structural system in a way that adversely affects the load bearing capacity,

- Buildings constructed in violation of the relevant legislation and the project in a way that adversely affects the structural system[♣],
- Buildings to be demolished by authorized public institutions for not being suitable for residential use, neglected, dilapidated or abandoned

In combination with the insurance rate in the region, the above exemption list undermines a comprehensive risk transfer considering the density of rural settlements in the region. Furthermore, this situation increases the uncertainty in the calculation of the total financial impact.

7.5. Casualties and Missing People

The latest official statement regarding the loss of life after the disaster was made by the interior minister in mid-April (bbc.com, 14.04.2023). Accordingly, the figure was determined to be 50.500 people. On the other hand, it is also known that new corpses were still found during the debris removal works after this time (e.g. on the 122nd day of the earthquake, a woman's body was found in the rubble in Adıyaman Province (06.06.2023) [Gazete Duvar, 2023]on the 135th day of the earthquake, a woman's body was recovered from the rubble in Hatay province (21.06.2023) [Yeniçağ Gazetesi, 2023], and on the 215th day of the earthquake, a body was found in the rubble in Hatay province (09.09.2023) [NTV, 2023]).

Unofficial numbers related to casualties given by different sources including national and local newspapers stated 50.783 people in ,Türkiye and 8.476 people in Syria (06.05.2023, Habertürk, 2023).

There are a number of reasons why local, national and international sources give different figures for the number of casualties and the number of people killed. During the first four months after the earthquake, when the EEFIT group conducted research, it was observed that these figures were frequently revised. The reasons for this may include the fact that the bodies of those who lost their lives, especially in rural areas, are usually buried by the locals without informing the relevant institution, that there are bodies that have not yet been found, and that data on the number of dead or missing people cannot be obtained accurately due to the high number of migrants in the region, which has a serious impact on the demographic structure (CNN TÜRK, 2023). According to a report prepared by the *Halkin Hukuk Burosu* (People's Law Office), a non-governmental organization, as a result of the work carried out in the earthquake zone between August 17-21, 7 months after the disaster, there are still missing bodies that have not yet been found (Gerçek Gündem, 2023).

It is necessary to carry out important studies on missing people and unidentified bodies in the earthquake area. It is also seen that there are both legal and ethical problems in this regard. Vedat Mercan, the Head of Public Security Department of the General Directorate of Security, informed the Turkish Grand National Assembly (TBMM) Earthquake Commission on March 25 that there were reports of 305 missing people, 81 of whom were children, and that the search for these people continued. Mercan also stated that 3,755 bodies were identified only by fingerprints and said, "We still have 1,297 citizens whose DNA samples we have taken, whose we have been able

[♣] If these are legalised through amnesties, then they can be insured. See: Cumhuriyet, 2020.

to locate the graves, but we have not yet been able to carry out identification procedures, and the studies are continuing." (Independent Türkçe, 2023)

For those whose bodies have been located but no action has yet been taken and whose bodies are reported to be still missing, a number of legal actions are required. In this regard, it is thought that there are especially troublesome processes waiting for the relatives of the missing. While the persons whose bodies were found in the buildings destroyed in the earthquake were recorded as deceased, the persons who could not be reached in the debris should be considered as deceased with the presumption of death or they should be filed to the court as missing person's claim. Yaşar University Faculty of Law Dr. Lecturer Elif Aydın Özdemir said, "For those who are known to have been buried under the rubble and whose bodies could not be reached, should file a missing person's claim on February 6, 2024 at the earliest, 1 year after the earthquake, and they are deemed absent and considered dead by a court decision." (Hürriyet, 2023)

According to the statement made by the Minister of the Interior on the 22nd of April (2023) regarding the missing citizens, it is reported that there is a total of 297 applications for missing persons. It is evaluated that 30 of them are in the age range of 0-6, 20 of them are in the age range of 7-12, and 36 of them are in the age range of 13-17. It was reported that 86 of the missing were children and the others were adults (Odatv, 2023). It is especially important to remember that children in earthquake zones are the most vulnerable population group. In this sense, there is a need for sensitive work on the protection of orphaned children or children who have lost their families in the region, both against post-traumatic stress disorder and for their shelter and protection in safe places. In this sense, the news about a 5-year-old child who was found in the Netherlands months after the earthquake, who is thought to be an earthquake survivor, who does not speak a word of Dutch and cannot understand how he got there, is an extremely important warning in this sense (BBC News Türkçe, 2023; Hatcakap on X, 2023).

It was also known that the number of Syrian refugees living in the provinces affected by the earthquakes is over 1.7 million people, as indicated in *Table 28*above. According to figures released in February 6100 Syrian migrants were claimed to have lost their lives in the earthquake (Yeni Akit, 2023). In a press release by the Minister of Interior on March 4, 2023, the number of Syrians who lost their lives in the earthquakes was stated as 4,267 (Odatv, 2023). Other unofficial sources claimed this number to be 6700 (Açık Radyo 95.0, 2023). The breakdown of this total for total for each affected by the earthquake not been disclosed. The number of injured is given as 107.204 according to official statements (TRT Haber, 2023). It is also considered that there are many Syrian refugees returning to their country after the earthquakes. Some non-governmental organizations and think tanks report that they envisage that after the earthquake, social pressures on Syrian refugees will tend to increase (Insamer, 2023; Voa Türkçe, 2023; Euronews, 2023; BBC News Türkçe, 2023).

7.6. Emergency Response: Search & Rescue

As per the updated Türkiye Disaster Response Plan (TAMP 2022), released immediately after the first earthquake in Pazarcık, a Level 4 emergency was declared and call of international assistance was issued through Emergency Response Coordination Centre (ERCC) (TERRA Report [Government of Türkiye, 2023]). Search

and rescue (SAR) personnel were deployed in the affected areas from the government, international SAR teams, NGOs and volunteers from the locality. The immediate SAR activities were challenging due to various reasons including: loss of access to affected regions as the transportation infrastructure was damaged, scarcity of rescue equipment, electricity blackouts etc. As per the TAMP plan, all provinces in Türkiye were assigned a set of first group and second group supporting provinces. However, several of the supporting provinces also were affected in the event, leading to a difficult situation. According to the press releases of Disaster and Emergency Management Agency (AFAD), about 9700 local SAR personnel and 9900 local support personnel and volunteers were working in the affected region on the day of the earthquake. Additionally, at least 105 countries and 16 international organizations pledged support to the victims and more than 40 of them sent SAR and medical teams, while even more sent emergency financial and material aid. The SAR deployment increased to more than 60000 national and 3251 international SAR personnel by day 2, and more steadily in the following days (*Table 35*). As per the Government of Türkiye (2023) TERRA report in March 2023, a total of 271,060 SAR personnel from all national and international organisations were deployed, along with 18,048 heavy machines, 75 aircrafts and 108 helicopters. The countries who sent SAR teams in the early days include the UK, USA, Germany, Hungary, Switzerland, Spain, Slovenia, Slovakia, Albania, Armenia, Azerbaijan, Croatia, El Salvador, Estonia, Iceland, India, China, Indonesia, Israel, Japan, Kenya, Malaysia, Mongolia, Netherlands, Pakistan, Poland, Qatar, UAE, Romania, Singapore, South Korea, Sudan, Thailand, Turkmenistan, Ukraine, Uzbekistan, Australia, Russia and Vietnam among others. At least 11 of the teams came with SAR dogs (Wikipedia, 2023).

It is noted that the coordination of general public and other SAR teams with the formal agency, AFAD was often difficult. The international or volunteering SAR, medical care and other support groups were reportedly kept waiting for prolonged amounts of time without being tasked with anything, and were not allowed to take their own initiative to help– such reports are specially prominent for Antakya, Hatay (https://twitter.com/thewizardofcero/status/1622777524743729153, T24 (26 Feb 2023)). Also for other locations, the international SAR groups are understood to have been kept under scrutiny and diligence of AFAD, which reportedly slowed down the operations.

Table 35: Emergency response deployment as per AFAD press releases from 06 Feb to 02 March 2023

Date	No of press releases	# of staff members working in the region	# Vehicles (Land)	# of vehicles (Air & Water)
06.02.2023	8	9698 SAR personnel 9876 Support personnel and AFAD volunteers	216 vehicles 1511 machines	18 planes (SAR) 4 helicopters 3 Drones
07.02.2023	4	Total 60,217 SAR personnel 3251 Foreign SAR personnel	Total 4,746 vehicles	88 air vehicles 10 ships
08.02.2023	4	Total 98,153 SAR personnel 5309 Foreign SAR personnel	Total 5,514 vehicles	122 air vehicles 10 ships

09.02.2023	4	Total 120,344 SAR personnel 6479 Foreign SAR personnel	Total 12,241 vehicles	160 air vehicles 22 ships
10.02.2023	3	Total 159,146 SAR personnel 7716 Foreign SAR personnel	Total 12,046 vehicles	166 air vehicles 26 ships
11.02.2023	4	Total 218,417 SAR personnel 8294 Foreign SAR personnel	Total 12,473 vehicles	184 air vehicles 26 ships
13.02.2023	1	Total 238,459 SAR personnel 9793 Foreign SAR personnel	Total 12,322 vehicles	246 air vehicles 26 ships
14.02.2023	1	Total 249,089 SAR personnel 9456 Foreign SAR personnel	Total 12,235 vehicles	246 air vehicles 26 ships
16.02.2023	2	Total 264,389 SAR personnel 11,488 Foreign SAR personnel	Total 12,600 vehicles	198 air vehicles 26 ships
19.02.2023	1	Total 245,198 SAR personnel	Total 12,681 vehicles	153 air vehicles 38 ships
21.02.2023	1	Total 242,392 SAR personnel	Total 13,700 vehicles	194 air vehicles 38 ships
24.02.2023	1	Total 239,977 SAR personnel	Total 13,224 vehicles	194 air vehicles 38 ships
01.03.2023	1	Total 234,636 SAR personnel	Total 18,040 vehicles	192 air vehicles 38 ships
02.03.2023	1	Total 228,591 SAR personnel	Total 18,048 vehicles	183 air vehicles

Fire stations responded in the first 24hrs. For instance, in İskenderun alone the fire stations saved 300 people and attended several local and large fires in the port. But they were inadequate for the scale of the event, as they lacked instruments and suffered damage themselves (ref). Similar circumstances prevailed for the Antakya fire station, where the earthquake damage made equipment vital for SAR inaccessible, leading to individual firefighters working on the ground on their personal discretion and on their own means.

There were concerns of an uneven distribution of emergency response, due to various reasons, including the immense geographic scale of destruction. In general, the

northern regions such as Kahramanmaraş and Gaziantep, received quicker support in the early days, while Southern regions, especially Antakya in Hatay received help with search and rescue much later, formal help arriving on the 3rd day. Our communication with the people of the affected areas shows that this uneven efficacy in SAR is interpreted in different lights: by some it is seen as ”normal” by some who report a deep understanding of the constraints of the institutions faced in these events including the vast geographic area needing help and the failure of transport infrastructure, and by some others interpreted as state's lack of capacity and emergency preparedness or yet a new manifestation of the discriminatory attitude of the state or the government towards non-Muslim or other minority groups and/or localities under local governance ran by the opposition. People of the locations where formal SAR operations were inadequate or non-existent took their own search and rescue initiatives, struggling especially in the face of the absence of needed equipment, medical care, light and other amenities as well as food and drinking water. There are reports that many had to find on their own (sometimes paying from their own pockets for it)equipment and/or other heavy machinery to clear the roads and/or lift debris around buildings to reach their loved ones. In some locations (predominantly Hatay, Antakya) some of these were stopped by AFAD as they were operations outside AFAD's coordination (Diken, 2023; BBC News Türkçe, 2023). AFAD was also criticised by some on the claims that they used heavy machinery without care and control, leading allegedly to death of those who were trapped under the debris, or breaking up of bodies (Platform24, 2023). The government block on Twitter platform in the days following the earthquake (8-9 February 2023) further hindered public coordination for SAR and rightfully received much criticism (Reuters, 2023).

7.7. Medical Response

Most of the hospitals in the region were not immediately operational, except for the ones with seismic isolators, such as the Dörtyol state hospital. Others were partially non-functional or operated from tents erected outside the hospital. A detailed account of the damage suffered by the hospital infrastructure is available in Section 6.1, under Infrastructure, along with some specific case studies. More than 26,000 medical professionals were deployed by the government in the region in the first month after the event, while the staff settled in the area were given an option to leave. Additionally several international medical teams were able to operate in the region, sent by countries including the UK, Italy, Bangladesh, Bosnia and Herzegovina, Bulgaria, Estonia, Hungary, India, Indonesia, Kyrgyzstan, Malaysia, Nepal, Philippines, Poland, Romania, etc. (Wikipedia, 2023). However, in the first couple of days after the earthquake, the medical service was overwhelmed and disrupted due to lack of equipment, resources and failure of associated infrastructure such as electricity and internet networks. By the third, most systems were able to function, following the supply of materials and recovery of related infrastructure (Government of Türkiye, 2023).

Over 80 field hospitals were set up across the region by national and international agencies, such as the Italian field hospital in Antakya (*Figure 241*), which was later gifted to the Turkish healthcare system. These were fully functional with mobile power stations and facilities to perform emergency operations. People were either getting treated in the field hospitals or getting referred to the functioning major hospitals farther away. However, communication regarding the functioning of the newly set up field

hospitals was noted to be challenging. Similarly, concerns about accessing routine healthcare for vulnerable populations (elderly, very young and pregnant) as well as for those who suffer from chronic illness needs were raised by the public in the region.

Figure 241: Italian field hospital in Antakya, Hatay

7.8. Displacement and Migration

7.8.1. Displacement

The numbers people made homeless, or displaced by the earthquake can be understood using two different methods. On the one hand, the numbers of damaged flats, and on the other hand, the numbers of people that are estimated to have either migrated or sought support for relief.

From the perspective of damaged apartments, the total published by the Ministry of Environment, Urbanization and Climate Change on 6 March 2023, there were 817,548 apartments either moderately damaged, heavily damaged, collapsed or to be demolished (See *Table 36* below).

Table 36: *Building damage assessment as of March 2023 and number of apartments to understand how many people were displaced by the earthquakes (Data from the Ministry of Environment, Urbanization and Climate Change, quoted in Government of Turkiye, 2023).*

Status	Number of buildings	Number of Apartments
Undamaged	860.006	2.387.163
Less/Slightly damaged	431.421	1.615.817
Moderately damaged	40.228	166.132
Heavily damaged	179.786	494.588
Collapsed	35.355	96.100

To be demolished	17.491	60.728
Not detected	147.895	296.508
Total	**1.712.182**	**5.117.036**

According to the Government's TERRA report, 2,273,551 people were directly faced with accommodation problems after the earthquake based on the numbers of moderately damaged, heavily damaged or collapsed. However, many of the families whose apartments are lightly damaged are also displaced because they do not wish to reside in the structure due to fear of earthquakes, even though they may be legally able to. This includes potentially an additional 1,775,235 apartments, if we do not include families whose houses are undamaged. Thus, there is somewhere between 900,000 and 2.6 million households that have been displaced by the earthquakes. The average household size across the earthquake region is 3.5 people (according to TERRA report), so the total number of people displaced by the earthquakes ranges from 3,150,000 to 9,100,000. The huge discrepancy between these numbers is due to whether families choose to reside in lightly damaged apartments or not. During the field mission, we met many families who were living in tents despite their houses having been assessed as lightly damaged or undamaged. Many people do not trust building damage assessment and were seeking a re-assessment to ensure that the house was safe. Families whose apartments are moderately damaged/heavily damaged or to be demolished are not legally able to stay in the building, however our communications in the area showed that some did, at least for some time and for part of the day, because of lack of other options, sanitation and safety concerns and for the need for privacy – adding further uncertainties to the above estimations

Looking at the data from the other angle, those who have sought support for relief – according to AFAD data from 3 March 2023, the total number of displaced people within the affected provinces is 2.5 million (*Table 37*). This includes people who are living in tent camps, containers or other state-provided accommodation within the earthquake-affected provinces. The International Organisation for Migration suggests that there is an additional 1.5 million or more people who are living in tents or containers that have been put up informally, either in small encampments, near roadways, next to their damaged houses or on private property (ReliefWeb, 2023).

It is estimated that there were also 1.55 million people who migrated outside the affected provinces to other provinces in Türkiye, which is discussed in more detail below. These numbers are decreasing since February/March due to migration back into the earthquake areas by primarily people who lived in rural areas to tend to their gardens and land.

Table 37: Number of people displaced by earthquakes, data based on those who have sought relief support (Source: IFRC, 2023)

Earthquake-displaced people	Estimated number of people
Displaced and staying in government accommodation in the affected provinces	2,500,000

Displaced and staying in informal accommodation in the affected provinces	1,500,000
Displaced and migrated outside affected provinces	1,550,000
Total	**5,550,000**

7.8.2. Migration

Across Hatay province and especially Antakya, our field observations show that city centres have become uninhabited following the earthquakes. Small business owners in a few of the neighbourhoods confirmed that most residents had left the city. It was observed that even the slightly damaged buildings were not occupied in Antakya or İskenderun. It is estimated from mobile phone data that 380,000 people left Antakya and migrated to Mersin, Eskisehir, Ankara, Antalya (Interview with Mayor of Hatay). Municipalities that have received substantial numbers of people such as Mersin and Ankara have faced considerable pressures due to high demands for rental housing and urban services and hence increasing rental values and unusually heavy traffic patterns, among others, so the impacts of the earthquake on urban areas is widespread and beyond the affected region. Safer-considered cities such as Ankara are known to have received migration from other earthquake prone cities, primarily Istanbul, due to fear caused by the Maras Events, therefore the migration is prompted by wider and more complex factors than solely and directly the devastation in the affected areas by the Feb 2023 earthquakes.

Anadolu Agency, citing official data from the governorates and published on 24 February 2023 shows migration stretched across Türkiye totalling 1,116,040 (*Figure 242*: and *Figure 243*). In the days following the earthquakes people could access free flights and transport out of the affected areas. It is observed that most migration has been to cities close by to the earthquake regions (Sağıroğlu et al., 2022). The numbers of those said to have left the earthquake region vary largely dependent on the source (Sağıroğlu et al., 2022). AFAD reported on 30 March 2023 that 1.55 million people migrated outside the affected provinces to other provinces in Türkiye. The TERRA report, which came out earlier suggested that 1.9 million has left, and the president reported on 1 March 2023 that 3.3 million people left the earthquake zone and 800 thousand people went to their villages (sondakika.com, 2023). In addition, more than 166,000 university students have transferred to other provinces to access education (Government of Türkiye, 2023).

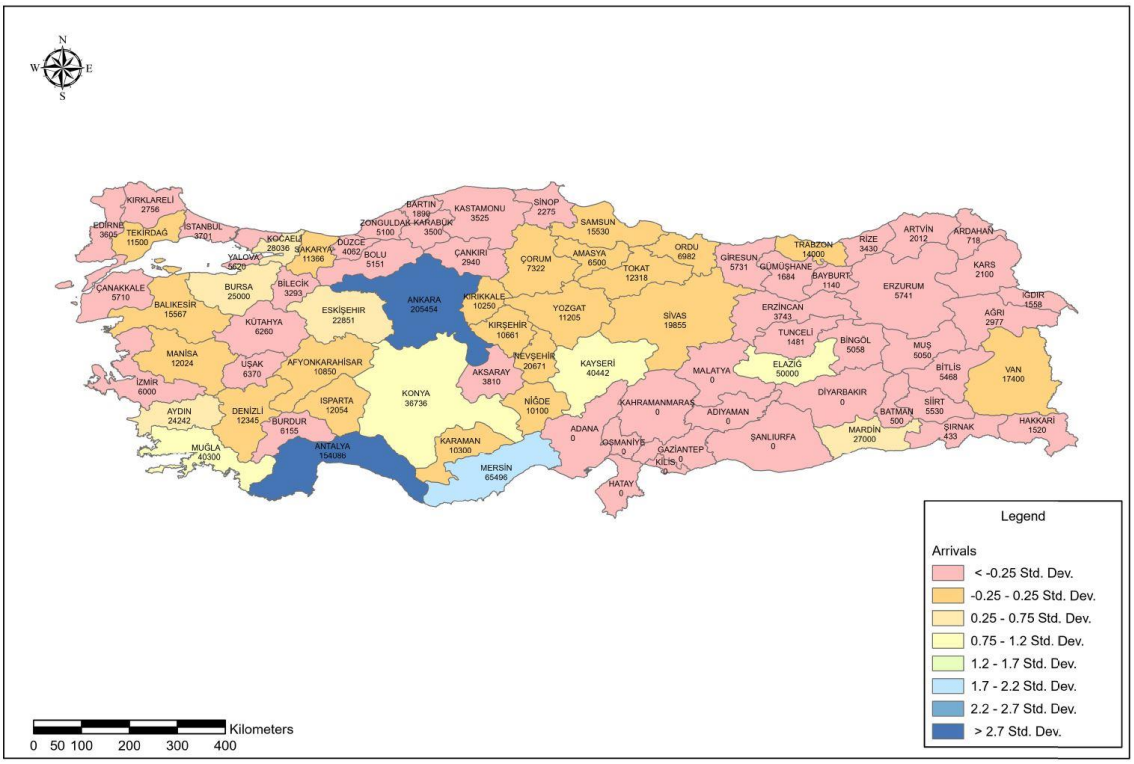

Figure 242: Map of estimated population movement as of 1 March 2023. Standard deviation (Std. Dev.) clearly shows which provinces are had the most in-migrantion following the earthquake (Map EEFIT team, based on data from Sağıroğlu et al., 2023)

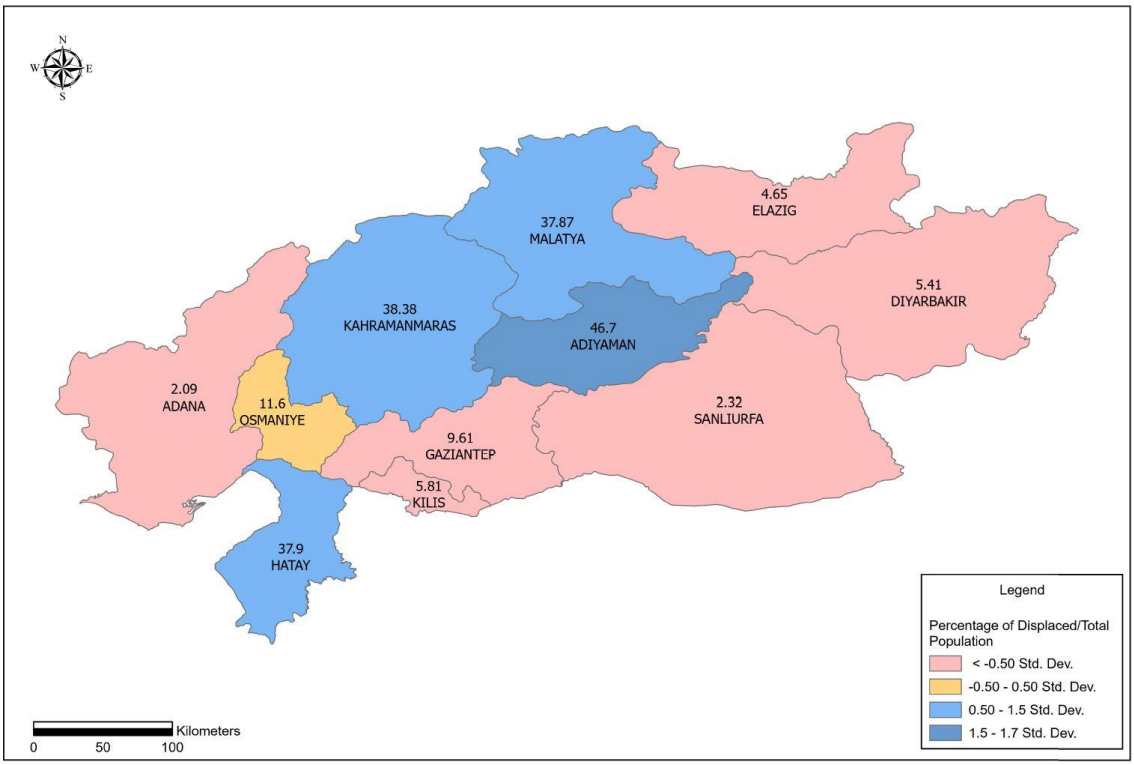

Figure 243: Map of estimated percentage of displaced/total population as of 1 March 2023. Standard deviation (Std. Dev.) clearly shows which provinces had the out-migration (Map EEFIT team, based on data from Sağıroğlu et al., 2023)

Earthquake-affected people who have migrated elsewhere are being supported by local governments in the relocation cities, including accommodation in hostels/hotels and containers, and given access to networks of relief supplies and support services. Some people access private rental housing, however the rents have increased considerably in recent years so for many this is unaffordable (Buğra Gökce on X, 2023)(see section below about rent subsidies). The government has issued statements against 'rent gauging' since the earthquake and warned homeowners to be fair in what they charge. People can also offer their homes for earthquake affected families to stay in for free or low rents, under the "May my home be yours" (*Evim Yuvan Olsun)* programme (https://www.evimyuvanolsun.org/).

The field team also observed that people have migrated within the earthquake area in search of housing or accommodation, including from the cities to villages or smaller towns, or from heavily affected cities to less-affected cities. For example, in the small town of Ilıca in north of Kahramanmaraş province, we met families who have come from Kahramanmaraş city centre to stay in tents there. People are migrating so they can access government temporary accommodation, and to move in the family homes in villages to avoid needing to pay expensive rents. As mentioned above, the President Erdogan reported on 1 March 2023 that 800,000 people had left to their villages.

The agricultural season is also a driver of migration and there is pressure on villages and small towns to enable people to come to the areas for the upcoming season. Rural settlements could return to normal faster for this reason. For example, in Çardak, a Chechenian village in the north of Kahramanmaraş, the community organisation (Kafkas Çeçen Kültür Derneği) was putting in place containers to house members, a community kitchen and bread oven. The population normally expands from 5000 to 10,000 people in the summer for the agricultural season, which is an important livelihood for the community. During our field visit, they explained that 200 people who were normally housed in the village were staying in hotels in Antalya owned by a businessman of Chechenian origins until the containers were ready.

It is estimated that 1.75 million Syrian refugees were living in the provinces affected by the earthquakes. Syrian refugees are required to register their residence in particular provinces. After the earthquakes, the Directorate of Migration Management announced that restrictions on temporary protection status holders to leave the province were lifted and the condition of obtaining a road permit document was relaxed to enable people to migrate to other provinces, this was originally for 90 days, and then reduced to 60 days. It was reported that Mersin was the most popular destination for Syrian migrants, with more than 50-60,000 people (Artı Gerçek, 2023). In an interview with staff of Mersin Municipality, it was explained that Syrian people were encouraged to move onto other provinces outside of Mersin because the volume of people was too great for the city to cope with at one time. It is also estimated that approximately 40-60,000 people have returned to Syria temporarily to deal with earthquake related matters, as the rules for crossing the border back into Syria were also relaxed after the earthquakes.

7.8.3. Rental Support

Households have access to government support to help pay for rent. In addition to an emergency of 10.000 TL per household, there was a payment of 15.000 TL for relocation support per household, and 3.000 TL/month for rent assistance to tenants

for a one-year period and 5.000 TL/month for rent assistance to homeowners for a one-year period. Anyone occupying a container, however, will not be eligible for rent support. Furthermore, financial support is only available for those whose house is moderately damaged, heavily damaged, collapsed for to be demolished; people whose homes are assessed as lightly damaged or not damaged are not eligible to apply for financial support.

In most of the country, it is not easy to find a rental house less than 5000-6000 TL and rents have increased nationally by 16% since February and more in destination cities like Mersin, Antalya and Ankara. In the earthquake region, it was estimated that rents have increased by 47% in Gaziantep Province and 25% in Hatay Province between February and April. Therefore, the rent support likely does not meet the needs of affected people, and consequently most will prefer to live in containers, or stay in their relatives' houses until permanent housing is available.

7.8.4. Return from the migration areas

It is estimated that, as of the end of April 2023 more than 20% of migrants have returned to their home provinces since the earthquake as more container housing was becoming available in the earthquake-affected region, and due to the high costs of rent in other cities. The United Nations High Commissioner for Refugees (UNHCR) has observed an increase in returns of Syrian refugees to the affected provinces as well, for similar reasons. However, lack of housing, education, trade, work and job opportunities will prevent many from returning until the situation is improved, or those who returned from going back to normal.

The government announced on 28 April that people could also apply for reimbursement of travel expenses to return to their provinces from which they migrated. This was deemed to be an important issue ahead of the May national elections, as voters could only cast their vote in the location where they were registered and people found it difficult to travel to their hometown. It is noted that Hatay airport remained closed up to 17 May to incoming passengers due to repairs on the runway.

It is expected that some migration will become permanent. In Mersin, the local government expected that up to 30% of migrants will stay permanently in Mersin, so the earthquake has the possibility of altering the country’s demographics and hence socioeconomics, having lasting impacts on many urban regions.

7.9. Temporary Shelters

As seen in Section 7.8, the number of households displaced by the earthquake could be anywhere between 900,000 and 2.6 million, depending on whether people are willing to stay in their lightly damaged houses and apartments or not. Housing these people is an immense challenge for the authorities. Tents were provided by AFAD nearly 50 hours after the first earthquake (TERRA report, March 2023), as well as other national and international organizations as mentioned below. Three types of temporary accommodation development have been observed in the area: (1) regular and formal temporary unit areas; (2) irregular and informal temporary units and areas. These are briefly explained below.

7.9.1. Regular and Formal Temporary Unit Areas:

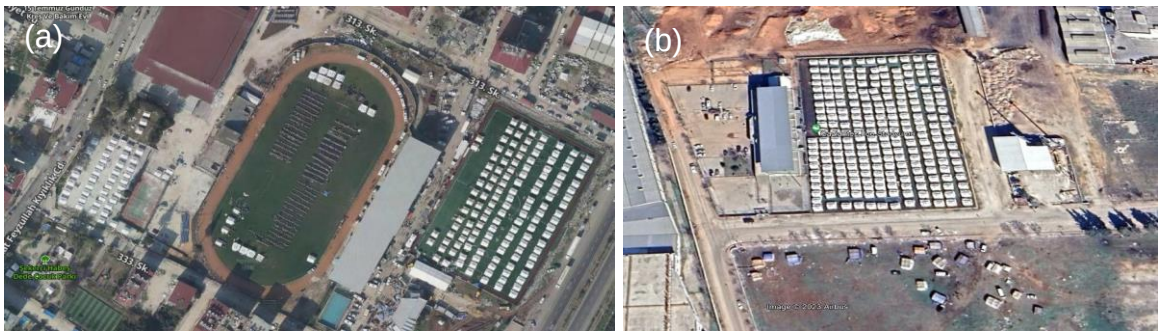

Figure 244: Regular and formal temporary housing units in (a) Kırıkhan / Hatay and (b) Gaziantep İlçe Stadyumu (football stadium) (source: Atlas Map, 2023)

These are temporary cities developed and organised by AFAD and other organisations such as Red Crescent, Municipal, National & International Institutions and NGOs. Many of these camps were receiving supplies from the AFAD network as well as other alternative networks of aid (see *Figure 244*). We visited a tent camp in Elbistan, which was managed by the local *Cemevi* (place of worship for Türkiye's Alevi-Bektashiyyah populations) (*Figure 245*a), a camp run by the local government in Ilıca (*Figure 245*b), a tent camp managed by Istanbul municipality in Samandağ (*Figure 245*c). Camps have been located on available open land, such as public open spaces within city centres, stadiums, military grounds, and vacant land. Some are set up near to field hospitals and distribution centers for easier logistics. People are generally choosing to stay in camps that are near to where their damaged house is located, although some people have moved locations in order to access the camps. Many camps are also housing the thousands of volunteers that have come to the affected region to support the relief effort.

Figure 245: Regular and formal temporary housing units visited during the field mission (a) Cemevi tent camp in Elbistan; (b) Tent camp run by local government in Ilıca; (c) Tent camp run by Istanbul Municipality in Samandağ and (d) Small encampment in İskenderun

There are other camps that are not run by government entities but rather they are more informal, some of them have received tents from AFAD and other donors, but the camp is not managed by an organisation, rather is it serviced through informal donations and services. Many Syrian people are living in camps like these. For

example, we visited a small camp set up on hospital ground in İskenderun (*Figure 245*d).

7.9.2. Irregular and Informal Temporary Units in Isolation or Groups:

These are temporary accommodation developed by locals and victims which are mostly close to areas where they were living before the disaster. The single units were set up by people to stay close to their houses, sometimes even attached to the house or located in its garden.

Figure 246: Irregular and informal temporary housing (source: Atlas Map, 2023)

Many tents were put up next to the damaged house or nearby to the property along the roadways (*Figure 247*a), and people were still able to access the damaged building for some of their needs, such use of toilets and shower, as well as access to kitchen/refrigerator. But they preferred to spend most of their time outside and sleep in the tents. This was also preferred for the fear of theft and the wish to stay close to their belongings. Some of the better examples include people being able to make comfortable makeshift camps in their gardens equipped with water supply for bathroom and kitchen needs, and shaded areas (*Figure 247*b). In other situations, tents have been erected along the roadways due to lack of space in the immediate vicinity of their homes leading to unsafe and noisy camps lacking privacy (*Figure 247*c). As rubble is cleared, more space is opened up for tents and encampments (*Figure 247*d). Others have created camps on public land, such as open spaces near to the municipal buildings. AFAD's policy is to have people moved into formalised camps to ease distribution of relief supplies, however many people do not wish to do this, and this can mean that they are left out of the formal distribution system, which points out a top-down and centrally manage approach. When we visited in mid-March, some people still did not have a tent, which has substantially changed till June.

Figure 247: Informal temporary housing units (a) Tent from AFAD near roadway, Göksun; (b) Private camp in garden, Samandağ, set up with water, toilets and cooking area; (c) Tents set up along the roadways, Ericek, north of Kahramanmaraş and (d) Tents set up in land where rubble has been cleared, Ericek

In a month following the earthquakes, 32 tent-cities were set up with over 360,000 tents accommodating close to 1,440,668 people. By end of February, 189 container cities have been located in 10 provinces, 2284 mobile baths and 5058 mobile toilets are also set up around such camps. *Table 38* and *Figure 248* shows the increase in number of temporary shelters in the disaster region according to the reference listed under *Table 38*. Number of container cities, containers and the people in accommodated in them in some of the provinces are listed in *Table 39*.

Table 38: Growth of tent and container cities in the disaster region until May 2023

Date	# of tent cities (tents)	# of container cities	# of people in tent cities	# of people in container cities	References
06/02/2023	- (21,996 tents)	-	-	-	(AFAD Press Release, 2023)
07/02/2023	- (54,511 tents)	-	-	-	(AFAD Press)
14/02/2023	- (227,762 tents)	- (48,271 containers)	-	-	(AFAD Press)
02/03/2023	332 (360,167 tents)	189 (90,914 containers)	-	-	(AFAD Press)
05/04/2023	345 (656,553 tents)	305 (49,202 containers)	2.626.212	78.718	(Yeni Asya, 2023)
30/04/2023	313 (806,000 tents)	806 (85,500 containers)	3,500,000		(İlke Haber Ajansı, 2023)

26/05/2023	-	352 (123,729 containers)	-	296,579 people	(Doğru Haber, 2023)

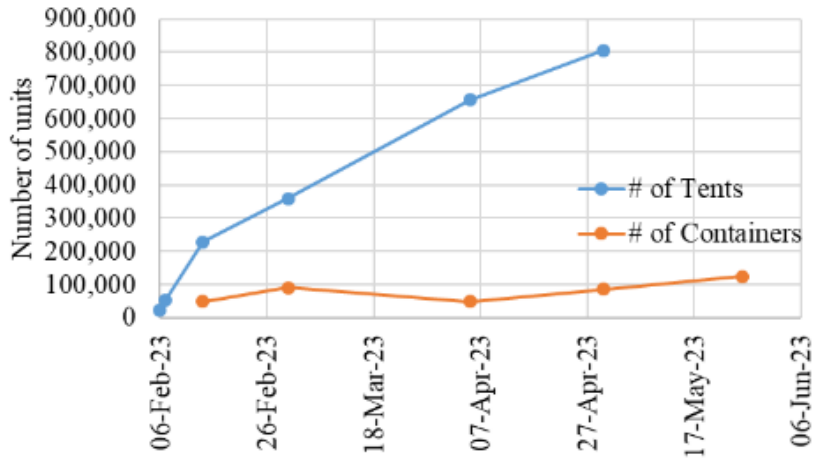

Figure 248: Growth of temporary shelter units in the disaster region

Table 39: Number of container cities in provinces until September 2023

Date	Province	# of container cities	# of people in container cities	Reference
25/04/2023	Nurdağı / Gaziantep	5 cities / 6.175 containers	20.000	(Ministry of Interior, 2023)
29/04/2023	Adıyaman	20 cities / 6.009 containers	24.000	Pehlül, 2023
17/06/2023	Malatya	51 cities / 18.000 containers	69.000	(Anadolu Agency, 2023)
27/06/2023	Kahramanmaraş	43 cities / 26.071 containers	90.939	(Anadolu Agency, 2023)
06/08/2023	Malatya	73 cities / 23.624 containers	97.421	(Anadolu Agency, 2023)
16/08/2023	Adıyaman	38 cities / 16.000 containers	56.000	(Precidency of Republic of ,Türkiye Directorate of Communications, 2023)
05/09/2023	Hatay	158 cities / 77.000 containers	> 150.000	(Doğru Haber, 2023)

In addition to tents and containers, temporary accommodation was provided in higher education dormitories and boarding schools, where possible. *Figure 249*a shows an example with identified locations for the temporary accommodation in an area within Antakya city. Additional assistance was provided by cruise ships in housing the earthquake victims in İskenderun (*Figure 249*b). We understood from our interview with the Mayor of Hatay in March that 100,000 tents were needed to supply the

metropolitan area. Although the current number of tents in the province is not known, Hatay has 158 container cities with about 77,000 containers in total, according to a report in the official news channel of the State- Anatolian Agency (AA).

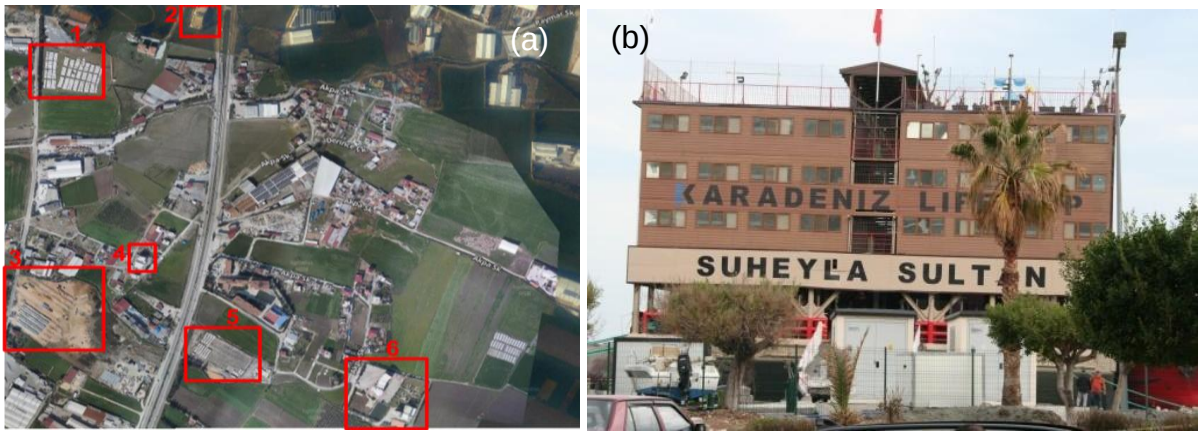

Figure 249: Temporary housing locations in Antakya (a) Temporary accommodation in Antakya - 1: Tent city, 2: Student hall (girls), Sabancı Dormitory, 3: Container city, 4: Student hall (boys), Gülbahçe Yükseköğretim Dormitory, 5: Possible area for container city. 6: Boarding School, Hatay Milli İrade Anadolu İmam Hatip High School; b) Karadeniz Lifeship Süheyla Sultan İskenderun

7.10. Relief and Early Recovery

7.10.1. Relief Supplies and Distribution

AFAD has assumed overall responsibility for the coordination of goods distribution. Every residential area or town has a distribution point where people can access water, food, toiletries, fuel and other necessities. Goods that are donated by other organisations, whether public or private, national or international, are also distributed through the AFAD system. During our field visit there was a high anxiety about humanitarian needs not being met and especially access to drinking and washing water, due to a lack of piped water supply in the most affected areas. Several residents recounted issues where goods distribution was unorganized leading to some people making off with mrore than what they need, while others did not have any. In Ericek, a town in Northern Kahramanmaraş, residents remarked that goods distribution was very stressful and we witnessed arguments at the distribution centre. At the same time, bagged coal had been dropped on the road and people from outside the camps were coming in cars and helping themselves (*Figure 250*). We also witnessed cases of bottled water being hastily distributed along the highway in Hatay, with some passers-by able to fill up their cars with bottled water. In Ilıca, at the tent camp, it was recounted that electric stoves were brought and left there, but they were all taken before being distributed to the residents. At the *Cemevi* tent camp in Elbistan, camp managers explained that they had changed the strategy of distribution to go around to each tent to ensure that all residents had equal access to relief goods in the camp. Some families were not able to access the relief system if they were not staying in the camps, and for example one family in Göksun were forced therefore to pay high commercial prices for water and other basic goods as they were staying outside of the camp.

Figure 250: Bagged coal dropped on the roadside in Ericek, March 2023.

7.10.2. Food Relief

In the early stages of the relief, hot food has been provided to people through a network of soup kitchens (*Aşevi*). At the height of the relief phase, there were more than 500 kitchens operating in the earthquake-affected areas to feed both survivors and volunteers. The kitchens are located in or near tent camps, and near strategic points in urban areas and villages, as well as in volunteer centres and field hospitals. Up to three meals a day are provided and many are run by religious groups and civil society groups. AFAD reported that on 3 March 2023, 3.882.000 hot meals were being delivered along with 4.000.000 loaves of bread daily. During the field visit we interviewed staff at the soup kitchen at St Ilyas Church in Samandağ (*Figure 251*). We were told that this kitchen they were producing 5000 meals in total daily. Each meal was provided in a take-out containers and people had to come and collect the meals. There was concern about the amount of waste from take-away containers. Although they had started by providing three meals per day, they had to reduce to this to two meals per day because of lack of water at the site to wash the equipment. Volunteers staffed the kitchen in rotations. The NATO kitchen which we visited in June 2023 was then producing 3000 meals per day and had a mess hall for eating in (*Figure 252*).

Figure 251: Soup kitchen at St Ilyas Church in Samandağ, March 2023

Figure 252: Soup kitchen at NATO Camp in İskenderun, June 2023

7.10.3. Post-Earthquake Trauma and Psycho-Social Support

According to AFAD press release, as of 3 March 2023, psychosocial support had been provided to 1.025.291 people, and 7392 personnel and 1655 vehicles were assigned to the disaster area (as of 1 March 2023).

Volunteer therapist, Caoimhe Butterly, who had been practicing in the Hatay region since the earthquake, explained (Interview March 2023) that the situation of people was one of high anxiety and trauma. She had been working to try to normalise people's responses, getting them to talk about what is happening in their body and why they are having the reactions that they are. She explained that children had been fainting during after-shocks, that people were having the trauma of having pulled bodies of family members from the rubble, seeing compressed body parts and faces and missing body parts. She explained that many people are still un-accounted for (more than 1000 at the time) and families are living with "ambiguous loss" – that is people who are still missing and one cannot accept that they are gone. She explained that some people are dealing with loss of entire families, for example she met one man who lost 42 family members as they were all staying in a hotel after a wedding. There are children who are still unable to speak six weeks after the earthquakes. Anxiety is also heightened as many people might not be with family members as they are separated in different cities. Many people are experiencing past mental health issues have come back again, for example suicidal feelings. Stress is made worse as many people do not have their basic humanitarian needs met. We also witnessed that many people working in first response, such as fire services were also suffering from low morale, which was exacerbated by a lack of suitable accommodation and supplies.

With regards to Syrian refugees the situation made is worse by depravities, for example some Syrian families still do not have access to tents or water on a regular basis. Many are undocumented workers and salaries have gone down, for example factories that were paying 120TL a day are now paying 70TL/day. Farm work used to be 100TL, now it is 50TL. Many Syrians who had moved to ,Türkiye 10-12 years earlier

and had assimilated into society are now finding themselves discriminated against as the relief system is divided between Turkish and Syrian families.

Some non-governmental organizations and think tanks think that after the earthquake, social pressures on Syrian refugees will tend to increase (Tatlı, 2023; Euronews, 2023; BBC News Türkçe, 2023; Erkılıç, 2023).

7.10.4. Safeguarding, Gender and Diversity

There have been many issues with regards to safeguarding in camps and tent areas. Many of the tents have been put up along roadways, which is unsafe, especially for children, as was communicated to us by some parents. One child died from drowning in a nearby waterbody. Tent camps have been flooded during rain events and affected by other storms and by floods (TTB, 2023; Robins, 2023; Ensonhaber, 2023). We also spoke to a women in Ilıca who told us that a young man had died from carbon monoxide poisoning in her tent camp. Reports from NGOs (cited in IFRC, 2023) outline that incidents of sexual assaults and violence against women, girls, LGBTQ and other at-risk individuals have been reported in the tent camps. Deteriorating socio-economic conditions are cited as a driver for this, as well non-gender disaggregated latrines. NGOs have also reported difficulties in accessing government helplines for domestic violence to report these attacks.

7.11. Demolishment and Debris Removal

According to the damage assessments conducted by the Ministry of Environment, Urbanization and Climate Change, 312,000 buildings containing 894,000 independent units have been determined to be moderately damaged, heavily damaged, collapsed, or required to be demolished immediately (Ministry of Environment, Urbanisation and Climate Change, 2023). Managing the construction and demolition waste of this catastrophic event extending over 11 provinces is an urgent need and top-priority. Between 116 million and 210 million tons of rubble, as indicated by the early predictions of UNDP, has generated, which is more than 10 times of what had generated after the 1999 Marmara Earthquake, which impacted on a more confined area. Monetary cost of this process accounts for US$113.5 million request for funding as part of UN's flash appeal (Kulu, 2023).

Demolishment practices proved problematic. Our interactions with the affected communities showed that accidental demolishment of the wrong building, as well as damaging the neighbouring building while demolishing one is commonplace. Further, the dust propagation induced by widespread demolishment especially in heavily damaged and tightly built-up city/town centres, such as Antakya and Kahramanmaras, was hard to bear. The particle counts measured by our field crews during the September-October visit in Antakya all indicated hazardous levels. Further, the vast amount of rubble that this widespread demolishment exercise comes with many risks if not handled properly due to the hazardous materials contained within the buildings. Asbestos, mercury, silica, and lead are among the dangerous materials that were set free either right after the earthquakes or the extensive demolishing campaign started soon after the rescue missions. It is crucial to state that the regulations forbidding the use and production of asbestos were put in place in 2010, which is much later than the construction date of many buildings in the disaster region. Experts interviewed by Reuters indicated that contamination from these hazardous materials over the long term may cause a larger human toll than the earthquake themselves, as these

materials can lead to a surge in cases of lung and other cancers, kidney disease, and nervous system disorders, as well as polluting the fertile lands and water resources (Toksabay et al., 2023).

Despite the risks of unplanned debris removal, it was observed that debris removal works were started before accomplishing search and rescue missions completely without a comprehensive analysis of where and how the waste materials from the rubble should be stored (Chamber of Mining Engineers, Türkiye 2023). This emergency removal reflex, which was observed also after the 1999 Marmara Earthquake (Baycan, 2004), resulted in an uncoordinated approach rather than a controlled and supervised scheme. Similar observations have been made by the EEFIT team members across the disaster zone, various dumping areas were used along the highways without any observable safety precautions which caused asbestos and other hazardous substances to be mixed into the air. Parallel to the statements of Chamber of Architects (2023a) and Gundogdu (2023), rubbles were observed to be emptied in close vicinity of agricultural areas, residential areas, and industrial zones in the nearby regions by disregarding the necessary controls and precautions. *Figure 253* and *Figure 254* are the satellite imageries showing the construction and demolition waste piles in Hatay and Kahramanmaraş. From the *Figure 253*, it can be seen that piles are extended over fertile lands and in close proximity to residential areas in Hatay. *Figure 254* shows another pile located very close to the city hospital of Kahramanmaraş.

Figure 253: Rubble piles nearby fertile land and residential area in Antakya, Hatay.

Figure 254: Rubble piles nearby NecipFazil City Hospital in Dulkadiroğlu, Kahramanmaraş.

Moreover, security personnel, military officers, and heavy machinery operators were observed unprotected against toxic dust. According to experts, asbestos-related diseases take many years to show their symptoms. Therefore, personnel in the field may not have a chance for compensation as it becomes harder to prove where they had been exposed to the toxic material (Toksabay et al., 2023).

Uncontrolled and wide management of construction and demolition waste management is a serious health and environmental issue not only for today but also

for the next generations. On the other hand, if handled carefully, risks can be avoided and many of the debris can be recycled (Baycan, 2004).

During the EFFIT follow up mission in June, the team observed in İskenderun and Antakya that waste was being sorted before being removed, with metals and appliances (white goods) taken out of the rubble for recycling. Many lorries full of twisted rebar were visible on the roads in the region. The rubble was being transported to dump sites around the cities, with a very high intensity of activity. We visited one dump site in Güneysöğüt near Antakya where 3000 lorries were working daily, between 8 am-12 midnight. There was intense dust pollution in the vicinity of the dumpsite, including where families were living nearby. We interviewed one family who were no longer able to eat the produce from their garden. We were also made aware that there were concerns of long-term environmental pollution from chemicals from the dumpsite leaching into the soil and nearby water sources (*Figure 255* and *Figure 256*).

Figure 255: Dumpsite at Güneysöğüt on 23 June 2023

Figure 256: Debris removal in Antakya, showing rebar separated for recycling, 22 June 2023

7.12. Reconstruction and– Housing Reconstruction/Site Selection Criteria Policies/Building Codes

In Türkiye, very similar approaches are generally observed in the site selection of permanent housing areas after disasters. It is possible to collect these basic criteria under two headings; the first is public lands, and the second is the solid ground criterion. The leading actor in the permanent housing processes after the earthquake is TOKİ, that is, the Mass Housing Administration established in 1984. TOKİ also cites the aforementioned site selection criteria in its statement regarding the Kahramanmaraş Earthquakes. TOKİ President Ömer Bulut reveals the criteria for housing in his statement (TOKI, 2023; Malatya Sonsoz, 22.02.2023). Accordingly, the ground, the distance to the fault line and the storey height are specified as the basic building production criteria (*Figure 257*). It is stated that the tunnel formwork system is also the basic building production system.

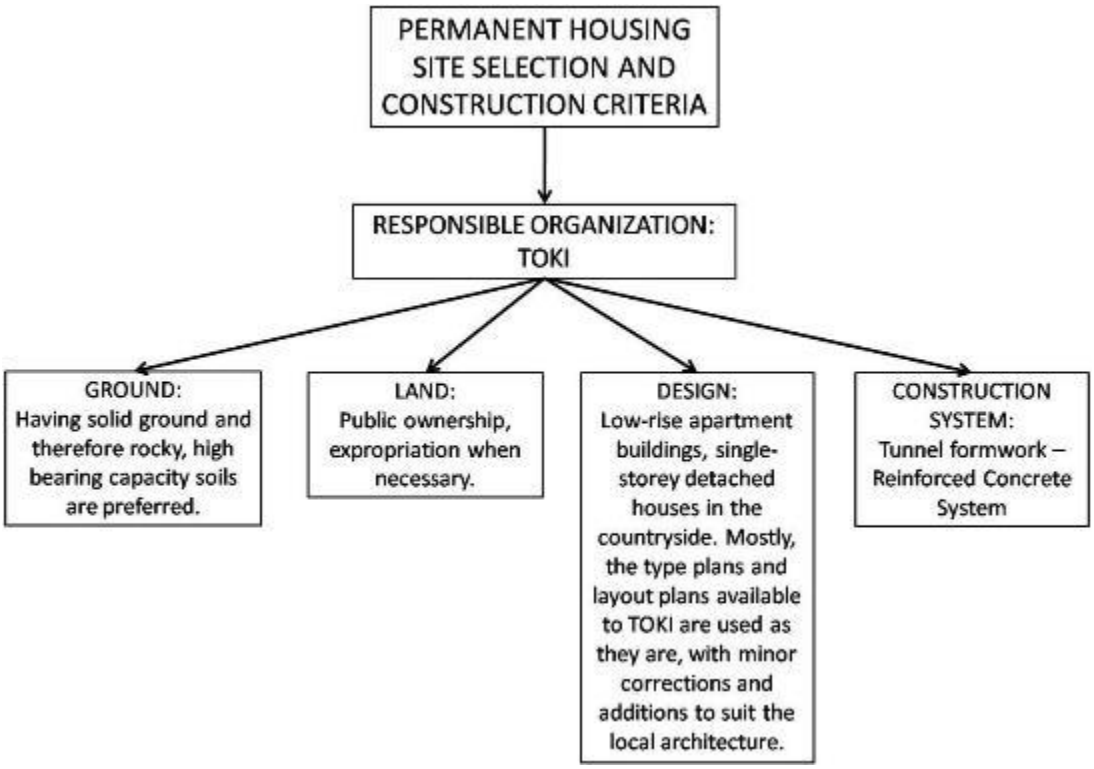

Figure 257: In its simplified form, permanent housing location selection and building production process application approach after the earthquake in Türkiye (Produced by the EEFIT-RRR Group).

Within the framework of the criteria put forward by TOKİ and therefore the Ministry of Environment, Urbanization and Climate Change, it is observed that site selection is made in mountain slopes or hilly areas, mostly agricultural areas, far from the city center.

The most typical example in the past for the large housing deficit that emerged after the earthquake in Türkiye was the 1999 Marmara Earthquake. After this earthquake, the construction of 42,587 houses was started. There has been a lot of discussions in terms of the site selection, design and construction processes of the permanent houses produced after the 1999 earthquake and the following processes. It is expected that these discussions will also guide the permanent houses to be built after the 6 February Kahramanmaraş Earthquakes. In general, the lack of user participation, neglecting the socio-economic and socio-cultural characteristics of the region, a design approach that ignores the architectural features of the region, traditional building production approach and local spatial needs, the distance of the created living spaces from the city centres are the first problems that come to mind (Suveyan, 2023. Erten, 2003) It may be possible to summarize the discussions on the production processes of permanent houses after the 1999 Marmara Earthquake in *Table 40*.

Table 40: Permanent housing problems after the 1999 Marmara Earthquake (Karaduman, 2002; Uzuner and Akıncıtürk , 2020)

Planning Problems	**Site Selection Problems**	**Design and Construction Problems**	**Socio-Cultural and Economical Problems**
Lack of holistic planning approach and community participation	The development of these areas close to green areas and forest areas will create environmental threats in the future.	Lack of designs suitable for changing family structures	Belonging to the place problems
Accessibility problems due to its distance from city center	With the spread of new housing areas towards the countryside, the distinctive texture of the countryside began to deteriorate.	Fine craftsmanship and material choices are of poor quality of housing units	Problems related to social life
Urban sprawl problems		Although it has been tried to be solved with the shopping areas, trade centers and schools envisaged in the residential areas, it is a problem that these facilities were not completed simultaneously with the housing constructions.	As a result of the variability in the economic value of the houses produced, economic inequalities occur among the owners of the houses.
Lack of regional data and user profile determination studies in the planning phase		Lack of user preferences	Lack of social facilities
Lack of interdisciplinary studies before, during and after the development of permanent housing areas. Social scientists, planners, architects, economists, sociologists etc. are needed in every phase of the development processes.			

The housing need that emerged after the February 6 Earthquakes is higher compared to the 1999 earthquakes. In the statement of the President and also in the institutional statements, it is stated that 650 thousand houses will be built in the disaster area (TCCB, 2023; Communication Directorate, 2023). It seems that the site selection studies for permanent residences in many different regions, especially in Hatay, have been completed and the construction of new residences has begun. Although it is stated that all the houses will be completed within 1 year, it seems very difficult to predict how long the process will be.

It may be possible to make an evaluation on permanent housing practices with the information obtained and observations made during the visits to the four cities (Hatay, Adıyaman, Kahramanmaraş and Malatya) which have been most affected by earthquakes. However, it is also considered that the housing production is at the very

beginning, the process will be long-term, and more detailed and new data on this subject will be available in new visits to the region in the future.

It has been observed that permanent housing areas in Hatay are far from the city center, and very close to agricultural lands and forest areas as well. It is understood that the primary criteria in the selection of these areas are the ground with a high bearing capacity and the public lands that provide rapid construction without any property problems (Chamber of Architects, 2023a).

Figure 258: Gülderen Neighbourhood Permanent Housing area in Antakya province

Lack of public participation can be asserted as one of the foremost planning and construction problems.

Figure 259: Hatay Altınözü Permanent Housing Area in Antakya province (TRT Haber, 03.05.2023)

The area of Kahramanmaraş Sütçü İmam University Agricultural Application and Research Center (SEKAMER) which conducting agricultural research, especially on walnuts and almonds in Dulkadiroğlu District Gafffarlı Mahallesi in the city center of Kahramanmaraş has been determined as a permanent residence settlement area and permanent housing construction works have started (Chamber of Architects, Türkiye (2023a) The fact that this area is a productive agricultural area and constitutes an important gene pool for a number of agricultural products, especially walnuts and almonds, raises the possibility that other dangers may arise with the selection of the area as a permanent housing area (Elmacıoğlu, 2023).

Figure 260: SEKAMER Area where the permanent housings will be constructed in Kahramanmaraş province.

Lack of public participation, proximity to the city center, and environmental problems can be asserted as the foremost planning and construction problems.

Örenli Neighborhood and İndere (Zey) Village, which are connected to the Center in Adıyaman, have been determined as permanent residential settlement areas; permanent housing construction works have started.

Figure 261: Örenli Permanent Housing Construction Site in Adıyaman province.

Figure 262: İndere Permanent Housing Construction Site in Adıyaman province.

It is necessary to assert as the lack of public participation, proximity to the city center, and environmental problems as the foremost planning and construction problems related to permanent housing process in Adıyaman province.

In Malatya province, it has been observed that the stages, which are the continuation of the existing TOKİ residences of the Gelincik Tepe permanent housing settlement area, have been converted into disaster housing and the construction continues. It was learned that the area is close to the Arslantepe Archaeological Site and archaeological findings were found in the construction area. It is understood that permanent housing settlements will increase the pressure of construction, and deterioration in the region.

Figure 263: GelincikTepe Permanent Housing Area in Malatya province.

Figure 264: Permanent Housing site under construction in June 2023, Gülderen Neighbourhood, Antakya

As a result, permanent housing practices have started in the disaster area, both in urban areas and in rural areas. The goal of quickly completing the process and relocating the homeless survivors to new residences is considered important. However, it has been observed that the problems encountered in the 1999 Marmara Earthquake are similar to those encountered and that there is a risk of recurrence in a wider area. For this reason, it will be important to closely monitor the problems that will arise in the continuation of the process and to produce solutions quickly.

References

Açık Radyo 95.0. (2023). 'At least 6,700 Syrians died in earthquake in Turkey'. Available at: https://acikradyo.com.tr/acik-gazete/turkiyede-depremde-en-az-6-bin-700-suriyeli-oldu [Accessed 2 Feb. 2024].

AFAD (2023). Available at: https://en.afad.gov.tr/about-the-disaster-area-affecting-the-life-of-the-general-public [Accessed 2 Feb. 2024].

AFAD (2023). Press Release. Available at: https://deprem.afad.gov.tr/press-release [Accessed 1 February 2024].

Akarsu, E. (2022). Natural Disasters and Epidemic Diseases During the Turkish Seljuk State Period (From Its Establishment to Its Collapse). Ph.D. thesis, Necmettin Erbakan University.

Albayrak, S. (2023). Deprem Hasarı Sanayiye Yansıdı. Available at: https://sanayigazetesi.com.tr/deprem-hasari-sanayiye-yansidi/ [Accessed 28 May 2023].

Anadolu Agency (2023). 69 thousand earthquake victims were placed in containers in Malatya.

Anadolu Agency (2023). 90,939 disaster victims were placed in containers in Kahramanmaraş.

Anadolu Agency (2023). Available at: https://www.aa.com.tr/tr/asrin-felaketi/kahramanmarastaki-konteynerlere-90-bin-939-afetzede-yerlestirildi/2931958 [Accessed 1 February 2024].

Anadolu Agency (2023). Available at: https://www.aa.com.tr/tr/gundem/malatyada-69-bin-depremzede-konteynerlere-yerlestirildi/2924579 [Accessed 1 February 2024].

Anadolu Agency (2023). In Malatya, 97 thousand 421 earthquake victims were placed in containers. Anadolu Agency (2023).. Available at: https://www.aa.com.tr/tr/dosya-haber/malatyada-97-bin-421-depremzede-konteynere-yerlestirildi/2962158 [Accessed 1 February 2024].

Arik, F.Ş. (1992). Earthquakes in Anatolia during the Period of Seljuks. Journal of Historical Research, 16(27), pp. 13-32.

Artı Gerçek (2023). More than 3 Million People Relocated: How Many Earthquake Victims Settled in Which Province? Migration. Published 20 March 2023. Available at: https://artigercek.com/guncel/3-milyonu-askin-insan-yer-degistirdi-hangi-ile-kac-depremzede-yerlesti-goc-243119h [Accessed 1 February 2024].

Atabey, İ.İ., Bozdoğan, K.B. (2012). The building inspection law applications: Example of Sivas. Engineering Sciences, 7(1), 119–128.

Atlas Map. Atlas Map Portal. Available at: https://atlas.harita.gov.tr/ [Accessed March 2023].

Aygün, B. (2005). Ecological Anthropology: Antakya. Ph.D. thesis, Ankara University.

Bahadir, G. (2013). The Formation Of Christianity In Antioch and Habib-i Neccar. Mustafa Kemal University Journal of Institute of Social Sciences, 10(23), pp. 207-214.

Bakir, M. (2021). Antiokheia: The City in the Shadow of Earthquakes (6th Century). Adnan Menderes University Journal of Institute of Social Sciences, 8(2), pp.229-243.

Bakirci, A., Soydan, E., Civelek, I.B. (2019). Turkey: Amendments to Building Inspection. Montaq.

Baycan, F. (2004, April). Emergency Planning for Disaster Waste: A Proposal based on the experience of the Marmara Earthquake in Turkey. In 2004 International Conference and Student Competition on post-disaster reconstruction "Planning for reconstruction," Coventry, UK.

Bayram, S., Aydınlı, S., Budak, A., Ora,l E. (2018). Ethical problems in the production and inspection of construction in Turkey. Pamukkale University Journal of Engineering Sciences, 24(3), 461–467.

BBC News Türkçe. (2023). Hundreds of Syrians in Turkey went to Syria after earthquake. 17 February. Available at: https://www.bbc.com/turkce/articles/crgz584x9gro [Accessed 1 February 2024].

BBC News Türkçe. (2023). Kahramanmaraş earthquake: Hundreds of Syrians in Turkey left for Syria after the earthquake. Available at: https://www.bbc.com/turkce/articles/crgz584x9gro [Accessed 2 Feb. 2024].

BBC News Türkçe. (2023). People living in Iskenderun, hit by the Kahramanmaras earthquakes: 'You were too late... Why didn't you come sooner?' Available at: https://www.bbc.com/turkce/articles/cmmv145pmj9o [Accessed 2 Feb. 2024].

BBC News Türkçe. (2023). Turkey asks Netherlands for information on '5-year-old earthquake victim'. Available at: https://www.bbc.com/turkce/articles/cg3dqdle18vo [Accessed 2 Feb. 2024].

Beyen, K., Erdik, M., Mazmanoğlu, C., Ekmekçioğlu, Z. (2003). The Seismic Activity of Antioch from Past to Present and the Assessment of the Actions to be Taken in the Light of an International Conference. Engineering Report Of Turkey, 423(1), pp. 51-53.

Bi Haber (2023). AFAD Volunteer: "We Waited at AFAD Hatay Directorate for a Day and a Half!" February 11, available at: https://www.youtube.com/watch?v=pu4V6WH_lJg (Accessed 22 January 2024).

Bikçe, M., Geneş, M.C., Gülkan, P., Kaçin, S. (2010). Investigation of Damage and Seismic Characteristics of Reinforced Concrete Framed Structures Based on the Mixed Approach of Combining Instrumental and Numerical Data. Tubitak Project, Middle East Technical University.

Büyüksaraç, A., Över, S., Geneş, M.C., Bikçe, M., Kacin, S., Bektaş, Ö. (2014). Estimating Shear Wave Velocity Using Acceleration Data In Antakya (Turkey). Earth Sciences Research Journal, 18(2), pp. 87-98.

Çelik, G.T., Ünal, C. (2017). Determination of problems in building inspection companies and the Adana example. Çukurova University Journal of the Faculty of Engineering and Architecture, 32(4), 71–78.

Ceyran, S., Elibüyük, M. (2012). Geographic Distribution of Earthquakes Causing Death in Türkiye (500 AD-2011). Tücaum VII. Coğrafya Sempozyumu, pp. 18-29.

Chamber of Architects, Türkiye. (2023a) 6 February 2023 Earthquakes Detection and Evaluation Report 2. 2 May. Available at: https://www.tmmob.org.tr/icerik/mimarlar-odasi-6-subat-2023-depremleri-raporu-2-tespitler-degerlendirmeler-ve-oneriler [Accessed 22 January 2024].

Chamber of Architects, Türkiye. (2023b) TMMOB February 6 Earthquakes 8th Month Evaluation Report. 10 October. Available from: https://www.tmmob.org.tr/icerik/tmmob-6-subat-depremleri-8-ay-degerlendirme-raporu-yayimlandi [Accessed 6 December 2023].

Chamber of Mining Engineers, Türkiye. (2023). 6 February 2023 Earthquake Report. 2 April. Available from: https://www.maden.org.tr/calismalar/raporlar/detay/6-subat-2023-deprem-raporu [Accessed 22 January 2024].

CNN TÜRK (2023). Day 134! What is the death toll in the earthquake, what is the current number of injured? How many buildings were destroyed and how many people died in which province? CNN TÜRK. Available at: https://www.cnnturk.com/turkiye/106-gun-depremde-olu-sayisi-ne-kadar-oldu-guncel-yarali-sayisi-kac-hangi-ilde-kac-bina-yikildi-kac-kisi-oldu [Accessed 2 Feb. 2024].

Communication Directorate. (2023). Disaster housing in the earthquake zone is rising rapidly. 5 June. Available from: https://www.iletisim.gov.tr/turkce/yerel_basin/detay/deprem-bolgesinde-afet-konutlari-hizla-yukseliyor [Accessed 1 February 2024].

Cumhuriyet (2020). Illegal structures were insured. Available at: https://www.cumhuriyet.com.tr/haber/kacak-yapilar-sigortalandi-1794650 [Accessed 2 Feb. 2024].

DASK (2023). DASK | Natural Disaster Insurance Institution | About DASK. Available at: https://dask.gov.tr/tr/dask-hakkinda [Accessed 2 Feb. 2024].

DASK (2023). DASK | Natural Disaster Insurance Institution | Interactive Earthquake Map. Available at: https://dask.gov.tr/tr/interaktif-deprem-haritasi [Accessed 2 Feb. 2024].

Değerliyurt, M., Çabuk, S.N., Aksu, R. (2014). Determination of Areas Suitable for Settlement for Sustainable Urban Development: The Case of Iskenderun City. Geographers Association International Congress Proceedings Book. Muğla Sıtkı Koçman University. Muğla. pp. 380-389.

Demirel, İ.O., Akansel, V.H., Bankir, Ş., Geneş, M.C., Erberik, M.A., Yakut, A. (2013). Analytical Evaluation of the Properties of Masonry Buildings in Antakya in Terms of Earthquake Performance. 2nd Turkey Earthquake Engineering and Seismological Conference. Hatay.

Demirtaş, R., Erkmen, C. (2019). Eastern Anatolia Fault System Earthquake Activity, Future Earthquake Potential, Researchgate.

Diken (2023). They were waiting for AFAD's approval: 'Cranes and diggers have been idle in Hatay for two days' - Diken. Available at: https://www.diken.com.tr/afadin-onayini-bekliyorlarmis-hatayda-vinc-ve-kepceler-iki-gundur-bos-bos-duruyor/ [Accessed 2 Feb. 2024].

Doğru Haber. (2023). How many containers were installed in the earthquake zone? Doğru Haber, 26 May. Available at: https://dogruhaber.com.tr/haber/933348-deprem-bolgesinde-kac-konteyner-kuruldu/ [Accessed 1 February 2024].

Ege, İ. (2014). Geomorphological Observations on Active Tectonics in the Antakya-Kahramanmaraş Graben. Mustafa Kemal University Journal Of Graduate School Of Social Sciences 11(26), pp. 71-88

Ekin, Ü. (2007). 1822 Halep-Antakya Earthquake and Its Impact on the Region. The Journal of Turkish Cultural Studies, 9(17), pp. 29-50.

Elmacıoğlu, L. (2023). Objection to the area where TOKİ will build a residence in Kahramanmaraş: "The gene center, which is one in Turkey and in three places in the world, should not be turned into a construction area." Independent TÜRKÇE, 11 March. Available from: https://www.indyturk.com/node/616116/haber/tokinin-kahramanmaraşta-konut-yapacağı-alana-itiraz-türkiyede-tek-dünyada-üç [Accessed 22 January 2024].

Ensonhaber. (2023). Fire broke out in a tent city in Adıyaman. 5 May. Available from: https://www.ensonhaber.com/3-sayfa/adiyamandaki-cadir-kentte-yangin-cikti [Accessed 20 December 2024].

Erdiş, E., Gerek, İ.H. (2012). Problems and solution suggestions in construction inspection process. Engineering Sciences, 7(1), 291–298.

Erel, T.L., Adatepe, F., Erel, T.L. (2007). Traces Of Historical Earthquakes In The Ancient City Life At The Mediterranean Region. Journal Of Black Sea/Mediterranean Environment, 13(3), pp. 241-252.

Erkılıç, O. (2023). The Syrians who went to their countries in the earthquake are returning. Available at: https://www.voaturkce.com/a/depremde-ulkelerine-giden-suriyeliler-geri-donuyor/7059313.html [Accessed 1 February 2024].

Erol, H. and Dede, M.S. (2022). A stakeholder-based review of the building inspection system in Turkey: The case of Yalova. Journal of Construction Engineering, Management & Innovation, 5(2), 95-106. DOI: 10.31462/jcemi.2022.02095106

Erten, G. (2003). Earthquake: Leaving a document on history: On permanent earthquake housing. Mimarlık, 309, Jan-Feb. Available from: http://www.mimarlikdergisi.com/index.cfm?sayfa=mimarlik&DergiSayi=10&RecID=488 [Accessed 1 February 2024].

Euronews. (2023). Some of the Syrians affected by the earthquake in Turkey are returning to their countries. 17 February. Available at: https://tr.euronews.com/2023/02/17/turkiyede-depremden-etkilenen-suriyelilerin-bir-kismi-ulkelerine-geri-donuyor [Accessed 1 February 2024].

Euronews. (2023). Syrians affected by the earthquake in Turkey are returning home. Available at: https://tr.euronews.com/2023/02/17/turkiyede-depremden-etkilenen-suriyelilerin-bir-kismi-ulkelerine-geri-donuyor [Accessed 2 Feb. 2024].

Gazete Duvar (2023). A woman's dead body was found in the rubble on the 122nd day of the earthquake. Gazete Duvar. Available at: https://www.gazeteduvar.com.tr/depremin-122nci-gununde-enkazda-kadin-cesedi-bulundu-haber-1622527 [Accessed 2 Feb. 2024].

Geçen, R., Ölmez, İ., (2018). Accessibility of Fire Brigades in Antakya (Hatay) in Emergency Situations. Journal Of International Social Research, 11(60), pp. 326-339.

Genes, M., Bikçe, M., Kaçin, S., Doğanay, E., Teköz, K., Abrahamczyk, L. (2011). Determination of Damage Vulnerability of Residential Multi-storey Reinforced Concrete Structures by Combining Instrumental and Numerical Data and Static Thrust Analysis. 1st Turkish Earthquake Engineering and Seismology Conference. Ankara.

Gerçek Gündem (2023). The Earthquake Observation Report revealed the severity: The prosecutor changed, the investigation returned to the beginning. Gerçek Gündem. Available at: https://www.gercekgundem.com/guncel/halkin-hukuk-burosundan-deprem-gozlem-raporu-savcilar-degistirildi-sorusturmalar-basa-dondu-434571 [Accessed 2 Feb. 2024].

Gokcebugra on X. (2023). Available at: https://twitter.com/gokcebugra/status/1660905916915499009?t=KExmHm47pMgQu5s39XGyQQ&s=08 [Accessed 2 Feb. 2024].

Goksunlular.com. (2024). Göksun Guide. Available at: http://www.goksunlular.com/?pnum=10&pt=G%C3%B6ksun+Rehberi [Accessed 2 Feb. 2024].

Government of Turkey (2023). Türkiye Earthquakes Recovery and Reconstruction Assessment (TERRA), 20 March 2023. Available from: https://www.sbb.gov.tr/wp-content/uploads/2023/03/Turkiye-Recovery-and-Reconstruction-Assessment.pdf [Accessed 5 June 2023].

Güler, M. and Karanuh, Z.D. (2018). Kentsel yaşam kalitesinin belirleyicisi olarak belediye hizmetleri ve stratejik planlar. In Mengi, A. and İşçioğlu, D. (Eds.), Küreselleşme Sürecinde Yerel Hizmet Yerel Siyaset (pp. 285-310). Ankara Üniversitesi Yayınları.

Gülkan, P. (2000). Building code enforcement prospects: The failure of public policy. Earthquake Spectra, 16, 351-374. https://doi.org/10.1193/1.1586159

Gündoğan, B. (2023). Deprem bölgesinde fahiş kira artışları konusunda devlet olarak gereğini yerine getiriyoruz. Anadolu Ajansı. Available at: https://www.aa.com.tr/tr/asrin-felaketi/bakan-soylu-deprem-bolgesinde-fahis-kira-artislari-konusunda-devlet-olarak-geregini-yerine-getiriyoruz/2830986 [Accessed 12 Sep. 2023].

Gunduz, A., Kaya, S. (2016). Hatay Studies -II. Antakya

Habertürk (2023). We didn't forget! It's been 3 months of indescribable pain... Here is the painful toll of the February 6 Kahramanmaraş earthquake! Habertürk. Available at: https://www.haberturk.com/son-dakika-haberleri-felaketin-uzerinden-3-ay-gecti-rakamlarla-6-subat-depremi-kahramanmaras-depreminin-bilancosu-3589109 [Accessed 2 Feb. 2024].

Hacıbaloğlu, D. (2003). Building Inspection in Turkey. Master's Thesis, Middle East Technical University, Ankara. Available from: https://open.metu.edu.tr/handle/11511/13568 [Accessed 29 May 2023].

Hatcakap on X (2023). Available at: https://twitter.com/hatcakap/status/1661752020435632134 [Accessed 2 Feb. 2024].

Hürriyet (2023). Those missing in the earthquake will be considered dead after 1 year. Hurriyet.com.tr. Available at: https://www.hurriyet.com.tr/gundem/depremde-kaybolanlar-1-yil-sonra-olmus-kabul-edilecek-42230220 [Accessed 2 Feb. 2024].

İlke Haber Ajansı. (2023). The number of containers established in the earthquake zone exceeded 85 thousand. İlkha Haber, 30 April. Available at: https://ilkha.com/guncel/deprem-bolgesinde-kurulan-konteyner-sayisi-85-bini-asti-326639 [Accessed 1 February 2024].

Independent Türkçe. (2023). Two applications for those missing and unidentified in the earthquake: Presumption of death and disappearance. Available at: https://www.indyturk.com/node/619791/haber/depremde-kaybolan-ve-kimli%C4%9Fi-belirlenmeyenler-i%C3%A7in-devreye-giren-iki-uygulama-%C3%B6l%C3%BCm [Accessed 2 Feb. 2024].

Insamer (2023). Issues of Post-Earthquake Migration and Resettlement of Refugees. insamer.com. Available at: https://www.insamer.com/tr/deprem-sonrasi-goc-ve-multecilerin-yeniden-yerlesimi-meseleleri.html [Accessed 2 Feb. 2024].

İstek, E. (2020). The City of Antakya through the Eyes of Travelers (Between the 10th and 19th Centuries). Journal of Pamukkale University Social Sciences Institute, (40), pp. 227-246.

Karaduman, N.E. (2002) The Evaluation of Permanent Housings Produced After East Marmara Earthquakes In 1999. Unpublished master's thesis. Istanbul Technical University, Turkey.

Kaya, S., Kıyılı, E. (2009). A look at natural disasters and epidemics that occurred in Antakya in the Middle Ages. Mustafa Kemal University Social Sciences Institute Journal, 6(12), pp. 403-418.

Kiliç, İ., Çoşkun, H., Uslu, H. (2013). Investigation of the Behaviour of Hatay Government House under Earthquake Loads. 2nd Turkey Earthquake Engineering and Seismological Conference. Mustafa Kemal University. Hatay.

Kocaoğlu, S.E. (2016). Examination of historical urban fabric of Antakya in terms of urban design and a case study. Master's thesis, Bartin University.

Korkmaz, H. (2006). The Relationship Between Soil Properties and Earthquake Effects in Antakya. Journal of Geographical Sciences, 4(2), pp. 49-66.

Kulu, L. (2023). Millions of tons of earthquake rubble await removal in Türkiye. United Nations Development Programme, 24 February. Available at: https://www.undp.org/press-releases/millions-tons-earthquake-rubble-await-removal-turkiye [Accessed 26 Jun. 2023].

Kural, R., Ünal, O. (2015). Investigation of the applications in Afyonkarahisar Province and the building inspection in the construction sector. Afyon Kocatepe University Journal of Science and Engineering, 15(3), 1–10.

Lom, N. (2011). Investigation and mapping of active faults in Antakya and its surroundings. Ph.D. thesis, Eurasian Institute Of Earth Sciences.

Maden, N., Beker, Y., Nazir, B. (2018). Observations of Natural Phenomena and Earth Sciences in the Chronicle of Theophanes. Blue Atlas, 6(2), pp. 118-137.

Malatya Sonsoz. (2023). Here are the 3 Most Important Criteria of TOKİ. 22 February. Available from: https://malatyasonsoz.com.tr/haber/15691956/iste-tokinin-en-onemli-3-kriteri [Accessed 1 February 2024].

Mavroulis, S., Mavrouli, M., Vassilakis, E., Argyropoulos, I., Carydis, P., & Lekkas, E. (2023). Debris Management in Turkey Provinces Affected by the 6 February 2023 Earthquakes: Challenges during Recovery and Potential Health and Environmental Risks. Applied Sciences, 13, 8823. https://doi.org/10.3390/app13158823

Ministry of Environment, Urbanisation and Climate Change of Republic of Türkiye. (2023). Reconstruction Process. Available at: https://www.csb.gov.tr/bakan-kurum-depremden-etkilenen-11-ilde-67-bin-konutun-ve-koy-evinin-yapim-surecini-baslattik-bakanlik-faaliyetleri-38517 [Accessed 22 January 2024].

Ministry of Interior of Türkiye. (2023). In Nurdağı, 85 per cent of the containers needed by earthquake victims have been installed. Turkish Republic Ministry of Interior, 25 April. Available at: https://www.icisleri.gov.tr/nurdaginda-depremzedelerin-ihtiyac-duydugu-konteynerlerin-yuzde-85i-kuruldu [Accessed 1 February 2024].

Mondaq (2019). Amendments To Building Inspection Legislation - Audit - Turkey. [online] Available at: https://www.mondaq.com/turkey/audit/800558/amendments-to-building-inspection-legislation [Accessed 3 Feb. 2024].

NTV (2023). 215th day of the earthquake: A body was found from the rubble during the foundation excavation. Ntv.com.tr. Available at: https://www.ntv.com.tr/turkiye/depremin-215inci-gunu-temel-kazisinda-enkazdan-ceset-cikti,XvQtLOu5rEOnEdzsLEq0rQ [Accessed 2 Feb. 2024].

Odatv (2023). How many Syrians died in the Kahramanmaras earthquake?. Odatv. Available at: https://www.odatv4.com/guncel/kahramanmaras-depreminde-kac-suriyeli-oldu-273287 [Accessed 2 Feb. 2024].

Odatv (2023). Minister Soylu counted them one by one: 297 missing, 86 of them children. Odatv. Available at: https://www.odatv4.com/siyaset/bakan-soylu-tek-tek-saydi-86-si-cocuk-297-kayip-281718 [Accessed 2 Feb. 2024].

Ömürbek, N., Karaatlı, M., Cömert, H.G. (2016). Evaluating construction auditing companies by using AHP-SAW and AHP-ELECTRE methods. Journal of Administrative Sciences, 14(27), 171–199.

Özdemir, R. (1994). Physical and Demographic Structure of Antakya in the Ottoman Period 1709-1860. TTK Belleten, 58(221), pp. 119-158.

Ozden, A.T. and Erbaş, M.S. (2023). A brief discussion paper on the ways and methods of local governments in accessing disaster risk information and data. Unpublished. [Contact information is typically not included in Harvard references.]

Ozden, A.T. and Erkilic, M.B. (2015). From Healing to Protective Disaster Coping Efforts: An Evaluation of Building Inspection Approaches within the Disaster Policies Developed between 1924 and 2010 in Turkey. Civil Engineering and Architecture, 3(4), 83-87, DOI: 10.13189/cea.2015.030404

Ozden, A.T. and Erkilic, M.B. (2015). From healing to protective disaster coping efforts: An evaluation of building inspection approaches within the disaster policies developed between 1924 and 2010 in Turkey. Civil Engineering and Architecture, 3(4), 83-87. https://doi.org/10.13189/cea.2015.030404

Özen, Ö., Türer, A., Şimşek, Ç., Dilsiz, A., Özden, B., Gölalmiş, M., Kaya, H., Korkmaz, Z.S., Korkmaz, H. (2007). Research and Development of Economical Seismic Isolation and Strengthening Methods of Masonry Structures Against Earthquakes. Tubitak Project, Middle East Technical University.

Ozer, C. (2019). Determination Of 3-D Crustal Seismic Velocity Structure Beneath Hatay and Surroundings. Journal Of The Faculty Of Engineering and Architecture Of Gazi University, 34(4), pp. 2215-2227.

Özonur, Ş. (2008). Crusader tate of Antioch. Ph.D. thesis, Marmara University.

Özşahin, E. (2010). A Geographical Approach At Natural Environment Problems In The Asi (Orontes) River Delta (Hatay/Turkey). Mustafa Kemal University Journal of Institute of Social Sciences, 7(13), pp. 445-475.

Özşahin, E. (2010). Assessment of Hatay Airport in terms of Geomorphological Features and Natural Risk. Turkish Studies, 5, pp. 4.

Özşahin, E. (2010). Evaluation of Hatay Site Selection in Antakya in terms of Geomorphological Features and Natural Risk. Balikesir University Journal of Institute of Social Sciences, 13(23), pp. 1-16.

Özşahin, E., Değerliyurt, M. (2013). Modeling Of Seismic Hazard Risk Analysis In Antakya (Hatay, South Turkey) By Using Gis. International Journal Of Innovative Environmental Studies Research, 1(3), pp. 31-54.

Özşahin, E., Özder, A. (2011). Temporal Change of the Relationship between Antakya City and Geomorphological Units (Hatay). Physical Geography Researches, 5, pp. 659-678.

Özşahin, E.,Kaymaz, Ç.K. (2013). An Example for the Evaluation of Disaster Culture: Antakya City. Turkey Earthquake Engineering and Seismological Conference, pp. 25-27.

Pala, M. & Demir, M.Ş. (2017). Building audit application in Southeastern Anatolia Region and problems of building audit and solutions for these problems. Journal of Engineering Science of Adıyaman University, 4(6), 20–33.

Perk, S., Ozer, C. (2019). Investigation Of Soil Properties Based On Accelerometer Stations Using Earthquake Recording: The Case Study Of Hatay, Turkey. Turk. J. Earthq. Res, 1(2), pp. 167-179.

Platform24 (2023). Hatay-Adıyaman: No AFAD, There is Negligence and Nepotism! Available at: http://platform24.org/yazarlar/5796/hatay-adiyaman--afad-yok--ihmal-ve-torpil-var [Accessed 2 Feb. 2024].

Polat, Z.A. (2019). Analysis of the regulation of “Zoning Reconciliation” in local governments. Planlama, 29(3), 202–209. https://doi.org/10.14744/planlama.2019.04796

Presidency of Republic of Turkiye Directorate of Communications. (2023). All beneficiaries in Adıyaman city centre were placed in containers. Directorate of Communications, 16 August. Available at: https://www.iletisim.gov.tr/turkce/yerel_basin/detay/adiyaman-kent-merkezinde-hak-sahiplerinin-tamami-konteynere-yerlestirildi [Accessed 1 February 2024].

PSB, Presidency of Strategy and Budget, Presidency of Republic of Türkiye. (2023). Türkiye earthquakes recovery and reconstruction assessment report. Available at: https://www.sbb.gov.tr/wp-content/uploads/2023/03/,Türkiye-Recovery-and-Reconstruction-Assessment.pdf

ReliefWeb, 2023. https://reliefweb.int/report/turkiye/ifrc-turkey-delegation-secondary-data-review-turkey-february-2023-earthquake-weekly-highlights-vol-16-5-april-2023

Reuters (2023). Anger over Turkey’s temporary Twitter block during quake rescue. Reuters. Available at: https://www.reuters.com/world/middle-east/anger-over-turkeys-temporary-twitter-block-during-quake-rescue-2023-02-09/ [Accessed 2 Feb. 2024].

Robins, A. (2023). Why did the flooding in the earthquake zone cause so much damage and loss of life? 16 March. Available from: https://www.bbc.com/turkce/articles/cye4lpprkn5o [Accessed 20 December 2024].

Sağıroğlu, A. Z., Ünsal, R., & Özenci, F. (2023). Post-Earthquake Migration and Human Mobility Situation Assessment Report. Ankara Yıldırım Beyazıt University Migration Policies Application and Research Centre (AYBÜ-GPM).

Sağıroğlu, A.Z., Ünsal, R., & Özenci, F. (2023) Deprem Sonrası Göç ve İnsan Hareketlilikleri Durum Değerlendirme Raporu. AYBÜ-GPM Rapor Serisi-15 (Güncellenmiş 2. Baskı: 15 Nisan 2023). Ankara: Ankara Yıldırım Beyazıt Üniversitesi Göç Politikaları Uygulama ve Araştırma Merkezi (AYBÜ-GPM).

Sargin, S., Dinç, Y. (2017). A Spatial Evaluation for the Protection of Cultural Heritage: Functional Change of Old (Traditional) Antakya Houses. Turkish Studies, 12(13), pp. 477-506.

Sert, Ö. (2018). The History of Disaster as Time-Space Expansion. Kebikec: Journal of Literature Research for the Human Sciences, (45).

sondakikacom (2023). President Erdoğan: 'We will lay a new future, a new life in front of our people'. Son Dakika. Available at: https://www.sondakika.com/politika/haber-cumhurbaskani-erdogan-dan-aciklamalar-2-15667512/ [Accessed 1 Feb. 2024].

Soylu, R. (2023). Turkey earthquake: Rents spike as survivors relocate west in search of safety. Middle East Eye. Available at: https://www.middleeasteye.net/news/turkey-earthquake-rent-prices-surge-migration-safe-homes [Accessed 12 Sep. 2023].

Subaşi, Ö. (2015). Natural Disasters That Occurred in Anatolia in the 11th Century. Atatürk University Turkic Studies Institute Journal, (54).

Suveyan, S. (2023). August 17 and February 6- What We Did and Couldn't Do After the Earthquake. Arkitera, 23 April. Available from: https://www.arkitera.com/gorus/17-agustos-ve-6-subat-deprem-sonrasinda-yaptiklarimiz-ve-yapamadiklarimiz/ [Accessed 1 February 2024].

T24. (2023) Antakya'daki arama - kurtarma çalışmalarından izlenimler: "Ses vere vere, bekleyerek öldüler". Available at: https://t24.com.tr/haber/antakya-daki-arama-kurtarma-calismalarindan-izlenimler-ses-vere-vere-bekleyerek-olduler,1094712 [Accessed 19 Jan 2024].

Tatlı, I. (2023). Post-Earthquake Migration and Refugee Resettlement Issues. Insamer, 06 March. Available at: https://www.insamer.com/tr/deprem-sonrasi-goc-ve-multecilerin-yeniden-yerlesimi-meseleleri.html [Accessed 1 February 2024].

TCCB. (2023). 'The silhouettes of permanent housing all over the earthquake zone began to rise.' 20 May. Available from: https://www.tccb.gov.tr/haberler/410/147228/-deprem-bolgesinin-dort-bir-yaninda-kalici-konutlarin-siluetleri-yukselmeye-basladi- [Accessed 22 January 2024].

Tekeşin, Ö., (2011). Investigation of Neotectonic Period Structures between Hatay (Antakya)-Samandağ. Ph.D. thesis, Eurasian Institute Of Earth Sciences.

Tercan, B. (2018). 1948'den bugüne imar afları. Mimarlık, 55(403), 20-26.

The Open Society Institute (2003). Ethnic, Religious and Language Groups: Towards a Set of Rules for Data Collection and Statistical Analysis. Available from: https://www.opensocietyfoundations.org/publications/ethnic-religious-and-language-groups-towards-set-rules-data-collection-and [Accessed 5 June 2023].

TMMOB Mimarlar Odasi. (2023). Mimarlar Odası 6 Şubat 2023 Depremleri Raporu - 2 Tespitler, Değerlendirmeler ve Öneriler. Available at: https://www.tmmob.org.tr/icerik/mimarlar-odasi-6-subat-2023-depremleri-tespit-ve-degerlendirme-raporu-yayimlandi

TOKI. (2023). TOKİ President Ömer Bulut: Strong and solid construction criteria of TOKİ will be applied. 22 February. Available from: https://www.toki.gov.tr/haber/toki-baskani-omer-bulut-tokinin-guclu-ve-saglam-yapi-kriterleri-uygulanacak [Accessed 22 January 2024].

Toksabay, E., Arranz, A., Chowdhury, J., et al. (2023). The toxic dust from Turkey's earthquakes. Reuters, 11 May. Available at: https://www.reuters.com/graphics/TURKEY-QUAKE/TOXINS/znvnbmyrzvl/ [Accessed 22 January 2024].

Topkara, N., Yücemen, M.S., Yilmaz, N., Deniz, A. (2019). Estimation of Earthquake Hazard for Antakya and its Neighbourhood by Stochastic Methods. 2nd Turkey Earthquake Engineering and Seismological Conference. Hatay.

TRT Haber (2023). The loss of life in the earthquake is 50 thousand 96 people. Available at: https://www.trthaber.com/haber/gundem/depremde-can-kaybi-50-bin-96-oldu-754477.html [Accessed 2 Feb. 2024].

TRT Haber. (2023) Rough construction of a block in the earthquake housing project in Hatay has been completed. Available from: https://www.trthaber.com/foto-galeri/hatayda-deprem-konutlari-projesinde-bir-blokun-kaba-insaati-tamamlandi/56128/sayfa-1.html [Accessed 1 February 2024].

TTB (2023). Turkish Medical Association draws attention to hygiene problems in tent cities. 28 April. Available from: https://bianet.org/haber/ttb-cadir-kentlerdeki-hijyen-sorununa-dikkat-cekti-277964 [Accessed 20 December 2024].

TÜİK (2023). Turkish Statistical Institute (TÜİK). Available at: https://www.tuik.gov.tr/.

Üsküplü, S. (2012). Preparation of earthquake scenarios of Hatay province and its surroundings by using GIS analysis techniques and comparison of these scenarios with historical earthquakes. Ph.D. thesis, Eurasian Institute of Earth Sciences.

Uzuner, E. and Akıncıtürk, N. (2020) An Evaluation of the Post-earthquake Urban Expansion Process: Kocaeli/ Gölcük Example. Resilience Journal, 4(1), 65-75.

Voa Türkçe (2023). Syrians who went to their country after the earthquake are returning. VOA Türkçe. Available at: https://www.voaturkce.com/a/depremde-ulkelerine-giden-suriyeliler-geri-donuyor/7059313.html [Accessed 2 Feb. 2024].

Wikipedia (2023). Wikipedia - Humanitarian response to the 2023 Turkey–Syria earthquake. Available at: https://en.wikipedia.org/wiki/Humanitarian_response_to_the_2023_Turkey%E2%80%93Syria_earthquake#:~:text=A%2072%2Dmember%20search%2Dand,those%20affected%20by%20the%20earthquakes [Accessed 2 Feb. 2024].

Wikipedia. (2024). Languages of Turkey. Available at: https://en.wikipedia.org/wiki/Languages_of_Turkey#cite_note-18 [Accessed 2 Feb. 2024].

World Bank and Global Facility for Disaster Reduction and Recovery (2023). Global Rapid Post-Disaster Damage Estimation (GRADE) Report: February 6, 2023 Kahramanmaraş Earthquakes-Türkiye Report.

Yeni Akit (2023). Shocking figure! Exactly one fifth of those died in the earthquake... Yeniakit.com.tr. Available at: https://www.yeniakit.com.tr/haber/sok-eden-rakam-depremde-hayatini-kaybedenlerin-tam-beste-biri-1733617.html [Accessed 2 Feb. 2024].

Yeni Asya. (2023). 345 tent cities and 305 container cities were established. Yeni Asya, 5 April. Available at: https://www.yeniasya.com.tr/gundem/345-cadir-kent-ve-305-konteyner-kent-kuruldu_580363 [Accessed 1 February 2024].

Yeniçağ Gazetesi. (2023). A woman's dead body was removed from the rubble on the 135th day of the earthquake. Available at: https://www.yenicaggazetesi.com.tr/depremin-135-gununde-enkazdan-kadin-cesedi-cikarildi-678954h.htm [Accessed 2 Feb. 2024].

Yesilbag, M. (2016). Hegemonyanın Harcı: AKP Döneminde İnşaata Dayalı Birikim Rejimi. Ankara Üniversitesi SBF Dergisi. [Details such as volume, issue, and page numbers are missing.]

Yücel, S.S. (2016). Evaluation based on calculation and device data under the earthquake impact of masonry type buildings. Master's Thesis, Iskenderun Technical University.

Yunatçi, A.A., Çetin, K.Ö. (2007). Probabilistic Seismic Hazard Analysis for Great Karaçay Dam and Hydroelectric Power Plant. 1st National Dam Safety Symposium and Exhibition. Ankara.

Zeyneloglu, S., Sirkeci, I., & Civelek, Y. (2016). Language shift among Kurds in Turkey: A spatial and demographic analysis. Kurdish Studies, 4, 25-50. doi:10.33182/ks.v4i1.405.

8. LAST WORD: WHAT HAS CHANGED?

The Türkiye earthquake sequence of February 2023 caused mass destruction over a very large geographical area. One year on from the earthquakes, the recovery and reconstruction efforts are still ongoing, with the aim of building back better and establishing resilient communities. The Government of Türkiye has allocated 15 billion Turkish liras (about 1.8 billion US dollars) for the reconstruction of housing and infrastructure. Various humanitarian partners have also provided different forms of assistance, such as cash transfers, livelihood support, education, and protection. In this final chapter, we have collated a series of situational updates and will highlight some ongoing concerns from the events of 2023.

Housing: The Earthquake Report prepared a year after the events by the Hatay Earthquake Victim Association states that 520,000 houses were deemed unusable in their province, and it is estimated that at least half of the families living in these houses will continue to live in tents and containers until they settle in permanent housing (Hatay Earthquake Victim Association, 2024). The same report states that a significant majority of people whose houses were moderately/severely damaged or completely destroyed has chosen not to settle in containers, and instead applied for rental support. However, many of these people faced difficulties in accessing suitable rental options due to rising rental prices and the insufficiency of existing housing stock, and while we understand that these people constitute the majority of those currently living in tents, there are no official audit or statistics on these statements. As in other post-earthquake contexts, the options available to owners and tenants of properties are starkly different. Only property owners are eligible to newly built permanent houses and there are no proposed solutions to date for tenants. *Figure 265* illustrates the housing options available to affected people.

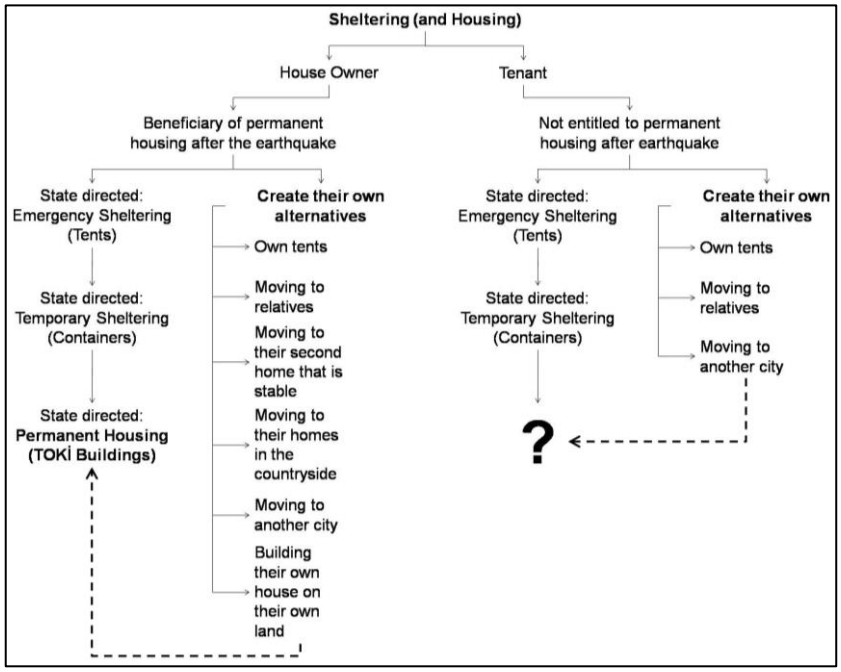

Figure 265: Sheltering and Housing options for disaster victims following February 6 (2023) Kahramanmaraş Earthquakes

To date, AFAD has paid 14.5 billion TL in rental assistance to earthquake victims. As of January 2024, the rental assistance payment to homeowner earthquake victims was increased from 5,000 TL to 7,500 TL (from 164.47 US $ to 246.71 US $) and the rental assistance payment to tenant earthquake victims was increased from 3,000 TL to 5,000 TL (from 98.68 US $ to 164.47 US $) (YirmidortTV, 2024). However, it is doubtful that rent subsidies are sufficient for accessing a tenancy in the earthquake zone. *Table 41* summarises a prices analysis for advertised rental properties in Antakya, drawing on data from "sahibinden.com", a widely used website for real estate for rent/sale in Türkiye. Our analysis shows that in Antakya, the central district of Hatay province, where the earthquake caused the heaviest damage, as of February 2024, 121 properties of different sizes were advertised for rent. As seen, the support provided by the government can barely cover the cost of even the smallest apartments in Antakya. As observed by many community groups, this, and other related factors are leading to dwindling population in the city. Further, earthquake survivors who chose to migrate to Türkiye's metropolitan cities such as Istanbul, Ankara and Izmir face much higher rent prices in these cities. Rental support for earthquake victims is expected to be offered only until the end of this year, which will exacerbate economic hardship for the affected people who cannot afford a property by 2025.

Table 41: Price analysis of apartments advertised for rent in Antakya. Data is obtained from: https://www.sahibinden.com/kiralik-daire/hatay-antakya?sorting=price_desc (accessed on 04.02.2024) ($1 = 30.4 TL).

Apartment Type - Size	**Number of Flats**	**Average Monthly Rental Cost** (This price does not include apartment service charges or the bills)
Apartment Flat - 1+0 (1 bedroom apartment flat)	2	4.750,00 TL (Between 5.500 - 4.000 TL) (*156,25 US $*)
Apartment Flat - 1+1 (1 bedroom and 1 sitting room apartment flat)	19	7.105,00 TL (Between 11.000 - 6.000 TL) (*233,71 US $*)
Apartment Flat - 2+1 (2 bedrooms and 1 sitting room apartment flat)	49	9.040,00 TL (Between 20.000 - 6.000 TL) (*297,36 US $*)
Apartment Flat - 3+1 (3 bedrooms and 1 sitting room apartment flat)	45	12.013,00 TL (Between 25.000 - 8.000 TL) (*395,16 US $*)
Apartment Flat - 4+1 (4 bedrooms and 1 sitting room apartment flat)	4	16.875,00 TL (Between 18.000 - 15.000 TL) (*555,10 US $*)
Apartment Flat - 5+1 (5 bedrooms and 1 sitting room apartment flat)	2	33.500,00 TL (Between 50.000 - 17.000 TL) (*1.101,97 US $*)

Permanent Housing (as of 1/2/2024): According to the data of the Turkish Ministry of Environment, Urbanization and Climate Change (TMoEUCC), 46,000 dwellings, which constitute the first phase of the permanent housing built after the February , 2023 earthquakes, are planned to be delivered in the first week of February (2024) in the provinces affected by the earthquakes (TRTHaber, 2024). Based on the same source, the number of dwellings to be delivered to the rightful owners in February-March 2024 is expected to be equal to 75,000.

The breakdown of the number of permanent TOKİ multistorey housing and low rise village houses (standard RC frame structures) under construction in Hatay is given in *Table 42* (TRTHaber, 2024). Based on this data, there is shortfall of around 78% between the number of TOKI housing units projected to be built in Hatay in the long term (146,000 units according to TRTHaber, 2024) and the housing units currently

under construction (32,314 units). Based on data published thus far by the TMoEUCC, we project that overall, considering all earthquake-affected provinces, 11.79% of the hosuign units planned for the beneficiaries have been completed by the government as of February 2024.

Table 42: TOKİ Permanent Housings which are under construction in the districts of Hatay Province. Data obtained from Ministry of Environment, Urbanization and Climate Change (TRT Haber, 2024).

District	TOKİ Housing	Village Housing
Antakya	12.823	316
Arsuz	1.188	494
Defne	3.069	127
Altınözü	364	900
İskenderun	3.986	157
Payas	1.351	-
Kırıkhan	2.576	1.088
Kumlu	303	7
Hassa	3.878	276
Samandağ	424	407
Dörtyol	2.060	-
Belen	292	87
Erzin	-	158
Reyhanlı	-	885
Yayladağı	-	680
TOTAL	**32.314**	**5.582**

Policy Changes Regarding Reconstruction: Despite the well-publicised role that the centrally governed risk management protocols played in this tragedy through legalisation of non-compliant buildings using amnesties and top-down land use decisions, we see that most recovery decisions are now also taken and implemented at a centrally managed fashion (*cf.* Erdoğan (2024) for the president's recent statements in Hatay), with no engagement with local stakeholders.

The recent "reserve area" law is a good example to this: this new law has recently been enacted to accelerate urban transformation after the 2023 earthquakes and to create new settlements in built-up areas at high seismic risk. According to this law, the TMoEUCC, TOKİ, municipalities, or real estate owners can declare vacant or existing residential areas as reserve areas, where operations such as expropriation, demolition, zoning plan changes and housing and social facilities construction are allowed to be carried out more quickly than they are under normal circumstances, owed to simplified bureaucratic protocols (TMoEUCC Istanbul Provincial Directorate, 2024). The reserve area law was implemented for the first time in Türkiye on an area of 270 hectares in Hatay. In this area, it is planned to demolish the buildings damaged or at seismic risk, and replace them with new residences (Cumhuriyet, 2023). The reserve area law has also started to be implemented in some neighbourhoods in Istanbul (TMoEUCC Istanbul Provincial Directorate, 2024).

Although the reserve area law provides an opportunity for safer built environments, it also brings along many risks. These include violation of property rights, displacement and eviction, loss of cultural heritage, environmental problems, disruption of social balances, and risk of corruption (Ortak Akil - Antakya, 2023). In Antakya and Defne, where the law has been implemented by the TMoEUCC (Gerçek Gündem, 2023) there is a lack of clarity as to what informs the decision-making and the declaration is perceived by many to pose the risk of dispossession and displacement of

approximately 50,000 people living in the region. We understand from various interviews that the affected residents have neither been consulted nor informed about the verdict or the details of the project that is to be implemented on their land (Gurses, 2024). The reserve area law has therefore been criticised as a practice that could harm the historical, cultural and environmental values of Antakya. Indeed, the Hatay Bar Association announced that it is preparing to file a lawsuit for the annulment of the law (*ibid*).

Similarly the recently launched law no. 7441 on the establishment of post-disaster reconstruction funds has been criticized for being vague in terms of how the funds will be created and allocated: The item 4 of the law states that the funds will be sourced from “a) All kinds of cash donations, aid, grants and loans originating from domestic and foreign sources; b) From the appropriation to be included in the budget for this purpose; c) Financing and resources provided by the Fund from domestic and foreign capital and money markets by being exempt from all restrictions in the legislation of institutions and organizations and d) From other income”. The funds raised this way are allowed to be tax-free and not be subject to usual auditing, and used at will and discretion of the Presidency (Resmi Gazete, 2023). The law is therefore a reminiscence of the funds creation processes associated with the *Türkiye Tek Yürek* donations programme, contributed to by many citizens in Türkiye and abroad, as well as governmental departments to raise money for the first response in the aftermath of the February earthquakes, and of the compulsory earthquake insurance (COI) in terms of the lack of commitment to the accountability in their use.

Civil Initiatives: On a more positive note, the team have seen numerous civilian or non-governmental initiatives to disentangle problems that led to the devastation from the events, and to inform recovery. *Sivil Düşün* is a EU programme supporting non-governmental organisations and activists working on post-disaster recovery. There are multiple accounts on X which release technically sound posts/threads on design and implementation flaws of buildings that collapsed at the earthquakes (e.g. @sharpquadratic) – a much needed endevour given the public prosecution work that was initiated right after the earthquakes to identify shortcomings of collapsed buildings has never yielded a publicly available set of information thus far.

Living Heritage is a collective composed of Hatay Deprem Dayanışması Derneği, TMMOB Chamber of City Planners and TMMOB Chamber of Architects as well as Architecture sans Frontières, among others, who recently released a statement for community-driven post-earthquake reconstruction in Antakya. They also highlighted in this document some of the ongoing problems in the area including the lack of basic infrastructure, its decreasing population, development driven displacement and the environmental and health hazards created by the debris removal and dumping programme. The main challenges faced by the affected communities a year on include:

1. **Lack of basic infrastructure and decreasing population**: Many people have left the city due to lack of housing and lack of access to basic infrastructure. Safe drinking water, food, sanitation and energy are scarce in supply. Healthcare, education, transport and employment are all very limited, this is leading to more people leaving the city.

2. **Ecological destruction and public health hazards**: The situation with respect to environmental and health impacts of rubble clearance and dumping persists, as these continue to be carried out without regard to legal safety measures and experts' warnings.
3. **Encroachment on natural and collective spaces**: There has been significant encroachment on open spaces and farmland following the earthquakes, because of tent sites and container camps, makeshift housing and dumping of rubble and other waste. This is eroding collectives spaces and natural environments. Issues of urban sprawl have been longstanding in Antakya and the post-earthquake decisions so far are making this situation worse. The selection of permanent housing sites on the outskirts of Antakya, and in farmland and natural areas will further exacerbate these issues as thousands of houses are to be built on these sites far from the city centre. There needs to be a balance between safety in reconstruction and in developing a sustainable and liveable city.
4. **Loss of sense of place, memory and vernacular heritage**: Restoring the 'sense of place' of inhabitants is important for repairing the city and a healthy recovery. This is not just about historical monuments but everyday spaces, like vernacular/traditional environments, markets and squares.
5. **Displacement, gentrification and touristification**: Local residents are very concerned about the gentrification and touristification of Old Antakya. This was already underway before the earthquake, but there are now opportunities for significant speculation. Low-income people and minorities are worries about being permanently displaced from their neighbourhoods.
6. **Personal safety and security**: Residents in Antakya are facing increased crime and theft resulting from abandoned areas and lack of proper lighting. There are also physical hazards caused by demolitions, falling debris and unstable structures, as well as a higher risk of traffic accidents due to the road conditions.

Key Messages from EEFIT

Reflecting on the findings from the missions and the information gathered a year on from the tragic events, the EEFIT team have two main areas of concerns. Firstly, there is a **lack of systematic and transparent data** hindering effective disaster management and post-disaster recovery. Data that is needed to make a comprehensive analysis of the vulnerability of the building stock, the design practices, the characteristics of the building stock, paperwork on planning and approval for building projects and inspection outcomes either do not exist or are not accessible. One year into the events, we are yet to attain, among other questions, the exact numbers of affected building stock, how and based on what criteria these are handled by the authorities, the construction age-earthquake performance relationship, and the social, economic and financial perturbations of the earthquakes within and beyond the eleven earthquake-hit cities.

The second is the **uncertainty**. An online survey was conducted by Hatay Planning Center (HPC) to comprehend and examine the perception of the recovery between August and October 2023. The findings from the responses of 5155 participants

(Antakya, 40%; Defne, 22%; Iskenderun, 13%, which aligns with the broader demographic structure) showed a sense of shared urgency of restoring the city to its previous state swiftly, enhancing daily living conditions, and fulfilling basic needs such as housing, education, and health, even after a considerable period of time elapsed. Similarly, the EEFIT team collected responses from 35 participants in the affected region in November 2023 (So et al., 2024), which showed that there was a desire for a safer built environment, accompanied however by an increased societal anxiety about the next big earthquake in Istanbul. The affected communities also expressed their frustrations and sadness for being left 'on their own' to navigate through the unclear, constantly changing and often-in-conflict official statements, and gauge what awaits them now and in the future.

We, as the EEFIT Team, would like to advocate for sustainable recovery following last year's tragedy, as well as for an improved seismic resilience and disaster management apparatus in Türkiye that encompasses:

a) **Inclusivity**: Disaster risk management and post-disaster recovery approaches which engage communities and other local stakeholders is key. Centrally imposed decisions are not in touch with the social, cultural and economic local context and therefore disruptive, and do clearly not contribute to overall resilience as history shows. There are several strong citizen's groups and professional organisations calling for greater participation in decision-making, and the need to work together with government bodies to develop plans that are inclusive.

b) **Mid-/long-term thinking**: Solutions to enhance resilience in a more sustainable way and respectfully to the environment, the rich local living cultures and the vernacular of the earthquake hit area in Türkiye require mid- / long-term thinking. With full appreciation of the matters which require urgent attendance, authorities should differentiate issues where haphazard and hasty decisions are likely to bring along potential unintended adverse consequences, which may be too difficult to solve in the future.

c) **Accountability and Data Transparency**: Lack of accountability underpins many pre-/post-disaster decision-making or action protocols in Türkiye. Institutional trust should be reinstated through political will, clear and publicly available data and penetrable and honest public discourses.

References

Ortak Akıl-Antakya (2023, Aralik 5). ANTAKYA ŞEHİR MERKEZİNDE REZERV YAPI ALANI İLANI HAKKINDA KAMUOYUNA DUYURU. Retrieved from Ortak Akıl-Antakya Platformu: https://www.ortakakilantakya.com

CNN Turk (2024, January 15). Rezerv alan yasası nedir? Rezerv alan düzenlemesi nasıl uygulanacak? Retrieved from CNN Turk: https://www.cnnturk.com/,Türkiye/rezerv-alan-yasasi-nedir-rezerv-alan-duzenlemesi-nasil-uygulanacak

Cumhuriyet. (2023, December 22). Rezerv alan nedir? Rezerv alanı ilan edilirse ne olur? İstanbul'da rezerv alanı ilan edilen yerler neresi? Retrieved from Cumhuriyet: https://www.cumhuriyet.com.tr/,Türkiye/rezerv-alan-nedir-rezerv-alani-ilan-edilirse-ne-olur-istanbulda-2154583

MoEUCC Istanbul Provincial Directorate (2024, February 01). Rezerv Yapı Alanı. Retrieved from Çevre, Şehircilik ve İklim Değişikliği İstanbul İl Müdürlüğü: https://istanbul.csb.gov.tr/rezerv-yapi-alani-i-3121

Erdoğan, O. (2024, February 4). “Merkezi yönetimle yerel yönetim el ele vermezse o şehre herhangi bir şey gelmez" . Retrieved from VOA: https://www.voaturkce.com/a/merkezi-yonetimle-yerel-yonetim-el-ele-vermezde-p-sehre-herhangi-bir-sey-gelmez/7470202.html

Resmi Gazete (2023, March 21). AFET YENİDEN İMAR FONUNUN KURULMASI HAKKINDA KANUN. Retrieved from Resmi Gazete: https://www.resmigazete.gov.tr/eskiler/2023/03/20230321-11.htm

Gercek Gündem (2023, November 26). Afet Yasası ilk Hatay'ı vurdu: Defne, Rezerv Alanı ilan edildi. Retrieved from Gerçek Gündem: https://www.gercekgundem.com/guncel/afet-yasasi-ilk-hatayi-vurdu-defne-rezerv-alani-ilan-edildi-442597

Gurses, O. (2024, February 2). Rezerv alanlar nasıl ilan ediliyor? Depremzede Damla Erdoğan'ın anlattıklarını dehşetle dinledim! Retrieved from Youtube: https://www.youtube.com/watch?v=gUDFExYHfPY

YirmidortTV (2024). Available From: https://www.yirmidort.tv/ekonomi/depremzedeleri-yakindan-ilgilendiriyor-kira-yardimi-uzatilacak-mi-151731 (Accessed on January 2024).

EEFIT

Earthquake Engineering Field Investigation Team

EEFIT is a UK based group of earthquake engineers, architects and scientists who seek to collaborate with colleagues in earthquake prone countries in the task of improving the seismic resistance of both traditional and engineered structures. It was formed in 1982 as a joint venture between universities and industry, it has the support of the Institution of Structural Engineers and of the Institution of Civil Engineers through its associated society SECED (the British national section of the International Association for Earthquake Engineering).

EEFIT exists to facilitate the formation of investigation teams which are able to undertake, at short notice, field studies following major damaging earthquakes. The main objectives are to collect data and make observations leading to improvements in design methods and techniques for strengthening and retrofit, and where appropriate to initiate longer term studies. EEFIT also provides an opportunity for field training for engineers who are involved with earthquake-resistant design in practice and research.

EEFIT is an unincorporated association with a constitution and an elected management committee that is responsible for running it activities. EEFIT is financed solely by membership subscriptions from its individual members and corporate members. Its secretariat is generously provided by the Institution of Structural Engineers and this long-standing relationship means that EEFIT is now considered part of the Institution.

This report can be downloaded from www.eefit.org.uk

EEFIT
c/o The Institution of Structural Engineers,
47 – 58 Bastwick St, London EC1V 3PS
Tel: +44 (0)20 7235 4535
Fax: +44 (0)20 7235 4294
Email: mail@eefit.org.uk
Website: http://www.eefit.org.uk